NBS SPECIAL PUBLICATION 378

Accuracy in Spectrophotometry and Luminescence Measurements

U.S. DEPARTMENT OF COMMERCE
National Bureau of Standards

Accuracy in Spectrophotometry and Luminescence Measurements

Proceedings of the Conference Held at the
National Bureau of Standards, Gaithersburg, Md.
March 22-24, 1972

Edited by

R. Mavrodineanu, J. I. Shultz, and O. Menis

Analytical Chemistry Division
Institute for Materials Research
National Bureau of Standards
Washington, D.C. 20234

U.S. DEPARTMENT OF COMMERCE, Frederick B. Dent, *Secretary*
NATIONAL BUREAU OF STANDARDS, Richard W. Roberts, *Director*

Issued May 1973

Library of Congress Catalog Card Number: 73-600066

National Bureau of Standards Special Publication 378

Nat. Bur. Stand. (U.S.), Spec. Publ. 378, 268 pages (May 1973)

CODEN: XNBSAV

Reprinted from the National Bureau of Standards
Journal of Research, Section A. Physics and Chemistry
Vol. 76A, Nos. 5 and 6, Sept.-Oct., and Nov.-Dec. 1972.

For sale by the Superintendent of Documents, U.S. Government Printing Office, Washington, D.C. 20402
(Order by SD Catalog No. C13.10:378). Price: $4.85, domestic postpaid; $4.50, GPO Bookstore

Abstract

This volume contains the 18 papers presented at the Conference on Accuracy in Spectrophotometry and Luminescence Measurements organized by the Analytical Chemistry Division of the National Bureau of Standards and held from March 22 to 24, 1972.

These papers discuss the problems encountered in accurate spectrophotometry and luminescence measurements of materials. They also define the status of these competences from the standpoint of basic principles, critical factors involved in the measurements, and the instrumental conditions which must be fulfilled to assure accurate measurements. Particular attention is given to the selection, production, and use of Standard Reference Materials in spectrophotometry and spectrofluorometry. Problems related to health are also covered in six of the papers, two of which include original contributions to the application of luminescence techniques to specific biochemical problems.

Key words: Accuracy, critical parameters; instrumentation; linearity; quantum efficiency; spectrofluorometry; spectrophotometry; standards.

Foreword

"When you can measure what you are speaking about, and express it in numbers, you know something about it; but when you cannot measure it, when you cannot express it in numbers, your knowledge is of a meager and unsatisfactory kind; it may be the beginning of knowledge but you have scarcely, in your thoughts, advanced to the stage of science," by William Thompson, Lord Kelvin, Popular Lectures and Addresses (1891-1894).

This work presents the formal Proceedings of the Conference on Accuracy in Spectrophotometry and Luminescence Measurements which was organized by the Analytical Chemistry Division of the NBS Institute for Materials Research. The Conference was held at NBS from March 22 through March 24, 1972. The papers contained in this volume have also been published in two consecutive issues of the Journal of Research of NBS, Volume 76A, Nos. 5 and 6, 1972.

This Conference brought together a number of leading authorities from the United States and from overseas whose broad knowledge and experience provided valuable scientific contributions to the various topics of the Conference. The papers assembled in these Proceedings focus attention on the problems associated with accuracy in spectrophotometry and luminescence measurements of materials, and define the status of these competences from the standpoint of basic principles, instrumental parameters, measurements, and Standard Reference Materials.

A major objective of the Conference was to provide the analytical chemist with the means to establish and maintain accuracy in spectrophotometric and luminescence measurements. The works presented in these Proceedings should contribute significantly to the advancement of spectrophotometric and luminescence measurements and constitute a solid ground for further progress.

W. Wayne Meinke, Chief
Analytical Chemistry Division

May 1973

Preface

This volume is divided in two parts. The first part consists of six invited lectures and four invited panel discussions on the subject of accuracy in spectrophotometry. The three invited lectures and five invited panel discussions, which constitute the second part of the volume, are devoted to the topic of accuracy in luminescence measurements.

These contributions are intended to interrelate theory and instrumentation with methodology for measuring "real samples" which are encountered in the general field of analytical chemistry, and more specifically in the fields of health and environment. The roles of the basic principles and instrumentation in the science of measurements are reflected in several papers. Three of these, by Clarke, by Mavrodineanu, and by Mielenz, represent parallel approaches to the evaluation of accuracy of spectrophotometers and serve to augment the other contributions. At the same time, independent measurements of a series of glass filters (NBS-SRM-930), serve to establish the magnitude of the bias in this calibration. In this manner a better understanding of the needs and limitations of a material in a measurement situation has been established. Points of view on the philosophy of spectrophotometric standards are expressed by Venable.

In the area of luminescence measurements, the three papers by Melhuish, by Crosby, Demas and Callis, and by Winefordner survey the basic problems and instrumental criteria. Their descriptions include a discussion of the state of the art and provide a clear prediction of the direction of future efforts. The two papers describing the absolute calibration of light sources and photodetector linearity by Rutgers, and by Sanders relate equally to both measurement problems. The three papers by Burke, Deardorff and Menis, by Reisfeld, and by Velapoldi, interface the instrumental performance with real sample measurements through the development of suitable material standards in spectrophotometry and spectrofluorimetry. On the other hand, the important areas of health and environment are extensively covered in four papers by Penton, Widdowson, and Williams, by Burnett, by Rand, and by Chen. They help to pinpoint the problems and progress associated with automation and clinical measurements. Finally, the papers by Udenfriend, and by Guilbault present insight into original contributions to the application of luminescence techniques to specific health measurement methodology.

This collection assembles in one volume valuable and original contributions, and constitutes a unique and important source of information which should serve equally well the workers in the field of research and applications of spectrophotometric and luminescence measurements.

The NBS Committee responsible for the organization of the Conference were Oscar Menis, general chairman and panel discussion moderator; James I. Shultz, associate general chairman; Radu Mavrodineanu, program chairman; Rance A. Velapoldi, associate program chairman; Robert W. Burke, arrangement chairman; and Sara R. Torrence, arrangement liaison.

The Conference had the encouragement of the National Institute of General Medical Sciences, who also cooperated with the National Bureau of Standards in supporting part of the work of the Analytical Chemistry Division. This work led to the design and development of instrumentation for high accuracy spectrophotometry; for the study, preparation and evaluation of liquid absorbance standards, and in the investigations related to solid compounds and inorganic ion glasses as Standard Reference Materials for spectrofluorometry. This support resulted in the issuance of a number of standards which assure that more meaningful measurements will be made in the field of biochemistry and related areas.

The undertaking of the Conference and publication of this book would not have been possible without the cooperation and assistance of many persons.

The important contributions of all speakers and the assistance of the session chairmen is acknowledged with deep appreciation.

The NBS Office of Technical Information and Publication, under the direction of W. R. Tilley, gave invaluable assistance to the publication of this volume; we wish to acknowledge in particular the assistance of Mrs. Betty L. Oberholtzer, Mrs. Bertha S. Darrow, and Mrs. Mary V. Betizel.

Within the Analytical Chemistry Division, special thanks are given to Mrs. Mary Pantazis for her tireless efforts in typing some of the manuscripts, and her diligent work in taking care of correspondence and program publications. Particular appreciation is expressed to Mrs. Rosemary Maddock for providing coordination and invaluable assistance in the many phases of preparing this volume. Special thanks are also extended to R. A. Velapoldi for his assistance in reviewing the papers on luminescence and for preparing the author index.

R. Mavrodineanu

J. I. Shultz

O. Menis

May 1973

Contents

PART I. SPECTROPHOTOMETRY

NATIONAL BUREAU OF STANDARDS SPECIAL PUBLICATION 378, Accuracy in Spectrophotometry and Luminescence Measurements, Proceedings of a Conference Held at NBS, Gaithersburg, Md., March 22–24, 1972 (Issued May 1973).

High Accuracy Spectrophotometry at the National Physical Laboratory

F. J. J. Clarke

National Physical Laboratory, Teddington, Middlesex, UK.

(June 5, 1972)

The techniques and equipment used at the National Physical Laboratory (NPL) to achieve high accuracy spectrophotometric measurements are described and discussed. The emphasis at NPL has always been on the determination of systematic components of error and their elimination or correction rather than on the attainment of mere precision, which is largely a matter of variance and resolution. The scales of regular transmittance, diffuse transmittance, total transmittance of scattering samples, regular reflectance, diffuse reflectance, total reflectance and radiance factor are determined, maintained, and made available in practical form to industry by combined use of a reference NPL manual spectrophotometer and commercial recording spectrophotometers.

The presentation will concentrate on transmittance measurements made with the reference instrument, which is designed specifically to allow separate investigation of the various possible sources of systematic error, processes that are not practicable with commercial spectrophotometers. The investigation of the linearity of the complete photoelectronic system has always been a key factor, and double-aperture devices have been used consistently at NPL for over 40 years to monitor the performance of this instrument and its predecessors. Besides instrumentation, the procurement of material standards of suitable quality is a major limitation of the art, and the types in use at NPL are described, including the recently developed Ceramic Colour Standards.

Key words: High accuracy spectrophotometry; photoelectronic linearity; reflectance; transmittance.

1. Introduction

Spectral measurements and techniques in the ultraviolet, visible and infrared regions of the electromagnetic spectrum fall into two general classes. The first involves work aimed at elucidating the physics and chemistry of the electronic, atomic, molecular and phase states of the materials involved, and this is the realm of the spectroscopist. The second involves work aimed at developing and using measurement techniques for accurate quantitative determinations of such properties as emissivity, radiance and radiant intensity of sources, transmittance, reflectance and radiance factor of passive materials, and responsivity of detectors. This is the realm of the radiometrist, photometrist and colorimetrist, but the techniques used (spectroradiometry and spectrophotometry) are of interest to scientists and technologists in many fields and industries because of their general usefulness. Those who develop the art are a very small minority compared with the users of the techniques and instruments, and are found usually at standardising laboratories and instrument manufacturers.

We may conveniently distinguish between spectroradiometry and spectrophotometry by means of an operational definition: spectroradiometry is concerned with the spectral properties of sources and detectors, whereas spectrophotometry is concerned with the spectral properties of material specimens. The work in these fields at the National Physical Laboratory (NPL) is currently organized in two Sections along just these lines: spectroradiometry forms part of the work of the Quantitative Spectroscopy Section under E. J. Gillham in Quantum Metrology Division, while ultraviolet, visible and near infrared spectrophotometry forms part of the work of Colorimetry and Photometry Section under myself in Metrology Centre. I regret to say that at present there is no programme of work at NPL on spectrofluorimetric standards, a subject still in its infancy but likely to become increasingly important. However fluorescent materials are measured for reflectance or diffuse transmittance as part of our spectrophotometric work, using either monochromatic illumination with broad-band detection or alternatively broad-band illumination with monochromatic detection, and the excitation and emission spectra can be distinguished from the reflected or transmitted components. Historically, spectrophotometric standards work in the ultraviolet and visible regions at NPL has always been closely integrated with colorimetry, and there is a very sound

reason for this: until relatively recently, the only users of spectrophotometers who really needed limit-of-the-art accuracy are those who use the instruments for colorimetric purposes. It was no accident that the colorimetrist Hardy at Massachusetts Institute of Technology (M.I.T.) set to work to design and develop the first commercially manufactured automatic recording spectrophotometer (The General Electric[1] instrument, ref. [1]) immediately following the establishment of the C.I.E. System of Colorimetry in 1931 and its widespread adoption by divers industries. That instrument remained unsurpassed for a great many years.

High accuracy spectrophotometry is needed for colorimetry because the chromaticity discrimination of the normal human observer is so fine that only very few of the instruments on the market can guarantee a commensurate accuracy in the derived colour specification. It may be pertinent to note that the colour industries generally use tristimulus filter colorimeters for differential measurements on production samples of known spectral profile, where speed and precision is more critical than freedom from possible systematic error, whereas spectrophotometers are used with tristimulus computation in cases where the spectral profile is unknown or likely to be variable and in cases where the highest absolute accuracy is required in colour specification. The development in recent years of colorant formulation by instrumental colour matched prediction systems [2, 3][2] nearly always involves spectrophotometers that are as accurate as are available on the commercial market and can be afforded by the firm involved.

The largest class of usage of spectrophotometers is by chemists, and except where their interests have been colorimetric, their demands have usually been for convenience, reliability, reproducibility and precision rather than for accuracy, for their uses are often diagnostic rather than critically quantitative. In cases where they have used spectrophotometric methods for determining concentrations, they have generally worked relative to standardised solutions and have not worried too much about the absolute accuracy of the optical density (absorbance) scales of their instruments. However, this situation is changing, and an increasing number of chemical and clinical applications are arising where high absolute accuracy is needed. Of the contributors to this Symposium, R. Mavrodineanu is probably best qualified to deal with these matters, and I will not myself comment further.

II. The General Nature of Errors and Accuracy in Spectrophotometry

Before considering in detail the methods of spectrophotometry and the equipment used at NPL, it is necessary to explain just what the term "high accuracy" can mean in this subject. It can mean several things: for instance one can distinguish between high quality commercial instruments and lower quality ones, and can say that by normal industrial and university laboratory criteria, high accuracy spectrophotometry is achieved when careful and competent staff are using a high quality instrument that is properly serviced when needed by the manufacturer or his agent. This approach may be embellished by ownership of several different designs of good quality instrument and the taking of an average of results from them or even some weighted mean, where the weighting depends on inspiration, prejudice or perhaps experience of their past history of divergences from the mean. However, such an approach is not acceptable for a standardising laboratory, or indeed any laboratory that aspires to making a determination to a known absolute accuracy, for it smacks of the "black box" approach which implicitly assumes that the manufacturers have somehow managed to build absolute accuracy into the photometric scale of the instrument or instruments. As it is well known from interlaboratory comparisons that different instrument types (and even different specimens of the same type) give systematic discrepancies that are experimentally significant in terms of their reproducibility and precision [4, 5, 6, 7, 8, 9], it is clear that it would be remarkable if even one instrument always gave a correct result. Since certain types of systematic errors are common to most instruments to some extent, it would also be remarkable if a mean result (or a weighted mean) could exactly or even approximately balance out the various sources of systematic error.

For the purposes of this Symposium we will take a more rigorous meaning of the term "high accuracy spectrophotometry." We will make no assumptions whatever about the validity of commercially manufactured equipment or about any calibration procedure which has been attempted by the manufacturer. We will question and test every aspect of the function of optical components or instruments which are used, and we will seek out, determine and correct for every systematic component of error which we can think of and discover, either in these component parts or in the complete reference instrument such as is described later.

Random components of error make their presence manifest in a rather obvious fashion, and most laboratories and text books are rather obsessed by them, with repeated use of phrases such as "signal-to-noise ratio" and similar concepts. Standardising laboratories should not be overconcerned with these problems, but rather with the systematic components of error. Random components of error are readily reduced by suitable statistical pooling of data from repeated runs, whereas systematic errors are not. A standardising laboratory can afford to and should make many more observations than an industrial laboratory normally would, and it usually becomes obvious as to how much reduction of variance by pooling is necessary. Again, I would point out that many laboratories are

[1] In order to adequately describe materials and experimental procedures, it was occasionally necessary to identify commercial products by manufacturer's name or label. In no instances does such identification imply endorsement by the National Bureau of Standards, nor does it imply that the particular product or equipment is necessarily the best available for that purpose.

[2] Figures in brackets indicate the literature references at the end of this paper.

unduly concerned with the statistical treatment of data, but this is not adequate to deal with the systematic errors that should be of most concern.

Excessive precision, arising from a combination of high resolution and good repeatability, is probably a bad thing since it tends to beguile even experienced staff into a false sense of security as to the real accuracy achieved. In the hands of inexpert staff the situation is worse, because of the confusion between the concepts of precision and accuracy that exists in so many minds. Of course, we must bear in mind that for many industrial purposes repeatability is more important than absolute accuracy. At this point we might note the difference between reproducibility and repeatability. Repeatability refers to the ability of an instrument to duplicate a result with a given sample presentation, and refers exclusively to the properties of the instrument. Reproducibility refers to the ability to duplicate a result when the sample presentation is repeated from scratch on different occasions i.e., when it is cleaned or prepared afresh, repositioned and realigned in the instrument. Reproducibility therefore refers to the whole measurement procedure and covers effects arising both from the instrument and the sample.

In general, components of errors are seldom purely random in nature or purely systematic, but tend to be intermediate in nature or rather closer to one aspect than the other. To assist in making this clear in practical terms, I have set out in figure 1 a classification of the more important types of error found in spectrophotometers in terms of their systematic or random nature, and it is instructive also to include for comparison the errors found in analogous instruments i.e., photometers, colorimeters, and abridged (filter) spectrophotometers. Some of these will be discussed in detail in section IV. Some of the errors which are partly systematic and partly random are very difficult to deal with, and these manifest themselves as errors which are systematically present for an unpredictable period and which then change to a different systematic error for another unpredictable period and so on. Such errors tend to be found in very complex systems, such as some of the more sophisticated double-beam automatic recording spectrophotometers, which may have several interlinked servos and feedback loops. This is one of the factors which has influenced us for decades at NPL in having a reference high accuracy spectrophotometer which is as simple as possible in function, with as little interaction as possible between its component parts, so that each aspect of its function can be separately investigated.

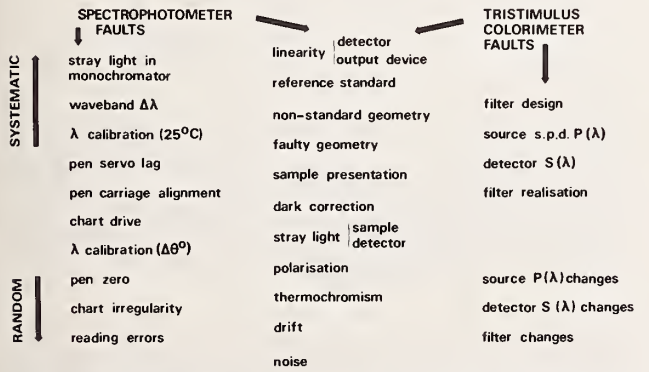

FIGURE 1. Classification of types of error found in spectrophotometers and colorimeters in relation to their random or systematic nature.

The term "high accuracy spectrophotometry" refers to quite different magnitudes of probable error when considering different types of measurement. The simplest case is measurement of direct transmittance i.e., with no scattered or diffused component of flux included, and the lowest attainable error levels are found here. The next least complicated case is measurement of direct (or specular) reflectance, again with no diffused or scattered component included, and error levels almost as low can be achieved, the additional errors arising from the necessary movement of the optical system. Measurement of radiance factor introduces additional errors in the conditions of illumination and view of the sample and uncertainties in the reference white standard used. Measurement of the total or of the diffused component of transmittance for scattering samples introduces the geometrical errors of integrating spheres (see later) and rather higher net error levels result, at least 0.2 percent in absolute value. In fact for this type of measurement and the remaining ones described below, the geometrical errors found in practice in the conditions of illumination and view are such that the monochromators and photoelectronic systems of good quality commercial spectrophotometers are often adequate to ensure the overall error level is not significantly increased. Measurement of total or of diffuse components of reflectance introduces not only the integrating sphere errors, but also the uncertainties in the reference white standards against which the samples are measured. Attainment of an error level of 0.2 percent in reflectance, while not impressive to a transmission spectrophotometrist, nevertheless qualifies for the term "high accuracy," because it cannot be attained reliably by using even an expensive commercial instrument in the usual way.

III. Spectrophotometric Equipment at NPL

Spectrophotometric standards at NPL are derived from measurements made on a specially constructed manual instrument (nonautomatic and nonrecording) known as the High Accuracy Spectrophotometer. This is the reference instrument, described in section III. A, and the performances of other instruments used in standards work are checked relative to it. Until about 25 years ago there were sometimes two and sometimes three manual spectrophotometers at work, these being used partly for establishing standards and partly for providing a calibration service for outside organizations. From then on the bulk of the outside calibration work was handled by two auto-

matic recording instruments, a General Electric and a Cary Model 10, and there was eventually only one manual instrument remaining, which became the reference instrument. In recent years the recording spectrophotometers mentioned above have been replaced by a Cary 14 and a Cary 14R with a number of improvements and accessory units, some designed and made at NPL, and these have now been interfaced to a local computer in an advanced time-sharing data handling system as described in section III. B.

In the spectrophotometric standards work at NPL the principle of substitution is strictly adhered to. This means that for double-beam instruments the measurement on a sample is sandwiched between measurements made on a reference standard ("Open" reading for absolute transmittance), and the second beam uses a comparison standard rather than a true reference standard.

In addition to the instruments used in spectrophotometric standards work, there are nowadays a number of other spectrophotometers at NPL, all regular commercial models and used as tools in a number of research and development projects, particularly by chemists. These are not instruments of the highest calibre, and are not used with any serious intention of obtaining accurate results, so we will not mention them further. One interesting exception concerns the work of S. C. Ellis and his colleagues in Radiation Science Division. Here a Cary 16 and an Optica CF4 are used to provide a calibration service in the dosimetry of hard radiation, the change in optical density in a photochemical actinometer being the measured indication of the previous irradiation [10]. The absolute accuracy of the optical density scale of these instruments at the appropriate UV and visible wavelength has been determined using transfer standards measured on our reference instrument described immediately below. The transfer standards were in the form of neutral density glass filters and cuvettes of accurately known pathlength containing known concentrations of pure potassium nitrate solution, so that this work also amounts to a new determination of the molar absorptivity of this material.

A. The NPL High Accuracy Spectrophotometer

The reference instrument for spectrophotometric standards at NPL is currently being completely rebuilt. The installation has been developed and improved in a piece-wise fashion over a number of years, first one portion being replaced or improved, then another, as the art has advanced in different areas at different times. In the earlier years much pioneer work was done by Preston [11, 12], Donaldson [13, 14, 15] and Harding [16]. An important milestone was in 1947 when a Hilger "Uvisir" (Müller-Hilger) quartz double-monochromator was introduced to supersede the use of series pairs of Hilger constant deviation prism monochromators, under the aegis of H. G. W. Harding, and from then to the present day one of these Uvisir instruments has formed the "fixed" portion of the optical system.

The principle of operation of the NPL reference instrument is, and always has been, deliberately simple. The layout is indicated in figure 2. A steady source (chosen for stability and output in the spectral region of interest) illuminates via the double-monochromator (chosen for aperture, freedom from stray light, wavelength adjustability and reproducibility) one of a pair of samples mounted on a two-position kinematic carriage. The transmitted or reflected light is collected over the required solid angle by suitable adjustable optics and assessed by a photoemissive detector (chosen for responsivity, stability and low dark current) which is dc coupled to a dc electrometer-input measuring system (chosen for high input impedance, low offset current and good zero and scaling stabilities). The single-beam principle is used throughout, both in optics and in electronics. No chopping or phase sensitive devices are used in the optical-photoelectronic system, though they may be used *within* electronic units such as stabilised dc supplies or digital voltmeters.

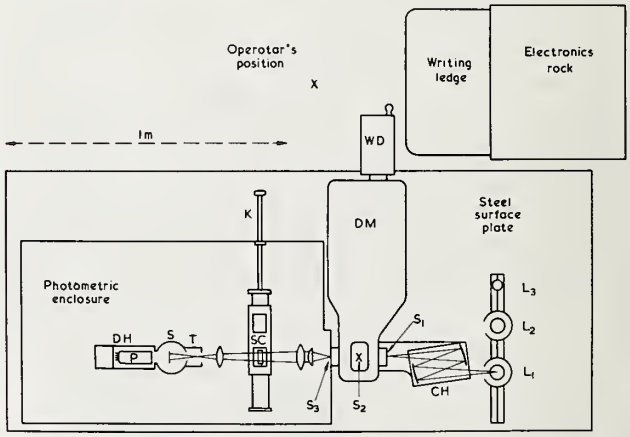

FIGURE 2. Layout of the NPL High Accuracy Spectrophotometer, 1966–1972. DM: double monochromator; WD: wavelength drum; S_1, S_2, S_3: entrance, intermediate and exit slits; CH: condenser mirror housing; L_1, L_2, L_3: alternative lamps for use in measurement or in wavelength calibration; SC: sample carriage; K: operating knob for SC; T: baffle tube; S: integrating sphere with central screen; DH: detector housing, containing a selected EMI 9558Q photomultiplier P.

This use of a dc single-beam technique for the past 40 years at NPL may strike an outside observer who has read the common text books in spectrophotometry and electronics as rather strange. The reason may be summarised by saying that the various developments in double-beam, chopped or phase-sensitive techniques have made their impact largely on the problems of coping with source instability, and improving detectivity, signal-to-noise ratio and repeatability, so that more read-out resolution can be used to obtain greater precision over a wider range of scan-speed, wavelength and waveband conditions. Signal-to-noise problems are inherently more serious in automatic scanning instruments because of the greater rate of information output required to reveal the

shape of a profile. However these techniques do nothing for absolute accuracy, and their most sophisticated employment in an advanced commercial recording instrument actually hinders attempts to determine systematic errors in the photometric values obtained (see sec. IV). For standards work there is no point in precision greatly exceeding the final accuracy that can be achieved after correcting for known systematic errors, whereas in ordinary commercial instruments where the systematic errors are sometimes rather serious, there is an advantage for many industrial purposes in having a rather better level of precision than can really be justified.

The basic measuring procedure is to take three types of reading in a preferred time sequence of the following character:

D R S R S R S R D

where D represents a dark reading, R a reference reading (for absolute transmittance work an "open" reading) and S a sample reading. The required photometric ratio is calculated initially as

$$(\bar{S}-\bar{D}) / (\bar{R}-\bar{D})$$

in terms of the mean values $\bar{S}$, $\bar{R}$ and $\bar{D}$ found, and a linearity correction is subsequently applied. This last is determined at intervals, and always immediately preceding and succeeding any limit-of-the-art determinations, as described in section IV. A. The use of a time-symmetrical sequence of observations is important in reducing the influence of "drift" on the results. Apart from shot-noise fluctuations and other short term instabilities, slow variations (drifts) of output are the main source of intrinsic photometric error in this technique. The time-symmetrical sequence will completely nullify the effect of drift, provided the drift be at a consistent rate and in the same sense. In practice the drift tends to be fairly consistent, and approximate nullification of drift effects is what is achieved with the technique. Irregular drift cannot be allowed for. As will be seen in the description of the installation that follows, great attention has been paid to reducing all possible sources of drift and instability.

The source most favoured for visible region work from 350 nm to 800 nm is a gas-filled lamp with single vertical coil, and a stock of a suitable design of 12V 48W obsolete-pattern automobile headlamps is used. The lamps are selected for freedom from filament distortion and striae in the bulb, such as would give rise to a seriously nonuniform irradiance in the field aperture of the monochromator. They are also aged and tested for stability prior to use in measurement, and a small proportion of these lamps are found to give rhythmic variation in output due to slow thermal oscillations in the convection currents in the gas filling: such lamps are rejected. The lamp is not simply held in a commercial fitting (bayonet or screw) but has soldered electrical connections to eliminate contact resistance. This type of source has not been improved for decades, but its operating stability has, due to advances in electronics. Whereas an operator used to monitor the lamp current with a precision vernier potentiometer and galvanometer, and vary a trimming rheostat accordingly (which controlled the current supplied from massive banks of lead-acid accumulators), nowadays the current through the lamp is automatically stabilised to typically a part in 10^5 over a 10 minute period by means of one from a range of custom-built variable dc-power supplies developed specially for photometric work at NPL. A light output stability of about ± 1 part in 10^4 is routinely achieved over a 10 minute period.

For near ultraviolet work in the region 280 nm upwards, the preferred source is nowadays a tungsten-halogen lamp, but we have not yet discovered a type which is ideal in all respects (but see section III. B). Although the stability should ideally be the same as with the conventional gas-filled lamp when run from the same stabilizer, we have not been able in practice to achieve the same stability of light output during measurements. For work at shorter wavelengths the deuterium arc has replaced the hydrogen arc as the preferred lamp, and although discharge lamps are inherently far less stable than incandescent filament lamps, the type we use gives a stability of rather better than 1 part in 10^3 over a 10 minute period.

The double-monochromator used up to the present is a Müller-Hilger instrument of aperture 60 mm×60 mm. In each component monochromator there is a double pass through each of two 30° natural quartz prisms, and the dispersions at all eight passes through such prisms are additive. The slit micrometers open the jaws symmetrically in all three cases, and fishtail templets allow the slit height to be varied at the entrance and exit slits. A prism instrument is preferred to a grating instrument for reduction of heterochromatic stray light, and for both manual and recording type instruments used in standards work a true double-monochromator is considered mandatory.

The light emerging from the exit slit enters a large light-tight photometric enclosure with matt black walls and measuring 1050 mm × 620 mm × 520 mm. This size of enclosure not only allows great freedom of optical configuration, with adequate room for baffles and light traps, but also reduces the influence of homochromatic stray light scattered or reflected from optical components and reflected from and round the enclosure. An extensive range of optical bench fittings and photometric components can be deployed to suit almost any kind of spectrophotometric measurement: direct transmittance, diffuse transmittance, total transmittance, direct reflectance at almost any angle, diffuse reflectance, total reflectance, or radiance factor at almost any angles of illumination and view. A kinematically designed sample carriage enables the sample or samples to be moved to accurately determined positions by remote control, these positions being located by stops that can be clamped at any position on the guides. All components are mounted on a 2100 mm × 900 mm steel surface plate conforming to Grade B of BS817 for long term stability.

The photodetector in the enclosure is held in a light-proof housing with a sliding shutter covering a 50 mm diameter port in a plate to which a 100 mm diameter integrating sphere can be screwed. The integrating sphere has two diametrically opposite portholes, the entrance port being the smaller, and light cannot pass directly from one to the other because of the presence of a central disc-shaped screen. This particular sphere is not used for measurements invoking integrating sphere theory (such as diffuse or total transmittance or diffuse or total reflectance) but is employed in direct transmittance and direct reflectance measurements to ensure that any movement of the beam or change in its size or distribution at the detector region will have no influence on the readings. This is important in measuring samples that are of nonideal optical quality, and the uniformity of the central screen is vital.

Until 1961 the photodetector used was a vacuum photoemissive cell of a type specially developed for accurate photometry, latterly Rank-Cintel Types VB39 or VB59 for good red response or VA39 with silica window for ultraviolet response. The VB59 cell is still currently the preferred detector used in white-light photometry such as the determination of luminous intensity or luminous flux of incandescent or discharge lamps: present photometer circuits are based on the impedance converter developed by Jones [17]. A succession of designs of dc electrometer amplifier null-balance detector systems had been developed over the years at NPL, especially by Preston [11], Harding [16] and Crawford [18]. In 1960 I started work on improving the photoelectronic system of Harding that was then in use, and found suitable operating conditions that would allow the EMI 9558 type of photomultiplier to be used in a linear fashion: until then photomultipliers were viewed askance by standards photometrists as being unstable and nonlinear as compared with single-stage vacuum photoemissive cells. At the same time, I developed two new designs of electrometer photocell amplifier, one of which (fig. 3) served for two years on the High Accuracy Spectrophotometer giving the best performance achieved at NPL with the null-balance method, and an accuracy of measurement as good as the digital voltmeter system which superseded it. The other design shown in figure 4 was invaluable in the investigation on Time-Ratio Photometry (see sec. V).

In the null-balance method traditional at NPL, the photocell amplifier has the task of detecting and displaying via a galvanometer spot deflection any change of potential difference between A and B in figures 3 or 4. Potential drop across the selected anode load resistor R is then balanced manually by means of a potential difference obtained from a precision potentiometer to give a null-output indication. As the potentiometer can easily have a stability and linearity in its dial-output relationship of order 1 part in a million, and as the null-detector circuit itself is not required to be very linear, there are no limitations on systematic accuracy except for those imposed by the intrinsic characteristics of the photodetector and its circuit. For the photocell amplifiers shown in figures 3 and 4 the relevant performance parameters were: input resistance approximately 10^{14} Ω, zero stability about 2 μV per 10 minutes, the open reading being up to 1.9 V.

The photodetector used nowadays is an EMI Type 9558Q photomultiplier with end-window S–20 (tri-alkali) cathode. The best tube used is one of a group specially selected by myself in terms of certain characteristics whose importance became clear as a result of unpublished researches into the use of photomultipliers for high accuracy work. The EHT supply used has only 1mV of ripple, noise or transients, which is

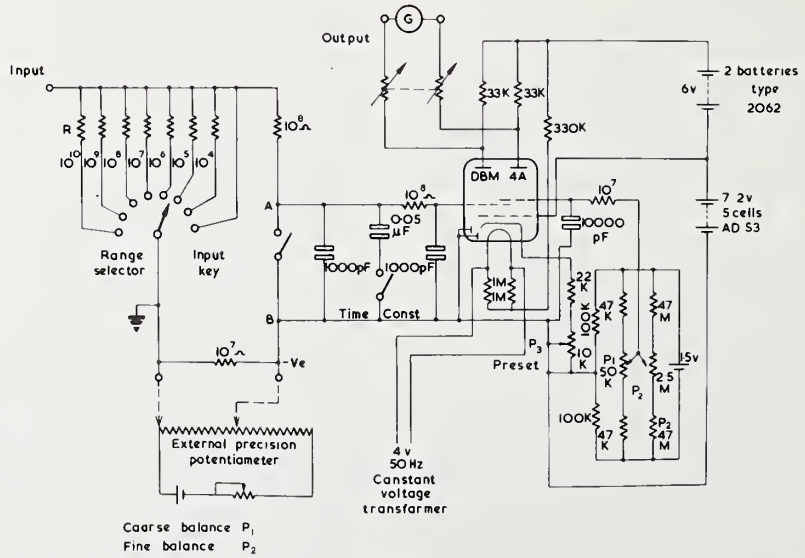

FIGURE 3. Photocell electrometer amplifier system developed by Clarke, as used 1961–1963 on NPL High Accuracy Spectrophotometer.

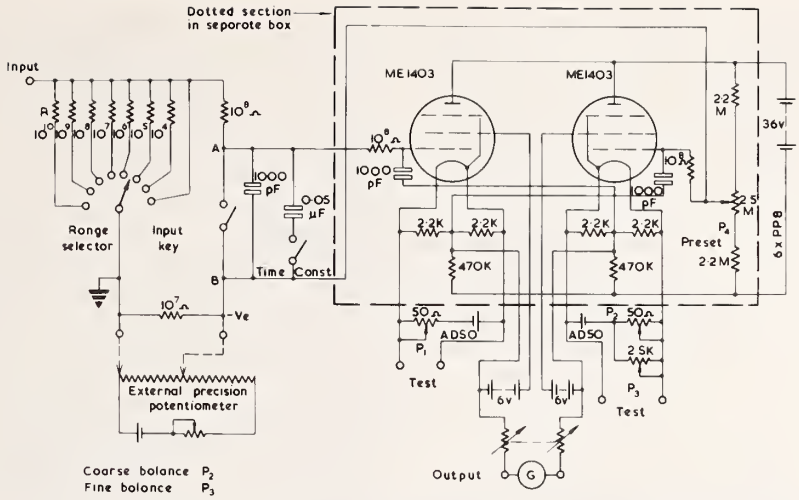

FIGURE 4. Photocell electrometer amplifier system developed by Clarke, as used in Time Ratio Photometry work on photomultipliers.

very important as the gain of an eleven-stage venetian blind type of photomultiplier is proportional to the 7.7 exponent of the EHT voltage. The low frequency noise in the photomultiplier output relevant to our dc usage conforms to the limiting value given by Schottky's Equation for shot-noise (allowing for the appropriate dynode enhancement factor of 1.3) while the dark current is equivalent to a stray flux of about 3×10^{-13} lumens of 2856 K Planckian radiation.

In 1963 digital voltmeters (DVM) became available with electrometer input circuits with input resistance of order 10^{11} Ω, offset currents of order 10^{-12} A, 10 μV sensitivity, scale lengths of 20,000 or more per range, linearity and stability commensurate with the resolution limit and a useful choice of sampling modes. The advent of these instruments and their satisfactory performance under rigorous tests caused me promptly to set aside the improved photoelectronic system I had introduced only 2 years before, and the system has remained substantially unaltered since. The present system is no more accurate than its predecessor but is quicker and more convenient to use and hence improves staff productivity.

The voltages developed across an anode load resistor (selected by PTFE wafer switch from a set with values 1 megohm, 3 megohm, 10 megohm, 30 megohm and 100 megohm) are measured by a Dynamco type 2020 or 2022 digital voltmeter. The coupling circuit sometimes used, figure 5, is of some interest as it incorporates a special compound filter to reduce low frequency noise while allowing a reasonable slewing rate to avoid lengthy waits for the potential change to become complete following interchange of photocurrent. A particular problem is that the potentiometric digital voltmeter has, and requires for common mode rejection, a twin-T mains frequency rejection filter with capacitors of value 0.1 μF and 0.2 μF in its input circuit, while we want to be able to use anode load resistors of value up to 100 megohms for certain high sensitivity measurements. The system would obviously be too

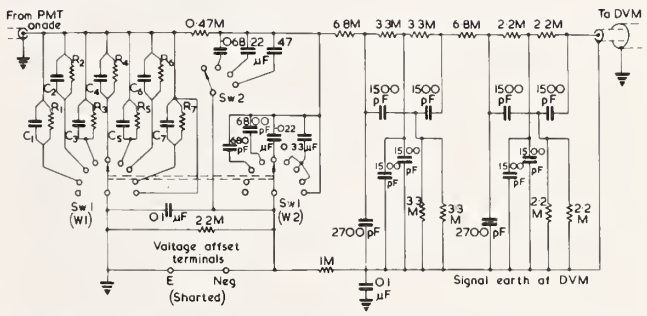

FIGURE 5. Special filter circuit for coupling anode of photomultiplier to a digital voltmeter sampling repetitively at mains frequency (50 Hz). The photometric ranging using Sw1 involves values of R_1 to R_7 of $10^8\Omega$ to $10^5\Omega$ in steps of about 3, and $RC = 0.02$ s for this first stage of low-pass filtering. Stage 2 is simple low-pass, with $RC = 0.016$ s for low values of load resistor, but tapered off for high values to compensate for stray capacitance in the phototube circuit. The time constant of this stage can also be augmented using Sw2. Stage 3 is simple low-pass, of $RC = 0.018$ s. Stage 4 is a twin-T network set to reject 34 Hz. Stage 5 is simple low-pass, of $RC = 0.018$ s. Stage 6 is a twin-T network set to reject 50 Hz.

sluggish if we used the normal filter provided, but as it can be switched out of circuit, this gives us the opportunity to provide our own external version. As figure 5 shows, a combination of four cascaded stages of R–C low-pass filtering and two stages of twin-T rejection filters tuned to 34 Hz and 50 Hz respectively are employed. Figure 6 shows the frequency response measured for such a filter, and indicates how successful the approach is in allowing low attenuation below about 5 Hz but a steep average roll-off above about 10 Hz.

This special coupling circuit was developed for special investigations and allows sector discs to be used validly over a range of speeds. A simpler coupling circuit is used for everyday work when 10^8 Ω resistors are not used. An alternative approach to the problem has been devised by Samways [19], and this has been used recently in spectroradiometric work at NPL.

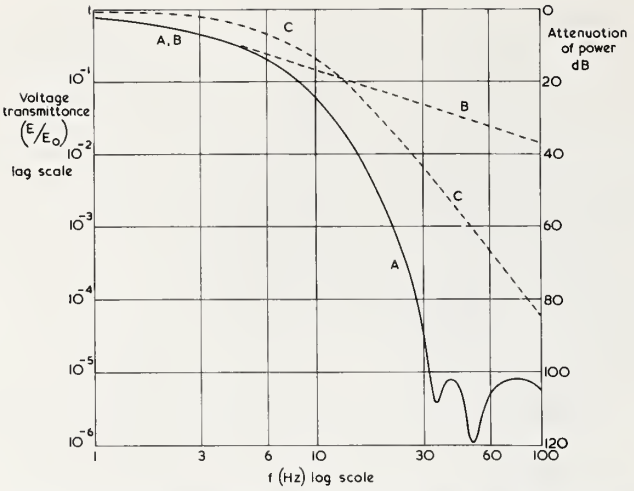

FIGURE 6. Transmittance versus frequency characteristic of special filter circuit (curve A). Note the 120 dB rejection at the sampling frequency of the DVM. Curve B shows the performance of a simple low-pass filter whose *RC* is set to 0.108 s to give an equivalent effect at low frequencies (<5 Hz). Curve C shows the effect produced by the 4 cascaded stages of simple low-pass filter present in the special filter circuit.

Because of the large number of optical configurations used to provide the different directions and solid angles of illumination and view and give different sizes of illuminated patch on the sample, it is impractical to show diagrams of them. Figure 2 shows a simplified indication of the optical arrangement used in measuring the direct transmittance of a small filter. However some of the points raised in section IV will give guidance on devising the most suitable optical layout.

The NPL High Accuracy Spectrophotometer is currently being rebuilt, and the double-monochromator to be used is a Hilger D300 which uses a double pass through a 60° Cornu prism of aperture about 55 mm × 55 mm in each monochromator section. A yet larger photometric enclosure measuring roughly 1300 mm × 900 mm × 700 mm will be used, and the sample carriage will employ a Schneeberger linear bearing as suggested by R. Mavrodineanu of NBS. The photoelectronic system is not being altered for ultraviolet and visible region work, but we are planning to add a synchronised detector chopped system for near infrared work in the region 800 nm to 2600 nm. This need arises because in 1967 Colorimetry and Photometry Section took over the responsibility for near infrared spectrophotometric standards (at up to 2600 nm) and until the present we have had no independent means of verifying the accuracy of our Cary 14 instruments in this region.

A number of checks and determinations of various kinds of systematic error are routinely made when working at high accuracy. These are detailed and discussed in section IV.

B. On-Line Data System for Automatic Recording Spectrophotometry

The bulk of the work in spectrophotometric standards and measurement services for outside organisations is performed on good quality recording spectrophotometers, and Cary 14 and Cary 14R instruments are used for these purposes. A detailed description of the Cary 14 instrument would be out of place here as it is a very well-known design and full details are obtainable elsewhere [20]. It is particularly noteworthy among commercial instrumentation for the size, freedom from stray light, wavelength calibration reproducibility and wide range of scan speeds of its prism-grating double-monochromator. In fact it is our experience that a wavelength value for a peak, trough or emission line can be determined more accurately with one of these recording instruments than with our reference manual instrument, and this is undoubtedly due to the ability to scan and record continuously and to the absence of stick-slip irregularities when scanning at even the slowest speed (0.05 nm/s).

Accessories available include the direct reflection attachment and the Model 1411 sphere. The direct reflection attachment uses the "V/W" optical arrangement after Strong [21] and invokes the use of a specimen compartment that is unusually large by commercial standards. In view of my comments on the importance of having a large compartment for the sample and supplementary optics in section III. A, it will come as no surprise to the reader to learn that we use this compartment unit in preference to the normal one for all direct transmittance work as well, and that we have built a duplicate ourselves for the second instrument. In addition we have a box extension above the lid which allows rather lengthy items to be measured a reasonable distance from either end, a feature which has proved very useful when measuring the envelope transmittances of photometric standard lamps.

The Cary 1411 sphere attachment is noteworthy among commercial instrumentation in having a pair of screens inside, between the reflectance sample and comparison ports and the detector port. This means that the largest source of systematic error found in the majority of commercial integrating spheres is taken care of, for without such screens the component of flux diffusely reflected directly to the detector port is grossly overweighted relative to the flux diffusely reflected in all other directions. The unit is provided with supplementary deuterium and tungsten sources for broad-band irradiation of samples, and the result is that a total of 30 measuring modes (combinations of source, detector and geometry of illumination and view) are available with our Cary 14 instrument and 32 modes with our Cary 14R. These are set out in table 1.

At the present time it is not practicable to determine the geometrical errors in integrating spheres by calculation. This is because classical integrating sphere theory depends on certain elegant simplifications which arise from the assumptions that a wall coating is uniform over its whole surface and that it is also Lambertian i.e., a uniform diffuser. Other common simplifications are to assume that samples are small enough to have a negligible effect on the

TABLE 1. Modes of measurement available for automatic recording spectrophotometry at NPL

Measurement with monochromatic irradiation and broad-band collection (geometry in brackets)	Source-Detector combination			Measurement with broad-band irradiation and monochromatic collection (geometry in brackets)	Source-Detector combination		
	Deuterium PMT	Tungsten PMT	Tungsten PbS		Deuterium PMT	Tungsten PMT	Tungsten PbS
Direct Transmittance $\tau(0°/0°)$	1	1	1*	Direct Transmittance $\tau(0°/0°)$	0	1	1
Diffuse Transmittance $\tau(0°/d)$	1†	1†	0	Diffuse Transmittance $\tau(d/0°)$	1	1	1
Total Transmittance $\tau(0°/t)$	1†	1†	0	Total Transmittance $\tau(t/0°)$	1	1	1
Direct Reflectance $\rho(8°/8°)$	1	1	1*	Direct Reflectance $\rho(8°/8°)$	0	1	1
Diffuse Reflectance $\rho(0°/d)$	1†	1†	0	Diffuse Radiance Factor $\beta(d/0°)$	1	1	1
Total Reflectance $\rho(8°/t)$	1†	1†	0	Total Radiance Factor $\beta(t/8°)$	1	1	1
Radiance Factor $\beta(0°/45°)$	1	1	0				

†Alternative version available with NPL Large Sphere Attachment.
*Available with Cary 14R instrument only.

mean sphere wall reflectance, that the other portholes are small enough to have a negligible influence on the spatial sampling of the flux collected from the sample and not to interfere with the interreflections needed for complete integration, and that the necessary screens are coated so as to be perfect reflecting diffusers i.e., with no absorption. The errors from these last three assumptions can be allowed for by theoretical analysis, but only by making use of the first two assumptions about the wall coating: in any case no analytical treatments to allow for real (nonideal) wall coatings have yet appeared. Some work on this problem has been going on recently at NPL by Ed. Fulton and myself using a numerical analysis method rather than an algebraic analysis approach, but results have only so far been obtained for particular cases, not the more intractable general cases.

Because of these theoretical difficulties in determining sphere errors, a practical approach has been adopted. An alternative sphere attachment for the Cary 14 instruments has been designed and constructed, and is known as the NPL Large Sphere Attachment [22]. The idea is to have available for use on the same instrument two comparable sphere reflectance attachments, both conforming as far as practicable with ideal requirements and yet with geometrical designs that differ as widely as possible. Any differences in measurements found with the two sphere attachments must then be due to their own errors, and not influenced by optical faults if any in the main instrument. To this end the sphere from a General Electric recording spectrophotometer (GERS) was used and modified, and a toroidal mirror system was used to couple the Cary 14 optics to it. The optical configuration of the two attachments are shown for comparison in Plates I and II, and apart from the size difference of the spheres (90 mm against 200 mm) the contrasted features are: wall coatings, smoked MgO for Cary

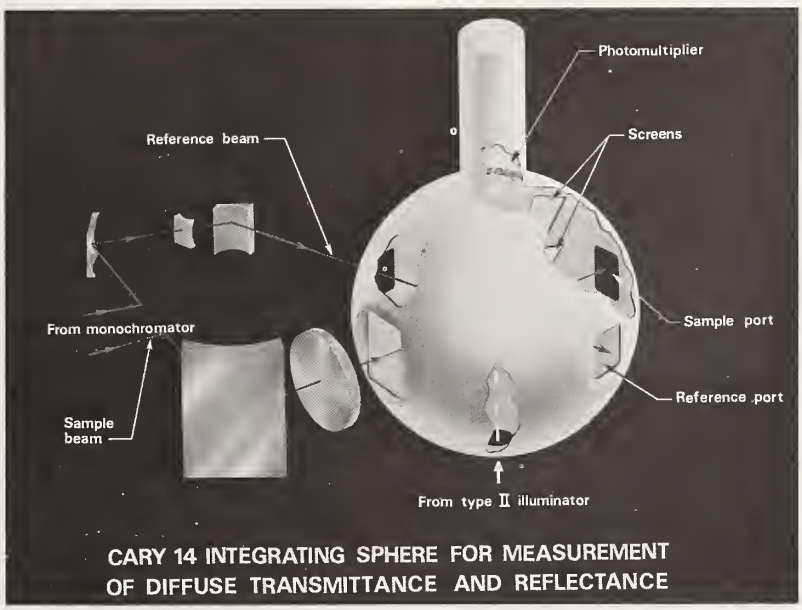

PLATE 1. Layout of the optical configuration of the Cary 1411 sphere attachment.

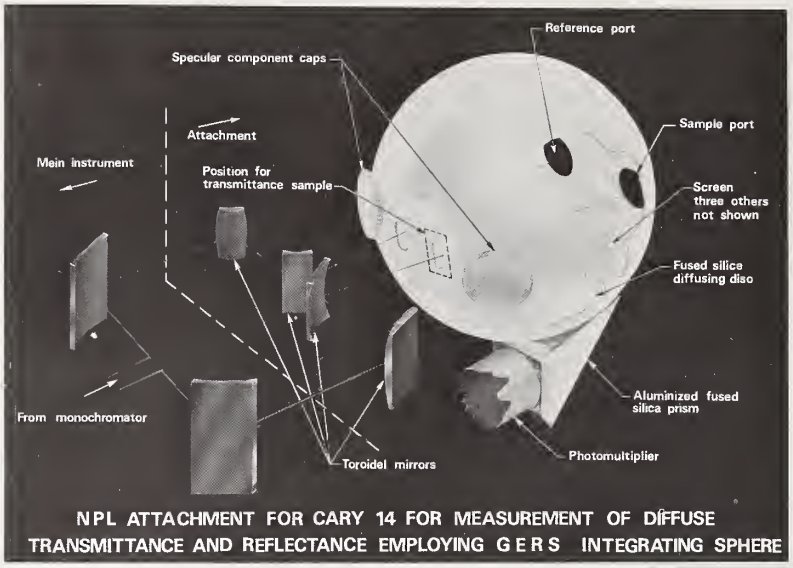

PLATE 2. Layout of the optical configuration of the NPL Large Sphere Attachment for a Cary 14 instrument.

1411, Distillation Products special $BaSO_4$ paint for GERS sphere; optical axes, perpendicular for Cary 1411, nearly parallel for GERS; photocell port, at top for Cary 1411, at bottom for GERS sphere; gloss traps, entrance ports for Cary 1411, separate ports for GERS sphere. The contrasted positions of the photocell port are very significant, as sphere coatings darken due to atmospheric dust and pollution in a systematically nonuniform way in the sense that the dirtiest portion is at the bottom and the cleanest is at the top. Apart from this, some measurements we made with a reflectance head on the freshly painted wall of a 1 m integrating sphere show that even fresh sphere coatings (judged visually to be uniform) are surprisingly nonuniform, and variations of several percent are normal. Both the Cary 1411 and the NPL unit have the necessary screens between the reflectance sample ports and the photocell port, but the NPL unit also has screens between entrance ports and the photocell port to make it fully valid for measurements of diffuse or total transmittance. The complete attachment is shown in Plate III.

The two recording spectrophotometers are interfaced in a time-sharing mode to a dedicated Micro 16P computer fitted with a core holding 16K words of 16-bit length and with a backing store facility in the form of a drum store holding 64K words. Two views of the complete installation are shown in Plates IV and V. As this spectrophotometer data handling system is unique and one of the most advanced yet developed, a description is worth including. The system was evolved from ideas provided jointly by staff of Instrumental Colour Systems Limited, Digico Limited and NPL, and a system schematic is shown in figure 7. The two spectrophotometers can be operated simultaneously and quite independently of each other, and this also applies to the real-time routines and user

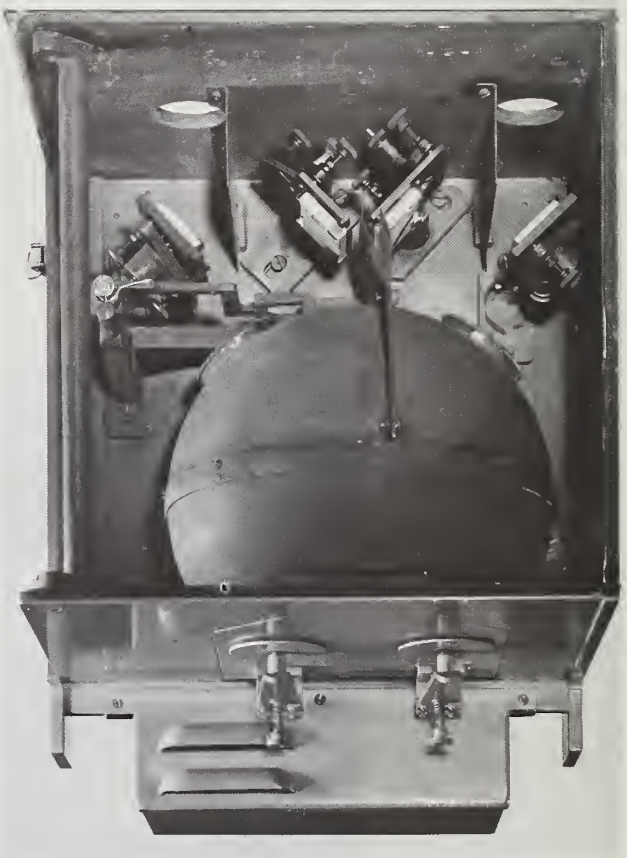

PLATE 3. View from above of the NPL Large Sphere Attachment showing the toroidal mirrors used to couple the Cary 14 optics to the GERS sphere used.

PLATE 4. View of the NPL on-line spectrophotometry data-system, showing the Cary 14 and 14R instruments. The near one is fitted with the Cary 1411 small sphere attachment, and the far one is fitted with the large sample compartment with box-lid extension for transmittance work on long samples.

PLATE 5. View of the NPL on-line spectrophotometry data-system, showing the dedicated Micro 16P computer with 16K of core to which the two spectrophotometers shown in the foreground are interfaced in a time-sharing mode for independent operation and processing.

programs whereby the instrument outputs are subject to digital noise filtering, normalising, referencing, dark correction, and radiometric photometric or colorimetric calculation as the case might be.

The user programs are in a high-level language called MATHCHAT, not unlike BASIC, and because the interpretive compiler is present in core under all normal conditions, the system seems very like a public telephone-modem linked time-sharing system based on a large processor, such as IBM's Call 360 or Honeywell-GE265. The avoidance of tedious double-

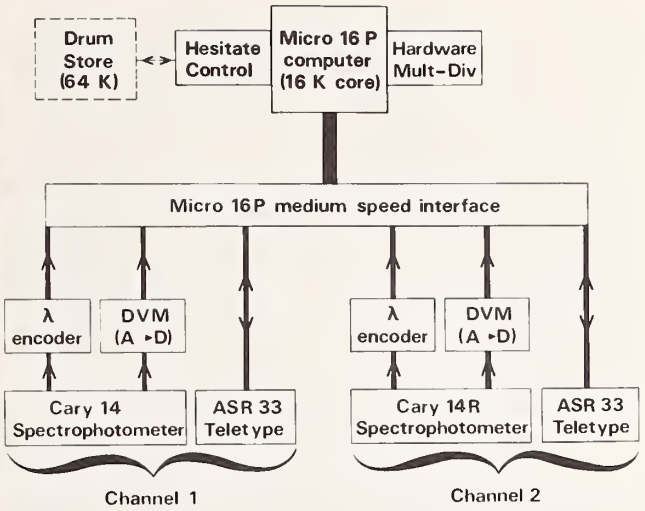

FIGURE 7. System schematic for the NPL's unique on-line data system (see text).

pass or triple-pass loading and compiling/assembling procedures, such as are currently common with small computers, is a tremendous advantage, as is the ability to instantly modify a user-program in a high-level language. One special feature of the language MATHCHAT, provided at our request, is that it allows subscripted integer arrays in addition to the usual real variables, simple or subscripted. This permits very efficient storage in core, particularly of spectral arrays for subsequent processing, as well as faster real-time operations, which can then use a hardware multiply/divide unit which reduces the time for a multiplication from about 1 ms to about 10 μs and for a division slightly longer.

Associated with each user area in core i.e., each "channel," are three peripherals, namely the photometric interface, the wavelength interface, and a ASR 33 teletype. "Reference" beam and "sample" beam photometric signals are extracted from a Cary 14 instrument at the feed to the slide wire potentiometer on the reference side and at the output from the multipot system on the sample side, so that the complete pen servo system is bypassed for the data system thereby avoiding possible troubles with nonlinearity, damage, dirty contact or displacement errors in the slide wire potentiometer and lag, nonideal damping, ill-defined temporal integration or mechanical troubles in the pen drive system. Signals are also extracted from the appropriate high-speed relays in the instrument to allow corresponding high-speed relays in the interface to provide proper synchronisation of sampling. The sample and reference values are read alternately each mains cycle by a digital voltmeter, and the values transferred to the appropriate buffer for real-time processing.

The wavelength value is also read into the same buffer each mains cycle by an absolute wavelength encoder coupled to the output shaft provided on the spectrophotometer to give a resolution of 0.1 nm. An

absolute encoder is preferred to the incremental type more commonly used in such systems because it avoids troubles from the operator starting at the wrong wavelength by mistake, problems with extraneous pulses (perhaps from power thyristor operation in a stabiliser in a neighbouring room) causing a gradual lack of registration between the wavelength and the record held in the register of an up-down counter, or perhaps momentary malfunction in the system. With an absolute encoder and wavelength being read at least once per 0.1 nm, momentary malfunction can only influence the current value, not future ones, and even if intermittent malfunction occurred, only a very small proportion of the data employed in the real-time routine described below would be affected.

The most advanced feature of our data system is the real-time procedure by which digital noise filtering is applied to the collection and initial processing of spectral data. Suppose that during a scan the wavelength encoder has just changed its indication to a new value 0.1 nm different from the last. During the time that it indicates the same wavelength (rounded to 0.1 nm) the sample and reference signals are collected and summed into separate registers, and the number of photometric values of each type is also held, so that on the next change of indication of 0.1 nm in wavelength value the arithmetic mean of the reference and sample beam values can be properly computed and their ratio taken. For ultraviolet and visible work the commonest scan speed used (1 nm/s) gives on average $2\frac{1}{2}$ reference and $2\frac{1}{2}$ sample beam readings per 0.1 nm interval. This process continues during the scan, but the arithmetically meaned photometric ratios are also multiplied by a special weighting factor or factors, depending on whether the wavelength value is at the time within one or more spectral "windows" within which piece-wise fitting of low order polynomials is required. The user can command the system to give at any required output wavelength λ_0 the value which would be obtained by making a least-squares fit of a cubic (or alternatively a quintic) to $(2n+1)$ photometric ratios, one for each 0.1 nm interval, where a wavelength range of this "window" extends from (λ_0-n) to (λ_0+n) in units of 0.1 nm.

The larger the value of $(2n+1)$, the more effectively is noise and variance filtered out, but if $(2n+1)$ becomes too large the portion of spectral profile being investigated within the "window" will not be properly represented by a portion of a cubic function, hence there is an optimum choice for $(2n+1)$ to suit the type of profile being measured. The largest value for $(2n+1)$ permitted is 101 and this implies a spectral "window" of ± 5 nm about the required value. However this "window" does not lead to anything like the amount of degradation in the spectral profile which would occur if a simple "running mean" were being evaluated over the same width of "window." When dealing with very sharp profiles the minimum value of $(2n+1)$ permitted is 3 for the cubic fit, which gives no data improvement over the initial photometric ratio at the wavelength required, apart from that arising in the first stage of data processing when a photometric ratio of arithmetic means of reference and sample beam readings is produced at each 0.1 nm interval. Obviously in such cases one uses a slow scan speed to allow the simple arithmetic means to give adequate noise reduction, and if one used a speed of 0.05 nm/s then the means of 50 reference and 50 sample beam readings are used to give the output data at 0.1 nm intervals.

The weighting factors used in executing the piece-wise cubic fit are automatically evaluated by a special algorithm as soon as the command choosing $(2n+1)$ is made prior to a spectral run, and the essential algebraic basis is given below.

For $(2n+1)$ equispaced ordinates extending from (λ_0-n) to (λ_0+n) in units of 0.1 nm in this case, the photometric value can be written $T(i)$, where $i=-n\ (1)+n$. The quadratic fitted value for $T(0)$ is $F(0)$, where

$$F(0)=\sum_{i=-n}^{n} W(i)\cdot T(i)$$

which is calculated during a scan. The weighting factors $W(i)$ are calculated beforehand, immediately the value of n is typed in:

$$W(i)=(S_4-S_2\cdot i^2)/[(2n+1)\,S_4-S_2^2]$$

where

$$S_2=\sum_{i=-n}^{n} i^2=(2n+1)\ (n+1)\ n/3$$

$$S_4=\sum_{i=-n}^{n} i^4=S_2\ (3n^2+3n-1)/5.$$

It should be noted that the general algorithm given here is that required for fitting a quadratic to any number of equispaced ordinates: owing to the fact that the odd-order terms in a polynomial do not influence the fitted value at the central ordinate of a symmetrical "window" (the only value we are using), the result of fitting a quadratic is identical to that of fitting a cubic, and that for a quartic is identical to that for a quintic, etc. [23]. As the algorithm becomes more difficult to derive for successively higher order polynomials, we obviously use the lower (even) order case that gives the same result. We also have the general algorithm for the piece-wise fitting of quartic (and hence quintic) polynomials, but it is omitted for brevity.

One particularly useful feature arising from the flexibility of the real-time procedure is that the spectral scan speed can be altered freely during a scan; for instance, a much slower scanned speed can be adopted when passing through a water absorption band in the near infrared than for the rest of the scan, which avoids certain well-known problems with slit or gain servos. Not only this, but the scan can be stopped and re-

started or even partly back-tracked and restarted without corruption of the acceptable part of the scan already produced.

The use of the backing store to hold an assortment of user program texts and standard data blocks as well as an image of the system software, compiler and maths packages is a great convenience, but is quite conventional and needs no further comment here.

What have proved to be the main advances in NPL's recording spectrophotometry given by the on-line data system? The main objective has been amply achieved, namely a major reduction in the staff time involved in all stages of standards work and calibration services for outside organisations, from making the measurements through various stages of data reduction to the final tabulations in our records or the despatch of a calibration report. The ease of producing and comparing data has led to anomalous operating conditions of the spectrophotometers being spotted more certainly. We have been gratified to find that the precision and repeatability of measurement has also been significantly improved, which suggests that the slide wire potentiometer and pen servo system of the Cary 14 instrument imposes a major limitation on its performance when used with a pen recorder output in the normal way. However we have not been deceived into imagining that the data system has necessarily reduced the systematic errors of measurement. Since we do not rely on commercial spectrophotometers to provide our scales of measurement, this is no great worry to us.

A considerable number of improvements have been made to the Cary 14 instruments and their accessories by NPL staff, but it would make a long and tedious discourse to describe them all and the majority of them are specific to the particular instrument. However one of the more minor improvements is worth mentioning as it can be applied to a number of other types of spectrophotometer as well as the Cary 14. This concerns the replacement of the RCA side-window photomultiplier type 1P28, used in the normal transmittance configuration, with one of the new EMI type 9670 tubes. We purchase these tubes specially selected for high near-infrared response, and they can be supplied with uniform sand-blasting of the silica side-window to give diffusion of light over the cathode. The diffusion is needed to reduce effects due to any displacement of the beam by the presence of the sample, and such sand-blasting is present in the special 1P28 tube supplied with the instrument. The great difference lies in the relative spectral responsivity of the S–10 type cathode as compared with the S–5 response of the normal or selected 1P28 tube, see figure 8. The limitations imposed by cathode responsivity only make their presence felt towards the ends of the spectral range that can be covered, and the lower quantum efficiency of the 9670 tube at wavelengths below about 590 nm is no practical problem. However at wavelengths above 600 nm the newer tube is clearly better, not merely because of higher spectral responsivity (which extends its range by about 150 nm) but particularly due to the much lower spectral gradient. Performance is improved in two ways: heterochromatic stray light reduction and a more gradual variation of the slit servo during a scan. Heterochromatic stray light itself is benefited in two ways in the 600 nm to 900 nm region: the lower spectral gradient would mean less shorter-wave stray light at a given slit opening, and the proportion of stray light for a given spectral gradient decreases markedly as slit width is reduced by the slit servo due to the higher absolute spectral responsivity in this region. The EMI 9670 is convenient as it is a plug-in replacement for the 1P28 tube, so that no modifications are necessary. While a tube with a S–20 response would be better still, figure 8, no compatible type is known to us.[3] A new compatible type has recently been announced by RCA with considerably extended red response, the C31025 series with Ga As or Ga In As cathodes, but I have not yet heard any satisfactory reports on these from other photometrists.

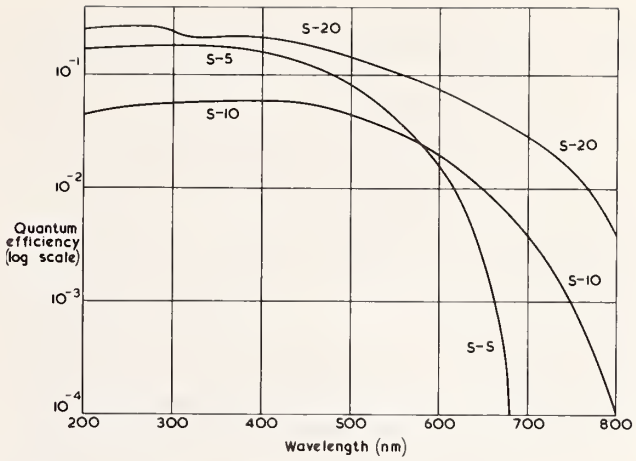

FIGURE 8. Spectral responsivity characteristic for EMI 9670 tube (S–10 cathode), a plug-in replacement for RCA 1P28 (S–5 cathode). The most desirable cathode type (S–20) is not available in compatible side-window designs.[3]

Another of the more minor improvements which is of general application concerns the choice of tungsten halogen lamp. Curiously in a double-beam system, we found that most of the types we tried gave rather poorer repeatability of measurement than the conventional gas-filled lamp originally supplied, and we attributed this to changes of filament position in relation to the rather striated silica envelopes used, which caused alterations in the light distribution at both slit and field aperture and which affected beam balance. We have found that an Atlas 30 V 250 W single-coil lamp type P1/8, running at 3400 K on full rating, has a particularly good quality envelope and gives both stable and efficient operation. The single coil filament allows one to tilt it to get maximum filling of the entrance slit using the Moiré effect,

[3]Subsequent to the Conference EMI have announced a compatible tube type 9785 with S–20 cathode.

and about 50 percent more throughput can be obtained than with the 120 V 650 W tungsten halogen source which the manufacturer can supply, while heating problems with the monochromator are eased.

IV. Determination and Correction of Systematic Errors

As described in section II, the spectrophotometrist seeking after high accuracy should concern himself much more with correction of systematic errors (and indeed avoiding them as far as possible) than with statistical exercises that relate to variance and random types of error. In the subsections 4.A to 4.D that follow some guidance is given as to how to deal with the more important types of systematic error. As the precise procedure depends on the details of the installation used, any description must refer to some particular type of configuration, and the NPL High Accuracy Spectrophotometer has been used as the model. It will become apparent that the procedures can easily be applied to any other instrument working on the same manual single-beam dc principle, but often not at all easily to a typical commercial instrument working on the double-beam chopped synchronous detection principle. While manufacturers have sometimes made drastic modifications so as to produce special versions of their instrument to investigate errors, this does not normally lie within the power of a user.

A. Linearity Correction, using the Double-Aperture or Multi-Aperture Methods

At NPL the preferred method of determining linearity errors in the photoelectronic system is the Double-Aperture method, and it has continued in use in high accuracy spectrophotometry for over 40 years. The method tests the linearity of response of the complete instrument system as it is set up for measurement of a sample, whereas other methods (sec. IV. B) often involve drastic modifications or major additions to the system or separate investigations on parts of the system i.e., the photocell, or amplifiers or potentiometer and the pen recorder or the digital readout, or some combination thereof. Provided that the method is sound, it therefore allows a single investigation of linearity to settle the question for the complete instrument at the time involved. The double-aperture method is the most accurate, sound, simple and foolproof technique that we know of for testing linearity in a manual single-beam dc-mode instrument.

Essentially, the only modification required to the system is the introduction of a double-aperture device into a suitable place in the optics. The advantage of this is that no change need necessarily be made to the system, and linearity testing can be commenced at any time. The most recent design in use at NPL since 1967 is shown in Plates VI and VII, and this was used as a model by R. Mavrodineanu for the one made for his new installation at NBS. We have devices with both square and circular aperture formats to suit different applications, and the sliding leaves are operated independently by Bowden cables from a pair of push-pull knobs each with a detent to permit the leaf to remain open. Leaf and knob are each spring-loaded to ensure that if the knob is not caught in the detent the leaf will always close fully. When closed all the edges of the leaf adjacent to the edge of an aperture are enclosed in closefitting slots to ensure that no light can leak through, and this requirement explains why a septum is used to separate the apertures. (Earlier designs have often not had this septum). The edges of

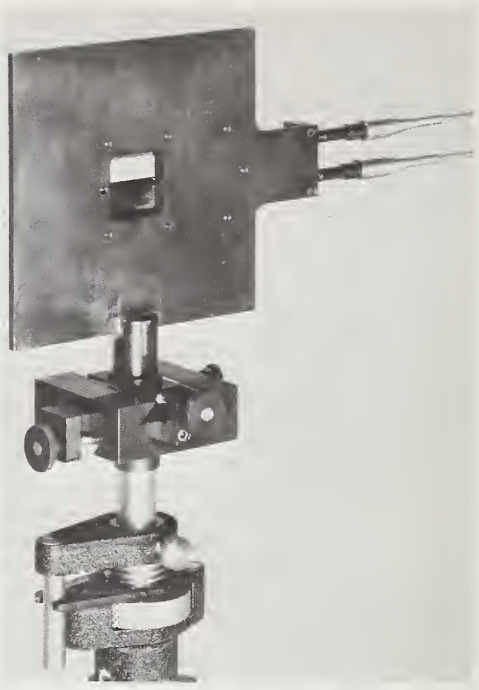

PLATE 6. NPL double-aperture device for linearity testing: general view of the side facing the incident radiation showing the bevelled edges.

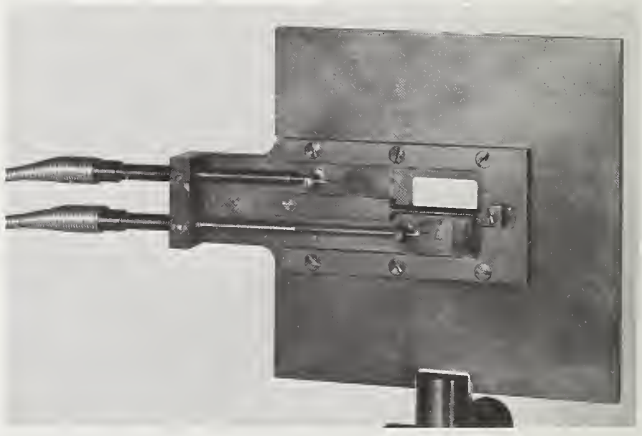

PLATE 7. NPL double-aperture device for linearity testing: detail of the side facing the detector system showing the mechanism and use of bevelling where possible.

the apertures are bevelled on both sides where possible, and the brass used in construction of the aperture plate and leaves is chemically blackened. This blackening leaves a weak specular component of reflection but very little diffuse component, and to prevent reflections of light back to some preceding optical component and thence back through one or both of the apertures, the whole device is slightly rotated about a vertical axis from the perpendicular orientation when being aligned.

The double-aperture device permits the departure from linearity of the complete instrument to be measured over any 2:1 step within the range of the photometric scale, and the procedure is first to place and align the device in a suitable part of the optical system (see later) and adjust the vertical position until the readings of each aperture (the other being shut) are approximately equal. If the readings from each aperture alone are A and B, those from both together are (A+B), and those with both shut are D, then a minimal sequence of readings is

$$D\ A\ B\ (A+B)\ (A+B)\ B\ A\ D$$

and this would be called a single-volley set. This is of course a time-symmetrical sequence to minimise drift and variance effects, and equal numbers of observations of each type are made to give equal statistical weight. For more accurate work, double-or-triple volley sets of observations are made for any particular 2:1 step. If the mean values of each type of reading are calculated then the linearity error ϵ is calculated as

$$\epsilon = [\overline{A+B} - (\bar{A}+\bar{B}) - \bar{D}]/[(\overline{A+B}) - \bar{D}].$$

The error ϵ is normally expressed as a percentage, and the correction to be applied to a measured photometric value of 50 percent over the corresponding part of the scale is $-\epsilon$.

But what if the photometric value to be corrected is not 50 percent, or is not measured over precisely the same part of the scale? To cope with the general case the procedure is to cascade the linearity testing in binary steps, so that if the first step involves output readings of full scale (f.s.) and 50 percent f.s., then the second step involves outputs of 50 percent f.s. and 25 percent f.s., the third step 25 percent f.s. and 12½ percent f.s., and so on. Various methods can be used to reduce the (A+B) reading of the nth step to the A reading of the $(n-1)$th step, such as reduction of lamp power, slit widths or use of a supplementary attenuator such as a filter. The settings of the successive steps to half the readings of the preceding step need not be closer than 1 percent of the value. This, and the fact that the A and B readings need not be equal to closer than 1 percent of the value, arises because the input-output relationship of the photoelectronic system, if not exactly linear, is always at least a smooth continuous function and approximately linear in any instrument that is in sound operating condition.

The method of linking the errors from each 2:1 step to form a series of points on a continuous error function is illustrated in figure 9. On the NPL reference instrument this function has always been found to be smooth and regular, but if it were not a regular smooth curve this fact might be missed due to the gaps between data points, especially at the upper end of the curve. Hence intermediate steps forming a second series of steps such as 70 percent f.s. and 35 percent f.s., 35 percent f.s. and 17½ percent f.s., etc. should be determined on any new or modified instrument. The 70 percent f.s. point is attached to the smooth curve drawn through the normal series 100 percent f.s., 50 percent f.s., 25 percent f.s., etc., and the points corresponding to 35 percent f.s., 17½ percent f.s. etc., are then linked to the assumed position for 70 percent f.s. as for the normal series. If the smooth regular curve assumed through the normal series of data points has been drawn correctly to fit the true error function, then the points at 35 percent f.s., 17½ percent f.s., etc., will also be found to lie on the curve. In general the second series will suggest some slight improvement in shape to the error function as in figure 9. A really sceptical standards man would then proceed to find a third series of value corresponding to some series like 85 percent f.s., 42½ percent f.s., 21¼ percent f.s., etc., and test the error function further.

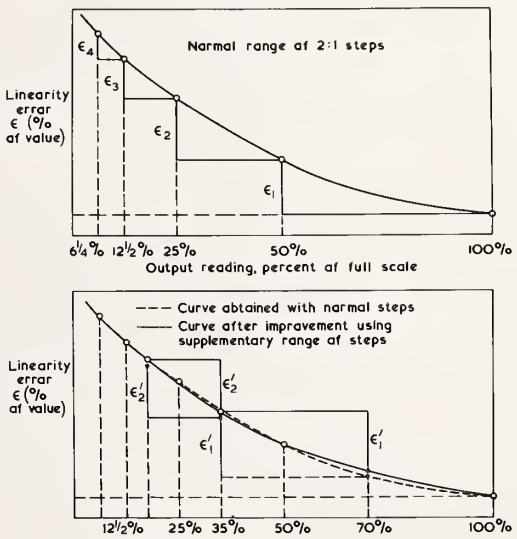

FIGURE 9. Upper diagram shows how the linearity error function is built up from the errors ϵ_1, ϵ_2 etc. found with each successive cascaded 2:1 step, starting with 100 percent full scale. Lower diagram shows how the linearity error function found with the normal cascaded 2:1 steps (dotted) may need altering to accommodate the errors ϵ'_1, ϵ'_2 found with a supplementary range of 2:1 steps, starting in this case at 70 percent full scale.

The double-aperture method may be regarded as completely sound if subject to the following conditions.

(1) Any additional component of reflected light introduced by the presence of a leaf blocking one aperture must not be allowed to pass to the detector

by the other aperture or by any other stray light path. This is met by keeping the double-aperture devices as far from other optical components on the illuminated side as practicable, by masking any bright parts of these components with black flock paper and by tilting the device slightly as mentioned before.

(2) By the same argument, there must be no alteration of reading from one aperture due to changes in interreflected components on the detector side of the device caused by alteration of the other aperture leaf. This is met by keeping the double-aperture device as far from optical components on the detector side as possible.

(3) There must be no relative change of light distribution at the double-aperture during a volley of observations. Apart from trying to prevent relative movement (not always completely possible, due to the need for adjustability and the opening and closing forces imposed), the light distribution should be as uniform as possible and slightly larger than the size of the double-aperture, so that to first order any relative movement produces no variation of reading.

(4) There must be no change of light distribution at the actual detector surface during a volley of observations, since an ideal filter inserted into the beam for measurement will cause no such change. In the NPL instrument the use of the integrating sphere as a diffusing device ensures that this condition is met. If the double-aperture device were focused onto the photocathode, the test would not be valid since when both apertures are open for (A+B) there would be two separate portions of the cathode acting like two photocells in parallel, and an intrinsic nonlinearity would not be detected if two photoelectron streams remained reasonably separate as in many types of photomultiplier.

(5) There must be no optical interference between the fluxes transmitted through each aperture. According to K. G. Birch of Optical Metrology Division, NPL this condition is met for all practical purposes in typically dimensioned equipment when conventional tungsten or discharge sources are used, provided that slit widths are not reduced below 0.002 mm during the linearity testing.

A consequence of (1) and (2) above is that at NPL we usually change the optical system within the photometric enclosure for linearity testing to allow the double-aperture device to be as far from other optical components as practicable.

The freedom from optical interference effects mentioned at (5) above arises because with slit widths commonly met with and with conventional sources the "coherence patch" at the double-aperture device is not large enough to straddle the septum, which is of order 3 mm wide. However to make doubly sure that interference effects cannot invalidate the test, the practice at NPL is to actually focus the double-aperture onto the target screen in the integrating sphere in front of the detector. Then even if the "coherence patch" were to cover the whole double-aperture, there would be no overlap of the fluxes from each aperture at the screen where they receive their first diffusion, so that no fringes could be formed there. The region of the slit image is the only place where fringes could be formed, and we make sure that the mirror or lens which images the double-aperture onto the target screen is not in this region as such fringes could interact with flaws, blemishes or dust particles to give readings capriciously high or low according to the precise relative positioning.

For systems employing temporal or spatio-temporal chopping of the light, a further condition must be met.

(6) There must be no change in the temporal features of the waveform reaching the detector between the three types of reading, A, B, or (A+B), whether of shape or phase: only a strict change of amplitude is permitted. This cannot be met if the light distribution of the beam alters at all during the sampling time, due to actual movement or due to sector-mirrors or rocking mirrors having a non-uniform reflectance due to poor coating, ageing, dust or pollution.

The requirement (6) arises because no ac-detector circuit (tuned narrow-band, synchronous sine-wave, synchronous square-wave, homodyne, heterodyne, or any other type) is ideal in the sense that it functions exactly as supposed, and changes of waveform shape or phase at a given amplitude will therefore generally cause a spurious change of output. This condition (6) can seldom be proved to be met in commercial instruments.

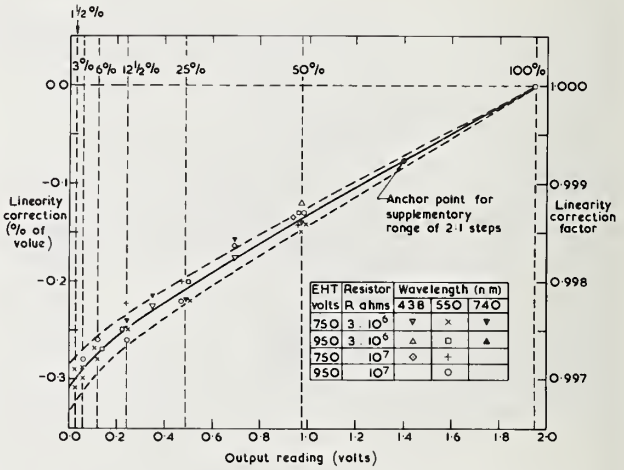

FIGURE 10. Linearity correction function of the NPL High Accuracy Spectrophotometer, showing corrections found for the range of EHT voltages, load resistors and wavelengths covered in one particular investigation. It happens that in this case the correction function is not sensitive to changes of operating conditions over a certain range of values, and a common curve is representative. The dotted curves show the probable error that would be quoted for the accuracy of the correction.

The linearity correction function of the NPL High Accuracy Spectrophotometer is shown in figure 10 in terms of results obtained before and after a particular programme of filter standardisation. The curve drawn for the normal sequence 50 percent f.s., 25 percent f.s., 12½ percent f.s., etc., has not been modified to suit the

sequence 70 percent f.s., 35 percent f.s., 17½ percent f.s., etc. Results are shown for the two values of dynode load resistor used, for different values of photomultiplier E.H.T., and for several wavelengths. Strictly speaking one should not assume that the correction required is the same when any of these key parameters is varied; however it can be seen that the correction function turned out to be not significantly different in any of the cases tested. In general, there is usually a preferred range of output current—E.H.T. combinations where an invariant and almost linear characteristic is obtained for the photocell. However departure from Ohm's Law behaviour of the load resistor is often a larger source of linearity failure than the photocell itself in well-designed systems, so each load resistor needs a separate investigation. As it has been found that the linearity correction function has remained stable over a period of several years, no attempt has been made to find load resistors that are more nearly ohmic in characteristic: a survey of resistors with thorough testing of all available types and ratings of interest would prove too costly to be justified in these circumstances.

It is not necessary to test linearity at different wavelengths unless it is thought possible that different mechanisms might then be operative in the photodetector. Some photocells do indeed have different characteristics in certain wavelength regions, usually at the long wave end of their spectral response. So when a new instrument or photocell is being tested for linearity, several wavelengths covering the whole range of spectral response should be used to check this point.

The multi-aperture method, commonly employing ten apertures, is but a variant of the double-aperture method, and is equally sound in principle. It has been used at NPL by lamp standards photometrists, whose needs are not quite so exacting as spectrophotometrists. In fact the multi-aperture method cannot be made as accurate as the double-aperture method with a given number of observations on a particular aperture combination, because it is impracticable to use a time-symmetrical sequence of readings which allow the values A, (A+B), (A+B+C), . . . (A+B+C+D+E+F+G+H+I+J) to be determined with equal and optimum accuracy relative to each other so as to produce ten points on the error function of equal uncertainty. To get results of equivalent accuracy, the demands on system stability are rather greater than with the double-aperture approach.

The double-aperture method allows the linearity correction required for any given 2:1 step to be determined to a few parts or less in 10^4, depending on the number of volleys of readings used. The accumulation of probable error for cascaded steps is illustrated in figure 10.

B. Linearity Correction, Using Other Methods

A great many approaches have been suggested over the years to the problem of determining linearity errors, and it is not proposed to review them critically in this paper as each would need a section equivalent to the preceding one to cover relevant points thoroughly. In this section some indications will be given as to why these other approaches are not preferred at NPL. In essence they nearly all amount to employment of a device or equipment which varies the irradiance at the photodetector in a predictable or calculable manner. Methods which involve the photocell being removed and tested away from the rest of the spectrophotometer can tell us much about the photocell but require supplementary investigations to be carried out on the rest of the photoelectronic system, for example on the Ohm's Law behaviour of the load resistors. Since even when this has been done, assumptions have to be made as to how the photocell might behave when in the instrument and connected into the system circuitry, such an approach cannot be regarded as foolproof. To give illustrations, temperature rises, magnetic fields, earth loops or cross modulation effects within an instrument can give rise to real or apparent linearity departures which have confused many an unwary investigator.

The double and multiple aperture methods are examples of the general principle of addition of fluxes, and the other methods which use this principle are equally sound but are difficult to implement experimentally with sufficient rigour. The use of several sources is clumsy as demands on the stability of the optics and the sources are great, and the apparatus is bulky. The device of using one source but multi-beam optics avoids severe source problems but leaves the problem of optical stability. Where beam-splitters are used for dividing or recombining the beams, the problems of polarisation, scatter and multiple reflections have to be faced, and where one source is used the interference effects are more likely to be troublesome than with the multi-aperture method because optical superposition of related wave fronts is more closely achieved. Beam-splitters are in general spectrally selective, and this makes their use for linearity testing difficult over a wide spectral range.

A pair of plane polarising devices used as polariser and analyser offers a possibility of producing a net transmittance varying predictably as a function of the angle of rotation of the analyser. Most polarisers (sheet polarisers, Brewster windows and electro-optic devices) are too poor in quality and too spectrally selective to be taken seriously, but polarising prisms of high quality have been used in attempts to obtain accurate linearity testing. The problem here is that the predicted law is only obeyed in practice over a limited range of optical density (absorbance) for as the "crossed" position is approached the optical density starts to change very rapidly making the orientation and alignment very critical, and at densities above unity the slightest flaw, surface blemish, or foreign particle on the intermediate surfaces causes partial depolarisation and hence a breakdown of the predicted law. Another problem is that the light passed by the analyser is plane polarised and at varying orientations, and most photodetectors are sensitive to polarisation effects to some extent. Unfortunately

it is not possible fully to depolarise plane-polarised light by means of a single diffusion, by reflection from smoked or pressed magnesium oxide or from opal glass, or by transmission through opal glass when its transmittance is of reasonable magnitude.

The inverse square law has often been used as a means of controlling the flux incident on a photocell in a predictable manner, but it is not good enough for work of the highest accuracy due to the non-uniform radiation field emitted by practical sources. If the source and detector apertures are finite, a correction to the inverse-square law has to be calculated using configuration integrals (a process sometimes called calculation of the mutual exchange coefficient), but this assumes a Lambertian (Cosine Law) behaviour of source emission and detector response. Practical sources and detectors never obey Lambert's Law closely. I myself have used pot opal glass as a secondary source, carefully masked to give a known aperture and with a tungsten ribbon source focused on the far side, but have not obtained good enough obedience to Lambert's Law: the departure from Lambert's Law is very difficult to measure by goniophotometry to sufficient accuracy to calculate an adequate correction, and is wavelength dependent. A "black body" source might prove acceptably Lambertian, but its defining aperture presents severe difficulties.

Variable apertures are another old favourite for producing a controlled attenuation of flux, but the method is generally unsound because of the impossibility of producing an optical beam in a spectrophotometer of uniform radiance cross-section. To overcome this the division of the aperture into numerous small variable apertures has been tried using combs, rotating grilles and venetian blind devices. The problem then becomes a geometrical one of realising the desired construction by precision engineering, and high accuracy cannot be achieved reliably. An alternative approach is to use fixed meshes or perforated screens as attenuators, but they too require calibration by some metrological procedure and this is unsound because not only is transmitted light lost in an instrument by diffraction but also for small apertures the effective area for transmission is less than the metrological area. This last point arises because radiant energy is absorbed for a distance of the order of its wavelength away from any metal edge: this effect of physical optics is too complicated to permit of any adequate calculations for a correction in any real situation.

Testing for obedience to Bouguer's Law or Beer's Law is another much used method of testing linearity, especially among chemists. However it is fallacious, for if these laws are verified for an instrument it only establishes that the photoelectronic system obeys a simple power law, not that the power (exponent) is exactly unity. In fact some particular faults in photoelectronic systems lead to precisely this type of nonlinearity, so that the method can be dangerously reassuring. Apart from this, Beer's Law seems to be exactly obeyed in remarkably few of the solutions that have been rigorously examined. The usual form of application involves cuvettes of varying path length or solutions of varying concentration. A variant is the technique suggested by Campbell in the 1930's but resurrected by Slavin and Porro [24], of grinding and polishing homogeneously absorbing glass to different thicknesses and verifying whether the density (absorbance) is proportional to thickness after allowing for reflection losses. This is equally fallacious of course.

Sector discs are an important method of accurate attenuation, and they are spectrally nonselective, not sensitive to polarisation and relatively easy to construct accurately and measure metrologically. If the Talbot-Plateau Law is obeyed the transmittance is linearly proportional to the angular opening. The problem is whether the detector really obeys the Talbot-Plateau Law: while many solid-state types do not, it happens that with suitable circuitry and choice of operating conditions vacuum photoemissive devices obey the law very closely indeed. This has led to the development of the technique of Time Ratio Photometry at NPL, as described in section V.

C. Heterochromatic Stray Light

The unqualified term "stray light" in spectrophotometry usually means heterochromatic stray light i.e., light transmitted by the monochromator that is outside the required or set waveband. There are in fact other types of stray light, referred to in the following section IV. D. Heterochromatic stray light arises from three main causes: general small angle and wide angle scatter from dust, blemishes and pollution of optical surfaces; stray reflections, especially where lenses or prisms are used; and unwanted orders of diffraction in grating instruments. General scatter is usually the worst culprit, and because of this it nearly always happens that the components of stray light become progressively smaller as their wavelengths depart further from the set wavelength.

The obvious approach in reducing errors is to purchase a high quality double-monochromator, and for guidance we would rank the different types of system in the following order for stray light: best is prism-prism, then prism-grating and finally grating-grating. However, even with such an instrument there are circumstances when significant heterochromatic stray light errors can arise. This is most commonly met at the long wave limit of ultraviolet and visible instruments, where a photomultiplier is used and particularly where a grating has been blazed for optimum performance in the awkward 280 nm to 340 nm region where one changes from an incandescent lamp to a hydrogen or deuterium arc. That choice of blaze has of course been dictated by the need to increase net response in this latter region and reduce heterochromatic stray light there, for this region is the second most suspect, apart from the region of short wave cut-off imposed by air and silica absorption at around 185 nm. For any source-detector combination the error is maximal where the net response is very low compared with the average over the usable range and

where the spectral gradient of response is steep, and this normally occurs near the limit of the usable range. It is for this reason that we are prepared to sacrifice peak quantum efficiency if necessary in order to obtain a less steep spectral gradient of response at the red end of the working range.

The general method of testing for errors is to use selective band or cutoff filters, and is well enough known to need no description here. It is important to check that introduction of the selective filter has no adverse optical effect. A convenient place to introduce such a filter into a common-path part of the system in a double-beam system is between the source and entrance slit, but this may alter the light distribution at both slit and field aperture and hence give a bias to the reading other than due to its absorption properties. It is therefore particularly important to adhere to the strict substitution principle in making the additional measurements. The same requirement applies equally when matched pairs of selective filters (even if of high quality and closely matched) are introduced into the sample and comparison beams of double-beam instruments.

D. Homochromatic Stray Light

Homochromatic stray light is any light which is present in addition to the light which has passed to the point in question along the optical system in the desired manner, and which is of approximately the same spectral distribution. Thus it means in practice all stray radiation except the heterochromatic stray light from the monochromator or any leakage of ambient light through chinks in the casing. (Leakage of ambient light becomes obvious if one switches off or covers all light sources in the room and blacks out the windows and one can then detect an alteration of output or of operating conditions, and this will not be commented on further.) Homochromatic stray light usually arises from specular or diffuse reflections, or from diffuse components of transmitted light in the case of transmitting elements of the system, and consists in general of light which has departed from its desired optical path and which somehow re-enters the system so as to be included with the required light being measured. There are so many mechanisms by which this can happen, and they are so particular to the precise optical configuration, that one cannot discuss the various possibilities in any general way. I will only mention therefore a few specific types of homochromatic stray light and how we deal with them.

Interreflections, involving specular reflections from optical surfaces or from bright metal components like slit jaws, and lens or mirror mounts, have two effects: if they involve the reflection from the sample itself then they impose a direct error on the photometric value being measured, whereas if they are independent of the sample itself they only impose an indirect error due to the spatial or angular distributions of illumination and collection not being quite as required. Tilting the sample usually reveals the direct type of error, but there is one circumstance (commonly met with in commercial instruments) where this is not necessarily so. I refer to the practice of placing a filter or cuvette at a slit image to minimise beam movements at a conjugate image formed at the detector. If an optical surface at a slit image is tilted slightly the reflected beam is deviated to cover a slightly different part of the aperture of the mirror or lens which has focussed the radiation, but a slit image will still be formed from the reflected light back at the exit slit of the monochromator, and it will not move. As slit jaws are bright-edged and either flat to the outside world or bevelled (often at 45°), and as monochromators often have plain windows there to prevent entry of the atmosphere or its pollutants, it is clear that there is usually a reflection back once more down the optical system towards sample and detector, and this will be focussed yet again to form an image at the specimen. Direct errors from interreflections can also occur on the detector side of the sample, especially if a bare (diffuserless) end-window photomultiplier receives light normally. In NPL standards work the sample is therefore never placed at a slit image if this can be avoided. The presence of both types of interreflection (i.e., involving the sample or not) can be checked most readily by eye using a dental mirror.

Both specular and diffuse reflections often occur at surfaces close to the beam and parallel to it, such as inner surfaces of lens or mirror mounts or tubes, and the cure is to add suitably shaped and dimensioned stops in the system. Stray specular reflections may strike the instrument casing or other parts and be diffusely or specularly reflected so as to "by-pass" the sample. This provides a further argument for a large photometric enclosure (sample compartment). This type of effect can cause serious errors in very dark samples, and a routine practice is to place a dummy (black) sample in the sample position and of identical dimensions to the sample and then take dark readings, and compare them with the more normal dark readings obtained by blocking the beam prior to entry into the photometric enclosure. The latter reading gives the photoelectronic system component of dark error (assuming there is no leakage of ambient light), whereas the difference in these readings gives the optical component of dark error. This procedure is very important in total and diffuse reflectance measurements, for small angle scatter in the sample beam optics preceding the integrating sphere causes a halo of scattered light surrounding the illuminating patch on the sample, both on the outer parts of the sample and on the sphere wall. In this case the "black" sample consists of a blackened cavity brought up against the sample port, and the error is usually the largest component of systematic error found in reflectance measurements, representing a zero offset ranging from roughly 0.1 percent in the infrared (2 μm) to roughly 0.5 percent in the ultraviolet (0.3 μm) in reflectance value but depending on the condition of the preceding optical surfaces. For transmittance measurements an opaque dummy is used, with a mirror or matt white surface attached in some cases to exaggerate particular types of stray light effect.

Samples should always be masked so as to cover their edges and have an opaque surround. This is to prevent by-passing of light, especially in small specimens, for it is not uncommon for stray reflections or small angle scatter to produce a weak flux distribution alongside or surrounding the beam: again I emphasise the use of the eye looking along the direction of the beam. The reference sample (or the absence of a sample for an "open" reading in absolute transmittance) must also have precisely the same masking present, to prevent systematic error. However these local masks on the sample carriage are not sufficient: it is also necessary to have a *fixed* mask as close as possible forming a locally limiting stop. This is to cover the possibility that the sample and reference masks do not assume the same position due to misalignment on the carriage or faulty adjustment of the stops on the carriage guides, or that they are not precisely the same size and shape. The fixed mask should either be slightly larger than the beam cross-section there, with clearance all round, or it should be smaller than the nearly uniform "core" of the beam cross-section. This is to obtain optimum photometric stability if one accepts that some slight relative movement of optical components might occur.

At NPL the direct interreflection error (involving the sample itself) is avoided by tilting the filter by an angle of order 1°, keeping the solid angle of illumination down to half-cone values of under 1°, avoiding forming a slight image at or near the filter, and catching the beam reflected back on to a piece of black velvet or flock paper placed just to the side of the exit slit. Even with such precautions, recent investigations with highly reflecting filters have shown that great care needs to be taken with metal-film or thin-film filters, and errors are likely to be appreciably greater than with normal absorbing filters.

Phenomena which can give rise to systematic errors in spectrophotometry are photochromism, thermochromism and fluorescence; but these could arguably be regarded as defects in the sample rather than defects in the measurement procedure. As with testing for heterochromatic stray light, the principles of testing for these phenomena are well known and largely common sense once the nature of the problem is understood, and further comment will not be made here.

E. Polarisation Errors

If we confine our attention to the normal isotropic materials used in standards and calibration work, then Fresnel's Equations tell us that for light incident or reflected at normal incidence polarisation has no effect on the measurement, while for angles near to normal polarisation effects are negligible. This is fortunate, for all monochromators produce a partial plane polarisation that is very significant, and it means that transmittance measurements are usually not subject to a significant error due to polarisation effects. For measurements of direct reflectance, diffuse reflectance or of radiance factor involving inclinations above 10° from normal however, certain precautions must always be taken as explained below.

The proportion of polarisation varies appreciably from monochromator to monochromator, so it is never satisfactory to quote a measurement which refers to the particular polarisation conditions (often not known reliably) in one particular instrument only. So we must specify "standard" conditions: but what are these? There are 3 obvious candidates: 100 percent *s*-polarised light, 100 percent *p*-polarised light, or randomly polarised light. The most generally useful value for a photometric quantity is the one which refers to randomly polarised light. Unfortunately randomly polarised incident irradiances and collector/detector systems not selective for polarisation are almost impossible to produce in instruments without sacrificing light by the use of heavy diffusion, and one therefore measures the quantity with a plane polariser present in either the irradiating or the collecting system or both, depending on which of these are inclined at appreciable angles to normal. This results in two (or sometimes four) measurements being made, and the required result for randomly polarised light is easily calculated from these as it is the arithmetic mean of the measurements.

V. Time Ratio Photometry

A few years ago O. C. Jones and I invented a new technique of photometry [25, 26] aimed at equalling or perhaps surpassing the accuracy achievable by the dc single-beam method, which relies as we have seen earlier on the close approximation to true linear behaviour of certain preferred types of photoemissive detector and on the fact that any slight non-linearity found in such systems is very stable and therefore accurately correctable by use of the cascaded double-aperture method of linearity testing. Our aim was to develop an independent scale for determining photometric ratios by which we could verify the validity of the existing method. At the same time we wanted the technique to be self-calibrating and not relying on corrections determined on another occasion, and also more suited to exploitation of modern developments in digital data techniques.

A. Talbot's Law and the Principle of Time Ratio Photometry

Talbot's Law, sometimes called the Talbot-Plateau Law, states that light fluctuating periodically above the critical fusion frequency of vision is exactly equivalent to steady radiation of the same average value, and the law was of course discovered (in 1834) in connection with the response of the human eye. Mathematically, if $F(t)$ is the periodically fluctuating light and R is the response evoked,

$$\mathrm{R}\{F(t)\} = R\{\bar{F}\}$$

where

$$\bar{F} = \int \frac{F(t)\,dt}{T}.$$

In 1913 Marx and Lichtenecker found that Talbot's Law applied also to vacuum photoemissive cells, as far as could be judged with the accuracy possible at that time. For a photocell that obeys Talbot's Law the mean photocurrent observed with a periodically fluctuating illumination is the same as that obtained if the incident flux is distributed uniformly throughout the duration of the period. For this to be true in practice, the associated electrical circuit must be linear and with an appropriate overall time constant. The linearity is necessary to prevent rectification, whereby energy can be transferred from the oscillatory terms to the constant term in the Fourier series for the chopped waveform as a function of time. In passing I would point out that linearity of the circuit elements is also necessary in the cognate case of tuned or phase sensitive detector systems, to prevent errors due to cross modulation.

In 1929 Carruthers and Harrison working at NPL [27], found strict obedience to Talbot's Law for a variety of photoemissive cells, including some that were markedly nonlinear as judged by their steady-state behaviour. It would not be out of place to emphasise that if a sector disc, whose opening is say 10 percent of its circumference, is inserted in a beam of light falling on a photocell obeying Talbot's Law, it is *not* correct to assume that the photocurrent falls to 10 percent of its former value. That will only be true if the photocell happens to have a linear characteristic as well as obeying Talbot's Law. What Talbot's Law does say is that the photocurrent falls to the same value that obtains if a 10 percent filter is inserted in the beam.

To consider the essence of the time ratio method, let us assume that one is trying to measure the transmittance of a filter. The method is, however, readily applicable to other types of photometric measurement. Imagine a steady beam of light illuminating a photoemissive cell with a suitable dc-measuring circuit. One needs a repetitive shutter, which opens and closes fully, and whose open-to-shut time ratio can be varied. The photocurrent obtained with the shutter open and the filter attenuating the beam is noted, then the filter is removed and the shutter sequence is started. The fraction of the total time during which the shutter is open is varied until the same photocurrent is obtained, then some accurate timing technique is employed to measure this time-ratio. The transmittance of the filter is then equal to the *fraction of time for which the shutter was open*, provided that the photometric detector obeys Talbot's Law. It is as simple as that.

The beauty of the method is that the shutter can be calibrated absolutely, in terms of time, in situ, and even simultaneously with the measurement as described later. Thus the shutter need not possess long term stability of characteristics: an adjusted value need only be held for a few seconds at a time.

It would be appropriate to break off for a moment to consider what is really happening, that a vacuum photoemissive device can adhere exactly to Talbot's Law yet give a slightly nonlinear response to steady radiation. The three important factors in this are:

Firstly, the cell has an intrinsic response time of order 10^{-9} second, which is much shorter than any chopping period that would be employed. Secondly, the cell has an instantaneous intrinsic response that is normally strictly linear, if it could be measured a few μs after a change of illumination with some suitable fast circuit, this instantaneous linearity not being affected by previous illumination. Thirdly, the cell possesses a relatively slow fatigue or drift characteristic whereby the observed photosensitivity changes progressively under illumination.

In our technique, if the cell obeys Talbot's Law, drift or fatigue do not affect the measurement, because the output produced by chopped radiation must suffer exactly the same drift or fatigue as that arising with steady radiation of the same average value. Otherwise the cell would not obey Talbot's Law.

B. Experimental Verification

We can now look at the experimental work carried out at NPL to see a selection of the evidence relating to the accuracy and the generality of Talbot's Law obedience in actual specimens of photoemissive detectors. The finer details of experimental technique and methodology will be omitted for brevity in this description of the work. Figure 11 shows the optical and electronic arrangement used in the initial studies. Later work has used modified systems of the same general kind. The variable shutter chops a slit image to provide a full on-off modulation with a fast rise time of a few microseconds, and for all our accurate fundamental work we have used a variety of sector discs. We have favoured mechanical or electro-mechanical shutters throughout, for such devices really do provide complete and stable modulation irrespective of wavelength, polarisation or angle of incidence.

A fraction of the light passed by the shutter is received via a beam-splitter at a supplementary gating photocell, which was a spare photomultiplier of no great quality. This had the function of simply opening and closing electronic gates rapidly to permit pulses from a stable 100 KHz oscillator to pass to counters as appropriate. Most of the light in the beam reached photodetector A, which in these first experiments was connected to one of several types of dc-electrometer current-amplifier via adjustable smoothing filters, the dc-null-balance technique being employed. The electrometer null-balance system shown in figure 4 was used for much of the work on photomultipliers. In some of the later experiments, a digital voltmeter was used to indicate directly the residual difference between the signal and a backing-off voltage: the backing-off technique proved very helpful in respect of the compromise needed between smoothing and slewing rate.

We have emphasised small transmission factors of order 1 percent in most of the work, due to the fact that the differences in waveform and instantaneous values between the test and comparison fluxes are then most pronounced, and impose the most difficult sampling conditions. Work on a vacuum photo-diode was carried

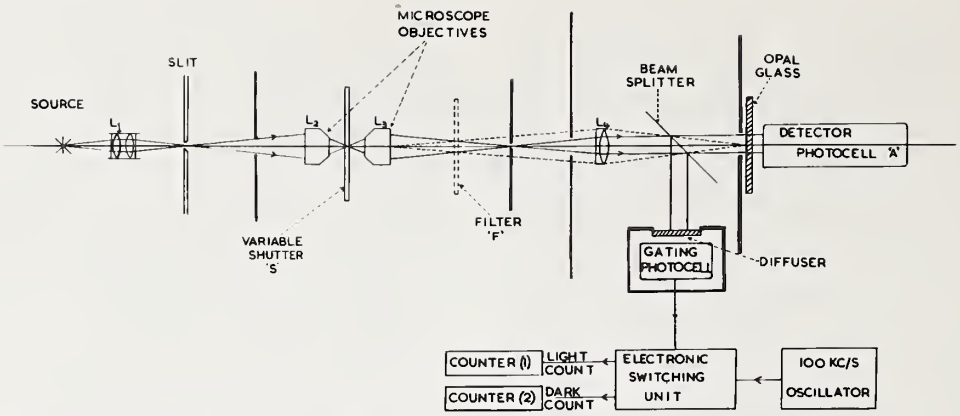

FIGURE 11. Optical and electronic system schematic for experiments on Time Ratio Photometry.

out by O. C. Jones and assistants, while work on photomultipliers was carried out by myself and assistants.

If Talbot's Law applies to some particular experimental configuration, then it follows that variation of flash frequency at constant mark to space ratio should have no effect on the output unless the frequency becomes so low that a sufficiently smoothed and readable output becomes impossible. The test is a necessary but *not sufficient* condition for Talbot's Law obedience. It was found that a simple vacuum photodiode, with capacitive smoothing of the anode circuit gives no significant change of reading as frequency is dropped to 2 Hz. With photomultipliers, it was found that discrepancies of up to a few percent of the value were obtained for a 1 percent sector if there was inadequate capacitance loading of either the anode or the last four dynodes. The reason for discrepancies with inadequate capacitance in the anode circuit is clear enough: with a reading of say 1 V dc, a 1 percent sector can give pulsed reduction of up to 100 V on the final collecting potential difference, leading to synchronised collapse of collection efficiency. The reason for Talbot's Law failure when the dynodes are not heavily loaded with capacitance is rather more interesting. For any one stage of a venetian-blind type of photomultiplier, there is a 0.7 power law relating stage-gain to applied volts. Since most of the output current is drawn from the last dynode, and most of the penultimate output current is drawn from the penultimate dynode, and so on, it is clear that there must be some voltage pulsing of the dynodes, which are usually fed from a chain of resistors. The voltage pulsing of the dynodes produces cross-modulation of the powers in the various terms of the Fourier series representing the square wave light modulation, and in this particular case some spurious rectification. By analogy with the old term "anode-bend demodulation," we can call this effect "dynode-bend demodulation."

Our dynode resistors are made as low in value as practicable, namely 100K, and we found that with 25μF per stage (giving $2\frac{1}{2}$ s time constant) we could eliminate the effect of dynode-bend demodulation. In fact recent measurements show no significant change for frequencies reduced to as low as 0.5 Hz, provided that the currents are kept down to the range where Talbot's Law is known to hold at frequencies above, say, 20 Hz. In fact with a 0.4 percent sector and peak anode currents of up to 4×10^{-4}A (far above the limit for linear behaviour under dc-conditions) no change was detectable to within ± 2 in 10 000 of the reading for 1 Hz, or ± 5 in 10 000 for 0.5 Hz. Larger output currents give progressively larger departures from Talbot's Law for a given gain or for a given flux. For a given output current, increasing the incident flux and reducing the gain to compensate will produce an increase in Talbot's Law error.

The most fundamental test for Talbot's Law obedience is to measure a sector transmittance by ratio of photo-currents, to correct for nonlinearities and compare the result with the true value. But what is the true value? This may be given by the time ratio technique:

$$\frac{T(o)}{T(t)}, \quad \text{or} \quad \frac{T(o)}{T(o) + T(c)}, \quad \text{or} \quad \frac{T(t) - T(c)}{T(t)}$$

where $T(o)$ is the total of "open" times, $T(c)$ is the total of "closed" times, and $T(t)$ is the total elapsed time during a counting period. However these ratios are only valid if $T(t)$ is either an exact number of chopping periods or else so large that the error due to the usual residual incomplete period is negligible. Further, the gating circuits must trigger at exactly 50 percent up the leading and trailing edges of the chopped waveform. These three versions of the sector transmission seldom agreed exactly, of course, and these divergences indicated our probable error.

Some results on this are shown in table 2. The linearity correction for the vacuum photo-diode and its circuit was negligible, whereas that for the photomultiplier and its circuit was finite. The linearity corrections were obtained from supplementary measurements by successive application of the *double-aperture technique* of absolute linearity correction. As explained in section IV. A this linearity correction allows properly for nonohmic behaviours of the load resistor as well as for true linearity de-

TABLE 2. Tests of Talbot's Law

METHOD OF MEASUREMENT	% Transmission		Effect of speed change from 30 f/s
	Sector A	Sector B	$\Delta \bar{R}$ %
Single Stage Cell			
Ratio of Photocurrents	1·473	3·126	<0·001 for speeds down to 2 f/s
Time-Ratio	1·474	3·129	
Computed from dimensions (uniform motor speed)	1·477	3·127	
Photomultiplier			
Ratio of Photocurrents	1·470		<0·003 for speeds down to 10 f/s
Corrected (for non-linearity)	1·473		
Time-Ratio	1·475		

parture of the photocell. A further estimate of the sector's transmission is given by metrology, difficulties arising here from uncertainties of the position of the true centres of rotation of these demountable sectors. The sectors were directly mounted on the shaft of a large dc compound-wound motor, and there was only inertial smoothing of any commutator pulsing. The data shown here indicate Talbot's Law obedience to within two or three parts in 100 000 of the "open" reading, and the discrepancies are of doubtful significance.

We now proceeded to apply time ratio photometry to measurement of a rather neutral absorbing glass filter of transmittance about 1 percent, and results are shown in table 3. To obtain reliable data a narrow-band green filter combination was used, so as to minimise effects due to nonneutrality of the test filter and changes in colour temperature of the lamp.

TABLE 3. Comparison of time ratio method with conventional photometry

METHOD OF MEASUREMENT	RESULT
(a) Transmission factor of filter measured directly by ratio of photocurrents in d.c. photometry	1·185% ± 0·001%
(b) The same, corrected for linearity departure	1·187% ± 0·002%
(c) Transmission factor of sector by timing	1·475% ± 0·001%
(d) Transmission of filter relative to sector, by ratio of photocurrent	0·806 ± 0·001
(e) Transmission of filter deduced from (c) and (d) i.e. by the time-ratio method	1·189% ± 0·002%

Only photomultipliers gave adequate data here, and in fact all the later work was done with photomultipliers. We measured the transmittance of the filter by direct ratio of photocurrents, and then corrected for linearity departure, giving the most accurate answer possible by conventional means. We then measured the transmittance of the sector then available that was closest in value to the filter, by the time ratio method, and followed this up by determining the transmittance of the filter relative to the sector by ratio of photocurrents. Ideally this last would have given a value close to unity had we had a closely matched sector-filter pair. As it was, the value of 0.806 required only a minimal linearity correction. The product of these last two measurements gives the transmittance of the filter by a simple form of time ratio photometry, and it will be seen that the residual discrepancy of 2 parts in 100 000 in "open" reading is not significant.

C. Generality of Talbot's Law With Various Operating Conditions in a Photomultiplier

A consequence of Talbot's Law is the invariance of the measured ratio of the transmittance of a sector disc to that of a filter. We later made up a special multi-component filter to match a certain 1 percent sector rather closely under conditions where Talbot's Law was known to hold, that is at low illuminations and low output currents. Table 4 shows results obtained when the flux and cathode current were fixed, and the gain and output current was varied over a wide range. The values S/F give the readings obtained with the 1 percent sector relative to the readings on the filter. Clearly, increasing the output current above a certain threshold level introduces progressively greater departures from Talbot's Law. Measurements of linearity errors under steady flux conditions showed not only no correlation in magnitude but these were of opposite sense. The Talbot's Law errors indicate some instantaneous saturation at the peak current levels, whereas the linearity checks show over-additivity due to dynode heating. When output current is held constant, it is found that as the flux is increased and the gain decreased to compensate, progressively larger errors arise. The results are general for all tubes tested

TABLE 4.

TALBOT'S LAW ERRORS, ϵ, FOR VARIOUS ANODE CURRENTS					
Gain	Ia (mean)	Ia (peak)	S/F	ϵ %	Δ lin.(st) %
$2{\cdot}6 \times 10^{3}$	$1{\cdot}9 \times 10^{-8}$	$1{\cdot}9 \times 10^{-6}$	0·984	0·0	0·00
$2{\cdot}6 \times 10^{4}$	$1{\cdot}9 \times 10^{-7}$	$1{\cdot}9 \times 10^{-5}$	0·984	0·0	0·00
$2{\cdot}6 \times 10^{5}$	$1{\cdot}9 \times 10^{-6}$	$1{\cdot}9 \times 10^{-4}$	0·972	−1·2	0·00
$2{\cdot}6 \times 10^{6}$	$1{\cdot}9 \times 10^{-5}$	$1{\cdot}9 \times 10^{-3}$	0·869	−11·7	+0·62
$2{\cdot}6 \times 10^{7}$	$1{\cdot}9 \times 10^{-4}$	$1{\cdot}9 \times 10^{-2}$	0·550	−44·1	+3·3
Fixed cathode current = 7×10^{-12} A. Sector of 1·0% Tube No. 6622					

502-591 O - 73 - 3

which were of the EMI 9558 type. Peak currents of up to about 2×10^{-5} A produce no significant error, if the gain is adequate.

The intercomparison of fatigue-curves of photomultipliers with equivalent chopped and steady fluxes provided an independent and convincing check on these facts. Such curves should be identical for devices that obey Talbot's Law, and this was indeed found to be the case.

Yet another consequence of Talbot's Law is that if a linearity test is made on equivalent steady and chopped radiation levels, the same result should be obtained. This powerful technique of measuring the difference between chopped and steady radiation linearity errors has also been applied to a number of photomultipliers using the sound double-aperture method, and once again it has been found that up to a certain threshold value of output current, no error occurs; above that level progressively increasing failures of Talbot's Law occur in the sense of "instantaneous saturation" of peak currents above about 2×10^{-5} A, confirming results mentioned earlier. This technique was also applied to investigating what happens as we vary the mark-to-space ratio or sector opening. Table 5 shows results from only 3 sectors out of a whole set with progressively varied transmittances that were used. This shows a very important result: it is not the mean value of current that determines the threshold for Talbot's Law failure: it is the peak current. This means that the presence of a specimen in a time-ratio spectrophotometer does not alter the optimum operating conditions, for the optimum operating conditions involve using currents slightly below the critical threshold for Talbot's Law failure.

TABLE 5.

TALBOT'S LAW ERRORS, ϵ, FOR VARIOUS SECTORS					
Sector τ	Ia (mean)	Ia (peak)	Δ lin.(ch) ($\times 10^{-4}$)	Δ lin.(st) ($\times 10^{-4}$)	$\epsilon \times 10^{4}$
0·40%	$9{\cdot}3 \times 10^{-8}$	$2{\cdot}3 \times 10^{-5}$	−10	−4	-6 ± 3
3·20%	$6{\cdot}4 \times 10^{-7}$	$2{\cdot}0 \times 10^{-5}$	−½	−1½	$+1 \pm 3$
75·04%	$1{\cdot}7 \times 10^{-5}$	$2{\cdot}3 \times 10^{-5}$	40	40	0 ± 5
0·40%	$1{\cdot}0 \times 10^{-6}$	$2{\cdot}5 \times 10^{-4}$	−40	−1	-39 ± 8
3·20%	$8{\cdot}1 \times 10^{-6}$	$2{\cdot}5 \times 10^{-4}$	−15½	14½	-30 ± 7
75·04%	$1{\cdot}9 \times 10^{-4}$	$2{\cdot}5 \times 10^{-4}$	477	542	-65 ± 9
Tube No. 5564		Net gain = 2×10^{5}			

I would like to mention two facts which reinforce our claims as to knowing the absolute uncertainties. Firstly, T. Quinn has used our time ratio techniques to determine the transmittance of certain sectors used in establishing the temperature scale at NPL and found consistency over long periods and with alternative timing and optical equipment to 1 or 2 parts in a million of the open reading, for sectors of 10 percent and 1 percent transmittance. Secondly, O. C. Jones designed a super-quality 0.4 percent sector which allowed metrology to 2 parts in a million. I measured this by ratio of photo-currents, corrected for linearity and produced a value that agreed to 1 part in a million of open reading, even though my probable error was 3 parts in a million of open reading.

D. Modes of Application

Three ways of applying Time Ratio Photometry to a double-beam automatic spectrophotometer will be briefly described below. There are in fact many other ways of using the principle. Figure 12 shows a system which uses fixed gating intervals from timer 28 and

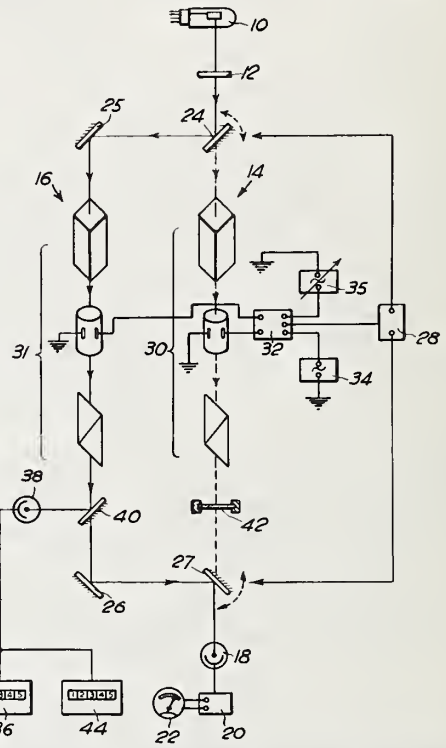

FIGURE 12. Schematic of one possible mode of application of Time Ratio Photometry to a double-beam spectrophotometer (see text).

gates 32 during which the null detector 18 looks at fixed amplitude, fixed duration pulses delivered by shutters 30 and 31. During the test phase pulses at fixed frequency are triggered by oscillator 34, and are attenuated by the specimen 42 to be equivalent to unattenuated pulses of lower frequency triggered by variable oscillator 35, which is controlled by the off-balance signal from null detector 18. A ratio of frequencies from counters 36, 44 energised by supplementary photocell 38 gives the transmittance.

Figure 13 shows a system in which a high frequency shutter 130 modulates a common portion of the optical train. A timer 128 controls the beam-switching and allows a fixed test phase interval. A shutter 131 allows the reference phase duration to be reduced so that the

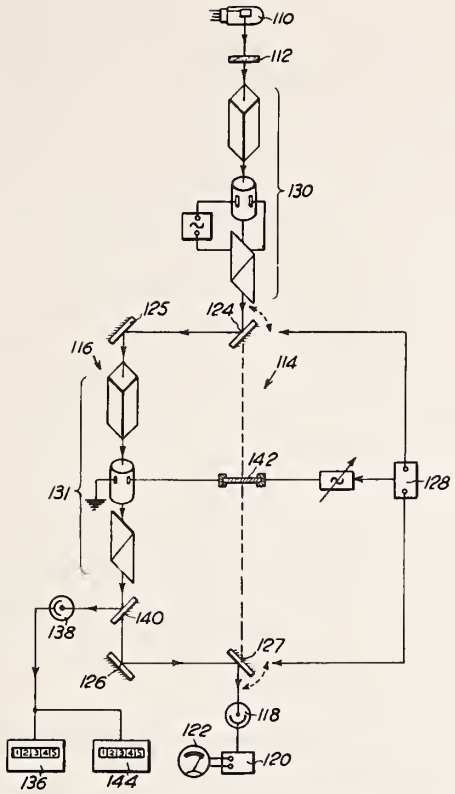

FIGURE 13. Schematic of another possible mode of application of Time Ratio Photometry to a double-beam spectrophotometer (see text).

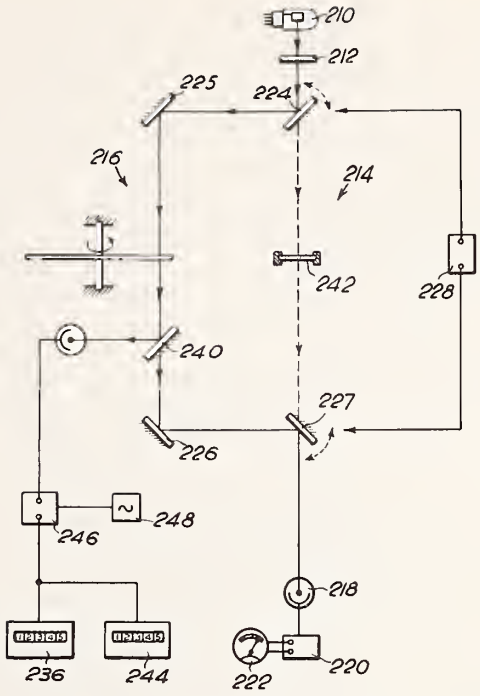

FIGURE 14. Schematic of another possible mode of application of Time Ratio Photometry to a double-beam spectrophotometer (see text).

reference flux is equivalent to the fixed duration but amplitude-attenuated test phase. A supplementary detector and two counters 136 and 144 allow the high frequency pulses from shutter 130 to be used to time the open durations that give a balance from null detector 118, with and without specimen 142 in place.

Figure 14 shows a system in which the gating intervals from timer 228 are fixed for test and reference phases. An intermediate-frequency variable mark-to-space shutter 216, such as a variable sector, is controlled by the off-balance signal from null detector 218 to achieve equivalence with the unchopped but attenuated flux passed by specimen 242. Timing is achieved by means of a supplementary detector, fixed frequency oscillator 248, gate 246 and counters as before.

Owing to the staff shortage in this field at NPL during the past few years, these ideas above have not been implemented in the sense that no Time Ratio Spectrophotometer for practical use has been built. The fundamental research described in sections V. A to V. C above was only performed on installations that could be described at best as abridged (filter) spectrophotometers. It remains for an instrument manufacturer to judge when the market would be ready for an automatic recording instrument that could achieve the accuracy which only a few of the world's standardising laboratories can at present achieve in a staff-intensive way with manual instruments of their own design. What is certain is that Time Ratio Spectrophotometry is ideally suited to on-line data systems with dedicated computers, since the technique is inherently digital.

VI. Material Standards for Spectrophotometry

A. Direct Transmittance

Absorbing glass filters form the most satisfactory transmittance standards in general, but they have their limitations, especially in respect of the spectral range available. It is desirable to separate out the effects of nonlinearity, heterochromatic stray light, wavelength calibration and wave band errors for diagnostic reasons, and this means that a neutral portion of the spectral profile must be used for holding or testing the photometric value. There are two classes of glass suitable for this: very neutral glasses such as Chance ON28, ON29, ON30 or ON31 or Schott NG3, NG4, NG5, NG11, or pseudo-neutral glasses such as Chance ON10, ON11A, ON31A or ON32A which have several broad smooth maxima and minima at different levels but are not selective enough to impose serious risk of heterochromatic stray light errors if measurements are made at the maxima or minima. These latter have the advantage that a single filter gives calibrations at several densities. Both classes of filter are used at NPL, and optical tolerances used in fabrication are that the flatness of the surface must be better than 1 fringe per cm and the parallelism

must be better than 15 s of arc. Such filters require several years to stabilise in transmittance because the surface reflection loss reduces progressively from the initial value (given roughly by Fresnel's Equations) due to the effect of the atmosphere and even modest cleaning procedures in leaching out metal oxide components from the surface of the complex glass, which lowers its superficial refractive index.

Because absorbing glasses cannot be used in the ultraviolet region satisfactorily, thin-film metal coatings on a good quality silica substrate are also used. These can be made very neutral, but it is difficult to avoid pin-holes or nonuniformity in manufacture, so a large illuminated patch must be used in measurement in order to obtain a representative result. They also require special care in measurement because of the high reflectance, and this is no trivial problem.

At NPL we prefer large material standards to small ones, so that a large enough illuminated area can be employed to ensure that blemishes or nonuniformities do not unduly affect the results, which can then be held to be representative of the sample. This provides a further reason for avoiding a slit image in the vicinity of the sample (see also sec. IV. D). The accuracy with which the dimensions and position of the illuminated patch on the sample need to be specified is obviously less critical with a large patch than with a slit image. At NPL the preferred size of sample is 50 mm x 50 mm, and the preferred patch size is about 15 mm x 10 mm. These dimensions give one considerable freedom in the optical configuration and so help with the problems of preventing homochromatic stray light.

Standard solutions, such as acid potassium dichromate, alkaline potassium chromate or potassium nitrate, are not used for holding our photometric scale in the ultraviolet or visible regions because of the additional uncertainties which are introduced in the preparation and handling of solutions. Interlaboratory comparisons have always shown greater discrepancies between measurements on solutions than on solid filters [6, 28, 29]. It should also be pointed out that the determination of the optical path length of a cuvette is a far from trivial problem in metrology, due to the presence of the outer pair of faces in addition to the inner pair being measured. It is possible to measure a 10 mm cuvette to an uncertainty of ± 0.002 mm, so that if a nominal density of 1 were being measured the uncertainty due to calibration error in the path length would be ± 0.0002. The method used at NPL to achieve this involves the use of a laser for alignment and a mercury source with interference microscope and standardised precision micrometer for measurement.

B. Direct Reflectance

Material standards of direct reflectance are very useful in allowing calibration by substitution with a fixed optical system, and a particularly stable type is kept at NPL. This was developed by myself some years ago and consists of a piece of Spectrosil grade fused silica which has had both surfaces ground and polished flat but wedged at an angle of 7° to each other. The front surface forms the standard of reflectance (roughly $3\frac{1}{2}$% in value) so that the reflection from the back surface has to be eliminated as otherwise it would give a second and displaced reflection as well as uncertainties due to interreflections. This elimination is done in two ways: its angle of reflection is 14° away from the required front surface reflection so that it can be excluded from the viewing system almost completely, and its magnitude is reduced to about 0.01 percent reflectance by means of a special coating applied to the back face. The performance of this coating is shown in figure 15, and the diffuse component of reflectance is even lower than the direct component. This means that with a near-flawless front surface, the standard has a negligible diffuse component of reflectance.

Studies of the polished surfaces of various glass types at NPL have shown that only pure silica is unaffected by the atmosphere and mild cleaning procedures. Our own spectrophotometric measurements show that the direct reflectance of these silica standards has not apparently altered over a period of years by an experimentally significant amount i.e., about ± 0.01 percent.

C. Diffuse Reflectance and Radiance Factor

A very extensive program of work has been going on for several years at NPL on these topics, and only an indication of this work can be given here. The process of determining the absolute scales of reflectance and radiance factor is fraught with difficulty, and has not yet reached a satisfactory conclusion. Claimed uncertainty levels of ± 0.5 percent quoted recently by several laboratories seem a little dubious in view of the discrepancies between them which extend over a range of more than 1 percent. The earlier determinations of Preston at NPL [30, 31] have not yet been surpassed for absence of systematic error by other laboratories, and the current investigation at NPL is far from complete. The primary standard is the perfect reflecting diffuser by definition, a theoretical abstraction. Secondary standards are pressings of analytical magnesium oxide or barium sulphate, which have replaced smoked magnesium oxide as being more reproducible. In fact a reproducibility of ± 0.1 percent in reflectance can be obtained with pressings, compared with up to ± 1 percent for the smoked preparation, and these pressings form our interim scale pending a satisfactorily accurate absolute scale. In the visible region the radiance factor for pressings of analytical grades for both barium sulphate and magnesium oxide is about 100 percent while the reflectance is about $98\frac{1}{2}$ percent.

Practical working standards in the form of ceramic materials are used in two forms. One of these is a special photometric opal glass MS–14 (replaced later by MS–20) which is only obtainable from U.S.S.R. This material is exceptionally white and neutral in the visible and near ultraviolet region, and

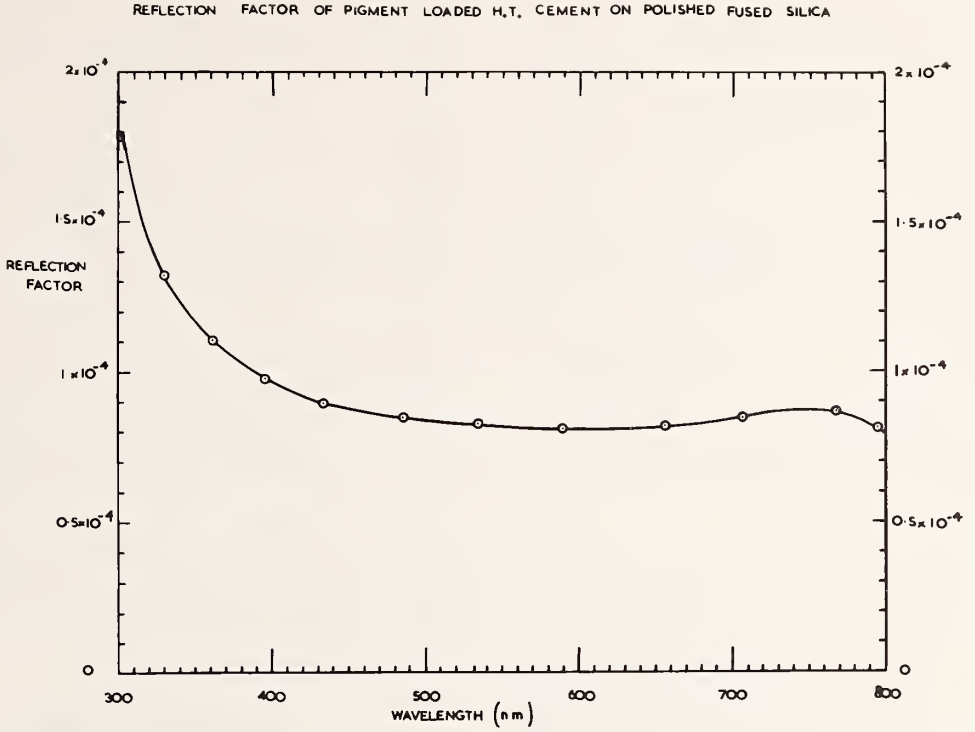

FIGURE 15. Direct reflectance profile for a special coating developed at NPL to reduce the rear reflection in working standards of direct reflectance. The standard is made from a wedged plate of Spectrosil fused silica polished on both surfaces, and the front surface reflection is the one required.

polishes well. It forms an excellent reference white standard for a reflection spectrophotometer, but of course needs calibrating against a secondary standard.

The other form of working standard used consists of sets of Ceramic Colour Standards. These were developed jointly by the British ceramics industry (especially British Ceramic Research Association) and NPL to provide durable, stable and uniform working standards in various nonwhite colours. They were developed mainly to provide a convenient means of testing the consistency of operation and accuracy of industrial colorimeters and spectrophotometers. Each set has a light grey of about 65 percent reflectance, a medium grey of about 30 percent reflectance and a dark grey of about 10 percent reflectance, these being used for testing linearity. In addition there are nine spectrally selective standards which are useful for testing wavelength calibration, waveband and stray light errors. The ultraviolet, visible and infrared diffuse reflectance profiles are shown in figures 16 to 20. Ceramic Colour Standards are more fully described in [32, 33, 34].

A thousand standards were manufactured by an automatic continuous process in a single batch for each colour type to give a statistically homogeneous population, and from these some sixty sets were purchased by NPL for its standardisation services. The remainder are available in uncalibrated form, and over half the stock has now been sold. The uncalibrated sets are very useful for transferring to them the calibration of an NPL-standardised set, especially in the case of a large company with several manufacturing plants at different sites: as the goniophotometric and spectrophotometric characteristics are closely similar, such a transfer is a purely differential measurement and can safely be done with a commercial instrument without systematic errors arising. NPL-standardised Ceramic Colour Standards are in use all over the world i.e., in Great Britain, The Netherlands, Norway, Germany, Italy, Switzerland, Hungary, U.S.S.R., Australia, Panama, Canada and, of course, the United States of America.

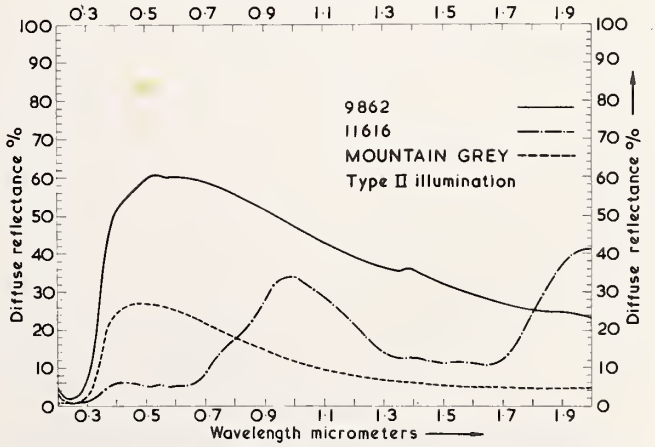

FIGURE 16. Ultraviolet, visible and near infrared diffuse reflectance profiles for the prototypes of the Light Grey, Medium Grey and Dark Grey Ceramic Colour Standards. The specular component was excluded in these measurements.

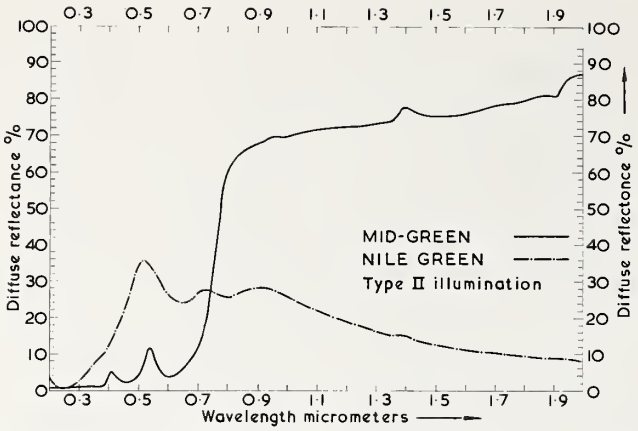

FIGURE 17. As in figure 16 for the prototypes of the Light Green and Dark Green Ceramic Colour Standards.

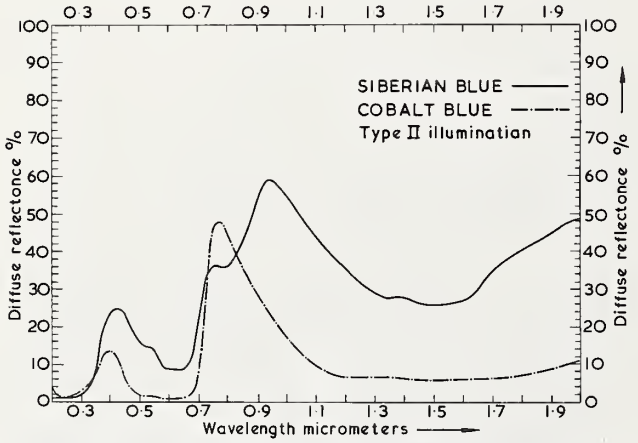

FIGURE 18. As in figure 16 for the prototypes of the Medium Blue and Dark Blue Ceramic Colour Standards.

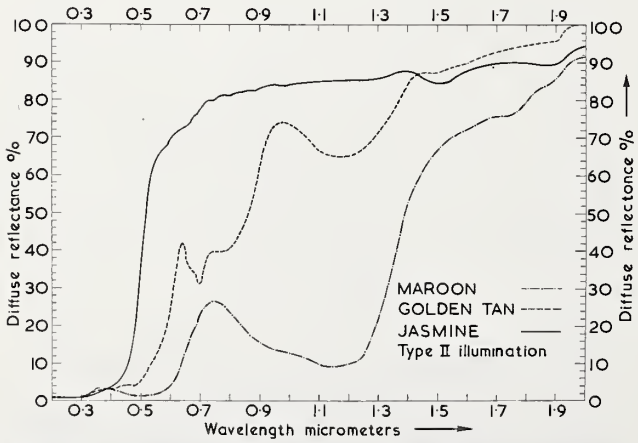

FIGURE 19. As in figure 16 for the prototypes of the Maroon, Brown and Yellow Ceramic Colour Standards.

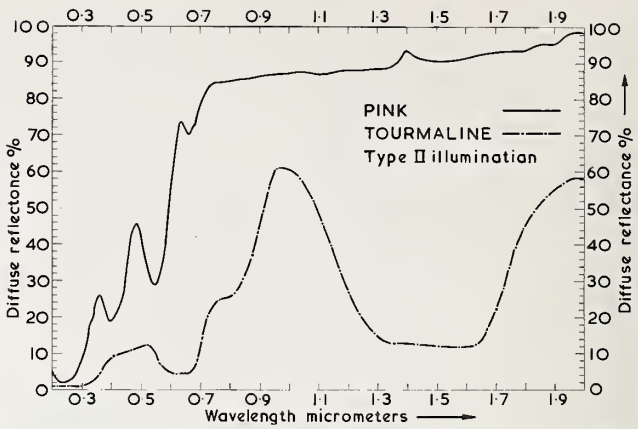

FIGURE 20. As in figure 16 for the prototypes of the Greenish Blue and Pink Ceramic Colour Standards.

The author wishes to express his thanks to the Institute of Materials Research, National Bureau of Standards for their generous assistance to facilitate his contribution to the Conference. The work described forms part of the programme of research of the National Physical Laboratory.

VII. References

[1] Hardy, A. C., Recording spectrophotometer, J. Opt. Soc. Amer. **25**, 305–311 (1935).

[2] Billmeyer, F. W., Precision and Accuracy of Industrial Color Measurement, Procs. Int. Colour Meeting, Lucerne, 445–456 (1965).

[3] Gailey, I., Visual versus instrumental colour matching, J. Soc. Dyers and Colorists **83**, 481–492 (1967).

[4] Edisbury, J. R., COLLABORATIVE TEST: Relative readings on twenty-eight Beckman spectrophotometers, Photoelec. Spectrom. Grp. Bull. **1**, 10–14 (1949).

[5] Gridgeman, N. T., Statistical analysis: the accuracy and precision of photoelectric spectrometry, Photoelec. Spectrom. Grp. Bull. **4**, 67–79 (1951).

[6] Edisbury, J. R., Some musings on errors in spectrophotometry, Photoelec. Spectrom. Grp. Bull. **5**, 109–114 (1952).

[7] Ketelaar, J. A. A., Fahrenfort, J., Haas, C., and Brinkman, G. A., The accuracy and precision of photoelectric spectrometers, Photoelec. Spectrom. Grp. Bull. **8**, 176–9 (1955).

[8] PSG Collaborative Test of 94 Recording Spectrometers, Photoelec. Spectrom. Grp. Bull. **16**, 443–467 (1965).

[9] Robertson, A. R. and Wright, W. D., International comparison of working standards for colorimetry, J. Opt. Soc. Amer. **55**, 694–706 (1965).

[10] Ellis, S. C., Problems in Spectrophotometry and their influence in Radiation Measurements, Symposium: Radiation Dose and Dose-Rate Measurements in the Megarad Range, NPL, 18–23 (UK Panel on Gamma and Electron Irradiation, 1970).

[11] Preston, J. S. and Cuckow, F. W., A photoelectric spectrophotometer of high accuracy, Proc. Phys. Soc. **48**, 869–880 (1936).

[12] Preston, J. S., Errors due to stray light in spectrophotometry, J. Sci. Instrs. **13**, 368–370 (1936).

[13] Donaldson, R., Spectrophotometry of reflecting materials, J. Sci. Instrs. **16**, 114–117 (1939).

[14] Donaldson, R., Stray light in monochromators, J. Sci. Instrs. **29**, 150–153 (1952).

[15] Donaldson, R., Spectrophotometry of fluorescent pigments, Brit. J. Appl. Phys. **5**, 210–214 (1954).

[16] Harding, H. G. W., Precautions necessary for accurate measurements of optical density standards, Photoelec. Spectrom. Grp. Bull. **4**, 79–86 (1951).

[17] Jones, O. C., An impedance converter for use with digital voltmeters, J. Sci. Instrs. **40**, 196–197 (1963).
[18] Crawford, B. H., Physical photometry, Notes on Applied Science No. 29, H.M.S.O., London, 1962.
[19] Samways, P. R., Optimum noise filter for dc measurements, J. Phys. **E 1**, 142–144.
[20] Bauman, R. P., Absorption Spectroscopy, p. 89 (Wiley; New York, 1962).
[21] Strong, J., Procedures in Experimental Physics, p. 376 (Prentice-Hall, New York, 1938).
[22] Clarke, F. J. J., Fulton, E. R., and Samways, P. R., An integrating sphere reflectance and transmittance attachment for use with a Cary 14 spectrophotometer, to be published.
[23] Hildebrand, F. B., Introduction to Numerical Analysis, p. 301 (McGraw-Hill, New York, 1956).
[24] Slavin, W. and Porro, T. J., Measurement of photometric accuracy in UV-VIS spectrophotometry, Procs. Pittsburgh Conf. on An. Chem. and App. Spect. (1960).
[25] Jones, O. C., and Clarke, F. J. J., A new photometric technique using a variable shutter device, Nature, **191**, 1290 (1961).
[26] Jones, O. C. and Clarke, F. J. J., Attenuation of Radiation, British Patent No. 1031781 (1962); US Patent No 3256444 (1966).
[27] Carruthers, G. H., and Harrison, T. H., Application of Talbot's Law to photoelectric cells with a non-linear illumination-current characteristic, Phil. Mag. S, 7, **7**, 792–811 (1929).
[28] Vandenbelt. J. M., A collaborative study of Cary spectrophotometers, J. Opt. Soc. Amer. **44**, 641 (1954).
[29] Vandenbelt, J. M., Collaborating readings with the Cary 14 spectrophotometer, J. Opt. Soc. Amer. **50**, 24 (1960).
[30] Preston, J. S., The reflection factor of magnesium oxide, Trans. Opt. Soc. **31**, 15–35 (1930).
[31] Preston, J. S., A new determination of the luminance factor of magnesium oxide, Procs. Phys. Soc, B, **65**, 76–80 (1952).
[32] Clarke, F. J. J., and Samways, P. R., The spectrophotometric properties of a selection of ceramic tiles, Report No. MC2, NPL (1968).
[33] Clarke, F. J. J., Ceramic colour standards, Procs. AIC Symposium, Color 69, Stockholm, 445–452 (Müsterschmidt, Göttingen, 1970).
[34] Clarke, F. J. J., Ceramic colour standards—an aid to industrial control, Printing Technology, **13**, 101–113 (1970).

(Paper 76A5–728)

NATIONAL BUREAU OF STANDARDS SPECIAL PUBLICATION 378, Accuracy in Spectrophotometry and Luminescence Measurements, Proceedings of a Conference Held at NBS, Gaithersburg, Md., March 22–24, 1972 (Issued May 1973).

An Accurate Spectrophotometer for Measuring the Transmittance of Solid and Liquid Materials

R. Mavrodineanu

Analytical Chemistry Division, National Bureau of Standards, Washington, D.C. 20234

(May 31, 1972)

The optical transmittance of solids and liquids as well as the molar absorptivity of various chemical species are parameters of fundamental significance in characterizing these materials. Meaningful transmittance data can be obtained only when the measurements are performed with well-known accuracy and precision. To perform such measurements, a high accuracy spectrophotometer was designed and assembled at NBS, Analytical Chemistry Division, and will be described in this paper. This single-beam instrument is composed of a constant radiation source, a monochromator, a sample carriage, an integrating sphere-photomultiplier assembly followed by appropriate electronics, and a read out system consisting of a digital voltmeter and a computer data acquisition and handling provision. The accuracy of transmittance measurements is determined by the light-addition principle used in conjunction with a two-aperture arrangement. The spectrophotometer can be used in manual or automatic modes of operation. A detailed discussion of the data obtained with this instrument, used in both modes, will be presented together with its application to the certification of solid and liquid Standard Reference Materials for checking the photometric scales of conventional spectrophotometers.

Key words: Absorbance; automation of accurate spectrophotometer; instrumentation, spectrophotometric; spectrophotometry, high accuracy; standard reference material in spectrophotometry; transmittance.

I. Introduction

Optical transmittance is due to an intrinsic property of matter and characterizes a particular transparent material. Since this parameter is not known a priori, it must be determined by experimental procedures.

True transmittance values can be obtained only by using accurate measuring techniques and by taking into consideration all factors which can affect and distort the data.[1]

Transmittance is the ratio of two radiation flux intensities. It is therefore necessary that the photometric scale of the spectrophotometer used to perform the measurements be accurate. The transmittance of a particular material is also a function of wavelength; hence the wavelength scale of the monochromator should also be accurate, and appropriate spectral bandpasses should be used. The measurements should be made using collimated radiations. Such radiations define unambiguously the actual path length through the transmitting medium, the reflection losses, and eliminate the effects of polarized radiations that are produced at the surface of the sample. Other important factors which must be considered are: homogeneity and stability of the sample, radiation scatter inside the sample, interference phenomena, stray radiation, polarization, fluorescence, temperature, particulate matter, and surface conditions. Since transmittance measurements depend on a diversity of factors, meaningful values can be obtained only by defining the experimental conditions for obtaining transmittance data [1, 2].[2] Spectrophotometers are used to perform two types of measurements:

(1) Quantitative determination of chemical species using the relation between optical transmission of the material, and the concentration as a measuring parameter. Under these circumstances, the photometric scale

[1] The optical transmittance of a solid material includes the reflection losses which occur at the air-solid interface.

The internal transmittance is defined as the transmittance of the material corrected for reflection losses (2). This internal transmittance can be calculated in principle from the transmittance by using the well known Fresnel equations (1, pp. 98 to 100).

For collimated radiation the reflectance R, for a material with an index of refraction, n, and an absorptivity, a, at wavelength, λ, is given through:

$$R_\lambda = \frac{(n_\lambda - 1)^2 + n_\lambda^2 a_\lambda^2}{(n_\lambda + 1)^2 + n_\lambda^2 a_\lambda^2}.$$

For a nonabsorbing material and collimated radiation:

$$R_\lambda = \frac{(n_\lambda - 1)^2}{(n_\lambda + 1)^2}.$$

For glass, n is approximately 1.5 in the visible region of the spectrum, and R will be about 4 percent at every air-glass interface.

When noncollimated radiation is used:

$$R_\lambda^\perp = \frac{\sin^2(\alpha - \beta)_\lambda}{\sin^2(\alpha + \beta)_\lambda}$$

for perpendicular polarized radiation, and

$$R_\lambda^\parallel = \frac{\tan^2(\alpha - \beta)_\lambda}{\tan^2(\alpha + \beta)_\lambda}$$

for parallel polarized radiation, where α and β are the angles of incidence and refraction, respectively.

In collimated radiation and in air, $\alpha = \beta = 0$ and $R^\perp = R^\parallel = R$.

[2] Figures in brackets indicate the literature references at the end of this paper.

of the spectrophotometer is calibrated in meaningful units, using a series of reference solutions having known concentrations of the species to be determined, rather than values of optical transmittance.

The accuracy of the measurements is related solely to the accuracy with which the concentration of the reference solutions is known and to the precision (stability, sensitivity, reproducibility) of the spectrophotometric method and instrument used. The accuracy of the photometric scale per se, is not a critical factor in such measurements.

The precision, stability, and reproducibility of the instrument can be checked before each series of measurements by careful use of solid or liquid reference filters having well established transmittance values.

(2) Determination of the optical transmission characteristics of solid or liquid materials, and the determination of molar absorptivities of chemical compounds. In both cases the accuracy of the photometric scale of the measuring instrument, among other things, is essential to provide true values. Ways to establish and check this important parameter are critically needed.

Since conventional spectrophotometers do not provide means to check photometric accuracy or to evaluate the possible sources of systematic errors, it was decided in 1969 to design and construct a research spectrophotometer on which transmittance measurements could be performed with well defined accuracy. Such an instrument would be used to determine optical transmittance of selected solids and liquids at various wavelengths. These materials can be used as standard reference materials (SRM's) to check the accuracy of the photometric scale of conventional spectrophotometers. The same certified SRM's could likewise be used to monitor the precision, stability, and reproducibility of those instruments [3, 4].

After a comprehensive examination of the literature in this field [5 to 34] arranged in chronological order, an instrument was developed which is similar in principle to the instrument at the National Physical Laboratory (NPL), Teddington, England, where a long tradition of high accuracy spectrophotometry exists. The instrument described in this work performs measurements of radiant energy in the visible and ultraviolet region of the spectrum, with well established and high photometric accuracy. Transmittance measurements on solids and liquids can be made with this instrument using collimated as well as noncollimated beam geometry. The wavelength accuracy and spectral bandpass achievable are adequate to avoid degradation of photometric accuracy, and the other interferences mentioned have been given careful consideration, and, in most cases, have been assessed quantitatively.

The transmittance measurements on the optically neutral glass filters discussed in this work have been made with a noncollimated beam geometry corresponding to an aperture of about f:10. The image of the exit slit of the monochromator (8 mm x 0.5 mm) was produced at the center of the entrance face of the filter. All measurements have been made against air for the nonattenuated radiation flux, and no correction for reflection losses was made. Transmittance measurements made with noncollimated radiation by projecting the image of the exit slit of the monochromator on the entrance face of the sample using an opening of f:10 (total angle of about 7° or 8°), may differ by several parts in 10^4 of the value when compared with similar measurements made with collimated radiations, as indicated in this Journal by K. Mielenz.

Noncollimated beam geometry was applied in this work to approach the measuring conditions used in most of the conventional spectrophotometers which are available today. A brief description of this instrument was given earlier in reference [3].

II. Description of the Instrument[3]

The high accuracy spectrophotometer, completed and tested in 1970, is a single beam instrument which contains the following components: (a) a constant radiation source, (b) a monochromator, (c) a sample holder, (d) a system to check the accuracy of the photometric measurements, (e) an integrating sphere attached to a photomultiplier-digital voltmeter unit, and (f) the data presentation system. Figure 1 illustrates schematically the arrangement of these various components. A circular neutral wedge is placed after the light source to select various levels of radiation intensities required for measurements. A description of the components is presented in the following sections.

a. **The Radiation Source.** Since the instrument is a single-beam type, it is essential that the radiation source be constant and homogeneous. Additional desirable conditions are: capability of monitoring the current supplied to the source and radiation similar to that from a Planckian radiator. The source is similar in design to that developed and used at NBS by H. J. Kostkowski and R. D. Lee of the Institute for Basic Standards. This source was duplicated in our instrument with the kind assistance of its developers.

The source is used in the spectral range 360 nm to 800 nm and consists of a tungsten incandescent filament lamp with a tungsten ribbon 8 mm long by 2 mm wide. The connections to the lamp terminals are soldered to minimize contact problems (see fig. 6). The direct current required to operate this lamp at approximately 3000 K is 18 A across a 6 V drop; our source is operated at 5 V and 15 A. The d.c. power supply is capable of delivering 15 V and 50 A, and can be operated in constant current or constant voltage modes. To achieve the constant current mode an external sensing resistor of 0.1Ω and 50 A and a current control circuit are placed in series with the power supply. A feedback voltage across this resistor is connected to the sensing system. The character

[3] The commercial instruments and parts used in the construction of the spectrophotometer are identified in the addendum.

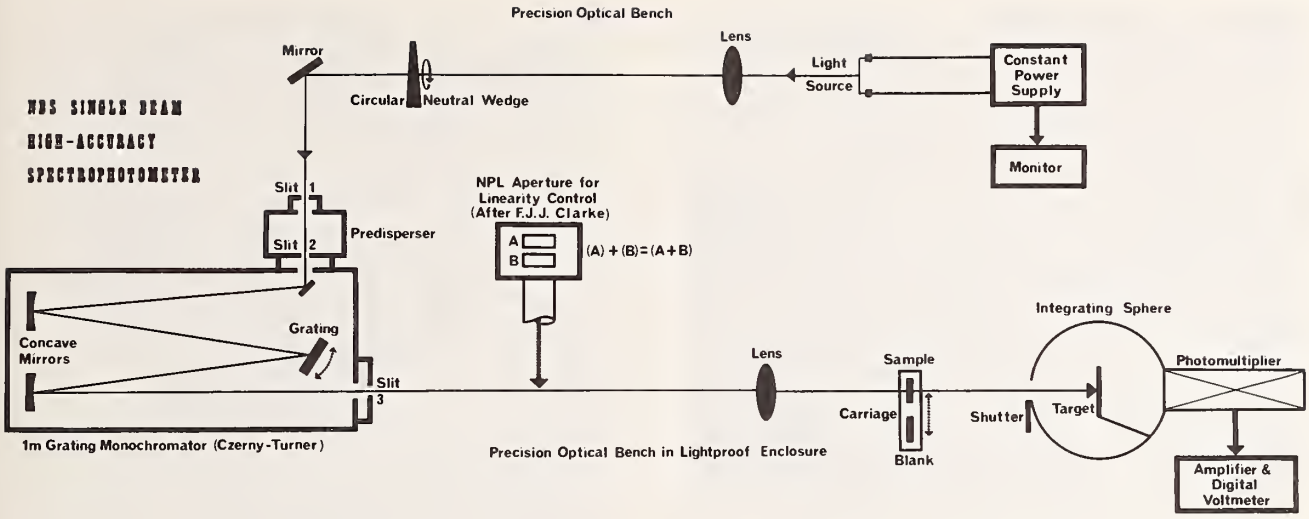

FIGURE 1. Principle of the single beam high accuracy spectrophotometer. The aperture unit is placed on the optical bench only when linearity measurements are performed.

istic of this function is the ability to automatically change its output voltage to maintain a constant current to the load resistor, which, in our case, is the lamp source. The nominal current regulation obtained is better than 0.01 percent, and the stability over an 8 hour period, at constant load temperature, is better than 0.02 percent. The stability of the current delivered to the lamp is monitored with a high accuracy potentiometer used in conjunction with a null meter. This meter is sensitive to variations in the current supplied to the lamp from 1 part in 1000 to 1 part in 1,000,000 per division (fig. 1 and fig. 14). The potentiometer is connected to the current source across a resistor (0.01Ω and 100 A) placed in series with the lamp.

The demagnified (2 to 1) image of the ribbon filament is projected on the entrance slit of the predisperser by a fused quartz (nonfluorescent SiO_2) lens whose focal distance is 254 mm and diameter is 44 mm. This and the other lenses used in the optical system, were calculated by K. Mielenz of the Institute for Basic Standards at NBS. The lenses are mounted in carriers which permit orientation in any position. A circular neutral wedge is placed between the light source and the predisperser. This wedge, evaporated inconel on a fused quartz disc (150 mm diam), is linear in density and provides a light attenuation of 100 to 1. The wedge is motor driven (1 rev. per s) to select proper radiation intensity levels as required by the measurements (figs. 2, 3, and 4). The radiation source used for measurements in the ultraviolet region to 275 nm is a single coil tungsten-bromine incandescent lamp (fig. 5) supplied by an adequate power source; below 275 nm, a deuterium discharge lamp is contemplated.

b. **The Monochromator.** The monochromator is a 1-m Czerny-Turner type grating instrument with a dispersion of 0.8 nm/mm. The flat grating has 1200 grooves per mm covering a surface of 100 x 100 mm. The monochromator is provided with a predispersing attachment to reduce the stray light (fig. 3). This pre-

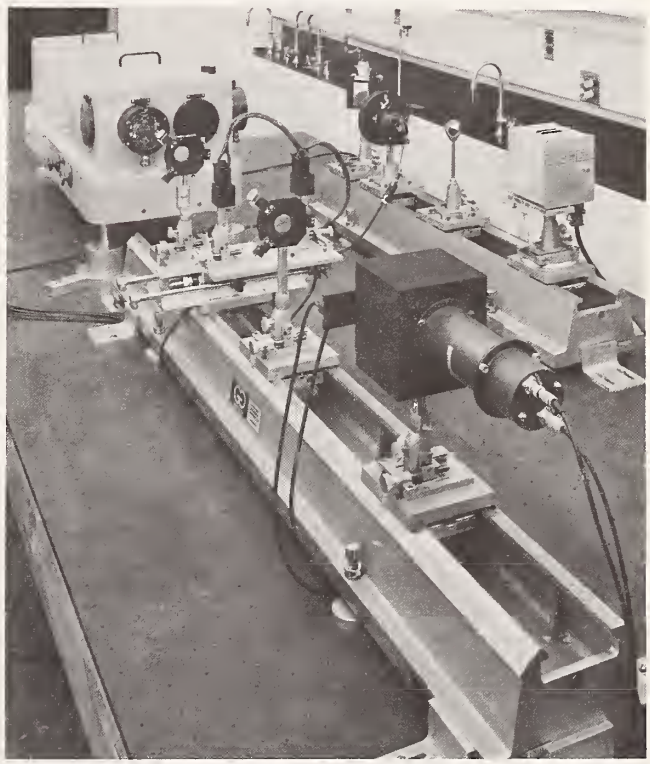

FIGURE 2. General views of the spectrophotometer. Rear: optical bench carrying the tungsten-halogen radiation source used for checking the alignment of optical components, followed by a quartz lens, the circular quartz neutral wedge, and a flat mirror. Left: the 1-m Czerny-Turner grating monochromator (the predisperser is not illustrated here). Front: optical bench carrying a quartz lens, the single-sample and blank carriage, a second quartz lens, and the integrating sphere with the photomultiplier housing.

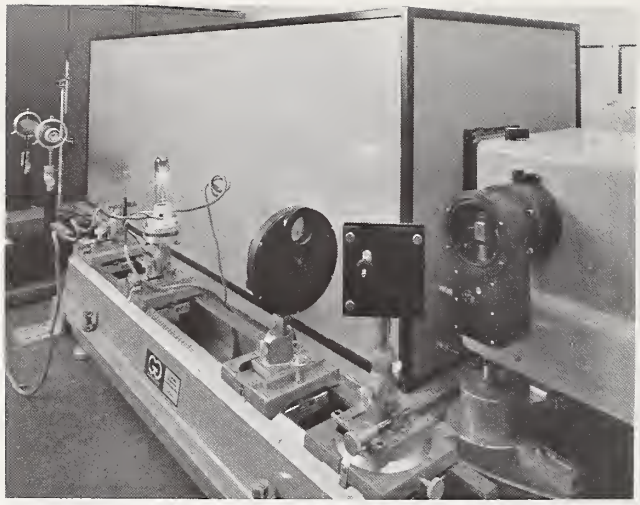

FIGURE 3. Close view of the tungsten ribbon filament lamp on its adjustable holder, followed by the quartz lens—circular neutral wedge assembly, and by the flat mirror in its adjustable holder. The 30° quartz prism Littrow-type predisperser is located at the entrance slit of the 1-m grating monochromator. Extreme left: neon gas laser used to check the optical alignment, and mercury discharge lamp for wavelength calibration. When in use, the tungsten ribbon lamp is surrounded by an enclosure with black walls (50 cm x 50 cm x 70 cm high). Rear: enclosure containing the optical units illustrated in figure 2.

disperser is a small quartz prism monochromator connected to the scanning system of the 1-m instrument. A wavelength counter permits readings to 0.1 nm and the scanning speed can be varied from 0.05 nm to 200 nm/min by a 12 speed synchronous electric motor.

The optical components are placed on precision lathe bed type optical benches which are 160 and 120 cm long, and are equipped with appropriate carriers provided with *x-y-z* adjustments.

c. **Sample Carrying Systems.** The spectrophotometer is provided with two sample carrying systems. One system measures one sample and its blank, while the other system permits sequential measurements for seven samples and eight reference reading positions against air, and can be operated manually or automatically through a computer interfaced with the instrument.

The single sample carrying unit consists of a platform provided with two vertical holders which can accept $\frac{3}{4}$-in (14 mm) rods and a variety of sample supports (fig. 2). These holders can be moved laterally through a rack and pinion arrangement. The platform is mounted on 4 ball bushings which ride on two horizontal rods and can be moved pneumatically across the optical axis. The pneumatic operation was recommended by G. E. Moore and J. T. Sterling of the Institute for Materials Research at NBS and by L. Owen, a guest worker at NBS. The travel distance is 8 in (20 cm) and the linear movement is smooth; the position of the platform and the sample in and out of the optical beam, can be reproduced within 0.025 mm. This unit is illustrated in figure 2

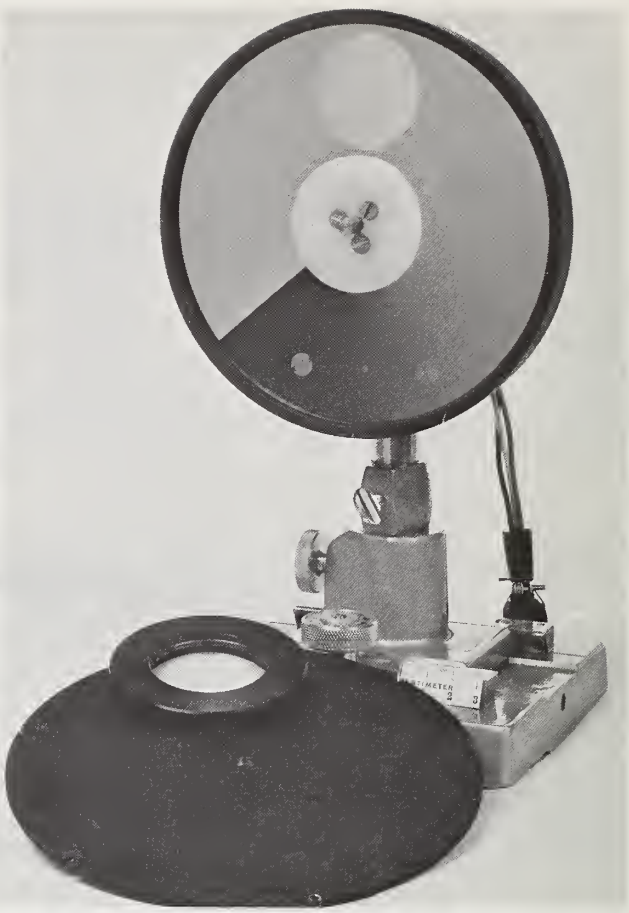

FIGURE 4. Close view of the circular, neutral wedge. The front plate which carries the fused silica lens was removed to show the fused silica disc with the evaporated metal layer.

and is located between the two quartz lenses. The sample holder is designed to accept conventional solid or liquid filter holders which fit most spectrophotometers. These holders are provided with a thermostating jacket, and can be rotated in the horizontal plane through a 10 cm diameter rotating table.

A filter holder which permits the rotation and scanning of the sample in the *x–y* direction is also available (fig. 7). It is provided with micrometer screws having a total linear motion of 25 mm with 0.01 mm per division. The seven-sample carrying unit is illustrated in figures 8 and 9 and consists of a semicircular aluminum-alloy plate placed horizontally on an appropriate carrier on the optical bench along the optical axis. This plate, which is 32 cm in diameter and 2.5 cm thick, can be rotated clockwise through a pneumatically operated precision ratchet system in increments of 12°. The stepwise rotation utilizes a solenoid valve which is operated electrically by a switch located outside the enclosure. This switch can be operated manually or automatically by computer (fig. 14).

FIGURE 5. Single coil tungsten halogen lamp in the adjustable holder.

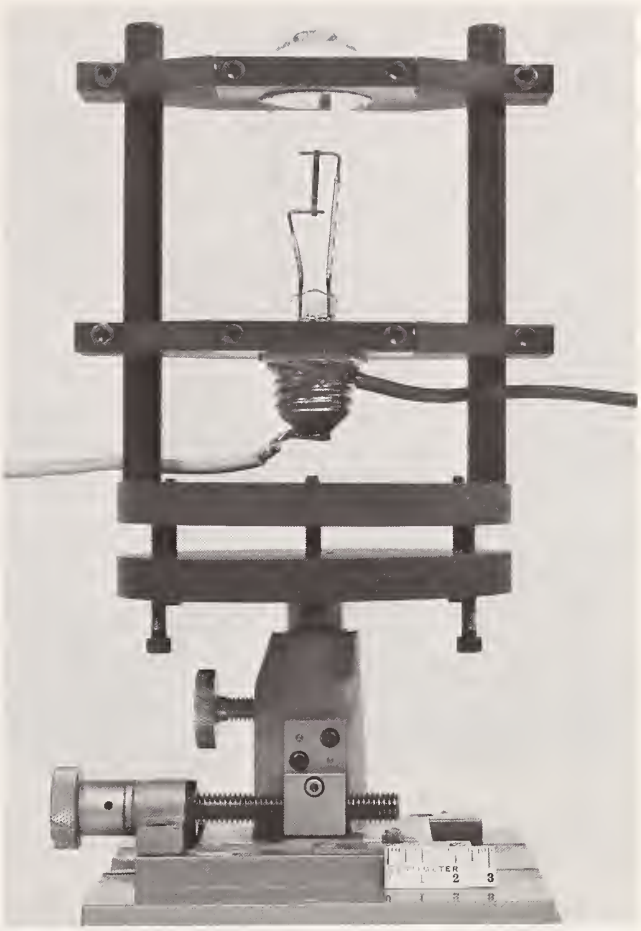

FIGURE 6. The tungsten ribbon filament lamp in the newly designed adjustable holder. The platform which carries the lamp is similar to that described in figure 5 and can be oriented in the horizontal plane through the six screws spaced around the edges of the platform at 60° intervals. Three screws push the platform while the other three pull.

The current-supplying wires are soldered directly to the lamp terminals to eliminate contact problems.

The semicircular plate carries seven sample holders similar to those used for the single sample system described earlier. The holders are placed at 24° intervals and are separated by blank spacings. About 1 atm of air pressure is used to operate the plate and the rotation is set at 2 s per 12° step when the automatic computer operating mode is used.

d. **System to Check the Accuracy of the Photometric Reading.** Since the high accuracy spectrophotometer is single beam, accurate photometric data are obtained when there is a linear relation between the measured radiation flux and the corresponding response of the photodetector.

Linearity of photodetectors can be measured by several means: the inverse square law [7, 15]; the use of optical elements having a known transmittance which can be determined by other means [17] and the light addition principle of Elster and Geitel using a plurality of light sources [5, 6, 8, 9, 10, 13, 18, 19, 20, 28, 31, 33, 34] or multiple apertures [11, 12, 14, 16, 21, 23, 25, 26, 27, 30]. A novel approach to the problem of accurate photometric measurements was described by O. C. Jones and F. J. J. Clarke [24, 29] and by F. Desvignes and J. Ohnet [32]. A critical discussion of some aspects of accurate spectrophotometry will be found in an NBS manuscript by Gibson and associates [22]. The radiation addition principle, using two apertures with one source of radiation, was chosen for our work. The aperture method for checking the linearity of photometric data was in use at the National Physical Laboratory from about 1930 onwards, and one form of it was described by Preston and Cuckow [11] in conjunction with a single beam spectrophotometer, using a five aperture screen. One year later, Buchmüller and König [12] described and used a two aperture unit. At NBS, Barbrow [14] used a 10 aperture arrangement, while Harding [16] and Cordle and Habell [25] at NPL described a two aperture system. Multiapertures were used by Hoppmann [21], Bischoff [23], Sanders [26] and Nonaka and Kashima [27]. Finally, Clarke [30]

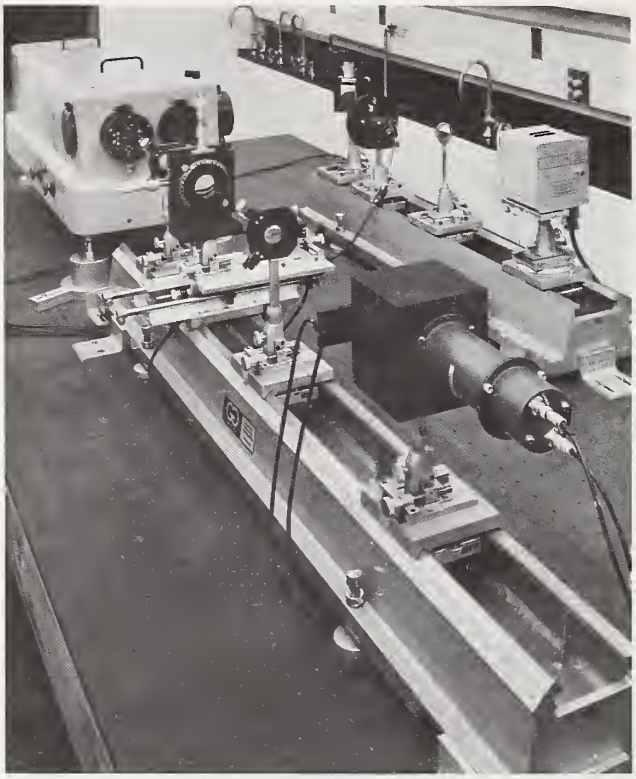

FIGURE 7. Same as figure 2 except for the sample holder which in this case is capable of rotating the sample 360° and to displace it in the *x-y* direction through the micrometer screws.

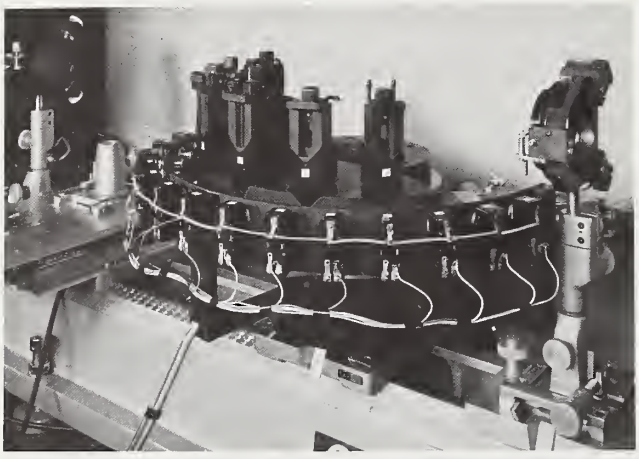

FIGURE 8. Circular platform carrying seven filter holders. The 15 position switches (7 sample positions and 8 blank positions) are visible along with the two quartz lenses. The exit slit of the monochromator is at left.

discussed in detail the use of a two aperture system to check the accuracy of photometric data obtained on the spectrophotometer at NPL. It is this two aperture system which is used at NBS.

The two aperture unit consists of a metal plate (130 mm by 100 mm) containing two rectangular

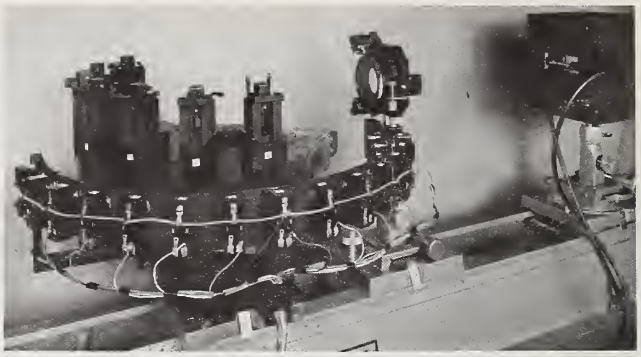

FIGURE 9. Same as figure 8. The pneumatic cylinder which rotates the circular platform through a ratchet mechanism is visible at the rear of the platform. The integrating sphere with its pneumatic shutter is seen at right.

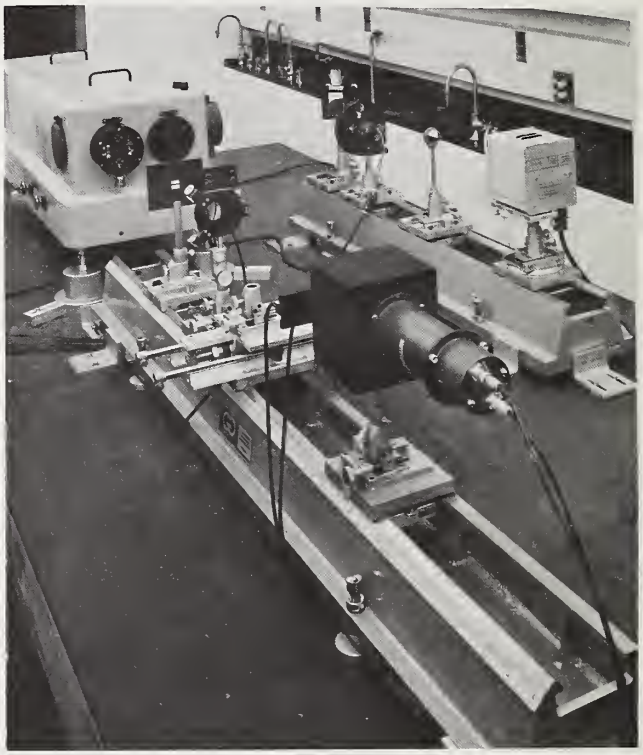

FIGURE 10. Same as figure 2. In this case the dual-aperture unit for linearity control is located on the optical bench after the exit slit of the monochromator.

windows, A and B, (20 mm by 8 mm) located one above the other (figs. 10, 11, 12). Each aperture can be closed by a light-tight shutter which is operated pneumatically by remote control (fig. 14). The aperture plate is placed in the optical path after the exit slit of the monochromator and *within* the optical solid angle of the instrument. The image of the apertures is then projected on the target of the integrating sphere. A fused quartz lens with a focal distance of 190 mm and a diameter of 60 mm is used for this purpose. The arrangement is illustrated in figure 10. No optical element

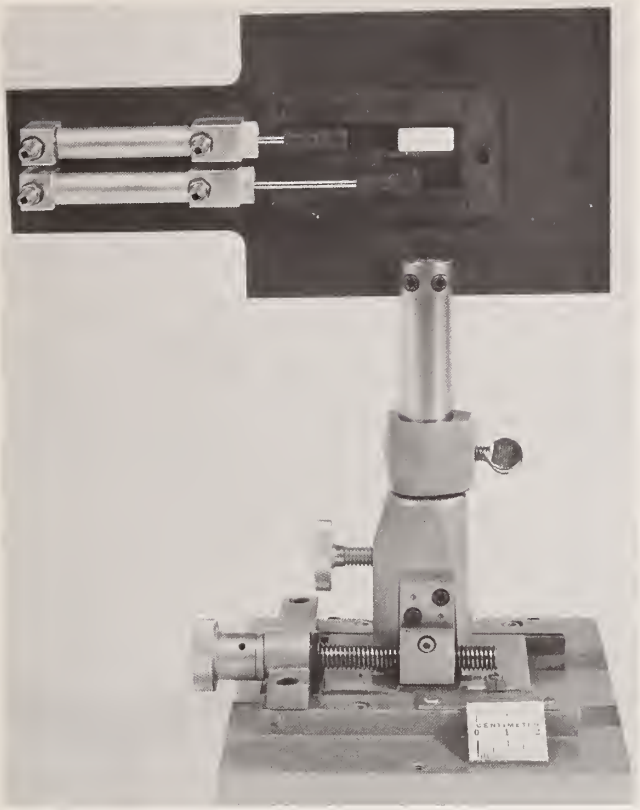

FIGURE 11. Detail of the dual-aperture unit showing its construction and the pneumatic system which operates the two shutters. One aperture is open, the other is closed.

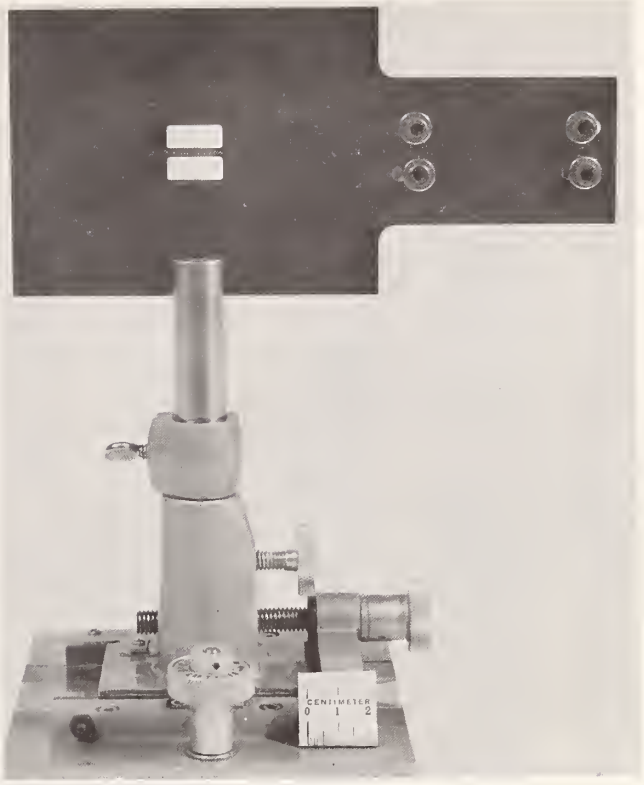

FIGURE 12. Front view of the dual-aperture unit, with both apertures open.

should be placed between the aperture plate and the monochromator. The linearity check consists of measuring the photocurrent produced when aperture A is open then closed, and then aperture B is open and then closed. The value of $(A)+(B)$ is compared with the values obtained with both apertures $(A+B)$ open. If the system is linear these two values should be identical:

$$(A)+(B)=(A+B).$$

If this is not the case, the system shows nonlinearity which is proportional to the amount by which the sum of $(A)+(B)$ differs from $(A+B)$. This difference is then used to correct the transmittance values measured on the solid or liquid filters.

e. **Integrating Sphere and Photomultiplier Arrangement.** The radiations emitted from the exit slit of the monochromator and passing through the aperture or the filter are received on the target of the integrating sphere. This sphere is illustrated in figures 2, 7, 9, and 10. A block of aluminum made from identical halves was cut to produce a half sphere in each block. The halves were joined together to form a hollow sphere. Its diameter is 125 mm and a target, made from a circular plate, 35 mm in diameter, is located at the center of the sphere. The front surface of the sphere has a 20 mm diameter opening. This opening can be closed by a shutter which is operated remotely by a pneumatic system. A 50 mm diameter opening is at the opposite end to which the housing of the photomultiplier is attached by an "O" ring to provide a light-tight joint. The inside of the sphere is coated using a suspension of $BaSO_4$; the outside is painted black.

Under these circumstances the sensitive surface of the photodetector receives the radiations originating from the exit slit of the monochromator only after these radiations have undergone at least two diffuse reflections.

The photomultiplier is a 50 mm flat-faced, silica end window tube with a 44 mm cathode and 11 venetian blind dynodes having CsSb secondary emitting surfaces. The cathode is an S−20 or tri-alkali type. The spectral range of this tube is from below 200.0 nm to 850.0 nm. The operating voltage used is 850 V. The photomultiplier output is supplied to a current-to-voltage converter consisting of an operational amplifier with high precision feedback resistors with values of 10^6, 3×10^6, 10^7, 3×10^7, and $10^8\Omega$. Dark current compensation is also available. This electronic system, described in figure 13 was designed and assembled by K. W. Yee of the NBS Electronic Instrumentation Section. The output from the current-to-voltage unit is connected to a digital voltmeter, illustrated in figure 14, with one microvolt resolution on the 1 V full scale range.

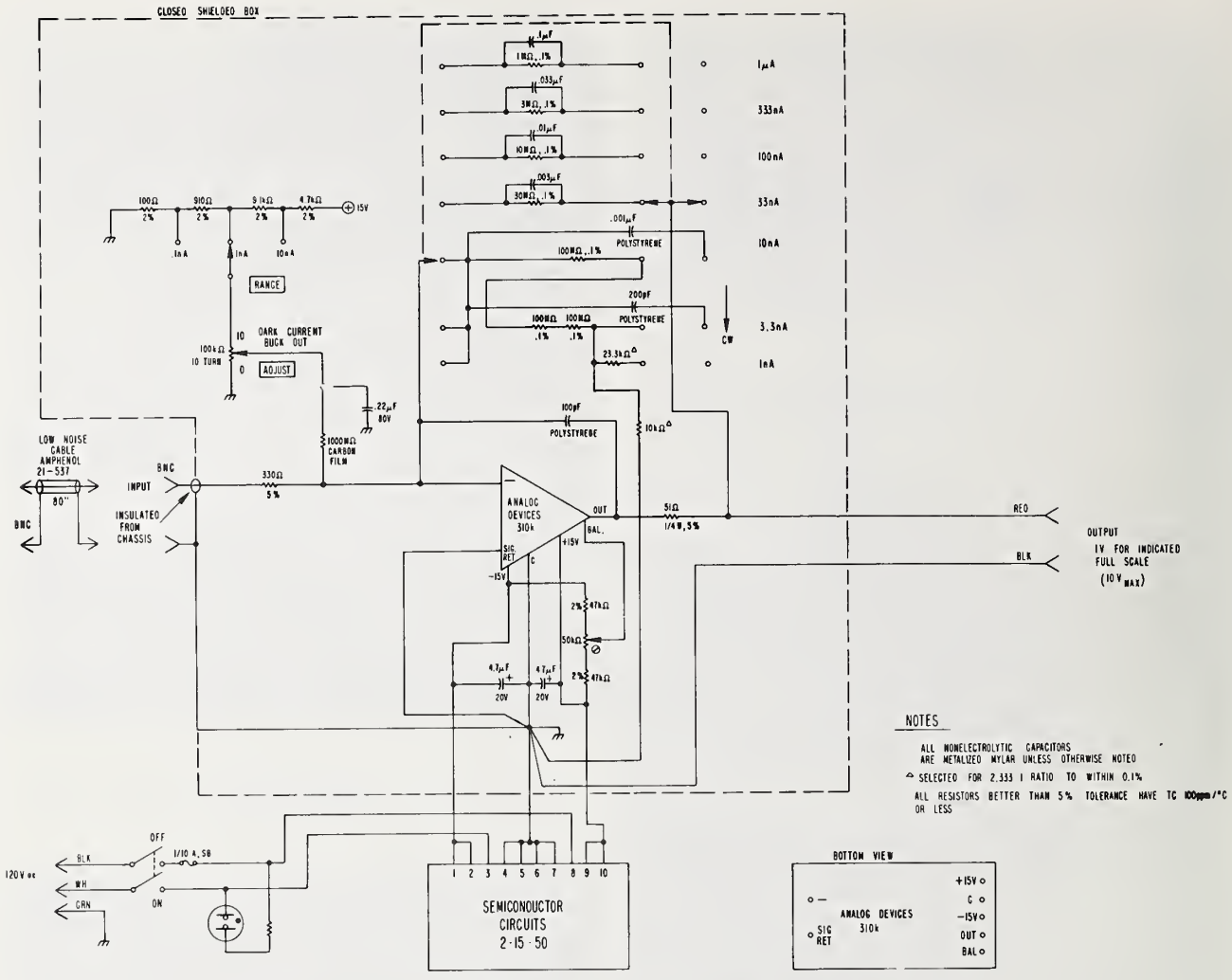

FIGURE 13. Schematic of the current-to-voltage circuitry. Courtesy of K. W. Yee.

The optical components located after the exit slit of the monochromator, including the photomultiplier tube, are enclosed in a light-tight box 200 cm long, 70 cm wide and 76 cm deep (fig. 3). The removable front panel is provided with a sliding door to permit rapid access to the filter-holder system. The box contains outlets for the compressed air which operates the apertures, sample carriage and integrating sphere shutter, and for the electrical connection from the photomultiplier. The inside walls are lined with thermal insulation painted black. When in use, all nonblack metal parts are covered with a black cloth to reduce stray light. The entire equipment is placed on a vibration isolation table 3.66 m by 1.52 m. The optical benches and the monochromator are secured by stops which are attached to the table surface. The alignment of the optical parts is made and checked periodically with a low-power laser shown in figure 3 (CW gas laser, output power 2 mW, λ 6328 Å) and with a high intensity tungsten-halogen lamp shown in figure 5.

f. **Data Collection and Presentation Systems.** The data output from the digital voltmeter (DVM), corresponding to the current generated at the photomultiplier tube by the radiations passing through the aperture system (A, B, $A+B$) or the samples (I) and blanks (I_0), can be obtained by visual means or computer operation. Both methods have been used in this work with good results. In the visual mode, the operator examines the digital voltmeter display and takes a mental average of the data. The display rate is adjusted to about one reading per second.

When measurements are taken by computer, the display of the digital voltmeter is adjusted to a faster rate; for instance, 10 to 20 data per second, depending on the capabilities of the instrument and measurement requirements. In our work, we use 10 data per second and collect 50 individual data for each measurement. This information is fed to the computer which calculates and prints the results as averages with the corresponding standard deviation, relative standard

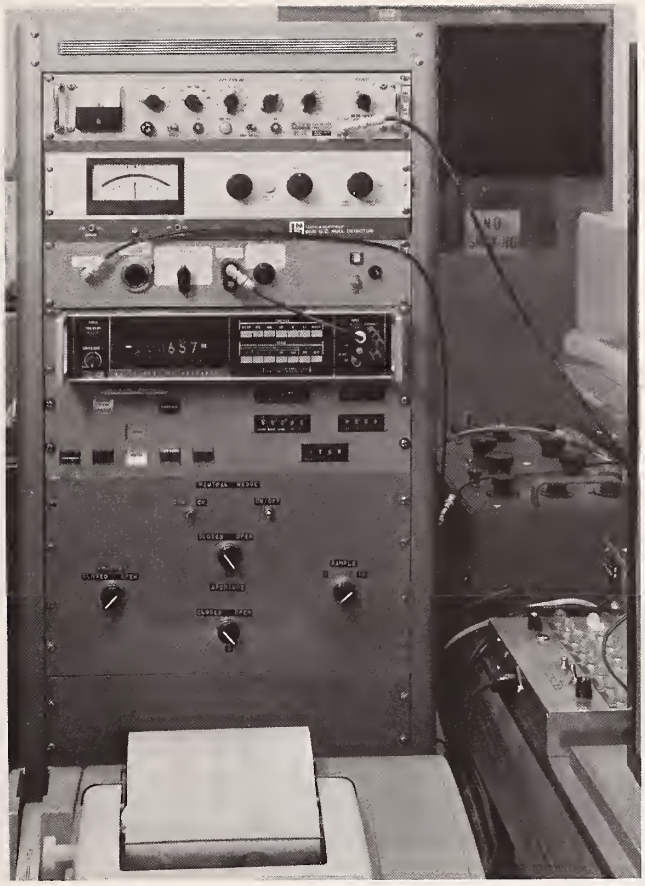

FIGURE 14. Console containing the power supply for the photomultiplier tube, the dc null detector, the current-to-voltage converter, the digital voltmeter, the command panel for computer operation, and the command panel for the pneumatic operation of the shutter, aperture system, and single sample carriage. The electric switches for operating the circular neutral wedge are also located on this panel.

Middle right: potentiometer for monitoring the dc current supplied to the tungsten ribbon filament lamp.

At bottom left: teletype for data presentation.

Right: light panel which indicates the position of the automatic seven sample holder.

deviation, and sample position number to identify the measurement. When transmittance measurements are made on individual samples or when linearity checks are performed, the readings are initiated manually for every position. When the seven sample holder is used for sequential measurements, the operation is performed automatically by the computer. It is programmed to take a predetermined number of individual DVM readings (50), print the arithmetic average, followed by the standard deviation, relative standard deviation, percent transmittance and sample position (fig. 15). At the conclusion of each measurement, the computer initiates a signal which rotates the holder to the next position. This is followed by the data taking and sample changing sequence until the measurements are stopped manually or automatically by a provision made in the computer program.

CALIBRATION OF SRM930 AT 440 NM 2-2-72
SAMPLE NUMBER AND POSITION:
1-70 IN 2; 1-79 IN 4; 2-79 IN 6; REFERENCE IN 8; 3-79 IN 10;
1-91 IN 12; 3-91 IN 14

POS	AV	S	S/AV	PERCENT T
1	.2001700E 01	.4388E-03	.2192E-03	
2	.6413441E 00	.3256E-03	.5077E-03	
3	.2001230E 01	.4320E-03	.2159E-03	32.044
4	.6528346E 00	.4804E-03	.7359E-03	
5	.2001040E 01	.4254E-03	.2126E-03	32.623
6	.4221110E 00	.2293E-03	.5432E-03	
7	.2000995E 01	.3041E-03	.1520E-03	21.095
8	.6560142E 00	.3189E-03	.4861E-03	
9	.2001402E 01	.4476E-03	.2236E-03	32.781
10	.2358762E 00	.1425E-03	.6039E-03	
11	.2001539E 01	.4114E-03	.2055E-03	11.785
12	.6739426E 00	.2848E-03	.4226E-03	
13	.2001205E 01	.4678E-03	.2338E-03	33.674
14	.2386761E 00	.1064E-03	.4456E-03	
15	.2001101E 01	.4150E-03	.2074E-03	11.927
1	.2001622E 01	.3187E-03	.1592E-03	
2	.6412983E 00	.1321E-03	.2060E-03	
3	.2002043E 01	.6139E-03	.3067E-03	32.036
4	.6526482E 00	.2474E-03	.3790E-03	
5	.2001551E 01	.4756E-03	.2376F-03	32.603
6	.4222282E 00	.2174E-03	.5149E-03	
7	.2001507E 01	.4355F-03	.2176F-03	21.095
8	.6562004E 00	.3344E-03	.5095E-03	
9	.2001529E 01	.5337E-03	.2667F-03	32.785
10	.2359933E 00	.1886E-03	.7992E-03	
11	.2001634E 01	.4532E-03	.2264E-03	11.790
12	.6741099E 00	.3418E-03	.5070F-03	
13	.2001589F 01	.6368E-03	.3182F-03	33.678
14	.2386828F 00	.1604E-03	.6720F-03	
15	.2001829E 01	.3388E-03	.1693E-03	11.924
1	.2002214E 01	.2826E-03	.1412E-03	
2	.6413472E 00	.3518E-03	.5486E-03	
3	.2001882E 01	.3882F-03	.1939E-03	32.035
4	.6526177E 00	.2513E-03	.3851E-03	
5	.2001741E 01	.3841F-03	.1919F-03	32.601
6	.4223418E 00	.2957E-03	.7000E-03	
7	.2002075E 01	.4892F-03	.2443F-03	21.097
8	.6562083E 00	.1365E-03	.2081E-03	
9	.2001871E 01	.3708E-03	.1852F-03	32.778
10	.2358786F 00	.1596F-03	.6767E-03	
11	.2002130E 01	.5036E-03	.2515E-03	11.782
12	.6740563E 00	.3022E-03	.4484F-03	
13	.2001997E 01	.4545F-03	.2270F-03	33.668
14	.2388354F 00	.1704E-03	.7133E-03	
15	.2002478F 01	.2975E-03	.1485E-03	11.928

FIGURE 15. Computer data presentation.

The programming of the entire computer operation was developed by J. Aronson, R. Freemire, and J. Wing. The computer-instrument interfacing was performed by F. Ruegg and R. Shideler of the NBS Analytical Chemistry Division, Technical Service Group, under the supervision of J. DeVoe.

III. Stability of the Electronic System

As a rule, before taking measurements with the spectrophotometer, a warmup period of one hour is required. The room temperature is kept at 24 ± 1 °C, and the relative humidity is 35 percent. The particulate matter is controlled through special filters which rates the room in the 100,000 class.

The dark current of the photomultiplier tube was measured by taking 15 replications each consisting of the average of 50 individual digital voltmeter readings. These measurements were made using 850 V at the anode. The average dark current under these circumstances produced 0.000682 V with a relative standard deviation of 0.71 percent.

In all of our work, a dark current buck-out arrangement was used. A series of measurements were performed to determine the stability of this dark current compensation. To this effect, 15 consecutive measurements, each representing the average of 50 indi-

502-591 O - 73 - 4

vidual digital voltmeter readings, were made and the average dark current value was 0.000024 V with a relative standard deviation of 23.1 percent.

Four tests were made to determine the stability of the electronic system and the radiation source using the computer data acquisition mode.

a. **Stability of the Current-to-Voltage Converter.** A constant voltage was supplied to the converter using the dark current compensation provided on the unit. Fifty individual measurements were taken every 5 seconds and the average value was printed along with its percent standard deviation. The measurements were then repeated 15 times and an average of the 15 values was calculated along with the corresponding percent standard deviation. These measurements were then repeated three times. The results are summarized in table 1. This table also presents the values for the first group and the average values and corresponding percent standard deviation for the two consecutive groups. It can be seen from the stability of the current-to-voltage unit that measurements can be performed with a reproducibility of about 0.0012 (at the 67% confidence level) expressed as percent standard deviation for a single determination. The time interval between the first and last group of measurements was 15 min.

TABLE 1. Stability of the current-to-voltage converter alone measured in three groups of 15 replications each

Replication	Average of 50 individual measurements; volts	Percent standard deviation
1	1.003494	0.0013_6
2	1.003496	0.0012_9
3	1.003482	0.0014_6
4	1.003507	0.0011_1
5	1.003515	0.0013_4
6	1.003508	0.0013_6
7	1.003497	0.0011_8
8	1.003498	0.0013_3
9	1.003505	0.0011_0
10	1.003510	0.0014_2
11	1.003518	0.0013_3
12	1.003521	0.0012_0
13	1.003522	0.0013_1
14	1.003507	0.0012_6
15	1.003527	0.0013_7
Average of replications	1.003507	First group
Percent standard deviation	0.0012	First group
Average of replications	1.003535	Second group
Percent standard deviation	0.0015	Second group
Average of replications	1.003545	Third group
Percent standard deviation	0.0010	Third group

b. **Stability of the Current-to-Voltage Converter Plus the Photomultiplier Tube Supplied with 850 V and in Total Darkness.** The measurements were made as previously described and the results are presented in table 2.

c. **Stability of the Current-to-Voltage Converter and the Photomultiplier Tube Supplied with 850 V and Exposed to the Radiation of a Tritium Activated Fluorescence Source.** A constant radiation source consisting of a tritium activated phosphor was placed before the integrating sphere and a series of measurements were taken following the technique described above. Table 3 shows the results.

d. **Stability of the Current-to-Voltage Converter, the Photomultiplier Tube Supplied with 850 V, and the Tungsten Ribbon Filament Lamp.** The same measuring procedure as mentioned in a, b, and c was used here. In this case, however, the incandescent tungsten lamp was used as the source of radiation. Table 4 summarizes the results of four groups of measurements over a period of 20 min. This last series of measurements indicate that the single-beam spectrophotometer is capable of producing measurements of radiation fluxes with a percent standard deviation of about 0.022_5 for single measurements with 2.00 V at the photomultiplier tube anode.

Table 3. Stability of the current-to-voltage converter and the photomultiplier tube at 850 V and exposed to the radiation of a tritium activated fluorescent source

Replication	Average of 50 individual measurements; volts	Percent standard deviation
1	1.536345	0.027_5
2	1.536326	0.030_2
3	1.536196	0.022_8
4	1.536289	0.023_5
5	1.536106	0.030_9
6	1.536117	0.031_4
7	1.535916	0.025_1
8	1.536065	0.023_8
9	1.536179	0.029_3
10	1.536003	0.023_3
11	1.536083	0.021_5
12	1.535961	0.026_3
13	1.536052	0.031_3
14	1.536095	0.026_6
15	1.536092	0.026_2
Average of replications	1.536122	First group
Percent standard deviation	0.0082	First group
Average of replications	1.535768	Second group
Percent standard deviation	0.0095	Second group
Average of replications	1.535522	Third group
Percent standard deviation	0.0054	Third group

accuracy with a low pressure mercury discharge lamp placed before the entrance slit of the monochromator. The following wavelengths were used for calibration: 3650.2 Å; 4046.6 Å; 4077.8 Å; 4339.2 Å; 4347.5 Å; 4358.4 Å; 4916.0 Å; 5460.7 Å; 5769.6 Å; and 5790.7 Å. If additional reference wavelengths are needed, a Cd-Hg or a He-discharge lamp could be used for calibration. The wavelength counter was then checked using the procedure recommended by Gibson [2], and a slit of 0.1 mm which is equivalent to an effective spectral bandpass of 0.08 nm. The deviation of the wavelength counter from the true value was found to be less than ± 0.1 nm; hence no wavelength correction was applied to the measurements discussed here.

V. Stray Radiation

Tests were made to determine the stray radiant energy (SRE) in the monochromator proper, as well as in the photometric arrangement. The measurement of stray radiation in the monochromator, that is, the radiation energy at wavelengths different from those of the nominal spectral bandpass transmitted through the instrument, is not easy or infallible. A detailed discussion of this instrumental parameter was given in an ASTM Tentative Method [35] and the procedure recommended in this work was used to determine SRE in the blue and yellow spectral range. In this procedure, a solution of methylene blue, which has a strong absorption in the range from λ 600 to 660 nm is used. The SRE using a slit of 1 mm (0.8 nm) was equal to or less than five parts in 10^5.

The SRE generated inside the photometric system is defined as the radiant energy which falls on the photosensitive detector without passing through the absorbing sample. This SRE is usually produced by reflections and scattering of radiations on the optical and mechanical parts located between the exit slit of the monochromator and the integrating sphere. The measurements were performed using a slit of 1 mm by placing a front surface mirror at the sample position, which reflects to the instrument all radiations received from the exit slit imaged at the mirror surface. The size of this image was about 8 mm high and 1 mm wide. In this way, a maximum SRE was generated in the spectrophotometer. The measurements were then performed at λ 577.3 nm, using a radiation flux intensity five times greater than that used in routine transmittance measurements, by determining the dark current of the photomultiplier with the shutter in the closed position at the integration sphere. An average dark current of 0.040 mV was observed. The mirror was then placed at the sample position, the shutter

TABLE 2. Stability of the current-to-voltage converter and the photomultiplier tube at 850 V in total darkness

Replication	Average of 50 individual measurements; volts	Percent standard deviation
1	1.012329	0.027_1
2	1.012342	0.048_8
3	1.012322	0.027_2
4	1.012320	0.033_8
5	1.012394	0.043_5
6	1.012421	0.015_3
7	1.012404	0.018_4
8	1.012406	0.029_6
9	1.012365	0.019_6
10	1.012402	0.019_1
11	1.012465	0.025_2
12	1.012412	0.061_5
13	1.012451	0.023_5
14	1.012417	0.029_8
15	1.012481	0.024_8
Average of replications	1.012395	First group
Percent standard deviation	0.0050	
Average of replications	1.012467	Second group
Percent standard deviation	0.0033	
Average of replications	1.012510	Third group
Percent standard deviation	0.0035	

In these measurements the stability of the direct current (nominal 5 V; 14 A) supplied to the tungsten ribbon lamp was monitored with the potentiometer, and the variation of this current was less than one part in 10^5 during a series of 15 consecutive measurements (5 min).

Following the four stability tests discussed earlier, a consecutive series of six measurements were made to determine the reproducibility of transmittance measurements. To this effect seven Schott NG–4 neutral glass filters were placed in the automatic sample carrying system and the data acquisition and sample changing operations were performed automatically through the computer unit. As mentioned previously, the sample carrying system can accept seven samples in positions 2; 4; 6; 8; 10; 12; 14, and eight intermediate positions 1; 3; 5; 7; 9; 11; 13; 15. The odd numbers correspond to measurements of the nonattenuated radiation beam passing through air and are marked I_0, while the even numbers correspond to measurements of the attenuated radiations after passing through the absorbing material and are marked I. The uncorrected transmittance, T, is then

$$T=\frac{I}{I_0}.$$

The radiation flux from the tungsten ribbon filament lamp was attenuated with the circular neutral wedge until a photocurrent corresponding to about 2.0020 V was obtained for the nonattenuated beam I_0. The photomultiplier tube was supplied with 850 V and the 30 MΩ resistor was used at the current-to-voltage converter. For every position, 50 digital voltmeter readings were taken by the computer at a rate of 10 to 15 per second. The average value was printed along with the sample position, the standard deviation, the relative standard deviation, and the transmittance values for the glass filters 2; 4; 6; 8; 10; 12; and 14:

$$T_2=\frac{I_2}{\frac{I_1^0+I_3^0}{2}};\quad T_4=\frac{I_4}{\frac{I_3^0+I_5^0}{2}};\quad T_6=\frac{I_6}{\frac{I_5^0+I_7^0}{2}};\ \text{etc. . . .}$$

until the seven glass filters were measured. This sequence was repeated six times and the results are given in table 5.

As can be seen from these data, the reproducibility of sequential transmittance measurements can be performed with an average standard deviation of 0.010 percent for a single determination.

IV. Wavelength Calibration

The wavelength scale of the monochromator is provided with a counter which indicates wavelength directly in ångstroms. This counter is checked for

Table 4. Stability of the current-to-voltage converter, the photomultiplier tube at 850 V, and the tungsten ribbon filament lamp

Replication	Average of 50 individual measurements; volts	Percent standard deviation
1	2.002395	0.038_0
2	2.001356	0.022_6
3	2.002145	0.024_7
4	2.000975	0.026_2
5	2.001944	0.020_7
6	2.000925	0.028_1
7	2.001832	0.026_1
8	2.000825	0.023_5
9	2.001551	0.026_3
10	2.000960	0.021_2
11	2.001739	0.023_1
12	2.000851	0.024_4
13	2.001729	0.028_2
14	2.000825	0.023_0
15	2.001557	0.024_4
Average of replications	2.001441	First group
Percent standard deviation	0.026	First group
Average of replications	2.001517	Second group
Percent standard deviation	0.012	Second group
Average of replications	2.000826	Third group
Percent standard deviation	0.025	Third group
Average of replications	2.001268	Fourth group
Percent standard deviation	0.027	Fourth group

Table 5. Reproducibility of transmittance measurements on seven Schott NG–4 glass filters No. 2; 4; 6; 8; 10; 12; and 14

Replication No.	Percent transmittance						
	2	4	6	8	10	12	14
1	33.327	21.711	12.236	50.990	33.377	20.906	13.473
2	33.325	21.710	12.237	50.983	33.377	20.903	13.471
3	33.321	21.711	12.241	50.992	33.383	20.900	13.474
4	33.320	21.708	12.240	50.988	33.375	20.901	13.470
5	33.323	21.710	12.239	50.983	33.379	20.901	13.474
6	33.325	21.710	12.238	50.986	33.377	20.904	13.470
Average	33.32	21.710	12.238	50.987	33.378	20.902	13.472
Percent σ	0.0080	0.0051	0.0150	0.0072	0.0083	0.0108	0.0141
Average percent σ				0.010			

was opened and measurements were made again. The average value found was 0.037 mV. This indicated that no SRE could be detected under the experimental circumstances.

VI. Linearity Control

The single-beam static optical system described in this work permits the unequivocal use of the radiation

addition principle by means of the double-aperture method for determining departure from linearity of the entire optical, photometric, and electronic system, and thus of the photometric accuracy of transmittance measurements.

The double-aperture and its positioning on the optical bench was described earlier. Its use will now be illustrated, and follows the procedure developed and used at the National Physical Laboratory.

Since the linearity of photometric data for a given photomultiplier tube depends on the anode voltage, the values at the current-to-voltage converter, and the ambient temperature, all measurements were made using identical experimental conditions. These same conditions were maintained when transmittance measurements were performed. Since the linearity is, within 1 part in 10^4, not usually a function of wavelength [36], all measurements were performed at λ 565.0 nm. A recent study of this parameter at NBS by Mielenz and Eckerle indicates that there may be a relation between wavelength and linearity at the level of 1 part in 10^5 [38].

The intensity of the radiation flux produced by the tungsten ribbon lamp was attenuated with the circular neutral wedge until a photocurrent equivalent to 2.0020 V was obtained when both apertures, A and B, were open. A setting of 850 V was used at the photomultiplier tube with a 30 MΩ resistor at the current-to-voltage converter. Fifty individual DVM readings were taken and the average value for $(A+B)$ was printed. Aperture B was then closed, and 50 DVM readings were taken. The average value for aperture A was printed. The average value for aperture B was then obtained in a similar manner by closing aperture A and opening aperture B. This sequence was repeated three times, ending with an $(A+B)$ value.

Identical measurements were made over a range of attenuation corresponding to 4 cascaded steps of 2 to 1 as illustrated in the actual example which follows:

Step 1	$(A+B)$	A	B
	2.0014_7	1.0159_6	0.9864_1
	2.0015_6	1.0159_9	0.9864_0
	2.0020_6	1.0160_9	0.9862_5
	2.0021_1	$1.01598 +$	$0.98635 = 2.00233$
Av.	2.00181		
Diff.	$2.00233 - 2.00181 = +0.00052$		
% Corr.	$= -0.026$		

Step 2	$(A+B)$	A	B
	1.0004_9	0.5102_0	0.4910_8
	1.0007_8	0.5099_6	0.4909_1
	1.0006_6	0.5100_4	0.4911_5
	1.0009_0	$0.51007 +$	$0.49105 = 1.00112$
Av.	1.00071		
Diff.	$1.00112 - 1.00071 = +0.00041$		
% Corr.	$= -0.041$		

Step 3	$(A+B)$	A	B
	0.5006_2	0.2565_7	0.2443_0
	0.5005_6	0.2567_3	0.2443_6
	0.5007_0	0.2566_5	0.2443_2
	0.5006_2	$0.25665 +$	$0.24433 = 0.50098$
Av.	0.50063		
Diff.	$0.50098 - 0.50063 = +0.00035$		
% Corr.	$= -0.069$		

Step 4	$(A+B)$	A	B
	0.2502_0	0.1287_2	0.1217_5
	0.2502_8	0.1285_6	0.1216_8
	0.2501_9	0.1285_4	0.1216_6
	0.2502_3	$0.12861 +$	$0.12170 = 0.25031$
Av.	0.25023		
Diff.	$0.25031 - 0.25023 = +0.00008$		
% Corr.	$= -0.031$		

The correction curve is established from these data by plotting voltages on the abscissa and the corresponding additive correction value on the ordinate. These are tabulated below and illustrated in figure 16.

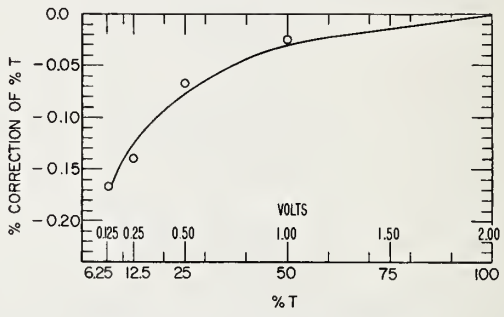

FIGURE 16. Linearity correction curve.

Voltage	% T	% Correction of % T
2.00	100	0.0
1.00	50	0.026
0.50	25	0.067
0.25	12.5	0.14
0.125	6.25	0.167

When transmittance measurements are performed, the I_0 reading is initially set with the circular neutral wedge to a value near 2.0020 V. The I value is then measured. If the initial $I_0 = 2.00214$ V and final $I_0 = 2.0022_8$ V and $I = 0.54220$ V, then percent T is:

$$\frac{0.54220}{\frac{2.00214 + 2.00228}{2}} \times 100 = 27.081$$

which is the noncorrected value. To correct this value, one takes from the ordinate of figure 16 the value corresponding to 0.54220 on the abscissa which, in this case, is 0.072. The corrected percent T value is then:

$$27.081 - \left(\frac{27.081 \times 0.072}{100}\right) = 27.061.$$

Mielenz and Eckerle have studied recently the double aperture method for testing photometric linearity, and have used a curve-fitting procedure for finding the nonlinearity correction rather than the method described earlier (38).

VII. Sample Position

A series of measurements were performed to determine the magnitude of error which could occur when the sample is oriented with its entrance face at an angle to the incoming radiation beam. The single sample holder provided with the rotating table, as described in section II, paragraph c, was used. Transmittance measurements were performed by producing the image of the exit slit of the monochromator at the entrance face of the sample (aperture f:10). The data are shown in table 6. The consequence of this condition on transmittance measurements is discussed by Mielenz in this Journal.

Table 6. Percent transmittance (*%T*), measured on three neutral glass filters 1.0; 1.5; and 2.0 mm thick at $\lambda = 440$ nm, at three angles of incidence

Angle of incidence	Filter 1.0 mm	Filter 1.5 mm	Filter 2.0 mm
Normal incidence	32.91_5	19.83_8	11.60_6
1°	32.89_9	19.83_3	11.60_4
2°	32.89_7	19.81_9	11.59_9
3°	32.88_1	19.81_2	11.58_9

Similar measurements were made to determine the identity of positions on the seven-sample automatic changer described in section II, paragraph c. For this experiment, seven neutral glass filters A; B; C; D; E; F; and G were used and were positioned in holders 2; 4; 6; 8; 10; 12; and 14 in three different arrangements as described by Garfinkel, Mann and Youden [39].

Table 7. Evaluation of the identity of the seven stations of the automatic sample changer

Percent Transmittance (*%T*) at station number (St. No.) 2; 4; 6; 8; 10; 12; and 14 for filters A, B, C, D, E, F, and G at $\lambda = 465.0$ nm

Run No.		A	B	C	D	E	F	G
I	*%T*	27.08	16.44	46.39	26.12	15.22	37.34	23.23
	St. No.	2	4	6	8	10	12	14
II	*%T*	27.07	16.40	46.39	26.11	15.21	37.34	23.23
	St. No.	14	2	4	6	8	10	12
III	*%T*	27.08	16.43	46.39	26.11	15.21	37.33	23.23
	St. No.	10	12	14	2	4	6	8

Transmittance measurements were then performed on all filters for the three different arrangements and the results are given in table 7. From these data it can be concluded that the seven stations are interchangeable and will produce measurements which will not differ by more than one part in one thousand.

VIII. Influence of Polarized Radiations on Transmittance Measurements

This effect was determined by measuring the transmittance of a Schott NG–4 neutral glass filter at four wavelengths using radiations emerging from the predisperser-monochromator unit, and by projecting the image of the exit slit (8 by 0.5 mm) at the entrance face of the filter with a convergent beam geometry corresponding to an f:10 opening. The glass filter was checked prior to measurements with a polariscope for freedom of internal tensions. Column one of table 8 shows the results obtained when transmittance measurements were made using the radiations produced by the spectrophotometer. Column two shows the results obtained when a polarizing sheet, with the vibration plane horizontal, was placed in front of the glass filter. The measurements obtained with the vibration plane in vertical position, are given in column three.

These measurements show that polarized radiations can affect transmittance measurements of solid glass filters when noncollimated beam geometry is used. This effect is predicted by the Fresnel equations mentioned in the introduction and should disappear when collimated radiations are used (1, pg. 100).

XI. Comparison of Transmittance Measurements

Two sets of solid filters were used in a comparative test to determine the reproducibility of transmittance measurements between two laboratories. One set was made from three neutral glass Schott NG–4 filters having nominal percent transmittances of 10; 20; and 30. The second set was made as described elsewhere [4]. Three evaporated metal (Inconel) on fused quartz (nonfluorescent) plates having nominal percent

Table 8. Effect of polarization on percent transmittance (%T) measured at four wavelengths on a Schott NG–4 glass filter

Wavelength nm	%T Produced by spectrophotometer	%T Polarizer, plane of vibration horizontal	%T Polarizer, plane of vibration vertical	% Difference $\%T_1 - \%T_3$
	1	2	3	
440.0	19.81_8	19.80_0	19.78_8	− 0.15
465.0	22.59_7	22.60_0	22.56_9	− 0.12
590.0	19.17_8	19.17_0	19.09_9	− 0.41
635.0	20.61_1	20.60_2	20.54_7	− 0.31

transmittances of 25; 50; and 75 were used. The transmittance measurements were performed on two sets of filters at the National Physical Laboratory (NPL) in England using their high accuracy spectrophotometer, and at NBS on the instrument described in this paper. The measurements at NBS were carried out before and after the measurements at NPL. All measurements were made with noncollimated convergent beam geometry. A rectangular surface of the filter about 3 mm by 8 mm was used at NPL and the beam was only slightly convergent. At NBS an area about 8 mm by 0.5 mm was used for the transmittance measurements.

The results given in table 9 indicate that an average difference of −0.19 percent of the values was obtained between the measurements carried out at NPL and at NBS. An average difference of −0.30 percent of the value was found when similar measurements were performed on the inconel-on-quartz filters, as shown in table 10.

X. Standard Reference Materials for Spectrophotometry

The need for providing means and materials to check the proper functioning of a spectrophotometer was discussed in some detail in previous publications [3, 4]. At that time it was established that the accuracy of the photometric scale is a critical and most demanding parameter in spectrophotometry. Hence, particular attention was given to a number of ways for checking this parameter. Investigations showed that solid colored glass filters, exhibiting optical neutrality over the spectral range from 400.0 nm to 700.0 nm, would constitute an acceptable Standard Reference Material (SRM). From the various colored glass filters available, Schott NG–4 "neutral glass" was selected, prepared and characterized. It is now offered by NBS as a means to check the photometric scale of spectrophotometers.

Table 9. Comparison between the percent transmittances (%T) measured on three Schott NG–4 glass filters at NPL and NBS

Wavelength nm	NBS, %T March 12, 1971	NBS, %T May 18, 1971	NBS, %T average	NPL, %T February 1971	% Diff. NBS to NPL
440.0	12.92	12.91	12.91_5	12.93	− 0.11
465.0	14.96_5	14.98	14.97_3	15.01	− 0.25
590.0	11.70	11.64	11.67	11.67	0.0
635.0	12.72	12.68	12.70	12.72	− 0.16
440.0	19.62_5	19.58	19.60_3	19.62	− 0.09
465.0	22.38_5	22.35	22.36_7	22.43	− 0.28
590.0	19.06	18.95	19.00_5	19.01	− 0.03
635.0	20.45_5	20.37	20.41_3	20.47	− 0.28
440.0	32.89	32.86	32.87_5	32.98	− 0.32
465.0	35.52	35.54	35.53	35.66	− 0.36
590.0	31.16_5	31.10	31.13_3	31.21	− 0.25
635.0	32.56_5	32.52	32.54_3	32.62	− 0.24

Average difference between NBS and NPL percent T values = − 0.19 percent.

Table 10. Comparison between the percent transmittances (%T) measured on three inconel-on-silica filters at NPL and NBS

Wavelength nm	NBS, %T 1	NBS, %T 2	NBS, %T average	NPL, %T	% Diff. NBS to NPL
450.0	24.87	24.88	24.87_5	24.93	− 0.22
550.0	23.78	23.82	23.80	23.86	− 0.25
650.0	23.38	23.39	23.38_5	23.46	− 0.32
450.0	49.35	49.33	49.34	49.56	− 0.44*
550.0	47.60	47.60	47.60	47.81	− 0.44
650.0	46.85	46.85	46.85	47.14	− 0.62
450.0	72.17	72.20	72.18_5	72.30	− 0.16
550.0	72.05	72.11	72.08	72.20	− 0.17
650.0	72.20	72.34	72.27	72.33	− 0.08

Average difference between NBS and NPL percent T values = − 0.30 percent.

*This filter had a flaw in the form of a crack which was sometimes visible and other times invisible. The larger differences found in the measurements of this filter may be due to this flaw.

SRM 930, developed in the Analytical Chemistry Division and available since March 1971 consists of three glass filters. Each filter bears an identification number, and the upper left corner has been removed to indicate correct orientation in the metal holder (fig. 17).

The transmittance measurements were made with the high accuracy spectrophotometer described in this paper, and are certified with an uncertainty of ±0.5 percent of the value. This uncertainty is the sum of the random errors of ±0.1 percent (2SD limit) and of estimated biases which are ±0.4 percent. These biases are due to possible systematic errors originating principally from the inherent inhomogeneity and instability of the glass as well as from positioning of the filter. Measurements were made at 24 °C, and variations within several degrees Celsius of this temperature will not significantly affect the calibration of the filters. The neutral NG−4 glass for the filters was provided by Schott of Mainz, Germany and is designated as "Jena Colored and Filter Glass." Nominal transmittance for a filter 1.5 mm thick is 20 percent at 400.0 nm wavelength and 32 percent at 700.0 nm wavelength. Between these limits the transmittance varies in a monotonic manner.

The filter is held in a frame and the size and shape of the filters and frames were selected, for practical considerations, to conform to the dimensions of the standardized cuvettes for which holders are supplied in most conventional spectrophotometers. The filters are approximately 1.0, 1.5, and 2.0 mm thick. Corresponding to these thicknesses are nominal transmittances of 30, 20, and 10 percent, respectively. These thicknesses were selected to provide a means for calibrating the photometric scale at three different levels.

The effective spectral bandpasses used to determine the certified values were equal to or smaller than 2.2 nm at 440.0 nm; 2.7 nm at 465.0 nm; 5.4 nm at 590.0 nm; and 6.0 nm at 635.0 nm. The transmittance measurements are made by producing the image of the slit (about 8 mm by 0.5 mm) using a convergent beam geometry with an opening of f:10 corresponding to an angle of 7° to 8° in the middle of the entrance face of the filter. This beam geometry was used to reproduce the average experimental conditions found in most of the conventional spectrophotometers available today. Prior to the certification, each filter is examined for surface defects and thoroughly cleaned. If, through handling, the surface of the filter becomes contaminated, it may be cleaned with a small soft brush attached to a rubber tube connected to a vacuum source [40]. If contamination results from fingerprints, they must be removed before making measurements. This may be accomplished by removing the filter from its holder, breathing lightly on it, and rubbing the surface gently with optical lens tissue. The clean filter is then properly positioned in its holder. To remove and replace the filter in the holder, the spring-loaded plate should be lifted with care to prevent damage to the filter. As little handling as possible is recommended. SRM 930 should be used according to the directions on the certificate; consult the manufacturer of the instrument if differences are obtained that exceed those specified by the manufacturer.

Under no circumstances should other cleaning procedures which make use of detergent solutions, organic solvents, etc. be applied.

When a filter has become contaminated beyond cleaning by the procedure described in the certificate, it should be forwarded to NBS. After proper cleaning, the filters will be checked and, if needed,

FIGURE 17. NBS Standard Reference Material 930 and calibration certificate.

recalibrated using the high accuracy spectrophotometer described in this work.

It was already stated that the accuracy of photometric scales defines only one of the parameters required for obtaining accurate transmittance values and molar absorptivities. Other factors must also be established. These are wavelength accuracy, adequate spectral bandpass, stray light, cell parameters (when solutions are measured), fluorescence, polarization, reflection, and temperature coefficient. Some of these variables were discussed in NBS Technical Notes 544 and 584 and are also examined in this paper.

The transmittance data given in the certificate which accompanies each SRM 930 depend not only on the intrinsic properties of the glass and the experimental measurement conditions, but on the surface state of the glass. This parameter varies with time and exposure conditions. When glass is exposed to normal room atmosphere and temperature, its surface is corroded to an extent depending on the composition, time of exposure, concentration, temperature and nature of the glass surface acting agents. This action produces a change in the reflecting and transmitting properties of the material [41]. For instance, a well-known phenomenon called "blooming" of the glass is due to the formation of an SiO layer at the surface of the glass. This layer, which increases the transmittance, acts as an antireflection coating. The speed with which such a layer is formed varies with the composition of the glass, the atmosphere and time. Generally speaking, several years are needed for a fresh surface to reach equilibrium. This, and similar

phenomena are presently being studied, along with means to stabilize the surface state of glass filters. Until more information is acquired in this field, we recommend that the colored glass filters issued as SRM 930 be rechecked annually to determine whether any physicochemical changes, which might affect the transmittance values, have occurred.

Another important factor is the need for defining and producing a clean glass surface. Until now the final cleaning of the NG–4 filters was made with redistilled ethyl alcohol and pure water (thermally distilled and deionized). Other cleaning procedures are under consideration. The use of isopropyl alcohol in vapor or liquid form associated with mild ultrasonic action is being investigated [41].

The transmittance characteristics of the SRM 930 limit the use of this material to the visible region of the spectrum from about 400 nm to the near infrared. Since the ultraviolet region, from about 200 nm is also important to the analyst who uses spectrophotometric methods, exploratory work is underway to select and certify solid material for checking the photometric scale in this spectral region. Optical filters exhibiting small transmittance-wavelength dependence in the spectral range 200 nm to near infrared can be obtained by evaporating thin semitransparent layer of a metal on a suitable transparent substrate [42, 4], and such filters have been considered in this work. The metals selected were inconel and chromium which exhibit adequate transmission characteristics and good adhesion to the substrate. The substrate was nonfluorescent fused quartz. A series of filters were prepared by the optical shop at NBS according to the following specifications: a number of nonfluorescent optical quality fused quartz plates, 10 mm × 25 mm and 1 mm thick, were cut and polished, Inconel or chromium metal was evaporated on the surface to produce nominal transmittances of 25, 50, and 75 percent. The surface bearing the evaporated metal was coated with a layer of optical cement which was transparent to the visible and ultraviolet radiations down to 230 nm. A clear plate of the same material was used to cover and protect the evaporated metal layer.

The filter assembly was then marked at one corner to insure its proper positioning and the finished filter was placed in a metal holder of conventional size (approximate o.d. 13 x 13 x 57 mm) fitting the cuvette holder found in most spectrophotometers. The metal holder was also marked at one side to permit positioning of the filter in a reproducible manner.

In addition to the evaporated metal filters, a number of units were prepared using only the clear uncoated fused quartz plates and assembled with the same optical cement. When desired, these clear filter assemblies could be used as reference samples in the blank compartment.

Before submitting the evaporated metal filters to transmittance measurements, a study was made of the effect of radiations on their transmittances. A filter was exposed to an accelerated test in which radiations had the same spectral distribution as the fluorescent lighting of the laboratory, except that they were 1000 times more intense. The filter was exposed for an equivalent of 36,000 hours of continuous irradiation. This test was made on a radiation accelerator made available by the Building Research Division of NBS. The percent transmittance was measured before and after the exposure and gave the following results:

	Transmittance, percent			
Wavelength, nm	250	380	500	650
Before exposure	44.48	51.35	48.90	47.41
After exposure	44.11	51.34	48.92	47.47

The relative standard deviation for a single determination of these measurements was 0.01 percent. As can be seen, the only significant relative change in transmittance of about 0.84 percent of the value occurred at 250 nm.

Several sets of these filters were calibrated at five selected wavelengths, 250 nm; 350 nm; 450 nm; 550 nm; and 650 nm, using the cleaning and measuring procedures outlined for Schott NG–4 colored glass neutral filters. The results indicated that the reproducibility of transmittance measurements is good (percent standard deviation 0.009 to 0.024) and is comparable to those obtained for the colored glass filters at all wavelengths except 250 nm. From the experimental data, it is evident that the transmittance of the evaporated metal filter at 250 nm is critical and, at present, no satisfactory explanation for this phenomenon can be given. A limitation of the evaporated metal filters is that they attenuate the intensity of radiation by *reflecting* a part of it, rather than absorbing. This can produce, in certain circumstances, undesirable stray light in the instrument and make the transmission measurements dependent on the geometry of the optical beam. However, since these filters are closer to optical neutrality than the colored glass filters, and since they can be used in the ultraviolet region as well, they were included in this work.

This limitation was apparent from the data obtained in a cooperative study conducted at C. Zeiss by A. Reule using conventional spectrophotometers. On the other hand, a similar comparative test, made on the same filters by F. J. J. Clarke at NPL has produced the results presented in table 10. One can observe that, in spite of the limitations mentioned above, an agreement within −0.30 percent of the value was obtained between NBS and NPL measurements at the indicated wavelength.

Further studies will be needed to assess unambiguously the transmittance characteristics of evaporated metal-on-quartz filters, with or without a protective quartz plate, and to assess their suitability as Standard Reference Materials to check the photometric scale of spectrophotometers in the ultraviolet and visible part of the spectrum.

XI. Addendum

The identification of commercial instruments and products, is given in the Addendum only to permit reproduction of the work described in this paper. In no instances does such identification imply recommendation or endorsement by the National Bureau of Standards, nor does it imply that the particular equipment or product is necessarily the best available for the purpose.

Radiation source for visible—Microscope lamps, type 18A/T10/1P–6V: General Electric Co., Lamp Division, Nela Park, Cleveland, Ohio 44112. For ultraviolet: Atlas single coil halogen (Bromine) lamp, type P1/8, 30V, 250W: GTE Sylvania, Inc., 6610 Electronic Drive, Springfield, Virginia 22151.

Power supply for microscope lamp, Kepco, Model JQE 15–50–M–VP: Kepco, Inc., 131–38 Sanford Avenue, Flushing, New York 11352. For tungsten-halogen single filament lamp: same manufacturer, Model JQE–36–30 Mt–VP.

Potentiometer: Leeds and Northrup Model K3 with null meter and power supply. Resistors: Leeds and Northrup 0.1, 50 A and 0.01, 100 A: Leeds and Northrup, Sumneytown Pike, North Wales, Pa. 19454.

Nonfluorescent fused silica: Dynasil Corporation of America, Berlin, New Jersey 08009.

Neutral Density Attenuator and $BaSO_4$ white paint: Eastman Kodak Co., Special Products Sales, Kodak Apparatus Division, Elmgrove Plant, Rochester, New York 14650.

Monochromator with predisperser: McPherson Instrument Corp., 530 Main Street, Acton, Massachusetts 01720.

Optical benches with carriers and x–y sample holder with micrometer control: Gaertner Scientific Corp., 1201 Wrightwood Ave., Chicago, Illinois 60614.

Lens holders: Ardel Instrument Co., Inc., P. O. Box 992, Jamaica, New York 11431.

Ball bushing and rails: Thompson Industries, Inc., Manhasset, New York 11030.

Pneumatic cylinders and accessories: Clippard Instrument Laboratory, Inc., Cincinnati, Ohio 45239.

Rotating table: Ealing Optics Division, 2225 Massachusetts Avenue, Cambridge, Massachusetts 02140.

Thermostating holders for glass cells and glass filters: Cary Instruments, 2724 South Peck Road, Monrovia, California 91016.

Pneumatic ratchet system: Allenair Corp., P. O. Box 350, 255 East 2nd Street, Mineola, New York 11501.

Black paint—Nextel 101–c 10 Black: Reflective Products Division 3M, 2501 Hudson Road, St. Paul, Minnesota 55101.

Photomultiplier tube EMI–9558QA: Gencom Division, 80 Express Street, Plainview, New York 11803.

Power supply for photomultiplier tube: Model 415B and digital voltmeter 8400A: John Fluke Manufacturing Co., P.O. 7428, Seattle, Washington 98133.

Thermal insulation: Photoshroud, Shumway Optical Instruments Corp., 2118 Beechgrove Place, Utica, New York 13501.

Vibration isolation table: Lansing Research Co., 705 Willow Avenue, Ithaca, New York 14850.

Low power laser; Model 195 cw gas laser, output power 2 mw: Optics Technology, Inc., 901 California Avenue, Palo Alto, California 94304.

Tritium activated fluorescent source, Beta light Marker HM–110: Canrad Precision Industries, Inc., 630 Fifth Avenue, New York, New York 10020.

Colored glass neutral filters, Schott NG–4: Fish-Schurmann Corp., 70 Portman Road, New Rochelle, New York 10802.

Spectral lamp: Oriel Optics Corp., 1 Market Street, Stamford, Connecticut 06902.

Polarization filters: Polaroid Corp., 119 Windsor Street, Cambridge, Massachusetts 02139.

Computer: 24K memory and 16 bit words. EMR computer, Division of Weston Instruments, Inc., Schlumberger Co., 8001 Bloomington Freeway, Minneapolis, Minnesota 55420.

The author gratefully acknowledges the assistance of the following persons, in addition to those already mentioned in the text:

F. J. J. Clarke, for the considerable assistance given through personal discussions on the philosophy and principles of high accuracy spectrophotometry at NPL.

Anne Compton, for advice and help during the experimental work carried-out at the high accuracy spectrophotometer at NPL.

G. E. V. Lambert, for information concerning glass filters (NPL).

K. D. Mielenz (NBS), for constructive discussions on the principles of spectrophotometry and for critically reviewing the manuscript.

W. H. Venable (NBS), for critically reviewing the manuscript.

K. L. Eckerle (NBS), for advice in measuring stray radiations and polarization produced in the monochromator.

C. R. Yokley (NBS), for advice on the radiation stability of incandescent tungsten filament lamps.

W. K. Haller (NBS), for valuable information on the properties of glass surfaces and optical glass filters.

H. H. Ku (NBS), for advice on interpretation of the data discussed in this paper.

NBS Instrument Shop, for constructing the mechanical parts described in this work.

NBS Optical Shop, for grinding the quartz lens used in this work.

D. S. Bright (NBS guest worker), for the programs written at various times during the initial phase of this work.

V. E. Gray (NBS), for assistance in performing the accelerated radiation tests.

H. J. Höfert and A. Reule (C. Zeiss, Oberkochen, Germany), for valuable information on linearity of

photodetectors and for demonstration of the radiation addition method.

R. J. Carpenter (NBS), for constructive discussions on electronic circuitry and photodetectors.

L. Marzetta (NBS), for advice and assistance in assessing various functioning parameters of photomultiplier tubes.

O. Menis, Section Chief, Analytical Coordination Chemistry (NBS), for approving and encouraging the work reported in this paper.

J. I. Shultz, Assistant Section Chief, Analytical Coordination Chemistry (NBS), for critically reviewing the manuscript.

XII. References

[1] Kortüm, G., Kolorimetrie-Photometrie und Spektrometrie, 464 p., 4th ed. (Springer-Verlag, 1962).

[2] Gibson, K. S., Spectrophotometry, Nat. Bur. Stand. (U.S.). Circ. 484, 48 pages (1949).

[3] Mavrodineanu, R., Spectrophotometry, instrumental development, O. Menis and J. I. Shultz, Eds., Nat. Bur. Stand. (U.S.), Tech. Note 584, pp. 9–21 (1971).

[4] Mavrodineanu, R., Solid materials to check the photometric scale of spectrophotometers, O. Menis and J. I. Shultz, Eds., Nat. Bur. Stand. (U.S.), Tech. Note 544, pp. 6–17 (1970).

[5] Elster, J. and Geitel, H., Un the comparison of light intensities by photoelectric methods, Ann. Physik, Chemie **48**, 625–635 (1893).

[6] Elster, J. and Geitel, H., The photoelectric effect on potassium at low light levels, Phys. Ztsch. **13**, 468–976 (1912).

[7] Koller, L. R., and Breeding, H. A., Characteristics of photoelectric tubes, General Electric Rev. **31**, 476–479 (1928).

[8] Campbell, N. R., The experimental proof of a fundamental photoelectric law, Trans. Opt. Soc. (London) **32**, 61–65 (1930–1931).

[9] Fleury, P., An addition method for the precise study of the variation of the current output of a photoelectric cell as a function of the incident luminous flux, Compt. Rend. Acad. Sci. (France) **199**, 195–197 (1934).

[10] Preston, J. S., and McDermott, L. H., The illumination response characteristics of vacuum photoelectric cells of the Elster-Geitel Type, Proc. Phys. Soc. (London) **46**, 256–272 (1934).

[11] Preston, J. S., and Cuckow, F. W., A photoelectric spectrophotometer of high accuracy, Proc. Phys. Soc. (London) **48**, 869–880 (1936).

[12] Buchmüller, F., and König, H., Precision measurements on incandescent lamps using selenium photocells, Assoc. Suisse Electriciens, Bulletin **28**, 89–99 (1937).

[13] Atkinson, J. R., Campbell, N. R., Palmer, E. H., and Winch, G. T., The accuracy of rectifier-photoelectric cells, Proc. Phys. Soc. (London) **50**, 934–946 (1938).

[14] Barbrow, L., A photometric procedure using barrier-layer photocells, J. Res. Nat. Bur. Stand. (U.S.), **25**, 703–710 (1940) RP1348.

[15] Kaiser, H., Photographic-photometric calibration of step filters, Spectrochimica Acta **3**, 518–537 (1947–1949).

[16] Harding, H. G. W., Precautions necessary for accurate measurements of optical density standards, Photoelectric Spectrometry Group Bulletin **4**, 79–86 (1951).

[17] Kortüm, G., and Maier, H., Dependence of photocurrent and illuminating intensity in photocells and photomultipliers, Z. Naturforschung **8A**, 235–245 (1953).

[18] Hansen, G., Check of photometric function of spectrophotometers, Mikrochimica Acta **1955**, 410–415.

[19] Hermann, W., Noise and linearity check on photomultipliers, Z. Naturforschung **12A**, 1006–1013 (1957).

[20] Reule, A., Checking the photometer scale of absorption instruments, Zeiss-Mitt. **1**, 283–299 (1959).

[21] Hoppmann, H., An instrument for checking the proportionality of physical radiation receivers, Technisch-Wissenschaftliche Abhandlungen Der Osram-Gesellschaft **7**, 306–312 (1958).

[22] Gibson, G. L., Hammond, H. K., III, Holford, W. L., and Nimeroff, I., Calibration of photometers, NBS Manuscript, Nov. 1, 1960.

[23] Bischoff, K., Measurement of proportionality of radiation receivers over a large radiation intensity range, Z. Instr. **69**, 143–147 (1961).

[24] Jones, O. C., and Clarke, F. J. J., A new photometric technique using a variable shutter device, Nature **191**, 1290 (1961).

[25] Cordle, L. C., and Habell, K. J., Photometry of telescopes and binoculars, National Physical Laboratory, Notes on Applied Science No. 14, 18 pp. (1962).

[26] Sanders, C. L., A photocell linearity tester, Appl. Optics **1**, 207–271 (1962).

[27] Nonaka, M., and Kashima, T., Linearity characteristics of multiplier phototubes, Japanese Journal Applied Physics **2**, 785–791 (1963).

[28] Höfert, H. J., and Loof, H., Calibration of photometric scales of a reflection photometer, Z. Instrumentenkunde **72**, 139–143 (1964).

[29] Clarke, F. J. J., Time ratio photometry, Lecture to the Optical Group of the Institute of Physics and the Physical Society (June 9, 1966).

[30] Clarke, F. J. J., High accuracy spectrophotometry of three filters, NPL, Report No. 3042, 14 pp. (Nov. 4, 1968).

[31] Reule, A., Testing spectrophotometer linearity, Appl. Optics **7**, 1023–1028 (1968).

[32] Desvignes, F., and Ohnet, J., Characteristics and measurement of properties of radiation receivers, Techniques Philips **N.6**, 1–18 (1968).

[33] Kunz, H., Representation of the temperature scale above 1337.58 K with photoelectric direct current pyrometers, Metrologia **5**, 88–102 (1969).

[34] Kostkowski, H. J., Personal communication (NBS 1970).

[35] ASTM Tentative Method of Estimating Stray Radiant Energy, ASTM:E 387–69T.

[36] Clarke, F. J. J., Personal communication (NPL, August 1970).

[37] Mielenz, K. D., and Eckerle, K., Accuracy of polarization attenuators (to be published), Appl. Optics (1972).

[38] Mielenz, K. D., and Eckerle, K., Spectrophotometer linearity testing using the double-aperture method, Appl. Opt. **11**, 2294 (1972).

[39] Garfinkel, S. B., Mann, W. B., and Youden, W. J., Design and statistical procedures for the evaluation of an automatic gamma-ray point-source calibrator, J. Res. Nat. Bur. Stand. (U.S.), **70C** (Eng. and Instr.), No. 2, 53–63 (1966).

[40] Edisbury, J. R., Practical Hints on Absorption Spectrophotometry (Plenum Press, New York, 1967).

[41] Holland, L., The Properties of Glass Surfaces (Chapman and Hall, London, 1964).

[42] Hass, G., and Thun, R. E., Editors, Physics of Thin Films (Academic Press, 1967).

(Paper 76A5–729)

NATIONAL BUREAU OF STANDARDS SPECIAL PUBLICATION 378, Accuracy in Spectrophotometry and Luminescence Measurements, Proceedings of a Conference Held at NBS, Gaithersburg, Md., March 22–24, 1972 (Issued May 1973).

Absolute Spectroradiometric Measurements

G. A. W. Rutgers*

Physical Laboratory Rijksuniversiteit Utrecht, Netherlands

(June 7, 1972)

There are two general methods for measuring a quantity of radiation emitted by a source. One can compare it with the radiation emitted by a standard source or one can measure the radiation with a detector calibrated in absolute units. When using the latter method, one must know the spectral transmittance factor of the optical components between source and detector.

In the present paper, a survey will be given of the standard sources available for spectroradiometry: cavity radiator, tungsten strip lamp, anode of the carbon arc, xenon arc and cascade arc. Several types of detectors such as the absolute bolometer and thermopile, with their properties, will be discussed.

Key words: Absolute spectroradiometry; absolute standard source of radiation; calibrated photodetector.

I. Introduction

If a physicist delivers a lecture for analytical chemists, he should take care that his language cannot lead to misunderstandings. From the Summary of Activities 1970/71 of the Analytical Coordination Chemistry Section (NBS Technical Note 584) it appears that the vocabulary used by physicists and chemists is not always the same. The main difference is in the use of the term *photometry*. For a physicist, particularly if he is engaged in the activities of the Commission Internationale de l'Eclairage (C.I.E.), photometry is the measurement of quantities referring to radiation evaluated according to the visual effect which it produces, as based on certain conventions [1].[1] These conventions require the evaluation to be done according to the international spectral luminous efficiency curve $V(\lambda)$, defined by C.I.E. in 1923. In *spectral* measurements of radiation, the $V(\lambda)$-curve does not play a part. Therefore, in my opinion, it is better to speak of *spectroradiometry* instead of photometry. In this terminology the main apparatus is a *spectroradiometer* instead of a photometer. Then the term *photometer* can be reserved for an apparatus, used to measure light (= visible radiation evaluated according to the $V(\lambda)$-curve) and the pleonasm in the expression "photometric scale in the visible region" can be avoided.

The following quantities will be used:

Spectral radiant intensity I_λ (in a given direction): Power emitted in that direction per unit of solid angle per unit of wavelength. Unit: W/m·sr,

Spectral radiance L_λ (of a source in a given direction): Power emitted in that direction per unit of projected area per unit of wavelength. Unit: $W/m^3 \cdot sr$,

Spectral irradiance E_λ: Radiant power received by a surface per unit area per unit of wavelength. Unit: W/m^3,

Spectral exitance M_λ: Quotient of the spectral radiant flux leaving an element of a surface by the area of that element. Unit: W/m^3.

It should be noted that the same definitions, without the adjective "spectral," can be used; then the units should be multiplied by m. Another point to be mentioned in the introduction is the usefulness of absolute measurements. Again referring to NBS Technical Note 584, the whole chapter on spectroradiometry is devoted to relative measurements, viz., the study of different color filters on behalf of radiometry. In these measurements, a constant radiation source and detector, reproducable samples and standard filters, and linearity of the detector in a wide range, are the most important requirements for the apparatus. However, there are other fields in which absolute measurements can give more information. For example, in line-reversal experiments, knowledge of the radiance of the background can give information on the radiance of a spectral line and therefore the number of transitions belonging to the line. Another example is the measurement of the spectral distribution of a radiation, emitted by an arbitrary source with either a continuous or a discontinuous spectrum. An example is the measurement of the radiance of a fluorescent surface.

By comparing the spectral distribution of the radiation with that of a standard source, an absolute measurement can be obtained if the geometry of the

*We have learned with sorrow during the publication of this paper of the death of Professor Rutgers on October 4, 1972.

[1] Figures in brackets indicate the literature references at the end of this paper.

measuring equipment is known.

From these examples, it will be clear that for absolute measurements sometimes a comparison is made with an absolutely calibrated source; in other cases, an absolute receiver will be used. In the latter case, the influence of the optical components between source and detector upon the measured quantities are often required.

In the following sections a survey will be given of:

(1) the standard sources available for spectroradiometry and their properties with respect to spectral radiance, accuracy and reproducibility,

(2) some detectors, used for absolute measurements, their calibration, reproducibility, accuracy and other properties, and

(3) some additional procedures used in absolute measurements.

Literature references will be far from complete; usually, references are given only to review articles and to special devices.

II. Spectroradiometric Standards

A. Black-Body Radiator

A radiator of which the spectral properties can be derived completely from theory is the *full radiator*, also called the *black-body radiator*. At a given temperature, T, the spectral distribution of the radiation emitted is only a function of the wavelength λ and is described by *Planck's law*. According to this law, the spectral *radiance*, L_λ, of a black-body as a function of λ is given by the relation:

$$L_\lambda = \frac{2hc^2}{\lambda^5} \frac{1}{e^{\frac{hc}{\lambda kT}} - 1} \qquad (1)$$

where h is the Planck's constant, c the velocity of light and k Boltzmann's constant. With $c_1 = 2\pi hc^2$ and $c_2 = hc/k$ (first and second radiation constant) eq (1) can be written[2]

$$L_\lambda = \frac{c_1}{\pi\lambda^5} \frac{1}{e^{hc/\lambda kT} - 1} \qquad (1a)$$

$c_1 = 3.7415 \times 10^{-16}$ W · m^2; $c_2 = 1.4388 \times 10^{-2}$ $m \cdot K$.

The spectral distribution (on the λ-scale) has a maximum at λ_m, given by the equation

$$\lambda_m \cdot T = 2.8978 \times 10^{-3}\ m \cdot K. \qquad (2)$$

For temperatures between 1200 and 3000 K, λ_m is situated between 2.4 and 1 μm, respectively (infrared region). The ratio of the radiances at e.g., 300 nm to those in the top increases from 2.4×10^{-5} at 1000 K to 0.0055 at 3000 K. Generally, the black-body radiator is more practicable for use in the infrared region than in the ultraviolet.

[2] The same expression without π in the denominator holds for the exitance M_λ.

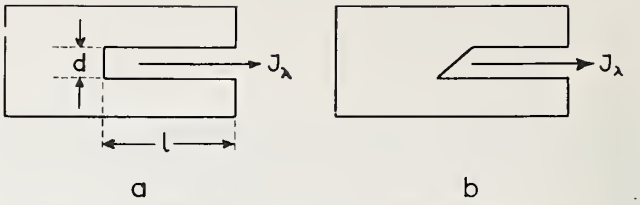

FIGURE 1. Simplified black-body radiators.

The most simple device is a hollow tube with a small hole in its (thin) wall, through which the radiation emerges. Another type is a rod with a hole drilled in its axis or a cavity of arbitrary shape (Hohlraumstrahler).

Deviations from ideal black-body conditions have been calculated, by Gouffé [2], De Vos [3] and recently by C. L. Sanders [4]. De Vos has shown that for a hole in a cylindrical rod (fig. 1a), the emissivity ϵ is between 0.978 and 0.997 if $1/d \sim 10$ and the inner wall has a reflection factor of 0.60. The lowest value of ϵ was found for a material with a specular reflection characteristic, the highest value for a material with perfectly diffuse reflection. For a cone-shape radiator, we measured a somewhat higher ϵ for a specularly reflecting wall. The first order approximation of ϵ in the general case (fig. 2) is, according to calculations by De Vos [3]:

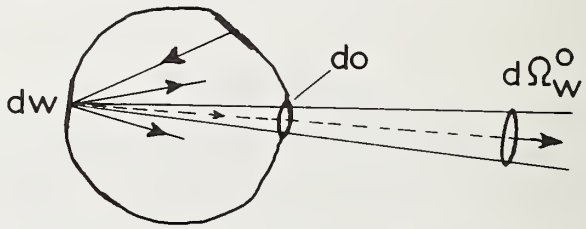

FIGURE 2. Cavity radiator to calculate the radiation loss through the hole $d0$.

$$\epsilon = 1 - r_w^{00} d\Omega_w^0$$

where r_w^{00} is the reflection factor of the element, dw, in the direction $d0 \leftrightarrow d0$ and $d\Omega_w^0$ the "loss" cone. In order to avoid specular reflection (large r_w^{00}), the element observed should not be perpendicular to the direction of observation (fig. 1b).

The temperature of the radiator must be measured according to the procedures described in the text of the International Practical Temperature Scale (IPTS 1968). For temperatures below the melting point of gold (1337.58 K = 1064.43 °C) down to 630.74 °C a thermocouple calibrated on three fixed points is used. Above the gold point, the temperature measurement is based on Planck's law. Here, the optical pyrometer can be used as a measuring instrument. Then, the radiation should be measured in a small wavelength region, usually at 650 nm, and the temperature is calculated from the ratio of the radiant intensities at the unknown temperature and at the gold point. The accu-

racy of radiation measurements with a black-body standard is related to the accuracy with which the temperature of the radiator can be measured. In order to obtain an accuracy of 1 percent in L_λ, the accuracy in the temperature required at some wavelengths and temperatures is mentioned in table 1.

TABLE 1

Accuracy needed in K for an error of 1 percent in L_λ

λ/T	1337	2000	2500	3800 K
300 nm	0.4	0.8	1.3	3.0
650 nm	0.8	1.8	2.8	6.5
2000 nm	2.5	5.4	8.2	17

The accuracy with which the gold point can be transferred to a visual pyrometer (650 nm) can be estimated to be 0.5 K and with a photoelectric pyrometer to 0.05 to 0.1 K (apart from inaccuracies in the gold point itself). A visual pyrometer calibrated at 650 nm with an accuracy of 0.5 K, has an inaccuracy of at least 3 K at 2500 K (ratio of radiances to be bridged about 2500). An accuracy of 1 percent in the visible region does not seem an excessive requirement for radiation measurements, but the figures in table 1 show that it is difficult to obtain this accuracy with a black-body radiator calibrated with a visual pyrometer. According to Gray and Finch [5], the accuracy of calibration of a visual optical pyrometer at 2500 K is about 7 K; for an automatic photoelectric pyrometer the accuracy is 0.6 K at 1337 K and 3 K at 2500 K. These authors conclude that "the accuracy attainable outside the standards lab is, at best, only moderate, even with the most careful work and frequent recalibration."

In conclusion, it can be stated that (1) the black-body radiator is, from a physical point of view, the best defined radiator, because its radiation does not depend upon the physical properties of the material of which it is made, (2) its calibration does not permit a higher accuracy than 1 to 2 percent in its radiance at $T \sim 2500$ K and $\lambda \sim 650$ nm. The use of the black-body radiator is restricted because of the auxiliary apparatus, such as a furnace of accurately adjustable temperature or a tube of high melting point. For laboratory purposes the tungsten strip lamp is perhaps less accurate but more practical. Nevertheless, black-body furnaces up to 2500 K have been constructed and successfully used for radiation measurements [4a].

B. Tungsten Strip Lamp

This section deals only with the tungsten strip lamp as a standard source for spectral radiance. In pyrometry, this source is also used as a secondary temperature standard, for instance for the calibration of commercial pyrometers.

The principal part of the strip lamp is a tungsten ribbon with a width of some millimeters and a length which varies for different types of lamp. The ribbon can be heated by an electric current up to a temperature of ~ 2360 K if the strip is mounted in an evacuated tube and to ~ 2800 K if the tube is filled with a noble gas. The spectral radiance L_λ is determined by the temperature of the strip and can be derived from Planck's law, multiplied by the spectral emissivity $\epsilon(\lambda, T)$ (Kirchhoff's law):

$$L_\lambda(\lambda, T) = \epsilon(\lambda, T) L_{b,\lambda}(\lambda, T). \tag{3}$$

In this formula $L_{b,\lambda}(\lambda, T)$ is the spectral radiance of a black-body at the same temperature, given by eq (1).

$\epsilon(\lambda, T)$ as a function of λ and T has been the subject of many investigations. A discussion of the measurements has been given elsewhere by Schurer [6] and the present author [7]. Since then, further results have been published [8]. For the visible region (at 660 nm) the new measurements are in agreement with the measurements by De Vos ([9] fig. 3), and the conclusion is, according to Schurer [6]: "The ϵ-values of De Vos, after correction with -0.5 percent ($\Delta\epsilon \sim 0.002$) for possible influences of stray light and diffraction offer in the u.v. and the visible up to 800 nm a set of data with the required accuracy and reliability" can still be maintained.

In the infrared at 2.6 μm (the largest wavelength in De Vos' measurements), the ϵ-values of Kovalev and Muchnik are about 5 percent higher than those of De Vos. According to Schurer [6], all previous measurements in the infrared at 2.6 μm have results which are from 5 to 10 percent lower than those of De Vos. It is difficult to explain why the differences between the results of different authors in the infrared are so much larger than in the visible region. They can be caused partly by different properties of the glass envelope of the lamps, partly by different properties of the tungsten strips themselves. More investigations in this spectral region seem to be needed to solve this problem.

At the shorter wavelengths, Buckley [10] has shown that a tungsten ribbon filament lamp with a sapphire window can also be used as a calibration source in the wavelength range 150 to 270 nm (ultraviolet). The ϵ-values, derived by Buckley from his measurements (at wavelengths between 150 and 200 nm), show a rather large uncertainty, but the relation to other measurements at 200 nm is very satisfactory.

The calibration of the lamp is usually performed by means of a pyrometer at one (650 nm) or two wavelengths. In this way the *luminance temperature* T_L[3] at that wavelength is measured and all uncertainties in the pyrometer calibration are transmitted to the ribbon calibration. The true temperature T is calculated from the relation (in Wien's approximation):

$$\tau(\lambda) \cdot \epsilon(\lambda, T) e^{-c_2/\lambda T} = e^{-c_2/\lambda T_L} \tag{4}$$

or

$$\frac{1}{T} - \frac{1}{T_L} = \frac{\lambda \ln \epsilon(\lambda, T) \cdot \tau(\lambda)}{c_2} \tag{5}$$

[3] Luminance temperature = temperature of the full radiator for which the spectral radiance at a specified wavelength is the same as for the radiator considered.

502-591 O - 73 - 5

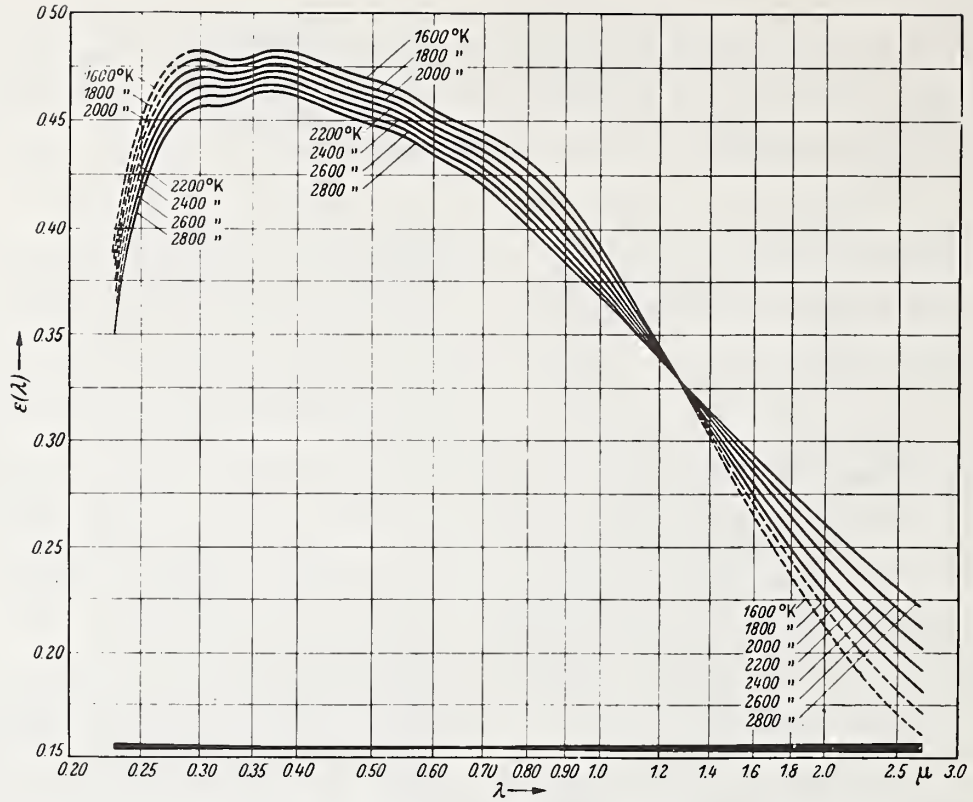

FIGURE 3. Spectral emissivity of tungsten as a function of wavelength and temperature after De Vos [9].

$\tau(\lambda)$ is the spectral transmission factor of the window. For $\lambda = 650$ nm and $c_2 = 1.4388 \times 10^{-2}$ m · K (5) can be written:

$$\frac{1}{T_L} - \frac{1}{T} = 1.041 \times 10^{-4} \lg \{\epsilon(\lambda, T) \cdot \tau(\lambda)\} \quad (5a)$$

Furthermore it should be kept in mind that there is a temperature gradient across and along the strip. The latter is smaller in the center part of the strip if the strip is longer and the end sections are folded back to the mounts. Detailed information for the use of the tungsten strip lamp is given, *a.o.* by Barber [11] and Kunz [12].

Usually, the current through the strip is supplied by a stabilized dc supply. A dc current can be measured with a great accuracy and electronically stabilized power supplies are commercially available. However, if a dc current is passed through the strip during a long time in the same direction, changes in the surface of the strip can be observed (De Vos [9], Quinn [13]). The grooves which are produced on the strip will have an influence upon its emissivity and therefore on the difference between true temperature and luminance temperature (Cf. eq (5a)). De Vos therefore recommended to reverse the current at regular time intervals.

One could also think on supplying the lamp with ac. Because of the finite heat capacity of the strip, it can be expected that the temperature of the strip changes periodically with the current and that a phase shift occurs between temperature and current. Measurements by Bezemer of our laboratory have shown that the temperature during a half-cycle of the 50 Hz supply changes between two values, T_{max} and T_{min}, which differ about 30 K at $T = 2000$ K for a tungsten strip of 20 x 2 mm and a thickness of 0.02 mm. If the temperature is measured with a visual pyrometer, no differences were found in the pyrometer readings for the same dc and ac (effective) current, because the eye is too slow to follow the 50-Hz fluctuations. If a chopping system is used, care should be taken that measurements are not made at a fixed point of the sine-wave.

The main reasons for nonreproducibilities in a particular strip lamp are:

(1) variations in the temperature because of changes in the position of the lamp (with respect to the vertical), typical for gas filled lamps [11],

(2) changes in the structure of the filament because of the direction of the current [9, 13],

(3) influence of the ambient temperature upon the calibration, particularly at low ribbon temperatures ($T < 1500$ K), and

(4) changes in the transmission factor of the window because of tungsten deposits. Evaporation of the tungsten has also an influence upon the ribbon itself.

Notwithstanding all these reasons for nonreproducibility, measurements of the spectral radiance of a number of lamps from different manufacture by Schurer [6] gave very satisfactory results. If all lamps were adjusted to the same luminance temperature at 650 nm, the spectral radiances at 280 nm did not deviate more than ±3 percent and at 2500 nm not more than ±2 percent.

For the user, the factors mentioned above mean that the lamp has to be recalibrated regularly. For absolute measurements, the accuracy is determined both by the accuracy of the calibration of the luminance temperature as a function of the lamp current and by the knowledge of the spectral emissivity of tungsten. In a review article such as this, the author cannot do much more than draw the user's attention to all the effects mentioned.

C. The Carbon Arc as a Standard for Spectroradiometry

A disadvantage of the tungsten strip lamp, inherent to the generation of the radiation, is the strong decrease in radiance with decreasing wavelength. At a temperature of 2800 K the maximum of the spectral radiance is at 950 nm; at 700 nm the radiance is still 74 percent of its maximum value, but at 300 nm it is only 0.3 percent of the maximum value. For a blackbody radiator, the relative slope of the radiance-wavelength curve in the visible and ultraviolet range of the spectrum decreases if the temperature increases. If $\epsilon(\lambda, T)$ does not change much with wavelength, a similar variation of radiance is found for other radiators. Therefore, one must look for a nearly grey radiator with a temperature as high as possible. In this respect, the anode of the carbon arc has favorable properties. Since the first measurements by Waidner and Burgess in 1904, the temperature and emissivity of the carbon and graphite anode have been subject of many investigations. A survey of these investigations has recently been given by Schurer [14]. The author drew attention to the remarkable differences in spectral reflectance of carbon, found by different investigators; they range from 1 to 30 percent, corresponding to emissivities of 99 to 70 percent.

First some words about the use of the carbon arc in practice. Generally, the arc is drawn between a horizontal anode (used as the radiance standard) and a vertical cathode. The electrodes must be mounted in a casing, which protects the arc from draught and the surroundings from radiation. Because of the rapid burning-off of the electrodes, their distance should be held constant, either manually or with an automatic device. It is often useful to make an enlarged image of the arc on a screen, on which the required position can be indicated. The arc is powered from a dc source, which should supply a current of about 10 A (for a low-current arc). To stabilize the arc, a ballast resistance is needed, which is usually chosen such that the voltage across the resistor is at least equal to that across the arc. Dependent on the quality of the supply, a ripple filter can be added to suppress a possible 50-Hz ripple of the supply source. Schurer did measurements on several electrodes from different manufacturers:[4]

Ringsdorff Werke G.m.b.H. (FRG), 6 different types, Ultra Carbon Corp. (USA), 5 different types, National Carbon Company (USA), 3 different types, Conradty (FRG), 3 different types. The data of these electrodes are collected in table 2. It can be seen that great variations in density and specific resistance exist in the different species. Much less variation was found in the current density at the overload point (current at which the arc starts hissing). Therefore, the variations in the temperature of the anode crater (the radiation source proper) are rather small. The lowest (true) temperature was found for Conradty-electrodes (3775 to 3785 K, ±15 K), the other temperatures range from 3790 K to 3865 K. The values of the spectral emissivity, found by Schurer for RWI anodes at arc temperature ranged from 96 percent in the ultraviolet, via 99 percent at 500 nm to about 96 percent at 1.5 μm. In some parts of the spectrum, the radiation from the arc itself can affect the observed anode radiance, particularly at

[4] In order to adequately describe materials and experimental procedures, it was occasionally necessary to identify commercial products by manufacturer's name or label. In no instances does such identification imply endorsement by the National Bureau of Standards, nor does it imply that the particular product or equipment is necessarily the best available for that purpose.

TABLE 2. Some data of the anodes, used by Schurer [14]

Manufacturer	Code	Kind of carbon	Density (10^3kg/m^3)	Resistivity ($10^{-6}\Omega$m)	Grain size	Overload A/mm^2
Ringsdorff	RWO	Graphite	1.79	7.7	Fine	1.12
	RWI	Graphite	1.59	7.5	Fine	1.07
	RWII	Lampblack	1.56	61	Fine	0.71
	RWIV	Graphite	1.78	7.2	Coarse	1.20
Ultra Carbon	U1	Graphite	1.75	7.2	Coarse	
	U2	Graphite	1.99	12.1	Fine	1.15
National Carbon	AGKSP	Graphite	1.66	6.4	Coarse	1.04
	SPK	Graphite	1.87	11.8	Fine	1.11
	L113SP	Lampblack	1.50	53	Fine	0.68
Conradty	Noris	Lampblack	1.20	96	Fine	0.6
	Noris vacuum	Coke	1.32	79	Coarse	0.75

those wavelengths where strong cyanogen bands are found and at wavelengths below 250 nm. Nevertheless, Schurer concluded "that the anode of a carbon arc in air offers a highly reproducible standard of spectral and total radiance." The total radiance, found for a RWO anode, appeared to be 3.84 W mm^{-2} $sr^{-1} \pm 1$ percent, of which 0.054 W $\cdot$ mm^{-2} sr^{-1} has its origin in the arc.

D. Some Other Standard Sources

Besides the standards, described in the foregoing sections, there are some radiation sources which, with certain restrictions, can also be used for absolute spectroradiometric measurements. Alternatives for the black-body radiator are the tungsten lamp, described by Magdenburg and Wende [15] and the black-body radiator after Quinn and Barber [16].

In the first case, a cylinder of tungsten foil is used with a slit in the surface. It can be used as a tungsten ribbon filament lamp, but with the possibility to measure $\epsilon(\lambda, T)$ of the tube by comparing the radiance of the tube and the slit. In the second case, a tungsten tube is used, which is observed end-on. Inside the tube is a bundle of tungsten wire, which is the proper source of radiation (fig. 4). It can be considered as a grey body with an emissivity as high as 0.95. The argon-filled lamp needs a current of 56 A at 12 V for a temperature of 2700 °C. Measurements by Jones [17] of the reproducibility of this lamp are promising and the Comité Consultatif de Photométrie of the Bureau International des Poids et Mesures, in its meeting of September 1971 has recommended to continue the study of this radiator.

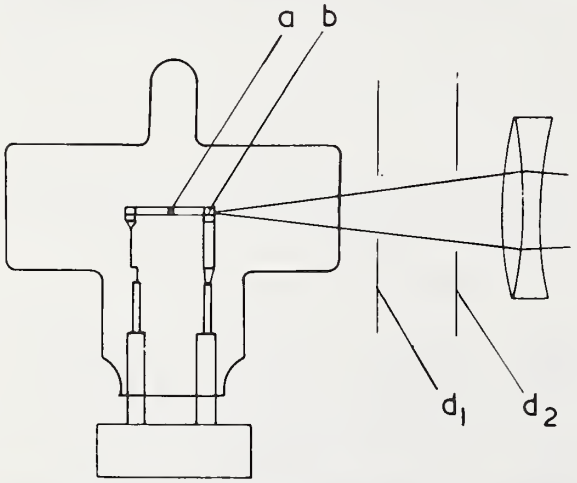

FIGURE 4. Quinn-Barber black-body radiator [16]. a, tungsten tube with tungsten wires; b, exit diaphragm, $\phi = 1$ mm; $d_1 d_2$ diaphragms for eliminating stray light.

For some spectroradiometric measurements, it would be worthwhile to have a background with a radiance still higher than that of the anode of the carbon arc. Attempts have been made to use the high-pressure xenon arc lamp for this purpose. Most investigations have been done for XBO–lamps of various wattage, made by Osram. For its use as a radiance standard one should take in mind that the discharge consists of two parts, the so-called "Plasmakugel," a small spot of high radiance situated just above the cathode and the column with a radiance which is about one quarter of that of the sphere. The spectral radiance of the sphere of XBO–900 lamp at 400 nm is about 1 W/$cm^2 \cdot sr \cdot nm$, that of the arc $\sim$ 0.3 W/$cm^2 \cdot sr \cdot nm$. The latter value is by a factor of 3 to 4 larger than the radiance of the anode of the carbon arc and by a factor of 200 larger than the radiance of the strip lamp at 2800 K, both at the same wavelength. In our laboratory ter Heerdt has measured the spectral distribution of the radiation emitted by different parts of the arc and investigates whether the reproducibility of the xenon-arc lamp is good enough for the use as standard source.

Another stable source of high spectral radiance is the cascade-arc of Maecker [18], a stabilized high current arc with a current of about 1000 A and a temperature of about 12000 K (fig. 5).

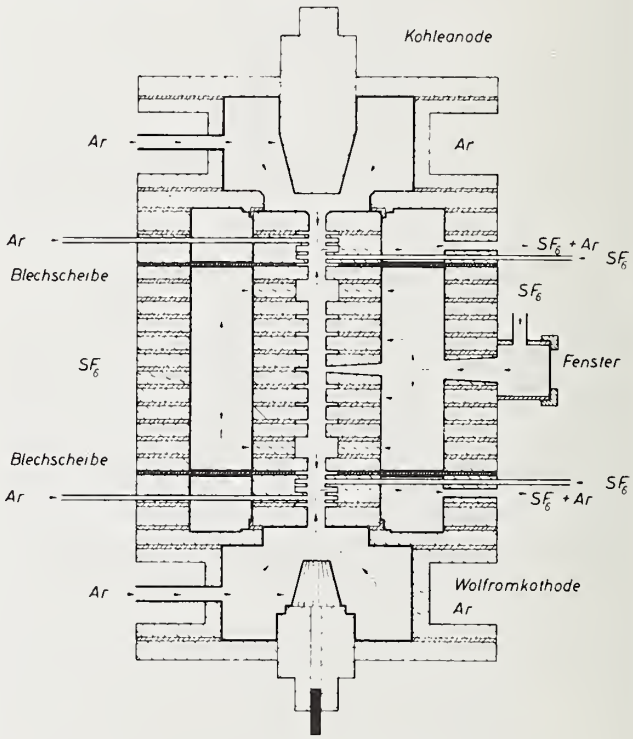

FIGURE 5. Maecker's cascade arc [18] between a carbon anode and a tungsten cathode. Around the arc the cooling discs. Argon is used here as protecting gas and SF_6 as the gas the properties of which are investigated.

The arc column burns within the bore of a stack of copper discs and has a diameter of about 5 mm. The spectrum consists of a strong continuous background on which spectral lines of the arc gas are superimposed. Most measurements up to now are related to the properties of the arc gas or gases at high temperatures, but it seems that this arc has also good properties for being used as radiation standard.

E. Irradiance Standards

All the standards mentioned in the foregoing sections are primarily meant for radiance standards. For absolute measurements of radiation, an irradiance standard can be required, that is to say a standard which causes a known spectral irradiance at the surface of a detector. If a black-body radiator is available, this can also be used as an irradiance standard if a diaphragm of known diameter is used. For the tungsten strip lamp this is more difficult to achieve, because the radiance is not constant along and across the strip. This makes it difficult to calculate the irradiance at a given distance from the lamp. More suitable standards for this purpose are the special tungsten filament lamps and quartz-iodine lamps, developed at the National Bureau of Standards [19].

An irradiance standard, which can also be used in the ultraviolet, is the UV-Normal by Krefft, Rössler and Rüttenauer [20], which consists of a high pressure mercury vapor lamp, run at dc, 2A, 200 W. An alternative is the Standard 75 lamp, 0.95 A, 80 W [21]. The spectrum consists of a weak continuum on which the mercury spectrum is superimposed. The spectral distribution has been measured *a.o.* by Rössler, van Stekelenburg [22], Coolidge and recently by Kok [21]. According to van Stekelenburg's measurements the differences between various lamps of a series are about 10 percent, the relative spectral distributions from different lamps are nearly equal. The UV-Normal gives an irradiance of 0.70 W/m^2 at a distance of 1 m at a wavelength of 365 nm (strongest line); at 296.7 nm this value is 0.10 W/m^2. The irradiance by the continuum at the same distance is 0.48 $mW/m^2 \cdot nm$ at 500 nm, 3.0 $mW/m^2 \cdot nm$ at 300 nm.

III. Absolute Radiometers

In the preceding section, standard sources have been described which can be used if absolute radiation measurements are required and a comparison of the unknown source with a standard source is possible. Another procedure for absolute measurements is to measure the radiation emitted by the unknown source directly with an absolute receiver, called also an *absolute radiometer.*

Most detectors used in optical measurements, such as the photomultiplier tube, the photoelectric cell etc., have a spectral responsivity which depends on the wavelength. Such a detector can be calibrated, either relatively or absolutely, with the help of a standard source, combined with a spectral apparatus or a series of interference filters. If the transmission characteristics of the spectral apparatus or the filters are known, the calibration can be made in absolute values. However, in many cases a relative spectral response curve is sufficient. We will come back to this procedure later on.

First we will pay attention to devices which offer the possibility of making an absolute measurement directly; that is to say, without using a standard source. In such a device the radiant energy or power absorbed must be compared with a quantity of energy or power of another form, usually a quantity of electric power. The apparatus, best suitable for this purpose and most thoroughly investigated is the *absolute radiometer*, belonging to the class of *thermal receptors.* Essentially, this type of receptor is independent of the wavelength of the incident radiation in the spectral region where the absorption factor (black surface) is independent of wavelength. The incident radiation is absorbed in, e.g., a metal foil which consequently increases in temperature. The increase in temperature can be measured in different ways, for instance with a thermopile or as a change in the resistance of the receiver, a *bolometer.*[5] Afterwards the metal foil can be heated by an electric current, which must be adjusted in such a way that an equal change in the detector element is caused.

One of the older instruments, based on this principle, is Wouda's bolometer [23], developed in the thirties in our laboratory. The radiation absorbing element in Wouda's bolometer is a manganin foil of 50 x 15 x 0.03 mm, blackened with carbon black on the front. On the back, a copper wire 50 μm in diameter is spread across the whole surface of the foil, as shown in figure 6.

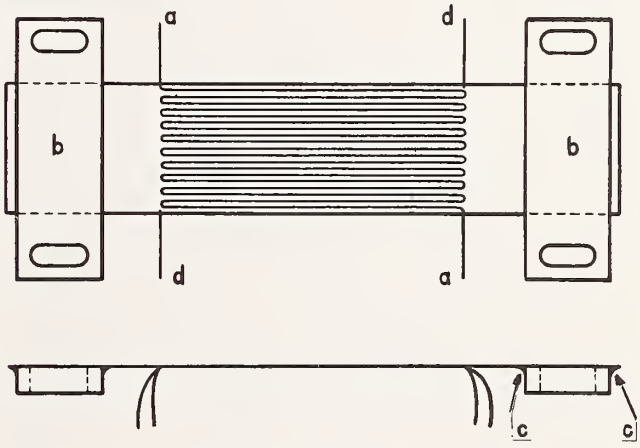

FIGURE 6. Wouda's absolute bolometer [23]. a,a = bolometer wire, $\phi = 50$ μm; b,b, copper clamps on which the metal foil is soldered (at c,c); d,d, potential wires.

A change in temperature of the receiver element by absorption of the incident radiation causes a change in the resistance of the copper wire, which can be measured with a Wheatstone bridge. Local differences in the temperature are eliminated by the shape of the wire which operates as an integrating device. Afterwards the foil can be heated with a known electric current; its resistance (nearly independent of temperature) is also measured in a bridge circuit. A similar element in the opposite arm of the bridge compensates for a possible influence of the surroundings. The heat balance equation is:

[5] According to [1], a bolometer is a thermal receptor in which the heating of the part that absorbs the radiation gives rise to a change in its electrical resistance. Here, bolometer is also used as a device where the receiver heats a resistor which resistance changes because of the heating of the radiation receiver (see Wouda bolometer).

$$\alpha EA = i^2R \qquad (6)$$

where E is the irradiance on the plane of the foil (W/m²), α the absorption factor of the foil, A its surface (m²), i the current which causes the same effect in the detector as the radiation and R the resistance of the foil. The accuracy is determined by the accuracy with which α, A, i, and R can be determined, the time constant by the heat capacity of the foil.

There is a difference between the heating of the copper wire by radiation or by the electric current through the foil, since in the first case the heat absorbed in the black layer has to pass this layer before it reaches the metal foil; in the second case the heat is produced inside the foil. Wouda has shown that the procentual error caused by this effect is $\sim \bar{\alpha}d/\lambda$ where $\bar{\alpha}$ is the heat loss per mm² and per °C of the frontside by radiation, convection and conduction of heat, d the thickness of the black layer and λ its heat conductivity. In the bolometer, used by Wouda, this correction was only 0.12 percent and was taken into account in the results of the measurements. Another point to be mentioned is the absorptance of the black layer. Carbon black has a reflection factor of 3–4 percent in the visible region; in the infrared beyond 4 μ the layer becomes more and more transparent. This can be avoided by the use of other layers, developed since then. Ultimately, Wouda claims an accuracy of 0.1 percent of his apparatus. Some years ago, we made a comparison between this bolometer and a thermopile, calibrated at the National Physical Laboratory, and found a difference of less than 1 percent. At that time, a more accurate comparison was not possible. An alternative device was designed by this author [24]. In this device the copper wire was replaced by a thin aluminum foil made by evaporation on the back of a mica foil. The receiver was a layer of evaporated manganin on the frontside of the mica foil. The accuracy was estimated to be better than 0.5 percent. Another alternative has been described by Bischoff of the Physikalisch-Technische Bundesanstalt [25] and by Gillham of the National Physical Laboratory [26].

In fact, Gillham developed three radiometers, of which the first one—an improvement of the older Guild radiometer—consisted of a circular metal disc, thermally insulated from its surroundings and provided with a number of thermocouples to measure its average temperature. The disc is heated either by the incident radiation or by an electrical heating element. Gillham made a new disc radiometer with a much smaller heat capacity and added a complete second receiver "identical to the first receiver, except that it looks in the opposite direction." The receiver and heating element are shown in figure 7. In his third radiometer, the *black-body radiometer*, the receiver is mounted in a cavity with an absorption factor sensibly equal to unity (fig. 8). This instrument has a sensitivity of 0.012 $V \cdot W^{-1}$ cm^{-2}, an area of the limiting aperture of 3.00 mm² and a time constant of 14 s. A comparison of the new instruments has shown that they agreed to within 0.2 percent.

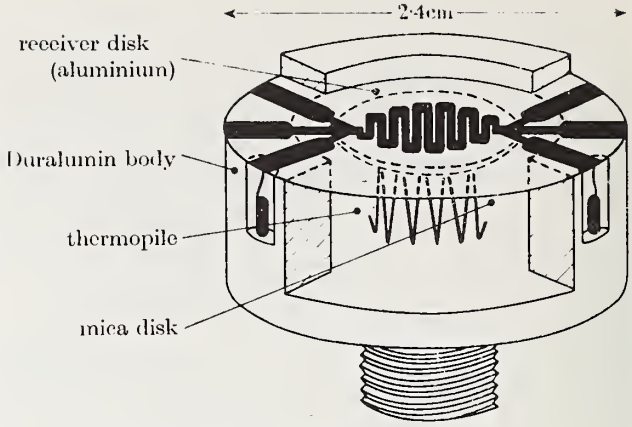

FIGURE 7. Gillham absolute radiometer [26].

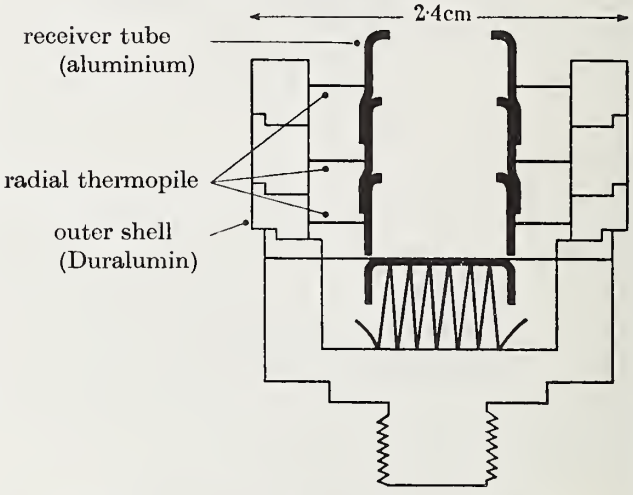

FIGURE 8. Gillham radiometer in a cavity [26].

At the National Standards Laboratory (Australia) a radiometer of the Gillham type has been used by Blevin et al. [27] for a new determination of the Stefan-Boltzmann constant. Preston [28] described a similar device, also intended for measuring the *energy* of radiation pulses. It had a rise time of $\frac{1}{4}$ s and a cooling time constant of 8 s.

An advantage of the black-body radiometer is that it is independent of the spectral characteristics of the black surface layer, used in the devices described above. It is often difficult to measure this absorption factor over a wide spectral region. Previously, Müller used a hemispherical mirror with the receiver in its center; the radiation is admitted through a hole in the mirror. The radiation which is reflected by the receiver impinges upon the mirror and is reflected back to the receiver. In this way the effective absorbance of the receiver can be increased.

Two other cavity-type radiometers have been developed and described in detail by Kendall and Berdahl [29]. One type is used in vacuum, the other either in vacuum or air. They are designed for measuring irradiances from about 0.10 mW/mm² to 8 W/mm² with an accuracy of 0.3 percent.

With all precautions taken, it seems possible to determine the total radiation on a certain plane with an accuracy of some tenths of a percent. For absolute spectral measurements the accuracy is much less. Intercomparisons by National Standardizing Laboratories of absolute spectral irradiance scales are carried out under the auspices of a committee on spectroradiometry of the Commission Internationale de l'Eclairage with C. L. Sanders as the chairman. All devices described above have a rather large area and time constant, and are generally not suited for measurements behind the exit slit of a monochromator. Therefore, the devices described must be considered as primary standard instruments, against which other radiation receivers, either nonselective or selective, can be calibrated.

IV. Additional Remarks Concerning Absolute Measurements

In the foregoing sections we have seen that for absolute measurements both absolute radiation standards and absolute receivers are available. For a proper use of these devices, several precautions have to be taken depending upon the aim of the measurements. The main problems in absolute radiometry are:

(1) the calibration of an arbitrary source in absolute units,

(2) the calibration of a selective receiver in absolute units.

In both cases the user is generally interested in the dependence of the quantities measured on the wavelength of the radiation emitted or received.

A. The Calibration of an Arbitrary Source

If an absolute standard source is available, both sources can be compared with the aid of a monochromator and an arbitrary receiver behind the exit slit. If the sources are comparable in size and spectral distribution, no special problems will be encountered. Both can sucessively be focused upon the entrance slit of the spectral apparatus and, if the receiver is a linear instrument, the ratio of the signals is a measure for the ratio in the radiances or radiant intensities. If the sizes or intensities of the sources differ considerably, a MgO- or $BaSO_4$-screen can be irradiated successively by the sources. Then, the radiances of the screen are compared. If the source to be calibrated has a spectrum composed of a continuous background and spectral lines superimposed upon the background (contrary to most standards described before, which have a rather smooth spectrum), the signal has to be separated into its component parts. This can be done in different ways:

(1) by variation of slit width. If for equal slit widths the width of the slits is changed, the intensity of the continuum leaving the monochromator is another function of this width than the intensity of the line radiation (intensity (:)$(\Delta\lambda)^2$ and $(\Delta\lambda)$ respectively under certain precautions [30]).

(2) with fixed (narrow) slits and continuous recording of the signal as a function of wavelength. The area between the total response and the interpolated continuum in the region of the line provides the radiant flux in the line. The slit width should be chosen in accordance with the dispersion and the slope of the spectral distribution curve. More about a similar method can be found in a paper by Bauer and Erb [31].

If an absolute receiver is available, one can either measure the radiant flux leaving the exit slit of the monochromator directly with the calibrated receiver or, if this receiver is not suited for this purpose (e.g., because his surface is too large and must be filled homogeneously), calibrate another receiver against the standard and use this one behind the exit slit (Cf. IV. B). In order to relate the signal of the receiver to the radiant intensity of the source to be calibrated, one must furthermore know the absorptance of the optical components between source and detector and the width of the spectral region transmitted by the monochromator. This last quantity is needed for the reduction of the measured signal to a quantity per unit of wavelength.

A method, which gives all the information needed, is schematically given in figure 9 (Krijgsman [32]). Two monochromators are required in crossed position. The source to be calibrated is focused on the entrance slit S_1 of the first monochromator (i.e., a double monochromator), which in its turn is successively focused on S_2 and S_3. S_3 is focused with lens L_3 in P. The spectral irradiance in P is measured with the absolutely calibrated receiver. Afterwards the image in P is replaced by the source K. The radiant intensity of K and its image (both in P) are compared with a second monochromator with arbitrary receiver or spectrograph but with a direction of dispersion which is perpendicular to that of the first one (S_4 perpendicular to S_3). The spectral region transmitted by the first monochromator can be derived from the shape of the region transmitted by the second monochromator. For detailed information on this method, the reader is referred to the literature.

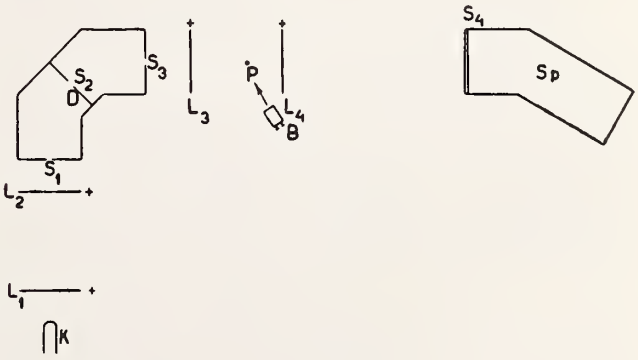

FIGURE 9. Krijgsman's arrangement [32] for the absolute calibration of an arbitrary source K. D, double monochromator with slits S_1, S_2, S_3; P, image of K; Sp, spectrograph with horizontal slit S_4.

B. Calibration of An Arbitrary Receiver

Here, also, the method depends upon the standard available, either a standard source or an absolute receiver. If a standard source is available, one can use either a series of interference filters or a monochromator to separate the radiation into individual wavelengths. In both cases the spectral transmittance of the wavelength-selecting device should be known. If a standard receiver is available, an arbitrary source can be used and the receiver to be calibrated can be compared to the standard receiver in an arrangement similar to that shown in the first part of figure 9 (both receivers in P). If the receiver has a spectral response curve with steep slope (or slopes), it might be necessary to calculate the effective wavelength of the radiation incident upon the receiver.

Factors, like nonlinearity, fatigue effects and area sensitivity of the receiver are not discussed here. But the user should not forget them in the evaluation of his measurements.

The author is much indebted to J. A. ter Heerdt for carefully reading the manuscript.

V. References

[1] Vocabulaire International de l'Eclairage. 3rd Ed. Publ. C.I.E. N° 17 (E–1.1) 1970.

[2] Gouffé, A., Aperture corrections for artificial black-bodies taking account of multiple internal reflections, Rév. d'Optique **24,** 1–10 (1945).

[3] De Vos, J. C., Evaluation of the quality of a black-body, Physica **20,** 669–689 (1954).

[4] Sanders, C. L., Thermodynamic considerations in realizing the primary standard of light. Metrologia **3,** 4, 119–29 (1967).

[4a] Suzuki, M., Nanjo, M., and Yoshié, K., Standards of spectral radiance and irradiance for the wavelength region of 0.25 to 2.5 μm. P–71.21, XVII–Session C.I.E., Barcelona 1971.

[5] Gray, W. T., and Finch, D. I., How accurately can temperature be measured? Physics Today **24,** 9, 32–40 (1971).

[6] Schurer, K., The tungsten striplamp and the anode of the carbon arc as radiometric standards. Thesis Utrecht 1969; The tungsten strip lamp as a standard of spectral radiance, Optik **28,** 400–406 (1968/69); Discussion of some uncertainties in the spectral emissivity of tungsten, Optik **28,** 44–53 (1968/69).

[7] Rutgers, G. A. W., Standards for photometry. Appl. Optics **10,** 12, 2595–99 (1971).

[8] Kovalev, I. I., and Muchnik, G. F., Normal spectral emissive power of tungsten etc., High Temperature **8,** 5, 983–88 (1970).

[9] De Vos, J. C., The emissivity of tungsten ribbon. Thesis Vrije Universiteit Amsterdam 1953; A new determination of the emissivity of tungsten ribbon, Physica **20,** 690–714 (1954).

[10] Buckley, J. L., Use of a tungsten filament lamp as a calibration standard in the vacuum ultraviolet. Appl. Opt. **10,** 5, 1114–18 (1971).

[11] Barber, C. R., Factors affecting the reproducibility of brightness of tungsten strip lamps for pyrometer standardization, J. Sci. Inst. **23,** 238–42 (1946).

[12] Kunz, H., Prüfen technischer Strahlungspyrometer, V.D.I.-Berichte Nr 112, 37–46 (1966).

[13] Quinn, T. J., The effect of thermal etching on the emissivity of tungsten, Brit. J. Appl. Phys. **16,** 973–80 (1965).

[14] Schurer, K., The spectral emissivity of the anode of a carbon arc, Appl. Opt. **7,** 3, 461–5 (1968).

[15] Magdenburg, H., and Wende, B., Über die Erzeugung Schwarzer Strahlung mit einer Wolfram-Lampe, PTB-Mitt. **74,** 431 (1964).

[16] Quinn, T. J., and Barber, C. R., A lamp as a reproducible source of near black-body radiation for precise pyrometry up to 2700 °C, Metrologia **3,** 1, 19–23 (1967).

[17] Jones, O. C., and Gordon-Smith, G. W., Utilisation d'une lampe à corps noir comme étalon de température de couleur et de luminance, Comité Consultatif de Photométrie 71–14 (Réunion Sept. 1971).

[18] Maecker, H., Fortschritte in der Bogenphysik. Proc. 5th Int. Conference on Ionization Phenomena in Gases, Munich 1961, 1793–1811.

[19] Stair, R., Schneider, W. E., and Jackson, J. K., A new standard of spectral irradiance. Appl. Opt. **2,** 11, 1151–1154 (1963).
Stair, R., Schneider, W. E., and Fussell, W. B., The new tungsten-filament lamp standards of total irradiance, Appl. Optics **6,** 1, 101–105 (1967).

[20] Krefft, H., Rössler, F., and Rüttenauer, A., Ein neues Strahlungsnormal, Z. techn. Phys. **18,** 20–25 (1937).

[21] Kok, C. J., Measurement of spectral irradiance of UV Normal and Standard 75 Lamps. Paper Committee E 1.2–C.I.E., Barcelona 1971.

[22] Proceedings 12th Congress C.I.E., Stockholm 1951, Committee 41 (Ultraviolet Radiation).

[23] Wouda, J., Nauwkeurige absolute intensiteitsmeting, Thesis Utrecht 1935.

[24] Rutgers, G. A. W., A new absolute radiometer, Physica **17,** 129–36 (1951).

[25] Bischoff, K., Ein einfacher Absolutempfänger hoher Genauigkeit, Optik **28,** 183–89 (1968).

[26] Gilham, E. J., Recent investigations in absolute radiometry, Proc. Roy. Soc. (London) A **269,** 249–76 (1962).

[27] Blevin, W. R., and Brown, W. J., A precise measurement of the Stefan-Boltzmann constant, Metrologia **7,** 1, 15–29 (1971).

[28] Preston, J. S., A radiation thermopile for cw and laser pulse measurement, J. Physics E: Sci. Inst. **4,** 969–72 (1971).

[29] Kendall, J. M. and Berdahl, C. M., Two black-body radiometers of high accuracy, Appl. Opt. **9,** 5, 1082–91 (1970).

[30] Morren, L., Une méthode de séparation des raies et du fond continu (etc.), 17th Session C.I.E. Barcelona 1971, Paper 71.08.

[31] Bauer, G., and Erb, W., Auswerteverfahren beim Vergleich eines Linienstrahlers mit einem Kontinuumstrahler, Optik **30,** 371–381 (1970).

[32] Krijgsman, C., De anode van de koolboog in lucht als standaardlichtbron, Thesis Utrecht 1938.

(Paper 76A5–730)

NATIONAL BUREAU OF STANDARDS SPECIAL PUBLICATION 378, Accuracy in Spectrophotometry and Luminescence Measurements, Proceedings of a Conference Held at NBS, Gaithersburg, Md., March 22–24, 1972 (Issued May 1973).

Accurate Measurements of and Corrections for Nonlinearities in Radiometers

C. L. Sanders

Division of Physics, National Research Council of Canada, Ottawa, Canada K1A OS1

(June 7, 1972)

The methods described in the literature for accurately measuring photocell linearity are surveyed and assessed. The effect of not measuring photocell linearity under the conditions used in the final apparatus are considered. Some of the conditions necessary for accurate assessment of the nonlinearity under working conditions are specified. The use of the NRC "Photocell Linearity Tester" to measure and correct for the nonlinearity of various receivers is described.

Key words: Nonlinearity; photocell linearity; photometric accuracy; radiation addition method.

I. Introduction

A radiometer is linear if at time, t_0, the response, $N(t_0)$, indicated by the radiometer is exactly proportional to the incident radiant flux, $\phi(t_0)$, i.e., $N(t_0) = \alpha\phi(t_0)$, where α is a constant. This is the ideal and is never exactly realized.

Our problem is to measure one radiant flux, ϕ_1, relative to another, ϕ_2. Thus, we want to know ϕ_1/ϕ_2 from the measurements N_1, and N_2. In general, ϕ_1 and ϕ_2 are functions of time since we must compare the two fluxes and thus cannot irradiate the receptor indefinitely with either flux.

In general, the response, $N(t_0)$, depends on the flux which fell on the receptor from the time the receiver was made up to time, t_0. It also depends on the electronic circuit associated with the receptor and on all of the things which control its behavior, such as component temperatures, power supply voltages, charges on its capacitors, magnetic fields, etc. Again, in the ideal case the response of the electronic circuit should depend only on $\phi(t_o)$, but in practice it will depend on $\phi(t)$ where t goes from $-\infty$ to t_0.

For accurate measurements, we must apply the two fluxes to be compared in a way which will, for the receptor and electronics used, produce a ratio which is precisely reproducible. We also must devise a method to measure and correct for the nonlinearity which is present at the time of the measurement.

The purpose of this paper is to describe the principal methods of reducing and measuring nonlinearity, to indicate the accuracies attained by each, and to point out a few of the merits or drawbacks in each. Hopefully this will aid in deciding which method is appropriate for a particular task, and also in deciding how many precautions are required to attain a specified accuracy. The reference list given is not intended to be complete, but rather to indicate a sufficient variety of methods.

II. List of Methods of Measuring and Correcting for Nonlinearity

1. Superposition (Additive) method. The superposition method is a basic physical method and is useful in all radiometric applications. It may be divided into two classes: (a) Multiple sources, (b) One source providing several independently interceptible beams.
2. Bouguer's Law.
3. Beer's Law.
4. A combination of the superposition method and Bouguer's Law as described by Hawes [1].[1]
5. Inverse Square Law.
6. Standard absorbing filters of either liquid or glass.
7. Standard reflecting materials.
8. Rotating sectors. WARNING: This does not measure all types of linearity because in the extreme case the flux is either ϕ or zero and nothing can be deduced about linearity.
9. Measurement of amplitude of harmonics or beat frequencies. Increases precision of measurements and speed of measuring nonlinearities.
10. Measurement of known radiant fluxes. Erminy [2] has shown how to provide the known radiant fluxes by the superposition method using three sources.

[1] Figures in brackets indicate the literature references at the end of this paper.

11. Null method eliminates nonlinearity. Lee and others use it in optical pyrometry by providing standard sources to match the test source.

12. Use of a linear receptor to calibrate a test receptor.

III. Summary of Methods of Reducing Nonlinearities and Increasing Accuracy

1. Kunz [3] has shown that one can attenuate the flux by a known amount using a sector and thus improve the results by keeping the average anode current in a photomultiplier low enough to make negligible the drift of dark current.

2. Jung [4] has demonstrated improved linearity by attenuating the larger flux with a sector. This is effective if the chopping rate is much faster than the time constant of the nonlinearity.

3. Jung [5] has demonstrated improved linearity by chopping the flux to be measured and then adding a steady flux, P_0, to the chopped flux to keep the average flux constant. The mixture of chopped and steady flux is then passed to a phase sensitive rectifier and the output caused by the chopped radiation is shown to be very linear provided the rectifier is linear. P_0 need not be measured.

4. Special circuits in photomultipliers to keep the dynode voltage independent of anode current have been developed. The linearity is improved by using an adequate cathode to first dynode voltage and maintaining a constant last dynode to anode voltage.

5. Low or zero load resistance for selenium (barrier layer) cells and silicon diodes improve the linearity.

6. Jones and Clarke [6] used a photocell obeying Talbot's Law and a variable sector measured by time ratio photometry to reduce nonlinearities in photometric measurements.

7. Potentiometric or feedback system to keep constant the input to electrometers increases the stability and precision of measurements. Vacuum photoemission diodes with a cylindrical anode are extremely linear.

A. Detailed Descriptions of Some Methods for Measuring Nonlinearities

1. *Superposition (Additive) Method*—In the superposition method with two sources fluxes ϕ_1 and ϕ_2 produce the responses N_1 and N_2. The combined flux, $\phi_1+\phi_2$, produces the response N_{12}. If $N_1+N_2=N_{12}$ then the photometer is linear. If $N_1+N_2\neq N_{12}$ the nonlinearity may be given by the factor $N_{12}/(N_1+N_2)$, as described by Sanders [7], where this factor may be used to correct the response at the scale position $(N_1+N_2)/2$. If $N_1\neq N_2$ the measured correction is only an average correction factor, which will have an error dependent on how the nonlinearity changes with response. Zero correction is assumed necessary at N_1+N_2.

Rotter [8] preferred to find the nonlinearity as a difference correction to the response. He assumed that the correction was zero at the value $N_1=N_2$, and then defined the correction at N_{12} by

$$k_2=N_1+N_2-N_{12}.$$

With Rotter's method, it is possible to make hand computations more easily.

a. Multiple Sources—Many descriptions have been given of the use of this method. Preston and McDermott [9] in 1934 reviewed some earlier papers and then described their linearity tests using six incandescent lamps inside an integrating sphere. The lamps which were screened from the diffuse viewing window could be switched on or off independently of one another. They were each adjusted to have a similar luminous flux. Each lamp was measured independently with the test cell and then in combinations of 2, 3, 4, 5, and 6. In this experiment, each lamp had to be switched on and stabilized before being used.

In most cases the photo cells tested decreased in sensitivity with the illumination on the receiver. They used blue, green, and red filters and found that the nonlinearity was worst for blue light. In some cases, increased anode to cathode voltage improved the linearity. Nonlinearities of up to 15 percent were measured. The best cell was an Osram KMV6[2] with a nonlinearity of 0.1 percent, at a ratio of 1:6 in flux. All KMV6 cells were not as linear.

It is possible that the nonlinearity was caused by decreased cathode to anode potential at the higher flux.

This type of nonlinearity can be avoided by using a cathode which is mounted at the end of a long cylindrical anode in the manner described by Boutry and Gillod [10]. The VB59 photodiode from Rank Cintel, England, which is very linear has the cathode mounted along the axis of the cylindrical tube with a small window in the metallized tube wall. The nonlinearity can also be avoided by using an auxiliary potential to cancel out the potential developed across the anode resistor, or by using the connections to an operational amplifier as described by Witherell and Faulhaber [11]. The operational amplifier decreases the anode load resistance by the factor $1/A$ where A is the open loop gain of the amplifier.

Other users of multiple sources have mounted the lamps in individual compartments and left the lamps lit and selected the flux by shutters. Erminy [2], Kunz [3], Jung [4], and Reule [12] used two or more sources which could be isolated by baffles or rotatable mirrors. See items below for more details on these applications.

Reule [12] described some linearity measurements on a Carl Zeiss DMR21 Recording Spectrophotometer. He used a method of testing the linearity of a single beam spectrophotometer which had earlier been described by Hansen [13]. This step source or supplementary light method uses the superposition principle. A supplementary source, S_S, provides an adjustable

[2] In order to adequately describe materials and experimental procedures, it is occasionally necessary to identify commercial products by manufacturer's name or label. In no instances does such identification imply endorsement by the National Bureau of Standards, nor does it imply that the particular product or equipment is necessarily the best available for that purpose.

amount of flux which is measured as N by the spectrophotometer in the single beam mode. S_S is blocked off and the internal source, S_I, in the spectrophotometer is adjusted to provide an equal reading. Both shutters are opened and the sum is noted. S_S is again blocked off and S_I is adjusted to give a reading equal to the sum. This stepping procedure is repeated until the top of the spectrophotometric scale is reached. Reule used steps of 20 percent as a compromise between good scale coverage and drifting errors.

The analysis of the measurements is complicated if there is drift of the zero, or drift of the readings caused by lamp drift. It is not possible to read below zero or above 100 percent.

Reule also described how to use a similar method for double beam operation. The agreement between the corrections for double and single beam operation was within 0.1 percent of full scale. The corrections necessary to correct for nonlinearity depended on wavelength, but were always less than 0.1 percent when a photomultiplier was used as the detector.

Reule was able to use identical geometry for the two sources so the measurements should be applicable to the measurements made with the spectrophotometer. The two sources are independent, so no interference can be caused by partial coherence.

b. One Source Providing Several Fluxes— This is a very convenient method, since it means that only one power supply is required to provide the two or more fluxes which are required, Since the source is usually a tungsten lamp, the voltage must be controlled with four times the stability which is required in the flux. The current should be controlled with about seven times more stability than that required in the flux. Thus, the power supply will be expensive and a considerable saving will result from using only one supply.

There is, however, a danger in deriving the two fluxes for the superposition method from a single source. The two fluxes may be coherent to some extent and this may cause errors in measuring the nonlinearity. In fact, Mallick [14] describes a method in which the departure of additivity of two intensities indicates the degree of coherence of the light vibrations at the two points. Since one cannot use the same measurement to determine both nonlinearity and coherence, it is necessary to be sure which or what combination of these phenomena one is measuring in a given experiment. The equation given by Mallick is

$$I(Q) = I_1 + I_2 + 2(I_1 I_2)^{1/2} |\gamma_{12}(\tau)| \cos [\alpha_{12}(\tau) - \delta].$$

One can see that if $\gamma_{12} = 1$ and the phase is correct, we can obtain a value of $I(Q) = 2(I_1 + I_2)$ in the case where $I_1 = I_2$. This is twice the value expected for incoherent sources. Similarly, $I(Q)$ could be zero if the phase was shifted by 180°. Admittedly these are the extreme cases. For some ideas on how to evaluate the possible errors in linearity measurements due to coherence, see Born and Wolf [15], Mielenz and Eckerle [16], and Bures and Delisle [17].

The coherence will depend on the wavelength, wavelength range, area of source, coherence in original source, angular separation of apertures, size of apertures, area of receiver, path lengths, difference in path lengths, and diffusion in the system. Thus, it would be advisable to use two different parts of the strip filament which acted as the original source. This may be accomplished in Sanders' [7] linearity tester by placing a thin prism in front of one-half of the pairs of holes. As shown in figure 1, this may be easily constructed by removing a 3° wedge from one-half of a circular glass plate with the thin edge of the wedge on a diameter. The plate may be positioned in front of the lens in the linearity tester with the diameter positioned relative to the master plate, shown in figure 2, so all the rays passing the upper half of the holes are deflected downward. A strip filament lamp has replaced the lamp with diffusing bulb. A photocell placed at the image of the lamp filament, will receive images from two separate parts of the vertical strip filament lamp. There may be some slight residual coherence due to interreflections in the lamp or by diffraction or stray light at the apertures, but it will be considerably reduced. If it is desirable to measure with monochromatic light or to extremely high accuracy, it would be advisable to use a diffuser before the receiver to remove even the residual coherence.

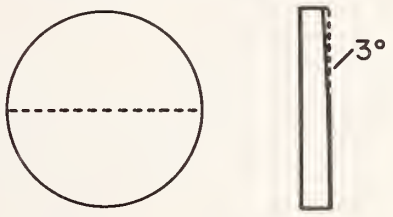

FIGURE 1. Circular glass plate with a 3 degree wedge removed from one half. This half deflects rays from 1 aperture of each pair of apertures in the linearity tester of figure 2.

The master plate in figure 2 has 18 apertures related in area as 1:1:2:2:4:4:8:8:16: . . . 64:128:128. This master plate is placed between a lens and the image of a lamp. Thus, each aperture as viewed from the image plane has a luminance equal to the luminance, L, of the source times, T, the transmittance of the lens. Thus, the irradiance from each aperture at the image is proportional to the area of the aperture. A rotatable disk with suitable holes can be positioned to transmit light through one hole or a pair of holes from the master plate. Thus, a range of illuminances of 1:256 are obtained at the image position. A receiver is placed at this position and the response measured for each aperture or pair of apertures, as shown in table 1, which is taken from Sanders [7]. For the whole series of measurements we must select one position which requires no correction. Sanders in 1962 used normalization at I_i, the maximum value. It is now believed that normalization at some fixed position on a scale would be more reasonable and advantageous in comparing nonlinearity measurements obtained at two different

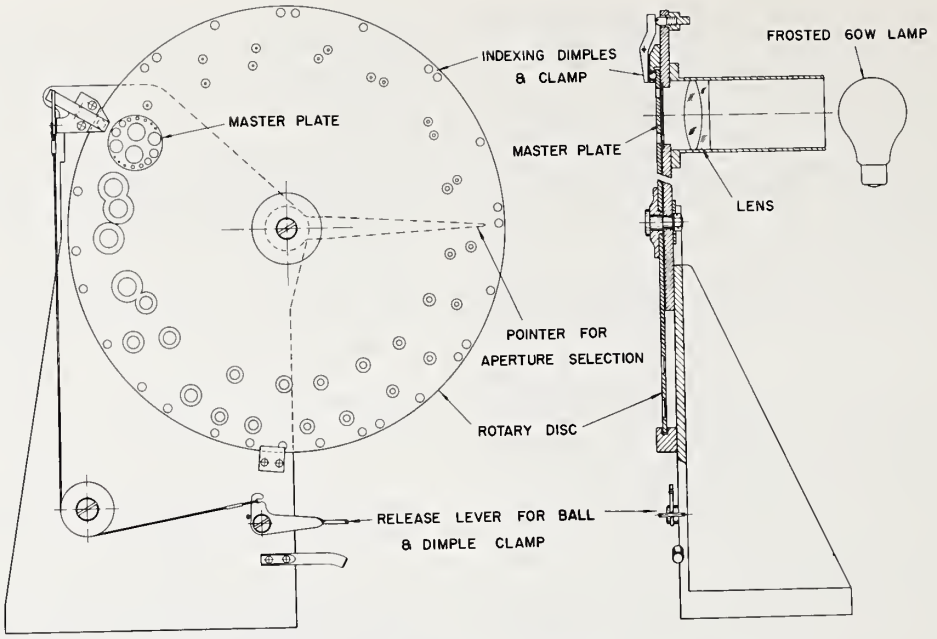

FIGURE 2. Sanders' Photocell Linearity Tester. (Courtesy, Applied Optics.)

times. With normalization at the maximum, one obtains the correction factors as shown in column 4, which are applicable to the responses shown in column 5. Using this apparatus, Sanders obtained correction factors for two detectors, the best of which was a vacuum diode photocell of Boutry and Gillod [10] which required a maximum correction factor of 0.997 over the whole range of 256:1. At the upper readings the correction required was less than 0.05 percent for a range of 30:1. The larger corrections with the smaller apertures may be caused by errors in measuring the smaller fluxes, by stray light, or by interference between partially coherent beams. The advantage of Sanders arrangement is that only one

TABLE 1. Determination of factors to correct readings to a linear scale

Net reading	Sum	Ratio	Correction factor[a]	Correction applies to reading
A			$\frac{Ii}{I+i}\cdot\frac{Hh}{H+h}\cdot\frac{Gg}{G+g}\cdot\frac{Ff}{F+f}\cdot\frac{Ee}{E+e}\cdot\frac{Dd}{D+d}\cdot\frac{Cc}{C+c}\cdot\frac{Bb}{B+b}\cdot\frac{Aa}{A+a}$	$\frac{A+a}{2}$
Aa	$A+$	$\frac{Aa}{A+a}$		
a				
B			$\frac{Ii}{I+i}\cdot\frac{Hh}{H+h}\cdot\frac{Gg}{G+g}\cdot\frac{Ff}{F+f}\cdot\frac{Ee}{E+e}\cdot\frac{Dd}{D+d}\cdot\frac{Cc}{C+c}\cdot\frac{Bb}{B+b}$	$\frac{B+b}{2}$
Bb	$B+b$	$\frac{Bb}{B+b}$		
b				
C			$\frac{Ii}{I+i}\cdot\frac{Hh}{H+h}\cdot\frac{Gg}{G+g}\cdot\frac{Ff}{F+f}\cdot\frac{Ee}{E+e}\cdot\frac{Dd}{D+d}\cdot\frac{Cc}{C+c}$	$\frac{C+c}{2}$
Cc	$C+c$	$\frac{Cc}{C+c}$		
c				
D			$\frac{Ii}{I+i}\cdot\frac{Hh}{H+h}\cdot\frac{Gg}{G+g}\cdot\frac{Ff}{F+f}\cdot\frac{Ee}{E+e}\cdot\frac{Dd}{D+d}$	$\frac{D+d}{2}$
Dd	$D+d$	$\frac{Dd}{D+d}$		
d				
E			$\frac{Ii}{I+i}\cdot\frac{Hh}{H+h}\cdot\frac{Gg}{G+g}\cdot\frac{Ff}{F+f}\cdot\frac{Ee}{E+e}$	$\frac{E+e}{2}$

Ee	$E+e$	$\frac{Ee}{E+e}$		
e				
F			$\frac{Ii}{I+i}\cdot\frac{Hh}{H+h}\cdot\frac{Gg}{G+g}\cdot\frac{Ff}{F+f}$	$\frac{F+f}{2}$
Ff	$F+f$	$\frac{Ff}{F+f}$		
f				
G			$\frac{Ii}{I+i}\cdot\frac{Hh}{H+h}\cdot\frac{Gg}{G+g}$	$\frac{G+g}{2}$
Gg	$G+g$	$\frac{Gg}{G+g}$		
g				
H			$\frac{Ii}{I+i}\cdot\frac{Hh}{H+h}$	$\frac{H+h}{2}$
Hh	$H+h$	$\frac{Hh}{H+h}$		
h				
I			$\frac{Ii}{I+i}$	$\frac{I+i}{2}$
Ii	$I+i$	$\frac{Ii}{I+i}$	1.000	Ii
i				

[a] Assuming no correction to reading of Ii.

moving part is required.

We have now modified it by cutting gear teeth on the edge of the large disk and driving the disk with a stepping motor with 500 steps per revolution. The positioning accuracy is adequate and it is no longer necessary to use the ball in the conical indentations to locate the disk exactly. A Slo Syn [18] Tape Control System operates the linearity tester. The Slo-Syn system was available for use since it was incorporated in 1968 into the spectroradiometer described earlier by Sanders and Gaw [19]. The apertures may be selected by punched paper tape in the order described in table 1 or in any other desirable way. It takes about 5 s to rotate the disk 180° so it is faster to proceed following approximately the order of table 1. One program used is to go through the table to the bottom and then to repeat starting from the bottom up. Nine zero readings are spaced fairly uniformly through this measurement cycle. The results are recorded on punched cards by means of a digital voltmeter. The measurements are analyzed by computer and a table such as table 2 is produced for each half-cycle.

The top line gives the description of the test. The next line shows the zero readings in volts which were recorded. The next line shows the eight averages of the successive pairs of adjacent zeros. The data in this table were obtained between the first and fifth zero. The table then follows the pattern set out in table 1. The data in table 2 are for a silicon diode connected to an operational amplifier to produce an effective 0.1Ω load resistance. The diode was a Pin 10 from United Detector Technology and was connected in the photovoltaic mode to an operational amplifier as described by Witherell and Faulhaber [11]. The silicon diode had a flashed opal glass in front of its V(λ) correction filter. Each measurement made after the cell had been illuminated for about 11 s. A 1 s reading was taken by the integrating DVM. The correction ratios in column 4 for a ratio of 1 : 2 in flux show a maximum deviation of 0.0026 from 1.0 at the response of 0.00567 V. This corresponds to a photocurrent of 0.00567 μA. The correction factor based on zero correction at the maximum reading is given in colmn 5. Here the correction is farthest from unity at the middle of the range, with the maximum departure of 0.0014 at 0.011 V. There is considerable variation from one measurement series to another and a number of repeat measurements were made.

Table 3 shows the correction factors for various selected voltage outputs for twelve repeat measurements on the same silicon diode. The first six lines are for a 1.5 s delay and the next six for an 11 s delay. The first line shows the response voltages at which linear

Table 2. Computer Output for Nonlinearity Measurements on a silicon diode

11 2102720006 TEST DIODE X1 12.45 AMPS 10 S, 1 S COUNT
0.000100 0.000100 0.000100 0.000120 0.000150 0.000120 0.000130 0.000110 0.000110
0.000100 0.000100 0.000110 0.000135 0.000135 0.000125 0.000120 0.000110

READING NAME	NET READING	SUM	CORRECTION RATIO	CORRECTION FACTOR	READING AT WHICH FACTOR APPLIES
A1	0.002500		1.0000	1.0013	0.002880
A12	0.005760	0.005760			
A2	0.003260				
B1	0.005060		1.0026	1.0013	0.005670
B12	0.011370	0.011340			
B2	0.006280				
C1	0.010360		0.9996	0.9986	0.011300
C12	0.022590	0.022600			
C2	0.012240				
D1	0.024660		0.9994	0.9991	0.024600
D12	0.049170	0.049200			
D2	0.024540				
E1	0.051370		0.9997	0.9997	0.047885
E12	0.095740	0.095770			
E2	0.044400				
F1	0.103610		1.0007	1.0000	0.087310
F12	0.174750	0.174620			
F2	0.071010				
G1	0.207140		0.9997	0.9992	0.179910
G12	0.359710	0.359820			
G2	0.152680				
H1	0.309115		1.0001	0.9995	0.359185
H12	0.718455	0.718370			
H2	0.409255				
I1	0.779645		0.9994	0.9994	0.786410
I12	1.571915	1.572820			
I2	0.793175				

Table 3. Correction factors at selected voltages for successive measurements on a silicon diode. Measurements 1–6 with a 1.5 s exposure before the reading. Measurements 7–12 with an 11 s exposure before the reading

Meas. No. Volts	0.003	0.006	0.01	0.05	0.10	0.30	0.50	0.70	1.00	1.30	1.50
1	1.0038	0.9986	1.0006	1.0005	1.0002	0.9993	0.9993	0.9994	0.9995	0.9998	0.9999
2	1.0057	1.0022	1.0008	1.0000	0.9998	0.9992	0.9993	0.9994	0.9996	0.9998	1.0000
3	0.9930	0.9982	0.9989	0.9998	0.9994	0.9990	0.9993	0.9993	0.9995	0.9998	0.9999
4	0.9979	0.9962	0.9989	0.9999	0.9997	0.9993	0.9994	0.9994	0.9996	0.9998	0.9999
5	0.9985	1.0035	0.9967	0.9999	0.9997	0.9992	0.9993	0.9994	0.9996	0.9998	1.0000
6	0.9943	0.9960	0.9974	1.0003	1.0003	0.9996	0.9995	0.9995	0.9997	0.9998	1.0000
7	0.9951	0.9968	0.9988	0.9993	0.9994	0.9992	0.9993	0.9994	0.9996	0.9998	1.0000
8	1.0004	0.9987	0.9994	1.0006	1.0010	0.9996	0.9993	0.9995	0.9997	0.9999	1.0000
9	1.0025	1.0043	1.0022	1.0013	1.0013	1.0002	0.9999	0.9998	0.9998	0.9999	1.0000
10	1.0038	1.0003	0.9990	0.9994	0.9998	0.9991	0.9994	0.9996	0.9998	0.9999	1.0000
11	1.0013	1.0013	0.9992	0.9997	0.9999	0.9994	0.9995	0.9994	0.9996	0.9998	0.9999
12	0.9977	0.9943	0.9936	1.0012	1.0012	0.9998	0.9995	0.9996	0.9998	0.9999	1.0000
Ave. 1–6	0.9989	0.9981	0.9989	1.0000	0.9999	0.9993	0.9994	0.9994	0.9996	0.9998	1.0000
Ave. 7–12	1.0013	0.9990	0.9987	1.0002	1.0004	0.9995	0.9995	0.9996	0.9997	0.9999	1.0000

interpolations were made to find the applicable correction factor. The next line shows the measurement number in column 1, followed by the correction factors for each voltage. The correction factors are quite consistent from one run to the next at voltages from 0.3 to 2.0 V. The average correction factors are

shown in the next to last line of table 3. The correction factor of 0.9995 is the farthest from unity. For this set of measurements the lamp used was a vacuum strip filament lamp.

The irradiance due to one aperture must not change when another aperture is opened. Interaction between one aperture and another may result from interreflections which depend on whether another aperture is open or closed. The precautions required to reduce these effects to the minimum possible have not been taken to date in the National Research Council (NRC) linearity tester. It seemed, previously, that the instability of the source or the receiver and its attendant electronic circuits, were the dominant sources of fluctuation and systematic error. Present developments suggest that some improvements would be warranted as follows. One could put antireflection coatings on all the optical surfaces, put light traps to collect major stray fluxes, make the aperture covers into light traps to prevent back reflected light when an aperture is closed and in general tighten up the experiment to ensure that all these effects produce negligible errors.

Nonaka and Kashima [20] made a series of measurements on several RCA photomultipliers of the types 1P21, 1P22, and 1P28. They used ten equal sized apertures in parallel light between two lenses which focussed the source on the receptor. Their measurements, made with a precision of about 0.1 percent, showed that the nonlinearity depended on the color of the light; on the position of radiation on the cathode; on the voltages (a) from the cathode to the anode, (b) from cathode to first dynode, and (c) from the last dynode to the anode. Nonaka and Kashima adjusted the radiation to obtain an anode current of 0.3 μA with all ten apertures open. They did not compensate for the voltage drop in the anode resistor and, hence, some nonlinearity will be caused by anode load feedback which results in a lower voltage from the last dynode to the anode as the anode current increases. At 500 V overall, the gain decreased with anode current, but at 1000 V overall, the gain usually increased with anode current. With 1000 V overall, the collection by the anode is complete, but the higher voltage produces a higher gain which with increasing incident flux causes enough voltage redistribution in the dynode chain to cause an increase in overall gain. This agrees with the analysis of Moatti [21] and Lush [22]. The nonlinearity was greater near the edge of cathode.

These measurements by Nonaka and Kashima, show that it is essential to measure the nonlinearities of a photomultiplier under the same optical and electrical conditions which will be used in obtaining the measurements to be corrected for nonlinearity. The nonlinearities can vary in the range ± 1.0 percent when these conditions are changed.

Rotter [8] analyzed the possibilities which existed for selecting and providing the irradiances to be measured in testing the nonlinearity of receptors by the superposition method. His treatment assumed that the irradiances were provided by a single stable source. A lens system with apertures graduated in size provided irradiances related in several different ways. Rotter analyzed the system with respect to the work involved and the accuracy produced.

He divided the measuring systems into two main classes:

1. Method in which more than two irradiances may be received at the same time.
   - 1.1. Method with, n, nearly equal sized openings, i.e., 1 : 1 : 1 : 1 : . . . .
   - 1.2. Method with gradation of the openings by a factor of two, i.e., 1 : 1 : 2 : 4 : 8 : 16 : 32 : . . . .
2. Method in which, at most, two irradiances are received at one time.
   - 2.1. Method with steps of pairs of equal irradiances increasing in size from one pair to the next by a factor of two, i.e., 1 : 1 : 2 : 2 : 4 : 4 : . . . .
   - 2.2. Method of increasing the size by steps of 62 percent which was first suggested and used by Rotter. These steps are arranged in size, according to the equation

$$A_i + A_{i+1} = A_{i+2}$$

except that the first two irradiances are equal in size, i.e., $A_0 = A_1 = 1$. The series then becomes 1 : 1 : 2 : 3 : 5 : 8 : 13 : 21 : 34 : 55 : 89 : 144.

For each method, Rotter gave the order of measurements, and the order of calculating the additive correction. As an example of this, the measurement program for Method 2.2 follows:

Reading	Irradiance	Correction
$N_{1'}$	1′	k_1
$N_{1',1}$	1′ 1	k_2
N_1	1	k_1
$N_{1,2}$	1 2	k_3
N_2	2	k_2
$N_{2,3}$	2 3	k_5

It is noted that each aperture is used in three consecutive readings, except aperture 1′, and the largest apertures are used only twice. The corrections k_i are found from

$$k_1 = 0 \qquad \text{(arbitrarily chosen)}$$

$$k_2 = N_{1'} + N_1 + 2k - N_{1',1}$$

$$k_3 = N_1 + N_2 + k_1 + k_2 - N_{1,2}$$

$$k_5 = N_2 + N_3 + k_2 + k_3 - N_{2,3}$$

$$k_8 = N_3 + N_5 + k_3 + k_5 - N_{3,5}$$

The calculations to find the corrections, k_i, are thus easily determined by additions and subtractions in this method, whereas that presented by Sanders requires extensive mulplication.

Rotter's analysis showed that the Method 1.1 using n equal sized apertures was very expensive (in the number of measurements required) compared to the other three methods, if the range was greater than 1 : 4

Thus, for the range 1:8, Method 1.1 required twice as many readings. For the range 1:64, it required about ten times as many. However, Method 1.1 is more likely to be used with eight sources and will cover a range of 1:8. Then the source will be raised in intensity by a factor of eight to cover the next factor of eight on the scale. With this procedure, the equal sized aperture method would only require twice as many readings as the other three.

In Rotter's analysis of the errors in the corrections relative to the errors caused by the source variations, he found that Method 1.1 produced correction values with errors between two and three times lower than those produced by the other methods. Thus, at least four repetitions of the measurements in the last three methods would be required to produce measurements with the same error as those obtained by a single set of measurements by Method 1.1.

It thus seems that the choice of the best method must be made based on other criteria, such as cost of the equipment, ease of use, or minimization of drifts.

Rotter described three physical arrangements of

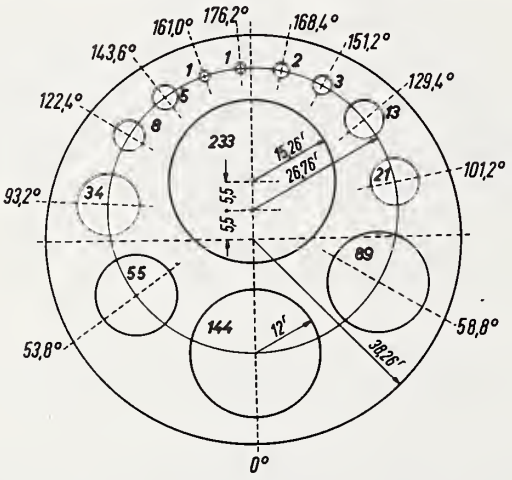

FIGURE 3. Rotter's aperture arrangement using 13 apertures with a sliding shutter on each. The angular position and relative diameter of each aperture is indicated. The outer circle indicates the outside diameter of the lens. (Courtesy, Messtechnik.)

apertures. One, reproduced in figure 3, has 13 apertures increasing in size by a factor of 62 percent, except for apertures 1 and 1′, which are equal. Each aperture is covered as required by a sliding shutter. The outer circle shows the size of the lens. This is a variation of Bischoff's [23] arrangement and makes good use of the lens area. The range covered is 1:377. The 13 sliding shutters make the method more complicated to use than that of Sanders or the one shown in figure 4 which was also given by Rotter.

This apparatus has two moving disks, B and C, with six apertures in each. The lens is outlined by the dotted circles enclosing both the smaller dotted circles D and E. These are apertures in a plate fixed in front of the lens. The numbers near the circles shown on the disks

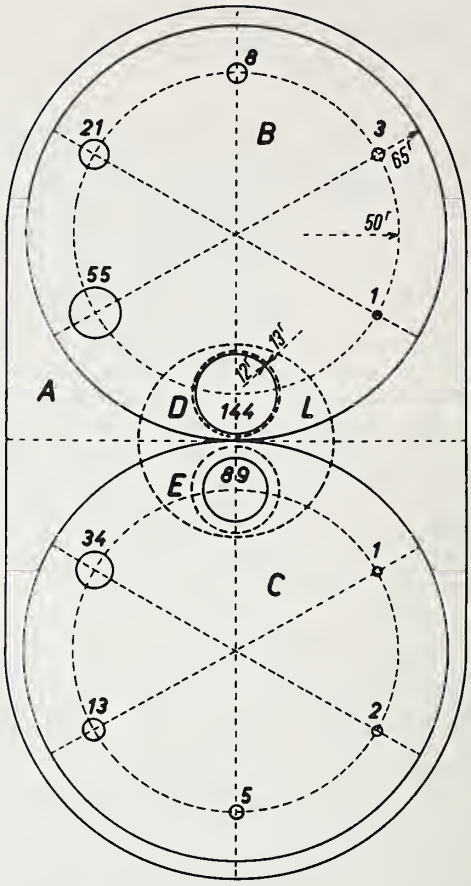

FIGURE 4. Rotter's aperture arrangement using two rotatable discs B and C with 6 apertures in each. Apertures D and E are in a disc before lens L with its outer diameter indicated by a dashed circle. (Courtesy, Messtechnik.)

indicate the relative area of these apertures. The disk B may be rotated to place any of the six apertures inside D or to cover D as required. The same applies to disk C relative to aperture E. The lens may be more effectively utilized if the holes D and E are oblong in shape and the largest holes in the disks are similarly distorted. This method of using two disks eliminates the requirement for a large number of moving parts. At the same time it requires less space and less accurate machining than Sanders linearity tester. Each disk remains stationary for three measurements as discussed above. The large disk in Sanders apparatus must be moved between the reading on A alone and the reading on A in combination with a. Thus there is a possibility of inexact reproduction of the flux through A or through a. Also, by using different disks in Rotter's apparatus, a different scaling of sizes may easily be selected. Also, disks B and C may be interchanged, which could be useful in eliminating certain errors.

2. Bouguer's Law—This law states that if filters a and b have transmittance T_a and T_b respectively, then the transmittance of the two filters placed one after the other in an optical beam, will be $T_a \times T_b$. Thus, if one

knows the transmittance of each of a set of filters, one can combine them to produce various transmittances to be used to test a photometric system.

The validity of the method is not always certain. Hawes [1] noted difficulties caused by transmittances changing with change of temperature, with age, with cleaning techniques, with interreflections, with nonuniformity of the filters, and with bandwidth of the transmitted beam. He found the system useful if one did not depend on the long term stability of the filter transmittance and took the proper precautions to control temperature, interreflections, uniformity and bandwidth.

Hawes, Bischoff [23] and others have noted that Bouguer's Law does not check for nonlinearity unless the transmittance of at least one filter is known by an independent method. See below under A(4) for Hawes' method which combines superposition and Bouguer's Law. Hawes found it necessary to select filters sufficiently uniform that a 1-mm aperture moving over the filter detected no changes larger than 0.01 in absorbance. He described an apparatus to use with a Cary spectrophotometer in making these measurements.

3. Beer's Law—This law states that log $(1/T)$ is proportional to the concentration of the solute in the solution, where T is the transmittance of a constant thickness of the solution. This is only true for monochromatic light unless T is independent of wavelength over the full extent of the measured radiation. This method is used in chemical analysis where the techniques are available to make the solutions properly and where the scientists may depend on the law in their analyses and know when it will be valid. Problems have been noted with particles growing in the solutions. Interreflections may change with concentration and the law may not be quite exact in all cases.

4. Combination of the Superposition Method With Bouguer's Law to Test a Spectrophotometer—Hawes [1] gave a useful set of criteria which should be met in selecting a method for calibrating photometric linearity in spectrophotometers. Hawes' method for spectrophotometry cannot be transferred to broad band photometry because the absorbing glass filters which are available are not exactly neutral. He used three Chance ON 10 filters about 1 mm thick. Two had transmittances of about 0.49 and the third about 0.57. He made the apparatus shown in figure 5. The solid block of metal with the two large holes is screwed firmly in place in the test beam of the Cary. Any one or any combination of the three filters may be placed in slots in the metal block, B. The possible selection of holes is: both open, *a* open, *b* open, or both closed, respectively, when no slide, slide *a*, slide *b*, or slide *c* is in the slot. The three filters cover both beams and are oriented, by the retainers shown at R, to prevent interreflections from reentering the optical beam. The test compartment is optically remote from the cathode of the photomultiplier in the Cary, so the beams from the two apertures fall on the same area of the cathode. It was necessary to insert and remove the slides by means

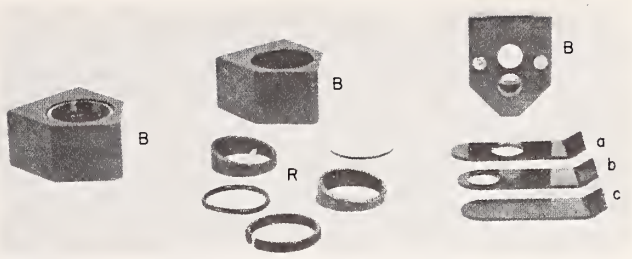

FIGURE 5. Dual aperture with filter assembly used by Hawes to determine and correct for nonlinearities. Fixed block B. Slides a, b, and c. Retaining rings R for three filters. (Courtesy, Applied Optics.)

of a flexible material in order not to disturb the position of the metal block. This procedure may also prevent temperature changes from being introduced by the fingers. It is not clear how the filters could be inserted and removed in the Bouguer Law tests without disturbing the position of the limiting aperture.

The slides produced a measurement at 100 percent on the scale and at two positions near 0.50 and at zero. Thus, using the superposition method, one could find the correction required near the middle of the scale and could use this to find corrected transmittances of filters 1 and 2. Hawes assumed that in the instrument the following relationship held over the whole scale:

$$I_{T'}/I_0 = T^{(1+e)} = T'$$

where e is the amount by which the exponent differs from unity, T is the true transmittance, $I_{T'}$ is the measured current with the filter in place, and I_0 is the current for 100 percent transmittance. Thus,

$$\log\ (I_{T'}/I_0) = (1+e)\ \log T = \log T'$$

and, from the measurements on filters 1 and 2 and those with the superposition method, e can be determined. Hawes calculated in absorbance rather than transmittance and applied a correction, eA, to each absorbance A.

Using two different photomultiplier tubes he found a difference of 0.07 percent in the transmittance when the two photomultipliers were used in the same instrument to measure the three component filter with a transmittance of 13.59 percent. The use of the value of e determined by the superposition method did not reduce the discrepancy. Hawes felt that the transmittance of one filter probably changed between the two sets of measurements. It thus remains to be shown whether the assumption of a constant value for e is valid and useful. If no sufficiently stable filters can be found, then it is questionable whether the corrections are necessary.

5. Inverse Square Law—the accuracies attainable

502-591 O - 73 - 6

with the inverse square law depend on the accuracy available in measuring: the distance from the source to the receiver, the uniformity with angle of the intensity of the source in the direction of the receiver, the size of the receiver, and the range of intensities required. It should be possible to refine the inverse square law method by measuring the angular distribution of intensity of the source over the largest solid angle which the receiver will subtend at the source. With this distribution and the cosine law to allow for the angle of incidence of the receiver surface, the flux incident on the receiver could be calculated for a number of distances. Changing the voltage on the lamp or inserting a filter would extend the range. Stray light due to reflections and due to diffraction caused by the baffles (see Blevin [24] would need to be given careful consideration.

6. Standard Absorbing Filters—See comments under Bouguer's Law. NBS filter sets described by Keegan, Schleter and Judd [25] are useful for detecting errors in a spectrophotometer and in keeping two or more spectrophotometers of similar geometry in agreement within a few tenths of a percent provided that the same filter set is used on both instruments.

7. Standard Reflecting Materials—Robertson and Wright [26] reported the results of measurements on grey ceramic tiles in a number of different laboratories. Standardized ceramic tiles [27], now available from National Physical Laboratory (NPL) or from the British Ceramic Tile Council, may be used for checking photometric linearity if the geometry of the spectrophotometer being used matches the geometry provided during the calibration.

8. Rotating Sectors—In some cases, sectors are used to reduce the average flux incident on a receptor or to measure the nonlinearity of a receptor. If the response produced by the intermittent flux is identical with that produced by a steady flux whose magnitude equals the mean magnitude of the intermittent flux taken over one period then the receptor is said to obey Talbot's Law. This does not necessarily mean that the receptor is linear. It just means that the nonlinearity is independent of whether the flux is chopped or steady. The faster the sector rotates the more likely it is that Talbot's Law will be valid. See parts B(1) and B(2) for applications of sectors to improve linearity of measurements. Kunz [3] describes methods used in accurate construction and calibration of sectors.

9. Measurement of Amplitude of a Harmonic or the Beat Frequency—Jung [4] described a very interesting, useful and rapid method of measuring the nonlinearity of receivers. In this method, two chopped beams of slightly different frequencies are combined on the receptor and the output of the receptor is examined at the difference frequency. Jung showed that the amplitude of this difference frequency is proportional to the nonlinearity if the nonlinearity is proportional to the flux. He also demonstrated that one could determine the time constant of the nonlinearity even if it was as small as a few milliseconds.

Jung assumed that

$$i = BP + CP^2 + DP^3 \tag{1}$$

with $|CP^2|$ and $|DP^3| \ll BP$ where B, C and D are constants, and i is the photocurrent and P is the incident flux. He defined NL_G as the nonlinearity measured by the superposition method at $i_1 + i_2$, where

$$NL_G\,(i_{1+2}) = 2\,\frac{i_{1+2} - (i_1 + i_2)}{i_{1+2}} \tag{2}$$

Using eq (1) to find the current, i_1 and i_2, for two fluxes $P_1 = P_2 = 0.5\ P$ and placing the currents in eq (2), we get

$$NL_G\,(i_{1+2}) \approx \frac{1}{B}\,(CP + \frac{3}{2}DP^2) \tag{3}$$

In the dynamic method, the flux, P_1, is modulated at frequency ω, and P_2 at ω_2, where $\omega_1 > \omega_2$. Jung proceeded to use a Fourier expansion to show that $A\ (\omega_1 - \omega_2)$, the amplitude of the frequency $\omega_1 - \omega_2$ is given by

$$A(\omega_1 - \omega_2) = \frac{1}{\pi^2}\,(CP^2 + \frac{3}{2}DP^3) \tag{4}$$

where the basic frequency ω_1, had the amplitude $A\ (\omega_1) = BP/\pi$. Jung then defined $NL_D(\hat{\imath})$ the nonlinearity at the maximum current, $i = i_{1+2}$, by

$$\begin{aligned} NL_D(\hat{\imath}) &= \pi A(\omega_1 - \omega_2)/A(\omega_1) \\ &= (1/B)\ (CP + (3/2)\ DP^2 \end{aligned} \tag{5}$$

under this assumption $NL_D = NL_G$ but the assumption of eq (1) is too simple because the photocurrent does not instantaneously change when P changes. Thus, Jung found it necessary to postulate

$$i = BP + CP^2\,(1 - \epsilon^{-(t/\tau)}) \tag{6}$$

where P is a function of time, τ is the time constant of the nonlinearity, and t is the time from commencement of the steady signal. By use of suitable expressions for i and P as a function of time and applying a Laplace transformation, Jung found that

$$NL_D\,(i, \omega\tau) = CP/B\ (1 + (\omega t)^2)$$

Thus by eq (3) with $D = 0$ and assuming that in the superposition method $t > \tau$, the relationship between NL_G and NL_D is

$$NL_D = NL_G/(1 + (\omega\tau)^2) \tag{7}$$

If the frequency of the chopper is 200 Hz and $\tau = 1$

ms, then $NL_D/NL_G = 0.4$. Thus one can find τ from the ratio of NL_D/NL_G.

The experimental arrangement used by Jung is

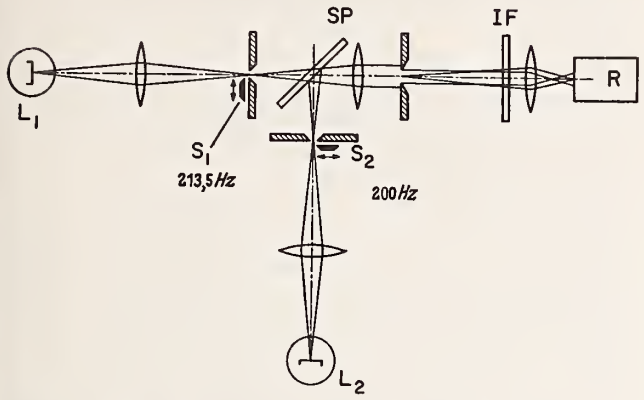

FIGURE 6. Jung's optical apparatus for dynamic measurement of nonlinearities. The semireflecting plate SP combines radiation from sources L_1 and L_2. The radiation is chopped by shutters S_1 and S_2. (Courtesy, Z. Angew. Physik.)

illustrated in figure 6. The oscillating shutters, S_1 and S_2, operate at frequencies of 213.5 Hz and 200 Hz, respectively. The semitransparent plate, SP, combines the beams from the lamps, L_1 and L_2, so they illuminate the receiver, R, identically. An interference filter, IF, could be used to isolate a narrow band of wavelengths.

The measuring circuit Jung used is shown in

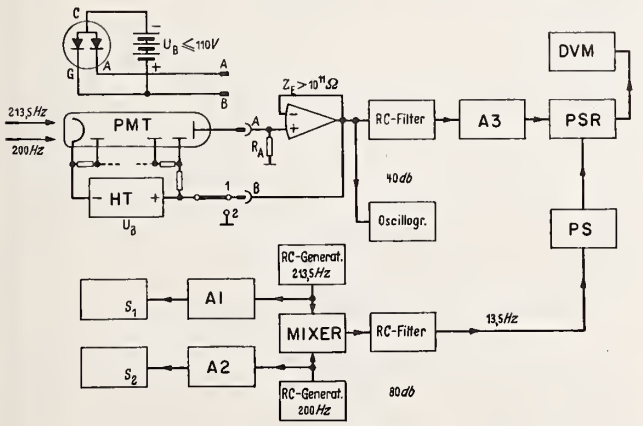

FIGURE 7. Jung's electronic apparatus for dynamic measurement of nonlinearities. A1, A2, and A3 are amplifiers. S_1 and S_2 are shutters. PS is a phase shifter and PSR a phase sensitive rectifier. (Courtesy, Z. Angew. Physik.)

figure 7. The oscillating shutters, S_1 and S_2, were driven by independent generators, G_1 and G_2, through power amplifiers, A_1 and A_2. The signals from G_1 and G_2 were fed to a mixer to produce the beat frequency at 13.5 Hz which was filtered by a filter, RC, to attentuate the base frequencies by 80 db. A phase shifter, PS, was required before the phase sensitive rectifier, PSR, and was adjusted to give maximum signal at the digital voltmeter, DVM. Provision was made for using either a photomultiplier, PMT, or a photodiode, Si. They could be connected at points A and B. In addition, B could be connected to either terminal 1 or 2. The first of these connections produces a voltage in the impedance transformer which keeps the voltage constant from the anode of the photomultiplier to the last dynode. The input impedance of the transformer is greater than $10^{11}\ \Omega$. This connection keeps the collection efficiency of the anode constant. The nonlinearity obtained by Jung using con-

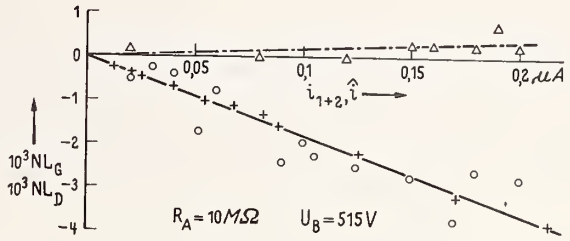

FIGURE 8. Jung's measurements on an EMI 9558 photomultiplier. Measurements without anode voltage compensation by the dc and dynamic method are shown respectively by circles and crosses. Those by the dynamic method with anode voltage compensation are shown by triangles. (Courtesy, Z. Angew. Physik.)

nection 1 for B is as shown by the triangles in figure 8. With B connected to position 2, there is a voltage drop produced in R_A by the anode current which causes the collection efficiency of the anode to decrease and causes nonlinearities, as shown by the crosses in figure 8. Jung's measurements by the dc superposition method with the point A connected to position 2 gave the results shown by circles.

There is much more scatter in the dc measurements than in the dynamic measurements. This instability may be partly caused by instability in the source, but also by drifting dark current caused by the large changes in average flux incident on the photomultiplier. Kunz [3] describes this effect in detail and his findings will be discussed further in B(1). Since the two measurements made without compensation of anode drop by Jung agree within the scatter, it is not possible to estimate a value of τ from eq (7). It only suggests that $\omega\tau \leqslant 1$.

As shown by the triangles in figure 8, the nonlinearity is much less when the change in the voltage across the anode resistor is compensated by connecting B to position 1. The sign of the nonlinearity is reversed as one would expect from Moatti [21] (see B4 below).

Jung's measurements on a silicon photodiode with 24 V bias and connected to give compensation of the voltage drop showed good agreement between the dynamic and dc method. The nonlinearity in this case was about 0.8 percent at 1 μA photocurrent.

Bressani, Brovetto and Rucci [28] described a method of testing nonlinearity of a photomultiplier by modulating the flux on a slit in front of a photomultiplier. The method depends on the modulation being exactly a sine function. Any nonlinearities in the receiver will produce the second harmonic which is

selected by a lock-in amplifier whose reference channel is driven by a frequency doubler from the oscillator, which also drives the oscillating mirror which modulates the beam. The 1 percent error in the linearity measurements was said to be due to the lock-in amplifier. This does not compare very well to the error of the phase sensitive rectifier used by Jung which Jung claimed was responsible for 0.05 percent of the error. The illumination at the slit must be uniform in Bressani's method and nonuniformity of sensitivity over the cathode must not be able to interfere, if the nonlinearity is to be measured correctly. This makes the potential of the method much lower than that of Jung's method using the beat frequency.

10. Measurement of Radiant Fluxes to Test Linearity—To the series of steps of irradiance which Rotter described, we should add that described by Erminy [2]. Erminy used three strip filament lamps,

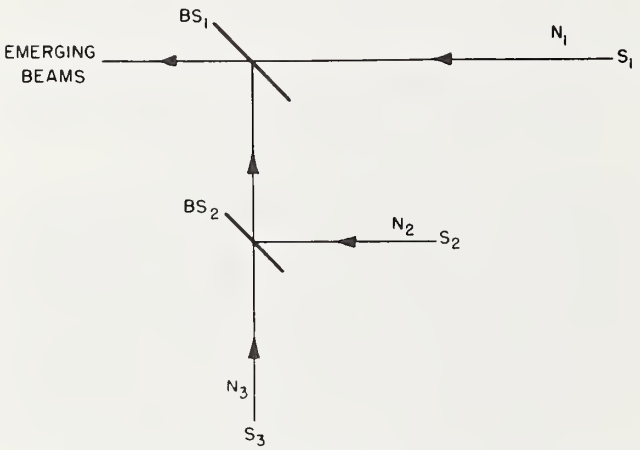

FIGURE 9. Erminy's arrangement using 3 sources for producing integral and fractional multiples of a radiance. (Courtesy, J. Opt. Soc. Amer.)

as shown in figure 9. The current on each lamp could be adjusted to provide selected levels of radiance. Each source could be blocked off with a shutter. Starting with N_0, Erminy showed how to obtain the radiances $mN_0/2^i$ where

$$m = 1, 2, 3 \ldots \text{ and } i = 1, 2, 3 \ldots .$$

Erminy used the device to obtain radiances which could be matched to the radiance of another lamp by a null detector. He produced in this other lamp a radiance scale obtained by additive means. The detector was not required to be linear or to have a good stability over a long period of time. Thirty seconds were required for each measurement.

In testing the nonlinearity of photocells, we are assuming their stability. The adjustment routine used by Erminy to provide a variety of radiances can also be used to provide irradiances with the same multiples, $mN_0/2^i$, and thus may be used to check the nonlinearity of photocells at a much greater variety of irradiances than can be obtained by the use of two sources. In producing an irradiance scale, one could, by appropriate optical means, adjust the irradiance from each source without changing the lamp current on the three lamps. An iris diaphragm, distance variation neutral wedge, etc. could be used with each source.

The two-step method can only produce irradiances differing by a factor of two, so one is very dependent on having a device which changes smoothly in nonlinearity as the irradiance increases. Erminy's arrangement can help to avoid such an assumption.

11. Null Method—Lee [29], in establishing the NBS pyrometric temperature scale, used Erminy's method with three strip filament lamps to calibrate a fourth lamp at 14 currents, so the radiances were in the proportion 0.007812 : 0.015625 : 0.03125 : 0.0625 : 0.125 : 0.25 : 0.5 : 0.67 : 1.0 : 1.5 : 2.0 : 3.0 : 4.0 : 6.0. Using $I = P(T_r)$, where $P(T_r)$ is a power function of T_r, he found seven coefficients to fit the 14 radiance temperatures T_r corresponding to the 14 currents. Tables were made using the equation so current could be related to temperature. A similar process could produce a (completely adjustable) radiance standard so the detector would need only serve as a null detector. It takes seconds for the lamp to stabilize at each temperature, but there may be some circumstances where this method should be used. The paper by Lee [29] describes the behaviour of strip filament lamps. Vacuum lamps are more stable than gas filled lamps, provided the temperature is kept low.

12. Use of a Linear Receptor to Calibrate a Test Receptor—Edwards and Jeffries [30] used a linear planar photodiode as a reference detector to measure the linearity of silicon diodes using a cathode ray oscilloscope as the display element. They were able to detect nonlinearities of 3 percent over a range of 10^5:1. Their applications involved measurements of pulses down to 3 ns duration. For slower tests, it should be possible to use, as a linear reference device, a vacuum photoemissive diode with an anode subtending almost all the solid angle surrounding the cathode.

B. Method of Increasing Linearity and Accuracy

1. *Selection and Operation of Photomultipliers for Measurement of High Flux Ratios*—Kunz [3] in a paper describing the development of a temperature scale above the gold point, listed the following 12 points to consider in the selection and use of photomultipliers:

(1) Photomultipliers with nonfocusing dynode systems are more suitable than other types.

(2) Photomultipliers with glass bases show smaller leakage currents than those with plastic bases.

(3) One should seek a photomultiplier with the smallest possible dark current leakage at the anode and dynode, e.g., 2.5×10^{-12} A at step voltages of 30 V. The insulation test should take place several hours after washing the base with very clean solvents and distilled water.

(4) Photomultipliers should be selected for the most constant possible sensitivity under changing illumina-

tion. In a check of the drift situation, particular attention should be paid to the drift following a decrease in illumination.

(5) For measuring uncertainties below 0.05 percent the EMI 9558 A photomultiplier must be operated only at photocurrents below 3×10^{-8} A.

In B2 and B3 below, Jung has shown that operation at considerably higher currents under special conditions can produce results of similar accuracy.

(6) With the EMI 9558 photomultiplier tube, operation with five (or eight) dynodes is possible, and, especially at small gains of 10 to 1,000 (or 30 to 10,000), is more advantageous if an initial drift causes interference when all stages are in use.

(7) The photomultiplier and its anode resistance must be installed in a housing with high thermal inertia or in a thermostatted housing.

(8) The anode resistance must have small voltage and small temperature coefficients.

(9) Anode feedback should be avoided by compensation or the provision of proper resistances.

(10) The capacitor in parallel with the anode resistance must have very low dielectric absorption.

(11) Interferences due to dielectric absorption in the electrometer input and its connecting cable must be avoided by suitable selecting or handling.

(12) In addition to the recommended application of rotating sectored disks for attenuation of the radiation, it may be necessary to incorporate simple supplementary filters in vibrating capacitor electrometers.

Kunz followed these rules and showed that an EMI 9558 was linear to about ± 0.005 percent at final electrode currents from 0.03 to 20 nA with an overall gain of either 30 or 300 and using the fifth dynode as the final electrode.

Kunz's paper should certainly be consulted by anyone wishing to improve their radiometric techniques.

2. Improving Linearity Using a Sector—After developing the dynamic (beat frequency) method of measuring nonlinearity and finding the relationship between NL_D and NL_G, Jung [5] proceeded to describe two methods of increasing the linearity of radiation measurements. The first method is to attenuate the strongest, P_2, of the two radiations which are being compared, with a sector with an opening which is such that the open time, D_S, relative to the period, T, is given by $D_S = P_1 T / P_2$. With this arrangement, the average irradiance from P_2 which reaches the receiver is equal to $P_2 D_S / T = P_1$. With the assumption of eq (6) for the type of nonlinearity and using a Fourier treatment, Jung showed that $\epsilon_D / \epsilon = 0$ for $\omega\tau \to \infty$ and $\epsilon_D / \epsilon = 1$ for $\omega\tau \to 0$. In this case, ω is 2π times the chopping frequency, and τ is the time constant of the nonlinearity. The errors, ϵ_D and ϵ, are respectively, the nonlinearity errors in the measurement with and without the attenuating sector. Thus if the nonlinearity appears much faster than the chopping period, the sector will not reduce the error at all, but if the nonlinearity appears slowly relative to the chopping period, the sector will reduce the nonlinearity. Note that the nonlinearity assumed in eq (6) is a nonlinearity proportional to the flux.

3. Improving Linearity by Adding a Steady Flux to the Weakest Flux of Two Chopped Radiations—Since some receivers, such as the silicon diode measured in figure 14, have a nonlinearity which is not proportional to the irradiance, Jung developed another method of increasing linearity in a receiver which has a nonlinearity that appears very quickly. The apparatus for comparing the radiant flux from P_1 and

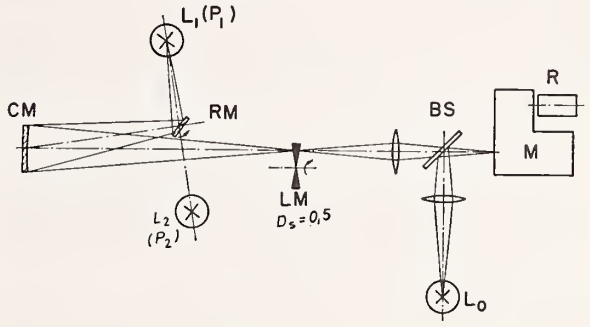

FIGURE 10. Optical arrangement for photometry of two radiances P_1 and P_2 selected by mirror RM. P_1 and P_2 are chopped. An adjustable radiation P_0 is added to the weaker radiation. (Courtesy, Z. Angew. Physik.)

P_2 by this method is illustrated in figure 10, taken from Jung. The rotatable mirror, RM, directs the radiation from either L_1 to L_2 to the concave mirror CM. The radiation is then chopped by LM, a 50 percent sector. During the time when radiation, P_1, from source, L_1, is falling on the receiver, R, radiation P_0 from L_0 is also incident on the receiver. P_0 is adjusted so the average chopped flux on the receiver from P_1 plus P_0 is equal to the average flux from P_2. The variation with

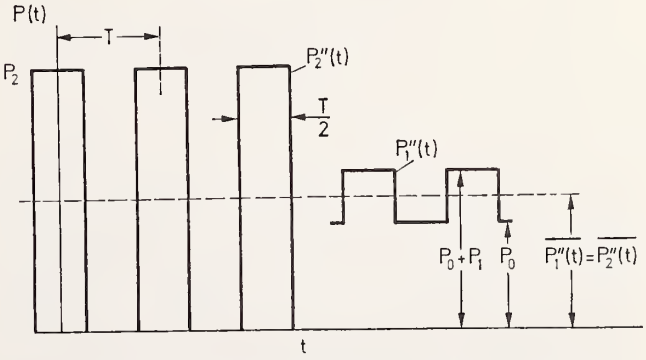

FIGURE 11. Time dependency of radiation on receptor. Radiations P_0, P_1 and P_2 are indicated. After chopping and recombination either $P_1''(t)$ or $P_2''(t)$ is incident on receptor. (Courtesy, Z. Angew. Physik.)

time of the incident flux on R is shown in figure 11. P_0, P_1, and P_2 indicate the steady fluxes. $P_1''(t)$ and $P_2''(t)$ indicate the respective incident flux depending on whether the mirror selects P_1 or P_2. The shutter on P_0 is also opened in the first case. A phase sensitive rectifier permits the chopped signal $P_1''(t)$ to be separated from the steady signal resulting from P_0. Again

Jung provided a theoretical treatment and showed that the nonlinearity should be eliminated completely if the nonlinearity is proportional to the flux.

If the photocurrent obeys eq (1), Jung showed that the quadratic part of the nonlinearity should be reduced by a factor of four.

Jung tested an EMI 9558 QB photomultiplier with the voltage divider network shown at the top of figure 12. This circuit provides a positive anode current-proportional nonlinearity of about $2 \times 10^{-3} \cdot \mu A^{-1}$ with a rise time of a little more than 1.3 ms. The rise time is caused by the capacitors across the last three stages. He used three methods of measurement:

(1) the usual dc superposition method,
(2) the superposition method where the combined beam was attenuated with a 50 percent sector,
(3) the dynamic method with the average frequency 206.5 Hz of the two signals.

The nonlinearity was measured over a wide range of anode currents. The respective results for the three

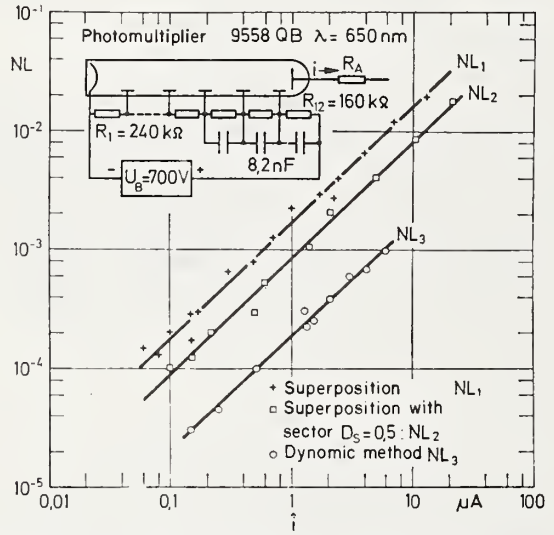

FIGURE 12. Jung's measurements of the nonlinearity of an EMI 9558 photomultiplier using 3 methods. (Courtesy, Z. Angew. Physik.)

methods are shown by NL_1, NL_2, and NL_3 in figure 12. The largest nonlinearity was measured by the first method. The sector attentuation of method 2 reduces the nonlinearity by a factor of 2. The dynamic method measures a nonlinearity less by a further factor of nearly 5. Jung showed that these results were consistent with the theory and indicated a rise time for the nonlinearity of 2.1 ms.

It remained for him to demonstrate experimentally that the method of providing equal average photocurrent by adding a steady flux to the weakest signal would produce improved linearity. For this purpose, he built the apparatus shown in figure 13. The equalization of average signal is accomplished by a voltmeter measuring the average voltage after IC, the impedance con-

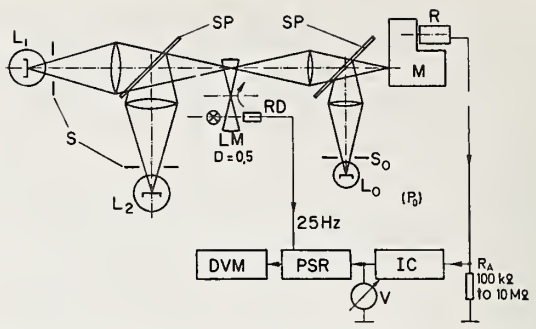

FIGURE 13. Apparatus for confirming the method of figure 10 by superposition. Radiation from sources L_1 and L_2 may be recombined or measured separately. Radiation from adjustable source L_0 is added until the voltmeter at the output of impedance converter IC reads a constant value. Phase sensitive rectifier PSR provides a signal to digital voltmeter DVM. Detector RD provides synchronization from chopper LM. (Courtesy, Z. Angew. Physik.)

verter. This is followed by PSR, the phase sensitive rectifier (controlled by a signal picked off RD, a detector, which is actuated by LM, the modulator) and a digital voltmeter. The results obtained by Jung are given

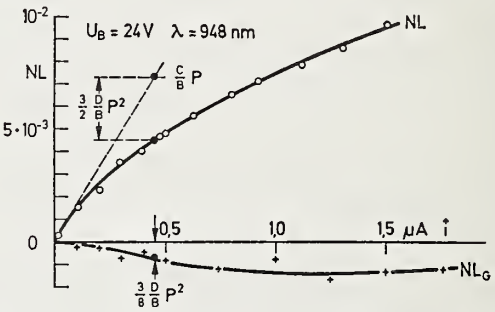

FIGURE 14. Jung's measurements of the nonlinearity of a silicon diode. NL for measurements by the dynamic method. NL_G for measurements with equalization of average current on the receptor. (Courtesy, Z. Angew. Physik.)

in table 4; column 1 shows the maximum anode current for each ratio of 2:1. Column 2 shows the nonlinearity for the method of figure 6, and column 3 the nonlinearity for the usual dc superposition method. The values in column 2 fluctuate in the range $\pm 0.2 \times 10^{-3}$, while the values in column 3 increase with anode current to 30×10^{-3} at 19 μA. We can see that Jung achieved a really vast improvement in linearity by maintaining the average light constant by adding a steady light during the presentation of the weaker flux.

After these measurements for a ratio of 1 : 2, Jung made measurements of P_1 relative to P_2 for ratios of 1 : 30 and 1 : 100. To obtain the true ratios, he measured i for each source without a modulator and corrected the i values using the values obtained from curve NL_1 of figure 12. The corrected ratio is given by

$$\frac{P_1}{P_2} = Q_= = \frac{i_1(1-NL_1(i_1))}{i_2(1-NL_1(i_2))}$$

The results for $Q_{=}$ are shown in column 4 of table 5. The ratio $Q_{\sim}$ from the use of P_0 to create constant average flux is formed without a correction of any kind. The values are given in column 6 of table 5. Column 7 shows the fractional difference between the two methods for the two flux ratios. These are respectively equivalent to agreeing in the measurement of transmittance of 0.03 to within 0.04 percent of the transmittance and agreeing in measuring a transmittance of 0.01 to within 0.06 percent of the transmittance.

TABLE 4

Max. Anode Current	Nonlinearity	
i μA	NL_0 (i = const)	NL_1 ($i \neq$ const)
0.20	$-0.18 \cdot 10^{-3}$	$0.35 \cdot 10^{-3}$
.40	.00	.70
.80	−.02	1.35
1.00	−.48	1.70
1.46	−.20	2.50
1.72	−.09	2.90
1.98	.21	3.30
2.78	.07	4.6
4.96	−.09	8.2
19.05	.10	30.0

pliers in photometry.

Finally, Jung applied the constant average light method to a silicon diode with a bias voltage of 24 V and obtained the points marked by crosses and the curve labelled NL_G in figure 13. The measurements for a ratio of 1:2 and using the usual dc superposition method are shown in figure 14 by circles and a curve marked *NL*. The values, NL_G, with a maximum of about 1.0×10^{-3} at 1 μA are much less in absolute value than the values *NL*. This shows that the equalization method also increases the linearity of receivers with curved nonlinearity characteristics. The nonlinearity may be high for a diode with a bias voltage applied. The bias makes the response fast and Jung may have used it biased for that reason.

4. Moatti [21] showed that in using a voltage divider network of equal resistors, to provide the voltages to the dynodes, one should expect a decrease of gain with anode current. Moatti suggested fixing the voltage from last dynode to anode. Lush [22] showed that this would produce an increase of gain with anode current and suggested introducing some resistance, in series with this fixed voltage, in the circuit from last dynode to anode. He showed that the optimum value of this resistance depended on the maximum anode current which would be drawn relative to the current in the voltage divider network. Land [31] experimented with the straight resistance network

TABLE 5

	D.C. method ($i \neq$ const)			Chopping method (i = const)		
	i μA	NL(i)	$Q_{=}$	i' μA	$Q_{\sim} = \frac{i_1}{i_2}$	$\frac{Q_{\sim}}{Q_{=}} - 1$
1	10.0909	$16.2 \cdot 10^{-3}$	32.295	10.0710	32.306	$0.34 \cdot 10^{-3}$
2	0.30756	$0.53 \cdot 10^{-3}$		0.31174		
1	12.2923	$20.0 \cdot 10^{-3}$	96.524	12.2048	96.580	$0.58 \cdot 10^{-3}$
2	0.12483	$0.22 \cdot 10^{-3}$		0.12637		

This is indeed a remarkable achievement, especially since one method requires no corrections for nonlinearity and the other requires a series of measurements of nonlinearity which must be combined to produce the final correction. It should be noted that Jung used vacuum tungsten strip lamps as sources with currents stabilized so their irradiance have a stability with time of 2×10^{-5}. The measurements were made with a photomultiplier at maximum currents up to 12 μA. Jung felt that the maximum measurement uncertainty was $\pm 0.7 \times 10^{-3}$ and resulted from noise and the nonlinearity of the phase-sensitive rectifiers.

If the procedure had been to add steady light to the weakest of two unchopped signals, in order to make a null reading, the added flux would need to be known to 0.0006 percent to achieve the same accuracy, but, in this constant average light method, P_0 need not be known. With the useful detail given by Jung we should all be able to make better use of photomulti-

and found that the changes in gain were about 1 percent if the ratio of the anode current to the current in the resistance network was less than 0.1. He suggested that this was good enough since instabilities would be this large.

W. Van de Stadt [32] in a short letter noted that "after exposure to a relatively high light flux (say, upwards of 10^3 times the NEP) the tubes exhibit 'memory', i.e. the anode current does not decrease to its previous dark current level after removal of the incident light flux. This memory effect may take several seconds to decay and is dependent in magnitude and duration on the light flux that generated it. The tube does recover to its original NEP given enough time."

Kunz [3] gave a detailed report on his experiences with dark current. His measurements on EMI 9558 photomultipliers gave results which indicate a time constant, of change in sensitivity after changing the incident flux, of between 8 and 16 min depending to

some extent on the anode current. The change of sensitivity was − 0.1 percent at 80 nA, − 0.4 percent at 330 nA and − 0.7 percent at 860 nA.

Kunz measured the dark current at the anode of an EMI 9558 photomultiplier tube with a gain of 300 and found that the dark current increased rapidly as the anode to last dynode voltage was increased. The anode current at 30 V was 1×10^{-12} A increasing to 5×10^{-12} A at 50 V. He found hysteresis with the current remaining higher, as the voltage was reduced, than it had been at the same voltage as the voltage was increased. When he measured the dark current at any of the dynodes from 5 to 10 he found that the hysteresis was reversed. The sign may be reversed because the dynodes emit photoelectrons, but the anode does not. However, on the dynodes the increase of dark current was fairly linear with last stage voltage. Because of the nonlinearity of dark current on the anode and because he found abrupt changes of anode dark current, Kunz preferred to use the measurements of current at one of the dynodes, rather than at the anode. He also wanted to use a low gain in most cases because he found it desirable to keep the current at the final stage below 30 nA.

5. Witherell and Faulhaber [11] discussed the operation of silicon diodes for photometric applications and gave data for silicon diode nonlinearity as a function of load resistance and cell current. They use the cell in the photovoltaic mode, i.e. without the bias used by Jung. They showed that the linearity improved by a factor of almost 15 for every decade decrease in load resistance. The nonlinearity also increased proportionally with cell current. With a load resistance of 1 Ω they found that the maximum nonlinearity was 0.1 percent for cell currents ranging from 50,000 nA to 0.5 nA.

For the short circuit condition the device is insensitive to temperature, about −0.1 percent/°C at 550 nm. They give the connections of the operational amplifier and also the properties of the amplifier and the cell which must be considered in using the cell in photometric applications. The bias voltage speeds up the response time so this will make Jung's measurements on the response time of the biased silicon diode inapplicable to the circuit used by Witherell and Faulhaber. Jung [4] measured at several wavelengths and found the nonlinearity of silicon diodes much more severe at long wavelengths. It would be interesting to know whether the same applies in the photovoltaic mode of operation.

6. Jones and Clarke [6] showed that it was possible to use a photomultiplier as a null device and thus to compare a larger flux, after transmission by a sector, with a weaker light which was unattenuated. They measured the opening in a adjustable sector by a photoelectric timing device. This method takes advantage of the fact that some receivers obey Talbot's Law, although they may be nonlinear when used to compare two steady irradiances of different size. The Jones and Clarke method can produce digital data directly from the timing procedure.

7. Jones and Sanders [33] showed that keeping the input voltage to an electrometer constant would improve the precision of measurements. This potentiometric method used an electrometer amplifier as a null device. It served at the same time to keep the voltage constant from cathode to anode of the vacuum photocell. This increased its linearity. The vacuum cell used had a cylindrical anode with the cathode at one end of the cylinder. The resultant device was precise and linear, but inconvenient to use since some knowledge of the signal was required in advance. Jones [34] later described a circuit which avoided this requirement and made it possible to measure accurately using a digital voltmeter. Similar techniques now use operational amplifiers.

8. Sauerbrey [35], in a private communication of his latest extension of Jung's method of constant average anode current, was able to show that with an average anode current of 10 μA on an EMI 9558 photomultiplier tube, it can be used with a nonlinearity of less than 0.1 percent. He investigated the effect of cathode-first dynode voltage, last dynode-anode voltage and second last dynode-last dynode voltage.

9. Schanda and Szigeti [36] showed that 50-W tungsten-halogen lamps with a single coil made by Tungsram were more stable in short term use than a 200-W lamp with a coiled-coil filament. The use of the former type could, therefore, improve results of spectrophotometry or spectroradiometry.

10. Davies [37] has recently shown that photomultipliers cleaned thoroughly, painted with silver paint which is connected to the cathode by a 10 MΩ resistor, and the use of the tube with no socket will reduce the dark current by as much as 1000 times. The dark current is more stable and is not increased after operation with anode currents up to 10 μA.

IV. Conclusions

The fundamental method of testing linearity is the superposition method. Several methods have been described and used to produce accuracies of 0.05 percent or better. Jung [4] has shown that nonlinearities can be measured quickly and precisely by a beat frequency method. His measurements do not always apply to the receptor as actually used, but his measurements suggested a method [5] of using receptors so they behave linearly or very nearly so. This method involves keeping the average anode current constant. The flux to be measured is chopped, a steady flux is added to the weaker and the alternating response is separated by a phase sensitive rectifier. The results are linear to 0.05 percent without correction for nonlinearity.

The accuracy of the phase sensitive rectifier may limit the accuracy of Jung's method. The accuracy and nonlinearities of the rectifier system would need

to be less than 0.01 percent if the error from this source is to be negligible.

Jung's method can only be used to measure steady radiation. For discharge lamps operated by ac, one might make a null comparison between a steady source and the periodic test source using one photometer. The steady source could then be measured using Jung's system. These measurements would need to be corrected for the residual nonlinearity as measured by the superposition method. This residual nonlinearity would be caused mainly by the increased space charges at higher photocurrents.

Sauerbrey has recently shown that with appropriate methods, a photomultiplier can be made to behave linearly, within 0.1 percent, at anode currents up to 10μA. This is in contrast to Kunz who used dc measurements and found that he needed to limit the maximum current to 0.03 μA on the last electrode to obtain results accurate to ± 0.005 percent.

Sauerbrey indicated that a photomultiplier tube which he tested did not obey the $1+e$ power function assumed by Hawes. It would, therefore, be advisable to check Hawes' assumption by the superposition method at several levels before using it in the Hawes' combination method.

For accurate measurements, tungsten strip filament lamps operating in a vacuum have been found necessary because of their better stability compared to gas filled lamps.

The receptor and its associated electronic circuit should be tested and used under the same conditions, if the measured nonlinearities are to be applicable. The nonlinearities are considerably altered by changing the resistance circuit in the dynode chain of the photomultiplier. Different resistance ratios are optimum for different types of tubes.

V. References

[1] Hawes, R. C., Technique for measuring photometric accuracy, Appl. Opt. **10**, No. 6, 1246–1253 (1971).

[2] Erminy, D. E., Scheme for obtaining integral and fractional multiples of a given radiance. J. Opt. Soc. Amer. **53**, 1448–1449 (1963).

[3] Kunz, H., Representation of the temperature scale above 1337.58 K with photoelectric direct current pyrometers, Metrologia **5**, No. 3, 88–102 (1969).

[4] Jung, H. J., Eine Dynamische Methode zur Messung der Nichtlinearitäten Fotoelektrischer Strahlungsempfanger. Z. Angew. Physik **30**, 338–341 (1971).

[5] Jung, H. J., Kompensation von Nichtlinearitäten bei Photoelektrischen Strahlungsmessungen. Z. Angew. Physik. **31**, 170–176 (1971).

[6] Jones, O. C. and Clarke, F. J. J., A new photometric technique using a variable shutter device, Nature **191**, 1290 (1961).

[7] Sanders, C. L., A photocell linearity tester. Appl. Opt. **1**, 207–211 (1962).

[8] Rotter, F., Die Prüfung der Linearität von Strahlungsempfängern, Z. Instr. **73**, 66–71 (1965).

[9] Preston, J. G., McDermott, L. H., The illumination-response characteristics of vacuum photoelectric cells of the Elster-Geitel Type, Proc. Phys. Soc. (London) **46**, Part 2, No. 253, 256–272 (1934).

[10] Boutry, G. A., and Gillod, P., Studies in Photoelectric Photometry. A Photoemissive Cell Specially for High Precision Measurements. (Laboratoire d'Essais Publications), No. 43, 32 (1939).

[11] Witherell, P. G., and Faulhaber, M. E., The Silicon Solar Cell as a Photometric Detector, Appl. Opt. **9**, 73 (1970).

[12] Reule, A., Testing Spectrophotometer Linearity. Appl. Opt. **7**, 1023–1028 (1968).

[13] Hansen, G., Prüfung der Fotometrischen Funktion von Spectralphotometern. Mikrochimica Acta, Heft 2/3, 410–415, (1955).

[14] Mallick, E., Measurement of the Degree of Coherence in Nonmonochromatic Light. Appl. Opt. **8**, 2501–2504 (1969).

[15] Born, M., and Wolf, E., Partially Coherent Light, Sec. 10.4.3 in Principles of Optics, p. 513, 4th Edition (Pergamon Press, New York, 1970).

[16] Mielenz, Klaus D., and Eckerle, Ken L., Spectrophotometer linearity testing using double-aperture method, Appl. Opt. **11**, 2294 (1972).

[17] Bures, J., and Delisle, C., Comptage des Photoélectrons Provenant de Points Statistiquement Indépendents et d'une Surface Etundue de Ia Photocathode. Can. J. Phys. **49**, 1255–1262 (1971).

[18] Slo-Syn Numerical Tape Control, Superior Electric Co., Bristol, Connecticut.

[19] Sanders, C. L. and Gaw, W., A versatile spectroradiometer and its applications, Appl. Opt. **6**, 1639–1647 (1967).

[20] Nonaka, M. and Kashima, T., Linearity characteristics of multiplier phototubes, Japan. J. of Appl. Phys. **2**, 785–791 (December 1963).

[21] Moatti, P., Linearité des Photomultiplicateurs. Effet des Courants de Dynodes. L'Onde Electrique XLIII, 787–793, July–August (1963).

[22] Lush, H. J., Photomultiplier linearity, J. Sci. Instr. **42**, 597–602 (1965).

[23] Bischoff, K., Die Messung des Proportionalitätsverhaltens von Strahlungsempfängern uber groβe Bestrahlungsstärkebereiche. Z. Instrum **69**, 143–147 (1961).

[24] Blevin, W. R., Diffraction losses in radiometry and photometry. Metrologia **6**, 39–44 (1970).

[25] Keegan, H. J., Schleter, J. C., and Judd, D. B., J. Res. Nat. Bur. Stand. (U.S.) **A66**, 203 (1962).

[26] Robertson, A. R. and Wright, W. D., International Comparison of Working Standards for Colorimetry, J. Opt. Soc. Amer. **55**, 685–706 (1965).

[27] Clarke, F. J. J., Ceramic Color Standards—An aid for industrial control, Printing Technology Magazine **13**, 101–113 (1969).

[28] Bressani, T., Brovetto, P., Rucci, A., A method for testing the linearity of a photomultiplier, Nucl. Instr. and Methods **53**, 41–44 (1967).

[29] Lee, R. D., The NBS photoelectric pyrometer and its use in realizing the International Practical Temperature Scale above 1063 °C, Metrologia **2**, 150–162 (1966).

[30] Edwards, J., and Jeffries, R. J., Automatic Linearity Tester for Photodetectors, J. Phys. E, Sci. Instr. **3**, 518–520 (1970).

[31] Land, P. S., A discussion of the region of linear operation of photomultipliers, Review of Scientific Instruments **42**, 420–425 (1971).

[32] Van de Stadt, W., Some remarks on photomultiplier tube behavior. Elec. Eng. **41**, 61 (1969).

[33] Jones, O. C., and Sanders, C. L. A High Precision Photoelectric Photometer. J. Opt. Soc. of Amer. **51**, 105–108 (1961).

[34] Jones, O. C., An impedance converter for use with digital voltmeters, J. Sci. Instr. **40**, 196–197 (1963).

[35] Sauerbrey, G., Private communication from PTB, Braunschweig, Germany.

[36] Schanda, J., and Szigeti, G., Stability of High Color Temperature Etalon Lamps, Preprint Paper No. 71.27 of Proceedings of CIE Session, Barcelona (1971).

[37] Davies, W. E. R., Reduction of dark current in photomultiplier tubes, Rev. Sci. Instrum. **43**, 556 (1972).

(Paper 76A5–731)

NATIONAL BUREAU OF STANDARDS SPECIAL PUBLICATION 378, Accuracy in Spectrophotometry and Luminescence Measurements, Proceedings of a Conference Held at NBS, Gaithersburg, Md., March 22–24, 1972 (Issued May 1973).

Physical Parameters in High-Accuracy Spectrophotometry

K. D. Mielenz

Optical Physics Division, Institute for Basic Standards, National Bureau of Standards, Washington, D.C. 20234

(May 31, 1972)

The measured apparent transmittance T_A of a filter or liquid sample depends on the beam geometry in the spectrophotometer. For focused light incident upon the sample, T_A is different for systems having different f-numbers, and also depends on the state of polarization of the light. These effects are eliminated when the incident light is collimated; in this case T_A approaches the "true" transmittance τ of the sample. Both modes of operation suffer from stray light and interference effects. The former may be reduced significantly by using mirror rather than lens optics, and the latter by suitable choice of the monochromator slit width. A new spectrophotometer based upon the above-mentioned design principles is described. The photometric precision of this instrument is shot-noise limited, permitting measurements to better than 10^{-4} transmittance units.

The double-aperture method of testing detector linearity to this level of precision is discussed. The conventional method of finding the nonlinearity correction can be replaced by a curve-fitting procedure giving better precision. Data on detector nonlinearity, and its dependence on wavelength, are presented.

Key words: High accuracy spectrophotometry, physical parameters; linearity test of photodetector; spectrophotometry, high accuracy.

1. Introduction

When the same sample is measured with two spectrophotometers the results often disagree by amounts several times greater than the precision of either instrument. An example of this is given in table 1, summarizing a recent NBS in-house intercomparison of two spectrophotometers both of which have precisions well below 10^{-4} transmittance units. When the measurements were repeated, it was found that the

Table 1. Results of comparative filter measurements. The high-accuracy spectrophotometers described in reference [1] and in this paper were used for this test

	Measured transmittance				Range of nonuniformity of filter (635 nm)
	440 nm	465 nm	590 nm	635 nm	
10% Filter					
Lab 1	0.1159	0.1356	0.1037	0.1136	
Lab 2	0.1145	0.1339	0.1024	0.1122	0.0005
Diff.	+0.0014	+0.0017	+0.0013	+0.0014	
20% Filter					
Lab 1	0.1980	0.2259	0.1916	0.2060	
Lab 2	0.1980	0.2259	0.1916	0.2061	0.0004
Diff.	0.0000	0.0000	0.0000	0.0001	
30% Filter					
Lab 1	0.3287	0.3553	0.3113	0.3255	
Lab 2	0.3289	0.3557	0.3115	0.3258	0.0001
Diff.	−0.0002	−0.0004	−0.0002	−0.0003	

filters were slightly inhomogeneous. This inhomogeneity is too small to account for the relatively large discrepancies for the 10 percent filter, but large enough to dismiss the agreement on the 20 percent filter as fortuitous, since no attempt had been made to measure the same area of these filters. Furthermore, the filters were found to be slightly dichroic in one laboratory, but not in the other. A similar interlaboratory test, which led to a small residual bias of roughly the same magnitude, is reported in reference [1].[1]

For the purposes of routine spectrophotometry, the level of agreement of these measurements is quite satisfactory, but not from the point of view of high-accuracy spectrophotometry. With well-designed modern spectrophotometers, it is possible to achieve repeatabilities of a few 10^{-5} transmittance units. Anyone using such advanced instrumentation cannot ignore discrepancies as large as those mentioned. As other cooperative tests have shown before [2], the above-mentioned results indicate that a part of the discrepancies must be attributed to the samples used. In view of this difficulty, spectrophotometric accuracy cannot be assessed by interlaboratory tests alone. In order to separate the effects of sample and instrument, it is necessary to identify the various possible sources of systematic errors for each of the spectrophotometers involved, and to take them into account before comparing results.

The main emphasis of this paper is on systematic errors due to beam geometry. It will be shown that different spectrophotometers are, indeed, likely to give different results. Conversely, it is entirely possible to obtain agreement between two instruments of similar design, but what was measured may not have been a meaningful material property of the sample.

Some of the beam-geometry errors are calculable by straightforward application of optical physics. These may be eliminated by numerical correction of the measured results. In other cases, the magnitude of the error must be determined experimentally. Ideally, a high-accuracy spectrophotometer should have off-axis mirror optics, and all measurements should be made in parallel light. Nevertheless, it is possible, although significantly more difficult, to perform accurate measurements using a conventional focused-beam spectrophotometer with lenses. Both types of instruments may suffer from systematic errors due to interference.

The particular samples discussed are glass filters, because these appear to be the most commonly used transfer standards for assessing spectrophotometric accuracy. A definition is given of what might be considered the 'true' transmittance of an ideal filter, followed by a discussion of some of the pitfalls of real filters.

The necessity to eliminate the systematic error due to nonlinear detector response is well recognized. It will be shown that the double-aperture [3] method can be adapted to yield the additive nonlinearity correction to $\pm 1 \times 10^{-5}$ transmittance units.

II. A New Spectrophotometer

Most of the measurements reported in this paper were performed with a new single-beam spectrophotometer designed as a research tool for spectrophotometric measurements with an accuracy exceeding that of conventional systems. The instrument is described elsewhere [4, 5] in greater detail; its design is shown schematically in figure 1.

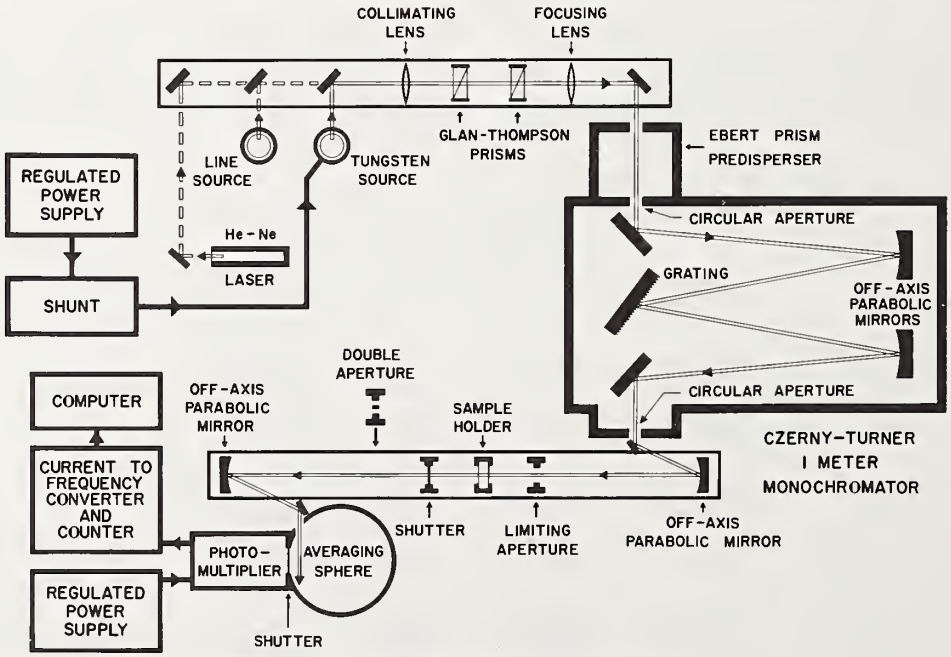

FIGURE 1. High-accuracy spectrophotometer.

[1] Figures in brackets indicate the literature references at the end of this paper.

The monochromator is an f/8.7 Czerny-Turner system with 1-m off-axis parabolic mirrors and a 1200-lines/mm plane grating blazed for 500 nm. The entrance and exit 'slits' are interchangeable circular apertures with diameters ranging between 0.25 and 1 mm, so that the exit aperture approximates a point source having a spectral band pass between 0.2 and 0.8 nm when the grating is used in the first order. This light is collimated by a 195-mm off-axis parabolic mirror, and focused into the detector by another. These two mirrors are mounted at the ends of a 120-cm precision optical bench; the space between them constitutes the sample compartment of the spectrophotometer. It will become apparent in this paper that this design; namely, the exclusive use of off-axis mirror optics, and the placement of the sample in a collimated and linearly polarized beam, constitutes the optimal beam geometry for high-accuracy spectrophotometry.

A large sample space was provided in this spectrophotometer, so that the beam geometries of other instruments can be simulated by means of lenses placed in the collimated beam. Several of the measurements reported in this paper were performed in this manner.

The light source is a tungsten ribbon lamp, rated for 6V and 18A, and connected to a regulated power supply using external sensing on a 0.1 Ω shunt rated for 50 A. Except for a possible linear drift in time, the radiant-flux output of this source is constant to better than 0.01 percent for periods of the order of 20 min. The flux into the monochromator is varied by variation of the lamp current or rotation of the first of the two Glan-Thompson prisms shown in figure 1. The second Glan-Thompson prism defines the state of polarization of the light. The source is focused on the entrance slit of the Ebert prism predisperser which precedes the grating monochromator.

A 2-mW helium-neon laser was installed in the system for alignment purposes, and spectral lamps are provided for calibration of the wavelength scale to a 0.02-nm accuracy.

The detector is an end-on photomultiplier tube attached to a 15-cm averaging sphere with an estimated efficiency of 20 percent. The photomultiplier tube has an S−20 cathode and 11 stages; the dynode chain is linear with a Zener diode between cathode and first dynode. Its power supply is voltage-regulated to 0.001 percent, and the anode current is measured by a current-to-frequency converter similar to that described by Taylor [6]. This converter and its associated high-precision counter were found to be linear to better than one part in 10^4, and to have a full-scale repeatability less than two parts in 10^5. The counter integrates over a 10-s interval.

The counter signals are recorded automatically on punched paper tape by means of a data acquisition and control system, which is also used as a computer terminal to process the recorded data.

Upon construction of the spectrophotometer, a series of tests was undertaken to determine its photometric precision. The signal currents generally drifted in time and exhibited random fluctuations superimposed upon this drift. Since all quantities measured with a spectrophotometer are ratios, the drift is of no concern provided it is linear in time, and provided that all readings are taken at fixed time intervals. Under these conditions the quantity affecting the precision of transmittance measurements is the standard deviation,

$$dI=\left\{\sum_{\nu=1}^{n}[I_\nu-I(\nu t)]^2/(n-1)\right\}^{1/2} \tag{1}$$

where $I_1, I_2, \ldots I_n$ are n successive readings of the same signal current I, and $I(\nu t)$ is their expectation value, obtained from a least-square fit of the measured data as a linear function of time, t.

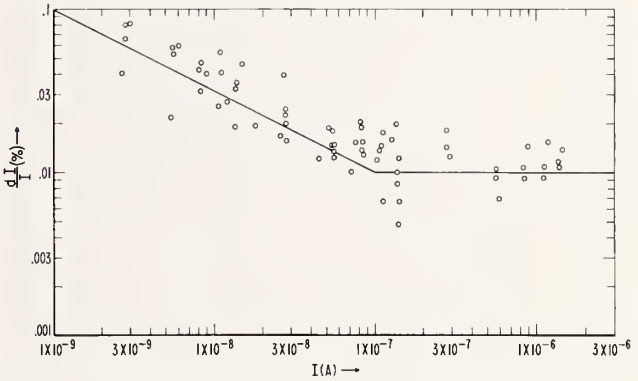

FIGURE 2. Photometric precision dI/I of spectrophotometer versus signal current I.

When plotted as shown in figure 2, the random error, dI, so defined, was found to be primarily a function of the signal current, I, itself independent of the particular combinations of lamp current, flux attenuation, wavelength, and photomultiplier dynode voltage used to produce any particular value of I. As indicated by the solid line, the relationship between dI and I is, approximately,

$$dI/I=\begin{cases}\sqrt{10/I}\times 10^{-7} & \text{if } I<10^{-7}\text{ A}, \quad (2a)\\ 10^{-4} & \text{if } I>10^{-7}\text{ A}, \quad (2b)\end{cases}$$

The low-current branch (2a) of this curve is due to photomultiplier shot noise. The limiting value (2b) for large signal currents is attributed to lamp noise.

Equations (2a, b) can be used to predict the random error,

$$dT=\left[\left(\frac{dI}{I}\right)^2+\left(\frac{d(TI)}{TI}\right)^2\right]^{1/2}, \tag{3}$$

with which this spectrophotometer will perform transmittance measurements. The result is that the standard deviation of a single measurement of transmittance is of the order of 10^{-4} transmittance units or less, provided that the signal current, I, for the 100

percent point of the transmittance scale is chosen to be equal or greater than 10^{-7} A. Measurements based on a series of repeated readings will then be reproducible to within a few 0.00001 transmittance units. This expectation was verified directly, when separate transmission measurements of neutral-density glass filters with nominal transmittances of 0.1, 0.2, and 0.3 were found to be repeatable to ± 0.00004.

III. The 'True' Transmittance of a Filter

The optical transmittance of a given sample,

$$T = \frac{\text{transmitted radiant flux}}{\text{incident radiant flux}}, \tag{4}$$

is not a well-defined property of matter. It depends on the form of the sample, on the path which the light travels, and is also a function of the polarization and degree of coherence of the light. Thus, it cannot serve a useful purpose in spectrophotometry unless constraints are imposed on sample and light beam so that the above ratio of fluxes is reduced to a meaningful material property. In the following, this limiting form of the optical transmittance, T, will be referred to as the 'true' transmittance, τ, of the sample.

As an example, consider an ideal glass filter; that is, a plane-parallel slab of homogeneous material of complex refractive index $\hat{n} = n(1 + i\kappa)$ and thickness,

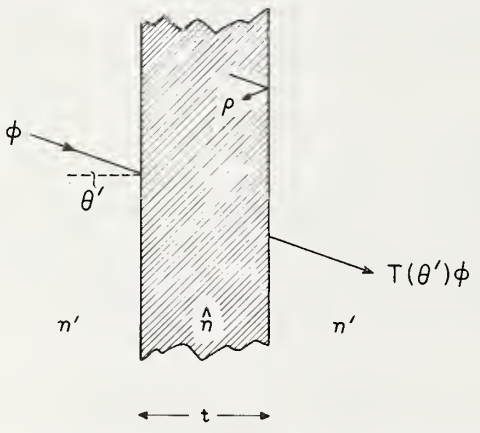

FIGURE 3. Notation used in calculating the transmittance of a filter.

t, bordered by identical media with refractive index, n', and illuminated by a linearly polarized plane wave of wavelength λ and angle of incidence θ' (fig. 3). Its optical transmittance is [7]

$$T(\theta') = \left| \frac{(1-\rho^2)e^{i\beta}}{1-\rho^2 e^{2i\beta}} \right|^2 \tag{5a}$$

where ρ is the appropriate Fresnel coefficient of amplitude reflection at each of the two boundary surfaces, given by

$$\rho_\perp = \frac{n' \cos\theta' - \hat{n} \cos\hat{\theta}}{n' \cos\theta' + \hat{n} \cos\hat{\theta}} \tag{5b}$$

for S-polarization and

$$\rho_\parallel = -\frac{n' \cos\hat{\theta} - \hat{n} \cos\theta'}{n' \cos\hat{\theta} + \hat{n} \cos\theta'} \tag{5c}$$

for P-polarization. Furthermore,

$$\beta = (2\pi/\lambda) t \hat{n} \cos\hat{\theta}, \tag{5d}$$

with $\hat{\theta}$ defined by Snell's law,

$$\hat{n} \sin\hat{\theta} = n' \sin\theta'. \tag{5e}$$

These equations indicate that T is a function of the angle of incidence and state of polarization of the light. Therefore, different transmittances may be measured for the same sample with spectrophotometers for which the angles of light incidence are different. In addition, the measured transmittance may vary when the polarization of the light is varied, so that a nonpolarizing filter may exhibit an instrument-dependent, apparent dichroism.

Equation (5a), which is based on the assumption of perfectly coherent light, also leads to an interference term. In practice, the degree of coherence of the light is different for different spectrophotometers, so that the actually observed interference effect will be more or less subdued. This may lead to further instrumental discrepancies of measured transmittances.

These sources of error are eliminated when transmittance is measured in collimated light at normal incidence, and under conditions such that interference is negligible. Then, eq (5a) is reduced to

$$T(0) = \frac{(1-r)^2 \tau_i}{1 - r^2 \tau_i^2} \equiv \tau, \tag{6a}$$

where r is the energy reflectance at normal incidence, given by

$$r = |\rho_\perp|^2 = |\rho_\parallel|^2 = \left| \frac{n' - \hat{n}}{n' + \hat{n}} \right|^2 \tag{6b}$$

for either state of polarization, and where

$$\tau_i = e^{-4\pi n \kappa t/\lambda} \tag{6c}$$

is the internal transmittance of the filter for normal incidence.

Equation (6a) is a function of the filter parameters, $\hat{n}$ and t, only [8], and may therefore be identified as the above-mentioned 'true' transmittance, τ, of the filter. Any departures of measured transmittance from this value of τ are to be considered errors.

IV. Requirements for Standard Filters

A few simple conclusions from eqs (6a, b, c) may serve here to demonstrate some of the difficulties in assessing spectrophotometric accuracy by measuring the same sample in different laboratories.

Differentiation of eq (6c) shows that the variation of τ_i due to a variation of sample thickness, t, is

$$\Delta\tau_i = \tau_i(\ln \tau_i)\Delta t/t, \tag{7}$$

which has an extreme value, $\Delta\tau_i = -0.37\Delta t/t$, if $\tau_i = 0.37$. Hence, it may be seen that t must be constant to at least 0.5 μm if the transmittance of a 2-mm thick filter is to be constant to 10^{-4} transmittance units. The filter must be plane-parallel to 0.1 milliradians if this requirement is to be satisfied over a 5-mm area. Equally stringent requirements must, of course, be imposed on the homogeneity of the filter material.

The importance of proper sample handling and cleaning may be illustrated by assuming the presence of a thin contaminating layer of thickness, t_1, and refractive index, n_1, on the filter surfaces. In this case, the Fresnel reflectance, r, in eq (6a) must be replaced by [9]

$$r_1 = \frac{n_1^2(n'-n)^2 + (n_1^2-n'^2)(n_1^2-n^2)\sin^2(x/2)}{n_1^2(n'+n)^2 + (n_1^2-n'^2)(n_1^2-n^2)\sin^2(x/2)}$$

$$\sim \frac{(n'-n)^2}{(n'+n)^2}\left\{1 + \frac{4n'n(n_1^2-n'^2)(n_1^2-n^2)}{n_1^2(n'-n)^2(n'+n)^2}\sin^2(x/2)\right\} \tag{8a}$$

where

$$x = 4\pi n_1 t_1/\lambda, \tag{8b}$$

and where it was assumed that $\kappa \ll 1$ and that $(n_1^2-n'^2)(n_1^2-n^2)/n_1^2(n'+n)^2$ is a small number [10]. In practice, the film may be water ($n_1 \sim 1.33$), oil ($n_1 \sim 1.47$), or some similar contaminant, so that $n_1 \sim 1.4$ may be taken as an average representative number. If $n' \sim 1$ and $n \sim 1.5$, then $r_1 \sim r - 12\sin^2(x/2)$, with r as the Fresnel reflectance (6b) of the uncontaminated surfaces. Hence, it is seen that the film acts as an antireflection coating; its effect on transmittance will be less than 10^{-4} transmittance units only if $2(r-r_1) \leq 10^{-4}$. According to (8b), the corresponding tolerance on the film thickness is $t_1 \leq 2\ 10^{-3}\ \lambda$, so that a layer only a few molecules thick may be troublesome. Repeated cleaning is likely to leave residual layers of at least this magnitude on the filter surfaces. A similar difficulty arises from the fact that the surfaces may gradually become leached by certain cleansing agents. The additional problem of dust is too well known to deserve more than passing mention at this point.

These examples show the large effect that inadequate samples and sample handling techniques may have on interlaboratory comparisons. Efforts are being made to develop more homogeneous filter materials, and to grind and polish them with greater precision, [11]. In the meantime some improvement may be achieved by more elaborate calibration procedures; for example, the calibration of a standard filter should be done by mapping. The filters must be cleaned with properly selected chemicals. They should also be recalibrated periodically, so that the user is made aware of any surface damage or accumulation of residual layers.

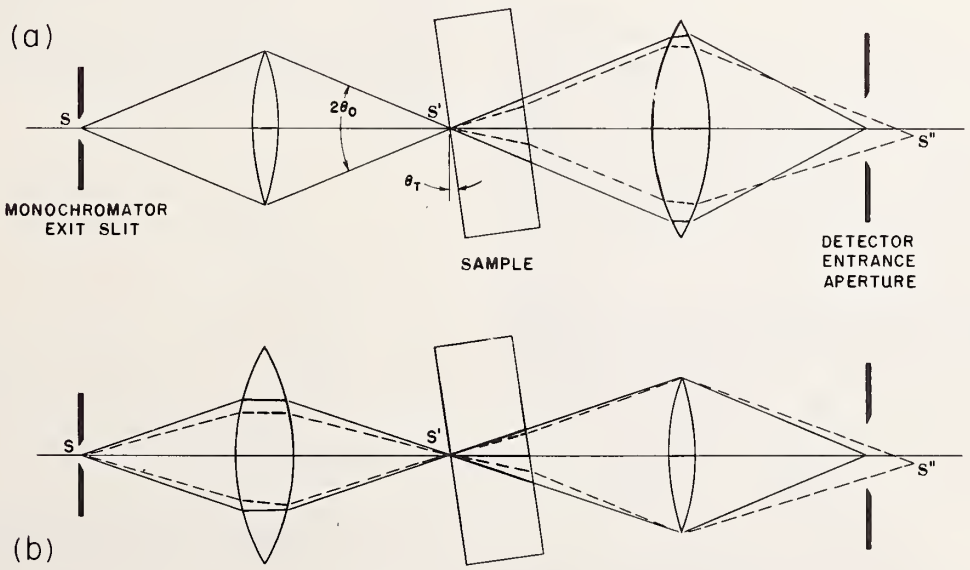

FIGURE 4. Path of light in focused-beam spectrophotometer before (———) and after (– – – – –) sample was inserted, and with (a) the first lens, and (b) the second lens as the limiting aperture.

V. Beam-Geometry Effects

The sample compartment of many spectrophotometers is designed as shown in figure 4, where the monochromator exit slit is focused into the sample by a lens, and is refocused into the detector by another. This beam geometry is preferred by most designers for intensity reasons (all of the flux from the slit is passed through the sample), but it will not yield the 'true' transmittance τ of eq (6a). The major systematic errors inherent in this design are due to beam displacement, interreflections, and oblique light incidence. These errors will be discussed now, in order to establish the conditions for which they are either negligibly small or may be eliminated by numerical correction.

A. Beam-Displacement Errors

The solid lines in figures 4a, b, show the path of light in a focused-beam spectrophotometer without the sample. As indicated by the broken lines, the sample shortens the effective distance between the intermediate slit image, S', and the second lens by an amount $t(1-1/n)$, so that the final slit image, S'', is shifted towards the detector. If the sample is not normal to the optic axis, S'' will also be shifted laterally. This causes different areas of the detector surface to be illuminated before and after the sample was inserted and, therefore, leads to errors because most detectors show a variation of sensitivity with illuminated area. This error must be avoided by passing the light through an averaging sphere before it reaches the detector. While this is a well-recognized fact, it is surprising that even some of the more elaborate commercial spectrophotometers are not equipped with averaging spheres. The inefficiency of spheres in some portions of the spectrum is no adequate reason not to use them at all.

Another error arises when the second lens is the limiting aperture of the beam, as in figure 4b. In this case, the insertion of the sample changes the effective aperture of the first lens, such that it collects less light than without the sample, resulting in too low a measured transmittance. It is easy to show, by measurements with either lens as the limiting aperture, that this error may be quite large. The results of such meaurements, listed in table 2, demonstrate the necessity to underfill the second lens.

TABLE 2. Measured transmittance of three neutral-density filters in focused light with (a) the first lens, and (b) the second lens as the limiting aperture (f/5)

(a)	(b)	(a)−(b)
0.10399	0.10303	0.00096
.31362	.31211	.00151
.58981	.58588	.00393

B. Interreflection Errors

Before the sample is inserted into the beam of a spectrophotometer with lenses, the radiant flux propagated toward the detector is, according to figure 5a,

$$\phi = T_1T_2(1 + R_1R_2 + \ldots), \tag{9a}$$

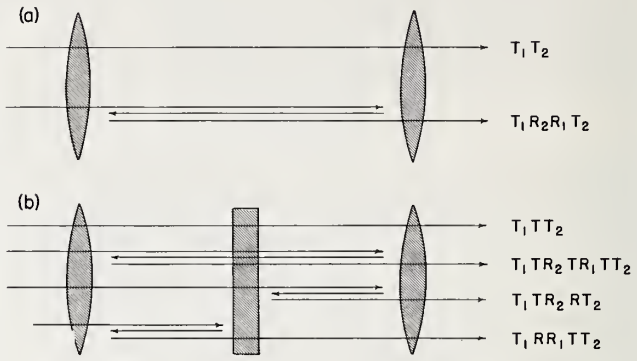

FIGURE 5. Reflected beams in a spectrophotometer with lenses.

where T_1, T_2, R_1, and R_2 are the transmittances and reflectances of the two lenses, and where any contributions due to four or more reflections are considered negligibly small. When the sample is placed in the beam, the transmitted flux is, as indicated in figure 5b,

$$\phi' = T_1TT_2(1 + R_1R_2T^2 + RR_2 + R_1R + \ldots), \tag{9b}$$

with T and R as the transmittance and reflectance of the sample.

As may easily be seen by measuring a sample with and without two clear glass plates on either side of it, the discrepancy between the ratio of these two fluxes and the transmittance, T, of the sample may be quite large. The results of such a measurement are plotted in figure 6, according to which the error is a monotonic function of transmittance and approaches 0.01 transmittance units for large values of T. This experiment represents a particularly bad case, but nevertheless, illustrates the seriousness of interreflection errors.

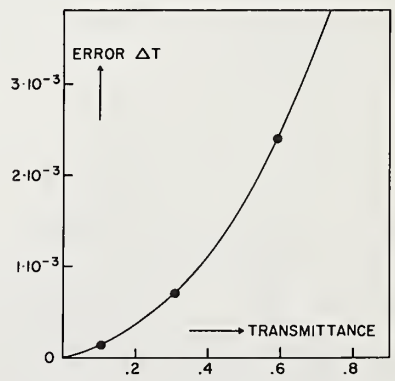

FIGURE 6. Difference ΔT in transmittance for three filters, measured between two clear glass plates and without them.

The main cause of the error is the fact that the insertion of the sample creates the two additional beams shown at the bottom of figure 5b. As is well known, these two beams may be prevented from reaching the detector by tilting the sample. This is indicated in figure 7 for the component reflected from the front surface of the sample and returned by the first lens. If this lens is biconvex, the light is focused into a real image, S_1, by the first surface of the lens, and into a virtual image, S_2, by the second. The

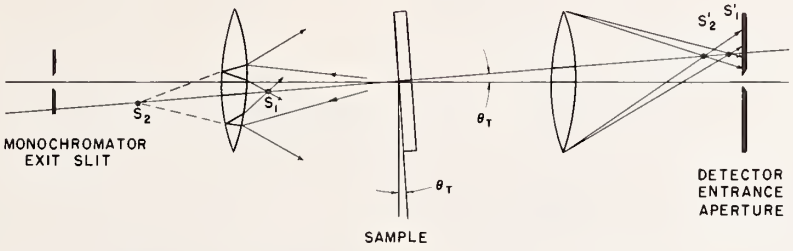

FIGURE 7. Elimination of interreflections by sample tilting.

right-hand side of the figure shows the corresponding images, S_1' and S_2', formed by the second lens, as well as the cones of light that must not pass through the detector entrance aperture. Figure 7 deals with only two of the eight ghost images thus formed, but it is clear that they all lie on the straight line shown, intersecting the optic axis at the tilt angle θ_T. Thus, it is always possible to eliminate the two bottom beams in figure 5b by sufficiently tilting the sample.

Just how much tilt is required is a very complicated function of beam geometry, and is best decided experimentally by measuring transmittance versus tilt angle until a plateau is reached. Such tests should be done under well-defined conditions for which the interreflection effect is large. A semireflecting nonabsorbing sample may be used. In this case the error, $(\phi'/\phi)-T$, is largest when $R=(1-T)=0.5$. According to figure 6, a clear glass or quartz plate also gives a large effect. In both cases, the dependence of reflectance on angle of incidence and polarization must be taken into account; otherwise a plateau may not be found. This is illustrated in figure 8. A 2-mm quartz plate was used, and data were taken for both, S and P polarization in the tilt plane of the sample [12]. According to section 5.3, below, the average of the S and P data is theoretically independent of angle for small values of θ_T. Thus, the figure indicates that a tilt angle of approximately 3° is necessary for this particular instrument.

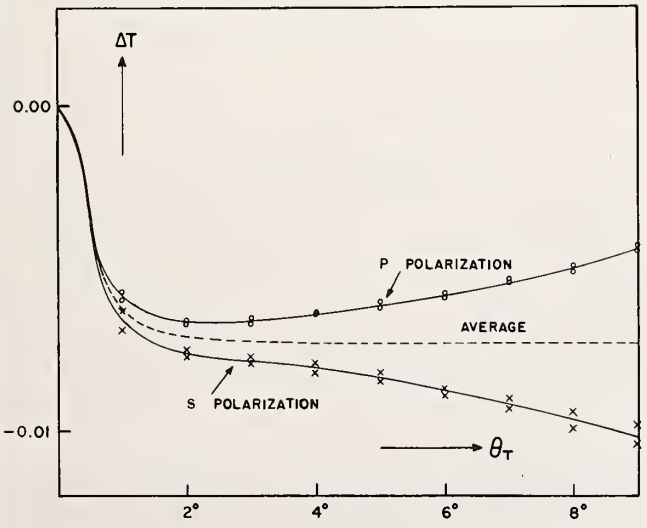

FIGURE 8. Difference ΔT in measured transmittance versus tilt angle for clear glass sample between lenses.

When enough tilt was introduced, the last two terms in eq (9b) may be omitted. Then the ratio of the two fluxes received by the detector becomes

$$\phi'/\phi = T\,\frac{1+R_1R_2T^2+\ldots}{1+R_1R_2+\ldots}$$

$$= T[1-R_1R_2(1-T^2)+\ldots]. \qquad (10)$$

The residual interreflection error given by this equation, is due to the fact that the direct beam in figure 5b has passed the sample once, whereas the remaining interreflected beam has passed it three times. This error cannot be eliminated by tilting.

Representing amounts of light which actually reach the detector, the quantities R_1 and R_2 in eq (10) are rather complicated functions of beam geometry. Nevertheless, it is clear that the residual error has a maximum, $T-\phi'/\phi=0.38\,R_1R_2$ for $T=0.577$, and, therefore, remains below 10^{-4} transmittance units as long as $\sqrt{R_1R_2}\leq 0.016$. In spite of the difficulty to assign numerical values to R_1 and R_2, it is likely that well-coated lenses will meet this requirement. Whether or not this is the case can be ascertained by means of a standard sample of about 60 percent transmittance which was calibrated on a lensless spectrophotometer.

C. Obliquity Errors

When defocusing and interreflection effects are eliminated, the remaining beam-geometry error of focused-beam spectrophotometers is due to oblique light incidence.

502-591 O - 73 - 7

Since θ' and $\hat{\theta}$ are small angles, and since the extinction coefficient, $n\kappa$, is also small, we have

$$\rho_\perp = \frac{n' - n}{n' + n}[1 + (n'/n)\theta'^2]. \tag{11a}$$

$$\rho_\parallel = -\frac{n' - n}{n' - n}[1 - (n'/n)\theta'^2]. \tag{11b}$$

as obtained by Taylor expansion of eqs (5b, c) to second order in θ' and θ, using Snell's law (5e), and letting $\hat{n} \sim n$. Similarly, eq (5d) leads to

$$\beta = (2\pi/\lambda)nt\,\{[1 - 1/2(n'\theta'/n)^2] + ik[1 + 1/2(n'\theta'/n)^2]\}, \tag{11c}$$

when second-order terms in κ are neglected.

With these approximations, the 'true' transmittance of eq (6a) becomes

$$\tau = \frac{(1 - r)^2\tau_i}{1 - r^2\tau_i^2} \tag{12a}$$

with τ_i as given by (6c) and

$$r = \left(\frac{n' - n}{n' + n}\right)^2. \tag{12b}$$

Similarly, eq (5a) is reduced to

$$T[\theta'] = \tau(1 + \gamma_i\theta'^2 \pm \gamma_r\theta'^2), \tag{13a}$$

$$\gamma_i = 1/2(n'/n)^2 \ln \tau_i, \tag{13b}$$

$$\gamma_r = 4(n'/n)r, \tag{13c}$$

where the upper and lower signs in (13a) pertain to S and P polarization, respectively, and where the interference term was again averaged. All terms in r^2 appearing in (13b, c) were neglected.

The two sources of error; namely, a decrease of internal transmittance due to increased path lengths at oblique incidence, and dependence of Fresnel reflectance on angle of incidence, appear as the separate terms involving γ_i and γ_r in (13a). These will be discussed in the following two sections.

1. Path-Length Error—In a focused-beam spectrophotometer, the average path of light through the sample is a function of the sizes and shapes of the monochromator exit slit and of the effective aperture of the focusing lens. In the following, it will be assumed that the slit is sufficiently short to be treated as a point source, and that the lens is underfilled so that the beam cross-section is rectangular because of the rectangular grating or prism aperture. For simplicity, the aperture will be assumed to be square, subtending the same angle $2\theta_0$ in both the horizontal and vertical planes. Furthermore, it will be assumed that the sample is tilted only in one of these planes. As before, the tilt angle will be denoted by θ_T.

Under these conditions, the average value of the squared angle of incidence θ'^2 in the tilt plane is, according to figure 4a,

$$(\theta'^2)_{av} = \frac{1}{2\theta_\delta}\int_{\theta_T - \theta_0}^{\theta_T + \theta_0} \theta'^2 d\theta' = 1/3(\theta_0^2 + 3\theta_T^2). \tag{14a}$$

In the remaining plane there is no tilt, so that

$$(\theta'^2)_{av} = 1/3\theta_0^2. \tag{14b}$$

The effective value of θ'^2 to be used in eq (13a) is the sum of these two. Therefore, the expected path-length error is

$$\tau - T = -\tau\gamma_i 2/3(\theta_0^2 + 1.5\theta_0^2) = -1/3(n'/n)^2\tau(\ln \tau_i)(\theta_0^2 + 1.5\theta_T^2). \tag{15}$$

If the Fresnel reflectance is small, this function has a maximum at $\tau_i = 0.37$. For this particular value of internal transmittance, and assuming $n = 1.5$, $n' = 1$, its magnitude is $\tau - T = 0.05\ (\theta_0^2 + 1.5\theta_T^2)$,

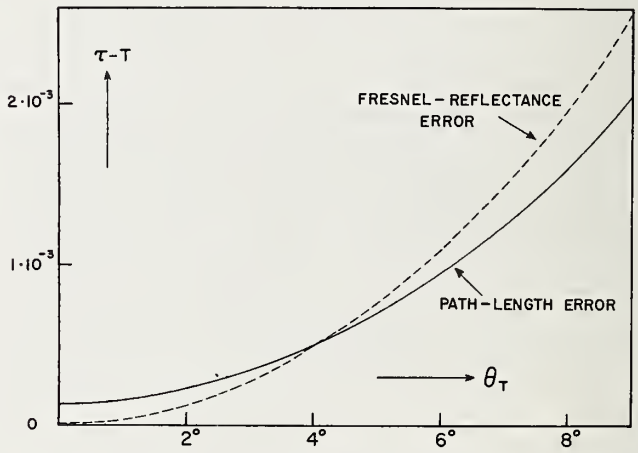

FIGURE 9. Maximal path-length error (for $\tau_i = 0.37$ and $\theta_0 = 0.05$ rad) and maximal Fresnel-reflectance error (for $\tau_i = 1.00$ and P polarization) versus tilt angle θ_T, as computed from eqs (15) and (16) with $n = 1.5$, $n' = 1$.

which is plotted in figure 9 as a function of tilt angle θ_T for an f/10 cone of light ($\theta_0 = 0.05$ rad). The graph shows that the effect of the cone angle, θ_0, is small, but that errors of the order of 10^{-3} transmittance units may be caused when the tilt angle is appreciable.

2. Fresnel-Reflectance Error—According to eq (13a) the effects of S and P polarization are approximately equal in magnitude, but opposite in sign. Therefore, they cancel when unpolarized light is used. For a symmetrical cone of light incident upon an untilted filter they cancel as well, because the roles

of S and P polarization are interchanged in any two perpendicular cross sections of the cone. Hence, Fresnel reflectance effects are observable only when polarized light is used, and when the filter is tilted.

Because of the opposing effects of S and P polarization in two mutually orthogonal planes, the effective value of θ'^2 to be used in this case, in the last term of eq (13a), is the difference of the two values in (14a, b). Therefore,

$$\tau - T = \pm \tau \gamma_r \theta_T^2$$

$$= \pm 4\tau(n'/n) r \theta_T^2, \qquad (16)$$

where the two signs pertain to the two cases in which the light is S or P polarized in the tilt plane.

This error is largest for large transmittances. If $n = 1.5$, $n' = 1$, $r = 0.04$, and $\tau = 0.92$, its magnitude is $\tau - T = 0.1\ \theta_T^2$, which is also plotted in figure 7. The figure shows that the Fresnel-reflectance error is of the same order of magnitude as the path-length error.

According to figure 10 the magnitude of this effect remains the same when a thin surface layer is present on the sample. The solid lines show the Fresnel reflectances for S and P polarization and for $n = 1.5$, $n' = 1$. As indicated by the broken lines, a thin layer of index $n_1 = 1.4$ and thickness $\lambda/100$ merely shifts these curves by a small amount. Thus, the angular dependence predicted by eq (16) remains unchanged, only the factor, r, on the right-hand side is changed insignificantly.

D. Elimination of Beam-Geometry Errors

The obliquity errors discussed in the previous section cannot be eliminated experimentally. In fact, they are increased by the necessity of tilting the sample in order to reduce the interreflection error. However, these obliquity errors can be predicted quantitatively and may, therefore, be removed by numerical correction of measured transmittances.

Thus, it should be possible to perform accurate measurements of 'true' transmittance with a conventional focused-beam spectrophotometer by eliminating defocusing and interreflection errors as indicated, measuring the tilt angle, and then applying a correction term, such as given by eqs (15) and (16) [13].

The same goal may be accomplished, in a much simpler fashion, by measuring in collimated rather than focused light. However, this cannot be done by simply repositioning the two lenses to make the light between them parallel. Such a beam geometry would still suffer from interreflection effects, so that the necessity to tilt the sample would reintroduce beam displacement and obliquity errors.

In order to avoid interreflections, it is necessary to use off-axis mirrors to collimate the light, and refocus it into the detector, as shown in figure 11. In this case, no significant portion of the light reflected from the sample will reach the detector, provided that the sample is normal to the beam and that off-axis mirrors are used in the monochromator as well. Each successive optical element will then reflect this light further toward the source, until some of it is returned by some lens on the source side of the monochromator. The final amount reaching the detector will be negligibly small.

To ensure that these conditions are realized, the imaging properties of the system must be quite good. Since a well-collimated beam cannot be derived from an extended source, it is necessary to equip the monochromator with small circular entrance and exit apertures rather than slits. Off-axis parabolas must be used rather than spherical mirrors to provide good imaging, so that the reflected light will still "fit" the monochromator apertures.

In addition, it is necessary to reduce the effects of spurious reflections by baffling, and by blackening of all component parts. The system must be aligned very carefully. This may be accomplished by means of an alignment laser and precision leveling devices for all components, including the sample holder.

The new spectrophotometer mentioned in section II, above, was designed and constructed in accordance with these guide lines. Returning the reflected light through the monochromator apertures was found to be a relatively easy alignment which, in addition to eliminating interreflections, also ensures that the samples are normal to the beam to within 1 milliradian. Therefore, no measurable obliquity errors are encountered and beam displacements will not occur, either. Unlike a focused-beam spectrophotometer, this instrument measures "true" transmittance without the necessity for elaborate precautions and numerical corrections.

The fact that this spectrophotometer is indeed effectively free from interreflection errors is demonstrated in figure 12. The figure shows the results of a

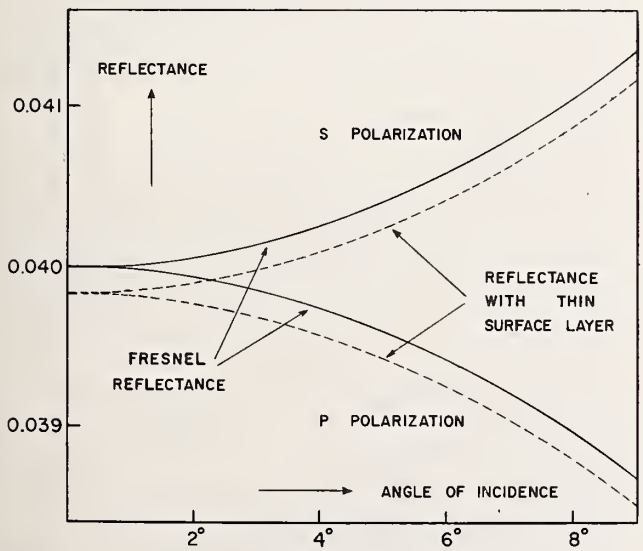

FIGURE 10. Computed reflectance of dielectric boundary ($n = 1.5$, $n' = 1$) with and without thin surface layer of thickness $\lambda/100$ and index 1.4.

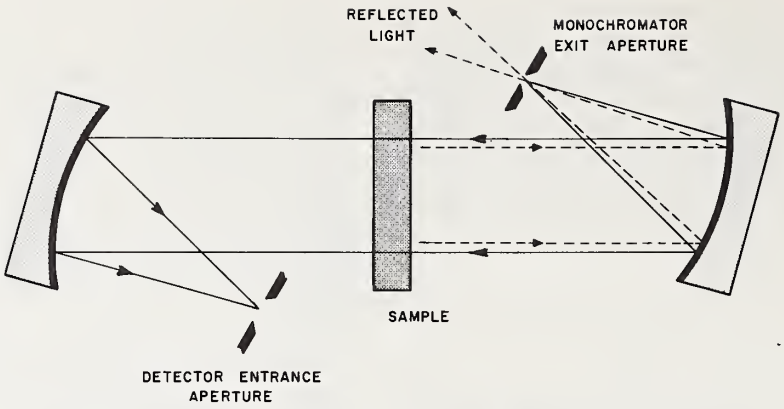

FIGURE 11. Elimination of interreflections by using collimated light at normal incidence and off-axis mirrors.

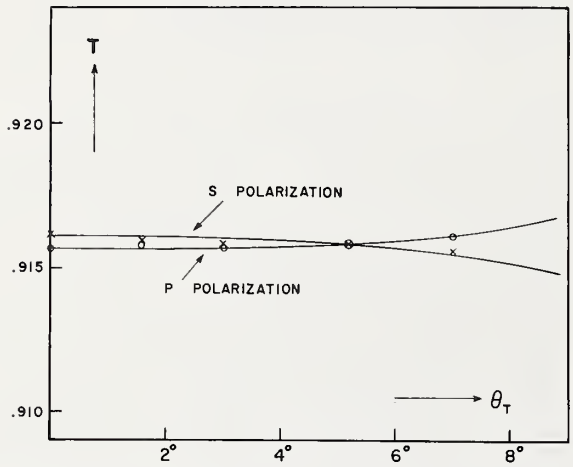

FIGURE 12. Measured transmittance T versus tilt angle for clear quartz sample between off-axis mirrors.

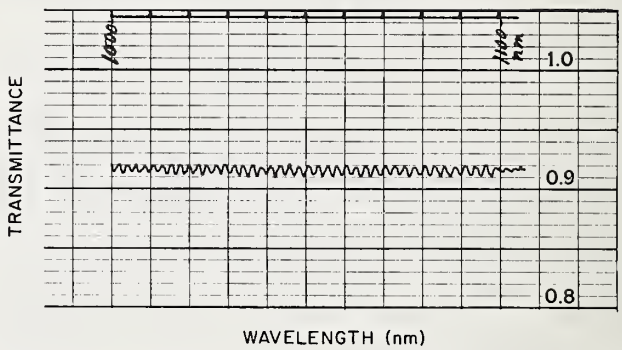

FIGURE 13. Measured interference effect for thin sample at near-infrared wavelengths.

tilting experiment similar to that of figure 8. There is no 'interreflection hump' near normal incidence as in the previous case, and the average of the measured transmittances for S and P polarization is the same for all tilt angles. The particular sample used (a clear quartz plate) was found to be slightly birefringent. This was verified by checking it between crossed polaroids.

VI. Interference Effects

Figure 13 demonstrates the possibility of interference effects in spectrophotometry. A recording spectrophotometer was used to measure the transmittance of a very thin glass plate ($nt \sim 0.24$ mm) at near-infrared wavelengths ($\lambda \sim 1.05$ μm). The observed modulation of transmittance of roughly 1 percent, due to interference fringes spaced 2.3 nm apart, is significantly smaller than would be expected from eq (5a), which predicts a fringe visibility of about 8 percent for this particular case. As already mentioned, this discrepancy arises from the partial coherence of the illuminating light.

Due to various 'smearing factors', such as localization of fringes, unequal amplitudes of interfering beams, and imperfect temporal or spatial coherence of the spectrophotometer beam, the effect is likely to be small in most practical situations. The particular type of interference observed and its magnitude are sample-dependent, and are also a function of the beam geometry of the spectrophotometer.

Unless the sample is plane-parallel by interferometric standards, the interference pattern will be of the Fizeau type, and will be localized in the sample. These fringes will be 'seen' to a greater extent by the detector of a focused-beam spectrophotometer (fig. 14a) than by that of a parallel-beam instrument. On the other hand, the latter is more susceptible to the Haidinger rings localized at infinity (fig. 14b) which occur when the sample is plane-parallel and is normal to the beam. Both types of fringes may result in a modulation of measured transmittance, such as shown in figure 13, when the spectrophotometer wavelength is scanned. The Fizeau fringe pattern may also cause a similar modulation of transmittance when the sample is moved across the beam at a fixed wavelength setting.

For most samples the reflectance r at the sample boundaries is small. Thus, two-beam rather than multiple-beam interference will be observed, and the fringe contrast will be small because of the large ratio

$1/r$ of the amplitudes of the two interfering beams. A further reduction of contrast may be attributed to the

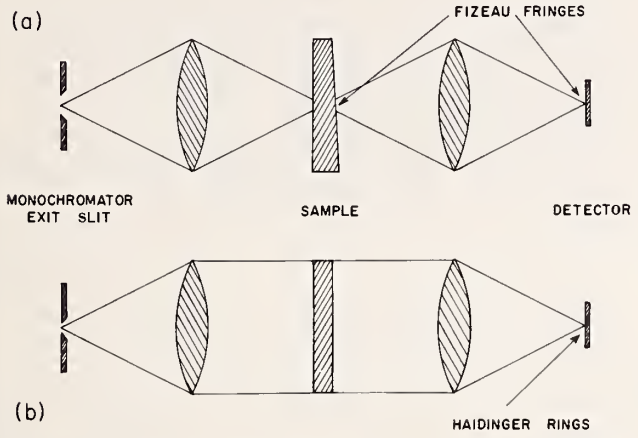

FIGURE 14. Localization of (a) Fizeau fringes, and (b), Haidinger rings in focused-beam and collimated-beam spectrophotometers.

finite degree of coherence of the interfering beams. The effect of imperfect temporal coherence is that the spectral fringe spacing, $\delta\lambda$, is generally significantly smaller than the bandpass $\Delta\lambda$ of the monochromator, so that the remaining net effect will be a much subdued average over several fringes. For example, $\delta\lambda = 0.04$ nm for a 2-mm filter of refractive index $n = 1.5$ at $\lambda = 500$ nm, whereas the normally used bandpass of the spectrophotometer described in section 2 is $\Delta\lambda = 0.8$ nm. In this case, the detector averages over twenty fringes and the reduction of contrast is at least twenty-fold. Lack of perfect spatial coherence may similarly lead to an averaging of several spatially separated fringes comprised within the spot size seen by the detector.

The over-all effect of these various factors is difficult to assess. Within the context of this paper it is only possible to estimate an upper bound of the effect on transmittance measurements with the spectrophotometer described here. Assuming the case of a perfectly plane-parallel, clear sample of optical thickness nt, arranged perfectly normal to the beam, the measured transmittance is [14]

$$T = \tau\left[1 + 2r\,|\,\gamma_{12}\,|\cos\left(\frac{4\pi}{\lambda}nt + \alpha_{12}\right)\right] \tag{17}$$

where τ is the average transmittance, r is the Fresnel reflectance of the sample boundaries, and

$$\gamma_{12} = |\,\gamma_{12}\,|\,e^{i\alpha_{12}} \tag{18}$$

is the complex degree of coherence of the interfering beams. The theory of partial coherence permits the computation of $|\,\gamma_{12}\,|$ as a function of the beam parameters [15]. For this particular spectrophotometer such computations show, for example, that a variation of measured transmittance as large as 3×10^{-3} transmittance units is possible for a sample of optical thickness 3mm measured at 500 nm and 0.8 nm bandwidth.

This result, although a worst-case estimate, indicates that interference must be reckoned with in high-accuracy spectrophotometry. The presence or absence of an effect should be ascertained experimentally whenever indicated. If present, the interference effect should be measured, and then averaged to obtain the 'true' transmittance of the sample.

Generally, the effect is largest for thin samples, small bandwidths, and long wavelengths. Thus, only sufficiently thick filters should be used as transfer standards for the assessment of spectrophotometric accuracy. Neutral-density filters are preferable since they permit the use of large bandwidths.

VII. Nonlinearity Correction

All spectrophotometers are subject to nonlinearity errors which must be eliminated by applying a correction, ΔT, converting the measured transmittance, T, into the true value

$$\tau = T + \Delta T. \tag{19}$$

A simple and yet accurate method to determine this correction is the method of light addition, based upon the fact that a linear system which gives readings $I(A)$ and $I(B)$ for radiant fluxes A and B will give a reading $I(A+B) = I(A) + I(B)$ when the two fluxes are added incoherently. The system is nonlinear and a correction must be applied if the ratio

$$1 + \sigma(A, B) = \frac{I(A+B)}{I(A) + I(B)} \tag{20}$$

is not equal to unity. The most practical implementation is the double-aperture method due to Clarke [3], in which the two fluxes are those transmitted by a pair of apertures which may be opened and closed separately or in combination. This method was used in the present work, and is discussed in detail in references [16] and [17].

The nonlinear detector response may be expressed in the form

$$I(\phi) = \eta\phi[1 + \epsilon(\phi)], \tag{21}$$

where

$I(\phi)$ = signal current minus dark current,

η = nominal detector sensitivity,
ϕ = radiant flux,
$\epsilon(\phi)$ = departure from linearity.

If the two apertures are equal in size, and if $\phi = A + B$ is the combined flux through both apertures, then, eq (20) may be written as

$$1+\sigma(\phi)=\frac{I(\phi)}{2I(\phi/2)}=\frac{1+\epsilon(\phi)}{1+\epsilon(\phi/2)}. \tag{22}$$

The measured apparent transmittance for a sample with true transmittance, τ, is

$$T=\frac{I(\tau\phi)}{I(\phi)}=\tau\frac{1+\epsilon(\tau\phi)}{1+\epsilon(\phi)}, \tag{23}$$

so that the required additive correction ΔT of eq (19) is given by

$$\Delta T=\tau\left[1-\frac{1+\epsilon(\tau\phi)}{1+\epsilon(\phi)}\right]. \tag{24}$$

These equations show that there is no straighforward functional relationship between the double-aperture datum, σ, and the nonlinearity correction ΔT. The former samples the detector response at the two points ϕ and 1/2 ϕ, but for the latter, we require the knowledge of $\epsilon(\phi)$ at a different pair of points, ϕ and $\tau\phi$. In the usual application of the double-aperture method, this difficulty is circumvented by using the fact that the multiplier of τ on the right-hand side of (23) happens to be the reciprocal of the right-hand side of (22), if $\tau = 1/2$. Thus, $[1+\sigma(\phi)]$ is the multiplicative correction to be applied when $\tau = 1/2$. Similarly, the correction factor for $\tau = 1/4$ is $[1+\sigma(\phi)][1+\sigma(1/2\,\phi)]$, and for $\tau = 1/2^n$ it is

$$\tau/T=\prod_{\nu=1}^{n}[1+\sigma(\phi/2^{n-1})]. \tag{25}$$

Thus, one can measure $\sigma(\phi)$, $\sigma(1/2\ \phi)$, . . . calculate the corresponding multiplicative corrections for $\tau = 1/2$, 1/4, . . ., and then draw a curve from which the correction may be read for arbitrary values of τ. This method is unsatisfactory because:

(a) The actually measured corrections are unevenly distributed along the τ-axis, with wide gaps between them in the regions of most interest.

(b) Most measurements are made at low light levels, where the correction is small and the experimental error is large.

(c) Each measured point depends on the previous ones, so that the errors accumulate as τ is decreased.

(d) The necessity to read the correction from a graph is awkward, especially if all other data are processed by computer.

These disadvantages can be overcome since, according to (22) and (24), ΔT is linked to σ through $\epsilon(\phi)$. Hence, it is possible to measure $\sigma(T\phi)$ for evenly distributed values of τ, process these data to find $\epsilon(\phi)$, and then calculate ΔT directly from (24). In order to do so, a lamp current is chosen so that the unattenuated flux, ϕ, through both apertures corresponds to the 100 percent point of the transmittance scale. After $\sigma(\phi)$ has been measured, the incident flux is attenuated in four 20 percent steps, and $\sigma(\tau\phi)$ is measured for $\tau = 0.8$, 0.6, 0.4, and 0.2. This series of measurements is repeated four times.

An example of the data so obtained is shown in figure 15. In all cases, the dependence of σ on T could

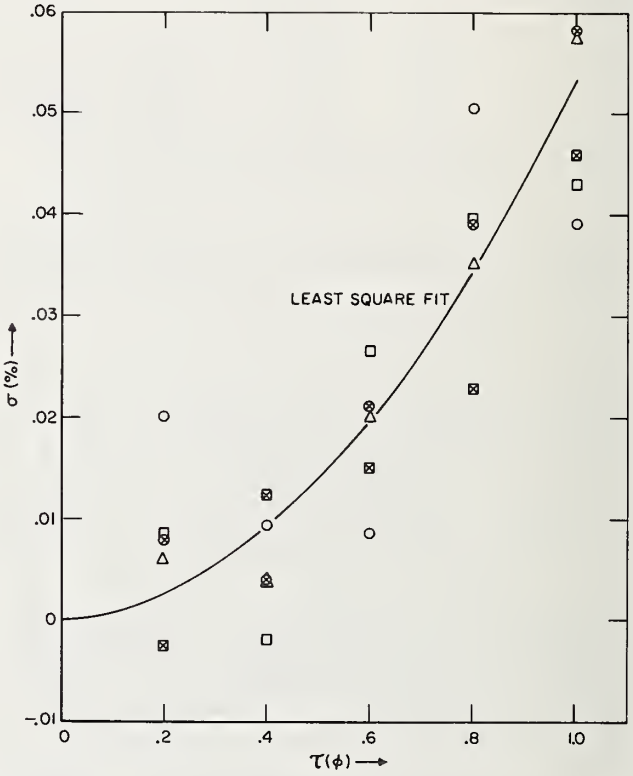

FIGURE 15. Measured dependence of the nonlinearity datum $\sigma(\tau\phi)$ on τ for $I(\phi) = 3 \times 10^{-7} A$ and $\lambda = 525$ nm.

be represented satisfactorily in the form of a parabola,

$$\sigma(\tau\phi)=a\tau+b\tau^2, \tag{26}$$

$$a=a(\phi),\ b=b(\phi), \tag{27}$$

where the coefficients, a and b, are determined from the measured data by least-square fitting, using the inverse variances of the measured values of $\sigma(\tau\phi)$ as weight factors. The use of a second-degree equation was justified by a statistical analysis with the residuals showing no patterns suggesting higher order terms.

Hence, we can calculate ΔT as follows. Letting

$$\epsilon(\phi)=\alpha\tau\phi+\beta(\tau\phi)^2+\ \ldots \tag{28a}$$

and then using eq (22), we find

$$\sigma(\tau\phi) = 1/2\ \alpha\tau\phi + 1/4(3\beta - \alpha^2)\ (\tau\phi)^2 + \ldots \qquad (28b)$$

to second order in ϕ, so that

$$a = 1/2\ \alpha\phi, \qquad b = 1/4(3\beta - \alpha^2)\phi^2, \qquad (28c)$$

according to (26, 27). Solving for α and β, and substituting the result into (28a),

$$\epsilon(\phi) = 2a\tau + 4/3(a^2 + b)\tau^2 + \ldots \qquad (28d)$$

and, therefore,

$$\Delta T = \frac{2aT(1-T) + 4/3(a^2+b)T(1-T)^2}{1 + 2a + 4/3(a^2+b)}, \qquad (29)$$

upon substitution of (28d) into (24) for $\tau = T$ and $\tau = 1$.

Thus the coefficients, a and b, can be stored in the computer after $\sigma(\tau\phi)$ was measured as described, and then ΔT may be calculated from eq (29) as required for arbitrary values of the measured apparent transmittance T.

As an indication of the precision of this method, table 3 lists the results obtained in two independent determinations of the nonlinearity correction. The two sets of final results for σ are in far better mutual agreement than the individual raw data of figure 15. The residual discrepancies of the additive correction, ΔT, never exceed 10^{-5} transmittance units.

For the particular spectrophotometer described in section II the nonlinearity correction was found to be independent of source polarization, free from interference effects, but slightly dependent on wavelength. This variation with wavelength (about 5×10^{-5} transmittance units or less between 400 and 750 nm) is taken into account in all measurements by means of a numerical interpolation formula derived from the measured values of ΔT for three wavelengths.

TABLE 3. Repeated measurements of σ and $\Delta T(\lambda = 525\ \text{nm}, I(\phi) = 3 \times 10^{-7}\ \text{A})$

T	First measurement		Second measurement	
	$\sigma \times 10^4$	$\Delta T \times 10^4$	$\sigma \times 10^4$	$\Delta T \times 10^4$
0.1	0.07	0.72	0.19	0.77
.2	.25	1.38	.45	1.46
.3	.52	1.96	.79	2.02
.4	.91	2.40	1.21	2.43
.5	1.39	2.67	1.70	2.66
.6	1.97	2.73	2.27	2.68
.7	2.66	2.53	2.92	2.45
.8	3.45	2.04	3.65	1.95
.9	4.34	1.21	4.45	1.14
1.0	5.34	0.00	5.33	0.00

The cooperation of K. L. Eckerle throughout this work is acknowledged with great appreciation. The design of the spectrophotometer was initiated by R. P. Madden, J. Reader, and J. Schleter. Various suggestions were made by C. E. Kuyatt, R. Mavrodineanu, and W. H. Venable.

VIII. References and Notes

[1] Mavrodineanu, R. J. Res. Nat. Bur. Stand. (U.S.), **76A** (Phys. and Chem.), No. 5, 405 (Sept.–Oct. 1972).
[2] Hawes, R. C., Appl. Optics **10**, 1246 (1971).
[3] Clarke, F. J. J., J. Res. Nat. Bur. Stand. (U.S.), **76A** (Phys. and Chem.), No. 5, 375 (Sept.–Oct. 1972).
[4] Mielenz, K. D., Eckerle, K. L., Madden, R. P., Reader, J., Appl. Optics (to be published).
[5] Mielenz, K. D., and Eckerle, K. L., Nat. Bur. Stand. (U.S.), Tech Note 729, 60 pages (June 1972).
[6] Taylor, D. J., Rev. Sci. Instr. **40**, 559 (1969).
[7] Born, M., and Wolf, E., Principles of Optics (Third Edition, Pergamon Press, 1965), Chapters 1 and 13.
[8] In all practical applications the surrounding medium is air. Most refractometers measure refractive indices with respect to air. In this case, the dependence of τ on n' is taken into account.
[9] Vasicek, A., Optics of Thin Films (North-Holland Publishing Co., 1960), Chapter 3.
[10] For $n' = 1$, $n = 1.5$, and $n_1 = 1.4$, the numerical value of this factor is -0.02. In addition, $\sin^2(x/2)$ is small for a very thin film. Further computations on this subject are presented in figure 10.
[11] Mavrodineanu, R., private communication.
[12] These measurements were performed by R. J. Bruening, NBS, on a goniophotometer with lenses for $\lambda = 546.1$ nm.
[13] It should be noted that the simplifying assumptions which led to eqs (13) and (14) may not apply. The correction terms must be derived for each spectrophotometer individually. A detailed knowledge of beam geometry is necessary for this purpose.
[14] Born, M., and Wolf, E., Principles of Optics (Third Edition, Pergamon Press, 1965), Chapter 10.
[15] Equation (19) was derived from the general expressions for $|\gamma_{12}|$ for small quasimonochromatic sources derived in K. D. Mielenz, Gas Lasers and Conventional Sources in Interferometry (Electron Beam and Laser Beam Technology, Academic Press, N.Y., 1968). For a uniformly illuminated circular aperture of angular radius $\alpha = a/2f$, the degree of spatial coherence is given by

$$|\gamma|_{\text{spatial}} = |(\sin A)/A|$$

where $A = k_0\alpha^2 t/2$, $k_0 = 2\pi/\lambda$. The degree of temporal coherence is the normalized Fourier transform of the spectral profile transmitted by the aperture, which in this case is

$$F(k = k_0) = \begin{cases} \sqrt{\frac{1}{4}a^2 - x^2} & \text{if } x^2 \leqq \frac{1}{4}a^2, \\ 0 & \text{otherwise,} \end{cases}$$

where $x = (k - k_0)dx/dk$ is the linear coordinate in the aperture plane, and where the aperture diameter is assumed to be much larger than the Rayleigh width of the grating. This leads to

$$|\gamma|_{\text{temporal}} = |2J_1(B)/B|,$$

where $B = atdk/dx$. Expressing $|\gamma_{12}|$ as the product of the degrees of spatial and temporal coherence, and substituting the result into (17), we obtain the numerical results quoted in section VI.
[16] Sanders, C. L., J. Res. Nat. Bur. Stand. (U.S.) **76A** (Phys. and Chem.), No. 5, 437 (Sept.–Oct. 1972).
[17] Mielenz, K. D., and Eckerle, K. L., Appl. Optics, **11**, 2294 (1972).

(Paper 76A5–732)

NATIONAL BUREAU OF STANDARDS SPECIAL PUBLICATION 378, Accuracy in Spectrophotometry and Luminescence Measurements, Proceedings of a Conference Held at NBS, Gaithersburg, Md., March 22–24, 1972 (Issued May 1973).

Liquid Absorbance Standards

R. W. Burke, E. R. Deardorff, and O. Menis

Institute for Materials Research, National Bureau of Standards, Washington, D.C. 20234

(June 14, 1972)

Errors in the measurement of the absorbances of liquid filters result from instrumental and chemical uncertainties. This paper presents a systematic study of these variables on the absorbances of selected filters. Three types of liquid filters are discussed. These are (1) individual solutions of high purity compounds, (2) composite mixtures and (3) aqueous solutions of organic dyes. The accuracy of the absorptivity data is established using NBS-calibrated glass filters. The magnitude of the errors arising from spectral bandpass, beam geometry, stray light, internal multiple reflections, and refractive index are delineated. Finally, as a practical outgrowth of this study, the development and issuance of NBS Standard Reference Material 931, Liquid Absorbance Standards for Ultraviolet and Visible Spectrophotometry, is described.

Key words: Absorptivity data; accuracy; liquid absorbance standards; Standard Reference Materials.

I. Introduction

In the use of filters for checking the accuracy of the photometric scale of spectrophotometers, one needs materials which exhibit absolute spectral neutrality. Such ideal filters are not available at present. The use of the materials which have been suggested is limited by instrumental and sample variables. For this reason, one must carefully specify conditions which define the other sources of errors.

The first part of this paper reviews several of the more important instrumental parameters and discusses their effects on absorbance measurements. Examples from the literature are given to illustrate the magnitude of the errors arising from spectral bandpass, stray light, nonparallel radiation, and multiple reflections. The second part presents some experimental studies of several materials which may serve as calibration "filters" or standards.

II. Instrumental Parameters

A. Wavelength Accuracy

The absorbances of most samples are sufficiently wavelength dependent that even in the most favorable regions of maxima and minima a wavelength error of 1–2 nm can produce absorbance errors of a few tenths of a percent. When performing measurements on the slopes of absorption peaks, the wavelength setting is obviously much more critical and errors are typically several percent per nanometer. Wavelength accuracy, therefore, becomes especially important when making absorbance measurements at, for example, an isosbestic point.

A line source provides the most definitive means for establishing the accuracy of the wavelength scale. The best single source is a mercury lamp which may be used throughout the range of 200–1000 nm. For calibration in the visible region, helium lines are also useful.

Gibson [1][1] has discussed the use of mercury and helium sources and has listed those lines best suited for wavelength calibration. Other sources which have been used include neon, cadmium, cesium, and sodium. The M.I.T. Wavelength Tables [2] summarizes the most prominent emission lines of these elements. Not all wavelengths are given and care must be taken in using any of these lines in order not to confuse closely adjacent lines with the one being checked. For those spectrophotometers having a hydrogen or deuterium source, the emission lines at 486.13 and 656.28 nm (H) or 485.99 and 656.10 nm (D) may provide convenient checks at these wavelengths.

Calibrated holmium oxide and didymium glasses may be useful secondary standards, particularly for checking recording spectrophotometers in which a dynamic check of the instrument is often desirable. The apparent absorption maxima of these filters, however, may vary with spectral bandpass. Therefore, for the highest accuracy, they should be calibrated for the spectral bandpass at which they are to be used.

In general, prism instruments require more frequent calibration than the grating type because their dispersion is temperature dependent. Corrections in the visible region are of the order of 0.1 nm per degree Celsius. Hysteresis effects must also be considered

[1] Figures in brackets indicate the literature references at the end of this paper.

and the wavelength settings should always be approached from the same direction.

B. Finite Bandwidth

Spectral bandpass differences undoubtedly account for a significant portion of the discrepancies in molar absorptivity values reported in the literature. Some have resulted from the employment of inadequate instrumentation; others have resulted from improper use of these instruments or complications arising from solution equilibria.

Increasing the spectral bandpass at an absorption maximum has two effects on apparent peak heights: (1) the observed values are always less than the true values and (2) the differences between the two are proportionally greater at higher absorbances. Thus, for a finite bandpass, a plot of absorbance versus concentration or path length will always have a smaller slope than it does in monochromatic radiation and, in addition, will be concave to the concentration axis. Figure 1 illustrates these effects. The reverse behavior will be observed for measurements at an absorption minimum. Meehan [3] has given a simple example which verifies these two effects mathematically.

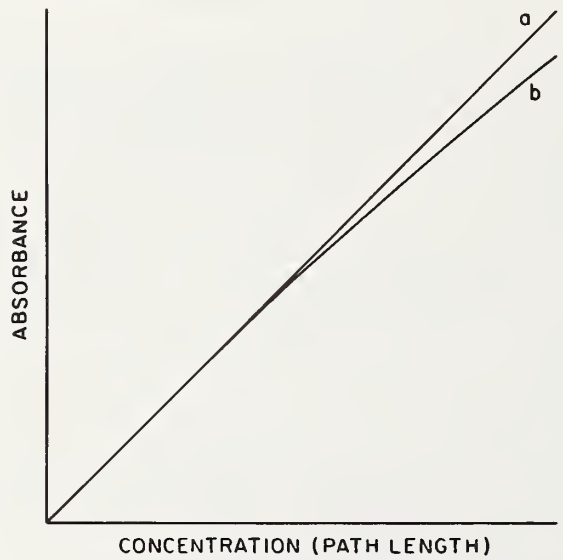

FIGURE 1. Effect of spectral bandpass on absorbance: (a) Monochromatic radiation (b) Finite bandwidth.

Consider that an absorbing system is illuminated by two monochromatic radiations of wavelengths λ_1 and λ_2 and that the Lambert-Beer law is obeyed at each wavelength with absorptivities a_1 and a_2. If the effective intensities of the two wavelengths are I_1 and I_2, respectively, the transmittance, T, is

$$T = (I_1 \cdot 10^{-a_1 bc} + I_2 \cdot 10^{-a_2 bc})/(I_1 + I_2) \qquad (1)$$

where b = path length and c = concentration. If λ_1 is the wavelength of maximum absorption so that $a_1 > a_2$, then

$$T = \frac{1}{(1+r)} \cdot 10^{-a_1 bc}[1 + r \cdot 10^{(a_1 - a_2)bc}] \qquad (2)$$

where $r = I_2/I_1$. The absorbance, A, defined as $-\log T$ is

$$A = a_1 bc + \log (1+r) - \log [1 + r \cdot 10^{(a_1 - a_2)bc}] \qquad (3)$$

which may be differentiated with respect to bc to give

$$dA/d(bc) = a_1 - [r(a_1 - a_2)10^{(a_1 - a_2)bc}]/ [1 + r \cdot 10^{(a_1 - a_2)bc}] \qquad (4)$$

At low absorbances

$$dA/d(bc)_{bc \to 0} = \frac{a_1 + r a_2}{1 + r} \qquad (5)$$

whereas when bc becomes large, $10^{a_1 bc} \gg 10^{a_2 bc}$ and the limiting slope is

$$dA/d(bc)_{bc \to \infty} = a_2. \qquad (6)$$

Thus, the limiting absorptivity at low absorbances is a weighted average of a_1 and a_2 while, at higher absorbances, it is equal to a_2, the smaller of the individual absorptivities.

The theory for the correction of spectral bandpass errors has been developed by Hardy and Young [4], Eberhardt [5], and Broderson [6]. Rigorous calculation requires integration of the relation

$$A_{obs} = \log \frac{\int I_\lambda S_\lambda d\lambda}{\int I_\lambda S_\lambda 10^{-A} d\lambda} \qquad (7)$$

where I_λ is the incident intensity and S_λ is the spectral sensitivity of the detector. Equation (7) emphasizes the fact that the observed absorbance depends not only on the shape of the absorption curve, but also on the wavelength distribution of the source and the detector response. If $I_\lambda S_\lambda$ is constant over the wavelength interval used, approximate corrections for spectral bandpass may be calculated by assuming a Gaussian shape for the absorption peak and a triangular slit function for the instrument. Some calculations are given in table 1 based on these assumptions. The tabulated values of A_{obs}/A agree closely with those observed experimentally for A up to 1. As shown by Broderson [6] however, for values of RBW larger than 0.5, A_{obs}/A also depends on A and the above treatment is no longer applicable.

C. Stray Light

Stray light is defined as any light outside the spectral region isolated by the monochromator that reaches the detector. It is produced by scatter from the optics and

TABLE 1. Dependence of A_{obs} on spectral bandpass at an absorption maximum under idealized conditions (see text)

RBW[a]	A_{obs}/A	RBW[a]	A_{obs}/A
0.0100	0.99995	0.0800	0.9970
.0200	.9998	.0900	.9962
.0300	.9995	.1000	.9954
.0400	.9992	.2000	.9819
.0500	.9988	.3000	.9604
.0600	.9983	.4000	.9321
.0700	.9977	.5000	.8987

[a] Relative bandwidth: Ratio of spectral bandwidth to half bandwidth of fully resolved peak.

walls of the monochromator and is present in varying amounts in all spectrophotometers.

Stray light can lead to varied problems in spectrophotometry. Spurious absorption bands may arise in some cases. More frequently, however, deviations from the Lambert-Beer law are produced. These deviations are positive if the stray light is absorbed and negative if it is not.

Extensive literature exists on the detection, measurement and minimization of stray light. Several of the more useful papers are those by Hogness, Zscheile and Sidwell [7], Perry [8], Slavin [9], and Poulson [10] in which additional references may be found.

The amount of stray light present is proportionally large in those wavelength regions where the transmission of the monochromator, the source intensity or the detector sensitivity are relatively low. These regions, which should first be checked, are 200–230 nm and 600–700 nm. If a tungsten lamp must be used in the range 350–400 nm, a visible cutoff filter should always be employed.

The quantitative assessment of stray light requires the use of extremely sharp cutoff filters. Slavin [9] and Poulson [10] have described a number of liquid and solid filters that may be used. Aqueous solutions of the alkali halides, for example, are extremely useful in the ultraviolet. Care must be taken, however, that light leaks in the cuvet compartment are not contributing to the observed results. The apparent stray light will not vary appreciably with slitwidth if only instrumental stray light is present. In a quick test for light leaks, the apparent stray light will decrease rapidly as the slits are opened.

The stray light error encountered most frequently in spectrophotometry produces a decrease in an absorption peak and leads to negative deviations from the Lambert-Beer law. If it is assumed that none of the stray light is absorbed by the sample, the measured absorbance is related to the true transmittance by the expression [9]

$$A_{obs} = \log\,[(1-T)\,S+T]^{-1} \qquad (8)$$

where S is the instrumental stray light expressed as a fraction. The effects of several levels of unabsorbed stray light on absorbance are given in table 2. Most samples absorb sufficiently in other regions of the spectrum to filter out a proportion of the stray light. Thus, indirect estimates of instrumental stray light based on deviations from linearity are generally low.

TABLE 2. Effect of unabsorbed stray light on absorbance

A	A_{obs}		
	$S=0.0001$	$S=0.001$	$S=0.01$
0.1	0.1000	0.0999	0.0989
.5	.4999	.4990	.4907
1.0	.9996	.9961	.9626
1.5	1.499	1.487	1.384
2.0	1.996	1.959	1.701

D. Nonparallel Incident Radiation

A perfectly parallel beam of radiation must come from a point source and can carry only an infinitesimal amount of energy. The light beam in a spectrophotometer always has some finite angular size. As a result, the average light path is greater than the perpendicular distance between the cuvet faces. Meehan [3] has considered the case in which the incident radiation is convergent or divergent in one dimension such as corresponds, respectively, to radiation focused by a cylindrical lens or leaving a narrow slit. If Θ and R are the angles of incidence and refraction, respectively, the path length of the extreme ray (fig. 2) is $b/\cos R$ and the absorbance of this ray is $A/\cos R$. Other rays enter at smaller angles and the observed absorbance is given by

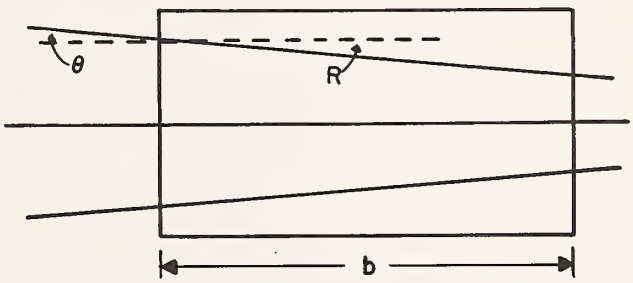

FIGURE 2. Nonparallel incident radiation [3]. Reprinted by permission of John Wiley & Sons, Incorporated.

$$A_{obs} = A/R_{max} \int_0^{R_{max}} 1/\cos\, R dR. \qquad (9)$$

For this relation to hold, the incident beam must be uniform over its cross section. Evaluation of this integral for R_{max} of 2–10° ($\Theta_{max}=2.7°$–$13.4°$) gives the following percent errors in A (table 3). Thus, for angles of incidence up to 5 degrees, the absorbance error is less than 0.1 percent.

E. Multiple Reflections

On passage of light through a cuvet containing solvent or sample solution, some radiation is reflected

Table 3. Dependence of absorbance error on nonparallelism of incident radiation

R_{max}, degrees	Θ_{max}, degrees	Percent error in A
2	2.7	0.020
4	5.3	.081
6	8.0	.18
8	10.7	.33
10	13.4	.51

at each of the two air-glass and the two glass-liquid surfaces. For perpendicular incidence, the fraction f reflected on passing from a medium of refractive index n_1 to a second having refractive index n_2 is given by the Fresnel expression

$$f=\left[\frac{n_1-n_2}{n_1+n_2}\right]^2 \tag{10}$$

For an air-glass surface, $f=0.04$ and for a glass-liquid surface, $f=0.0035$. When more than one surface is involved, the effects of multiple reflections must be considered. The essential question when dealing with liquid filters is whether the solvent completely compensates for such reflections. According to Goldring et al. [11], it does not. They consider the case where the reflections from all surfaces perpendicular to the light beam on the two sides of the sample are grouped together to form two effective reflection coefficients, r_1 and r_2, as shown in figure 3. Considering only first and second order reflections, the observed absorbance is

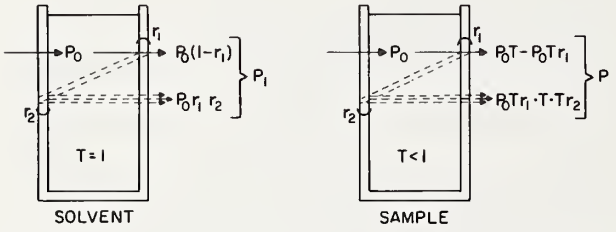

Figure 3. Internal multiple reflections [11]. Reprinted by permission of the American Chemical Society.

$$A_{obs}=\log\frac{P_1}{P_2}=\log\frac{P_0}{P_0T}\frac{(1-r_1+r_1r_2)}{(1-r_1+r_1r_2T^2)} \tag{11}$$

which, after transformation and series expansion, can be reduced to the following expression:

$$A_{obs}=A+0.4343\,(1-T^2)\,\frac{r_1r_2}{1-r_1}. \tag{12}$$

Considering only the reflections from the two cuvet faces and that $r_1=r_2=0.05$, the variation of A_{obs} with A is

A	0.1	0.2	0.5	1.0	2.0
A_{obs}	0.1004	0.2007	0.5010	1.0011	2.0011

Thus, because of internal multiple reflections, the measured absorbance should always be larger than the true absorbance with the percentage difference being greatest at low absorbances. Verification of these deviations is difficult experimentally. Goldring et al. [11], however, have suggested ways of minimizing reflection effects. These include positioning the cuvet at a small angle to the beam and stopping down the detector surface, immersing the cuvet in a fluid contained in a larger rectangular cuvet turned at an angle to the beam, or by using a cuvet with prismatic windows. In each case, the effective path length must be determined separately. Other alternatives consist of using cuvets constructed of absorbing materials or immersion of a glass filter into the sample. For a limited wavelength range, reflection errors can also be reduced by coating the external window surfaces with anti-reflection layers.

In addition to reflections from the cuvets, reflections from other surfaces must also be considered. Gibson [1] has pointed out that reflections may occur from the surfaces of the slit and detector and has suggested a means for checking this source of error. A thin glass plate is placed in its normal position at right angles to the beam and then at a small angle from this position. In the second position the reflected energy is directed out of the beam while scarcely affecting the true absorbance.

F. Cuvets

The majority of absorbance measurements are performed on solutions and, in such instances, the cuvet becomes an integral part of the measurement system. Presently, the uncertainty in the length of the light path can be a limiting factor in the determination of molar absorptivity. Nonparallelism of the end windows can be of even greater consequence. However, the effect can be minimized by using the same cuvet orientation for all measurements. The uncertainty in path length is nevertheless greater.

Cuvets are available in a variety of shapes and sizes and may be made of glass or silica. Construction remains largely an art and cuvets may vary considerably in their quality. Two methods of assembly are commonly used. These are: (1) fusion using only heat and (2) the use of intermediate, low-melting glasses. At present, each has its disadvantage. The first technique is the more desirable, but our experience, primarily with rectangular cuvets, indicates that the edges are not always completely fused. These surfaces exhibit capillarity and may become serious sources of contamination. Under such conditions, the cleaning of these cuvets is difficult, if not impossible. The use of low-melting fluxes on the other hand can produce strains because of differences in coefficients of expansion and cuvets so constructed are generally more fragile.

Cuvets are frequently offered in matched sets. This may be considered more of a convenience than a necessity since this terminology is normally used only to describe the transmission of the window material.

Path length and parallelism of end plates are of more fundamental importance. Unfortunately, no generally accepted tolerances have been established in this country for the construction of cuvets. The British Standards Institution, however, has published a set of specifications [12] which merit our consideration and possible adoption. They recommend that the path length be specified to ± 0.02 mm and the end windows be flat over a defined beam area to four Newton fringes per centimeter in mercury green light. It should be feasible for greater accuracy, especially for the 10 mm cuvets, to calibrate a limited number by appropriate metrology techniques to ± 0.01 mm.

III. Evaluation of Selected Liquid Filters

This section is a report of our efforts to develop well characterized liquid absorbance standards. Three general types of liquid filters are discussed. These are (1) individual solutions of high purity materials, (2) empirical mixtures and (3) aqueous solutions of organic dyes. Much of the emphasis has been placed on determining the optimum conditions for preparation of these filters and, once established, what the absorbing species or ionic compositions of these systems are. By combining this information with the instrumental considerations developed in the first part of this paper, it is hoped that the resulting data represent a step toward obtaining more meaningful absorptivity measurements.

A. Instrumentation

Absorbance measurements at a fixed wavelength were performed manually on a high precision double-beam spectrophotometer provided with a double monochromator. The accuracy of the photometric scale of this instrument was established with the NBS high-accuracy spectrophotometer described by Mavrodineanu [13]. The wavelength scale was checked with a mercury lamp. Potassium halide solutions [9, 10] were used to assess stray light in the ultraviolet.

Room temperature was maintained between 24 to 26 °C. The cuvet compartment and jacketed holders were thermostated by a circulating water bath. Copper-constantan thermocouples were used to measure temperature differences between the bath and the sample solution.

An electronic feeler gauge [13] was used to measure the path length of the 10 mm rectangular cuvets normally used. Solutions, assumed to obey Beer's law, were used for calibrating the 1 mm cuvets.

The accuracy of the microbalance was established with NBS-calibrated weights. Class A, 1-liter volumetric flasks were checked gravimetically. All dilutions were subsequently made by volume. To minimize errors from cell positioning, borosilicate, Pasteur-type pipets were used to transfer solutions to and from the cuvets.

B. Individual Solutions of High Purity Compounds

1. Potassium Dichromate. Numerous attempts have been made to use chromium (VI) solutions as ultraviolet absorbance standards. In the early studies [7, 14, 15, 16, 17] alkaline solutions of potassium chromate were preferred. More recently, potassium dichromate in slightly acidic media has been described [18, 19, 20]. The absorption spectra of these two systems are quite different with the latter giving the more desirable arrangement of maxima and minima (fig. 4).

The approximate composition of chromium (VI) solutions may be derived from the following equilibria:

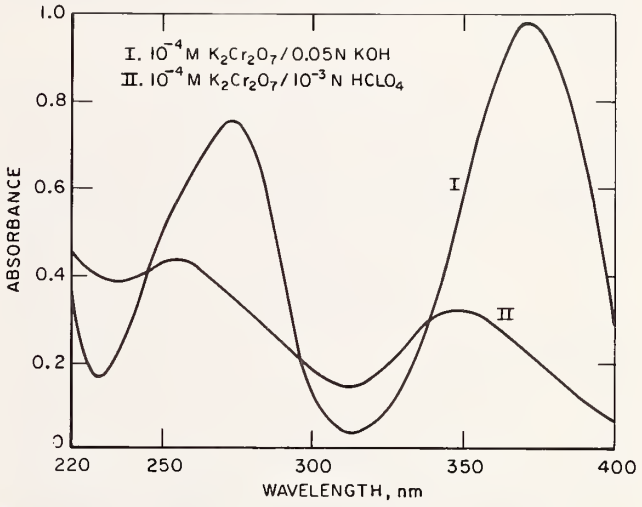

FIGURE 4. Absorption spectra of 10^{-4} M Cr (VI) in 0.05 N KOH and 10^{-3}N $HClO_4$.

$$H_2CrO_4 \overset{K_1}{=} H^+ + HCrO_4^- \tag{13}$$

$$HCrO_4^- \overset{K_2}{=} H^+ + CrO_4^{=} \tag{14}$$

$$2HCrO_4^- \overset{K_3}{=} Cr_2O_7^{=} + H_2O. \tag{15}$$

Some values reported for the equilibrium constants K_1, K_2, and K_3 at 25 °C are as follows:

$K_1 = 0.16$ [21]

$K_2 = 3.2 \times 10^{-7}$ [22] and 3.0×10^{-7} [23]

$K_3 = 43.7$ [21], 35.5 [24] and 33.0 [25].

Thus, at a pH greater than 10, chromium (VI) exists almost entirely as $CrO_4^{=}$ ions while, in weakly acidic solutions, the predominant species is $HCrO_4^-$ which partially dimerizes to $Cr_2O_7^{=}$. The amount of dimer will increase with increasing chromium concentration. The formation of H_2CrO_4 or $CrO_4^{=}$ can be essentially eliminated by maintaining the acidity near pH 3.

Much of the uncertainty that has arisen from the use of acidic potassium dichromate solutions as potential absorbance standards can be attributed to the dimerization reaction (eq (15)). It is primarily this equilibrium which leads to the observed deviations from Beer's law. Because of the range of values reported for K_3, one of the first objectives of the present study was to redetermine this constant. The spectrophotometric method was chosen and is described in some detail below.

a. **Spectrophotometric Determination of the Dimerization Constant for: $2HCrO_4^- = Cr_2O_7^= + H_2O$.** If $HCrO_4^-$ and $Cr_2O_7^=$ are the only Cr(VI) species present with molar absorptivities ϵ_1 and ϵ_2, respectively, the apparent molar absorptivity, ϵ_m, will be given by

$$\epsilon_m = (1-\alpha)\epsilon_1 + 1/2 \cdot \alpha\epsilon_2 \tag{16}$$

where α is the fraction of total chromium in the dichromate form. From eq (15) the thermodynamic equilibrium constant of the dimerization reaction is

$$K_3 = \frac{[Cr_2O_7^=]}{[HCrO_4^-]^2} \cdot \frac{\gamma_2}{\gamma_1^2} \tag{17}$$

or, in terms of α

$$K_3 = \frac{\alpha}{2(1-\alpha)^2 Cr_T} \cdot \frac{\gamma_2}{\gamma_1^2} \tag{18}$$

where γ_1 and γ_2 are the activity coefficients of $HCrO_4^-$ and $Cr_2O_7^=$, respectively, and Cr_T is the total chromium concentration. Because the ionic strength never exceeded 0.01, the activity coefficients may be treated by the Debye-Hückel expression [25]

$$-\log \gamma_i = \frac{AZ_i^2 I^{1/2}}{1 + I^{1/2}} \tag{19}$$

where Z is the ionic charge, I is the ionic strength and A has a value of 0.509 l/mol at 25 °C. Equations (16) and (18) can be rewritten to give, respectively,

$$\epsilon_m = \alpha(1/2\ \epsilon_2 - \epsilon_1) + \epsilon_1 \tag{20}$$

and

$$\log K_3 = \log \frac{\alpha}{2(1-\alpha)^2 Cr_T} - \frac{2AI^{1/2}}{1 + I^{1/2}}. \tag{21}$$

Assuming a value of K_3, one can calculate from eq (21) the α values at various total chromium concentrations. If the choice of K_3 is correct, the measured values of ϵ_m should lie on a straight line of slope $(1/2\ \epsilon_2 - \epsilon_1)$ and intercept ϵ_1, as seen from eq (20). The best value of K_3 is then determined by the method of least squares.

1. Experimental Procedure

The chromium (VI) solutions used in the subsequent studies were prepared from NBS SRM–136c, potassium dichromate, which had been dried at 110 °C for two hours. The distilled water was shown to be free of reducing impurities by titration with a dilute potassium permanganate solution. Perchloric acid was used to maintain the pH at 3.0 ± 0.1.

The optimum wavelengths for the determination of K_3 were chosen as follows: Two solutions were prepared, one containing 391 mg $K_2Cr_2O_7$/l and the other, 40.0 mg $K_2Cr_2O_7$/l. The former was transferred to a 1.023 mm cuvet and the latter to a 10.00 mm cuvet. A differential scan was then made on a recording spectrophotometer equipped with a 0–0.1 absorbance (full scale) slidewire, using the less concentrated solution as the reference. The resulting spectrum is shown in figure 5. Relatively large differences in absorbance are seen in the wavelength regions near 275 and 385 nm even though the total number of chromium atoms in each light path is the same. Thus, it is in these two regions that the largest deviations from Beer's law should be observed. Three wavelengths were subsequently selected in each region for the determination of K_3–390, 385 and 380 and 280, 275 and 270 nm, respectively.

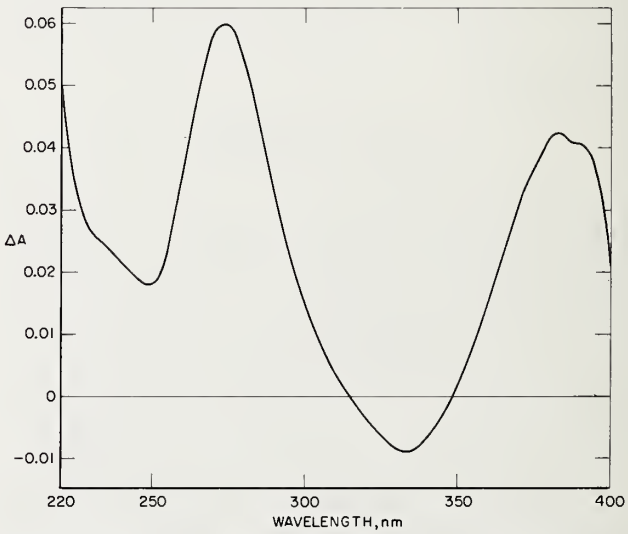

FIGURE 5. Difference spectrum of 391 mg $K_2Cr_2O_7$/l in 1.023 mm cuvet versus 40.0 mg $K_2Cr_2O_7$/l in 10.00 mm cuvet; pH = 3.

2. Results

The apparent molar absorptivities calculated from absorbance measurements on the four chromium concentrations used for the determination of K_3 are given in table 4. Using the method of least squares, these ϵ_m values were plotted against the α fractions calculated from eq (21) for various assumed values of K_3. The molar absorptivities were weighted according to the reproducibility of the absorbance measurements. A computer was used for all calculations.

A typical graph of the residual standard deviation of the experimental ϵ_m values from the best straight line fit is shown in figure 6 for K_3 values of 28 through 36. The minimum in this curve is the best estimate of K_3 and, for the case shown, is 32.6. The K_3 values at the six wavelengths are summarized in table 5.

TABLE 4. Apparent molar absorptivities, ϵ_m, of $K_2Cr_2O_7$ solutions at 25 °C; pH = 2.9 ($HClO_4$)

$K_2Cr_2O_7$ Conc. mg/l	ϵ_m l/mol^{-1} cm^{-1}					
	390 nm	385 nm	380 nm	280 nm	275 nm	270 nm
100.06	589.2	748.7	865.1	1579.3	1718.6	1881.0
400.48	714.1	878.6	997.8	1758.2	1914.4	2069.8
699.86	806.2	973.8	1094.0	1890.0	2053.5	2208.0
1000.27	875.9	1045.6	1166.5	1988.2	2161.5	2313.6

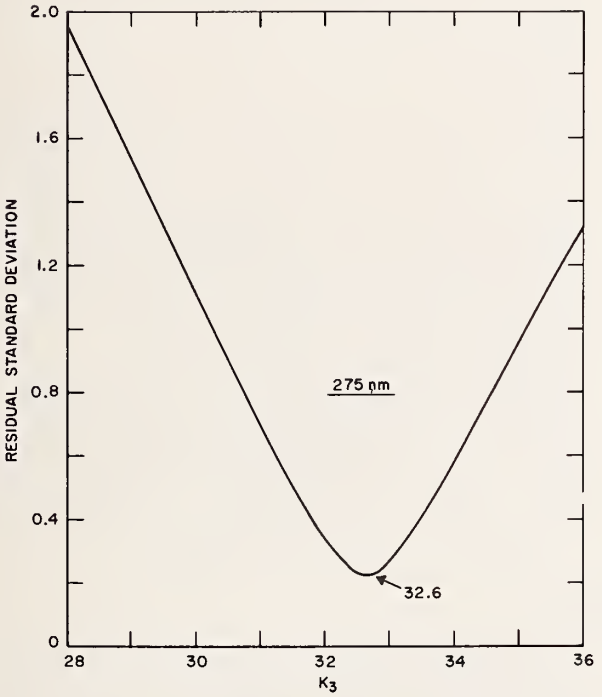

FIGURE 6. Least squares determination of K_3.

TABLE 5. K_3 values at 25 °C as determined at several wavelengths

λ, nm	K_3
390	32.4
385	33.3
380	33.8
280	33.5
275	32.6
270	31.6
Avg.	32.9
Std. Dev.	0.8
Rel. Std. Dev.	2.5%

b. Absorption Spectra of $HCrO_4^-$ and $Cr_2O_7^=$. The absorbances of three solutions containing nominally 20, 40, and 60 mg $K_2Cr_2O_7$/l (pH = 3.0 ± 0.1) were measured in a 10.00 mm cuvet at 5 nm increments over the wavelength range of 220–400 nm. A close approximation of $\epsilon(HCrO_4^-)$ was obtained by extrapolating the apparent molar absorptivities to zero chromium concentration. This extrapolation is simplified since the variation of α is nearly linear over this concentration range. Similar absorbance measurements were performed on three solutions containing 1000 mg $K_2Cr_2O_7$/l using a 1.023 mm cuvet and the corresponding α value was calculated from eq (21), with $K_3 = 32.9$. The first approximations of $1/2 \cdot \epsilon(Cr_2O_7^=)$ values were obtained by substituting the extrapolated $\epsilon(HCrO_4^-)$ results and the above α value into eq (20). The $\epsilon(HCrO_4^-)$ and $1/2 \cdot \epsilon(Cr_2O_7^=)$ values were then refined by successive approximations. The calculated absorption spectra of these two ions are shown in figure 7.

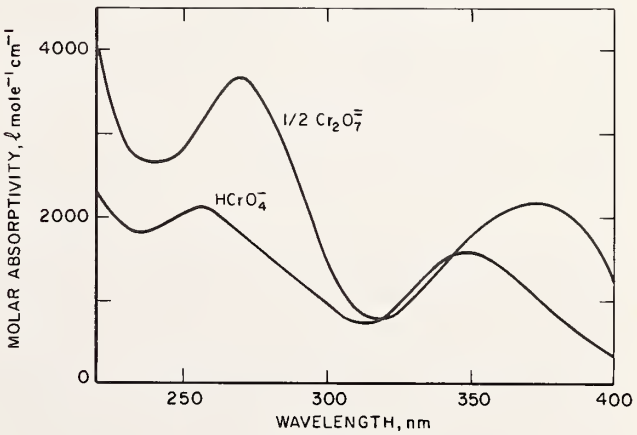

FIGURE 7. Absorption spectra of $HCrO_4^-$ and $Cr_2O_7^=$.

c. Molar Absorptivities of $HCrO_4^-$ and $Cr_2O_7^=$ at 350, 313, 257, and 235 nm. As shown previously in figure 4, the absorption spectrum of weakly acidic solutions of $K_2Cr_2O_7$ exhibit maxima at 350 and 257 nm

and minima at 313 and 235 nm. These maxima and minima do not shift significantly over the concentration range of 20–100 mg $K_2Cr_2O_7$/l. This is considered a practical range for most applications since it yields absorbances of about 0.1–1.5 for a 10 mm cuvet.

The molar absorptivities of $HCrO_4^-$ and $Cr_2O_7^=$ at 350, 313, 257, and 235 nm were determined by the procedure described above and are given in table 6. The $\epsilon(HCrO_4^-)$ values are estimated to be accurate to ± 0.5 percent. Because of the imprecision of the K_3 determination, the uncertainty of the dichromate molar absorptivity values may be as large as ± 5 percent.

Table 6. Molar absorptivities, ϵ, of $HCrO_4^-$ and $Cr_2O_7^=$ at 25 °C

	ϵ, l mol^{-1} cm^{-1}			
	350 nm	313 nm	257 nm	235 nm
$HCrO_4^-$	1576	711	2100	1804
1/2 $Cr_2O_7^=$	1788	823	3156	2688

Table 7 shows the agreement between the experimental and calculated apparent molar absorptivities for five concentrations of potassium dichromate in dilute perchloric acid (pH = 2.92 ± 0.02). The experimental values are the averages obtained on five individual samples measured at each concentration. The 95 percent confidence limits for any given set of measurements was 0.1 percent. The α values used are also given. These are seen to vary nearly linearly over the range of chromium concentrations employed.

d. Optimum pH and Choice of Acid. The chromium (VI) solutions used in this study were prepared in dilute perchloric acid media having a pH of about 3. This acidity was selected because the existing equilibria data indicated this pH limited the formation of either H_2CrO_4 or $CrO_4^=$ to less than 0.1 percent of the total Cr (VI) concentration. Perchloric acid was chosen instead of sulfuric to prevent the formation of chromate-sulfate complexes. Tong and King [24] and Davies and Prue [25] noted slight differences in the absorbances of dilute perchloric and sulfuric acid solutions after correcting for differences in ionic strength. They attributed these differences to mixed complex formation. More recently, Haight et al. [26] have shown that the conversion of $HCrO_4^-$ to $CrSO_4^=$ is quantitative in 1 *M* HSO_4^- solutions and that absorption spectrum of this complex is significantly different from the $HCrO_4^-$ spectrum.

Because most of the previous work reported in literature has been done in sulfuric acid, it was considered of interest to intercompare these two systems. The results are shown in each acid between pH 2 and 3. At 350 nm the results obtained in perchloric acid are consistently 0.1–0.2 percent higher than in sulfuric; at 235 nm, they are lower. The relatively large increase in absorptivity at 235 nm at pH 1.90, together with the above considerations, suggest the formation of additional chromium (VI) species in systems employing dilute sulfuric acid solutions. (See table 8.)

e. Effect of Temperature. The absorbances of a solution containing 60 mg $K_2Cr_2O_7$/l in dilute perchloric acid (pH = 3) were measured over the temperature range of 17 to 37 °C. The percentage change in absorbance for wavelengths of 350, 313, 257, and 235 nm is shown in figure 8. The results are uncorrected for

Table 7. Experimental and calculated values (E, C) of the apparent molar absorptivity of $K_2Cr_2O_7$ at 25 °C; pH = 2.9($HClO_4$)

$K_2Cr_2O_7$ Conc. mg/l	α		ϵ_m, l mol^{-1} cm^{-1}			
			350 nm	313 nm	257 nm	235 nm
20.22	0.0090	E	1577.6	713.5	2113.6	1814.7
		C	1577.9	711.9	2108.7	1812.1
		Diff.	−0.3	+1.6	+4.9	+2.6
40.09	0.0178	E	1579.9	713.3	2120.8	1820.2
		C	1579.8	713.0	2118.8	1819.7
		Diff.	+0.1	+0.3	+2.0	+0.5
60.12	0.0262	E	1581.4	713.8	2127.2	1827.1
		C	1581.5	713.8	2126.7	1827.2
		Diff.	−0.1	0.0	+0.5	−0.1
80.17	0.0344	E	1584.0	715.0	2137.6	1835.8
		C	1583.3	714.8	2135.3	1834.4
		Diff.	+0.7	+0.2	+2.3	+1.4
99.92	0.0423	E	1585.5	715.6	2144.0	1841.5
		C	1584.0	715.0	2143.7	1841.4
		Diff.	+1.5	+0.6	+0.3	+0.1

TABLE 8. Apparent absorptivities, a, of sulfuric and perchloric acid solutions of $K_2Cr_2O_7$ at 25 °C; $K_2Cr_2O_7$ conc. = 0.050 g/l

		a, l g^{-1} cm^{-1}			
	pH	350 nm	313 nm	257 nm	235 nm
H_2SO_4	1.90	10.71_0	4.83_7	14.44_4	12.43_7
	1.98	10.71_2	4.83_9	14.44_0	12.41_8
	2.20	10.72_2	4.83_9	14.42_9	12.40_2
	3.00	10.73_3	4.84_4	14.42_7	12.38_1
$HClO_4$	1.99	10.72_7	4.84_8	14.44_8	12.39_6
	3.08	10.74_0	4.84_5	14.43_4	12.38_3

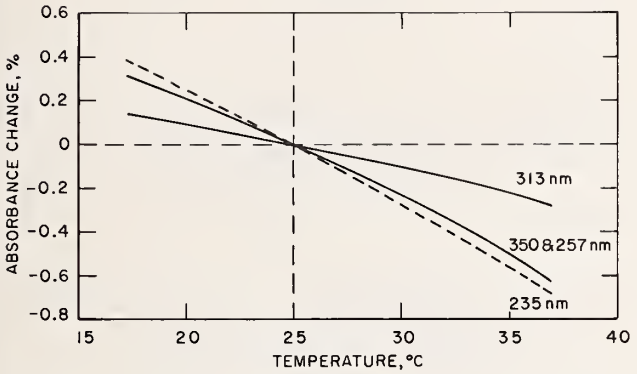

FIGURE 8. Change in absorbance with temperature for acidic solutions of $K_2Cr_2O_7$; pH = 3 ($HClO_4$).

thermal expansion of the solvent. The absorption minimum at 313 nm exhibits the smallest temperature dependence (− 0.02 percent per °C) while the maxima at 350 and 257 nm and the minimum at 235 nm have temperature coefficients of − 0.05 percent per °C over the range 20 to 30 °C.

f. $K_2Cr_2O_7$ in 0.05 M Na_2HPO_4 and 0.05 M KOH. To overcome some of the difficulties in handling strongly alkaline chromate solutions, Johnson [27] has recommended dissolving $K_2Cr_2O_7$ in 0.05 M Na_2HPO_4 at pH 9. The apparent molar absorptivities obtained in this medium and in 0.05 M KOH are given in table 9. As seen from the data, both systems appear to exhibit deviations from Beer's law of about three parts per thousand over the concentration range studied. Although this deviation is the same magnitude and direction predicted from uncompensated internal multiple reflections discussed previously, we have not been able to demonstrate experimentally that such reflections are responsible for the observed results. Studies in which the cuvet windows are coated with various anti-reflection layers are continuing however.

TABLE 9. Apparent molar absorptivity of potassium chromate in 0.05 M Na_2HPO_4 and 0.05 M KOH at 25 °C

	0.05 M Na_2HPO_4		
		ϵ_m, l mol^{-1} cm^{-1}	
K_2CrO_4 Conc., $M \times 10^5$	pH	373 nm	274 nm
7	9.2	482_7	370_3
14	9.1	482_0	369_7
21	9.1	481_3	369_2
	0.05 M KOH		
7	.....	483_0	370_5
14	.....	482_4	369_8
21	.....	481_4	369_1

From a consideration of the equilibrium data, the absorbances in the two systems should be nearly identical. The ionic strength of the 0.05 M Na_2HPO_4 is 0.15 and, from Neuss and Rieman's work [22], the ionization constant for the reaction $HCrO_4^- = H^+ + CrO_4^=$ is approximately 9×10^{-7} mol/liter. Thus, at pH 9.1, only about 1 in 1000 chromium atoms is present as $HCrO_4^-$. Since this species is less absorbing than $CrO_4^=$ at 373 and 274 nm, the apparent molar absorptivities in 0.05 M Na_2HPO_4 should agree with those obtained in 0.05 M KOH to within 0.1 percent.

The absorbance of alkaline chromate solutions decreases with increasing temperature at both absorption peaks. Between 17 and 37 °C, the temperature coefficient at 373 nm is − 0.09 percent per °C; at 274 nm, it is − 0.06 percent per °C.

2. Potassium Nitrate. Aqueous solutions of potassium nitrate exhibit a nearly symmetrical absorption peak with λ_{max} at 302 nm. This system has been studied extensively by Vandenbelt [14] and by the British Photoelectric Spectrometry Group in two collaborative tests [28, 29]. Molar absorptivities reported vary from 7.06 to 7.20 liter mol^{-1} cm^{-1}. This range of values undoubtedly results in part from the fact that KNO_3 solutions deviate significantly from Beer's law.

Careful reexamination of this system has yielded the following apparent molar absorptivities (table 10). These are seen to decrease rather markedly with increasing potassium nitrate concentration. Several factors conceivably contribute to this behavior. In addition to possible multiple reflection effects already discussed some ionic interactions are undoubtedly possible in this system because of the relatively high concentrations of solute required coupled with the fact that the N—O bond in the nitrate ion has some polar character.

The potassium nitrate used in the above study was analyzed for commonly encountered impurities. After drying at 110 °C, the water content was less than 0.02 percent. Flame emission analyses [31] indicated the following levels of alkali and alkaline earth impurities

502-591 O - 73 - 8

(in parts-per-million): Li (< 0.2); Rb (13); Mg (0.2); Ca (1); Sr(4) and Ba (< 2).

At 302 nm, the absorbance of KNO_3 solutions decreases with increasing temperature. Over the range 17 to 37 °C, the temperature coefficient is −0.14 percent per °C.

Solutions stored for up to six months showed no measurable change (≤ 0.1 percent) in absorbance. Edisbury [29] has cautioned, however, that some solutions may develop bacterial whiskers on standing. Sterilization may be effected by prior boiling of the distilled water.

TABLE 10. Apparent molar absorptivity, ϵ_m, of aqueous solutions of potassium nitrate at 25 °C

KNO_3 Conc., M	ϵ_m, l mol^{-1} cm^{-1} 302 nm[a]
0.028	7.16_0
.056	7.14_2
.084	7.12_7
.112	7.10_6
.140	7.09_1

[a] Spectral bandpass = 1.0 nm

3. Potassium Hydrogen Phthalate. High purity potassium hydrogen phthalate (KHP) is readily available. It is presently issued by the National Bureau of Standards as a primary acidimetric standard. Its use in the preparation of buffer solutions of known pH is well established. It has also been used as a spectral standard in the comparative evaluation of spectrophotometers [11, 32].

The absorbance of KHP solutions is dependent on acidity, as shown in figure 9. In the present study, dilute perchloric acid solutions were employed to minimize changes in ionic composition as a function of pH. Acid concentrations much above 0.1 N could not be used because of the precipitation of potassium perchlorate. Subsequently, all solutions were prepared to contain 10 ml of perchloric acid per liter with a pH of 1.3.

Ringbom [21] has given the first ionization constant of phthalic acid as 1.6×10^{-3} at 25 °C at an ionic strength of 0.1. At the pH used, the absorbing system consisted of 97 percent phthalic acid and 3 percent hydrogen phthalate ions. Table 11 summarizes the absorptivity values obtained on these solutions.

Absorbance decreases at the 275.5 nm maximum and increases at the 262 nm minimum with increasing temperature. Over the range 17 to 37 °C the temperature coefficients are −0.05 percent and +0.05 percent per °C, respectively.

Perchloric acid solutions of KHP (NBS–SRM 84g) were examined for possible fluorescence, using a high sensitivity spectrofluorometer. With 280 nm excitation, a faint fluorescence was detected with λ_{max} at approximately 350 nm. The possible effects of this fluorescence on the absorbance data remain to be established.

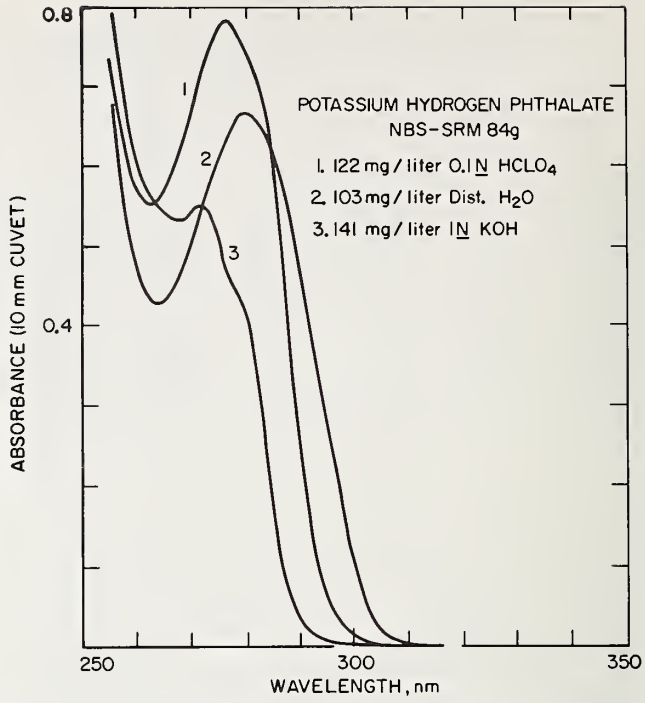

FIGURE 9. Absorption spectra of KHP solutions at different acidities.

TABLE 11. Apparent absorptivity, a, of potassium hydrogen phthalate in dilute perchloric acid at 25 °C; 10 ml $HClO_4$/liter

NBS SRM 84g Conc., g/l	a, l g^{-1} cm^{-1} 275.5 nm	262 nm
0.034	6.33_2	4.49_4
.142	6.31_9	4.48_9

4. Cobalt and Nickel Sulfates and Perchlorates. Aquo cobalt (II) and nickel (II) ions have relative broad absorption peaks with λ_{max} at 512 and 394 nm, respectively (fig. 10). Solutions of either may serve as useful absorbance standards. Most of the attention to date, however, has been directed at cobalt sulfate which was first recommended by Gibson [1].

In this study, the apparent molar absorptivities of $Co(H_2O)_6^{+2}$ and $Ni(H_2O)_6^{+2}$ were examined in sulfate and perchlorate media. All solutions were prepared from the high purity metals by dissolution in H_2SO_4–HNO_3 or $HClO_4$–HNO_3 acids. Nitrate was removed by repeated fuming until the acidity was reduced so that on dilution to volume, a pH of 1 could be obtained. The results obtained in the two acid media are given in table 12. The values in sulfate solution are significantly higher than in perchlorate media for both cobalt and nickel, suggesting that some complexation of these ions by $SO_4^{=}$ or HSO_4^{-} has occurred. A differ-

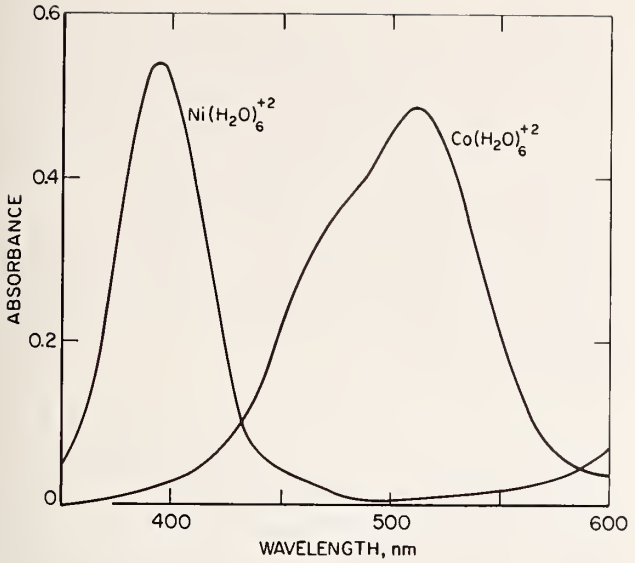

FIGURE 10. Absorption spectra of $Ni(H_2O)_6^{+2}$ and $Co(H_2O)_6^{+2}$.

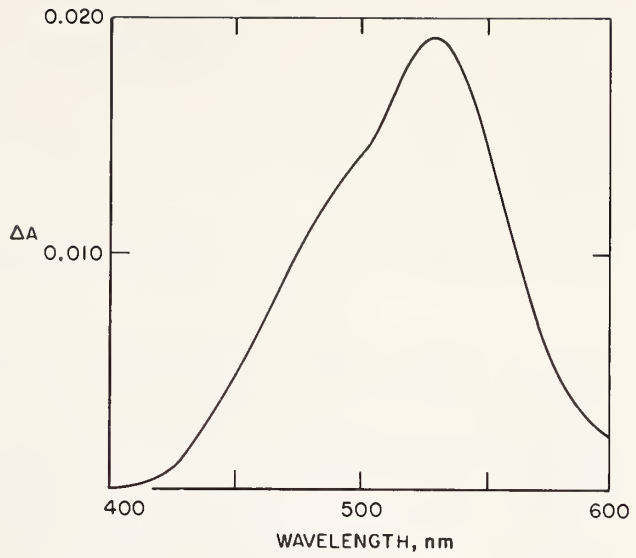

FIGURE 11. Differential spectrum of cobalt sulfate versus cobalt perchlorate; 10 mm cuvets; pH = 1.

TABLE 12. Apparent molar absorptivities, ϵ_m of acidic solutions of cobalt and nickel ions at 25 °C; pH = 1.0

Co Conc. g/l	ϵ_m (512 nm) l mol^{-1} cm^{-1} Sulfate	Perchlorate
2.4	4.88_1	4.80_3
12.0	4.86_9	4.79_1

Ni Conc. g/l	ϵ_m (394 nm) l mol^{-1} cm^{-1} Sulfate	Perchlorate
2.3	5.16_7	5.09_0
11.5	5.15_4	5.07_7

ential spectrum of 0.2000 molar cobalt solution in sulfate against the same cobalt concentration in perchlorate media is shown in figure 11. In sulfate solution, the formation of a second cobalt species with $\lambda_{max} = 528$ nm is indicated. Similar behavior was also observed for nickel.

The absorbances of cobalt and nickel solutions at their maxima are temperature dependent and increase with increasing temperature. Between 17 and 37 °C the temperature coefficients are 0.18 and 0.14 percent per °C at 512 and 394 nm, respectively. To explain their nuclear magnetic resonance data on cobalt(II) solutions, Swift and Connick [33] have suggested that the octahedral $Co(H_2O)_6^{+2}$ complex is in equilibrium with the tetrahedral $Co(H_2O)_4^{+2}$ complex and that formation of the latter is favored by increasing temperature. By analogy with halide complexes, the tetrahedral configuration would be expected to be approximately one hundred times more absorbing than the octahedral complex. A very small shift in this equilibrium could result in a relatively large change in absorbance and thereby account for the large temperature coefficient of this system. The same explanation may also be valid for nickel solutions.

C. Liquid Filters of Improved Optical Neutrality

Two approaches have been used in an attempt to improve the optical neutrality and extend the wavelength range of liquid filters. One is based on the use of empirical mixtures, while the other employs water-soluble, organic "black" dyes.

In 1946, Thomson [34] described the preparation of a grey inorganic solution consisting of chromic, cobaltous and cupric sulfates and potassium dichromate. This solution, however, does not transmit below 300 nm. To extend the wavelength range farther into the ultraviolet, a second exploratory solution (henceforth referred to as the NBS composite) was prepared in which the cupric and potassium dichromate components of the Thomson mixture were replaced by *p*-nitrophenol. The absorption spectra of these solutions are compared in figure 12 to a commonly used glass filter (Chance ON–10). The NBS composite was prepared in dilute sulfuric acid and had a pH of 1. No fluorescence was observed under these conditions.

Over the range 250–600 nm, the NBS composite exhibits several broad maxima and minima whose absorbances are less dependent on spectral bandpass than the Chance ON–10 glass. Examples are given in figure 13 at two wavelengths for each.

The possible use of either Thomson solution or the NBS composite as an absorbance standard is limited by two factors, both of which arise from the presence of chromium (III) in these mixtures. First,

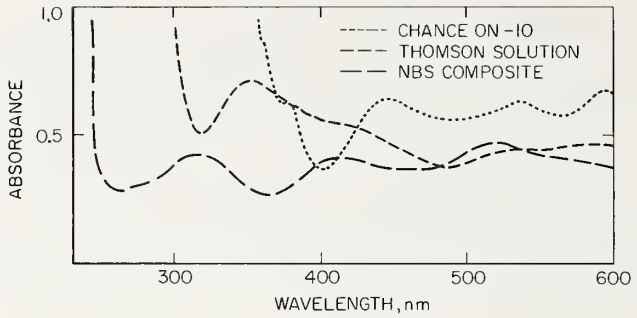

FIGURE 12. Absorption spectra of Thomas solution, an NBS composite and a Chance ON–10 glass.

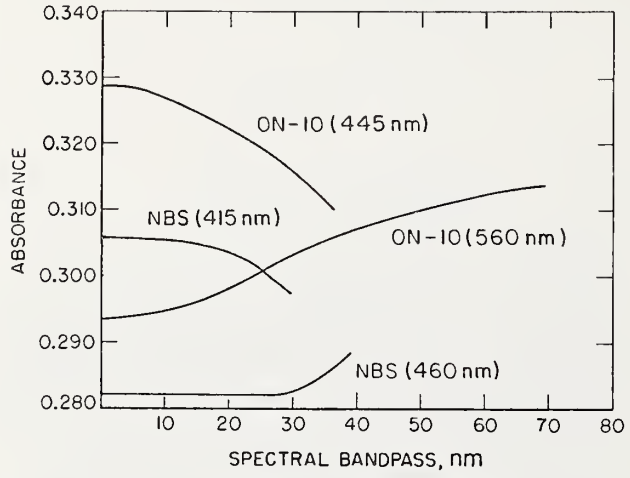

FIGURE 13. Variation of absorbance with spectral bandpass for NBS composite and Chance ON–10 glass.

an initial "aging" of 6–8 weeks period is needed in order to achieve adequate spectral stability at room temperature. Secondly, and even more critical for our purpose, is that the absorbances of the aged solutions exhibit a nonreversible temperature dependence. They must therefore always be stored at the temperature at which they were aged.

Hall and Eyring [35] have studied the constitution of chromic salts in aqueous solution and have suggested that during the aging process $Cr(H_2O)_6^{+3}$ ions polymerize to yield species of the type

$$\left[(H_2O)_5Cr{-}\overset{H}{O}{-}Cr(H_2O)_5 \right]^{+5},$$

$$[(H_2O)_4Cr \begin{array}{c} H \\ O \\ O \\ H \end{array} Cr(H_2O)_4]^{+4}$$

and

$$\left[(H_2O)_5{-}Cr{-}\overset{H}{O}{-}Cr(H_2O)_4{-}\overset{H}{O}{-}Cr(H_2O)_5 \right]^{+7}$$

in which the observed increase in acidity is explained by the formation of —OH bridges. Recent studies [36] have shown that temperature, initial pH and the type of anion present significantly affect the equilibrium composition. Although refluxing can reduce the aging period from several months to several hours, this is of no practical advantage since the high temperature products, on cooling, are no longer stable.

In addition to the investigation of empirical mixtures, several water-soluble organic dyes have also been studied. Some typical absorption spectra are shown in figure 14. All of these dyes have high absorptivities and the concentrations used were of the order of 50 milligrams per liter.

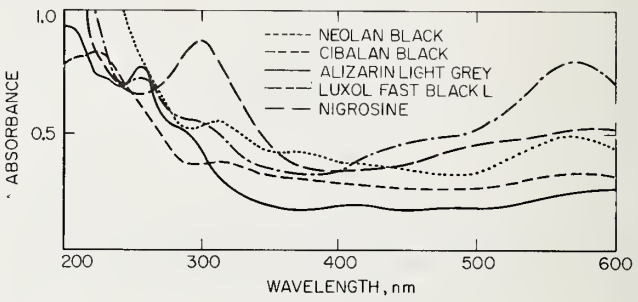

FIGURE 14. Absorption spectra of aqueous solutions of selected dyes.

Cibalan Black [37], Neolan Black [37] and Alizarin Light Grey [38] were selected for further evaluation. Aqueous solutions of these dyes were found insensitive to pH over the range 2–9, not affected by heat and relatively light fast. Solutions continuously exposed to fluorescent light exhibited an absorbance change of about 1 percent over a period of two months. These initial results appeared sufficiently promising to warrant purification and more extensive testing. Members of the Organic Chemistry Section have assisted in this effort. The purification of these dyes has proven extremely difficult, however, and yields of only a few hundred milligrams of each have been obtained. Much larger quantities are needed if these dyes are to be used as Standard Reference Materials. More efficient purification procedures are presently being sought.

D. Standard Reference Material (SRM) 931

The first liquid absorbance standard to be issued by the National Bureau of Standards is SRM 931. The preparation and certification of this Standard Reference Material are described below.

The filters were prepared by dissolving high purity cobalt and nickel in a mixture of nitric and perchloric acids. The weights of cobalt and nickel were chosen so that the absorbances of their aquo complexes were approximately equal at their absorption maxima. The absorbance of nitrate was adjusted to a comparable level by evaporation and subsequent addition

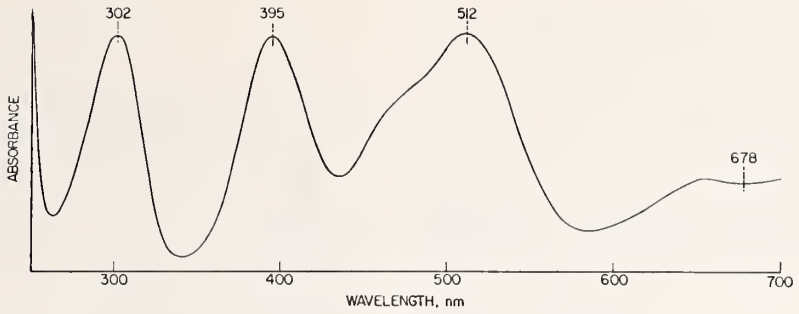

FIGURE 15. Typical absorption spectrum of SRM 931.

of small amounts of nitric acid. The final pH of these mixtures was about 1.

An absorption spectrum of a typical filter is shown in figure 15. The peaks at 302 and 512 nm are due to absorption by NO_3^- and $Co(H_2O)_6^{+2}$, respectively. The peak at 395 nm and the plateau at 650–700 nm are due to $Ni(H_2O)_6^{+2}$.

The filters are supplied in 10 ml ampoules which have been prescored for easy opening. An SRM unit consists of three sets of filters, each set containing a "Blank" (0.1N perchloric acid) and three absorbance levels of the filter. Each set is packaged in an individual tray for added convenience.

The filters were calibrated by randomly selecting ampoules from each lot. The certified absorbances are as follows:

TABLE 13. Certification of NBS SRM 931

	Net absorbance[a]			
	Wavelength and (Bandpass), nm			
Filter	302(1.0)	395(1.7)	512(2.0)	678(6.5)
"A"–'Blank'	0.307 ± 0.003	0.304 ± 0.003	0.303 ± 0.003	0.115 ± 0.002
"B"–'Blank'	0.608 ± 0.005	0.605 ± 0.005	0.606 ± 0.005	0.229 ± 0.003
"C"–'Blank'	0.906 ± 0.007	0.907 ± 0.007	0.911 ± 0.007	0.345 ± 0.003

[a] Net absorbances "A"–'Blank,' "B" –'Blank,' and "C"–'Blank' were determined using 10.00 mm cuvets at 25.0 °C.

The uncertainties are given at the 95 percent confidence level and include a possible systematic error of ±0.5 percent.

Absorbances are certified at 25.0 °C. Absorbances at other temperatures in the range 17 to 37 °C may be calculated using the formula:

$$A_t = A_{25}[1 + C_A(t-25)]$$

where: A_t = Absorbance at temperature t (°C)
A_{25} = Absorbance certified at 25.0 °C
C_A = Fractional change in absorbance per °C

The values of C_A at the four wavelengths are given below.

λ, nm	C_A
302	−0.0014
395	+0.0014
512	+0.0018
678	+0.0014

The absorbances of these filters will also depend on the spectral bandpass used. To insure that the measured absorbances do not differ by more than ±0.1 percent from the true values, the effective spectral bandpass should not exceed 1.5, 2.0, 3.3, and 8.5 nm at 302, 395, 512, and 678 nm, respectively.

IV. Conclusion

The availability of well characterized materials from which the analyst prepares his own solutions is preferable to the issuance of ampouled liquids. Although the former are not as convenient to use, they offer potentially greater accuracy because of their better stability.

The potassium dichromate and potassium hydrogen phthalate used in this study are issued by NBS as primary oxidimetric and acidimetric standards (SRM 136c and 84g, respectively). The potassium nitrate is presently issued as a thermal analysis standard (SRM 756). A product of comparable purity may be

obtained by repeated recrystallization of reagent-grade material from distilled water. The cobalt and nickel solutions are best prepared from the high purity metals which are commercially available.

To certify absorptivities for these materials, one must resolve the question as to how well these systems obey Beer's law. For acidic potassium dichromate, the increased dimerization of $HCrO_4^-$ to $Cr_2O_7^=$ with increasing chromium concentration primarily accounts for the relatively large deviations observed. With potassium nitrate, one can only speculate that ionic interactions are enhanced at the higher concentrations. In neither instance are these deviations sufficiently large to limit the usefulness of these materials as liquid absorbance standards. Such deviations do require that the absorptivity data be used with proper precautions.

Additional studies are needed to explain the 0.2–0.3 percent deviations from Beer's law obtained for the various concentrations of alkaline chromate, potassium hydrogen phthalate, cobalt perchlorate and sulfate, and nickel perchlorate and sulfate. Although internal multiple reflection effects appear to be of the proper magnitude to account for these differences, initial attempts to measure such effects with magnesium fluoride-coated cuvets have not been successful. While extremely durable, magnesium fluoride reduces reflections by about 50 percent and more efficient coatings will probably be needed to resolve this problem. If internal reflections are responsible for the observed deviations, the absorptivity data given should not be corrected when using liquid absorbance standards for checking the accuracy of the photometric scale since these reflections are included in every measurement. However, in the determination of molar absorptivity, which is considered a fundamental property of the material, appropriate corrections should be applied. Until this question can be resolved, it is recommended that these materials be used at concentrations which yield an absorbance of at least 0.5 when measured in a 10 mm cuvet. With this restriction, it is believed that the uncertainty of the absorptivity data does not exceed ± 0.5 percent at the 95 percent confidence level.

The authors wish to express their appreciation to Radu Mavrodineanu for providing the calibrated Schott filters and to David S. Bright for performing the computer calculations on the $HCrO_4^-/Cr_2O_7^=$ equilibrium.

V. References

[1] Gibson, K. S., Nat. Bur. Stand. Circular 484 (1949).
[2] Harrison, G. R., M.I.T. Wavelength Tables (John Wiley & Sons, Inc., New York, N.Y., 1969).
[3] Meehan, E. J., 'Treatise on Analytical Chemistry', Kolthoff, I. M., and Elving, P. J., Editors, Part 1, Volume **5**, Chapter 54 (John Wiley & Sons, Inc., New York, N.Y., 1964).
[4] Hardy, A. C., and Young, F. M., J. Opt. Soc. Am. **39**, 365 (1949).
[5] Eberhardt, W. H., J. Opt. Soc. Am. **40**, 172 (1950).
[6] Broderson, S., J. Opt. Soc. Am. **44**, 22 (1954).
[7] Hogness, T. R., Zscheile, F. P., and Sidwell, A. E., J. Phys. Chem. **41**, 379 (1937).
[8] Perry, J. W., Photoelectric Spectrometry Group Bull. **3**, 40 (1950).
[9] Slavin, W., Anal. Chem. **35**, 561 (1963).
[10] Poulson, R. E., Appl. Opt. **3**, 99 (1964).
[11] Goldring, L. S., Hawes, R. C., Hare, G. H., Beckman, A. O., and Stickney, M. E., Anal. Chem. **25**, 869 (1953).
[12] British Standard 3875, British Standards Institution (1965).
[13] Mavrodineanu, R., Nat. Bur. Stand. (U.S.), Tech. Note 584, 178 pages (1971), O. Menis and J. I. Shultz, Eds.
[14] Vandenbelt, J. M., Forsyth, J., and Garrett, A., Anal. Chem. **17**, 235 (1945).
[15] Haupt, G. W., J. Opt. Soc. Am. **42**, 441 (1952).
[16] Haupt, G. W., J. Res. Nat. Bur. Stand. **48**, 414 (1952).
[17] Vandenbelt, J. M., and Spurlock, C. H., J. Opt. Soc. Am. **45**, 967 (1955).
[18] Gridgeman, N. T., Photoelectric Spectrometry Group Bull. **4**, 67 (1951).
[19] Ketelaar, J. A. A., Fahrenfort, J., Haas, C., Brinkman, G. A., Photoelectric Spectrometry Group Bull. **8**, 176 (1955).
[20] Vandenbelt, J. M., J. Opt. Soc. Am. **50**, 24 (1960).
[21] Ringbom, A., Complexation in Analytical Chemistry, (John Wiley & Sons, Inc., New York, N.Y., 1963), p. 294.
[22] Neuss, J. D., and Rieman, W., J. Am. Chem. Soc. **56**, 2238 (1934).
[23] Howard, J. R., Nair, V. S. K., and Nancollas, G. H., Trans. Faraday Soc. **54**, 1034 (1958).
[24] Tong, J., and King, E. L., J. Am. Chem. Soc. **75**, 6180 (1953).
[25] Davies, W. G., and Prue, J. E., Trans. Faraday Soc. **51**, 1045 (1955).
[26] Haight, G. P., Richardson, D. C., and Coburn, N. H., J. Inorg. Chem. **3**, 1777 (1964).
[27] Johnson, E. A., Photoelectric Spectrometry Group Bull. **17**, 505 (1967).
[28] Edisbury, J. R., Photoelectric Spectrometry Group Bull. **1**, 10 (1949).
[29] Edisbury, J. R., Photoelectric Spectrometry Group Bull. **16**, 441 (1965).
[30] Malitson, I., private communication.
[31] Rains, T. C., private communication.
[32] Ewing, G. W., and Parsons, T., Anal. Chem. **20**, 423 (1948).
[33] Swift, T. J., and Connick, R. E., J. Chem. Phys. **37**, 307 (1962).
[34] Thomson, L. C., Trans. Faraday Soc. **42**, 663 (1946).
[35] Hall, H. T., and Eyring, H., J. Am. Chem. Soc. **72**, 782 (1950).
[36] Burke, R. W., and Deardorff, E. R., Nat. Bur. Stand. (U.S.), Tech. Note 544, 153 pages (1970), O. Menis and J. I. Shultz, Eds.
[37] Ciba Chemical and Dye Company, Fair Lawn, New Jersey.
[38] Industrial Chemicals Division, Allied Chemical Corporation, Buffalo, New York.

(Paper 76A5–733)

NATIONAL BUREAU OF STANDARDS SPECIAL PUBLICATION 378, Accuracy in Spectrophotometry and Luminescence Measurements, Proceedings of a Conference Held at NBS, Gaithersburg, Md., March 22–24, 1972 (Issued May 1973).

Accurate Measurement of Molar Absorptivities

Robert W. Burnett

Clinical Chemistry Laboratory, Hartford Hospital, Hartford, Connecticut 06115

(June 7, 1972)

The key to accurate measurement of molar absorptivities is a thorough understanding of the sources of error which appear throughout the measurement procedure. Sources of determinant error will be listed with comments on estimating their magnitude and eliminating them where possible. Sources of random error will be discussed as well as the propagation of both random and determinant errors. There is discussion of the need for accurate values of molar absorptivities using examples from clinical chemistry. Finally, the proper use of accurate absorptivity values in the clinical chemistry laboratory will be considered. Here, emphasis is on the need for a quality assurance system which includes routine checks on such things as wavelength calibration and photometric accuracy of spectrophotometers, calibration of analytical balances, and quality of incoming reagents.

Key words: Molar absorptivity in clinical chemistry; random errors in molar absorptivity; systematic errors in molar absorptivity.

I. Introduction

Absorption spectrophotometry in the visible and ultraviolet is undoubtedly one of the most valuable tools available to the analytical chemist. In clinical chemistry, roughly 60 percent of all determinations performed utilize this technique. It is natural, therefore, that in the quest for more meaningful data, considerable attention is focused on accuracy in spectrophotometry, and specifically on accurate measurement of molar absorptivities. In this paper the important sources of error which affect molar absorptivity measurements are reviewed and the propagation of the individual errors is discussed. In addition, some of the rationale underlying the increasing interest in accuracy in spectrophotometry is discussed, with particular reference to clinical chemistry.

The key to accurate measurement of molar absorptivities is careful attention to the various error sources which are present in the measurement process. The problem discussed here is that of establishing a molar absorptivity uncertainty which is no greater than one part per thousand. With this in mind, we will be concerned with individual sources of error down to a level of one or two parts per ten thousand, recognizing that many errors contribute to the final uncertainty. This point is demonstrated more formally in the brief discussion of error propagation. Much of the material presented on errors is in the nature of a review; it is thought that this may be useful since discussions of the various errors are somewhat scattered in the literature, and the mathematical complexity of some of the original discussions may obscure their practical implications. Reference is made to earlier papers for many of the mathematical details.

Molar absorptivity, ϵ, may be defined by Beer's law as

$$\epsilon = \frac{AM}{bc} \tag{1}$$

where A is absorbance, M is the molecular weight of the solute, b is the effective path-length in centimeters and c is the solution concentration in grams per liter. The units of ϵ are thus $1 \cdot \text{mol}^{-1} \cdot \text{cm}^{-1}$. Two restrictions apply to eq (1); first, the equation is valid only for monochromatic radiation, and second, the ratio of absorbance to concentration is constant only for ideal solutions. The former restriction will be commented upon later and the latter is not usually a problem because measurements are ordinarily made at concentrations below 10^{-3} mol $\cdot l^{-1}$ where deviation from ideal behavior may be ignored. A related problem sometimes encountered is commonly known as a chemical deviation from Beer's law, which occurs when the concentration of the absorbing species does not increase linearly with solute concentration. Examples of this behavior are well known and the effect will not be commented upon further, except to note that the acid chromium (VI) system, which has been recently studied by Burke, et al. [1][1], is a particularly important system of this type because of its common use as an absorbance standard. It is emphasized that adherence to Beer's law over a range of concentrations

should never be assumed in the absence of supporting experimental data. In contrast to the chemical sources of error, the items discussed below may be classed as instrumental and procedural sources of error in the measurement process.

[1] Figures in brackets indicate the literature references at the end of this paper.

II. Systematic Errors

A. Gravimetric and Volumetric Errors

Although these error sources may seem rather obvious, they deserve mention both for completeness and because certain components are probably often ignored. Analytical balances must be calibrated using weights certified by the National Bureau of Standards. The solution temperature at which absorbance measurements are made must be known and the solvent density at this temperature should be used in calculating the solution concentration. Accurate temperature measurement is especially important when the solvent has a high coefficient of thermal expansion; for example, chloroform shows a volume expansion of 1.3 parts per thousand per °C near room temperature. In addition, it is interesting to note that the relatively low heat capacity of many organic solvents means that they are much more sensitive to heating effects than is water. Chloroform shows 27 times the volume expansion of water for an equal heat input.

Where gravimetric technique is employed in measuring both solute and solvent, it is necessary to take the apparent specific volume of the solute into account in calculating the concentration, the relationship being

$$c=\frac{1000\ W_x\rho}{W_s+W_x\rho\bar{v}} \tag{2}$$

where c is concentration in grams per liter, W_x is weight of solute in grams, W_s is weight of solvent in grams, ρ is solvent density in g/cm³ and $\bar{v}$ is solute apparent specific volume in cm³/g. This is especially important for solutes of relatively high molecular weight and low molar absorptivity, in which case the correction due to $\bar{v}$ can approach one part per thousand.

Finally, it must be remembered that in any weighing process which involves displacement of air, a buoyancy correction must be applied. The magnitude of this correction depends on the difference in density between the weights used and the material being weighed. For water, the correction is about one part per thousand and it is only slightly smaller for most solids. Buoyancy corrections for single-pan balances have been discussed in detail by Burg and Veith [2] and by Lewis and Woolf [3].

B. Path Length Errors

To obtain highly accurate absorbance measurements, the cell path length must obviously be known with very high accuracy. Electromechanical devices known as electronic gauges have been used for this purpose. In expert hands and with careful calibration and repetitive measurements, these instruments are capable of establishing the path length of a cell to ± 0.0001 cm, which for a standard one-cm cell is a relative accuracy of one part per ten thousand. In addition, the measurement may be made at any point on the cell window so that the parallelism of the windows is also readily checked. The magnitude of the error which may be introduced by accepting the nominal value for cell-path length is not commonly appreciated. At the National Bureau of Standards, in a series of measurements of fourteen cells with a one-cm nominal path-length, thirteen deviated from the nominal value by greater than one part per thousand and five were in error by greater than 1 percent [4]. As will be seen, this may easily be the most significant error source in a molar absorptivity measurement. An accurate measurement of cell path length will not suffice to eliminate all path length errors, however. Several additional factors which can influence the *effective* path length are discussed below.

C. Beam Alignment Errors

A significant error due to nonparallel incident radiation appears whenever the most extreme angle which the light rays make with a line normal to the cell windows exceeds about 3°, as shown in figure 1a.

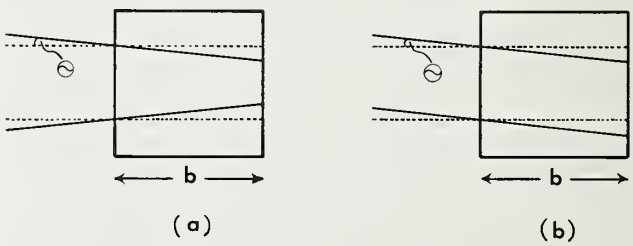

FIGURE 1. (a) Increase in effective path length due to nonparallel incident radiation. (b) Increase in effective path length due to improper cell orientation.

This increases the effective path length and, therefore, the observed absorbance. At an absorbance of one, the error is five parts per thousand when the most extreme rays deviate from the normal by 10°; if the maximum deviation is 5° the error is under one part per thousand. Exact corrections depend on the refractive index of the solution and must be obtained by numerical integration [5]. Proper cell orientation is also critical since cell windows must be normal to the incident radiation. Any other orientation will result in a longer light path through the cell, as shown in figure 1b. This effect is significant at deviations greater than 1° and increases with Θ^2, the approximate relation being

$$\delta=\frac{\pi^2\Theta^2}{64{,}800\ n^2} \tag{3}$$

where δ is the fractional path length error, Θ is the angle of incidence of the beam, in degrees, and n is the refractive index of the solvent. The error function is shown graphically in figure 2 for $n = 1.33$.

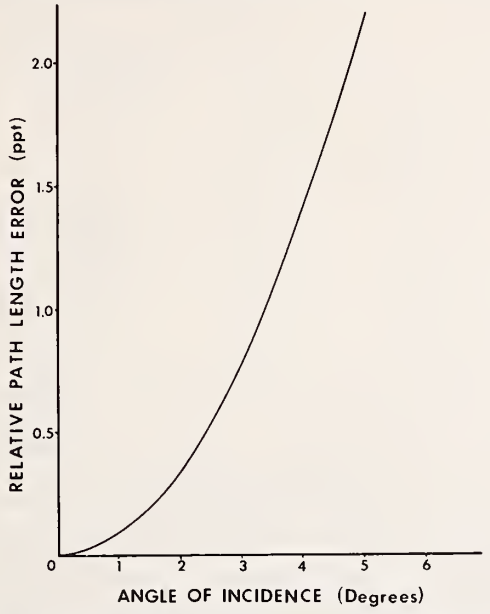

FIGURE 2. Relative path length error (parts per thousand) due to improper cell orientation, for $n = 1.33$. From eq (3).

D. Reflection Errors

When light passes from one medium with refractive index n_1 to another with refractive index n_2, a fraction of the light is reflected at the interface. If the angle of incidence is zero (light beam normal to the interface) the Fresnel relation for the fraction reflected, is

$$f = \left(\frac{n_1 - n_2}{n_1 + n_2}\right)^2. \tag{4}$$

An air-glass interface may be roughly represented by using $n_{air} = 1.0$ and $n_{glass} = 1.5$, in which case $f = 0.04$, i.e. 4 percent of the incident light is reflected. Reflection losses can be partially compensated by subtracting the apparent absorbance of pure solvent from the absorbance of the solution in an identical cell. Unfortunately, this still leaves an important error which is due to multiple reflections within the cell. The major component of this error is due to light which enters the cell, is reflected back into the solution from the rear window (the window nearest the detector), is reflected again at the forward window, and reaches the detector having traversed the solution three times. This problem has been considered by Goldring, et at. [6] who derived the following approximation for ΔA, the increase in apparent absorbance due to multiple reflections,

$$\Delta A = 0.434(1 - T^2)\left(\frac{f_1 \cdot f_2}{1 - f_1}\right) \tag{5}$$

where T is the solution transmittance, f_1 is the fraction of light reflected at the rear window (considering both interfaces) and f_2, the fraction reflected at the forward window. Equation (5) may be rewritten in terms of the relative absorbance error δ,

$$\delta = \frac{(0.434 - e^{-2A})}{A}\left(\frac{f_1 \cdot f_2}{1 - f_1}\right) \tag{6}$$

Figure 3 shows how δ varies with A for the condition $f_1 = f_2 = 0.04$. This should be recognized as the minimum error which is possible since only the reflections

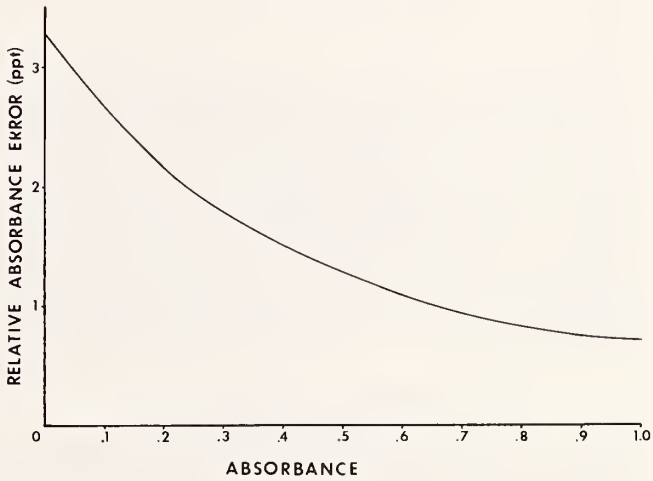

FIGURE 3. Relative absorbance error (parts per thousand) due to multiple reflections at cell windows. From eq (6) with $f_1 = f_2 = 0.04$.

at the air-glass interface are considered. In practice, it may be found that reflections from other surfaces close to the light path are significant, and f_1 and/or f_2 may be much greater than 0.04 [6], although this should not be the case in well-designed instruments.

E. Effect of Finite Slit Width

Since nomenclature in this subject is not completely standardized, the following definitions are given: slit function plot is the plot of photon flux emergent from the exit slit *versus* wavelength; spectral bandwidth is the width at half-height of the slit function plot; natural bandwidth is the width at half-height of the absorption band; bandwidth ratio is the ratio of the spectral bandwidth to the natural bandwidth. Since Beer's law is valid only for monochromatic light, the use of a band of radiation, albeit narrow, introduces an error unless the absorption spectrum is extremely flat in the region of interest. The mathematical formulation of this problem has been dealt with by several authors [7–9] and usually involves the assumptions of a triangular slit function plot and a Gaussian shape for the absorption band. The results obtained show that the observed absorbance is lower than the true absorbance and that the error is a function of the bandwidth ratio, as shown in figure 4. Strictly speaking, the error magnitude is

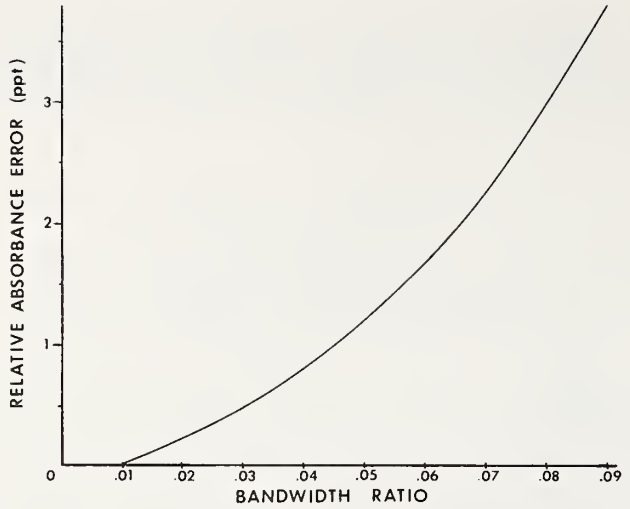

FIGURE 4. Relative absorbance error (parts per thousand) due to finite slit width (9, 10).

also a function of absorbance, but this dependence is negligible as long as the bandwidth ratio is less than 0.4 [9].

F. Stray Radiation

As used here, stray radiation means radiation appearing at the detector with wavelengths outside the envelope defined by the slit-width and monochromator dispersion. This radiation may be either unabsorbed or partially absorbed by the sample. The variation with wavelength of source intensity, monochromator transmission and detector sensitivity are all factors which affect the amount of stray radiation present. For the case where the radiation is unabsorbed it can be shown [11] that the observed absorbance is less than the true absorbance by an amount, ΔA, equal to

$$\Delta A = \log (1 - r + 10^{A} r) \qquad (7)$$

where r is the fraction of stray radiation present. Table 1 shows the relative absorbance error caused by the presence of 0.1 percent and 0.01 percent unabsorbed stray radiation. It must be emphasized, however, that if a solution has intense absorption bands at other than the wavelength for which the monochromator is set, the mathematical formulation is considerably more complex. The error may be somewhat less than is shown in table 1, although there is also the case where the fraction of stray radiation absorbed is greater than the fraction absorbed at the wavelength of interest. In this case, the observed absorbance is greater than the true absorbance. Measurement of stray light has been discussed by Slavin [12] and Poulson [13] among others and extensive correction tables given by Opler [14]. Naturally, the fraction of stray light appearing at the detector will be relatively high in those regions where source output or detector sensitivity is low, or when working at high absorbances.

TABLE 1. Absorbance error due to unabsorbed stray radiation

A	$\frac{\Delta A}{A} \times 1000$ (parts per thousand)	
	$r = 0.001$	$r = 0.0001$
0.1	1.12	0.11
.2	1.27	.13
.3	1.44	.14
.4	1.64	.16
.5	1.88	.19
.6	2.15	.22
.7	2.48	.25
.8	2.87	.29
.9	3.34	.33
1.0	3.89	.39

G. Wavelength and Absorbance Accuracy

The spectrophotometer should be calibrated for both wavelength and absorbance as close as possible to the points where they will be used. Obviously the measurements will be no better than the uncertainty of the calibration system. The error in absorbance at an absorbance maximum, due to a systematic bias in wavelength setting, is a function of the width of the absorption band of the compound of interest. The relative absorbance error is shown in figure 5, and was calculated assuming a Gaussian band shape and

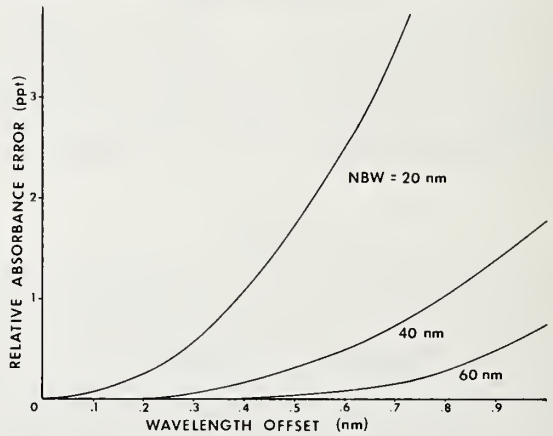

FIGURE 5. Relative absorbance error (parts per thousand) due to wavelength scale inaccuracy, for absorption bands of various natural bandwidths (NBW).

neglecting the effect of finite slit-width. With regard to absorbance calibration, it may be noted that if it is feasible to use solutions as absorbance standards, the systematic errors due to path-length, beam alignment and multiple reflections may be partially compensated in the calibration. On the other hand, if the accuracy of the photometric readings is established by other, more sensitive means such as testing the summation of photon flux (light addition principle), then these

errors must be accounted for separately.

The important sources of systematic error in spectrophotometry have been summarized in table 2. As used in the table, a positive error is one for which the apparent absorbance is greater than the true absorbance.

TABLE 2. Systematic error sources in spectrophotometry

	$\Delta A/A$ Range (parts per thousand)
Solution temperature	−2 to +2
Solute apparent specific volume	0 to −1
Buoyancy correction	+0.2 to +1
Cell path-length	−10 to +10
Cell orientation	0 to +1
Multiple reflections	+0.5 to +3
Finite slit-width	0 to −1
Stray radiation	0 to −1
Wavelength offset	0 to −1

III. Random Errors

In any analytical process, random errors occur whenever an instrument setting is made or a reading is taken. In the simplest type of measurement of a molar absorptivity, significant random errors can be introduced at two points; first, the weighing of solute and solvent, and second, the measurement of the solution absorbance. The approach which should be taken is first to consider means of minimizing the errors and then to estimate the magnitude of the residual errors. The random errors associated with weighing are minimized simply by using a balance of adequate sensitivity in the range of interest. If the residual error is estimated to exceed one part in ten thousand, the actual magnitude should be determined by experiment.

Random error associated with absorbance measurements is a rather difficult topic to treat theoretically, and the simplifying assumptions found in many discussions may be misleading. The objective is to determine the point on the absorbance scale where the relative absorbance error, $\Delta A/A$, is a minimum. Of the many components which can influence this, the one which often represents the limiting factor is the detector. The most commonly employed detector in high precision spectrophotometers is the photomultiplier. Briefly, the principal advantage of this device is that for low photocathodic currents the signal-to-noise ratio varies with the square root of the current, while photodiodes show a direct proportionality between these two quantities. Thus, at the relatively low levels of light intensity commonly encountered in spectrophotometry, it can be shown that photomultipliers operate at a higher signal-to-noise ratio than do photodiodes. Mathematical derivations for a single-beam instrument have been recently presented by Ingle and Crouch [15]. An analysis has also been given for a double-beam photomultiplier instrument [16] where it is shown that the minimum relative absorbance error is obtained near $A=1.0$ and does not vary significantly between $A=0.5$ and $A=1.5$.

It should be kept in mind that the random error is actually a complex function of several variables, and the consensus is that the procedure to be recommended is to experimentally determine $\Delta A/A$ as a function of absorbance for the particular instrument to be used. After appropriate steps have been taken to minimize the error associated with each measurement, the residual random error component may be reduced further by performing multiple measurements. This will be commented on in the following section.

IV. Propagation of Error

After all errors discussed above have been minimized and measured, it is necessary to ask how the residual error components combine to give an overall uncertainty in the molar absorptivity. The simplest case is that where only single measurements are made, in which case the errors in weighing and in reading solution absorbance will be propagated as systematic errors. If F is any function of three independent variables, $F=f(a,b,c)$, with associated bounds of systematic error, Δa, Δb, and Δc, the bound for the error in F is given [17] by

$$\Delta F=\left|\frac{\partial F}{\partial a}\right|\Delta a+\left|\frac{\partial F}{\partial b}\right|\Delta b+\left|\frac{\partial F}{\partial c}\right|\Delta c \qquad (8)$$

Applying this relation to eq (1) yields the expression for the uncertainty in ϵ,

$$\Delta\epsilon=\left(\frac{M}{bc}\right)\Delta A+\left(\frac{AM}{b^2c}\right)\Delta b+\left(\frac{AM}{bc^2}\right)\Delta c \qquad (9)$$

Because of the particular form of eq (1), a simplification obtains from writing the result as a relative uncertainty

$$\frac{\Delta\epsilon}{\epsilon}=\frac{\Delta A}{A}+\frac{\Delta b}{b}+\frac{\Delta c}{c}. \qquad (10)$$

This equation expresses the important result that the relative error in ϵ is just the sum of the relative errors in absorbance, path length and concentration.

Finally, it is noted that the random error component of $\Delta\epsilon$ can be reduced by performing repetitive measurements. If multiple absorbance measurements are made on the same solution, ΔA may be decreased, but Δb and Δc are unaffected and contribute to $\Delta\epsilon$ as before. If many solutions are prepared and measured independently, both ΔA and Δc may be reduced, although since the reduction of the random error is proportional to $\sqrt{n}$, an improvement by a factor of two or three is all that may be practical. Moreover, it is clear that systematic errors are unaffected by repetitive measurements and will always contribute a constant amount to the final uncertainty in molar absorptivity.

V. Spectrophotometric Accuracy in Clinical Chemistry

Although much attention has been focused on precision in clinical analysis, there is increasing recognition of the importance of accuracy. In a thoughtful discussion on the status of the clinical laboratory sciences, Young, et al. state [18]:

> "While day-to-day . . . reproducibility . . . is necessary for results to be meaningful within a single institution, it is essential that the results are also accurate if they are to have long-term validity or are to be compared with results from other laboratories."

A prerequisite for accuracy in many clinical analyses is an accurately known molar absorptivity. An important example is found in clinical enzymology where measurements of enzyme activities in blood serum account for 15 to 20 percent of all tests performed in the clinical chemistry laboratory. These activities are measured spectrophotometrically as the rate of utilization of substrate or rate of appearance of product of the enzyme-catalyzed reaction, and reported values are given in units of micromoles per minute per unit volume of serum. In these tests, standardization in the usual sense is not feasible and accuracy of results is directly dependent on the accuracy of absorbance measurements and accuracy of the value assumed for the molar absorptivity of substrate or product.

The problem is complicated further by the fact that a molar absorptivity is not a solute property, but may vary markedly with changes in solvent, pH or concentrations of other components in the solution. This is pertinent because of the many different conditions of temperature, pH and buffer composition which are routinely employed in clinical enzymology. A panel appointed by the International Federation of Clinical Chemists is currently engaged in considering referee methods for enzyme assays in clinical chemistry. It is significant that the goal of the panel is to recommend methods with a systematic bias no greater than ± 1 percent. If this is to be achieved, it will probably be necessary to know the molar absorptivity of the substrate or product to within one or two parts per thousand.

A compound of particular interest in this connection is nicotinamide adenine dinucleotide (NAD) which is a required coenzyme in many reactions of clinical importance. NADH, the reduced form of NAD, has a characteristic absorbance maximum at 340 nm, and rate reactions involving this couple are commonly followed by measuring absorbance at 340 nm as a function of time. The accepted value of 6220 $1\ mol^{-1} \cdot cm^{-1}$ for the molar absorptivity of NADH at 340 nm was determined in 1948 by Horecker and Kornberg [19]. It is not widely appreciated that their seven experimental values ranged from 5930 to 6310. These authors considered 6220 to be a minimum value and estimated a possible error of 2 percent in their assigned value. Sources of error connected with the spectrophotometer were not discussed. Thus, our best estimate of this important constant may be more realistically stated as 6200 ± 200, and this uncertainty alone may account for as much as a 2 to 3 percent systematic bias in many of our enzyme assays.

Another area where accurate molar absorptivities could be used to advantage is that of monitoring quality of incoming reagents, especially those used as standards. Bilirubin is an example of a compound which is widely used as a standard, but which has been notorious for variations in purity among the several commercial sources. The availability of purified bilirubin from the National Bureau of Standards (SRM 916) and the determination of its molar absorptivity makes possible the elimination of an important source of systematic error in this test and makes interlaboratory comparison of results feasible. It is emphasized that monitoring incoming reagent quality is only one aspect of an effective quality assurance program in clinical chemistry. Other items which should be routinely checked include wavelength and absorbance accuracy of spectrophotometers, following the practical suggestions of Rand [20], calibration of balances and thermometers, and reagent water purity. Each of these items deserves attention in order to make further progress toward the goal of increased accuracy in clinical chemistry.

VI. Summary

The determination of molar absorptivities with an overall uncertainty not greater than one part per thousand is possible only if consideration is given to the several sources of error which have been discussed. Systematic errors whose magnitude and direction are both known may be corrected. This leaves random errors and systematic errors for which only an estimation of magnitude is available, which are used in estimating the overall uncertainty of the molar absorptivity value from eq (10). The need for accurate molar absorptivities has been discussed, using examples in clinical chemistry. These values, used in conjunction with a comprehensive quality assurance program, form the basis for increasing accuracy in many clinical chemistry tests, which will result in clinical laboratory data which are more useful than that presently available.

VII. References

[1] Burke, R. W., Deardorff, E. R., and Bright, D. S., in Nat. Bur. Stand. (U.S.), Tech. Note 584, O. Menis and J. I. Shultz, Eds. (1971), p. 27.
[2] Burg, W. R., and Veith, D. A., J. Chem. Educ. **47**, 192 (1970).
[3] Lewis, J. E., and Woolf, L. A., J. Chem. Educ. **48**, 639 (1971).
[4] Matwey, J., Analytical Chemistry Division, National Bureau of Standards, personal communication.
[5] Meehan, E. J., in Treatise on Analytical Chemistry, I. M. Kolthoff, and P. J. Elving, Eds., Part I, Vol. **5**, (John Wiley & Sons, New York, N.Y., 1964), p. 2776.
[6] Goldring, L. S., Hawes, R. C., Hare, G. H., Beckman, A. O., and Stickney, M. E., Anal. Chem. **25**, 869 (1953).
[7] Hardy, A. C., and Young, F. M., J. Opt. Soc. Am. **39**, 265 (1949).
[8] Eberhardt, W. H., J. Opt. Soc. Am. **40**, 172 (1950).

[9] Broderson, S., J. Opt. Soc. Am. **44**, 22 (1954).
[10] Cary Instruments, Model 16 Spectrophotometer Instruction Manual.
[11] Meehan, E. J., in Treatise on Analytical Chemistry, I. M. Kolthoff and P. J. Elving, Eds., Part I, Vol. **5** (John Wiley & Sons, New York, N.Y., 1964), p. 2776.
[12] Slavin, W., Anal. Chem. **35**, 561 (1963).
[13] Poulson, R. E., Appl. Opt. **3**, 99 (1964).
[14] Opler, A., J. Opt. Soc. Am. **40**, 401 (1950).
[15] Ingle, J. D., and Crouch, S. R., Anal. Chem. **43**, 1331 (1971).
[16] Optimum Spectrophotometer Parameters, Applied Physics Corporation Application Report AR14–2 (1964).
[17] Ku, H. H., J. Res. Nat. Bur. Stand. (U.S.), **70C** (Eng. and Instr.), No. 4, 263–273 (Oct.–Dec. 1966).
[18] Young, D. S., Scott, C. D., and Cole, E. B., Clin. Chem. **17**, 818 (1971).
[19] Horecker, B. L., Kornberg, A., J. Biol. Chem. **175**, 385 (1948).
[20] Rand, R. N., Clin. Chem. **15**, 839 (1969).

(Paper 76A5–734)

NATIONAL BUREAU OF STANDARDS SPECIAL PUBLICATION 378, Accuracy in Spectrophotometry and Luminescence Measurements, Proceedings of a Conference Held at NBS, Gaithersburg, Md., March 22–24, 1972 (Issued May 1973).

Problems Associated With the Need for Standardization in Clinical Spectrophotometric and Fluorometric Measurements

James R. Penton, Graham M. Widdowson, and George Z. Williams

Research Institute of Laboratory Medicine Institute of Medical Sciences, San Francisco, Calif. 94115

(June 5, 1972)

There is a growing demand in clinical chemistry for analyses to be performed in a manner allowing comparisons of results among laboratories and, from time to time, in the same laboratory. Reliable comparability requires adequate procedures of standardization for spectrophotometric and fluorometric instruments and methods. Problems with chemical and instrumental standardization are discussed.

For assays where the substance to be measured is available in suitable form, primary chemical standardization is justifiably popular. Relatively unsophisticated instrumentation can be used to compare measurements of unknown samples with such standards. Because primary standards meeting all necessary criteria are not available for many assays of clinical significance, standardization must depend on precision and accuracy of the instrumentation used, and on accurately compiled values of chemical-optical properties for the materials of interest. The task of compilation is outside the capability of the routine laboratory and should be provided by a reliable central agency. If an individual laboratory is to use the agency's compiled values, that laboratory must have available precise, accurate and reasonably inexpensive instrumentation along with reliable absorbance, fluorescence, and wavelength calibration standards.

Key words: Clinical standards; standard reference materials; standardization, spectrofluorometric; standardization, spectrophotometric.

I. Introduction

Spectrophotometric analyses in the routine clinical chemistry laboratory are performed within a unique framework. This framework imposes conditions responsible for many of the problems of inaccuracy and lack of standardization in clinical chemistry. The factors comprising this framework include:

a. Workload—many clinical chemistry laboratories are performing in excess of a quarter of a million analyses each year, and this number has been growing in the United States at a rate as high as 15 percent per annum.

b. Time—to enable prompt action by a physician, results are nearly always required on the day the specimen is collected; quite often results are needed within an hour. A twenty-four hour service must usually be maintained.

c. Range of analyses—as many as 40 different determinations are commonly available on request with a wide range of "special investigations" available by arrangement.

d. Type of sample—analyses are most commonly performed on serum or plasma, a viscous, protein-rich complex matrix available in restricted quantity.

e. Cost—clinical chemistry determinations contribute to the rising costs of health care; therefore the laboratory director must be cost-conscious, though not at the expense of precision and accuracy.

f. Personnel—the competent clinical chemistry technician must master a growing number of techniques, and operate a wide range of instrumentation that depends on many different principles.

As long ago as 1947, Belk and Sunderman [1][1] suggested the need for standardization in the clinical chemistry laboratory. They distributed aqueous solutions of glucose, chloride, urea and calcium, serum for measurements of total protein and albumin, and citrated whole blood for measurements of hemoglobin concentration, to a number of laboratories in Pennsylvania. They revealed wide discrepancies between results from different laboratories analyzing identical

[1] Figures in brackets indicate the literature references at the end of this paper.

specimens. For example, 27 of 41 laboratories obtained urea nitrogen results more than 5 mg/100 ml from the actual concentration of 45 mg/100 ml. That poor accuracy of results was a worldwide problem was demonstrated by similar reports from Australia [2], Britain [3], Canada [4], and New Zealand [5].

A major change in the operation of most routine clinical chemistry laboratories during the last 15 years has resulted from the introduction of mechanized and automated analytical equipment, both of the discrete sample and continuous flow type. That the introduction of such equipment can improve day-to-day precision of laboratory results has been demonstrated by Mitchell [6]. Gowenlock [7], reporting on an interlaboratory trial in Britain in 1965, concluded that apart from potassium determinations in serum, laboratories using AutoAnalyzer[2] (Technicon Instruments Corporation, Tarrytown, N.Y.) methods produced more consistent results. Many laboratories now have quality control schemes usually checking the precision of results either by using pooled human sera, commercial control sera or, in the United States, by participating in the College of American Pathologists' Quality Assurance Service.

It might be assumed that the introduction of mechanized and automated equipment, together with the use of quality control techniques, would by now have improved accuracy and thus interlaboratory agreement. The results of the latest surveys are not always reported in a comparable way to those of Belk and Sunderman [1], making such judgment difficult. For example, the College of American Pathologists' Quality Evaluation Program for 1971 divided the results for a given determination into groups according to the type of analytical method used; no overall range, or range for results within a group, was given. The results of the national quality control scheme in Britain, however, give the individual results obtained by each laboratory. Figure 1 (taken from the British scheme for a week in September 1969) shows the wide distribution of results from different laboratories when aliquots of identical serum specimens were analyzed for uric acid.

Even if there has been a slight improvement in the accuracy of results since 1947, the performance of clinical chemistry laboratories still falls far below that which should be expected.

A precise analytical method is not necessarily accurate and herein probably lies a major cause of the problem. Lack of accuracy in spectrophotometric methods of analysis may be caused by several factors including lack of suitable standards, inadequate colorimeters and spectrophotometers; and poor specificity of the chemical reaction. The latter factor is outside the scope of this discussion. Though there is frequently an interdependence between the chemical and instrumental aspects of analysis, we will consider them separately.

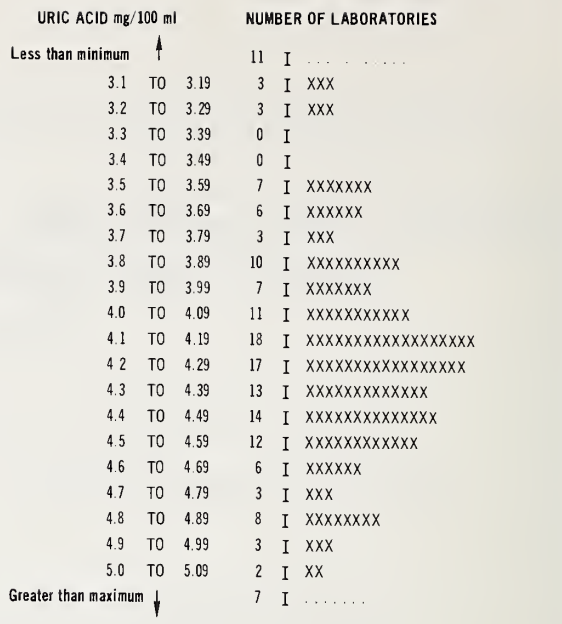

FIGURE 1. Histogram of uric acid results obtained when aliquots of a serum specimen were analyzed by 164 laboratories in the United Kingdom, during September, 1969. Courtesy of the Department of Health and Social Security, United Kingdom Committee on Standards and Quality Control in Clinical Biochemistry.

II. Instrumental Considerations

To function appropriately within the described framework of clinical chemistry requirements, a spectrophotometric analytical system must satisfy certain criteria. Those criteria concerned with economics, i.e., initial cost, operating cost and analytical rate, will, for the purpose of this discussion, be considered satisfied; only those criteria directly affecting standardization will be considered. Generally, these criteria are:

a. Instrument specifications adequate for standardization of the analysis.
b. Instrument meets specifications.
c. Instrument can be easily operated to verified attainable performance.
d. Instrument performance routinely verified in quality control program.
e. Operators understand behavior of instrument if measurement limits are exceeded.

Satisfaction of the criterion of adequate specification implies a thorough knowledge of the measurement characteristics of the instrumental system and of the interaction of those characteristics with those of the chemical system. It is essential to know: the range of absorbance which the spectrophotometric device will be required to measure, the wavelength at which measurements must be made, spectral band widths of absorption spectra to be investigated, temperature

[2] In order to adequately describe materials and experimental procedures, it was occasionally necessary to identify commercial products by manufacturer's name or label. In no instances does such identification imply endorsement by the National Bureau of Standards, nor does it imply that the particular product or equipment is necessarily the best available for that purpose.

characteristics of both instrumental and chemical systems, and calibration stability of the instrumental system.

Once the necessary characteristics of the instrument system have been defined, performance must be verified. An adequate evaluation of instrument performance requires reference materials of independently verified quality. These materials may be used to check wavelength accuracy, spectrophotometric linearity and, if necessary, spectrophotometric accuracy.

A. Wavelength

Several wavelength tests are available. In instruments where its use is convenient, Rand [8] recommended the mercury vapor lamp as a calibration source because of its many well defined emission lines. Where use of a mercury vapor lamp is inconvenient because of mechanical considerations, the sharp absorption bands of didymium and holmium oxide glass filters [8, 9] can furnish useful calibration points. These same filters, however, must *not* be used for spectrophotometric linearity and accuracy tests. Their narrow absorption band widths, which suit them for wavelength testing, make their transmission much too sensitive to wavelength setting accuracy.

B. Spectrophotometric Linearity

Reule [10] pointed out that spectrophotometric linearity is a necessary, but not a sufficient, condition for spectrophotometric accuracy. He noted that scale readings could be linear with light absorbance change but differ from true absorbance by a nonunity factor. On this basis, he objected to the use of absorbing materials to test spectrophotometer performance; and he suggested a precise test method using carefully controlled additions of light. Reule's method is not suitable for general clinical laboratory use because of its complexity. However, the information he presents is fundamental to understanding of linearity and accuracy tests.

Only spectrophotometric linearity is required in many clinical chemistry assays. In these cases, Reule's objection to tests based on substances which obey the Lambert-Beer law is negated and stable solutions of substances with broad absorption bands near the wavelengths of interest may be employed. Acidic solutions of cobalt ammonium sulfate and alkaline solutions of potassium chromate [11] have been suggested by NBS. Rand [8] favored acidic potassium dichromate (available from NBS as Standard Reference Material 136c). Buffered solutions of reduced nicotinamide adenine dinucleotide (NADH) may be useful if their marginal stability is taken into account. Solutions carefully prepared from materials of known ancestry can serve as useful spectrophotometric linearity benchmarks in both wide and narrow bandwidth spectrophotometers.

An instrumental characteristic which can markedly reduce the linear range of a photometric device is stray light [12]. Results of an experiment in our laboratory illustrate the effect of stray light and are shown in figure 2. These data were obtained on an AMINCO Rotochem (American Instrument Company, Silver Spring, Md.) from determinations of the transmittance of solutions of NADH in 0.1 mol·l^{-1} phosphate buffer (pH = 7.4). Measurements were taken at 340 nm, both with and without a minus-visible 360 nm cutoff filter in the photo detector window. The fall-off of linearity seen at low transmittance without the filter results from stray heterochromatic light "sneaking past" the monochromating element and into the photo detector without being attenuated by the absorption bands of the sample. The filter recommended by the manufacturer in this example is typical of the "stray light" and "order-sorter" filters found on prism and grating monochromators. Mis- or disuse of such filters can degrade the performance of even the best spectrophotometer to a level far below the specifications upon which its procurement was based.

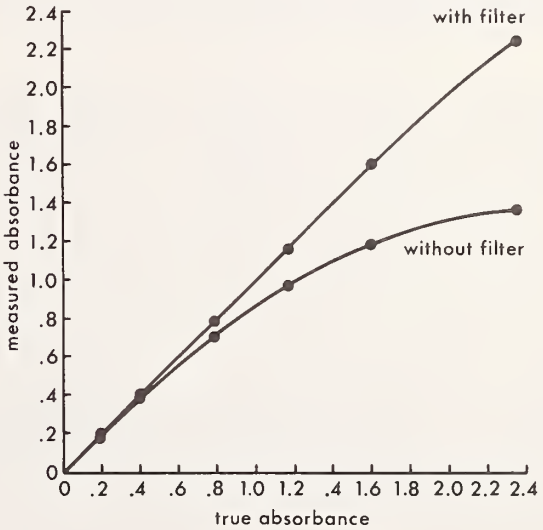

FIGURE 2. Absorbance of NADH solutions measured at 340 nm with and without stray light filter.

C. Spectrophotometric Accuracy

When the goal of instrument testing is verification of spectrophotometric accuracy, several pitfalls appear beyond those associated with linearity. Even though linearity tests may be satisfied in characterizing the spectrophotometric performance of wide bandwidth devices, in most cases these instruments are not capable of spectrophotometric accuracy. The data in figure 3 were obtained in our laboratory from solutions of buffered *p*-nitrophenol measured at 404 nm in an AMINCO Rotochem. The curves show that increasing spectral bandwidth causes apparent absorbance decreases from the "true" absorbance measured on the Beckman DU (Beckman Instruments Inc., Fullerton, Calif.) at 0.6 nm bandwidth; linearity remains good. If the instrument under test is of adequately narrow

502-591 O - 73 - 9

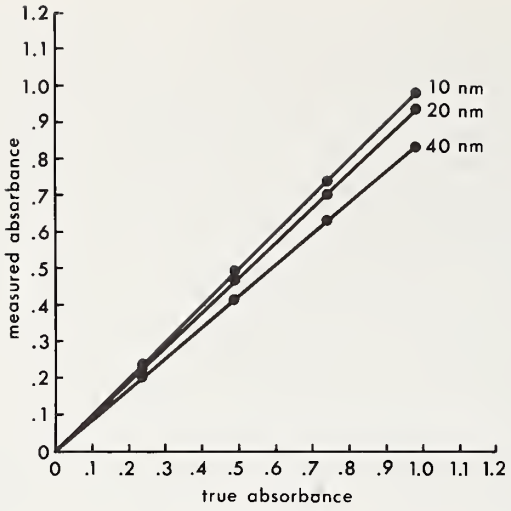

FIGURE 3. Absorbance of *p*-nitrophenol solutions measured at 404 nm with bandwidth of 40 nm, 20 nm and 10 nm; plotted against true absorbance.

bandwidth to warrant investigations involving spectrophotometric accuracy, then the materials used to assess this must be considered. In obtaining the NADH results described in figure 2, we noticed that the measured absorbances were lower than predicted from weight concentration and the accepted molar absorptivity of NADH reported by Horecker and Kornberg [13]. Solutions of NADH (Sigma > 98% purity) from two lot numbers were prepared in phosphate buffer, and their absorbances measured at 340 nm on a Beckman DU spectrophotometer. Our calculated molar absorptivities were approximately two-thirds of the expected value. When the indirect determination based on enzymatic conversion of nicotinamide adenine dinucleotide (NAD) to NADH described in [13] was duplicated, molar absorptivities in good agreement with the reference value were obtained. The source of this discrepancy has not yet been resolved, but it is obvious that direct use of NADH as a spectrophotometric accuracy-test material must be approached with caution.

Slavin [14] discussed the relative merits of liquid and solid test materials for spectrophotometric accuracy assessment and concluded that the requirements of convenience and stability favored use of solid materials. He described applications of the Chance-Pilkington (England) ON–10 neutral filter glass and of perforated metal screen filters. Copeland, King and Willis [15] described the use of the NBS carbon yellow filter glass as absorbance standard for the 540 nm assay of cyanmethemoglobin but lamented the strong wavelength dependence (0.0083 A/nm) of the filter at the desired wavelength.

Wavelength dependence is a criticism common to most reference materials proposed for use in spectrophotometric accuracy tests, especially when such tests are conducted in the environment of the clinical chemistry laboratory. Each material requires considerable discretion in choice of wavelength range for which it is used. If the material is used where its absorbance is strongly wavelength-dependent, then seemingly trivial errors in wavelength calibration can lead to decidedly nontrivial errors in spectrophotometric accuracy assessments. Since the Beckman DU used by Copeland, King, and Willis [15] has a wavelength accuracy of about ± 0.4 nm, this measurement on the NBS carbon yellow filter could have been in error by 0.0035 A units from wavelength inaccuracy alone.

D. Functional Considerations

Problems resulting from inadequate wavelength accuracy, spectrophotometric linearity and spectrophotometric accuracy may be minimized by using extreme care in specifying and verifying a spectrophotometric system, but we ask what are the implications of poor performance of these functions in the nonideal world of the clinical chemistry laboratory.

In enzyme assay by kinetic measurements, the rate of substrate conversion is calculated from molar absorptivity and absorbance change with time. When substrates and conversion products have relatively narrow spectral bandwidth absorption curves, accurate calculation of the concentration from absorbance and molar absorptivity will depend on accuracy of wavelength setting. To illustrate the effect of wavelength dependence, we performed assays of serum alkaline phosphatase using conversion of *p*-nitrophenyl phosphate to *p*-nitrophenol. Measurements of kinetic rates were made at the correct wavelength of 404 nm and at "erroneous" wavelengths of 414 nm and 424 nm. The results in table 1 show that the apparent activities are considerably lowered by errors in wavelength.

TABLE 1. Effects of wavelength on apparent activity of alkaline phosphatase

Sample number	Activity* (I.U./L) at 30 °C		
	404 nm	414 nm	424 nm
1	38.3	35.4	28.8
2	68.9	64.3	51.4
3	59.8	56.3	45.4
4	38.3	34.7	28.5
5	57.4	53.2	41.5
6	50.0	46.3	36.6

*Activities are the average of two assays.

Even in the assays in which comparison measurements are made between standard and unknown samples, spectrophotometric linearity is required, except in the trivial case where the standard and the unknown have exactly the same light transmittance. With instruments of nominally acceptable linearity, there is still danger that unknown samples may be encountered with transmittance outside the verified range of linearity, and routine treatment of such samples will cause reduction in precision of the measurement. This loss of precision stems from either

or both of two sources. The more severe effect results from measuring in a range of transmittance below that for which the spectrophotometer is linear. Necessity for verification of linearity for each individual instrument is obvious because some commonly used clinical colorimeters have significant deviations from linearity at absorbances as low as 0.5 (Association of Clinical Biochemists' (A.C.B.) reports [16, 17]).

Another serious, but less apparent, source of precision loss results from measuring at transmittances far removed from 0.368 (Absorbance = 0.434). Near this transmittance Beer's law calculations yield the lowest relative concentration error ($\Delta C/C$) for any given uncertainty in transmission measurement [18, 19]. Willard, Merritt and Dean [20] show the relative concentration error, resulting from a transmittance measurement uncertainty of 0.4 percent, to range from 8.2 percent at 0.95 T through 1.1 percent at 0.40 T to 8.7 percent at 0.01 T.

The assay of enzymes by kinetic rate determination often requires measurement of small changes in absorbance. Many spectrophotometers commonly used for direct concentration assay do not have absorbance resolution adequate to measure these small differences precisely. Absorbance is proportional to concentration of the absorbing species in direct measurements. Therefore, for a given relative error in absorbance measurement, the relative error in concentration is the same; e.g., if an absorbance measurement is 0.500 ± 0.002, then the relative error is $\pm(100 \text{ percent} \times 0.002/0.500)$ or ± 0.4 percent, and the relative error in concentration calculated from this absorbance measurement also will be ± 0.4 percent.

However, if the same spectrophotometric error (± 0.002) is present in an instrument used to measure a kinetic rate, the relative error on the assay results may be much worse. When the enzyme aspartate aminotransferase (SGOT) is determined by a common kinetic rate method [21], the absorbance change observed for samples from normal subjects is of the order of 0.01 per min at 30 °C. Typical absorbances for two readings taken 2 min apart are 1.000 and 0.980 and the difference, 0.02. In the worst case, when the measurement errors for each of the two readings are additive, the relative error could be $\pm(100 \text{ percent} \times 0.004/0.020) = \pm 20$ percent. The fundamental problem is that of measuring precisely small differences in large numbers. Thus, small relative errors in each of the two measurements can lead to large relative errors in the value derived from their difference.

This fundamental problem of precisely measuring small differences is further aggravated by the widespread use of instruments with digital display or printout of readings. While digital displays do much to reduce likelihood of operator reading error, they conceal the fact that precision of absorbance measurement is more difficult to obtain at low transmittances. It is apparent on a meter scale, linear for percent transmission, that the range of 1.0 to 2.0 absorbance occupies only 9 percent of the entire transmission scale; hence a technician may be leery of making readings in this range. But if a digitial display shows 1.931 for one absorbance reading and 1.968 for another, the operator is likely to interpret those readings as exact when, in fact, they are very probably quite inaccurate.

If an analog (continuously variable) signal is to be displayed digitally, an analog-to-digital conversion must occur. The accuracy with which the number displayed represents the original analog signal depends on the sophistication of conversion circuitry; that accuracy is not absolute and can be quite poor.

As an example, we calculated the absorbance resolution of General Medical Sciences—Atomic Energy Commission (GeMSAEC) spectrophotometric systems. These systems employ analog-to-digital conversion circuitry with resolutions of $1/2^{10} \approx 0.1$ percent (ten bit) or $1/2^{12} \approx 1$ in 0.025 percent (12 bit). The best absorbance resolution deliverable by these two converters at several absorbance levels is shown in table 2. The difference in resolution between the two converters is apparent.

Table 2. Absorbance resolution for 10 and 12 bit analog-to-digital converters

	ΔA	
A	10 Bit	12 Bit
0.0	0.00054	0.00014
.3	.00108	.00027
.7	.00174	.00043
1.0	.00546	.00135
1.5	.01773	.00436
2.0	.05798	.01378

E. Routine Instrument Performance Verification

Although the necessity for initial verification of instrument performance is undeniable, relatively little has been done to incorporate separate instrument checks into the clinical laboratory quality control program. For example, this omission may permit an undetected malfunction to reduce the linear range of the spectrophotometer. Samples of normal concentration could still give accurate readings, but abnormally high concentration samples would produce readings falling outside the range of the instrument's linear response. To be sure, use of control samples simulating abnormal assay values would reveal this fault, but at the expense of complete re-run of all samples assayed preceding discovery of the difficulty.

Several wavelength and absorbance verification devices are available in readily usable form. Examples are the convenient Gilford (Gilford Instrument Laboratories, Oberlin, Ohio) calibration device for their 300–N Microsample Spectrophotometer, and the Arthur H. Thomas (Arthur H. Thomas Company, Philadelphia, Pa.) didymium and holmium oxide filter glasses supplied with an adapter to fit into any sample carrier designed to hold standard 1 cm square cuvettes. However, it must be emphasized that it is appropriate *use*, and not mere possession of verification devices such as these, which standardize laboratory performance.

F. Operator Considerations

Even an instrument system which is capable of meeting all necessary specifications will not reliably perform accurate analyses if that system is not designed to be easily operated in the proper manner. However, it is difficult to visualize a more ergonomically efficient spectrophotometer than the Gilford 300–N. We have seen this instrument used to measure absorbances greater than 3.0; used to measure absorbance at two wavelengths without readjusting the zero setting; calibrated with the zero-set control and even operated from a cold start with *no* adjustment checks; all by experienced and presumably well-trained technicians who should know better. An undetermined but undoubtedly large contribution to poor quality control arises from improper operation of laboratory equipment, due to poor instrument design and poor operator understanding.

III. Chemical Standardization

Radin, in 1967, [22], reviewed the definition and use of standards and the standard materials available to the clinical chemist, and discussed the limitations of various so-called standards. His view that "there is actually very little in the way of official definitions of standards for the clinical chemist" was reinforced by a joint report of the National Academy of Sciences, National Research Council Subcommittee on Reference Materials [23]. The situation has improved since that time, as evidenced by the reports of Young and Mears [24], Meinke [25], and Zief and Michelotti [26]. The improvement has been due to the introduction by the National Bureau of Standards of Standard Reference Materials (SRM) for use in clinical chemistry. To July, 1971, these include cholesterol, urea, uric acid, creatinine, calcium carbonate, bilirubin, D-glucose, potassium chloride, tris (hydroxymethyl) aminomethane, tris (hydroxymethyl) aminomethane hydrochloride and glass filters for spectrophotometry.

The importance of the SRM's must not be underestimated; however, they represent a solution to only part of the problem. The clinical laboratory worker must be aware of errors which may occur despite the availability of SRM's; stability of standard solutions is particularly important. The variable stability of solutions of uric acid is well known, while Gowenlock [7] showed that in part, the lack of interlaboratory agreement for the determination of serum urea could be attributed to deterioration of aqueous urea standards containing no preservative. In a few cases, SRM's when used in aqueous solution are not ideal standards in clinical chemistry. Recently, we were investigating the determination of uric acid by an adaptation of the supposedly specific uricase neocuproine method [27], both manually and on the Beckman DSA–560. Unable to get 100 percent recovery of uric acid added to pooled human serum, we discovered that the slope of the standard uric acid curve (using SRM) can be varied according to the amount of bovine albumin added. When the concentration of bovine albumin is approximately 7.0 g/100 ml, 100 percent recovery of added uric acid is attainable.

A large number of routine clinical chemistry laboratories are using multichannel analyzers of both continuous flow and discrete sample type. Aqueous standard solutions containing a mixture of known amounts of all the substances commonly being determined in the routine clinical chemistry laboratory are not available. Multichannel machines are therefore being calibrated with commercially supplied calibration sera for which values for each determination have been assigned by the manufacturers. That wide differences may occur between the values obtained on the same machine with sera from different manufacturers, and even between lots from the same manufacturer, has been reported by Childress [28] and Helman, Reingold and Gleason [29]. These differences may occur for a variety of reasons, e.g., variation in weight or homogeneity of material. The Scientific and Technical Committee of the Association of Clinical Biochemists (A.C.B.) [30] reported variation in dry content from vials (all of the same lot number) of some manufacturer's control sera to be as high as 13.80 percent C.V. Six of the 10 brands investigated had coefficients of variation of over 2.0 percent. The deviation of the weight of the contents of these vials could be correlated to the deviation in analytical results obtained when these vials were reconstituted.

Data from our laboratory (table 3) shows the percentage deviation from the mean dry weight content of 10 vials of control sera compared with the percentage deviation from the mean analytical value for several determinations performed on the contents of each vial. The 10 vials were selected at random from a box of 40 vials (all of the same lot number); great care was taken to assure the correct amount of water was added to each vial. Replicate aliquots from each vial were analyzed in the same run. Excellent agreement was obtained between replicate analyses from the same vial for all the determinations. The variation in dry weight content of the vials is unacceptable, however. If the contents of each vial is representative of a homogeneous batch, one would expect the deviations from the mean assay values to be the same as the deviations of the weight values; this is not the case. Most batches of control sera from manufacturers are not subject to the large errors shown here. The large errors, however, pose the question of how frequently smaller and less easily recognized errors occur. The results showing variability of vial content were obtained on what was described by the manufacturer as control serum, not calibration serum. However, the same manufacturing standards are required for both control and calibration purposes.

Amador, Massod, and Franey [31] compared the values they obtained for aspartate aminotransferase in three commercial control sera with the values assigned by the manufacturer and found differences of 11 to 17 percent (possibly due to the manufacturer failing to provide sufficient details of the method they used to assign the values). In a more recent paper, Dobrow and Amador [32] reported a similar study for lactate

Table 3. Percentage deviation from the mean dry weight content $\bar{x}$ of 10 vials of control sera compared with the percentage deviation from the mean analytical value for several determinations performed on the contents of each vial

Vial	Percent deviation from $\bar{x}$ dry content	Percent deviation from $\bar{x}$ analytical value				
		Total protein	Phosphate	Uric acid	Calcium	Magnesium
1	−1.4	−3.2	−3.3	−0.9	−1.5	10.2
2	1.9	1.4	2.7	5.6	0.7	−5.5
3	2.1	1.4	2.7	5.6	0.7	−10.8
4	−2.1	−1.7	−3.3	−3.0	0.7	10.2
5	−2.1	−1.7	−3.3	−5.2	−1.5	5.0
6	1.8	4.4	5.7	3.4	0.7	−5.5
7	−2.2	−1.7	−3.3	−5.2	−1.5	5.0
8	−2.2	−1.7	−3.3	−5.2	0.7	5.0
9	1.8	2.9	2.7	3.4	0.7	−5.5
10	2.3	−1.7	2.7	3.4	−1.5	−5.5

dehydrogenase, aspartate aminotransferase, alkaline and acid phosphatase, and amylase. They concluded that the activities stated by six of the eight manufacturers were doubtful or unacceptable in more than 50 percent of the sera tested. Bowers, Kelley and McComb [33] have shown that in some assay procedures, animal alkaline phosphatases (often used in commercial control sera) do not behave identically to human serum alkaline phosphatase.

These findings clearly indicate that currently available calibration sera should not be used directly as calibration materials for any analytical procedure.

Cali [34] suggested recently that SRM's make verification of commercial calibration sera possible; this statement is correct only if referee methods of analysis are available for use in conjunction with the SRM's. NBS will publish the first referee method for the determination of calcium shortly. The availability of referee methods and SRM's will do much to improve standardization in large laboratories. However, in small laboratories, where the problem is greatest, shortage of manpower and equipment does not permit analysis of calibration sera by referee methods. We suggest that NBS consider the production of reference sera with values for the common routine determinations assigned through use of their own SRM's and referee methods. These NBS reference sera would be used by laboratories to check commercial sera used for daily calibration of multichannel analyzers.

An alternative to the production of reference sera by NBS may be a certification program for commercial products. An example of the way in which an independent laboratory can be used for standard and reagent certification has been demonstrated by the cyanmethemoglobin certification program of the College of American Pathologists, as described by King and Willis [35].

In the meantime, the situation could be improved if the manufacturers used greater care in the preparation of calibration sera. When assigning values to calibration sera, they should indicate the exact methods used for this purpose. Values for aspartate aminotransferase and alkaline phosphatase, for example, are frequently said to have been assigned using the Karmen [36] or Bessey, Lowry, and Brock [37] methods, respectively. Almost certainly, modifications of these methods (with regard to substrate concentration buffer type, etc.) have been used, resulting in quite different activities from the original methods.

IV. Conclusions

1. Spectrophotometric analyses in the routine clinical chemistry laboratory are performed within a unique framework.

2. The accuracy of results in clinical chemistry laboratories falls far below the level that should be expected.

3. Choice of instrumentation must be based on a thorough understanding of both the characteristics of the instrument and the assays which must be performed.

4. Except in the case of inadequate absorbance resolution, instrument availability does not generally limit clinical laboratory performance.

5. Materials for verification of instrument performance are often not available in a form suitable for routine use in the clinical laboratory.

6. *Referee analytical methods* are needed for use in conjunction with NBS *standard reference materials.*

7. The only materials currently available for calibration of multichannel analyzers are commercially prepared sera. Because of ill-defined methods of assigning values and poorly understood properties of enzymes from non-human sources, unverified use of these materials for calibration is highly undesirable.

8. The situation with regard to calibration sera could be improved by:

a. Greater care in the manufacture of calibration sera and provision of information concerning the *exact* method used to assign values to the material.

b. Certification of commercial calibration sera by an independent laboratory using NBS standard reference materials and referee methods.

c. Preparation by NBS of reference sera, to which values are assigned using standard reference materials

and referee methods. Such reference sera could be used by laboratories to assign values to new batches of commercial sera.

9. The most sophisticated and versatile spectrophotometric system can yield standard results only when operated within its limitations. Chemical and serum reference materials must be used with due regard for their limitations. It is axiomatic then that, to understand and fully control what he *can* do, the laboratory operator must also understand what he *cannot* do with analytical apparatus and methods. He must be able to recognize *bad* results as bad and be able to interpret these mishaps to correctly evaluate laboratory performance just as the physician should interpret *good* laboratory results in diagnosis of the patient's physiologic performance.

V. References

[1] Belk, W. P., and Sunderman, F. W., A Survey of the Accuracy of Chemical Analyses in Clinical Laboratories, American Journal of Clinical Pathology **17**, 853 (1947).

[2] Hendry, P. I. A., Proficiency Survey in Clinical Chemistry, 1961. Report of Adelaide Meeting, p. 8. College of Pathologists of Australia, 1961.

[3] Wootton, I. D. P., and King, E. J., Normal values for blood constituents: Inter-hospital differences, Lancet **I**, 470 (1953).

[4] Tonks, D. B., A Study of the accuracy and precision of clinical chemistry determinations in 170 Canadian laboratories, Clinical Chemistry **9**, 217 (1963).

[5] Desmond, F. B., A clinical chemistry proficiency survey. New Zealand Medical Journal, **63**, 716 (1964).

[6] Mitchell, F. L., Quality Control in a Large Laboratory, Proceedings of the Association of Clinical Biochemists, **4**, 38 (1966).

[7] Gowenlock, A. H., Results of an interlaboratory trial in Britain, Annals of Clinical Biochemistry, **6**, 126 (1969).

[8] Rand, Royden H., Practical spectrophotometric standards, Clinical Chemistry **15**, 839 (1969).

[9] Edisbury, J. R., Practical Hints on Absorption Spectrometry (Hilger and Watts, London, 1966).

[10] Reule, Alfred, Testing spectrophotometric linearity, Applied Optics **7**, 1023 (1968).

[11] Haupt, Geraldine W., An alkaline solution of potassium chromate as a transmittancy standard in the ultraviolet, Journal of the Optical Society of America **42**, 441 (1952).

[12] Poulson, Richard E., Test methods in spectrophotometry: Stray-light determination, Applied Optics **3**, 99 (1964).

[13] Horecker, B. L., and Kornberg, Arthur, The extinction coefficients of the reduced band of pyridine nucleotides, Journal of Biological Chemistry **175**, 385 (1948).

[14] Slavin, Walter, Photometric standard for ultraviolet-visible spectrophotometers, Journal of the Optical Society of America **52**, 1399 (1962).

[15] Copeland, B. E., King, J., and Willis, C., The National Bureau of Standards carbon yellow filter as a monitor for spectrophotometric performance, The Journal of Clinical Pathology **49**, 459 (1968).

[16] Colorimeters with Flowthrough Cells—A Critical Assessment of Four Instruments, Scientific Report No. 1. Association of Clinical Biochemists, England (1965).

[17] Colorimeters—A Critical Assessment of Five Commercial Instruments, Scientific Report No. 2. Association of Clinical Biochemists, England (1966).

[18] Ayres, Gilbert H., Evaluation of accuracy in photometric analysis. Analytical Chemistry **21**, 652 (1949).

[19] Ringbom, Anders, Uber die Genauigkeit der Colorimetrischen Analysenmethoden I. Zeitschrift für Analytische Chemie **115**, 332 (1939).

[20] Willard, H. H., Merritt, L. L., and Dean, J. A., Instrumental Methods of Analysis (Van Nostrand, New Jersey, 1965).

[21] Amador, E., and Wacker, W. E. C., Serum glutamic-oxalacetic transaminase activity. A new modification and an analytical assessment of current assay techniques, Clinical Chemistry **8**, 343 (1962).

[22] Radin, N., What is a standard, Clinical Chemistry **13**, 55 (1967).

[23] Report by the Sub-Committee on Reference Materials, Committee on Analytical Chemistry Division of Chemistry and Chemical Technology, National Academy of Sciences—National Research Council: Standard reference materials as viewed by the laboratory supervisor—A status report, Analytical Chemistry **40**, 24 A (March 1968).

[24] Young, D. S., and Mears, T. W., Measurement and standard reference materials in clinical chemistry, Clinical Chemistry **14**, 929 (1968).

[25] Meinke, W. W., Standard reference materials for clinical measurements, Analytical Chemistry **43**, 28 A (May 1971).

[26] Zief, M., and Michelotti, F. W., Clinical chemistry: A challenge for high purity standards and reagents, Clinical Chemistry **17**, 833 (1971).

[27] Morgenstern, S., Flor, R. V., Kaufman, J. H., and Klein, B., The automated determination of serum uric acid, Clinical Chemistry **12**, 748 (1966).

[28] Childress, C. C., An Improved Technique for the Standardization of the SMA 12 AutoAnalyzer, Advances in Automated Analysis, 1970, p. 167, Technicon International Congress.

[29] Helman, E. Z., Reingold, I. M., Gleason, I. O., Plea for standardization of commercial calibration materials for automated instruments, Clinical Chemistry **17**, 1144 (1971).

[30] A note from Scientific and Technical Committee, Association of Clinical Biochemists, News Sheet, United Kingdom, p. 11 (Aug. 1971).

[31] Amador, E., Massod, M. F., Franey, R. J., Reliability of glutamic-oxalacetic transaminase methods, American Journal of Clinical Pathology **47**, 419 (1967).

[32] Dobrow, D. A., and Amador, E., The accuracy of commercial enzyme reference sera, American Journal of Clinical Pathology **53**, 60 (1970).

[33] Bowers, G. N., Kelley, M. L., and McComb, R. B., Precision estimates in clinical chemistry. Variability of analytic results in a survey reference sample related to the use of a nonhuman serum alkaline phosphatase, Clinical Chemistry **14**, 595 (1967).

[34] Cali, P. J., SRM's and verification of commercial standards, Clinical Chemistry **18**, 172 (1972).

[35] King, J. W., and Willis, C. E., Cyanmethemoglobin Certification Program of the College of American Pathologists, American Journal of Clinical Pathology **54**, 496 (1970).

[36] Karmen, A., A note on the spectrophotometric assay of glutamic-oxalacetic transaminase in human blood serum, Journal of Clinical Investigation **34**, 131 (1955).

[37] Bessey, O. A., Lowry, O. H., and Brock, M. J., A method for the rapid determination of alkaline phosphatase with five cubic millimeters of serum, Journal of Biological Chemistry **164**, 321 (1946).

(Paper 76A5–735)

NATIONAL BUREAU OF STANDARDS SPECIAL PUBLICATION 378, Accuracy in Spectrophotometry and Luminescence Measurements, Proceedings of a Conference Held at NBS, Gaithersburg, Md., March 22–24, 1972 (Issued May 1973).

The Role of Spectrophotometric Standards in the Clinical Chemistry Laboratory

Royden N. Rand

Department of Pathology, University of Pennsylvania, and William Pepper Laboratory, Hospital of the University of Pennsylvania, Philadelphia, Pa. 19104

(June 7, 1972)

It is obvious that erroneous data reported to a physician may adversely affect patient welfare. Currently, acceptable limits of accuracy and precision are poorly defined. It should be recognized, however, that the spectrophotometric measurement step in an appropriate analytical procedure is critical and inapparent error may occur. Spectrophotometric measurements, both manual and automated, are extensively used in the clinical chemistry laboratory. At least 1,000,000 such measurements per day on rather diverse equipment are made in this country; yet, few standards exist. Results of intra-lab surveys suggests that performance could be improved. The various ways in which spectrophotometry is used will be illustrated and a discussion of possible errors resulting from nonstandardized instrumentation will follow. There is pressing need for well defined and easily usable standards for wavelength, photometric accuracy, photometric linearity, stray light, as well as NBS specifications for optical cuvettes.

Key words: Clinical spectrophotometry, accuracy, precision; optical cuvettes; spectrophotometric standards, clinical.

I. Introduction

It is not widely appreciated that spectrophotometric methods represent the principal measurement techniques used in the clinical chemistry laboratory. A recent text lists 147 analytical techniques; of these, 84 require the use of spectrophotometry [1].[1] The twenty-five most widely used techniques at the William Pepper Laboratory are spectrophotometric.

The numbers of spectrophotometric analyses performed in any active hospital are impressive. At the Pepper Laboratory, for example, of 450,000 analyses per year about 300,000 require the measurement of the absorbance of light. We, therefore, make 800–1,000 spectrophotometric measurements per day. Other information allows us to estimate that more than 1,000,000 spectrophotometric tests are performed daily in the clinical laboratories in this country [2]. When it is realized that the growth-rate of clinical chemistry is approximately 15 percent per year, then a perspective of present requirements for accuracy and precision is immediately recognized.

Given the information that spectrophotometric measurements are so widely used, it seems strange that suitable standards are not readily available and in widespread use. It seems appropriate, therefore, for this communication to discuss:

1. The accuracy and precision requirements for clinical chemical measurements.
2. The use of spectrophotometry in the laboratory.
3. The present "state of the art" of spectrophotometric measurements.
4. The various types of spectrophotometric errors and how such errors may relate to the accuracy and precision requirements discussed in section III.
5. The type of standards which are required.

II. Nature of Clinical Laboratory Data

For the fields other than medicine, it is relatively easy to describe how the quantitative data of the analytical laboratory are used. Several examples can be cited:

1. The analysis of steel yields information that helps control quality, composition, and costs.
2. The analysis of gold is required to protect the purchaser's investment.
3. The analysis of the products of organic synthesis may verify composition and help optimize yield of desired products.
4. Quantitative analysis of biochemical systems helps elucidate reaction mechanisms.

[1] Figures in brackets indicate the literature references at the end of this paper.

In general, therefore, quantitative analysis can be used to obtain data that are used theoretically or empirically, in rather well defined ways.

By comparison, it is difficult to show clearly and unambiguously how quantitative clinical laboratory information is used in the practice of medicine. For example, while a change in the butterfat content of milk of 0.2 percent can be recognized as economically significant, a comparable change in the total protein content of serum, although easily measured, cannot be so easily interpreted. In general, small changes in the levels of medically important substances are difficult to interpret. Nevertheless, the clinical chemistry laboratory does quantitative analysis. It may be instructive, therefore, to describe how these data may be used.

A. Generalized Use In Diagnosis

Although recent studies of logic of diagnosis avoid dealing with the precise role of laboratory tests, it is generally recognized that they play a key role in medical decisionmaking [3].

When a physician sees a patient presenting certain signs and symptoms, he forms a hypothesis about the possible diseases compatible with them. He may then order one or more laboratory tests, the result of which will help confirm or negate the hypothesis. Given the likelihood of a disease, the expected increase or decrease in specific serum constituents helps confirm the presence of the disease. This use of laboratory data is essentially qualitative. That which is sought, is evidence of change in blood level clearly outside the normal range. Such use of laboratory information implies only moderate requirements of precision and accuracy.

From the viewpoint of the analyst, however, the perspective changes considerably. The concentration ranges of biologically important substances varies from micrograms to grams per deciliter. Further, the maximum concentration ranges encountered in disease may vary from 1.5 times the mean normal value to as much as 50 or greater. Because of this, the only possible means of assuring consistent information within and between laboratories, between analyst and between days, is to perform analyses with well defined and characterized methods, making measurements with the use of high purity standards and *instruments known to be calibrated correctly.*

B. Specific Diagnosis

To a limited extent, quantitative analysis provides specific diagnostic information. This is obviously true when the analytical procedure provides information concerning the amount of an abnormal substance—such as a paraprotein—present in a body fluid. There are, though, only a limited number of instances where this is the case, and indeed, few of these analyses use spectrophotometric procedures. Some substances normally in blood appear to vary within narrow limits. Examples of this are calcium and other electrolytes as well as total protein and albumin within an individual [4, 5]. Further research in this area using measurements of high accuracy and precision may show how minimal abnormalities in levels of such substances are related to disease.

C. Therapy Related Decisions

An extremely important aspect of quantitative blood analysis is in relation to therapeutic decisions. The determination of such substances as sodium, potassium, hemoglobin, bilirubin, and certain drugs are commonly encountered examples. The accurate quantification of these substances seems to be required for consistent and reliable medical decision-making. For example, in fetal Rh incompatibility, pediatricians feel that a bilirubin level of 20 mg/dl suggests a high risk of significant brain damage and, thus, will intervene with exchange transfusion. Similarly, routine control of electrolyte levels following surgery requires impressive quantitative support from the laboratory. Another example is the quantification of the blood levels of therapeutic drugs to insure optimal response without toxicity. Accuracy and precision seem most clearly related to patient welfare for this application of quantitative analysis, where therapeutic decisions may depend on a blood level of some substance.

III. Accuracy and Precision Requirements

The discussion, to this point, suggests that accuracy and precision requirements of clinical laboratory determinations have not been rigorously defined. Several recent articles, however, have discussed the problem. The most comprehensive are by Barnett, entitled "Medical Significance of Laboratory Results," and Campbell and Owen, entitled "Clinical Laboratory Error in Perspective" [6, 7]. In both, the authors attempt to derive acceptable limits of variability for commonly used tests on the basis of the consensus of highly qualified physicians,[2] table 1 summarizes some of their findings.

The range of values for one standard deviation seems to be rather broad. For example, in Campbell and Owen, glucose was thought to require a reproducibility of 0.8–3.6 mg/dl; Barnett concludes that 5.0 mg/dl is acceptable. This variability may be due to the fact that the requirements for reproducibility were obtained by a consensus technique. Since there seems to be no current theoretical or experimental approach to the problem, consensus is the only means of arriving at these specifications.

Neither paper makes an explicit distinction between accuracy and precision. The medical decision levels represent the value at which a decision may be made and the variability represents the allowable precision limits. Although these are stated to be one standard deviation, it should be at least questioned as to whether these would not better represent two standard devia-

[2] Using operations research techniques in his doctoral dissertation, Cavanaugh has studied the probable effects of laboratory error for three commonly used tests [8]. He, too, found it necessary to use a consensus of informed medical expertise to elucidate the impact of laboratory error. He concludes that a "cost per laboratory error" can be computed and that this has meaning in terms "loss of life and limb." The concept is intriguing and Cavanaugh's challenging approach should be further explored.

Table 1. Acceptable Analytical Reproducibility

From Barnett [6] and Campbell and Owen [7]

Test	Decision level[1] [6] *mg/dl*	Acceptable reproducibility[2] [6] *mg/dl*	Acceptable reproducibility[2] [7] *mg/dl*
Glucose	120	5.0	0.8 −3.6
Urea	27	2.0	0.9 −2.4
Calcium	11	0.25	0.03–0.33
Chloride[3]	90	2.0	0.6 −2.7
Phosphate	4.5	0.25	0.14–0.25
Sodium[3]	130	2.0	1.0 −2.6

[1] Level at which a medical decision may be made.

[2] 1 S.D. in appropriate units.

[3] Units for chloride and sodium are milliequivalents per liter, mEq/l.

tion limits. In any case, the listed precision limits are certainly achievable as one standard deviation limit and probably for two standard deviation limits, by careful work.

For our purposes, it is not necessary to decide whether one figure or another is acceptable and correct. We may use them as guidelines to maximum acceptable error. In fact, we shall use Barnett's figures later in this paper to help elucidate some aspects of analytical error and, perhaps, better understand some of the requirements of spectrophotometric practice.

IV. Spectrophotometry in the Clinical Laboratory

A. Instrumentation

1. *Wide Band Instruments*—Wide band instruments are of many types and varieties with spectral bandwidths greater than 10 nm. These may be simple filter colorimeters or reasonably sophisticated spectrophotometers. Older instruments are null point type, whereas newer models are direct reading. Some are very simple; some are relatively complicated with highly stabilized electronics and digital absorbance readouts.

2. *Narrow Band*—The more expensive grating and prism ultraviolet visible type, narrow spectral bandwidth instruments are less commonly encountered. These may be single or double beam.

3. *Devices Used in Automation*—The most commonly encountered are double beam, interference filter, transmission type equipment.[3]

B. Type of Analyses Performed With Each Kind

1. *Wide Band*—The wide band instruments are primarily used for manually performed procedures in the visible area of the spectrum. In general, reagents are added to react with the substance being quantified either directly in the fluid being analyzed or in a protein-free filtrate. A color is produced, sometimes after the application of heat, and its light absorbing characteristics are compared to those obtained with standards similarly treated.

2. *Narrow Band*—The most important applications of the narrow band instruments are: (1) the determination of enzymes, (2) toxicologically significant substances, (3) the direct absorptiometry of compounds such as bilirubin or uric acid, and (4) identification of unknown substances. In general, for these uses, absorptivities are used to compute the unknown concentrations.

3. *Photometric Instruments Used in Automation*—These instruments are used in a manner similar to the wide band instruments. They generally operate in the visible area of the spectrum and colors of standard compounds are compared to colors obtained with biological specimens.

[3] Strictly speaking these are not true double beam systems. One beam, of course, passes through the colored sample; the other passes through a filter of the same transmittance and is sensed by a separate photocell. Thus only variations in the output of the source can be compensated.

V. "State of the Art" Spectrophotometric Measurement in the Clinical Laboratory

A. Wide Band Instruments

Few studies have been published on the significance of wide band instruments. A major study, however, was "Colorimeters—A Critical Assessment of Five Commercial Instruments" by Broughton and colleagues [9]. The participants studied two models of five manufacturer's instruments. The most significant performance factors were thought to be: (1) reproducibility (2) sensitivity (3) linearity. The overall design of the instrument, the accompanying sample cells and accessories were also critically discussed.

Stable solutions yielding absorbances of 0.05–0.55 were used to evaluate reproducibility. Typically, ten readings were made without resetting zero, then ten additional readings completed the series. Linearity was studied over a wide range of concentrations for five different chemical procedures, using five separate wavelengths. Sensitivity was defined as the ratio of the slope of the calibration curve to that obtained in a narrow band instrument.

A summary of their findings is found in table 2. Detailed examination of the paper makes clear that of the five wide band instruments examined, only one could be relied upon to yield calibration curves linear to an absorbance of 1, as well as sustaining a sensitivity in the range of 0.7 to 1. Although it is obviously unfair to extrapolate conclusions from this study to include all wide band instruments, it may be that many instruments of this type will exhibit some limitations on performance. It seems evident that the presence of such problems may limit the reliability of any analyses performed with such equipment. Standards for linearity and sensitivity evaluation are sorely needed.

Further evidence supporting this point may be found in a survey for wide band instruments performed in New York State [10]. Relevant data are found in

TABLE 2. Performance of Selected Wide Band Colorimeters

Reproducibility—when expressed as coefficient of variation, it varied from 1–3 percent at an absorbance of 0.1; above an absorbance of 0.4 it was 1 percent or less.

Linearity—varied from a continuous curve to linearity through an absorbance of one. Many instruments are linear only to absorbance of 0.5–0.6. Instruments of same make and type frequently showed significant differences in performance.

Sensitivity—widely variable, from a low of 21 percent to a high of 120 percent. Instruments of same make and type frequently showed significant differences.

Summary of data found in Broughton, et al. [9].

table 3. The three types of instruments listed are ones commonly found in clinical laboratories in this country. Three points are important:

1. The range of results reported for any solution, for any type of instrument is distressingly wide. For example, for instrument 1 and solution B, 95 percent of the instruments fall between 0.413 and 0.513.
2. There are significant deviations from linearity for instruments 2 and 3.
3. The relative sensitivity for instruments 2 and 3 are unimpressive.

The reasons for these poor results are not clear. Again, the need for appropriate standards and their frequent use seems very clear.

TABLE 3. Performance of Wide Band Spectrophotometers [1]

Instrument [2]	Bandpass *nm*	Number of instruments	Absorbance		Deviation in linearity	Relative sensitivity
			Solution A [3] 0.0500*M*	Solution B [3] 0.100*M*		
					percent	*percent*
No. 1	20	75	0.228 ± 0.012	0.463 ± 0.025	+1.5	95
No. 2						
10 mm	30	34	.191 ± 0.017	.382 ± 0.039	0	81
12 mm	35	58	.197 ± 0.011	.386 ± 0.022	−1.8	82
19 mm	35	67	.193 ± 0.013	.368 ± 0.027	−4.9	79
No. 3						
10 mm	20	33	.202 ± 0.022	.395 ± 0.044	−2.5	84
12 mm	20	74	.214 ± 0.011	.416 ± 0.018	−1.8	82
19 mm	20	51	.206 ± 0.008	.400 ± 0.019	−3.2	85

[1] Vanderlinde, R., Instrumentation Survey—Visible Spectrophotometry. Report of Laboratories for Clinical Chemistry, New York State Dept. of Health, June 7, 1971.

[2] Millimeter designation refers to the size of the test tube used to hold sample.

[3] Solutions A, B = 0.0500 M, 0.100 M cobaltous ammonium sulfate in 1 percent (v/v) H_2SO_4 read at 510 nm; all values corrected to 10 mm light path.

B. Narrow Band Instruments

It might be supposed that the performance of narrow band instruments would be more impressive than the wide band types. Unfortunately, this is a generalization not substantiated by published data. Several surveys bear this out:

1. Even if one looks only at the data for potassium nitrate, data from the world survey conducted by the Photoelectric Spectrophotometry Group [11], indicate a spread of results for both absorbance and peak wavelengths that is unacceptably broad.
2. In mid 1971, the College of American Pathologists (CAP) surveyed narrow band spectrophotometers in a number of clinical laboratories in the United States [12]. Solutions in sealed ampules included potassium dichromate (25, 50, 100 mg/l in 0.01 N H_2SO_4); Thomson Solution ¼, ½ full strength); alkaline potassium chromate (40 mg/l in 0.05 N KOH). Data for some of these solutions are summarized in figure 1. The means and two standard deviations, as well as coefficients of variations are graphically shown. At 257 nm, the intra-instrument variability is aston-

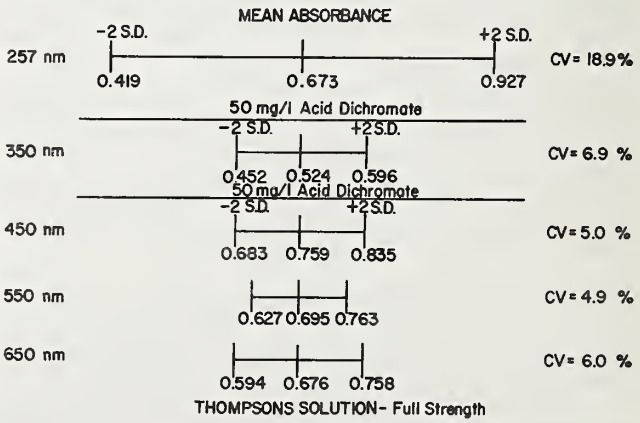

FIGURE 1. Performance of narrow band spectrophotometers in the United States.

Data from the report of the Subcommittee on Instrumentation, College of American Pathologists (1971).

ishingly high; at the other wavelengths, the coefficient of variation varied from 5–7 percent.

3. By contrast, a number of laboratories in New York State were surveyed at about the same time by the New York State Department of Health [10]. Some of these data are shown in figure 2. By comparison, the variability of instruments in the New York State survey was remarkably low.

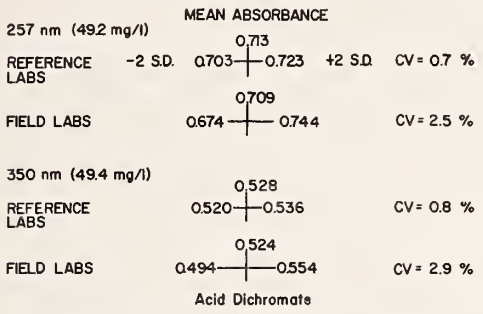

FIGURE 2. Performance of narrow band spectrophotometers in New York State.

Data from Vanderlinde, R., Report of a Survey, N.Y. State Department of Health (1971).

If the CAP results are representative of the range of spectrophotometric performance in this country, then we need to be concerned with the effect of such variable performance upon accuracy and precision. This point is amplified in table 4. The data represent the absorptivity of acid dichromate computed from the CAP survey for three concentrations. Shown are the high, low and mean values as well as data obtained in our laboratory. It is obvious that any analyses requiring an absorptivity for conversion of absorbance to concentration would be seriously in error, if a literature value were used.

It is also worth noting that the currently accepted value of 10.69 for the absorptivity of acid dichromate (in 0.1 H_2SO_4) was not met even at the mean [13]. Our values were also somewhat low. By contrast, we obtained 10.65 and 10.63 for the 50 mg/l and 100 mg/l solutions in the New York State survey.

TABLE 4. Absorptivity of Potassium Dichromate in 0.01 H_2SO_4[1]

		(350 nm)
25 mg/l	High	12.24
	Mean	10.48
	Low	8.72
	Pepper Lab	10.36
50 mg/l	High	11.92
	Mean	10.48
	Low	8.04
	Pepper Lab	10.58
100 mg/l	High	11.83
	Mean	10.09
	Low	8.35
	Pepper Lab	10.38

[1] College of American Pathologists, Instrumentation Survey, May 1971 [12].

It is difficult to feel complacent about the reliability of measurements on narrow band instruments in the clinical labs in this country. When variability of ± 10 percent to ± 39 percent can occur, then surely the accuracy of analyses performed on such equipment must be severely questioned.

C. Automatic Instrumentation

To this author's knowledge, no studies of the photometers used in automatic instrumentation have been published. However, intra-laboratory surveys of analytical variability have been conducted [14]. Results have been analyzed by separation of the data from those laboratories using automatic methods from those using manual techniques. Typical data are shown in table 5. The reasons for the scatter in both instances include poor standardization and photometric variability. It would seem in order, therefore, to suggest that the photometric performance of automatic instrumentation should be studied in order to

TABLE 5. Results of an Intra-Laboratory Trial in Britain [1]

Substance [2]	Manual methods				Autoanalyzer methods			
	Number	Mean concentration	S.D.	Range [3]	Number	Mean concentration	S.D.	Range [3]
Phosphorus	A. 131	3.037	0.406	1.2 to 9.3	35	2.860	0.273	2.3 to 3.7
	B. 135	7.758	1.231	3.1 to 10.4	35	7.906	0.576	6.6 to 9.0
	C. 134	4.458	0.469	3.1 to 5.5	35	4.666	0.243	4.0 to 5.3
Urea	A. 59	121.80	15.33	15 to 164	113	126.23	6.62	108 to 140
	B. 61	67.03	7.94	53 to 86	112	65.32	4.89	45 to 92
	C. 60	79.73	9.60	52 to 123	112	81.96	4.81	63 to 100

[1] From Gowenlock, A. H., Ann. Clin. Biochem. 6, 126 (1969).

[2] Samples A + B were dried sera; Sample C, aqueous solution.

[3] Range includes reported results; mean and S.D. are best estimates.

assess the magnitude of the photometric component of analytic error. At the least, linearity specifications and standards seem to be required.

VI. Common Sources of Spectrophotometric Error and Their Possible Effect on the Accuracy and Precision of Clinical Chemical Analyses

A. Wide Band Instruments

1. *Wavelength*—Wavelength error is of considerable significance if colored substances with sharp absorption bands are analyzed. This is true, of course, because the rate of change of absorbance with wavelength will probably be high enough to cause a significant absorbance error. Usually, however, colored materials with appreciable broad absorption bands are analyzed in wide band instruments. Hence, clinical chemical analysis of this sort is little affected by wavelength error over moderate intervals, particularly if standards are run concurrently. On the other hand, it is well known that the optimum wavelength for any procedure is at the peak of absorbance. It follows that evidence of wavelength accuracy is implicit for reliable definition of this optimum wavelength.

2. *Photometric Accuracy*—It is difficult to give photometric accuracy unambiguous meaning in wide band instruments [13]. Thus, accurate absorbance measurements are not really possible in this type of instrument.

Some idea of the magnitude of the errors involved can be gained by study of table 6. This table summarizes an experiment in our laboratory in which a dilute solution of reduced nicotinamide adenine dinucleotide (NADH) was made in phosphate buffer at pH 7.4. Concentration 1 was twice concentration 2. These solutions were placed in 19 mm internal diameter test tubes and read against a phosphate blank in wide band grating instruments of 10 and 20 nm bandpasses. The same test tubes were used in both instruments and the readings were completed within a few minutes.

Table 6. Absorbance of NADH in Two Wide Band Instruments at 340 nm. [1,2,3]

Instruments	Bandpass	Concentration 1	Concentration 2	ΔA
1	10 nm	0.304	0.156	0.148
2	20 nm	0.233	0.126	0.107

[1] NAHD dissolved in 0.1 M phosphate buffer at pH 7.4.

[2] Concentration 2 was one-half concentration 1.

[3] 10 mm round test tubes used for photometric readings.

Several conclusions are immediately obvious from these data: (1) Instrument 1 shows a more nearly linear relation of absorbance to concentration. (2) Instrument 2 gives absorbances significantly below instrument 1. (3) If NADH coupled enzymes were being assayed and the NADH concentration changed from C_1 to C_2, instrument 2 would have given an apparent enzyme activity 20 percent below instrument 1. Such differences, traceable to instrumentation, are most distressing. This is further evidence that the accuracy of spectrophotometric measurements in wide band instruments is questionable and may lead to significant error.

3. *Photometric linearity*—The wide band instruments used in most laboratories are assumed to be linear through an absorbance of 1.0. Earlier in this paper were cited data indicating variable performance of wide band instruments with respect to linearity [8]. It seems clear that the percentage error due to unsuspected nonlinearity is a function of the actual deviation and the absorbance at which nonlinearity becomes evident. Absorbance errors of more than 10 percent could be due to nonlinearity.

4. *Photometric Sensitivity*—Again, the British are to be credited for recognizing that linearity and photometric sensitivity are both important instrument parameters [9]. If an instrument is linear through an absorbance of one, then the slope of the line relating absorbance to concentration is a function of a number of variables. These include: (1) sample size, (2) absorptivity of colored complex, (3) optical path, (4) dilution factor, (5) photometric response. Since the slope and sensitivity may be altered by more than one factor, it is difficult to weight the photometric component and assign its contribution to analytical error. Indeed, there seems to be no general agreement as to what constitutes optimum sensitivity.

Some indication of the scope of the photometric problem may be obtained by reference to data found in table 7. This table lists for a few determinations the acceptable uncertainties pointed out by Barnett and shown in table 1 [6]. If we use actual absorbance-concentration relationships found for each of these, then for each of Barnett's uncertainties, we may compute a minimum change in absorbance which must be sensed and sensed repeatably. These are shown in

Table 7. Required Sensitivity of Absorbance Measurements

Analyte	Medical decision level *mg/dl.*	Absorbance sensitivity required *(Autoanalyzer)*	Absorbance sensitivity required *(Manual)*
Glucose	120 ±5	0.013	0.005
BUN	27 ±2	0.010	0.080
Uric Acid	6 ±0.5	0.067	0.022
Calcium	11 ±0.25	0.035	0.080
Phosphate	4.5± .025	0.016	0.080

From Barnett [6].

column 3 for Autoanalyzer [4] procedures in our laboratory and in column 4 for manual procedures as described in a text [14]. Inspection of these data show the following; (1) The minimum sensitivity required is 0.005 absorbance and the maximum is 0.080. (2) Of the 10 values listed, five require a sensitivity of 0.022 or less. It seems likely that few current wide band instruments can consistently measure differences of 0.005; by the same token differences of 0.080 should easily be measured. It should also be realized that absorbance differences of 0.022 require, in general, measurement of transmittance values that differ by 1 percent or less. Thus, even to meet Barnett's broad tolerances requires spectral measurements of high sensitivity and precision.

B. Narrow Band Instrumentation

Narrow band spectrophotometers are used for the determination of a number of substances, some of which are listed in table 8. In addition to these, the

Table 8. Determinations Performed With the Use of Narrow Band Spectrophotometers

Bilirubin
NADH—coupled enzymes
Alkaline phosphatase (kinetic—using sodium dinitrophenol phosphate)
Barbiturates
Diphenylhydantoin
Doriden
Tolbutamide
Hemoglobin derivatives
Uric acid at 292 nm

partial characterization of the purity of standards by the determination of molar absorptivity is growing in importance. This use is discussed in this Journal by Burnett. (See figs. 1 and 2).

Our purpose in this section is to assess the significance of commonly encountered spectral errors and their effect on the analytical reliability of the determinations involved. It would be beyond the scope of this article to exhaustively catalog each of the various determinations. Rather, we may take two different procedures and discuss some aspects of each.

First, let us consider the spectrophotometric determination of bilirubin [1]. Typically, a 1 to 50 dilution of serum may be made and the absorbance determined at two wavelengths, (455 and 575 nm). The 455 nm wavelength represents the bilirubin peak; the 575 nm peak may be used to correct the bilirubin absorbance for the contribution of hemoglobin. In table 9 some computations are based on two assumptions: (1) what we are dealing with is a hypothetical serum in which no interference from hemoglobin or other absorbing substances exist, (2) that the absorptivity of bilirubin in serum at 455 nm is 60.1.

If we refer to Barnett's paper we may note that the usual medical decision level for serum bilirubin in the newborn infant with hemolytic disease is 20 mg/dl and that the uncertainty of the bilirubin measurement at this level should be $\pm$ 1.5 mg/dl. One can, then, compute the expected absorbances that might be obtained at upper and lower limits; and this is shown in table 9, column 4.

It is to be noted that on the high side, the expected absorbance is 11 percent above the nominal and on the low side is 8 percent of the nominal. The "allowable" spread is in the range of 15–20 percent of the mean. In the previously cited CAP survey, the range of values reported for Thomson's solution at 450 nm, was 10 percent of the mean. Since one-half of the "allowable" variation could be accounted for by spectrophotometric error, only 5–10 percent remains for all other sources of error. It seems evident that reduction of the measurement error could significantly reduce analytical error. If this were so, the allowable limits might be set even lower than stated by Barnett.

Similarly, in table 10 some hypothetical computations with respect to NADH are made. That which is assumed is: (1) the "true" molar absorptivity of NADH is 6.2×10^3, (2) a 10 percent high or low absorbance error can occur in any instrument, (3) the "true" absorptivity is used to compute enzyme activity in international units.

If such absorbance error occurs, then in column 3

Table 9. Absorbance of Bilirubin Solutions and Medical Decisions [1]

Substance	Decision level	Upper and lower limits [2] *mg/dl*	Absorbance at limits	Absorbance difference	Percent of decision level
Bilirubin		21.5	0.457	0.046	11
	20 mg/dl.		.411		
		18.5	.379	.033	8

[1] Assumes a direct spectrophotometric procedure reading at 455 nm, an absorptivity of 60.1 and a dilution of 1/50 and no hemoglobin interference.

[2] See Barnett [6].

[4] In order to adequately describe materials and experimental procedures, it was occasionally necessary to identify commercial products by manufacturer's name or label. In no instances does such identification imply endorsement by the National Bureau of Standards, nor does it imply that the particular product or equipment is necessarily the best available for that purpose.

Table 10. Spectrophotometric Error and Effective Molar Absorptivity of NADH and Its Effect on Computed NADH-Coupled Enzyme Levels

NADH level	Absorbance	Molar absorptivity	Apparent enzyme activity (*U*)	Enzyme activity (corrected for apparent absorptivity) (*U*)
Normal enzyme concentration			(Expected)	
7.8 mg/dl.	0.700	6.2×10^3	32.4	
10 percent low	0.630	$7\ \times10^3$	32.4	28.6
10 percent high	0.770	5.7×10^3	32.4	35.0
Elevated enzyme concentration			(Expected)	
		6.2×10^3	404	
10 percent low		$7\ \times10^3$	404	358
10 percent high		5.7×10^3	404	437

The high and low absorbance values are assumed as possible errors. See figure 1 for justification.

are listed the apparent molar absorptivities corresponding to the erroneous readings. In column 4 are listed activities for a hypothetical NADH coupled enzyme in the high normal range and a typical elevated enzyme activity. If we ignore the error occurring in the absorbance measurements of the enzyme activity itself, then in the last column are listed the "true" values assignable to these two enzyme activities based on NADH absorptivity corresponding to the high and low errors. The large differences are obvious.

Now this has the appearance of a quantitative argument; it is not intended to be so. It is, rather, a model to show the effect of spectrophotometric error on a clinically important determination. That such error can occur is attested to by the data in figure 1, from the CAP survey. Two coefficients of variation at 350 nm were observed to be 13.8 percent.

The common sources of spectral error in narrow band instruments are well understood. Wavelength error, nonlinearity, photometric inaccuracy, and stray light are major contributors. Standards for each of these are needed urgently.[4]

C. Automatic Instrumentation

Let us consider the photometers in use in automatic analyzers. The basic photometric requirements seem clear enough: (1) Given a chemistry which is linear, it is expected that the photometer output would exhibit basic conformance to the Beer-Bouguer Law over the range of transmittance of 0.1 to 1.0. (2) The sensitivity should be such that the desired or optimum absorbance concentration relationship is achieved and sustained from determination to determination.

In our hands, the various automatic analyzers seem to yield adequately linear calibration lines through an absorbance of one.[5] Linearity should not be considered apart from sensitivity since considerable flexibility exists with respect to possible ratios of sample to reagent. We may define the appropriate sensitivity as that which will yield a change in absorbance per defined detection limits (see table 2) clearly within the capability of the photometric system. This can be done by selection of the appropriate sample size; however, one may be hampered because the concentration of analyte which spans the 0–1 absorbance range may be so small as to require a large number of dilutions and re-running of samples. Some compromise is usually accepted.

An experiment was performed to evaluate the ability of an Autoanalyzer to discriminate small changes in concentration. Phosphate solutions in the range 3.23 to 4.73 mg/dl were prepared by dilutions of weighed reagent grade phosphate salt. These were analyzed on an Autoanalyzer (modified Sumner technique [17]), on three separate days. On each day, the standards used in the routine lab were utilized to prepare calibration curves. These were linear over the concentration range 1 mg/dl to 12 mg/dl (absorbance range 0.065 to 0.710). The equation of the standard line was computed by linear regression; this equation was then used to compute the values obtained for the weighed materials. Some of the data are summarized in table 11.

Over the three experimental days, the determined values group very closely with the maximum range not exceeding 0.22 mg/dl. Although all estimates are lower than the weighed-in values, the worst case underestimates by only 0.18 mg/dl. (See day 2–3.12 mg/dl.) Thus it would appear that at least for aqueous material, we can easily estimate phosphorus within 0.25 mg/dl. This falls within the specifications cited by Barnett [6].[6]

VII. Current Needs for Spectrophotometric Standards

The National Bureau of Standards has a current program related to spectrophotometric standards.

[4] It is recognized that there are other sources of error which also contribute. Among these are variability in optical path dimensions, scatter of sample, fluoresence of sample, reflections, etc. Some of these were reviewed in a classic paper which indicates compelling obstacles to the determination of absolute absorbance [16]. Our argument here is that elimination of major sources of error would allow analytical accuracy at a level rarely approached. The question of the measurement of absolute absorbances and the elimination of all sources of error is a most difficult matter. The major effort now, however, should be to reduce within and between instrument variability and error to less than 1 percent.

[5] This statement does not imply that there is evidence that all Autoanalyzer determinations are inherently linear. Some are; some are not.

[6] It is possibly significant to mention that a skilled operator used the instrument. Furthermore, there is no evidence that the same sensitivity would apply to proteinaceous materials To obtain data of this quality, standards must be run each time the analyzer is operated, at the very least.

Table 11. Ability of an Autoanalyzer to Distinguish Small Changes in Concentration Using Aqueous Phosphate Standards

Weighed concentration *mg/dl.*	Found *mg/dl.*			High–low range *mg/dl.*
	Run 1	Run 2	Run 3	
3.23	3.27	3.15	3.25	
	3.27	3.05	3.16	0.22
		3.15	3.25	
	Mean of 3 determinations = 3.19			
3.46	3.50	3.42	3.42	
	3.43	3.51	3.42	0.16
		3.42	3.34	
	Mean of 3 determinations = 3.43			
3.69	3.69	3.60	3.59	0.19
	3.69	3.60	3.50	
	Mean of 3 determinations = 3.61			
4.32	4.26	4.34	4.19	0.15
	4.26	4.34		
	Mean of 3 determinations = 4.29			
4.73	4.73	4.70	4.61	0.12
	4.73	4.61	4.61	
	Mean of 3 determinations = 4.66			

Current research has been summarized in this Journal and in another publication [18].

A major contribution of this program is the current availability of calibrated Schott NG Glass. These glasses, mounted in a convenient holder, are most useful for checking photometric accuracy in the visible range.

Other standards are also needed, if we are to hope for spectrophotometric measurements of uniformly high accuracy and precision. A summary of these follows:

A. Wavelength Standards

Suitable wavelength standards of universal applicability are strongly indicated. These should be usable in both narrow and wide band instruments.

B. Photometric Accuracy and Linearity

Although the current NG glasses are excellent, it appears that a more neutral glass, optically more homogeneous, would allow calibration to ± 0.1 percent relative transmittance. The capability of use in the ultraviolet would be a most important specification. Additionally, these glasses should be usable in wide band instruments.

Chemical standards are also needed for both narrow and wide band instruments for primary use in linearity and sensitivity evaluation. These would also be useful when necessary to prove that accurate spectrophotometric measurements can be made with liquids. This in contrast, of course, to proof that the photometric accuracy of an instrument, itself, is acceptable. Chemical standards should also be available for checking the linearity and sensitivity of the photometers used in automatic analyzers.

Stray light, of major significance in ultraviolet measurements, needs a standard method for its measurement.

Spectrophotometric grade cuvettes need to be specified with respect to optical path length and wedge. A standard method of measurement needs to be established. Dr. Barnett's paper, I believe, indicates the importance of cuvette error in spectrophotometric systems.

Last, but not least, it should be emphasized that independent means for defining and measuring photometric accuracy need continued research. The presence of the high accuracy instrument at the Bureau should afford a useful tool for study of the problems related to this fundamental question.

VII. Summary

This paper has discussed the role of spectrophotometric standards in the clinical laboratory. Its underlying thesis is that errors in the color measuring step of photometric analysis have largely been ignored. Errors occurring in this step can and do contribute significantly to analytical error. It can be shown that errors traceable to the color measuring step can be of a magnitude such that medical decisions are made more difficult or may cause harm to the patient.

The assistance of Mrs. A. Ritz in obtaining some of the data in this paper is recognized with pleasure. The criticism of D. Arvan, who read the entire manuscript, was most helpful.

IX. References

[1] Tietz, N. W., Ed., Fundamentals of Clinical Chemistry (W. B. Saunders Co., Philadelphia, Pa., 1970).
[2] Brownfield, R. L., personal communication.
[3] Feinstein, A. R., Ann. of Int. Med. **61**, 564 (1964).
[4] Gordan, G. S., Loken, H. F., Blum, A., and Teal, G. S., Metabolism **11**, 94 (1962).
[5] Cotlove, E., Harris, E. K. and Williams, G. Z., Clin. Chem. **16**, 1028 (1970).
[6] Barnett, R. N., Amer. J. Clin. Path. **50**, 671 (1968).
[7] Campbell, D. G. and Owen, J. A., Clin. Biochem. **1**, 3 (1967).
[8] Cavanaugh. E. L., Doctoral Dissertation, Univ. of Calif., Berkeley, Calif. (1968).
[9] Broughton, P. M. G., Riley, C., Cook, I. G. H., Sanders, P. G., Braunsberg, H., Colorimeters—A Critical Assessment of Five Instruments, Assoc. Clin. Biochemists (1966).
[10] Vanderlinde, R., Report of A Survey, N.Y. State Dept. of Health (1971).
[11] Anon., Photoelec. Spectrometry Group Bull. **16**, 441 (1965).
[12] Anon., Report of the Subcommittee on Instrumentation, Coll. of Amer. Path. (1971).
[13] Rand, R., Clin. Chem. **15**, 839 (1969).
[14] Gowenlock, A. H., Ann. Clin. Biochem. **6**, 126 (1969).
[15] Anon., Clinical Methods Manual, Bausch & Lomb, Inc., Rochester, N.Y. (1965).

[16] Goldring, L. S., Hawes, R. C., Hare, G. H., Beckman, A. O. and Stickney, M. E., Anal. Chem. **25,** 869 (1953).
[17] Sumner, J. B., Science **100,** 413 (1944).
[18] Menis, O. and Shultz, J. I., Eds. Nat. Bur. Stand. (U.S.) Tech. Note 544, 151 pages (Sept. 1970), and 584, 175 pages (Dec. 1971).

(Paper 76A5–736)

NATIONAL BUREAU OF STANDARDS SPECIAL PUBLICATION 378, Accuracy in Spectrophotometry and Luminescence Measurements, Proceedings of a Conference Held at NBS, Gaithersburg, Md., March 22–24, 1972 (Issued May 1973).

Spectrophotometric Standards

W. H. Venable, Jr.

Institute for Basic Standards, National Bureau of Standards, Washington, D.C. 20234

(May 31, 1972)

To be useful, spectrophotometric measurements must be believable and practical. The basic standard for any believable spectrophotometric measurements is the ability to accurately compare fluxes of radiation within the framework of a well-defined geometry. The emphasis in the program proposed for the Institute for Basic Standards is to develop such ability over the broadest range of spectrophotometric measurements. Establishing such a basis will enable the National Bureau of Standards to render real assistance to those who deal with the problem of making practical measurements

Key words: Photometric accuracy; standards, spectrophotometric.

Spectrophotometric standardization is probably best described as elusive. This is not to say that it is an animated being which goes skulking from one hiding place to another, nor is it something which cannot be obtained. Rather, its elusiveness lies in the extreme care required to define what is to be measured and to make sure that something else is not being measured instead. Very seldom is there a one-to-one relationship between the spectrophotometer output and the desired quantity. To standardize a useful spectrophotometric measurement is to determine what *actual* relationship exists.

This assertion can best be illustrated in terms of very high accuracy measurements. The careful worker in spectrophotometry, as it is presently applied, can in general feel confident of an accuracy of plus or minus 0.005 in transmittance in the visible range and, under very favorable circumstances, attain a confidence to 0.002. Very high accuracy measurement for the purposes of this discussion would correspond to confidence to within less than 0.001 in transmittance in the visible, with corresponding degradations in the more difficult wavelength regions and for more difficult geometries. At this level, the effects to be discussed are very important and can determine success or failure in achieving the desired accuracy. It should also be borne in mind that where the accuracy really counts is in determining the desired property of the material being investigated, which is seldom completely or even partially an optical property. If the coupling between the property of interest and the measured spectrophotometric quantity is weak, as is the case in many health and environmental measurements, it may be necessary to achieve a very high spectrophotometric accuracy in order to measure the desired property even crudely. Consider as an example some of the factors which enter into the problem of determining the concentration of a solute in a solution, such as:

a. Linearity—Although it is important to know the linearity of an instrument, knowing it is not sufficient to assure accuracy in measuring transmittance, since many other factors contribute to producing the spectrophotometer output. It should also be noted that gages, such as filters, which have been calibrated on one instrument cannot provide a highly accurate means of determining the linearity of another instrument, since gages have a number of properties which are measured in different ways by different instruments.

b. Image Shift—Since inserting a medium in the beam changes the optical path length, the focus, and hence the way the receiver is illuminated, will be changed. Also, if the sample is tipped, as is sometimes done to reduce the effect of interreflections, the light reaching the receiver will be shifted laterally. If the receiver is at all sensitive to such variations in illumination, the spectrophotometer will measure this effect as well as transmittance.

c. Reflections—In the usual arrangement of a solution in a cuvette, there will be four surfaces at which reflections occur, and multiple reflections between these surfaces contribute to the spectrophotometer output in most cases. If there are any transmitting glasses such as lenses or windows in the spectrophotometer, there can be additional effects due to reflections from these.

d. Index of Refraction—The index of refraction of a solution fluctuates strongly in the wavelength range occupied by an absorption line. This change in refractive index will in turn cause image shifts and changes in reflections within that range of wavelengths.

502-591 O - 73 - 10

This again will appear as a part of the spectrophotometer output.

e. Identification of properties—Even if a spectrophotometer were made to measure transmittance perfectly, transmittance per se is often not the property of interest. Transmittance is a complex quantity which depends upon the measurement geometry and several properties of the sample, and thus is not simply related to a single property such as the concentration of a solute in a solution.

The foregoing discussion has dealt with some of the interactions between spectrophotometer and test sample. There are, of course, other sources of difficulty such as scattering of light by the sample, changes in the sample with temperature and stray light from the monochromator. All of these also contribute to the spectrophotometer output.

The point to be made here is that if high spectrophotometric accuracy is to be achieved, these effects must be accounted for. The electronics, optics, detectors and readouts of the spectrophotometers available have been greatly improved, so that these instruments can be made much more stable and more sensitive than they were five or ten years ago. The result has been more than an order of magnitude improvement in precision, but there has been no corresponding improvement in accuracy. Improving accuracy can only come about through concerted efforts by instrument makers, standards laboratories, and those who need to perform very accurate spectrophotometric measurements.

Instrument makers should at the very least make the optical layout of each instrument known *in complete detail* so that the owner or prospective owner can see what stands in the way of his achieving the accuracy he needs. It would also be a great contribution if each new instrument intended for high accuracy work were designed for accuracy in a particular type of measurement, without undue concern that it give the same "numbers" for a given filter that last year's instrument gave.

The standards laboratory has a many-faceted role in standardization for high accuracy. Research should be conducted to find how the magnitude of each of the various contributions to error can be determined, to find in which case corrections can be made, and in such cases give practical procedures for making the corrections. When special gages are needed to aid in a particular step of calibration, the standards laboratories should see that these are available and that all the pertinent properties of these gages are made known. For example, for very high accuracy work, the absorbance, index of refraction, thickness and scattering properties of a filter should be supplied by the standards laboratory instead of just a transmittance value. For such work it makes no sense for a standards laboratory to pass out gages with a "best value" of some single property attached. The standards laboratory must maintain a versatile, thoroughly evaluated, and carefully documented measurement system in order to perform its own work and evaluate the work of others. Also, the standards laboratory must constantly be aware of new developments in spectrophotometry and maintain a close liaison with all groups involved in the measurements in order to assist everyone, including the standards laboratory itself, to achieve the needed measurements.

The ultimate responsibility for standardization of very high accuracy measurements lies in the person or persons performing the measurements. The user must take the steps necessary to determine what stands in the way of his obtaining the particular data he desires with his particular instrument and make appropriate corrections. The operator of the spectrophotometer may have the knowledge and experience to do this on his own, or he may have to rely heavily on instructions provided by others, but he is the one who must standardize his measurements.

What has been described is spectrophotometric standardization for very high accuracy—standardization for the future, since very high accuracy spectrophotometry is not being used at the present. However, factors such as those listed in the early part of this discussion contribute to any measurement, and they should be considered when making measurements at any level of accuracy. The cost in effort to obtain very high accuracy measurements will be great, so it is extremely important to attempt them only where the anticipated benefits will be correspondingly great—they certainly should not be attempted when not really needed. Very high accuracy measurements *can* be obtained with diligence on the part of those making the measurements, and support for such measurements *can* be provided by instrument makers and standards laboratories, but a change in attitude and approach by all may be required before they are achieved.

To be useful, spectrophotometric measurements must be believable and practical. The basic standard for any believable spectrophotometric measurements is the ability to accurately compare fluxes of radiation within the framework of a well-defined geometry. The ability to relate the results of such measurements to a property which is to be determined can only be achieved through careful interpretation of the spectrophotometric output based on considerations such as those described above. The emphasis in the program being proposed for the Institute for Basic Standards is to develop a strong measurement capability over the broadest possible range of spectrophotometric measurements. Establishing such a capability will enable the National Bureau of Standards to render real assistance to those who deal with the problem of making practical measurements for a given application.

(Paper 76A5–737)

PART II. LUMINESCENCE MEASUREMENTS

NATIONAL BUREAU OF STANDARDS SPECIAL PUBLICATION 378, Accuracy in Spectrophotometry and Luminescence Meosurements, Proceedings of a Conference Held ot NBS, Gaithersburg, Md., March 22–24, 1972 (Issued Moy 1973).

Absolute Spectrofluorometry

W. H. Melhuish

The Institute of Nuclear Sciences, Department of Scientific and Industrial Research
Private Bag, Lower Hutt, New Zealand

(July 11, 1972)

The last 10 years has seen the increasing publication of the emission spectra of organic, inorganic and metal-chelate compounds, but there is no agreed method of presentation of such spectra. In the few cases where corrected emission spectra have been published, there is often no mention of the units used for the intensity coordinate or the method used for correcting spectra. A method of reporting absolute fluorescence spectra originally put forward in 1962 will be reexamined and improved. The two best known methods for calibrating spectrometers for absolute spectrofluorometry: (a) standard tungsten lamp, (b) quantum counter method, will be critically examined, and the limitations and possible improvements in accuracy will be proposed. The criteria for an emission standard will be examined and the use of emission standards for calibrating spectrofluorometers discussed. It is suggested that the distribution of emission standards to laboratories measuring corrected fluorescence spectra and the analysis and publication of the results should be done in the near future.

Key words: Actinometers; calibration of spectrofluorometers; detectors, absolute; fluorescence spectra, corrected; quantum counters; spectrofluorometers, design; spectrofluorometry, absolute; standard lamps; standards, fluorescence; thermopiles.

I. Introduction

Although fluorescence from organic molecules or molecular complexes has been used for many years as a method of trace analysis especially in biochemical and medical work, it was not until the introduction of commercial spectrofluorometers in the 1950's that fluorescence spectra began to appear in the literature in any great numbers. The selectivity and accuracy of analysis were greatly improved by measuring fluorescence spectra and also it became possible to recognize organic molecules in very dilute solution from their fluorescence spectra. The use of fluorescence spectra in many photophysical investigations such as determination of quantum efficiencies of fluorescence, studies on the configuration of ground and excited states, electronic energy transfer and so on, has become increasingly important in the last 10 or 15 years [1, 2].[1]

The emission spectrum recorded by a spectrofluorometer, unlike an absorption spectrum, is greatly distorted by the response function of the instrument (sensitivity as a function of wavelength), and by artefacts such as scattered light in the analyzing monochromator. The response function of the spectrofluorometer is determined by the transmission of the monochromator as a function of wavelength, the spectral sensitivity of the detector (usually a photomultiplier tube) and the variation in transmission and focusing properties of lenses (if used) with wavelength. The response function can only be reliably measured by using a source of known spectral energy distribution. Absolute spectrofluorometry, therefore, is mainly concerned with the problem of obtaining sources with accurately known spectral distributions.

Despite increasing publication of fluorescence spectra, especially in the last 10 years, it is disappointing to find that most spectra have not been corrected in any way and are thus of limited use to other workers. In the few cases where corrected spectra have been published, it seems customary to give the intensity "in arbitrary units" and provide no information on the dimensions of the units or the method used for correction. Those who publish fluorescence spectra should take note of a joint statement made by a number of investigators in 1962 [3] which stresses the importance of reporting the method of correction, subtracting "background fluorescence" and using appropriate units (e.g. quanta s^{-1} per unit wave number interval). This list has been extended by Demas and Crosby [4] to include those factors which are important when measuring quantum efficiencies of fluorescence from emission spectra.

In view of the fact that absolute calibration of spectrofluorometers is an exacting task requiring equipment not available in many laboratories, it would seem important to encourage the use of fluorescence emission standards. These can be used in three ways: (a) for presentation alongside the spectrum being investi-

[1] Figures in brackets indicate the literature references at the end of this paper.

gated so that the reader can correct the spectrum from the most recently known figures for the standard, (b) for calibrating spectrofluorometers, (c) for use in a ratio spectrofluorometer to give the ratio of the unknown to standard at each wavelength. Some standards have already been proposed [5, 6, 7], but new ones need to be found, especially in the ultraviolet and near infrared regions.

In this account of absolute spectrofluorometry, no attempt has been made to completely review the literature. The reader will find further references in the recent review article on photoluminescence quantum yields by Demas and Crosby [4]. Rather the emphasis will be on the experimental methods in absolute spectrofluorometry with a critical examination of methods of calibration, suggestions for improving accuracy and recommendations on nomenclature.

II. Definitions

A. Units

The recommended radiometric and photometric units as defined by the Système International d'Unitès (SI), are the joule (J), the watt (W) and the lumen (lm). The symbols and defining equations for quantities used in emission studies are:

radiant energy	$= Q$ (J)
radiant flux, φ	$= dQ/dt$ (W)
irradiance, E	$= d\varphi/dA$ (W m^{-2})
spectral irradiance, $E(\lambda)$	$= dE/d\lambda$ (W m^{-2} nm^{-1})

The spectral irradiance, $E(\lambda)$, is commonly used to record the output of black bodies and tungsten lamps. Unfortunately, there are no SI units for photon quantities and in this review we will use the nomenclature recently recommended by Muray, Nicodemus, and Wunderman [8]. The authors propose placing a "q" as a subscript on radiometric quantity to denote a photon quantity. Thus the photon units for some of the emission quantities would be:

photon energy	$= Q_q(h\nu)$
photon flux, φ_q	$= dQ_q/dt$ ($h\nu$ s^{-1})
photon irradiance, E_q	$= d\varphi_q/dA$ ($h\nu$ s^{-1} m^{-2})
photon spectral irradiance, $E_q(\lambda)$	$= dE_q/d\lambda$ ($h\nu$ s^{-1} m^{-2} nm^{-1})
or $E_q(\tilde{\nu})$	$= dE_q/d\tilde{\nu}$ ($h\nu$ s^{-1} m^{-2} (cm^{-1})$^{-1}$)

In the past, the quantity $E_q(\tilde{\nu})$ has been variously labelled I, q, B, $Q(\tilde{\nu})$, etc., but the new symbol would appear to be less confusing and we recommend its adoption.

B. Presentation of Emission Spectra

The integrated corrected emission spectrum is proportional to the fluorescence efficiency. The most useful quantity for photochemists is the quantum fluorescence efficiency which is proportional to $\int_0^\infty E_q(\lambda)d\lambda$ or $\int_0^\infty E_q(\tilde{\nu})d\tilde{\nu}$. Thus the most useful spectra for publication are $E_q(\lambda)$ or $E_q(\tilde{\nu})$ spectra in which the maximum of the curve is given as $E_q(\tilde{\nu}) = 1.00$. Many workers report fluorescence spectra on a wavelength scale, but a wave number scale is to be preferred especially when vibrational structure is present. It is important to remember that the shapes and positions of the peaks of fluorescence spectra depend on the units used. This is illustrated in figure 1. Here $E(\lambda)$ and $E_q(\tilde{\nu})$ for quinine in 1 N H_2SO_4 are plotted on the same graph. The relation between the various units for emission spectra can be shown from the work of Ejder [9] to be:

$$\lambda^3 E(\lambda) = \lambda^2 E_q(\lambda) = \lambda E(\tilde{\nu}) = E_q(\tilde{\nu}).$$

Thus emission spectra can be readily transformed by multiplying by the appropriate power of λ; e.g. an $E_q(\tilde{\nu})$ spectrum can be converted to an $E_q(\lambda)$ spectrum by multiplying by λ^{-2}.

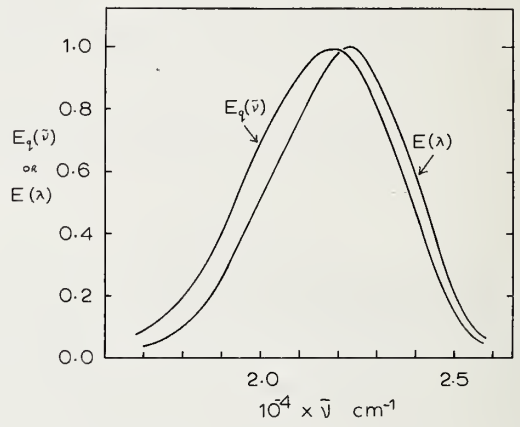

FIGURE 1. $E_q(\tilde{\nu})$ and $E(\lambda)$ spectra of quinine (10^{-4} M) in N H_2SO_4.

C. Glossary

The following abbreviations will be used in the following text, diagrams and tables:

FS = front surface
SV = side view
φ_f = quantum efficiency of fluorescence
OD = optical density or absorbance
PM = photomultiplier
M = monochromator
QC = quantum counter
TP = thermopile
$S(\tilde{\nu})$ = spectrofluorometer response function required to give $E_q(\tilde{\nu})$ emission spectra
λ = wavelength (nm)
$\tilde{\nu} = 1/\lambda$ = wave number (cm^{-1}).

III. Equipment

A. Excitation Sources

Undoubtedly the most popular exciting source for fluorescence is the high pressure xenon lamp in combination with a wide aperture grating monochromator. In order to get sufficient light at wavelengths shorter than 300 nm, it is common to use lamps of 450 watts or larger and these have the advantage of being somewhat more stable than the lower wattage lamps. If a very intense exciting source is needed, a medium or high pressure mercury lamp can be used with appropriate filters. When measuring the fluorescence spectra of concentrated solutions, powder or single crystals where front surface illumination is necessary (Sec. V), stray light from the exciting monochromator can be a problem, especially if the fluorescence emission from the sample is weak. Stray light can either be light appearing in the second or higher orders, or instrumental scatter of many wavelengths. This second type of instrumental scatter is easily demonstrated by placing the eye at the exit slit of the excitation monochromator when its wavelength is set in the UV region. Interference from second order stray light can be greatly reduced by using suitable nonfluorescent cutoff filters or bandpass filters [10]. Unfortunately few commercial spectrofluorometers have filter holders and it is necessary to have them fitted. Double grating monochromators will reduce instrumental scattered light to a large extent, but the throughput is also reduced. Good practical discussions on the use of filters and monochromators is given by Kortüm [11] and Parker [2].

The amount of stray light from a Gillieson type monochromator (as modified by Schroder [12]) when a mercury lamp is placed at the entrance slit is shown in figure 2, dashed line. The wavelength setting was 365 nm, the bandwidth was 20 nm and the 390 lines/mm grating was blazed at 350 nm. The light output was scanned with a Jarrell-Ash[2] 1/4 meter grating monochromator. The units are φ_q for the mercury lines and $E_q(\tilde{\nu})$ for the continuum. A Wratten 2 C filter (λ cutoff at 390 nm) was placed at the entrance slit of the 1/4 meter monochromator to eliminate errors due to scattering and multiple diffraction of the intense line in the analyzing monochromator (see Sec. III, B). The stray mercury lines may be further reduced by choosing a suitable bandpass filter for the exciting line.

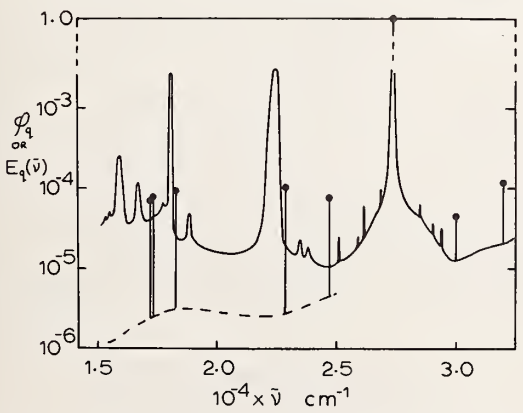

FIGURE 2. Stray light in excitation and analyzing monochromators. ● = mercury lines.

Dashed line: stray light from excitation monochromator set as 365 nm with a mercury lamp at entrance slit, and a 2c filter at exit slit.

Solid line: spurious peaks due to stray light in analyzing monochromator set at 365 nm, with a mercury lamp at the entrance slit.

B. Analyzing Monochromators

The most readily available and least expensive monochromator is the single grating instrument based on the Ebert-Fastie or Czerny-Turner mountings (fig. 3, b and c).

The Gillieson mounting (fig. 3a) is sometimes used in monochromators intended for excitation purposes. Most commercial instruments use single grating monochromators and provided one is aware of their limitations, they are adequate for measuring the rather broad fluorescence spectra given by organic molecules in solution. The advantages of grating monochromators over prism ones are: (a) linear wavelength dispersion, (b) high aperture and (c) easy interchange of gratings for different spectral regions. However, the grating monochromator generally has higher scattered light and the overlapping of orders can be a problem.

The most important source of stray light in a grating monochromator, particularly one of large aperture, is

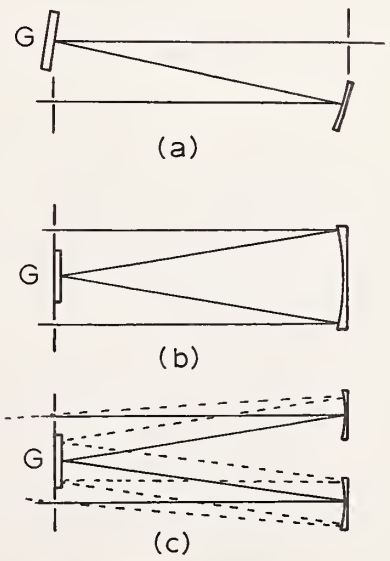

FIGURE 3. Types of grating monochromators: (a) Gillieson, (b) Ebert-Fastie, (c) Czerny-Turner. (G = plane grating).

[2] In order to adequately describe materials and experimental procedures, it was occasionally necessary to identify commercial products by manufacturer's name or label. In no instances does such identification imply endorsement by the National Bureau of Standards, nor does it imply that the particular product or equipment is necessarily the best available for that purpose.

multiple diffraction. One possible pathway for double diffraction is shown by the dashed lines in Figure 3c. This well known problem has not been quantitatively investigated until recently [12, 13]. Multiple-diffracted light can be reduced with a mask, but this reduces the transmission of the monochromator. An experimental determination of stray light in the Jarrell-Ash 1/4 meter grating monochromator with a grating blazed at 600 nm is shown in figure 2, solid line. The exciting wavelength was 365 nm and the baffle inside the monochromator was removed for these measurements. Many of the spurious peaks shown are due to multiple diffraction as may be proved by removing the exciting light with a Wratten 2 C filter; the peaks disappear, but the stray mercury lines from the excitation monochromator are not affected. This spurious light is particularly troublesome when scattered exciting light cannot be avoided as when measuring multicrystalline material from the FS or measuring solutions with a very low fluorescent intensity. In these cases it is advisable to remove the exciting light with a sharp cutoff filter and make corrections for any fluorescence absorbed by the filter. The minimizing and correction of stray light in spectrofluorometry will be further discussed in Section V, A.

C. Detectors and Amplifiers

The detector used in spectrofluorometry is the photomultiplier. End-window photomultipliers are to be preferred, since there is no grid in front of the photosurface to obstruct the narrow light beam from the exit slit of the analyzing monochromator. A quartz window photomultiplier with an S–20 photosurface has been found to have good sensitivity over the range 220 to 800 nm. A modern tube such as the EMI type 9698 QB has a very low dark current ($\sim 10^{-10}$A) and does not need cooling.

For fluorescence spectral measurements in the range 800 to 1100 nm, a cooled photomultiplier with and S–1 sensitivity curve is commonly used. It is possible that an uncooled P–I–N silicon diode may prove to be a more useful detector in this wavelength region [14], but unfortunately the surface areas of silicon photodiodes presently available are too small to be useful in spectrofluorometry.

For amplification of photocurrents of $\geq 10^{-12}$ A, solid state electrometers of the type described by Weinberger [15] are quite adequate and inexpensive. Selectable time constants ranging from 0.1–2 s. should be included in the amplifier to improve the signal-to-noise ratio. Photocurrents less than 10^{-12} A are best measured by photon counting. Not only is it possible to use simple amplifiers and discriminators [16, 17] but greater accuracy with shorter sampling times is achieved [18]. It should be noted that the photocathode should be at ground potential when the photomultiplier is used for photon counting to minimize noise due to current leakage from the photocathode.

D. Design of Spectrofluorometers

Parker [2] has discussed the design of spectrofluorometers and several instruments have been described in the literature [19-22]. Few instruments, however, are completely satisfactory if they are required to perform a number of different functions, and we believe the following criteria should be examined before building a spectrofluorometer:

(a) There should be space around the sample so that heating and cooling baths, flow cells, liquid helium Dewars, etc., may be fitted.
(b) The instrument should be double beam in order to eliminate light source fluctuation and have the ability to measure excitation spectra.
(c) The sample should be capable of being observed from the front face and from the side.
(d) Excitation light source should be easily exchangeable.
(e) There should be space for fitting filters at the exit beam of the excitation monochromator and at the entrance slit of the analyzing monochromator.
(f) Space should be available for fitting chopping discs, e.g., for measuring phosphorescence spectra.
(g) The scanning speed should be accurately adjustable over a wide range.
(h) Amplifiers should have adjustable time constants to improve the signal-to-noise ratio.

A design used in this laboratory which meets all of these requirements is shown in figure 4. Three con-

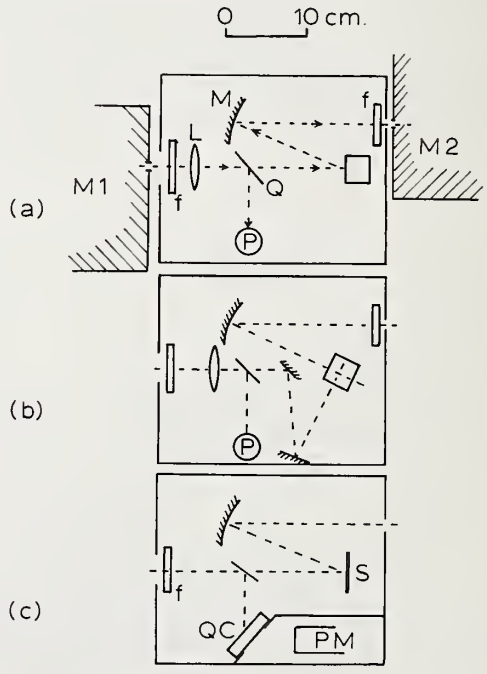

FIGURE 4. Spectrofluorometer design. M1, M2 = monochromators, Q = quartz beam splitter, f = filters, M = spherical aluminized mirror, P = photocell, PM = photomultiplier, QC = quantum counter, S = scatterer, L = quartz lens.

figurations are shown: (a) for measuring fluorescence spectra using FS excitation, (b) for measuring fluorescence spectra with SV and (c) configuration for calibrating the analyzing monochromator and photomultiplier, using the quantum counter method (Sec. IV, C). Light shields have not been shown on the diagram. Excitation spectra can be measured by replacing P in figure 4a with a quantum counter. The two signals from the monitoring photocell (or quantum counter photomultiplier) and the analyzing photomultiplier are amplified by electrometers and led to a ratio recorder of the type described by Haugen and Marcus [19]. Components are held rigidly on a series of optical benches contained in a hinged box between the two monochromators.

The spectrum recorded by spectrofluorometers is usually an uncorrected one plotted on a wavelength scale. The correction of the spectrum and replotting on a wave number scale is very laborious and instruments for the direct correction of spectra, as they are recorded, have been described [22, 23]. However these corrected curves must still be replotted if a wave number scale is required. The use of small, inexpensive on-line computers is becoming increasingly common and in the future it is likely that these will be used to correct both ordinates and plot the spectrum directly. The only additional equipment needed for the spectrofluorometer is a digital voltmeter with binary coded decimal (BCD) output and several stepping motors. Interfacing to a small computer such as the PDP–8 presents no problems.

IV. Calibration Methods

A. Introduction

The emission spectrum recorded by a simple spectrofluorometer, i.e., one without built-in automatic correction devices, is distorted not only by the scattering artefacts described in Section III, B, but also by the wavelength dependence of the detector and monochromator transmission. Only two calibration procedures for determining this response function have so far been developed. The first method depends on the assumption that a tungsten lamp operated at a color temperature, T_c, has a spectral distribution of a black body at T_c K multiplied by the emissivity ($\epsilon(\lambda)$) of tungsten:

$$E(\lambda) = \frac{8\pi hc\,\lambda^{-5}\,\epsilon(\lambda)}{[\exp(0.01438/\lambda T_c)] - 1} \qquad (1)$$

where λ is in meters.

This emission standard is then used to calibrate the system as described in Section IV, B.

The second method makes use of an intense source of light and a monochromator. A detector of known response measures the watts (or quanta s^{-1}) emerging from the exit slit at various wavelengths. This calibrated source is then used to determine the response function of the spectrofluorometer. These two methods will be critically examined in Sections B and C, following.

It is important to note that the spectrofluorometer is not being calibrated under precisely the same conditions that pertain to the measuring of fluorescence spectra. Errors may arise if: (a) different areas of the grating or prism are illuminated; (b) different areas of the photomultiplier photocathode are illuminated; or (c) if the calibration curve depends on the plane of polarization of the light.

B. Tungsten Lamp Calibration

Vavilov [33], one of the first to measure a corrected fluorescense spectrum, made visual spectrometric comparisons between the output of a tungsten lamp of known color temperature and the radiant flux from a fluorescent solution. The greatest source of error in the use of tungsten lamps appears to be the uncertainty in the spectral emissivity ($\epsilon(\lambda)$) of tungsten. To overcome this error, Stair et al. [24] at the National Bureau of Standards, Washington, D.C., individually calibrate tungsten strip lamps against a high temperature black body, and it is probable that these lamps (type U90) are the most accurate spectral radiant sources presently available. The uncertainty in output ranges from a maximum of 8 percent at short wavelengths to 3 percent at long wavelengths [24]. A description of the use of a standard tungsten lamp is given by Christiansen and Ames [25]. Certain precautions must be taken in the use of standard tungsten lamps. The lamp housing dimensions, the position and the current used must be precisely as specified and the radiance must be taken normal to the tungsten strip from a small area in the middle.

The output of tungsten lamps is very low in the near UV region and care must be taken to correct for stray light by the filter subtraction method [25]. We have found in practice that it is not possible to use the NBS standard lamp below about 340 nm when calibrating a single grating monochromator and photomultiplier, owing to excessive stray light.

A good standard lamp, such as the NBS type U90 is expensive, difficult to use and has a limited lifetime. The usual practice is to compare the standard lamp against an inexpensive lamp which is used as a secondary standard. Such lamps are commercially available. Care must be taken with secondary standards that errors are not introduced by reflections from the glass envelope. Lippert et al. [5] made a secondary standard lamp which was filled with argon and backed by a horn-shaped absorber of the sort used in Raman spectroscopy.

C. Calibrated Emission Monochromator

The idea of taking a xenon lamp and monochromator and measuring the radiant flux from the exit slit in order to calibrate a monochromator and photomultiplier appears to have first been advanced by White et al. [26]. They used fluorescein in NaOH to detect the number of quanta s^{-1} emerging from the mono-

chromator over the wavelength range 250 to 300 nm. Melhuish [27] and Parker [28] describe the method in more detail. Since the accuracy of the method depends primarily on the detector used to measure the radiant flux, we will discuss detectors in more detail below (Sec. IV, D). A fixed fraction of the flux from the exit beam of the exciting monochromator is reflected [27] or scattered [28] into the analyzing monochromator and the photomultiplier current measured at each wavelength. Eastman [29] scatters the light into the analyzing monochromator with colloidal silica (Ludox) in order to have a geometry close to what will be used when measuring fluorescence spectra. In calculating the correction factor, $S(\tilde{\nu})$, it is important to allow for the wavelength dependence of the scatterer and the transmission characteristics of the quantum counter window and any beam splitters used in the optical system. For the apparatus used in this laboratory (fig. 4c),

$$S(\tilde{\nu}) = \frac{\varphi_q(\tilde{\nu})M(\tilde{\nu})W_1(\tilde{\nu})}{W_2(\tilde{\nu})\int_0^\infty R(\tilde{\nu})d\tilde{\nu}}$$

where $\varphi_q(\tilde{\nu})$ = relative number quanta s^{-1} observed by the detector
$M(\tilde{\nu})$ = reflectivity of scatterer
$W_1(\tilde{\nu})$ = transmittance of the quartz beam splitter
$W_2(\tilde{\nu})$ = transmittance of the quantum counter window
$R(\tilde{\nu})$ = recorder deflection

Equation (2) is strictly valid only if $S(\tilde{\nu})$ is constant over the bandwidth of slit used in the analyzing monochromator, typically 4 to 6 nm. A preliminary calibration is made using equation (2) to determine $S(\tilde{\nu})$. The correct calibration factor is then calculated from

$$S_{\text{corr.}}(\tilde{\nu}) = \frac{\varphi_q(\tilde{\nu})M(\tilde{\nu})W_1(\tilde{\nu})}{W_2(\tilde{\nu})\int_0^\infty [S(\tilde{\nu}_0)/S(\tilde{\nu})]R(\tilde{\nu})d\tilde{\nu}} \quad (3)$$

where $S(\tilde{\nu}_0)$ is the correction factor at the center of the scanned band. $S_{\text{corr.}}(\tilde{\nu})$ will usually differ from $S(\tilde{\nu})$ by not more than 2 or 3 percent, except in the region of 700 to 800 nm where the photomultiplier sensitivity changes very rapidly with wavelength. This procedure allows one to choose any slit width for the excitation and analyzing monochromator and is the most reliable method to use. Very little error is introduced if peak heights instead of $\int_0^\infty R(\tilde{\nu})d\tilde{\nu}$ are measured provided, (a) the bandwidth of the light leaving the excitation monochromator is 4 or 5 times less than the bandwidth of the analyzing monochromator and, (b) $S(\tilde{\nu})$ does not change rapidly over the bandwidth defined by the slit of the analyzing monochromator. Calibration by measuring peak height was used by Melhuish [27] and Parker [28], a procedure which was justified because $S(\tilde{\nu})$ did not change rapidly with wavelength over the wavelength range investigated.

It has been pointed out by Børresen and Parker [30] that any silica focusing lenses in the excitation monochromator system can cause calibration errors because a constant area of the scatterer receives varying amounts of the exciting flux depending on the wavelength, while the quantum counter measures the total photon flux in the beam.

The accuracy of this method of calibration rests on the accuracy of the response of the detector measuring $\varphi_q(\tilde{\nu})$ (Sec. IV, D) and on the accuracy to which the spectral reflectivity factor $M(\tilde{\nu})$ is known. Aluminum films were used in the calibration technique described previously [27] because if these are prepared by rapid evaporation at low pressure, the reflectivity is constant over a wide wavelength range [31]. The reflectivity of magnesium oxide seems to be less well known. Values published by Benford, Schwartz and Lloyd [32] were obtained using an integrating sphere. Multiple scattering in the sphere could result in a lower reflectivity at some wavelengths, than for a single scattering. We have recently found that the spectral reflectivity of fresh MgO (1 mm thick) to be the same as a freshly deposited aluminum film to within ± 1.5 percent from 340 to 800 nm (fig. 5). There was a slight decrease (~ 3 percent) at 300 nm, the shortest wavelength investigated. Good values of $M(\tilde{\nu})$ for single scattering from MgO are clearly needed, especially since the MgO scatterer is used in the determination of absolute quantum efficiencies of fluorescence [43].

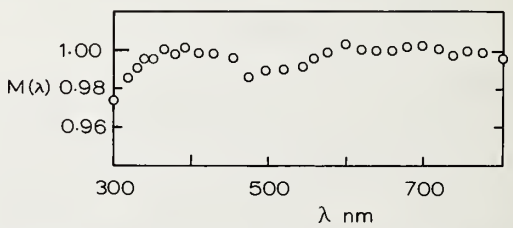

FIGURE 5. Reflectivity ($M(\lambda)$) of freshly deposited MgO versus a fresh rapidly deposited aluminum surface.

D. Detectors

The calibration of the emission monochromator by measuring the energy of quanta s^{-1} from the exit beam requires a detector with an accurately known spectral response. Three detectors have been used for this and each of these will be critically examined.

(1) Thermopiles: These detectors are coated with a layer which absorbs the radiation, causing the heating of a number of thermopiles. The thermoelectric current must be amplified with a high gain, low drift current amplifier. Thermopiles are generally compensated for changes in ambient temperature, but warm objects, such as the human body or a hot lamp housing, can cause changes in output. The absorbing coating on

thermopiles (lamp black or blackened gold) is often assumed to absorb all UV, visible and infrared light, but this is not true. The reflectivity of lamp black is known to increase in the UV region and so for a properly calibrated thermopile, the reflectivity of the actual coating on the junctions ought to be measured. The response curves of three thermopiles measured by Christiansen and Ames [25] differ considerably from each other (40–80 percent at 250 nm) so that it cannot be assumed that all thermopiles have a constant sensitivity over a wide wavelength range. The chief disadvantage of the thermopile is its low sensitivity. The measurement of the output of the emission monochromator becomes very difficult as a result of the narrow bandwidth required (1 to 3 nm) for calibration of the analyzing monochromator and photomultiplier. The wide wavelength response of a thermopile might actually be a disadvantage since stray infrared energy in the beam would also be detected. White et al. [26] and Rosen and Edelman [21] have used thermopiles for calibration purposes on the assumption of the flat energy response.

(2) Quantum Counters: Early investigations by Vavilov [33] showed that the energy efficiency of many dyes in solution was approximately proportional to the exciting wavelength (i.e. φ_f independent of λ) except near the absorption maximum. Further work by Anderson and Bird [34], Harrison and Leighton [35] and Bowen [36] showed that for many dyes, φ_f was independent of wavelength over a wide range and that such solutions could, therefore, be used to determine quanta s^{-1} in the UV and visible region by measuring the fluorescent flux from a fairly concentrated solution of the dye. Rhodamine B (4 g/l in ethylene glycol) was first tested and used as a wide range quantum counter by Melhuish [37]. An important innovation of this new quantum counter was to move the photomultiplier so that no directly transmitted light could be detected. It was now possible to reliably measure the quanta s^{-1} in a broad fluorescence band even if the tail of the band extended beyond 600 nm. The preferred geometry for a quantum counter is that of Parker [38] which not only avoids errors from directly transmitted light, but uses the full thickness of the quantum counter as a filter (fig. 4c). By comparing the rhodamine B quantum counter with a thermopile [27, 39] it has been shown that the response of the quantum counter is constant to within about ± 5 percent from 220 to 600 nm. Deviations which are observed may in fact be due to the thermopile and not the quantum counter [27]. Another method of testing a quantum counter is to use one for measuring excitation spectra. For an ideal quantum counter, the excitation spectrum should agree with the absorption spectrum, provided that φ_f is independent of λ and the OD of the fluorescent solution being measured does not exceed 0.05. A series of substances may be selected to cover a wide wavelength range and by limiting the excitation range to only one electronic band, the probability that φ_f changes with wavelength is reduced. Figure 6a shows the percent deviation of the excitation spectrum from the absorption spectrum for solutions of 2 aminopyridine, quinine, 3 aminophthalimide, proflavine, fluorescein, rhodamine B and methylene blue using a rhodamine B quantum counter in the apparatus shown in figure 6b. Solutions were freshly prepared since deterioration occurred when the solutions were exposed to light. The φ_f of quinine in 1 N H_2SO_4, for example, was 25 percent too low at 310 nm if left for three days in the light. The dashed line in figure 6a shows the comparison of a thermopile with the rhodamine B quantum counter [27].

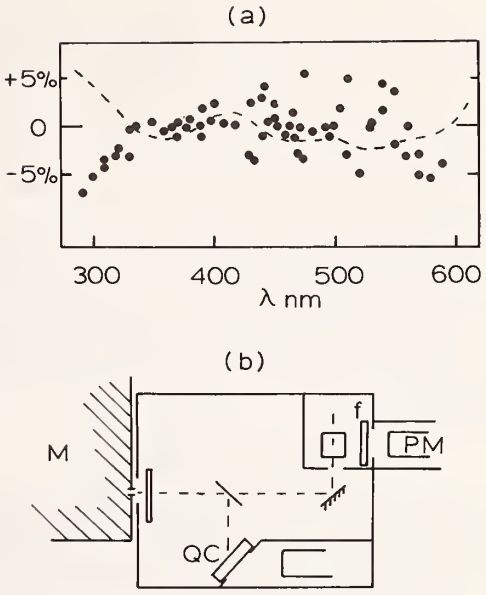

FIGURE 6. (a) Deviation of excitation spectra from absorption spectra (±3%).
(b) Apparatus for measuring excitation spectra.

Methylene blue has been used as a quantum counter by Seely [40]. A 1.5 g/l solution of methylene blue in ethylene glycol can be used from 520 to 700 nm, but it is about 50 times less sensitive than the rhodamine B quantum counter when both are used with an S–20 photomultiplier.

The advantage of the quantum counter over the thermopile is its high sensitivity. Moreover, if several different fluorescent compounds are used as quantum counters, all of which give the same response, we can be reasonably assured that we are actually measuring the quanta s^{-1} in the beam. The apparatus needed for calibrating an analyzing monochromator and photomultiplier using a quantum counter is illustrated in figure 4c. The excitation monochromator has a bandwidth of 1 to 2 nm and the analyzing monochromator a bandwidth of 4 to 8 nm. A filter cutting off at 350 nm is inserted at f (fig. 4c) when calibrating between 400 and 700 nm. The outputs from the amplifier connected to the quantum counter and the photomultiplier amplifier are fed to a ratio recorder. It is important to refer back to a particular wavelength from time to time, to correct for drift in the system.

(3) Actinometers: At least one author [26] has calibrated the output of an emission monochromator using the uranyl oxalate actinometer. The quantum yield of the more sensitive ferrioxalate actinometer has been measured as a function of wavelength by Parker and Hatchard [42] and could probably be used for calibration, although long exposure times would still be required. The wavelength response of the actinometer is not constant and its yield at different wavelengths must be measured against a detector such as the thermopile. Thus, the accuracy of the yield versus wavelength of the actinometer can be no better than the thermopile, which, as we have seen above, may not be very well known especially in the UV region.

E. Polarization Effects

The transmission of a grating monochromator depends on the direction of polarization of light incident on the entrance slit. Thus the correction factor, $S(\tilde{\nu})$, which has been measured for completely unpolarized light will not apply to plane polarized light. Figure 7 shows the correction curves for a Jarrell-Ash 1/4 meter monochromator (blaze = 600 nm) and a 9698–QB (S–20) photomultiplier. If the fluorescence spectrum being measured is not completely depolarized the correction factor $S(\tilde{\nu})$ obtained for unpolarized light cannot be used for correcting the spectrum. The true spectrum might be obtained using a polarizer at the entrance slit of the analyzing monochromator and recording $\parallel$ and $\perp$ spectra, correcting each by the appropriate $S(\tilde{\nu})$ curve and adding. It is also important to recognise that the $S(\tilde{\nu})$ depends on the plane of polarization when investigating polarization of emission spectra using a grating monochromator.

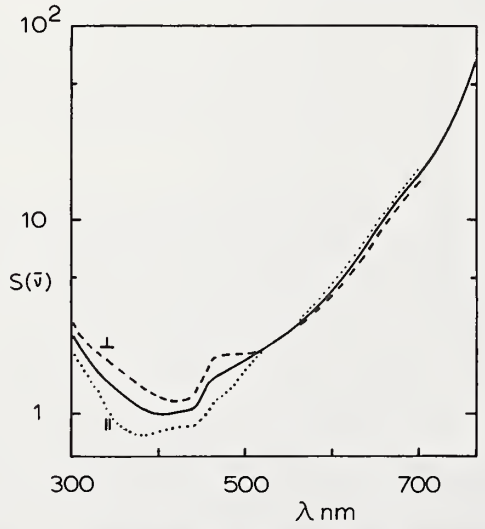

FIGURE 7. Correction curves $[S(\tilde{\nu})]$ for a grating monochromator and photomultiplier ——— = unpolarized light, ····· = polarization $\parallel$ to grating rulings, - - - - - - = polarization $\perp$ to grating rulings.

The light from the exit slit of a grating monochromator is also polarized to some extent, the degree of polarization varying with the wavelength setting. Hence, in using this light to calibrate an analyzing monochromator as described in Section IV, C, it is important to depolarize the light by scattering off a magnesium oxide scatterer. The use of an aluminum reflector can sometimes give errors of 10 percent or more and, therefore, should not be used.

V. Methods of Measuring Spectra

A. Dilute Solutions

When the absorption spectrum overlaps the fluorescence spectrum, a true fluorescence spectrum, free from reabsorption effects, can only be obtained in dilute solution. It is important that the cell be blackened with matt black paint on three sides, if observation is from the front surface, or two sides, if viewed from the side. The use of side viewing reduces stray exciting light which is particularly important if the exciting wavelength is within the emission band. Stray light is due to the following causes:

(a) fluorescence of the solvent and cell material
(b) Raman and Rayleigh scattering by the solvent molecules
(c) scattering of light at interfaces or from dust in the solution.

Stray exciting light can often be reduced by filtering the solution to remove solid particles and this should be done as normal practice. Sometimes it is possible to choose a light filter which prevents stray exciting light from reaching the inlet slit of the analyzing monochromator, but does not absorb any of the fluorescence. Stray background light should always be checked after the measurement of the fluorescence spectrum by filling the cell with clean solvent and rescanning. Any stray light is then subtracted from the observed fluorescence spectrum.

Most spectrofluorometers measure fluorescence emitted at right angles to the exciting beam (SV mode). The decrease of fluorescence in these instruments as the concentration of the fluorescence is increased, sometimes attributed to concentration quenching, is actually a geometric effect caused by a shift in the region of absorption in the cell towards the front surface where it cannot be seen. Thus, at high concentrations of solute, the fluorescence must be observed from the same side as the exciting light enters (FS mode). FS viewing may also be used for dilute solutions; in fact, more fluorescence can be collected by the analyzing monochromator than in the SV mode. However, stray exciting light scattered from the front face of the cell will be much larger than in the SV mode. We have found that a 5×10^{-6} M (3 parts per million) solution of quinine in H_2SO_4 excited at 365 nm to be the lowest concentration that can be used in the FS mode before stray light becomes excessive.

Before correcting the fluorescence spectrum it is important to see if the refractive index of the solvent varies over the emission band scanned since the amount of light entering the slit of the analyzing monochromator from the fluorescent solution is proportional to n^2. For a fluorescent solute in benzene, for example, the photon irradiance increases by 3 percent from 434 to 588 nm as a result of dispersion in liquid benzene.

B. Concentrated Solutions and Crystals

When the absorption coefficient of the sample for the exciting light is so high that absorption is virtually complete in the first millimeter or less of the sample, fluorescence must be observed from the front surface. The scattering of exciting light into the analyzing monochromator now becomes a problem, especially if the sample is multicrystalline. Furthermore, it is not usually possible to measure a blank for crystalline samples. Although the use of a double monochromator for analyzing the fluorescence helps, the only real solution is to use a sharp cutoff filter to remove the exciting light. If the fluorescence emission falls within the region where the filter absorbs, the transmission of the filter must be measured and the observed fluorescence spectrum corrected for absorption by the filter.

A more serious error arises from reabsorption of fluorescence if the absorption and fluorescence spectra overlap. This error can be corrected by making use of the equation for reabsorption of fluorescence for the special case of front surface viewing [43]. For highly absorbing solutions where shifts in the region of absorption can be neglected, this equation becomes

$$dB(\lambda') = A f(\lambda') d\lambda' \alpha_\lambda (1 + \varphi K' + \varphi^2 K'' + \ldots) \int_0^l \exp\left[-(\alpha_\lambda + \alpha_{\lambda'} x) z\right] dz \qquad (4)$$

where a prime refers to fluorescence, unprimed to the exciting light,

A = constant
$f(\lambda')$ = true (corrected) fluorescence spectrum
$dB(\lambda')$ = observed (corrected) fluorescence spectrum
$\alpha = 2.303\,\epsilon C$ where ϵ = molar extinction coefficient and C = molar concentration
x = sec $[\sin^{-1}(\sin \theta/n)]$ where θ = angle between the exciting beam ($\perp$ to the cell face) and the observing beam and n = refractive index of the solvent
l = thickness of the cell
z = distance from the front face
$K', K'', \ldots$ = reabsorption-emission factor [43]
φ = absolute quantum efficiency of fluorescence.

Equation (4) can be simplified further if absorption of the exciting light is sufficiently high that

$$\exp -(\alpha_\lambda + \alpha_{\lambda'} x) \ll 1$$

and it is assumed that all the K factors are equal. Then

$$dB(\lambda') = [A/(1-\varphi K)][\alpha_\lambda/(\alpha_\lambda + \alpha_{\lambda'} x)] f(\lambda')\, d\lambda'. \qquad (5)$$

Since the first term in square brackets is independent of λ, the observed spectrum $dB(\lambda')$ may be corrected by multiplying by $(\alpha_\lambda + \alpha_{\lambda'} x)/\alpha_\lambda$ at each wavelength.

Perylene in ethanol has a large overlap between absorption and fluorescence spectra and this compound has been used to test eq (5). The fluorescence spectra of 5×10^{-4} M and 10^{-6} M solutions of perylene in a 10 mm cell is shown in figure 8. The solution was excited and observed from the front surface. The spectrum was corrected using the rhodamine B quantum counter method (Sec. IV, C and D) using an MgO scatterer. The cell was blackened on 3 sides and corrections were made for stray light with solvent in the cell. The bandwidth of the analyzing monochromator was 1.5 nm. The spectrum of the 5×10^{-4} M solution, when corrected by eq (5) (Open circles, fig. 8) agrees well with the 10^{-6} M spectrum.

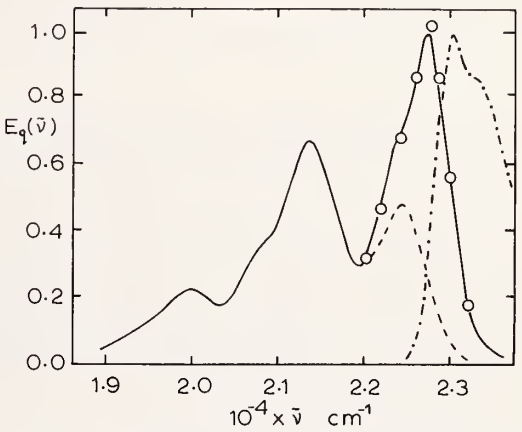

FIGURE 8. Fluorescence spectra of perylene in ethanol, $\lambda_e = 365$ nm, FS. ——— $= 10^{-6}$ M, - - - - - $= 5 \times 10^{-4}$ M, - · - · - · = absorption spectrum.

By using a very thin cell and choosing an excitation wavelength where α_λ is as large as possible, the reabsorption effect can be minimised. Thus, 5×10^{-4} M perylene in a 0.2 mm-cell when excited at 404 nm gives a fluorescence spectrum almost identical ($\pm 3\%$) with the 10^{-6} M spectrum in the 1-cm cell.

C. Narrow Bands

The measurement of a fluorescence spectrum with narrow bands require narrow slits and a slow scanning speed. As a rough guide to the settings needed to record a spectrum without significant error, we may use

the equation of Petrash [44] which states that the error in a recorded band of Gaussian or dispersion shape is approximately proportional to

$$(\gamma^{-5} d\lambda/dt)^{4/9} \tag{6}$$

where $d\lambda/dt$ = scan rate and γ = half-line width. Thus, if the time constant of the spectrofluorometer is adjusted so that the error in the recording is no greater than 1 percent, the scanning rate would have to be reduced nearly 100 times to record a band of one-tenth the width with the same accuracy. An incorrect setting of scanning rate or time constant is easily observed by stopping the scan on the steeply rising part of the band and observing any subsequent movement of the pen to a higher reading.

D. Reporting Corrected Fluorescence Spectra

The most useful fluorescence spectrum for publication is one measured in very dilute solution where errors due to reabsorption of fluorescence are negligible. However, there are several other factors which could influence the shape of the spectrum and, therefore, the author should give a complete description of the measuring conditions. These are listed below (see Ref. 3). Conditions (a) to (d) are the most important, but the complete list should be given if the spectrum is suggested as a standard.

(a) If a standard tungsten lamp is used for calibration, describe the origin and the accuracy of its spectral distribution. Were corrections made for scatter in the monochromator? (See Sec. IV, B.)
(b) If a standard fluorescent substance is used, give the author and list the factors (d) to (m) below.
(c) If a quantum counter, thermopile or actinometer is used for calibration, give full details of the detector. Describe the system used with particular reference to the spectral reflectance of the scatterer used.
(d) Clearly state the units used for the fluorescence flux; $E_q(\tilde{\nu})$ = quanta s^{-1} per unit wave number interval is preferred.
(e) Were corrections made for stray background light using the pure solvent? (See Sec. V, A.)
(f) State the geometry of the apparatus, whether front surface or side viewing and the dimensions of the cell.
(g) Give the bandwidth of the analyzing monochromator.
(h) The source, purity and concentration of solute should be stated.
(i) The solvent used and method of purification should be noted.
(j) The temperature should be given.
(k) Was the cell blackened on any of its faces?
(l) State the excitation wavelength and its spectral purity.
(m) Give φ_f, if known.

Some commercial spectrofluorometers record absolute fluorescence spectra. It is important to know what units are used for the fluorescence flux and convert to quanta s^{-1} per unit wave number interval, if necessary. These instruments use thermopiles or correction cams in order to automatically correct the emission spectrum and their accuracy is, therefore, uncertain. In reporting fluorescence spectra obtained with these instruments, it would seem desirable to include the spectrum of one or more standards.

E. Future Developments

If the time comes when there are a sufficient number of precisely known standards covering a wide wavelength range, a double beam spectrofluorometer, which takes the ratio of the fluorescence fluxes of the unknown and standard at such wavelength, would overcome the necessity of calibrating the analyzing monochromator and detector. If the observed ratio of unknown to the standard at the frequency is $R(\tilde{\nu})$, then

$$Eq\ (\tilde{\nu})_x = Eq\ (\tilde{\nu})_s \times R(\tilde{\nu})$$

where subscript x = unknown, and s = standard.

Lippert et al. [5] describe a double beam spectrofluorometer of this design using a 13 Hz chopping frequency. The advantage of a double beam system is that fluctuation in the exciting light or in the gain of the photomultiplier does not influence the recorded spectrum.

VI. Standards

A. Introduction

An absolute emission standard is ideally one which satisfies the following criteria:

(a) Broad wavelength range with no fine structure
(b) Small overlap between absorption and fluorescence spectra
(c) Easily obtained and purified
(d) Stable
(e) High φ_f
(f) Spectrum independent of exciting wavelength
(g) Clear, free from scattering centers
(h) Completely depolarized emission.

A standard with a broad emission band with no peaks is important so that the spectrum does not depend on the resolution of the analyzing monochromator. A high φ_f and a reasonably high OD at the exciting wavelength are both important to reduce errors due to stray light (Sec. V, A). A number of absolute standards have been proposed, notably by Lippert et al. [5], but the quinine spectrum is the only one measured by a number of authors. The new standard 2-amino pyridine proposed by Rusakowicz and Testa [45] covers approximately the same wavelength range as 2-naphthol and is to be preferred since it does not have the temperature effects shown by the latter.

The effect of reabsorption of fluorescence on the emission spectrum has been discussed in Section V, B. Although standards should be measured in very dilute solution where reabsorption has no effect, sometimes spectra are determined at high concentrations. It is important, therefore, to have some idea of what region of the standard spectrum might be affected by reabsorption. The upper limit of the error due to reabsorption is given by eq (5). The term $A=\alpha_\lambda/(\alpha_\lambda+\alpha_{\lambda'}x)$ has been included in tables 1 to 5 to show the wave number region where reabsorption errors can be expected.

B. Individual Standards

1. Quinine in sulfuric acid (fig. 9). Table 1 lists the determination since 1941 of the absolute fluorescence spectrum of quinine. Many of these figures have been taken from rather small diagrams and are therefore not accurate to better than ± 3 percent. All spectra have been converted to $E_q(\tilde{\nu})$ spectra using the appropriate conversion factors.

We have found that for a 10^{-4} M solution of quinine viewed from the FS, the spectrum is unaffected by: (a) varying the sulfuric acid concentration from 0.1 to 2 N, (b) varying the exciting wavelength from 260 to 390 nm, (c) measuring three different brands of quinine. Thus the differences between the published quinine spectra are almost certainly due to calibration errors. The largest deviations are found for those spectra determined from a tungsten lamp calibration.

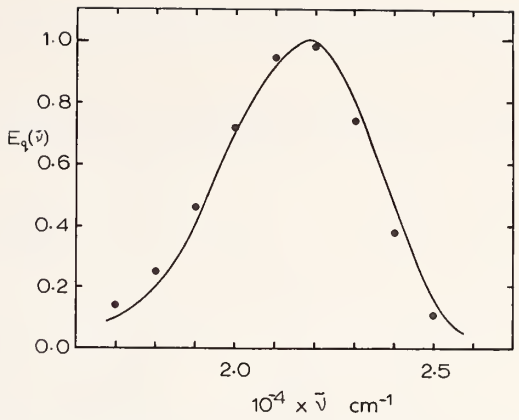

FIGURE 9. Quinine, 10^{-4} M in N H_2SO_4 (25 °C, $\lambda_e = 365$ nm). ● = Lippert [5].

TABLE 1. Absolute fluorescence spectrum of quinine in H_2SO_4 ($\lambda_e = 365$ nm)

$10^{-3}\times\tilde{\nu}$ cm^{-1}	A[a]	$E_q(\tilde{\nu})$										
25	0.95	0.07	0.105	0.105	0.135	0.105	0.15	0.10	0.16	0.14	0.15	0.152
24	.98	.36	.43	.375	.37	.375	.46	.37	.47	.46	.49	.480
23	1.00	.78	.80	.740	.79	.74	.80	.78	.80	.78	.83	.810
22		.99	.99	.980	.99	.98	1.00	.99	.99	.99	.99	1.00
21		.92	.91	.950	.92	.97	0.92	.97	.92	.97	.93	0.915
20		.56	.67	.715	.68	.75	.70	.74	.70	.77	.70	.710
19		.35	.40	.460	.40	.47	.42	.41	.42	.51	.42	.405
18		.20	.215	.240	.20	.26	.21	.21	.24	.26	.21	.200
17		.....	.104	.140	.09	.16	.10	.....	.11	.11	.08	.095
Ref.		47	6	5	48	7	27	21	46	29	22	41
Solvent		2N	2N	0.1N	0.1N	1N	1N	1N	0.5N	0.1N	.....	1N
Mode		*FS*	*FS*	*FS*	*SV*	*FS*	*SV*	*SV*	*SV*	*SV*	*SV*	*FS*
Conc(M)		10^{-5}	10^{-5}	10^{-3}	2×10^{-6}	5×10^{-3}	2×10^{-6}	10^{-5}	2×10^{-5}	.....	.....	10^{-4}
Calibration[b]		*L*	*L*	*L*	*L*	*L*	*L*+*Q*	*T*	*Q*	*Q*	*Q*	*Q*

[a] $A=\alpha_\lambda/(\alpha_\lambda+\alpha_{\lambda'}x)$

[b] L = tungsten lamp calibration, Q = quantum counter calibration
T = thermopile calibration

2. 2-Naphthol (fig. 10). Lippert et al. [5] have published the absolute fluorescence spectrum of 2×10^{-4} M 2-naphthol in a 0.02 N, pH 4.62 acetate buffer at various temperatures. In using this standard, the temperature and the composition must be known, and the concentration and pH of the buffer must be exactly as specified by Lippert. Børresen [46] has published the absolute emission spectrum of a 10^{-4} M

solution of 2-naphthol using an instrument calibrated with the rhodamine B quantum counter. The results are given in table 2.

We have also checked the spectrum using the quantum counter method of calibration and found good agreement with Børresen's results, but rather poor agreement with Lippert.

3. 3-Amino phthalimide (fig. 11). A comparison of Lippert's spectrum with the absolute spectrum recently measured in this laboratory is given in table 3.

TABLE 2. Absolute fluorescence spectrum of 2-naphthol in 0.02 *N* acetate (pH 4.62 − 4.68) ($\lambda_e = 313$ nm)

$10^{-3}\times\tilde{\nu}$ cm^{-1}	A[a]	$E_q(\tilde{\nu})$						
30	0.51	0.220	0.380	0.220	0.36	0.370	0.220	0.345
29	.93	.860	.900	.860	.90	.900	.860	.930
28.5	.99	.980	.995	.980	.97	.980	.980	1.00
28	1.00	.980	.955	.980	.97	.970	.985	.950
27		.745	.680	.740	.71	.745	.750	.715
26		.625	.590	.620	.62	.628	.630	.620
25		.780	.800	.770	.72	.750	.790	.825
24		.915	.930	.900	.80	.842	.930	.895
23		.810	.785	.795	.65	.630	.825	.670
22		.550	.515	.535	.41	.390	.565	.405
21		.300	.245	.295	.22	.224	.305	.235
20		.140	.092	.135	.095	.125	.145	.135
Ref.		5	49	5	46	41	5	41
Temp. (°C)		24	24	23	22.7	22.7	25	25
Conc. (M)		2×10^{-4}	10^{-5}	2×10^{-4}	10^{-4}	5×10^{-5}	2×10^{-4}	5×10^{-5}
Mode		FS	SV	FS	SV	FS	FS	FS
Calibration[b]		L	$Q+L$	L	Q	Q	L	Q

[a] $A = \alpha_\lambda/(\alpha_\lambda + \alpha_{\lambda'}x)$

[b] L = tungsten lamp calibration. Q = quantum counter calibration

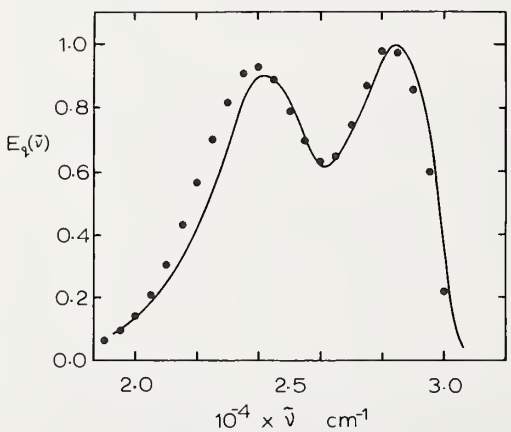

FIGURE 10. 2-Naphthol, 5×10^{-5} *M* in 0.02 *N* acetate, pH 4.62 (25 °C, $\lambda_e = 313$ nm). ● = Lippert [5].

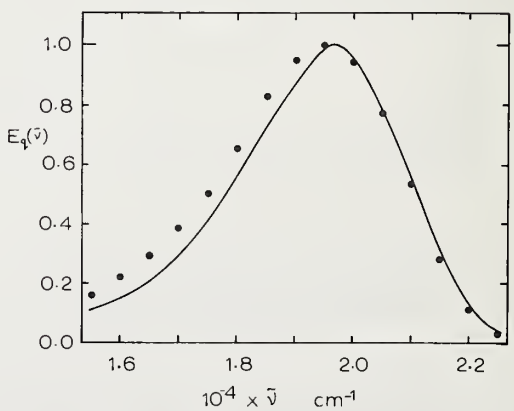

FIGURE 11. 3-Aminophthalimide, 2×10^{-4} *M* in *N* H_2SO_4 (25 °C, $\lambda_e = 365$ nm). ● = Lippert [5].

TABLE 3. Absolute fluorescence spectrum of 3-amino phthalimide in H_2SO_4 at 25 °C $\lambda_e = 365$ nm

$10^{-3} \times \tilde{\nu}$ cm^{-1}	A[a]	$E_q(\tilde{\nu})$	
23	0.97	0.01	—
22.5	.99	.03	0.04
22	1.00	.110	.125
21.5		.280	.308
21		.530	.560
20.5		.775	.790
20		.945	.955
19.5		1.000	.990
19		0.950	.875
18.5		.825	.725
18		.650	.565
17.5		.500	.402
17		.385	.290
16.5		.295	.207
16		.220	.151
15.5		.160	—
Ref.		5	41
Conc. (M)		5×10^{-4}	2×10^{-4}
Mode		FS	FS
Solvent		0.1 N	1 N
Calibration[b]		L	Q

[a] $A = \alpha_\lambda / (\alpha_\lambda + \alpha_{\lambda'} x)$

[b] L = tungsten lamp calibration, Q = quantum counter calibration

4. *m*-Dimethylamino nitrobenzene (DNB) (fig. 12). Lippert et al. [5] measured the absolute emission spectrum of DNB in 30 percent benzene and 70 percent hexane. Table 4 compares this spectrum with the one measured in this laboratory. The spectrofluorometer was calibrated with rhodamine B and methylene blue quantum counters. A disadvantage of this standard is its low φ_f and this, coupled with the fact that the instrumental sensitivity is decreasing in the region of the emission spectrum, results in a poor signal-to-noise ratio.

TABLE 4. Absolute fluorescence spectrum of *m*-dimethylamino nitrobenzene at 25 °C in 30 percent benzene, 70 percent hexane ($\lambda_e = 365$ nm)

$10^{-3} \times \tilde{\nu}$ cm^{-1}	A[a]	$E_q(\tilde{\nu})$	
22	0.93	0.03	0.10
21	.98	.235	.41
20	1.00	.610	.80
19		.935	1.00
18		.975	0.86
17		.825	.68
16		.615	.48
15		.405	.31
14		.235	.17
13		.110	—
Ref.		5	41
Conc. (M)		10^{-4}	5×10^{-4}
Mode		FS	FS
Calibration[b]		L	Q

[a] $A = \alpha_\lambda / (\alpha_\lambda + \alpha_{\lambda'} x)$

[b] L = tungsten lamp calibration, Q = quantum counter calibration

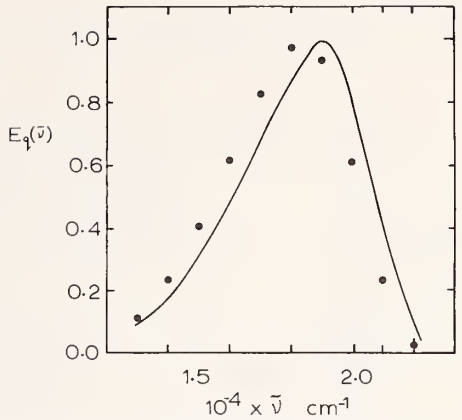

FIGURE 12. *m*-Dimethylamino-nitrobenzene, 5×10^{-4} M in 30 percent benzene, 70 percent hexane (25 °C, $\lambda_e = 365$ nm). ● = Lippert [5].

5. 2-Aminopyridine (fig. 13). The corrected fluorescence spectrum of 2-aminopyridine determined by Rusakowicz and Testa [45] using a tungsten lamp for calibration is given in table 5. The spectrum measured

TABLE 5. Absolute fluorescence spectrum of 2-aminopyridine in H_2SO_4 at 25 °C

$10^{-3} \times \tilde{\nu}$ cm^{-1}	A[a]	$E_q(\tilde{\nu})$	
31	0.64	0.03	0.05
30.5	.82		.145
30	.94	.17	.325
29.5	.97		.540
29	1.00	.575	.686
28.5			.840
28		.93	.960
27.5			1.000
27		.99	0.980
26.5			.920
26		.805	.790
25.5			.660
25		.52	.530
24.5			.405
24		.26	.310
23.5			.222
23		.138	.148
22.5			.102
22		.068	.075
Ref.		45	41
Solvent		0.1 N	1 N
Conc.		10^{-5}	10^{-5}
Mode		SV	FS
Calibration[b]		L	Q
λ_e nm		285	313

[a] $A = \alpha_\lambda / (\alpha_\lambda + \alpha_{\lambda'} x)$

[b] L = tungsten lamp calibration, Q = quantum counter calibration

in this laboratory using the quantum counter method of calibration is in good agreement with their spectrum.

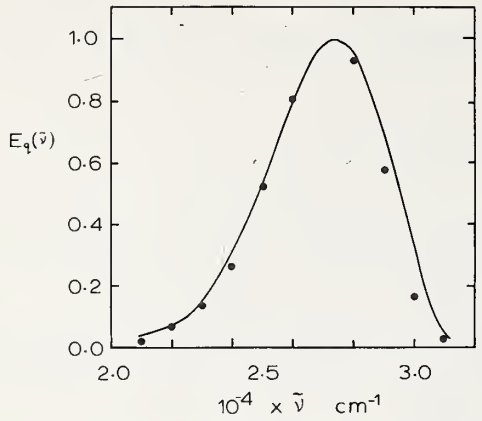

FIGURE 13. 2-Aminopyridine, 10^{-5} M in N H_2SO_4 (25 °C, $\lambda_e = 313$ nm). ● = Rusakowicz and Testa [45].

C. New Standards

The greatest lack, at present, is for standards in the ultraviolet and near infrared regions of the spectrum. Reisfeld et al. [50] recommend thallium activated potassium chloride as an emission standard in the UV region. For the red and near infrared regions, rhodamine B and methylene blue might be used since these substances have a high φ_f. Preliminary measurements in this laboratory (fig. 14) indicate that these two would cover the range 18,000 to 12,000 cm^{-1}.

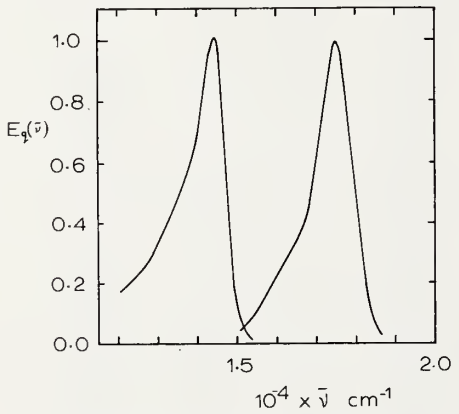

FIGURE 14. Rhodamine B, 5×10^{-6} M and methylene blue, 5×10^{-5} M in ethanol (25 °C, $\lambda_e = 436$ nm).

VII. References

[1] Birks, J. B., Photophysics' of Aromatic Molecules (John Wiley and Sons, Inc., New York, N.Y., 1970).

[2] Parker, C. A., Photoluminescence of Solutions (Elsevier, New York, N.Y., 1968).

[3] Chapman, J. H., Förster, Th., Kortüm, G., Lippert, E., Melhuish, W. H., Nebbia, G., Parker, C. A., Phot. Soc. Group Bull. No. 14, 378 (1962), Appl. Spectroscopy **17**, 171 (1963); Z. Anal. Chem. **197**, 431 (1963).

[4] Demas, J. N., and Crosby, G. A., J. Phys. Chem. **75**, 991 (1971).

[5] Lippert, E., Nagele, W., Seibold-Blankenstein, I., Staiger, W., Voss, W., Z. Anal. Chem. **170**, 1 (1959).

[6] Kortüm, G., and Hess, W., Z. Phys. Chem. NF **19**, 9 (1959).

[7] Melhuish, W. H., J. Phys. Chem. **64**, 762 (1960).

[8] Muray, J. J., Nicodemus, F. E., Wunderman, I., Appl. Opt. **10**, 1465 (1971).

[9] Ejder, E., J. Opt. Soc. Amer., **59**, 223 (1969).

[10] Bennett, H. F., and McBride, W. R., Appl. Opt. **3**, 919 (1964).

[11] Kortüm, G., Kolorimetrie, Photometrie u. Spektrometrie 4th ed. (1962) (Springer-Verlag, Berlin, 1955).

[12] Mitteldorf, J. J., and Landon, D. O., Appl. Opt. **7**, 1431 (1968).

[13] Pribram, J. K., and Penchina, C. M., Appl. Opt. **7**, 2005 (1968).

[14] Fisher, R., Appl. Opt. **7**, 1079 (1968).

[15] Weinberger, R. G., Elect. Aug. 30, 58 (1971).

[16] Akins, D. L., Schwartz, S. E., Bradley-Moore, C., Rev. Sci. Instrum. **39**, 715 (1968).

[17] Lampton, M., and Primbsch, J. H., Rev. Scient. Instr. **42**, 731, (1971).

[18] Jones, R., Oliver, C. J., and Pike, E. R., Appl. Opt. **10**, 1673 (1971).

[19] Haugen, C. R., and Marcus, R. J., Appl. Opt. **3**, 1049 (1964).

[20] Turner, G. K., Science **146**, 183 (1964).

[21] Rosen, P., and Edelman, G. M., Rev. Sci. Instrum. **36**, 809, (1968).

[22] Cundall, R. B., and Evans, G. B., J. Sci. Instr. (J. Phys. E.) **1**, 305 (1968).

[23] Lipsett, F. R., J. Opt. Soc. Amer. **49**, 673 (1959).

[24] Stair, R., Johnston, R. G., Hallbach, E. W., J. Res. Nat. Bur. Stand. (U.S.), **64A**, 291 (1960).

[25] Christiansen, R. L., and Ames, I., J. Opt. Soc. Amer. **51**, 224 (1961).

[26] White, C. E., Ho, M., Weimer, E., Anal. Chem. **32**, 438 (1960).

[27] Melhuish, W. H., J. Opt. Soc. Amer. **52**, 1256 (1962).

[28] Parker, C. A., Anal. Chem. **34**, 502 (1962).

[29] Eastman, J. W., Photochem. and Photobiol. **6**, 55 (1967).

[30] Børresen, H. C., and Parker, C. A., Anal. Chem. **38**, 1073 (1968).

[31] Hass, G., and Waylonis, J. E., J. Opt. Soc. Amer. **51**, 719 (1961).

[32] Benford, F., Schwartz, S., Lloyd, G. P., J. Opt. Soc. Amer. **38**, 964 (1948).

[33] Vavilov, S. I., Phil. Mag. **43**, 307 (1922); Z. Phys. **42**, 311 (1927).

[34] Anderson, W. T., Bird, L. F., Phys. Rev. **32**, 293 (1928).

[35] Harrison, G. R., Laighton, P. A., Phys. Rev. **38**, 899 (1931).

[36] Bowen, E. J., Proc. Roy. Soc. **154A**, 749 (1936).

[37] Melhuish, W. H., N.Z. J. Sci. and Tech. **37B**, 142 (1955).

[38] Parker, C. A., Nature **182**, 1002 (1958).

[39] Yguerabide, J., Rev. Scient. Instr. **39**, 1048 (1968).

[40] Seely, G. R., J. Phys. Chem. **73**, 125 (1969).

[41] Melhiush, W. H., unpublished. Apparatus used shown in figure 4a.

[42] Hatchard, G. G., Parker, C. A., Proc. Roy. Soc. **235A**, 518 (1956).

[43] Melhuish, W. H., J. Phys. Chem. **65**, 229 (1961).

[44] Petrash, C. G., Opt. and Spect. **6**, 516 (1959).

[45] Rusakowicz, R., and Testa, A. C., J. Phys. Chem. **72**, 2680 (1968).

[46] Borresen, H. C., Act. Chem. Scand. **19**, 2089 (1965).

[47] Kortüm, G., and Finckh, B., Spect. Act. **2**, 137 (1941).

[48] Parker, C. A., and Rees, W. T., Analyst **85**, 587 (1960).

[49] Unpublished (1962) using the apparatus in Ref. 27.

[50] Reisfeld, R., Honigbaum, A., and Velapoldi, R. A., J. Opt. Soc. Amer. **61**, 1422 (1971).

(Paper 76A6–741)

NATIONAL BUREAU OF STANDARDS SPECIAL PUBLICATION 378, Accuracy in Spectrophotometry and Luminescence Measurements, Proceedings of a Conference Held at NBS, Gaithersburg, Md., March 22–24, 1972 (Issued May 1973).

Absolute Quantum Efficiencies

G. A. Crosby*

Department of Chemistry, Washington State University, Pullman, Washington 99163

J. N. Demas

Department of Chemistry, University of Virginia, Charlottesville, Virginia 22901

and

J. B. Callis

Department of Chemistry, University of Washington, Seattle, Washington 98105

(July 11, 1972)

Recent developments in several areas of chemistry, laser technology, photodetector instrumentation, and calorimetry are surveyed, and their probable impact on the measurement of quantum yields is assessed. Chemical developments include: (a) synthesis and design of new luminescent molecules that could possibly serve as standards, (b) application of improved separation techniques to provide samples of extreme purity, and (c) advances in photochemistry that portend the development of wide-range chemical actinometers. The potential use of lasers in quantum-yield measurements and their advantages over conventional sources for application in both optical and calorimetric techniques are pointed out. New methods of quantum-yield measurements, based on the novel characteristics of laser pump sources, are suggested, including the feasibility of measuring yields under time-resolved conditions and of employing internal standards. The possible lifting of wavelength restrictions on both laser sources and detector devices and the implications of these developments for extending the spectral range of quantum-yield measurements are discussed. The current status of calorimetry for determining yields is surveyed, and the impact of recent technology on the feasibility of developing calorimetric methods competitive with optical methods is assessed.

Key words: Calorimetry in quantum yields; laser, use in quantum yields; photodetectors in quantum yields; quantum efficiencies.

I. Introduction

The explosive developments of science and technology in the last quarter century have been mirrored in the steady rise of optical methods in chemistry, physics, and biology. Today the use of fluorescence and phosphorescence in fundamental and applied investigations is routine. Initially focussed on frequency and relative intensity measurements, the effort during the last few years has begun to encompass determinations of efficiencies of large classes of luminescent materials. Such a measurement, the quantum-yield determination, is one step removed in difficulty from recording energy, measuring relative luminescence intensity, or monitoring rate of decay (at least for times beyond a microsecond) of excited species. The result is that developments in quantum-yield technology have lagged behind those in the other areas. Recently, however, the technological advances relevant to quantum-yield measurements and the increased interest in obtaining efficiencies signal that a comprehensive analysis should be carried out on the present needs for accurate quantum efficiencies and an assessment be made of the current developments in the methods of determining them.

The present article is not an attempt to review the field of quantum-yield measurements. Although considerable space is devoted to optical and calorimetric methods for determining yields, no attempt has been made to review these techniques adequately either. (For a comprehensive review of optical methods, see ref. [1].[1]) Rather the thrust of the present article is to point out a few of the obvious needs for accurate yield information, to note some of the current progress in

*Prepared during the tenure of AFOSR (NC)–OAR, USAF, Grant No. AFOSR–72–2207.

[1] Figures in brackets indicate the literature references at the end of this paper.

instrumentation technology and chemistry that may lead to better yield determinations, and to suggest a few avenues of investigation that appear ready for development. Our remarks are restricted mainly to solutions and rigid glasses. For readers interested in yields from solid materials, we direct them to the review article by Lipsett and to the original literature [2–10]. Gas phase determinations are also not discussed, although recent publications show that the field is expanding [11–13].

II. The Importance of the Quantum Efficiency

The luminescence quantum efficiency of a compound (Φ) is defined as the fraction of molecules that emit a photon after direct excitation by the source. The terms absolute yield, quantum yield, yield, and efficiency are all used interchangeably throughout this article.

Recent research developments in many areas of physical, chemical, and biological research have reached a stage where the lack of absolute quantum efficiencies is seriously hampering further progress. We enumerate here a few areas where such information could be decisive. In theoretical chemistry, studies of radiative and especially radiationless processes have been proliferating [14–18]. The role of various terms within the Hamiltonian (vibronic, spin-orbit) [19–22] and the effect of substituents on both radiative and radiationless rate constants of isolated molecules are under scrutiny [23–25]. The interactions of excited species with the host molecules in condensed phases are not well understood, but some information is beginning to accumulate [26, 27]. Reliable efficiencies are needed on many classes of molecules to test the predictions implicit in the formalisms and to unearth new problems.

An especially important fundamental problem concerns the limits of applicability of the Strickler-Berg equation [28] for obtaining radiative lifetimes of excited states from the inverse absorption processes [29]. Serious discrepancies exist between the measured natural radiative lives (τ_{0_m}), as obtained from the equation $\tau_{0_m} = \tau_f/\phi_f$ where τ_f is the fluorescence decay time and ϕ_f is the fluorescence quantum yield, and those calculated by the Strickler-Berg relation. These discrepancies exist for simple molecules (e.g., SO_2) [30] and for larger systems such as diphenylpolyenes [31]. The lifetimes can be anomalously long [32, 33] or anomalously short [34]. Large intermolecular [33] or intramolecular configurational changes [34] have been invoked to rationalize the results. More quantum efficiencies are required to quantify the experimental situation.

A second problem in the application of the Strickler-Berg equation involves the selection of degeneracy factors for upper (g_u) and lower (g_l) states involved in the transitions when application is made to formally forbidden transitions ($S \rightarrow T$). For hydrocarbons at the usual refrigerant temperatures ($\geq$ 50 K) a value of $g_u = 3$ is reasonable, since the level splitting is much smaller than kT and thermal equilibrium is established among the nearly isoenergetic levels. For systems where spin-orbit coupling is large, such as encountered in d–d [35] and charge-transfer [36, 37] excited states, the splittings may be comparable to or even greater than kT. Then measured quantum yields and lifetimes are expected to be temperature dependent, and the Strickler-Berg relation can only really be applied and tested after careful studies of temperature-dependent decay times [38] and quantum yields [39] have been carried out. Reliable quantum efficiencies for many model systems are needed.

Another area where reliable quantum efficiencies are lacking, and one where the role of experimental yields can be decisive, is in determining the effects of deuteration on the radiationless rate constants for degrading excitation energy. Theoretical classifications of radiationless processes according to "strong" and "weak" coupling limits have been made. In the first case, no important deuterium effects on radiationless rates are predicted; in the latter, large changes due to deuteration are expected [40]. Few systems have been studied experimentally to distinguish these coupling limits. It is manifest that major decisions about the relative importance of various mechanisms for fundamental radiationless processes could be made from quantum-yield comparisons of deuterated and nondeuterated molecules [41–43].

The present status of organic photochemical research also warrants the effort of measuring accurate luminescence yields. Particularly important is a knowledge of efficiencies for organic molecules that can be used as energy donors or acceptors in photosensitization experiments. Reliable yields on series of closely related molecules whose singlet or triplet states span important energy regions would aid substantially in the design of experiments to test mechanisms of energy transfer and to control photochemical products. The need for yields of organic systems is compounded by the fact that mixed solvents and unconventional pure solvents are sometimes necessary. Thus, the known efficiencies of compounds must be extrapolated into systems where conditions differ radically from those prevailing during the original determinations.

Not only total quantum yields, as defined initially, but yields from particular levels in molecules exhibiting multiple level luminescence are needed. Such quantities are of paramount importance for assessing relative quenching rates of excited singlet and triplet levels, for obtaining efficiencies of intersystem crossing, and for relating measured quantities to theoretically defined parameters. The processes associated with a typical organic system are illustrated in figure 1. In terms of the rate constants displayed on the figure, we can define: $\phi_f = k_f/(k_f + k_{q_f} + k_{is})$, $\phi_p = k_p/(k_p + k_{q_p})$, and $\phi_{is} = k_{is}/(k_{is} + k_f + k_{q_f})$. It is obvious that Φ, the total measured quantum yield as defined earlier, equals $\phi_f + \phi_p$ provided the only processes occurring after excitation are those depicted in the figure. It is also clear that the sum of ϕ_f and ϕ_{is} may or may not be unity depending upon the existence of singlet quench-

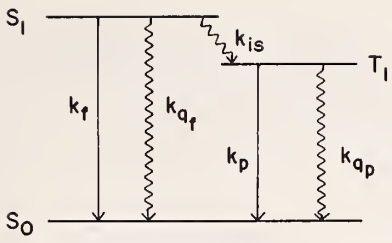

FIGURE 1. Principal pathways of degradation of an excited organic molecule. ⟶, radiative decay; ⇝, radiationless decay. k_f= radiative rate constant for depopulating S_1; k_{q_f}= radiationless rate constant for depopulating S_1; k_{is}= radiationless rate constant for converting from S_1 to T_1; k_p= radiative rate constant for depopulating T_1; k_{q_p}= radiationless rate constant for depopulating T_1. $k_f/(k_f+k_{q_f}+k_{is})=\phi_f$ (quantum yield of fluorescence from S_1). $k_p/(k_p+k_{q_p})=\phi_p$ (quantum yield of phosphorescence from T_1). $k_{is}/(k_{is}+k_f+k_{q_f})=\phi_{is}$ (quantum yield of intersystem crossing).

ing (k_{q_f}). A particularly important quantity is ϕ_{is}. It measures the efficiency of populating the triplet state, thus producing a reactive species responsible for many photochemical reactions and frequently serving as an efficient energy donor.

Several methods have been proposed to determine ϕ_{is} [44–51]. Different photophysical properties and processes have been utilized and ingenious techniques have been devised to extract ϕ_{is} from the data. Nonetheless, the methods rely eventually on the measurement of a photoluminescence quantum yield. A fundamental question raised by these measurements of intersystem crossing yields is whether the sum of $\phi_f+\phi_{is}$ is indeed unity. The equality has been shown to hold for a number of aromatics [52–57] and for porphin and its derivatives [58]. Exceptions abound, however, [59] and the experimental situation is still unclear [60]. Accurate and extensive quantum-yield measurements are necessary in order to establish or refute the stated equality as a fundamental (or rarely violated) law of luminescence. For pyrene, k_{f_q} is reported to be negligible at 77 K but competitive with k_f at room temperature [61].

The role of quantum-yield measurements in providing information on biologically important systems is expanding rapidly. Reports of quantum yields of naturally occurring bases [62] as functions of pH are providing insight into the possible fundamental physiological functions of these materials. Useful information on conformations and the nature of the excited states of biopolymers [63–65] has been provided from fluorescence measurements on oligonucleotides and polynucleotides containing fluorescent purine analogs. Some of the reported quantum yields are extremely low dictating new demands for accurate quantitative measurements at low light levels.

The real power and usefulness of fluorescent probes in biological systems are becoming appreciated. A typical example is 2-*p*-toluidinyl-6-naphthalenesulfonate (TNS), one of a series of compounds that are practically nonfluorescent in water but strongly fluorescent in organic solvents or when bound to protein molecules. This substance can be used as an extrinsic fluorescent chromophore for the study of protein conformations [66, 67], in the study of nitrogen antibody interactions [68], in following protein conformational changes produced by metal ion binding [69], and in elucidating enzyme activation processes [70]. In spite of its obvious importance it is significant that the mechanism by which the fluorescence of this molecule is changed by the medium is still not well understood. Spectroscopic studies, including detailed and accurate quantum-yield determinations, are of fundamental importance for molecules of this type and should be actively sought.

The need for quantum yields of inorganic molecules is also manifest and growing. Especially those materials classed as inorganic coordination compounds, usually containing some organic moieties, deserve considerable attention. This class of molecules, long utilized empirically in fluorescence metal analysis, has only relatively recently been recognized as providing candidates for electro-optical devices [71], for fundamental studies of radiative and radiationless transitions [35, 36], and for energy donors in inorganic photochemical studies [72]. The real possibility of engineering these molecules to have predetermined frequency ranges, high yields, and appropriate chemical properties [73] opens up a whole range of new experiments that were not possible just a few years ago. Needed, however, is detailed information on their spectroscopic properties, especially their absolute efficiencies, and the temperature dependences thereof. The near infrared region, virtually inaccessible at present to quantum-efficiency measurements can possibly be made accessible by the use of complexes possessing low-lying emitting levels, particularly those molecules displaying charge-transfer luminescence. Yet, few yields of these compounds have been measured, and none, to our knowledge, of compounds emitting beyond 800 nm.

We digress here to present some information on a few representative transition-metal complexes whose unique luminescence properties are not yet well recognized. Complexes of ruthenium(II), osmium(II), and iridium(III) with π-conjugated ligands display visible and near-UV absorption spectra dominated by strong charge-transfer absorption bands of high intensity ($2000 \leqslant \epsilon \leqslant 20{,}000$, where ϵ is the molar absorptivity) (figs. 2, 3, 4). In the case of osmium(II) complexes, the absorption bands extend well into the red region of the spectrum. Upon irradiation these molecules emit light with good efficiencies at low temperature ($>10\%$), and some are still reasonably efficient at room temperature in fluid solution. In figures 2 and 3 it is seen that the quantum yields are independent of wavelength, a property of fundamental and applied importance.

Other spectroscopic properties of interest of these molecules are evident in figure 4. One sees that each emission spectrum consists of a unique electronic band. This is a feature characteristic of all these systems at

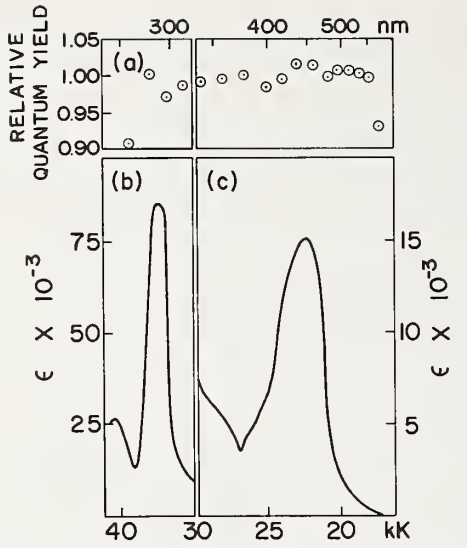

FIGURE 2. Relative quantum yield (a) and absorption spectrum (b, c) of tris(2,2′-bipyridine)ruthenium(II) chloride in methanol at room temperature: (a) 0.2 g/5 ml in a 1-cm cell, (b, c) 6.7×10^{-5} *M* in a 1-cm cell. The first and last yield points are less accurate than the others. [Ref: J. N. Demas and G. A. Crosby, J. Amer. Chem. Soc. **93**, 2841 (1971).]

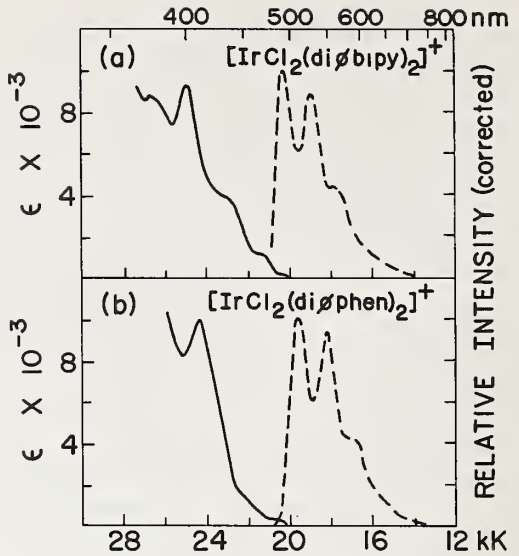

FIGURE 4. Absorption (———) and luminescence (- - -) spectra of phenyl-substituted iridium(III) complexes in ethanol-methanol glass (4 : 1, *v/v*) at 77 K. (a) *cis*-dichlorobis(4,4′-diphenyl-2,2′-bipyridine)-iridium(III) chloride, (b) *cis*-dichlorobis(4,7-diphenyl-1,10-phenanthroline)iridium(III) chloride. [Ref: R. J. Watts and G. A. Crosby, J. Amer. Chem. Soc. **94**, 2606 (1972).]

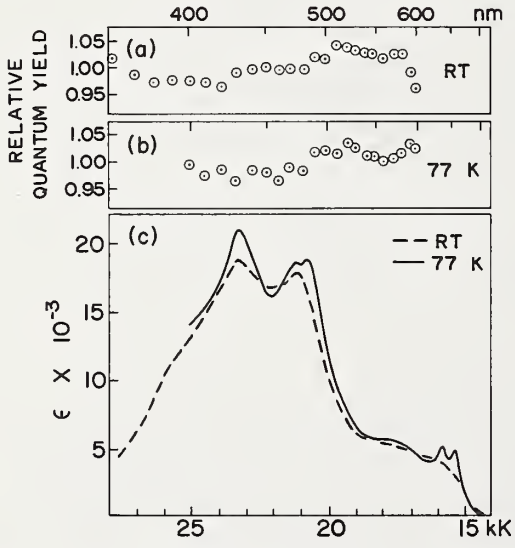

FIGURE 3. Relative quantum yields (a, b) and absorption spectra (c) or tris(1,10-phenanthroline)osmium(II) iodide in ethanol-methanol (4:1, *v/v*): (a) 4.5×10^{-7} *M* in a 1.76-cm cell at room temperature; (b) 4.5×10^{-7} *M* in a 1.76-cm cell at 77 K (glass); (c) - - -, 9.0×10^{-6} *M* in a 10-cm cell at room temperature; ———, 7.12×10^{-5} *M* and 1.42×10^{-5} *M* in 1.76-cm cells at 77 K (glass). [Ref: J. N. Demas and G. A. Crosby, J. Amer. Chem. Soc. **93**, 2841 (1971).]

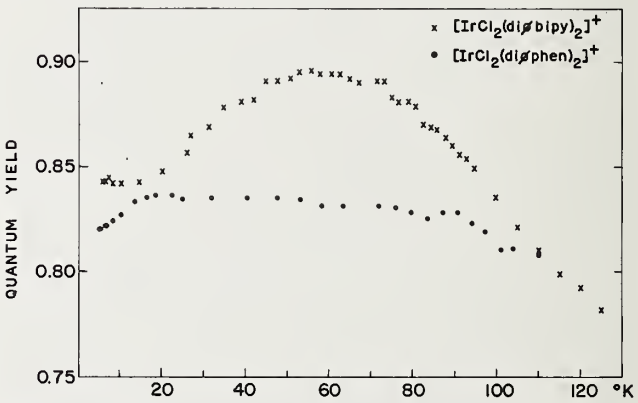

FIGURE 5. Temperature dependence of quantum yields. ×, *cis*-dichlorobis(4,4′-diphenyl-2,2′-bipyridine)iridium(III) chloride. ○, *cis*-dichlorobis(4,7-diphenyl-1,10-phenanthroline)iridium(III) chloride. Both molecules were dissolved in poly(methylmethacrylate) and irradiated with ~ 365 nm radiation.

temperatures above 77 K [35–37]. Furthermore, the measured decay times are on the order of microseconds, thus falling between those limits normally encountered for established fluorescences and phosphoresences. Finally, the capability of tuning the frequency by ligand change is apparent.

Additional spectroscopic features of importance are evident in figure 5. Not only are the yields of some of the molecules extremely high but, also, for some of them, the efficiencies are virtually temperature independent over large ranges. Because of the favorable chemical properties of these substances and their unique luminescence behavior, considerable fundamental information concerning the excited state properties of transition-metal complexes can be gleaned

from studies of their photoluminescences. Particularly important are accurate determinations of quantum yields as a function of temperature [38, 39]. Their possible value as fluorescence standards and as components in chemical actinometers is discussed below.

III. Standards

The absolute determination of quantum yields is a measurement fraught with difficulties. Understandably, workers have resorted to the much more convenient and rapid technique of measuring yields relatively, i.e., by comparison with known standards. Perforce, this procedure shifts a major burden of the accuracy of the final figure to the standard. Thus, the real need for more and better standards. Compounding the problem is the necessity to have standards for various solvents, for various temperature ranges, for wide ranges of wavelengths, and for different states of matter (solid, plastic, glasses, solutions). This is a stiff order. When one considers the importance of standards, the small number of well-studied ones, and the disconcerting disagreement of reliable workers on the actual reported efficiencies, the magnitude of the problem of obtaining good standards is revealed. [Relative yield measurements are so much easier to perform than absolute ones, however, that the demand for absolute standards will continue to increase.] An account of commonly used standards and an assessment of the reliability of their yield values are available [1]. Additional information on common standards and some interesting suggestions for new ones are contained in the article by Testa [74]. Many workers choose standards possessing favorable chemical properties for relative measurements even though the accuracy of some of the "standard" yields is not well substantiated.

The incidence on the market of commercial instruments that can measure yields routinely also increases the need for standards. In fact, institution of a program to remeasure old standards and search for new ones has considerable merit, in our opinion. If a bank of reliable standards could be built and marketed, which would provide checks on both research results and instrumentation throughout the country, a mass of misinformation would be clarified, and future additions of shoddy yield data to the literature would be measurably reduced. Such a program seems appropriate for the National Bureau of Standards.

At this juncture we wish to point out again the unusual optical properties of inorganic complexes, especially those of ruthenium, osmium, and iridium described above. It is our contention that they deserve serious study as candidates for standards, as well as for numerous other applications in spectroscopy and photochemistry. Because their properties can be modified by ligand substitution, ligand modification, and change of counter ion, it is possible to design them to have specified frequencies, high yields, and desirable solubilities. Thus, molecules can be engineered to dissolve in most common solvents. Their potential as quantum-yield standards should be studied, especially if internal standards (see below) were employed.

Finally, we wish to call attention to recent developments in purification procedures that bear on the accuracy of quantum-yield measurements. Chemical purity of any fluorescent compound is always desired; for quantum-yield standards it is a stringent requirement. This aspect of quantum-yield work has been repeatedly emphasized [1, 29, 75], not only for quantum-yield measurements but for emission spectroscopy in general. Intense light sources commonly employed to measure low yields exacerbate the impurity problems. The use of lasers dictates adherence to criteria for chemical purity far stricter than those normally applied [76]. Increases in detector sensitivity and the employment of high aperature equipment to monitor weak emitters place still greater demand for high standards of chemical purity. The availability of image intensifier tubes adds a new dimension to the impurity problem [77].

The virtues of thin-layer chromatography, column chromatography, and zone refining as supplements to the classical chemical techniques for obtaining high purity are relatively well known. Not commonly appreciated, however, are the remarkable chemical separations obtainable with the use of dextran molecular sieves in column chromatography. Although usually employed for biochemical separations, the effectiveness of molecular sieves for purifying inorganic materials is not common knowledge [78]. Indeed, the usual conception of the primary mechanism responsible for such separations (dominant role of molecular size) leads one to predict that molecules of similar size and shape should not be separable with such procedures. Yet, separations of isomeric, six-coordinated complexes of transition metals have been accomplished [73]. In fact, the discriminatory ability of the Sephadex gels to separate the components of reaction mixtures is so acute that surface adsorption activity must be at work in addition to steric effects [79].

Because of the many desirable features of gel filtration chromatography as a purification technique we strongly recommend its use both for purifying fluorescence standards and for preparing samples in general. For transition-metal complexes where reaction mixtures can produce a host of chemically and spectroscopically similar molecules, efficient separations are mandatory. In many cases gel filtration provides a superb answer to the problem.

IV. Quantum Efficiencies by Optical Methods

The first reliable method for measuring quantum yields by an optical technique was introduced by Vavilov in 1924 [80]. The method is a substitution technique employing a solid scatterer as a standard. The experiment requires two basic measurements. First, the detector monitors the sample luminescence that is generated by total absorption of the excitation light focussed to a point in the cell. Then the detector

records the light diffusely scattered by a magnesium oxide surface substituted for the original cuvette. From these data and some ancillary measurements, the absolute quantum yield can be computed. A detailed description of the technique including the derivation of equations is given in reference 1. Basic improvements on the method were the introduction of a quantum counter by Bowen in 1937 [81] and the incorporation of the refractive index correction by Förster in 1950 [82]. Refinements by McClure et al. [83] in the early 50's and the introduction of the rhodamine B quantum counter in 1955 by Melhuish [84] resulted in a method of measurement that has produced some of the most accurate quantum yields available.

In 1957 Weber and Teale [49] made a step forward by the introduction of solution scatterers for standards. This technique introduces its own special problems and limitations but is easier to carry out than the basic Vavilov method [1]. Numerous workers have devised improvements and modifications of both the Vavilov and the Weber-Teale methods for determining quantum yields, yet the measurements are still relatively tedious to perform and have many associated problems.

The difficulties inherent in absolute procedures and the demand for yield measurements on hosts of compounds have led workers to devise simple relative methods for performing the measurement. In these methods the yield of an unknown is compared with the "known" quantum yield of a standard material. Relative methods fall into two categories, optically dense and optically dilute. In the former, concentrated solutions are employed to absorb all the incident flux; in the latter, dilute solutions insure negligible diminution of the excitation beam across that part of the sample viewed by the detector. Optically dense quantum-yield measurements relative to a standard can be made extremely rapidly and are subject to moderate errors provided the substances satisfy somewhat rigid requirements. The accuracy can be low due to effects associated primarily with high concentrations. Optically dilute methods generally avoid problems created by solute-solute interactions and, due to the availability of high quality spectrofluorometers and their components, have become the preferred techniques for obtaining yields.

An analysis of optically dilute methods, the useful equations and their limits of validity, and the problems associated with this kind of measurement are contained in reference 1. We refer the interested reader to this review and the references therein. We wish to point out here, however, two problems associated specifically with yields obtained by optically dilute procedures that modern laser technology should admirably solve, (a) inaccurate (high) yields caused by strong light from a broad band source leaking through the filter system and (b) inaccurate yields produced by uncertainties in the effective absorbances of samples over the finite bandpass of the filters or monochromator excitation system (see *Lasers*, below).

For routine determinations of quantum yields by optical methods, the use of optically thin solutions versus optically thin standards is probably the best method available. The reported reproducibility is quite good (1–2%), and the agreement between laboratories is excellent (<5%) for some molecules. Considerable improvement in accuracy is to be expected from substituting lasers for conventional sources and from incorporating modern electronics and detectors into the systems. Although frequently reported with high precision [35–37], the accuracy of quantum yields obtained from substances dissolved in rigid glasses may not be high in spite of the good reproducibility. The relative importance of polarization errors is especially vexing to assess for rigid systems, and more work on this aspect of the optically dilute methods is badly needed [85].

Finally, we reiterate that both the optically dense and optically dilute techniques are still relative ones. Whatever systematic errors are built into the standards will be reflected in the results. Accurately measured standards are urgently needed.

A. Recent Developments in Instrumentation

We turn now to highlight some recent instrumentation advances that bear on optical methods of determining quantum yields. Lasers are by far the most important development, but the significance of available high sensitivity Raman instrumentation and recent improvements in photodetectors deserve attention.

1. Lasers

Lasers are now available in a wealth of types, powers, and configurations. The salient features of the most common varieties are reviewed in table 1. This list is by no means complete. In many cases, commercially available items are listed, and data have been drawn frequently from the manufacturer's literature. It should be further noted that specialized design frequently can improve many of the listed characteristics. In addition, because of the rapid advances in laser technology, this table will surely be obsolete by the time it is printed. The interested reader should consult the latest issues of the laser trade journals (e.g., *Laser Focus* and *Laser Sphere*) and other technical journals for up-to-date information. An especially valuable source is reports on advanced seminars in laser technology [86].

Most significant for luminescence and quantum-yield work is the high continuous wave (cw) powers available in the near UV and visible from argon lasers. The continuous tunability of the cw pumped dye lasers and their remarkably narrow line widths are also particularly noteworthy. Pulsed nitrogen lasers with their extremely short duration pulses and UV frequencies are ideally suited for most lifetime measurements and even for nanosecond photolysis. By driving a dye laser with a nitrogen laser and selecting the wavelength with an intracavity grating, one can preserve the extremely short durations and relatively high powers (one to two orders of magnitude in power are sometimes lost), but the added feature of continuous tunability from the

TABLE 1. Characteristics of selected lasers

Continuous Wave Lasers

TYPE **Discrete Line Lasers**	λ, nm	POWERS	MONOCHROMATICITY
Ar [a]	351.1 + 363.8; 457.9; 472.7; 476.5; 488.0; 496.5; 501.7; 514.5; 528.7	20 mW to 2 W	< 0.001 Å
Kr [a]	350.7 + 356.4; 476.2; 482.5; 520.8; 530.9; 568.2; 647.1; 676.4; 752.5; 799.3	20–500 mW	< 0.001 Å
Tunable Lasers			
cw pumped dyes with intracavity λ selection [a]	520–690	10–160 mW	0.1 Å normal to 0.001 Å

Pulsed Lasers

TYPE **Discrete Line Lasers**	λ, nm	POWERS	MONOCHROMATICITY	DURATION, nsec
N_2 [b]	337.1	1–10 1–100 kW peak 0.5 W average	~1 Å	5–10
Nd^{3+}-YAG	266 (frequency quadrupled), 13 lines from 473 to 679 (frequency doubled), 13 lines from 946 to 1358	1–5 kW peak 10–100 m W average	< 1 Å	100–400
Ruby	694 (Q-switched)	100 MW peak 1 J per pulse	0.1 Å	20 [d]
	347 (frequency doubled)	10 MW peak	0.1 Å	20 [d]
Tunable Lasers				
Flashlamp pumped dyes [c]	340–>650	0.25 J/pulse 600 kW peak 25 mW average	< 1–10 Å	100–500 [d]
N_2-laser pumped dyes [b]	360–>650	2–150 μJ/pulse 1–10 kW peak 1–50 m W average	< 1–20 Å	2–10 [d]
Nd^{3+}-YAG pumped dyes [e]	540–670 and 270–340	20–700 W peak 0.2–25 mW average	< 1 Å	
Parametric oscillator [e]	650–3000	50–700 W peak 1–10 mW average	≤ 1 Å to 0.001 Å	70–150

[a] Data for lasers from Spectra-Physics and Coherent Radiation.
[b] Data for AVCO Everett Research Lab. lasers.
[c] Data for Synergetics Research, Inc. lasers and from references [88, 89, 90, 91].
[d] Mode locking can yield picosecond pulses (< 0.1 nsec), although spectra bandwidth will usually be increased. See references [90, 91].
[e] Data for Chromatix laser.

near UV through the visible is obtained. These characteristics are ideal for carrying out time-resolved spectroscopy, a powerful fundamental and analytical tool. The large pulse energies available from the flash-lamp-pumped dye lasers are also attractive for some studies, and systems can be built for minimal cost [87–89].

From table 1 the benefits accrued from replacing conventional light sources with a laser source are manifest. The powers available far exceed those normally obtained from even wide bandpass conventional sources. This power gain, however, can be obtained at no loss in spectral purity, and for most molecular systems one can treat the sample absorbance as constant over the excitation line. Thus, one of the significant sources of error mentioned above in quantum-yield and excitation-spectra determinations is eliminated. The higher powers available from the lasers also permit the use of more dilute solutions; this reduces the trivial errors of self absorption and secondary emission.

In addition to the high powers and narrow line widths, lasers have other advantages. Typically, the laser beam is of very small size. A cw argon laser, for example, has a beam diameter of 1 to 2 mm. It is highly coherent and can be focussed to an essentially diffraction limited spot. This high degree of focusability is commonly exploited in Raman work where the laser is directed down the long axis of a microcapillary. The use of a microcapillary cell would also yield significant advantages in luminescence spectroscopy. There would be negligible reabsorption, and the source composed of the emitting volume would be a near line. Thus the emissions could be focussed extremely efficiently onto the entrance slit of an emission monochromator, even for very narrow emission bandpasses. Such a system could not be used with even moderately photosensitive materials, however, unless a flow system were employed. Microcapillary cells have a further disadvantage for comparative work due to the higher precision required for reproducible alignment.

There seems little doubt that the wavelength range, the pulse duration, and the available powers of most of the types of lasers will be greatly improved. With progress in mode-locking [90–92] it seems reasonable to anticipate that the dye lasers will yield repetitive, stable, and continuously tunable subnanosecond pulses extending from the UV to near-IR regions. Such a tunable, short duration source would represent truly a delta function excitation flash for luminescence lifetime measurements and time-resolved spectroscopy, with little sacrifice in power or spectral purity. For dye lasers especially, considerable improvements in peak and average power are anticipated as the pulsed nitrogen lasers become more efficient. Wavelength range limitations of tunable dye lasers will almost certainly become relaxed as the dyes are frequency doubled into the UV, and new dyes will surely extend the available range well into the infrared. Already the entire range between 7000 and 11,700 Å has been covered by pumping photographic film sensitizer dyes with Q-switched ruby lasers [93]. A number of parametric oscillators has been constructed that exhibit continuous tunability from 7000 to 20,000 Å, and efficiencies of 45 percent have been reported [94].

Referring to the optical quantum-yield methods sketched above, we cannot think of a technique that would not benefit substantially from the replacement of the conventional light source with the laser. We have no doubt that where low cost is not a prime factor, but accuracy is of paramount importance, lasers will eventually become the excitation source of choice. This statement applies to calorimetric methods also.

2. *Raman Instrumentation*

The developments of laser Raman spectroscopy have yielded a whole new line of optical components that are admirably suited for luminescence and quantum-yield measurements as well. One of the principal areas of progress is monochromator technology. Quite fast, extremely-low stray-light, double monochromators have been produced. Stray light in these devices is so low that one can scan to within a few wave numbers of the laser line pump. Such superb stray light rejection makes them a natural choice for luminescence and quantum-yield measurements, especially when laser excitation is employed. It is noteworthy that much of the impetus for the development of very high power krypton and argon lasers also stemmed from the needs of the Raman spectroscopist.

Photomultipliers have also undergone enormous improvements. By reducing the effective photocathode size and cooling the tubes to reduce the dark current, the dark backgrounds have been reduced to a few counts per second (e.g., tubes of the IT&T[2] type). All this has been accomplished with an extended red response S–20 photocathode, which may exhibit a quantum efficiency of several percent beyond 800 nm.

Thus the modern unmodified Raman instrument using an argon laser source represents a nearly ideal excitation-detection system for luminescence, at least when the molecules absorb in the region of the laser lines. The ready availability of these Raman spectrometers within many laboratories also adds to their attractiveness for such work. Almost any further advances in Raman technology are certain to be adaptable with benefit for making luminescence measurements and for determining quantum efficiencies.

3. *Photodetectors*

In addition to the restricted area tubes used in Raman spectroscopy, there have been other significant advances in detector technology. RCA, for example, has introduced a line of gallium arsenide and indium-doped gallium arsenide extended red-response

[2] In order to adequately describe materials and experimental procedures, it was occasionally necessary to identify commercial products by manufacturer's name or label. In no instances does such identification imply endorsement by the National Bureau of Standards, nor does it imply that the particular product or equipment is necessarily the best available for that purpose.

photomultipliers. The gallium arsenide tubes typically have quantum efficiencies of 1.4 percent at 860 nm. With indium doping, the red response is further extended, and RCA will supply tubes having efficiencies of 1 percent at 950 nm, 0.2 percent at 1000 nm, and 0.1 percent at 1060 nm. In addition to having remarkably deep infrared penetration, these tubes have quite low dark currents even at room temperature; in most cases they can be regarded essentially as a quantum jump better than the old infrared tubes with S–1 response. Further improvements seem likely since gallium arsenide photosensitive surfaces have been prepared having maximum quantum efficiencies of 80 percent [95].

Semiconductor diodes are also improving. Germanium diodes of the type used in nuclear instrumentation make superb optical detectors [96]. They can have large areas ($> 1\ \text{cm} \times > 1\ \text{cm}$) and sensitivities comparable to photomultipliers. Their noise equivalent power (NEP) is $\sim 10^{-15}$ W/Hz$^{1/2}$ from the visible to beyond 1600 nm. Their stability and near quantum flat response of ~ 0.6 has led to the suggestion that they be used as replacements for thermopile radiation detectors [96].

When operated in the avalanche mode, these photodiodes have many of the characteristics of photomultipliers. They still have the high quantum efficiencies of the solid state photodiodes but also exhibit a limited gain multiplication. Typically, their sensitivities stretch well into the near infrared. Texas Instruments, for example, has introduced a series of silicon and germanium photodiodes packaged with amplifiers (TIXL 74–76). For the silicon system, the NEP at 900 nm is less than 5×10^{-13} W/Hz$^{1/2}$. For the germanium ones, the NEP is $\sim 2 \times 10^{-12}$ W/Hz$^{1/2}$ at 1060 nm or $\sim 6 \times 10^{-12}$ W/Hz$^{1/2}$ at 1540 nm. With properly biased photodiodes, single photon counting is even possible. With germanium photodiodes, NEP's of $\sim 10^{-13}$ W/Hz$^{1/2}$ at 1500 nm have been realized. Germanium devices are usable to beyond 1700 nm [97]. It seems reasonable that further improvement in these avalanche devices will yield even higher sensitivity in the near-IR region. It is even possible that they will become competitive with photomultipliers in the visible-UV regions. In a spectrophotometry application weak transient absorption during flash photolysis has been detected in the 0.6—1.1 μ region with the aid of an inexpensive silicon photodiode [98].

If the major source of noise in an optical experiment is due to the photon statistics, then the signal-to-noise ratio depends upon the square root of the quantum efficiency of the detector. Thus for high light level experiments the high quantum efficiency of photodiodes is a distinct advantage for noise discrimination, especially in the near infrared.

B. New Experimental Techniques

1. Internal Standardization

Internal standardization is frequently used in analytical chemistry. To date, however, we are aware of no use of an internal standard for quantum-yield measurements. This failure has been a result of the experimental difficulties involved rather than because of any undesirable fundamental features of the technique itself. In fact, internal standardization is probably one of the more elegant and useful techniques for accurate relative quantum-yield determinations. The method appears especially feasible in view of modern instrumental developments.

In the internal standardization procedure both the unknown and standard would be contained in the same solution. The emission spectra of the two compounds would then be run in a single scan of the emission instrument. From the relative emission intensities of the standard and the unknown and their absorbances one would then calculate the efficiency of the unknown relative to the standard by normal procedures. The advantages of such a procedure are numerous. Since the standard and unknown are in the same solvent and cell, refractive index corrections are all but nonexistent, and radiation trapping is essentially identical between both samples. Errors introduced by cell mismatch are eliminated. There are, of course, serious restrictions on the method. The standard and the unknown must emit in well-resolved spectral regions (by means of time-resolved spectroscopy, even this restriction may be lifted). They must also absorb at the same wavelength.

Several experimental difficulties must be considered closely if satisfactory results are to be obtained using an internal standard. Because the standard and unknown are present in the same solution, great care must be taken to prevent any bimolecular quenching or energy-transfer processes, since their occurrence would modify the yields of the species present [99]. As long as one is using optically dilute solutions, there is no problem with long-range energy transfer of the Förster-type. This would not, however, always be true if optically dense solutions were employed.

Diffusion-controlled processes must also be considered. One can readily show that even if a sample has a component with a lifetime as long as 1 μs that is quenched by the other one at the diffusion controlled limit (10^{10} M^{-1} s^{-1}) then the concentration of the second species must exceed 10^{-6} M to cause 1 percent quenching of the first. Since optically dilute measurements are usually carried out at optical densities less than 0.01, then any second component with $\epsilon \geq 10^4$ at the exciting wavelength would introduce a negligible error. Of course, if the first compound has a lifetime of less than 1 μs or the quenching proceeded with a rate less than the diffusion-controlled limit, then this already weak restriction would be relaxed still further. For example, if the standard's lifetime were 10^{-8} s (a typical fluorescence lifetime), then the maximum permissible concentration of the second species would be 10^{-4} M; this would permit molecules with $\epsilon \geq 10^2$ to be measured. The same arguments apply to the second component. Most materials and standards would have coefficients satisfying this condition in some region. Thus, because of bimolecular

quenching it appears that the internal standardization technique is largely limited to optically dilute measurements. Consequently, all of the restrictions and limitations on any optically dilute method are present [1].

The remaining serious difficulty or source of error envisioned in a procedure employing an internal standard is that inherent in accurately calibrating any spectrometer over a wide wavelength range. Also, some compounds have extremely wide emission bandwidths; then difficulty will be encountered in obtaining satisfactory standards. Transition-metal complexes, as discussed above, may possibly be designed for appropriate standards. Sensitivity, even when working with low yield substances under optically dilute conditions, does not appear to present a severe limitation for the method.

In summary, we believe that the use of an internal standard in relative quantum-yield determinations deserves serious consideration for investigation and development. If well-defined standards become readily available, the method could eventually become one of the preferred ways of running high-accuracy yield determinations.

V. Quantum Efficiencies by Actinometric Methods

The principle of the actinometric method for measuring quantum yields is conceptually simple. One merely surrounds the sample completely with an actinometer solution, measures the apparent intensity of the emitted radiation, and then, using the same type of actinometer solution, monitors the intensity of the excitation beam. If the irradiated solution is totally absorbing, the ratio of the two intensities is the absolute quantum yield. Whereas actinometers are capable of measuring absolute intensities, this technique is, in fact, a relative method since the absolute yield of the actinometer need not be known. To our knowledge, this method has not been used for measuring optically excited luminescence efficiencies. It has, however, been utilized in a suitably modified form for measuring chemiluminescence yields [100].

The principal reason for the nonadoption of an actinometric method is experimental. Most actinometers have quantum yields that are strongly wavelength dependent, and their absorption characteristics make it difficult to arrange to have all of the emitted light absorbed over the very wide wavelength ranges encountered in molecular luminescences. Because of these factors it is difficult to obtain an accurate measurement of the intensities of both the excitation beam and the broad molecular emission with the same actinometer. With the advent of new sources and actinometers, however, actinometric methods may achieve a useful place in absolute quantum-yield measurements.

Before launching into speculative discussion we point out that the potassium salt of *trans*-$[Cr(NH_3)_2(NCS)_4]$ (Reinecke) is an excellent wide-range actinometer covering the 300 to 600-nm region [101]. Its yield has been measured over an extended wavelength range, and it is reasonably sensitive. Unfortunately, it is not without its shortcomings. To absorb most of the emitted light in the 300 to 600-nm range, rather concentrated and/or thick solutions are required (about 1.5 cm at a concentration of 5×10^{-2} *M*). The compound also exhibits a slow but bothersome thermal decomposition. Finally, there is a slight, although perhaps not real, variation of the quantum yield with wavelength, a variation that is, however, small enough that reliable corrections could be made. No one has confirmed the original yields, and the initial data were taken at somewhat greater wavelength intervals than would be desirable for precise corrections. Notwithstanding these objections, Reinecke's salt is even now usable as a wide-range actinometer for yield determinations.

Recent photochemical investigations portend the development of additional wide-range actinometers. Demas and Adamson [102] have found that tris(2,2′-bipyridine)ruthenium(II) sensitizes, by a diffusion-controlled process, the redox decomposition of tris(oxalato)cobaltate(III). Since the donor has a broad, intense absorption, it is quite easy to obtain, with thin solutions, total absorption of incident light from the UV to beyond 500 nm. The decomposition of the $[Co(C_2O_4)_3]^{3-}$ may be readily monitored spectrophotometrically (unfortunately not with quite the high sensitivity of the ferrioxalate). Furthermore, since the efficiency of population of the donor level is believed to be unity and to occur virtually instantaneously following excitation, the system has a decomposition yield that is inherently wavelength independent and that has a broader range than most other actinometers. In its present form, their system is not, however, a useful actinometer. With modifications it, or a related system, may become practical.

Lasers make the actinometric method for measuring yields appear even more attractive. The excellent focusability of lasers permits an extremely small entrance aperture to be used and thus minimizes the error due to loss of radiation through the excitation port. Also, because the laser beam is inherently well collimated, one could use relatively dilute solutions in very long cells and irradiate down the cylindrical axis. In this way trivial reabsorption effects would be minimized. A device built along these lines might look much like a condenser with the outer cooling jacket filled with the actinometer solution. Of course, any measurement based on an optically dilute method would be subject to the normal corrections, and the optically dense method would be prone to its usual inherent errors. In spite of these objections, common to all optical quantum-yield measurements, it seems that the actinometric method has distinct possibilities even now with potassium Reinecke, and it will probably become more attractive with time, especially as the developments in modern inorganic photochemistry gain momentum and uncover new photochemical reactions and sensitizers.

VI. Quantum Efficiencies by Calorimetric Methods

Although measurement of quantum efficiencies optically involves generally familiar instrumentation, this statement cannot be made about calorimetric procedures. Recently, however, developments in technology point toward a gaining importance of calorimetry in the field of quantum yields, and we wish to discuss some of them. Because of their relative unfamiliarity, we present here a more detailed account of the various methods employed in calorimetry than was included above for the optical methods.

Calorimetric methods of measuring quantum yields are based on the assumption that energy absorbed from a beam of light incident upon a solution of fluorescent molecules is either lost through reemitted photons or degraded to heat by radiationless processes. The objective of calorimetric techniques is to measure the energy yield of these radiationless processes, Y_h, which is defined as the ratio of heat energy produced to incident photon energy absorbed. Y_h is obtained by measuring the ratio of the heating produced by irradiation of the fluorescent sample to the heating produced by irradiation of a nonfluorescent sample that absorbs the same fraction of the excitation energy.

In the absence of photochemistry, the fluorescence [103] energy yield is the complement of Y_h and the quantum yield of fluorescence is related to it by the formula

$$\Phi = (\bar{\nu}_a/\bar{\nu}_f)(1-Y_h) \tag{1}$$

where $\bar{\nu}_a$ and $\bar{\nu}_f$ are the average frequencies (cm^{-1}) of absorbed and fluorescence photons, respectively, defined by the formulas

$$\bar{\nu}_a = [\int I_a(\lambda)A(\lambda)d\lambda/\lambda]/[\int I_a(\lambda)A(\lambda)d\lambda] \tag{2}$$

$$\bar{\nu}_f = [\int I_f(\lambda)d\lambda/\lambda]/[\int I_f(\lambda)d\lambda] \tag{3}$$

$I_f(\lambda)$ and $I_a(\lambda)$ are the fluorescence and excitation intensities at wavelength λ, $A(\lambda)$ is the percent absorbance of the sample with a pathlength equal to the cell dimension, and the integrals are over the fluorescence and excitation bands, respectively. Since $\bar{\nu}_f$ and $\bar{\nu}_a$ are easily measured with high precision by standard photometric techniques, they will not be discussed further here [1, 29].

Several important factors favor calorimetric methods for the determination of absolute quantum yields: (a) The method serves as a valuable independent check of the assumptions used in photometric techniques for measuring Φ_f; in particular, corrections for experimental geometry, index of refraction changes, and polarization effects are largely eliminated. (b) Using relatively crude apparatus, some workers have obtained values of Y_h with a precision comparable to those obtained by other methods [29]. (c) The calorimetric method works well with samples that emit in the near infrared where the sensitivity of optical techniques is relatively low. Recent developments in photodetectors are alleviating this problem, however (see above).

With the usual procedures and components, the principal disadvantages and limitations of the method have been the following: (a) The insensitivities of the calorimeters used thus far have forced workers to use highly absorbing samples; consequently, large corrections for reabsorption of the fluorescence [29, 104] are required. (b) The method has been limited to substances possessing high quantum yields. (c) Measurements have been confined to liquid samples at room temperature. (d) Methods devised thus far have been tedious and time consuming to perform.

Recent advances in calorimetry, especially in the technology of light sources and transducers, and improvements in methods of data acquisition portend wider acceptance of the technique for obtaining quantum efficiencies. The generality, sensitivity, and ease of performance of calorimetric methods will undoubtedly improve. Our purpose here is to review some of the advances in methods and components and to indicate possibilities for still greater improvements.

A. Calorimeters

The calorimetric apparatus consists of an excitation source, a means for selecting a bandwidth of the incident radiation, and a calorimeter to measure the heat energy produced during irradiation. The science of calorimetry is a mature field of endeavor, and the reader desirous of a general background in the subject is referred to the several books and recent reviews now available [105–108]. Let us begin our discussion of calorimetric apparatus by considering the constraints on the calorimeter imposed by the requirements for measuring quantum yields. First, provision must be made for admitting the exciting light. Second, the calorimeter must be designed so that all fluorescence escapes the cell. Third, since the sample will not be uniformly irradiated, the average or total heating must be detected. Fourth, the calorimeter must be very sensitive. In general, the sensitivity requirements will depend on the energy of the incident radiation, the absorbance of the sample, and the value of the quantum yield to be measured. A straightforward analysis of the propagation of errors in the calorimetric method shows that in order to measure a value of $\Phi_f = 0.5$ with a precision of 1 percent, the heating of the nonfluorescent sample must be measured with a precision of 0.1 percent.

It is shown later that most calorimeters detect the heating power produced by steady state irradiation. If the incident radiation power is 100 mW, and we are using samples that absorb 10 percent of the beam or less to avoid reabsorption effects, then our calorimeter must be capable of measuring a heating power of 10 μW with a signal-to-noise ratio of unity.

It is now obvious that the method for detecting heat flow in the calorimeter must be very sensitive. Most

calorimeters use temperature transducers to measure heat flow. One figure of merit, useful for evaluating temperature transducers, is their noise equivalent temperature (*NET*) given by the following expression

$$NET = [N/S(\Delta f)^{1/2}] \text{ deg/Hz}^{1/2} \quad (4)$$

where N is the noise voltage developed by the transducer, S is the voltage sensitivity of the transducer, and Δf is the noise bandwidth. The *NET* is defined as the temperature change required to generate a signal-to-noise ratio of unity when the detector noise is referred to a one cycle bandwidth.

One common method for measuring temperature changes in calorimetry is by means of a thermopile. Generally, the limiting noise in this device is due to the Johnson noise of its resistance. For a 100-junction copper-constantan thermopile of 100 Ω resistance, the *NET* is calculated to be 0.2 μdeg/Hz$^{1/2}$. The tiny voltages associated with these devices can be conveniently measured by means of a commercially available nV amplifier such as the Keithley Model 148. The construction of thermopiles is an art and is discussed by Hill [109], Howarth [110], and Evans [111].

Resistance thermometers have also been used for calorimetric work. Larsen [112] has shown that the sensitivity of platinum resistance thermometers operated by an ac bridge approaches the theoretical limit imposed by the Johnson noise of the device. He gives a *NET* of 20.5 μdeg/Hz$^{1/2}$ for a commercially available 500 Ω platinum resistance thermometer. These tranducers are very stable with time, are smaller in size than thermopiles, and do not require reference junctions.

The use of thermistors in calorimetry has been discussed by Meites et al. [113]. Previously, these temperature transducers have been criticized for calorimetric work because of long term instabilities [112]. Meites et al. found, however, that operation of selected and aged 100 K thermistors at low power levels (18 μW) allowed reliable detection of temperature changes of 10 μdeg by means of a dc bridge and recording potentiometer. The *NET* as predicted by consideration of the Johnson noise is even lower, 0.7 μdeg/Hz$^{1/2}$. Attainment of this resolution will probably require use of an ac bridge and phase sensitive detection. Thermistors also offer advantages due to their small sizes and fast response times.

In addition to temperature transducers, one can also employ volume transducers to measure heat flow. The volume change, ΔV, produced at constant pressure in response to a heat change, ΔQ, is given by the formula

$$\Delta V = \alpha \Delta Q / C_p \rho \quad (5)$$

where α is the thermal expansion coefficient of the sample, ρ is its density, and C_p is its heat capacity per gram. A simple dilatometer for measuring volume changes in calorimetric experiments has been used by Seybold, Gouterman, and Callis [29]. In their apparatus, the sample is contained in a cell open to the atmosphere only through a capillary tube. The volume of the solution is visually monitored as it expands up the capillary. Volume changes as small as 7×10^{-5} cm^3 can be measured; for a 10-cm^3 ethanol sample this corresponds to a temperature rise of 7×10^{-3} °C. Further increases in sensitivity in capillary dilatometers can be obtained by using a travelling microscope [114] or a photocell to measure changes in the height of the liquid in the capillary.

A greatly improved technique for measuring volume changes has been developed by Callis, Gouterman, and Danielson [44]. These workers use a capacitor microphone to detect volume changes. They claim a noise equivalent volume (*NEV*) change of 4×10^{-10} cm^3 referred to a 1-Hz bandwidth, which corresponds to a *NET* of 0.04 μdeg/Hz$^{1/2}$ for heating 10 cm^3 of ethanol. In addition to its sensitivity, this technique has other advantages: (a) The volume change is independent of the size of sample irradiated, whereas the magnitude of the temperature change depends on the size of the sample. (b) Equation (5) is valid even though a uniform temperature is not established if, at all points, ΔT is small enough so that the equation holds locally. Thus, the sample need not be stirred. (c) The response time of this apparatus is limited only by the transit time for sound in the cell. Disadvantages of the volumetric technique are: (a) The electronics, as originally devised by Callis et al. are ac coupled. Use of a capacitance bridge can overcome this disadvantage, however. (b) The apparatus is sensitive to vibration and acoustical noise and therefore must be isolated from both. (c) For water, an important solvent, $\alpha/\rho C_p$ is ~10 times lower than for organic solvents.

All of the calorimeters we shall discuss in this paper are surrounded by an isothermal shield, and thus all can be characterized by the same energy flow equation

$$dH/dt = FY_h P(t) - KH(t). \quad (6)$$

$H(t)$ is the heat energy retained in the sample, F is the fraction of incident power absorbed by the solute, $P(t)$ is the incident radiation power, and K is the first-order heat loss constant under the assumption that all heat losses are newtonian. We have neglected heating due to absorption by the solvent and reabsorption of fluorescence photons. These effects are discussed elsewhere [1].

Two cases of eq (6) may be distinguished: (a) When the heat loss term is negligible, the calorimeter is an adiabatic one. (b) When the heat loss term is large, the calorimeter is a conduction calorimeter. When the heating input is exactly balanced by an equal cooling, then the calorimeter is known as a compensation calorimeter.

Let us first consider the use of the conduction type calorimeter as employed by Alentsev [104] for measuring Y_h. The calorimeter consists of a thin cell suspended in a chamber whose walls are maintained at a constant temperature. Temperature changes are measured by means of a thermopile. The measuring

junctions are arranged symmetrically around the lateral wall of the cell, and the reference junctions are buried in the isothermal wall. The major source of heat loss is through the thermopile itself. A schematic of the apparatus is shown in figure 6. Since temperature changes are measured, we can use the relationship $H(t)=C_p[T(t)-T_0]$ to convert eq (6) to a form involving the instantaneous temperature.

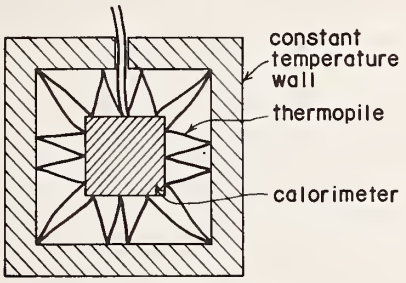

FIGURE 6. Conduction calorimeter.

$$dT(t)/dt=[FY_hP(t)/C_p]-K[T(t)-T_0] \quad (7)$$

where T_0 is the temperature of the wall. For steady state irradiation (P constant), the solution to eq (7) is

$$T(t)-T_0=FY_hP(KC_p)^{-1}[1-\exp(-Kt)]. \quad (8)$$

After a time $t \gg 1/K$ the maximum temperature rise, ΔT_m, is reached.

$$\Delta T_m=FY_hP(KC_p)^{-1}. \quad (9)$$

The ratio of ΔT_m for the fluorescent sample to ΔT_m for a nonfluorescent sample that absorbs the same fraction of incident light gives Y_h, provided K and C_p are the same. For a given energy input, ΔT_m can be maximized by using the lowest value of K and C_p. As used for determination of Y_h, the conduction calorimeter may be thought of as a power measuring device, and thus a factor of merit is its noise equivalent power (*NEP*), which is defined as the power input required to generate a signal-to-noise ratio of unity when the detector noise is referred to a 1-Hz bandwidth. For the conduction calorimeter

$$NEP=NET(K)C_p \quad (10)$$

where the *NET* is that of the temperature transducer used. For a *NET* of 1 μdeg, a heat capacity of 10 cal/°C and a K^{-1} of 10 min, one obtains a *NEP* of 0.07 μW. In practice, the best conduction calorimeters [115] exhibit a *NEP* of 0.2 μW; but even this value is far better than that obtained by Alentsev. The limit of sensitivity of this apparatus is apparently determined by the temperature stability of the environment of the calorimeter [115]. Design and construction of conduction type microcalorimeters is discussed extensively by Evans [111] and by Calvet and Prat [115, 116]. In the most advanced designs [111, 115, 116], the experiment is conducted differentially, i.e., the temperature difference between the irradiated sample in one cell and an identical unirradiated sample in a twin cell is measured. This technique greatly increases the long term stability of the apparatus and is to be recommended for any type of dc calorimetry.

As employed for conventional calorimetric measurements, conduction calorimeters are not stirred. This is possible if a large number of thermocouples is distributed evenly over the surface of the calorimeter so that the average surface temperature is measured. For fluorescence measurements, however, it is ideal to have all of the fluorescence escape the cell. Thus, the thermopiles should occupy only a tiny fraction of the cell surface. The cell must be stirred. Unfortunately, stirring produces its own heating, which gives rise to additional noise in the system [111].

Perhaps the major disadvantage of using conduction calorimeters is that long times are required for measurement. For a K^{-1} equal to 10 min, one must wait at least 1 h for the sample to come into equilibrium, and additional time will be taken waiting for the temperature to stabilize.

Some recent work by Chastel and Tachoire [117] suggests that the commercially available and highly perfected Tian-Calvet conduction microcalorimeter may be used in a virtually unmodified form in conjunction with a pulsed light source. The calorimeter is shown schematically in figure 7. The cell is made of glass or quartz, which is surrounded by a metallic "can" whose inside is coated with a totally absorbing black substance. The thermocouples are

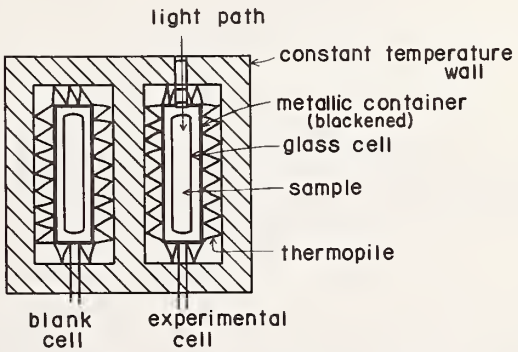

FIGURE 7. Tian-Calvet conduction microcalorimeter modified for quantum-yield determination.

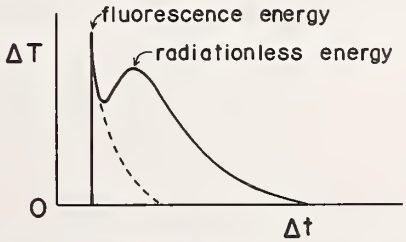

FIGURE 8. Thermogram from Tian-Calvet microcalorimeter.

affixed to the metallic cell. Irradiation of the sample produces a double flux of light and heat. The light is converted to heat through absorption by the metallic cylinder. A recording of the temperature as registered by the thermocouples versus time in the form of a thermogram would be expected to yield the results shown in figure 8. The first peak is due to light absorbed at the cylinder; the second is due to heat diffusing from the sample produced by radiationless processes. If the response times of the apparatus to heat and light are determined, then it is easy to separate the two responses and obtain the energy yields. Chastel and Tachoire have obtained excellent results on energy yields of flash sources for photography in this manner.

A second type of calorimeter, which can be used for measurements of Y_h, is a heat flow compensation calorimeter. The design of such calorimeters has been discussed by Sturtevant [118]. In these devices, heating produced by irradiation is balanced by an equal amount of cooling power supplied by a thermoelectric module. The null heating point is sensed by a temperature transducer. Thus, the cooling power supplied is a direct measure of the energy input power. An apparatus is shown schematically in figure 9. This device

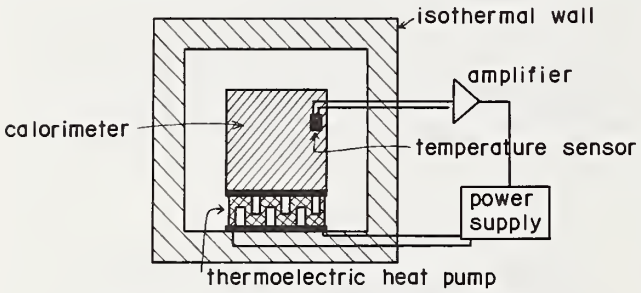

FIGURE 9. Heat flow compensation calorimeter.

is also essentially a power measuring apparatus, and its factor of merit is given by the *NEP*, which is related to the *NET* of the temperature sensor, as follows:

$$NEP = NET(C_p)\tau^{-1} \tag{11}$$

where τ is the time constant of the temperature detection. To minimize the *NEP*, one desires the lowest values of heat capacity and *NET* and the longest time constant. For a $NET = 1$ μdeg, $C_p = 10$ cal/°C, and $\tau = 10$ the *NEP* is 4.2 μW. This type of calorimeter may also be used in a differential mode where the difference between an irradiated and unirradiated cell is measured.

Adiabatic calorimeters are a third possibility for Y_h measurements. They have been employed in this manner by Seybold, Gouterman, and Callis [29] and by Gudmundson et al. [119]. In these devices one attempts to eliminate heat transfer between the calorimeter and its surroundings. Because of the tiny temperature changes involved, this ideal is best approached by conducting experiments in a constant temperature jacket calorimeter for short time periods so that heat losses are negligible. As with conduction calorimeters, adiabatic calorimeters can be used with steady or pulsed sources. If the sample is irradiated by a steady light source, the temperature rise can be measured as a function of time. In this case, the calorimeter may be thought of as a power measuring device, and the minimum detectable power level will be related to the *NET* of the temperature sensor by the formula

$$NEP = NET(C_p)\Delta t^{-1} \tag{12}$$

where Δt is the maximum time after the start of irradiation at which a measurement can be made. For the isothermal jacket calorimeter this condition will be $K\Delta t \ll 1$ where K is the rate of newtonian heat loss. For a *NET* of 1 μdeg, a C_p of 10 cal/°C, and a Δt of 100 s, a *NEP* of 0.42 μW is obtained. If a pulsed light source is used, the net temperature rise is measured. In this case, the calorimeter determines the integral of the incident power, and thus a figure of merit is the noise equivalent energy change, *NEE*, which is just the *NET* of the temperature sensor times the heat capacity of sample and calorimeter. Thus, for a *NET* of 1 μdeg and a 10 cal/°C heat capacity, we obtain a *NEE* of 10 μcal. This method is attractive because pulsed light sources of high energy are readily available (e.g., pulsed lasers), and heating due to absorption of fluorescence by the calorimeter can be separated by its time dependence.

Thus far, all of the types of calorimeters we have discussed are, in principle, capable of measuring very low power levels and will allow elimination of reabsorption corrections. They all have a common single disadvantage, however. The measurements are performed near zero frequency and are tedious and time consuming. Further, the temperature of the calorimeter and surroundings must be controlled to the *NET* of the temperature sensing device if the lowest possible *NEP* of the calorimeter is to be realized.

Currently, a new technique for calorimetric measurements of Y_h, which can overcome some of the disadvantages of conventional calorimetry, is under development. Essentially the apparatus is the flash calorimeter of Callis, Gouterman, and Danielson [44] shown in figure 10. It consists of a glass cuvette, one wall of which is the compliant diaphragm of a capacitor microphone. The valve attached to one side of the cell serves as a capillary leak so that the liquid can slowly enter or leave the cell. This prevents slow pressure changes that would occur in a completely closed cell subject to temperature drifts and the dc component of repetitive excitation.

Because of the fast response time of this apparatus, the exciting light is modulated, and the resultant heating is detected at the frequency of the modulation by phase sensitive techniques. The advantages of ac methods of doing experiments is well known [120]. Briefly, all experiments are contaminated with noise, some of which has a $1/f^n$ frequency dependence. This latter noise is dominant in calorimetric measure-

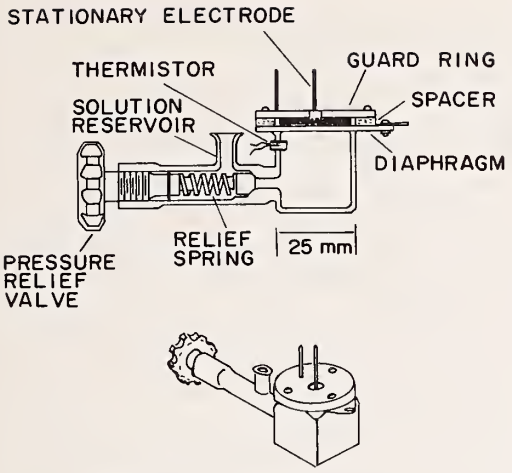

FIGURE 10. Flash calorimeter.

ments, which are performed at low frequencies where thermal drifts are important. By modulation one can shift the frequency domain of the experiment to a point where noise due to thermal drifts is no longer important and thermostating can be eliminated. By means of phase sensitive detection, very narrow bandwidths can also be obtained, further discriminating against noise.

Due to these advantages, it is worthwhile to consider in more detail this new method for determining Y_h. Assume that the light intensity has the time dependent form

$$P(t) = P_0(1 + \cos \omega t). \tag{13}$$

P_0 is the steady state power in cal/s and ω is the modulation frequency. The heating in the cell in response to the excitation is given by eq (6). We may combine eqs (5) and (6) to obtain a differential equation for the time dependence of the volume change

$$dV(t)/dt = [\alpha F Y_h/\rho C_p] P(t) - K'V(t) \tag{14}$$

where K' is the first-order rate constant for removal of the excess volume change and is given by

$$K' = \alpha K/C_p + K''. \tag{15}$$

In this expression, K'' is the rate constant for the capillary leak. Integration of eq (14) gives for the steady state solution

$$V(t) = Y_h P_0(\cos \omega t)/\rho C_p \omega \tag{16}$$

where we have assumed that $\omega \gg K'$.

The amplitude of the signal will, therefore, be inversely dependent upon the frequency of modulation. In practice, the experiment should be done at the lowest frequency commensurate with unimportant $1/f$ noise. This apparatus, like the other calorimeters discussed, is also a power detector, and its *NEP* will be given by

$$NEP = NEV(C_p)\rho\omega/\alpha. \tag{17}$$

For a *NEV* of 10^{-10} cm^3, $\rho C_p/\alpha = 4 \times 10^2$ cal/cm^3, and $\omega = 1$ s^{-1}, we obtain a *NEP* of 0.2 μW. In addition to its great sensitivity, the advantages of this technique over others we have thus far discussed are the elimination of elaborate thermostating and the execution of measurements rapidly.

An alternative method for using the flash calorimeter is to employ a pulsed exciting source. If a fairly high repetition rate is achieved, the volume change can be stored in a computer and averaged over many repetitions. If the noise is random, then the improvement in signal-to-noise ratio will increase as the square root of the number of experiments averaged.

B. Light Sources

The ideal light source for calorimetric measurements must be of high intensity, stable with time, and of high spectral purity. Thus far, only conventional noncoherent light sources have been used. Tungsten lamps are very stable with time but give useful output only in the visible region of the spectrum; further, their high infrared output is difficult to remove. High pressure mercury and mercury-xenon arc lamps appear to be the most useful of the noncoherent light sources. They generate high-intensity pressure-broadened lines in the visible and ultraviolet, produce a tolerable infrared output, and can be easily stabilized. Monochromatization of light from noncoherent sources has been achieved through use of solution filters, but complete removal of infrared light is not possible. In contrast, interference filters can be fabricated to specification and will remove most unwanted infrared radiation.

Potentially the most useful light sources for calorimetric yield measurements are lasers, just as they are for optical quantum-yield measurements. As discussed above, there are now commercially available several different types of cw gas lasers that lase at a variety of frequencies in the spectral region 320 to 650 nm. The 2-W argon ion laser is a good example (see table 1). Other gas phase lasers commercially available and of possible use in calorimetry are Kr, He-Ne, He-Cd, Se, and Xe. The amplitude stability of these lasers can be made as high as 0.1 percent. Generally, there is some noncoherent plasma radiation in the beam, but this may be removed by interference filters and the use of long pathlengths. The principal drawback to these devices is that their outputs are limited to specific lines, and it is always desirable to excite a molecule at the maximum of its absorption. The availability of the laser-pumped dye lasers should remedy this problem. The narrow line widths, stable outputs, and tuning capabilities over wide spectral regions make them prime candidates for sources in calorimetric quantum-yield determinations.

502-591 O - 73 - 12

If a pulsed light source can be used, then the flash-lamp-pumped dye laser is an ideal choice. As discussed previously, these sources can be tuned continuously in the region 340–600 nm using several different dyes, and their extension farther into the infrared is already at hand. Good short term amplitude stability and high energies per pulse are commercially available in coaxially pumped systems.

C. Conclusions

Calorimetric methods for measuring quantum yields have been little used in the past because of the difficulty of making the measurements and, to some extent, because of the average photochemist's unfamiliarity with the techniques. Recent advances in the technology of calorimetry, the progress in transducer design, and the availability of laser excitation sources promise considerable improvements in the rapidity and accuracy of calorimetric methods. These improvements should lead to wider appreciation of this powerful technique for attacking the fundamental problem of measuring radiative and radiationless efficiencies of excited molecular systems.

VII. References

[1] Demas, J. N., and Crosby, G. A., J. Phys. Chem., **75**, 991 (1971).
[2] Lipsett, F. R., Progr. Dielectrics, **7**, 217 (1967).
[3] Saxena, V. N., Ind. J. Pure Appl. Phys., **9**,407 (1971).
[4] Saxena, V. N., Rense, W. A., and Bruner, E. C., Jr., J. Opt. Soc. Amer., **60**, 865 (1970).
[5] Thornton, W. A., J. Electrochem. Soc., **116**, 286 (1969).
[6] Bruner, E. C., Jr., J. Opt. Soc. Amer., **59**, 204 (1969).
[7] Hammer, A., and Wolf, H. C., Phys. Status Solidi, **33**, K25 (1969).
[8] Nygaard, K. J., Brit. J. Appl. Phys., **15**, 597 (1964).
[9] Kristianpoller, N., J. Opt. Soc. Amer., **54**, 1285 (1964).
[10] Allison, R., Burns, J., and Tuzzolino, A. J., ibid., **54**, 747 (1964).
[11] Al-Ani, Kh., and Phillips, D., J. Phys. Chem., **75**, 3662 (1971).
[12] Borisevich, N. A., and Tolstorozhev, G. B., Bull. Acad. Sci., USSR, Phys. Ser., **34**, 574 (1970).
[13] Nakamura, K., J. Chem. Phys., **53**, 998 (1970).
[14] Robinson, G. W., and Frosch, R. P., ibid., **37**, 1962 (1962).
[15] Robinson, G. W., and Frosch, R. P., ibid., **38**, 1187 (1963).
[16] Siebrand, W., in The Triplet State, A. B. Zahlan, Ed. (Cambridge University Press, London, 1967), p. 31.
[17] Siebrand, W., J. Chem. Phys., **47**, 2411 (1967).
[18] Siebrand, W., ibid., **46**, 440 (1967).
[19] Lin, S. H., ibid., **44**, 3759 (1966).
[20] Bixon, M., and Jortner, J., ibid., **48**, 715 (1968).
[21] Henry, B. R., and Siebrand, W., ibid., **54**, 1072 (1971).
[22] Burland, D. M., and Robinson, G. W., ibid., **51**, 4548 (1969).
[23] Rusakowicz, R., and Testa, A. C., Spectrochim. Acta, **27A**, 787 (1971).
[24] Klueger, J., Fischer, G., Fischer, E., Goedicke, Ch., and Stegemeyer, H., Chem. Phys. Lett., **8**, 279 (1971).
[25] Lentz, P., Blume, H., and Schulte-Frohlinde, D., Ber. Bunsenges. Phys. Chem., **74**, 484 (1970).
[26] Sharafy, S., and Muszkat, K. A., J. Amer. Chem. Soc., **93**, 4119 (1971).
[27] Eastman, J. W., Spectrochim. Acta., **26A**, 1545 (1970).
[28] Strickler, S. J., and Berg, R. A., J. Chem. Phys., **37**, 814 (1962).
[29] Seybold, P. G., Gouterman, M., and Callis, J., Photochem. Photobiol., **9**, 229 (1969).
[30] Douglas, A. E., J. Chem. Phys., **45**, 1007 (1966).
[31] Birks, J. B., and Dyson, D. J., Proc. Roy. Soc., Ser. A, **275**, 135 (1963).
[32] Briegleb, G., Trencseni, J., and Herre, W., Chem. Phys. Lett., **3**, 146 (1969).
[33] Kobayashi, T., Yoshihara, K., and Nagakura, S., Bull. Chem. Soc. Japan, **44**, 2603 (1971).
[34] El-Bayoumi, M. A., Dalle, J. D., and O'Dwyer, M. F., J. Amer. Chem. Soc., **92**, 3494 (1970).
[35] Demas, J. N., and Crosby, G. A., ibid., **92**, 7262 (1970).
[36] Demas, J. N., and Crosby, G. A., ibid., **93**, 2841 (1971).
[37] Watts, R. J., and Crosby, G. A., ibid., **94**, 2606 (1972).
[38] Harrigan, R. W., and Crosby, G. A., Abstracts, 163rd National Meeting of the American Chemical Society, Boston, Mass., April 1972, Phys. 105.
[39] Hager, G. D., and Crosby, G. A., 1972, unpublished results.
[40] Englman, R., and Jortner, J., Mol. Phys., **18**, 145 (1970).
[41] Lim, E. C., and Bhattacharjee, H. R., Chem. Phys. Lett., **9**, 249, (1971).
[42] Ricci, R. W., Photochem. Photobiol., **12**, 67 (1970).
[43] Thomas, T. R., Watts, R. J., and Crosby, G. A., J. Chem. Phys. (in press).
[44] Callis, J. B., Gouterman, M., and Danielson, J. D. S., Rev. Sci. Instrum., **40**, 1599 (1969).
[45] Bonnier, J. M., and Jardon, P., J. Chim. Phys. Physicochim. Biol., **67**, 577 (1970); **66**, 1506 (1969).
[46] Bonnier, J. M., Jardon, P., and Blanchi, J. P., Bull. Soc. Chim. Fr., **12**, 4787 (1968).
[47] Wilkinson, F., and Dubois, J. T., J. Chem. Phys., **39**, 377 (1963).
[48] Förster, Th., Ann. Physik, **2**, 55 (1948).
[49] Weber, G., and Teale, F. W. J., Trans. Faraday Soc., **53**, 646 (1957).
[50] Pringsheim, P., Fluorescence and Phosphorescence (Interscience Publishers, Inc., New York, N.Y., 1949).
[51] Bowers, P. G., and Porter, G., Proc. Roy. Soc., Ser. A, **299**, 348 (1967).
[52] Medinger, T., and Wilkinson, F., Trans. Faraday Soc., **61**, 620 (1965).
[53] Horrocks, A. R., Medinger, T., and Wilkinson, F., Chem. Commun., 452 (1965).
[54] Medinger, T., and Wilkinson, F., Trans. Faraday Soc., **62**, 1785 (1966).
[55] Horrocks, A. R., Kearvell, A., Tickle, K., and Wilkinson, F., ibid., **62**, 3393 (1966).
[56] Horrocks, A. R., Medinger, T., and Wilkinson, F., Photochem. Photobiol., **6**, 21, (1967).
[57] Horrocks, A. R., and Wilkinson, F., Proc. Roy, Soc., Ser. A, **306**, 257 (1968).
[58] Gradyushko, A. T., Sevchenko, A. N., Solovyov, K. N., and Tsvirko, M. P., Photochem. Photobiol., **11**, 387 (1970).
[59] Ermolaev, V. L., and Sveshnikova, E. B., Acta Phys. Polon., **34**, 771 (1968).
[60] Seybold, P. G., and Gouterman, M., J. Mol. Spectrosc., **31**, 1 (1969).
[61] Kropp, J. L., Dawson, W. R., and Windsor, M. W., J. Phys. Chem., **73**, 1747 (1969).
[62] Gill, J. E., Photochem. Photobiol., **11**, 259 (1970).
[63] Leng, M., Pochon, F., and Michelson, A. M., Biochim. Biophys. Acta, **169**, 338 (1968).
[64] Pochon, F., Leng, M., and Michelson, A. M., ibid., **169**, 350 (1968).
[65] Ward, D. C., Reich, E., and Stryer, L., J. Biol. Chem., **244**, 1228 (1969).
[66] Edelman, G. M., and McClure, W. O., Accounts Chem. Res., **1**, 65 (1968).
[67] Stryer, L., Science, **162**, 526 (1968).
[68] Winkler, M., J. Mol. Biol., **4**, 118 (1962).
[69] Kingdon, H., Fed. Proc., **26**, 842 (1967).
[70] McClure, W. O., and Edelman, G. M., Biochemistry, **6**, 567 (1967).
[71] Crosby, G. A., Harrigan, R. W., and Watts, R. J., patent applied for.
[72] Demas, J. N., and Adamson, A. W., J. Amer. Chem. Soc., **93**, 1800 (1971).
[73] Watts, R. J., and Crosby, G. A., ibid., **93**, 3184 (1971).
[74] Testa, A. C., Fluorescence News, **4**, No. 4, 1 (1969).
[75] Gill, J. E., Photochem. Photobiol., **9**, 313 (1969).
[76] Spencer, R. D., Vaughan, W. M., and Weber, G., in Molecular Luminescence, E. C. Lim, Ed. (W. A. Benjamin, New York, N.Y., 1969), p. 607.

[77] Ness, S., and Hercules, D. M., Anal. Chem., **41**, 1467 (1969).
[78] Druding, L. F., and Kauffman, G. B., Coordin. Chem. Rev., **3**, 409 (1968).
[79] Clifford, H. J., Ph. D. dissertation, University of New Mexico, 1971.
[80] Vaviloy, S. I., Z. Phys., **22**, 266 (1924).
[81] Bowen, E. J., and Sawtell, J. W., Trans. Faraday Soc., **33**, 1425 (1937).
[82] Förster, Th., Fluoreszenz Organischer Verbindungen (Vandenhoeck-Ruprecht, Göttingen, Germany, 1951).
[83] Gilmore, E. H., Gibson, G. E., and McClure, D. S., J. Chem. Phys., **20**, 829 (1952); **23**, 399 (1955).
[84] Melhuish, W. H., New Zealand J. Sci. Tech., **37**, 142 (1955).
[85] Almgren, M., Photochem. Photobiol., **8**, 231 (1968).
[86] S.P.I.E. Seminar Proceedings, Developments in Laser Technology, Vol. 20, University of Rochester, 1969.
[87] Hanna, D. C., and Smith, R. C., Sci. J., **5**, 53 (1969).
[88] Goldstein, A., and Dacol, F. H., Rev. Sci. Instrum., **40**, 1597 (1969).
[89] Furumoto, H. W., and Ceccon, H. L., IEEE, J. Quant. Electron., **6**, 262 (1970).
[90] Soffer, B. H., and Linn, J. W., J. Appl. Phys., **39**, 5859 (1968).
[91] Snavely, B. B., Proc. IEEE, **57**, 1374 (1969).
[92] DeMaria, A. J., Glenn, W. H., and Mack, M. E., Phys. Today, **24**, 19 (1971).
[93] Sorokin, P., Sci. Amer., **220**, 30 (1969).
[94] Smith, R. G., Anal. Chem., **41**, 75A (1969).
[95] Tansley, T. L., and Ralph, J. E., J. Phys. D, **3**, 807 (1970).
[96] Mathur, D. P., McIntyre, R. J., and Webb, P. P., Appl. Opt., **9**, 1842 (1970).
[97] Haecker, W., Groezinger, O., and Pilkuhn, M. H., Appl. Phys. Lett., **19**, 113 (1971).
[98] Melhuish, W. H., J. Phys. E, **4**, 60 (1971).
[99] Bojarski, C., Kusba, J., and Obermüller, G., Z. Naturforsch., **A26**, 255 (1971).
[100] Weller, A., and Zachariasse, K., Chem. Phys. Lett., **10**, 424 (1971).
[101] Wegner, E. E., and Adamson, A. W., J. Amer. Chem. Soc., **88**, 394 (1966).
[102] Demas, J. N., and Adamson, A. W., Manuscript in preparation.
[103] The term fluorescence is used here in the general sense, i.e., to include all radiative processes whether spin allowed or spin forbidden.
[104] Alentsev, M. A., National Research Council of Canada Technical Translation TT-433, Zh. Eksp. Teor. Fiz., **21**, 133 (1951).
[105] Brown, H. D., Ed., Biochemical Microcalorimetry (Academic Press, Inc., New York, N.Y., 1969).
[106] Wadsö, I., Quart. Rev. Biophys., **3**, 383 (1970).
[107] McCullough, J. P., and Scott, D. W., Ed., Experimental Thermodynamics, Vol. 1 (Plenum Press, Inc., New York, N. Y., 1968).
[108] Weissberger, A., Ed., Techniques of Organic Chemistry, 3d ed, Vol. 1 (Interscience Publishers, Inc., New York, N.Y., 1959), Ch. 10.
[109] Hill, A. V., Trails and Trials in Physiology (Edward Arnold, London, 1965).
[110] Howarth, J. V., Quart. Rev. Biophys., **3**, 429 (1970).
[111] Evans, W. J., in Biochemical Microcalorimetry, H. D. Brown, Ed. (Academic Press, Inc., New York, N.Y., 1969), Ch. 14.
[112] Larsen, N. T., Rev. Sci. Instrum., **39**, 1 (1968).
[113] Meites, T., Meites, L., and Jaitly, J. N., J. Phys. Chem., **73**, 3801 (1969).
[114] Zamyatnin, A. A., Russ. J. Phys. Chem., **45**, 567 (1971).
[115] Calvet, E., and Prat, H., Recent Progress in Microcalorimetry (translated by H. A. Skinner)(The Macmillan Co., New York, N.Y., 1963).
[116] Calvet, E., and Prat, H., Microcalorimetrie (Masson, Paris, 1956).
[117] Chastel, R., and Tachoire, H., Rev. Gen. Elec., **77**, 871 (1968).
[118] Buzzell, A., and Sturtevant, J. M., J. Amer. Chem. Soc., **73**, 2454 (1951).
[119] Gudmundsen, R. A., Marsh, O. J., and Matovich, E., J. Chem. Phys., **39**, 272 (1963).
[120] Wilson, E. B., Introduction to Scientific Research (McGraw-Hill Book Co., Inc., New York, N.Y., 1952).

(Paper 76A6-742)

NATIONAL BUREAU OF STANDARDS SPECIAL PUBLICATION 378, Accuracy in Spectrophotometry and Luminescence Measurements, Proceedings of a Conference Held at NBS, Gaithersburg, Md., March 22–24, 1972 (Issued May 1973).

Phosphorimetry*

J. D. Winefordner

Department of Chemistry, University of Florida, Gainesville, Florida 32601

(July 26, 1972)

Phosphorimetry in the past has received limited use because the precision of reproducibility was inadequate, there were solvent limitations, and preparation of test specimens was difficult and time consuming. Detection limits have now been lowered by more than two orders of magnitude by using a rotating capillary sample cell, a more stable excitation-source power supply, and aqueous solvents. These steps have also increased precision by more than an order of magnitude. Considerable reduction in time and effort of sampling and measurement has been effected compared to phosphorimetric measurements made with standard procedures and commercial equipment. Twenty microliters of aqueous solution is all that is required to fill a quartz capillary cell by capillary action. Capillary cells filled with aqueous solutions do not crack when cooled to 77 K or when returned to room temperature. Rotation of the sample cell minimizes effects due to cell orientation and thus improves precision. Reduction of background phosphorescence results in improved accuracy of analysis. A study was made of the influence of methanol-water mixtures and of sodium-halide aqueous solutions on the magnitude of phosphorescence signals from several substances and of the effect on signal-to-noise ratios. The optimum solvent system for many phosphorimetric measurements is discussed. Analytical results are given for several organic substances measured by phosphorimetry at 77 K. These results are compared with those from previous studies by older methods.

Key words: Aqueous solvents in phosphorimetry; phosphorimetry; rotating capillary cell; solvents for phosphorimetry.

I. Introduction

Phosphoresence is a type of photoluminescence in which radiation is emitted by a molecule following radiational excitation of the molecule by means of radiation of higher energy than the emitted radiation. Phosphorescence involves two singlet-triplet transitions and as a result has a longer lifetime than fluorescence which involves two singlet-singlet transitions. Because the first triplet level of a molecule with an even number of electrons has lower energy than the first excited singlet level of the same molecule, phosphorescence also involves lower energy transitions than fluorescence, and so the phosphorescence spectrum of a given molecule occurs at longer wavelengths than the fluorescence spectrum of the same molecule. The mechanism of the production of phosphorescence is well known [1–3][1] and so will not be discussed. This manuscript is concerned with the analytical uses of phosphorescence for quantitative analyses of organic molecules—called phosphorimetry. Zander [4], Winefordner, McCarthy, and St. John [5], Winefordner, St. John, and McCarthy [6], McCarthy [7], and Winefordner, Schulman, and O'Haver [8] have reviewed and described the instrumentation, the methodology, and the uses of phosphorimetry.

Phosphorimetry has been used during the past decade for a limited number of quantitative analyses, e.g., the analysis of impurities in polycyclic aromatic hydrocarbons [9–11], in coal tar fractions [12], in air [13–15], and in petroleum fractions [16–18], the analysis of inhibitors in petroleum products [19], the analysis of pesticides, fungicides, oils, etc., in foods [20–25], and the analysis of amino acids and pharmaceuticals in biological fluids [27–35]. It is evident that up to now, phosphorimetry has been utilized only sparingly as an analytical tool for quantitative analysis and has been confined primarily to those cases where other analytical methods, such as fluorimetry and absorption spectrophotometry, either cannot be used due to lack of sensitivity or presence of interferences or give ambiguous results, and so additional analytical information is desirable. In fact, fluorimetry and absorption spectrophotometry have often been used for quantitative analyses which could quite well have been performed with greater precision, accuracy, and speed by means of phosphorimetry. The lack of use of phosphorimetry (with commercial spectrofluorimeters with phosphoroscope attachments) for quantitative analysis has been a result of the following factors: (i) the greater complexity and time to carry out an analysis due to the use of small sample cells which are difficult

*Research was carried out as part of a study on the phosphorimetric analysis of drugs in blood and urine, supported by a U.S. Public Health Service Grant (GM–11373–09).

[1] Figures in brackets indicate the literature references at the end of this paper.

to clean, fill, align, and empty, the need for solvents which form clear, rigid glasses at liquid nitrogen temperatures, and the use of liquid nitrogen for sample cell cooling; (ii) the poor precision and accuracy of measurements due to the difficulty of alignment of the sample cell in the Dewar flask containing the coolant, due to the poor source stability—particularly long term drift, and due to the ease of contamination of glassware, cells, and solvents; and (iii) the marginal sensitivity (limits of detection) for many molecules due to light losses resulting from the excessive number of optical surfaces, the small sample cells, and the use of the phosphoroscope (mechanical chopper) which cuts out more than 75 percent of the measured signal as compared to continuous excitation-measurement. In this manuscript, the instrumental methods utilized in the author's laboratory to eliminate or minimize the above limitations will be described and typical analytical data indicating the improvement in results will be given.

II. Typical Commercial Phosphorimeter

In order to compare the improvements made in phosphorimetric instrumentation, it is necessary to describe the typical commercial phosphorimeter. A block diagram of a typical commercial spectrophotofluorimeter with rotating can phosphoroscope which has been used by the author (e.g., AMINCO SPF[2] with phosphoroscope assembly) is shown in figure 1. The source of excitation energy is generally a continuously-operated xenon arc lamp driven from a well-regulated dc power supply so as to minimize long-term drift. A portion of the source radiation is introduced into the excitation monochromator to produce a small spectral band of excitation radiation which is focused upon the sample cell, usually a quartz tube (containing sample) which is placed in a quartz Dewar flask which contains a coolant (usually liquid nitrogen) for freezing the sample (see fig. 2). A fraction of the phosphorescence emission is observed by the emission monochromator, and the wavelength region of interest is thus presented to the transducer, usually a multiplier phototube with an S–4 or S–5 response. In the averaging dc measurement systems, frequently employed in commercial spectrophotofluorimeters, the current (usually 10^{-6} to 10^{-9} A) is amplified and either read out directly from a meter face or on a time base or x–y recorder (the x–y recorder is most frequently employed when utilizing one of the monochromators in the scanning mode for recording of spectra, and the time-base recorder is often used for quantitative measurements at one set of excitation and emission wavelengths).

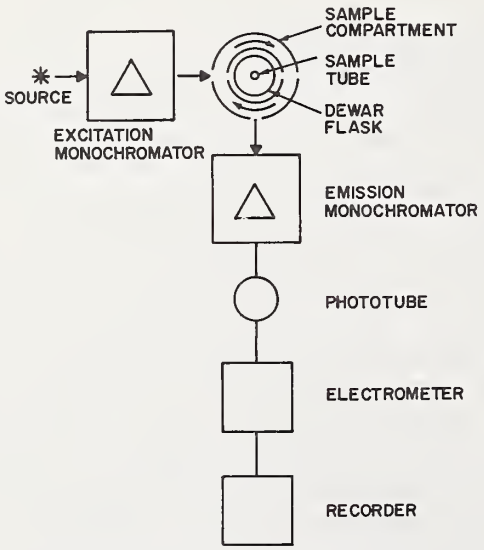

FIGURE 1. Block diagram of typical commercial analytical spectrophotofluorimeter with phosphoroscope attachment.

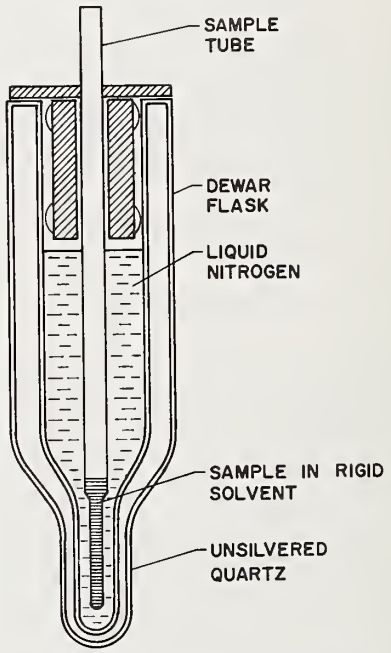

FIGURE 2. Schematic diagram of typical commercial sampling system for phosphorimetry.

A means for terminating exciting light and allowing measurement of a portion of the phosphorescence radiation without interference from the intense, scattered, incident radiation and the faster decaying fluorescence radiation must be included in the phosphorimeter design. The instrument diagrammed in figure 1 utilizes a typical rotating-can phosphoroscope, shown in greater detail in figure 3. In operation, the sample is excited for a short time through a window in the can; the can rotates to terminate excitation, after

[2] In order to adequately describe materials and experimental procedures, it was occasionally necessary to identify commercial products by manufacturer's name or label. In no instances does such identification imply endorsement by the National Bureau of Standards, nor does it imply that the particular product or equipment is necessarily the best available for that purpose.

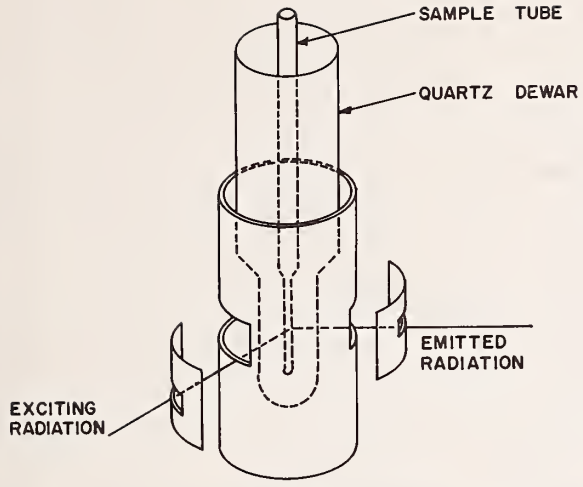

FIGURE 3. Schematic diagram of a typical rotating can phosphoroscope.

which another window is presented to the detection axis. The phosphorescence signal is observed through this window until the window moves off-axis, then the process is repeated. The instrumental response time constant employed in the dc measurement systems used with such phosphorimeters is usually made sufficiently large so as to provide a steady phosphorescence signal at all but the slowest phosphoroscope speeds.

Other means of modulation, such as the Becquerel disc phosphoroscope and pulsed source-gated detector systems, are not used in commercially available phosphorimeters. The pulsed source-gated detector system is by far the most versatile and potentially the most useful analytical system for phosphorimetry. All improvements discussed in this manuscript will be with respect to the system described above and shown in figure 1.

III. Instrumental Improvements in Phosphorimetry

A. Solvent Selection and Sampling Technique Improvements

Phosphorescence is generally not observed in liquid solutions at room temperature because radiationless deactivation due to collisions which occur within the lifetime of the excited molecule result in low phosphorescence quantum yields [36] producing phosphorescence signals buried within the phosphorescence background noise [37]. Therefore, all analytical phosphorimetric studies have been carried out in rigid media [4–8]. The criteria previously used to select a solvent for phosphorimetry have been: solubility of the analyte; low phosphorescence background (easy to purify); and formation of a clear, rigid glass at 77 K (boiling point of liquid nitrogen which is a safe, inexpensive, optically transparent coolant).

Unfortunately few solvents, particularly very polar ones, form transparent glasses at 77 K [38–40]. Ethanol is an excellent polar solvent for phosphorimetry. Small volume percents of water, mineral acids, and strong bases can also be combined with ethanol to produce clear rigid media at 77 K. The most popular mixed solvent has been EPA (a 5:5:2 volume ratio of diethyl ether, isopentane, and ethanol). Unfortunately, these solvents either do not have good solubility characteristics or result in irreversible changes of many organic species, particularly those of biological importance. Solvents, which are crystalline or severely-cracked at 77 K, have been used for some qualitative studies [41–44] but have generally been ignored or discounted as solvents for quantitative measurements. Scattering [45] and surface reflections [46] have been cited as reasons for not using snowed media [4–8] in analytical studies. The cracks or crystals create optical inhomogeneities in the medium which result in nonreproducible phosphorescence signals. Freed and Vise [29], as well as Parker and Hatchard [47], have suggested the use of an internal standard (spectrally removed from the molecule of interest) to be used as a reference to compensate for variations in sample positioning and cracking of the medium. The use of an internal standard offers a reasonable solution to the problem of sample positioning and occasional cracking; however, the choice of an internal standard satisfying the above criteria and not undergoing chemical or physical interaction with the compound being studied is extremely difficult and time consuming. In addition, the use of an internal standard is not applicable to the case of snowed or cracked media because the phosphorescence signal may be influenced by the extent of scattering, which can be wavelength dependent as long as the effective particle size is small [48, 49].

An alternative to the internal standard technique was suggested first by Hollifield and Winefordner [50] and later improved upon by Zweidinger and Winefordner [51] and still later by Lukasiewicz, Rozynes, Sanders, and Winefordner [52], and by Lukasiewicz, Mousa, and Winefordner [53, 54] all of whom used a rotating sample cell assembly to average all orientations of the sample cell, thus resulting in greater precision and accuracy of phosphorometric measurements in clear, rigid glasses [50], in rigid organic snows [51], and in rigid, aqueous snows [52–54]. In addition, there are no difficulties encountered with sample positioning and alignment.

Lukasiewicz, et al. [52–54] have added another great improvement to allow the measurement of aqueous or predominately aqueous solutions at 77 K by means of phosphorimetry. These workers used an open quartz capillary cell as the sample cell. Sample solutions ($\sim 20\ \mu l$) fill the cell by capillary action, and the sample cell is then rotated as described above. As a result of the open capillary cell, these cells with predominately, or pure, aqueous solutions do not crack when rapidly cooled to liquid N_2 temperatures or when warmed back to room temperature by use of a heat gun. Of course, the major advantage of using aqueous or aqueous-organic solutions in phos-

phorimetry are: most biochemical species are more soluble in aqueous solutions than in the solvents needed to produce clear, rigid glasses at liquid nitrogen temperatures; the solution conditions, e.g., pH, ionic strength, etc., can be varied for optimal analytical results; water is easier to obtain in higher phosphorimetric purity than most organic solvents; and contamination problems are less when water can be used to clean glassware, cells, and equipment.

The rotating sample cell assembly currently being used is a modification of the one described by Hollifield and Winefordner [50]; the present system, described in detail by Zweidinger and Winefordner [51] and modified by Lukasiewicz, et al. [52–54], is shown in figure 4. The rotating assembly consists primarily of a Varian A60–A high resolution NMR spinner assembly (Varian Associates, Palo Alto, Calif.) mounted on an AMINCO phosphoroscope sample compartment in place of the usual lid. The pressure cap of the spinner assembly is covered with black tape to ensure a completely light-tight sample compartment. The rotating sample cell is driven by a flow of nitrogen gas or air taken from a compressed gas cylinder. The sample cell must have a 6 mm o.d. and be about 25 cm long. The sample rotation is maintained at some constant speed between 450 and 1400 rpm; the actual speed is unimportant as long as it is constant during a series of measurements and can be assured by means of a normal two-stage regulator and a rotameter flow meter to monitor the gas flow rate. The normal quartz sample cells used by Zweidinger and Winefordner [51] were 5 mm o.d. and 3 mm i.d., whereas the quartz capillary cells used by Lukasiewicz, et al. [52–54] were 5.0 mm o.d. and 0.90 mm i.d. The cells were made of synthetic, high-purity, optical-grade quartz (Quartz Scientific Co., Eastlake, Ohio for the capillary tubing and Amersil, Inc., Hillside, New Jersey for the normal tubing).

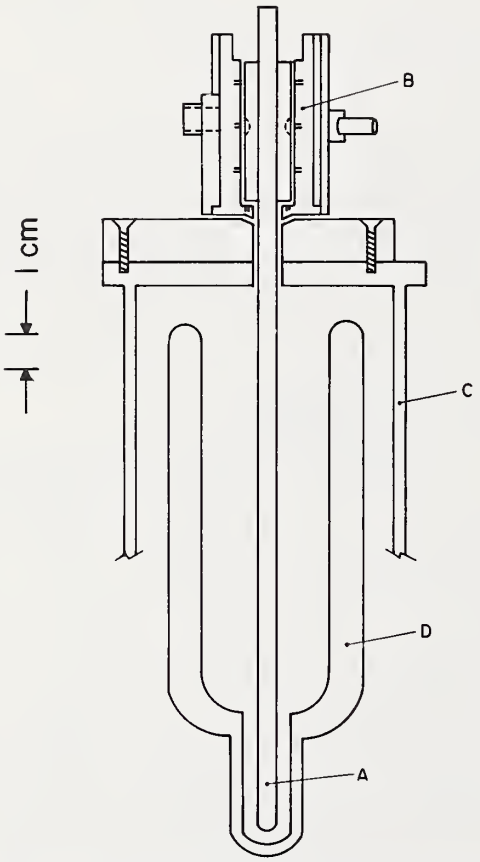

FIGURE 4. Schematic diagram of rotating sample cell assembly [51].
A. Quartz sample cell
B. Varian (909614–04) spinner assembly for NMR
C. Aminco light cover mount
D. Aminco quartz Dewar flask

The inherent photoluminescence of the quartz resulted in an appreciable "phosphorescence" background, especially with the capillary cells. However, the long-lived luminescence of the quartz cells could be minimized by mounting an excitation polarizer oriented perpendicular to the sample cell length between the sample cell housing and excitation monochromator entrance slit. Luminescence excitation spectra of the long-lived component of the quartz capillary sample cells are shown in figures 5 and 6. It can be seen from the results in figure 6 that the lowest background was obtained when both polarizers were used. For quantitative work, however, use of both polarizers is undesirable because each polarizer has a low transmittance and the loss of sensitivity is compounded. The background resulting when only one polarizer was used in the excitation beam was slightly higher than that obtained with two polarizers but still approximately 100 times lower than the background obtained without the use of the excitation polarizer.

The improvement in precision of measurement when the normal sample cell was rotated as opposed to not rotated is given in table 1. It should be stressed that the rotating sample cell holder, even when used in the stationary aligned mode (no rotation), can provide and increase in precision of as much as tenfold over the same cell in random orientation. When the normal sample cell is rotated, a further improvement in precision of about twofold is obtained (see table 1). It is interesting to note that the precision for snowed and cracked matrices is not significantly different from that for an ethanolic, clear matrix. The stationary, randomly oriented sample cell measurements were considerably more precise than those obtained by Hollifield and Winefordner [50] because of the close tolerances of the present rotating sample cell system. One great advantage of using the rotating sample cell is the simplicity of positioning the cell. After the normal sample cell is cleaned and filled (requires about five minutes), the cell with the Teflon (du Pont) turbine is simply dropped into place and spun by flow

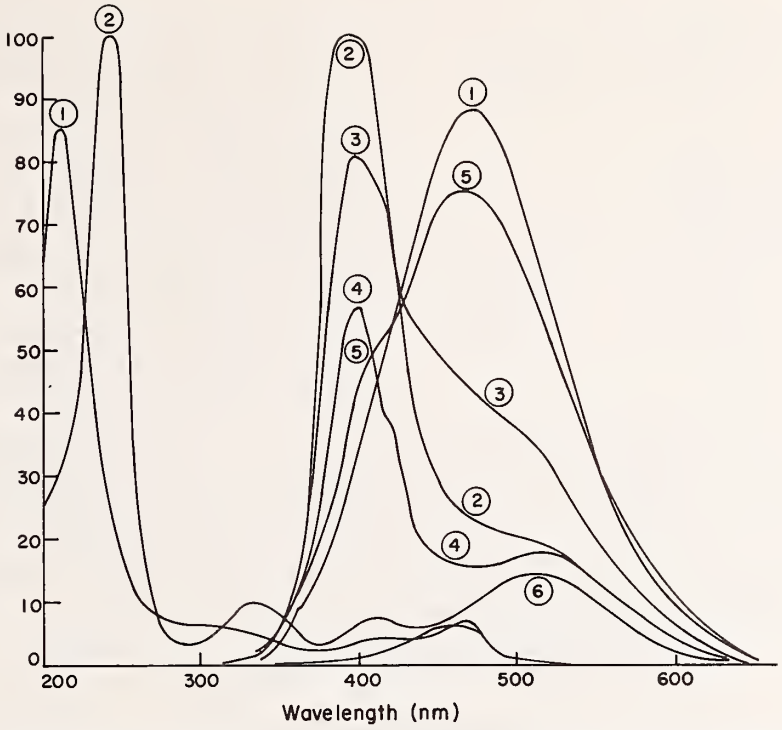

FIGURE 5. Excitation and emission spectra of long-lived component of quartz capillary sample tube (no polarizer used) spectra 1, 2, 3, 4, 5, and 6 corresponding to excitation at wavelengths 210, 240, 230, 250, 220, and 280 nm respectively.

TABLE 1. Precision of phosphorescence measurements [a] for clear glasses and snows using rotating sample cell assembly [51]

Number of determinations	Nature of matrix	Relative percent standard deviation: Stationary [a,d] random orientation	Stationary [a,e] aligned	Rotating [a,f]
4	Clear [b]	8.7	1.3	0.8
6	Clear [b]	6.0	0.5	0.8
5	Cracked [b]	13.7	3.4	1.4
11	Clear [b]	3.1	0.9	0.3
10	Clear [b]	2.9	2.8	1.0
5	Snow [c]	3.6	1.6	0.9
10	Snow [c]	2.8	0.8	0.6
10	Snow [c]	2.7	2.4	0.7

[a] Phosphorescence measurements were made on 1.6×10^{-5} M sulfanilamide solutions which give a signal five orders of magnitude above phototube dark current. The normal rotating sample cell was used.

[b] Ethanol solvent.

[c] Isooctane : ethanol, 4 : 1, v/v mixture as solvent.

[d] This column is indicative of the reproducibility obtainable with the commercial sampling system.

[e] This column gives results for the rotating normal sample cell assembly but with the normal cell stationary in the assembly.

[f] This column gives results for the rotating normal sample cell assembly but with the normal cell rotating in the assembly.

of compressed air. As a result of spinning the cell, the inner filter effect is also minimized.

A series of 10 replicate determinations of 1 μg/ml 2-thiouracil in 10 percent v/v methanol-water were measured to determine the precision obtainable with the rotating quartz capillary cell. The relative standard deviation obtained was 1.5 percent. This is an improvement of nearly an order of magnitude over the stationary quartz capillary tube system used by Lukasiewicz, Rozynes, Sanders, and Winefordner [52], and compares favorably with the standard deviations of results obtained with normal rotating sample cells (see table 1). The major noise contribution in the system with the rotating capillary cell arises from wobble of the cell caused by the loose fit of the turbine sleeve in the spinner assembly. If the capillary cell were held rigidly by the turbine sleeve so that no wobble occurs on rotation the precision would probably be comparable to the best data reported in table 1 for the larger, normal quartz, sample cell.

B. Improvements in Precision and Accuracy of Phosphorimetry

The relative percent standard deviations obtainable with the typical commercial system shown sche-

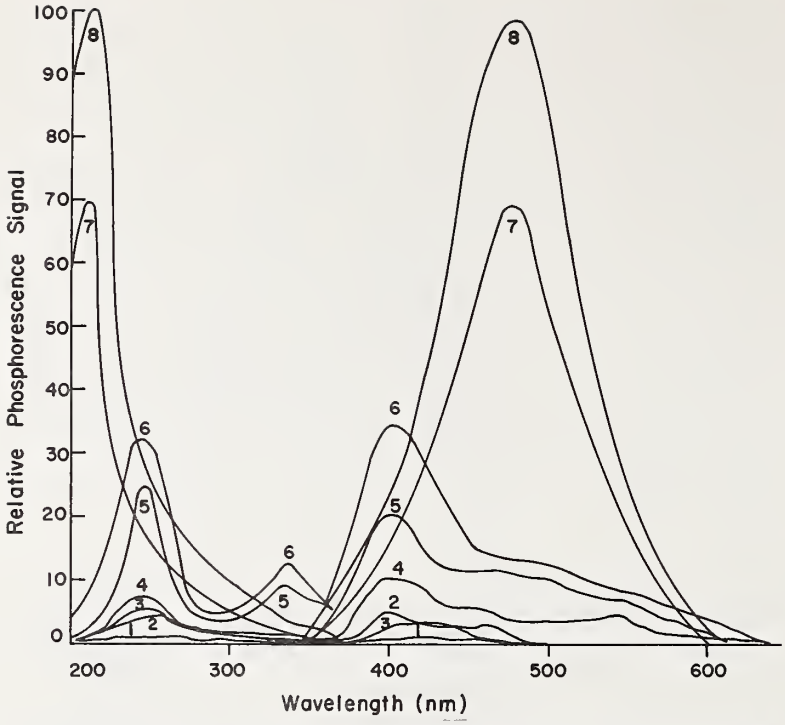

FIGURE 6. Excitation and emission spectra of long-lived component of quartz capillary sample tube, using polarized radiation; orientation of polarizers with respect to vertical axis of cell as follows [52]:

	Excitation	Emission
1.	⊥	∥
2.	∥	∥
3.	⊥	⊥
4.	∥	⊥
5.	∥	no polarizer
6.	⊥	no polarizer
7.	no polarizer	⊥
8.	no polarizer	∥

Spectra 1 thru 6 were obtained with a gain of 5-fold; full-scale approximately equal to twice level of dark current of multiplier phototube. Spectra 7 and 8 were obtained with a gain of unity.

matically in figure 1 are given in table 1. By using the rotating sample cell system as well as a more stable xenon lamp power supply, the precision of phosphorimetric measurements can be increased by as much as tenfold (see data in table 1). In addition, the contamination of glassware, solvents, and sample cells with phosphorescent impurities seriously limits precision of measurements, particularly at low concentrations of analyte. Zweidinger, Sanders, and Winefordner [55] have described techniques for cleanup of sample cells and glassware. These authors recommend cleaning the sample cells and glassware used in solution preparation in an ultrasonic cleaner for about 30 seconds or in concentrated nitric acid if there is serious contamination; when contamination is extremely serious the item can be heated in an oven or placed directly in a flame. Of course, solvents used in phosphorimetry should be purified by distillation, zone freezing, or some other separation method. It should be stressed that distillation of demineralized

water results in a solvent of extremely low phosphorescence background compared to ethanol, EPA, or any other commonly used organic solvent.

By use of an elliptical source condensing system and a more stable xenon lamp power supply, it was possible to reduce drift and noise by about tenfold as compared to those obtained with the standard power supply in the commercial phosphorimeter. The elliptical source condensing system is commercially available (in our case, from American Instrument Co., Inc., Silver Spring, Maryland). The xenon lamp power supply system was assembled using a highly regulated power supply (Harrison Lab Model 6268 A, Hewlett-Packard, Palo Alto, Calif.) operating in the constant current mode at 7.5 A (150 W lamp) with the addition of the starter circuit shown in figure 7.

A comparison of phosphorescence signals and signal-to-noise ratios obtained with the rotating normal sample cell and the Zweidinger, Sanders, and Winefordner [55] sample cell cleanup procedure with the earlier cleanup procedure of Tin and Winefordner [56] is given in table 2.

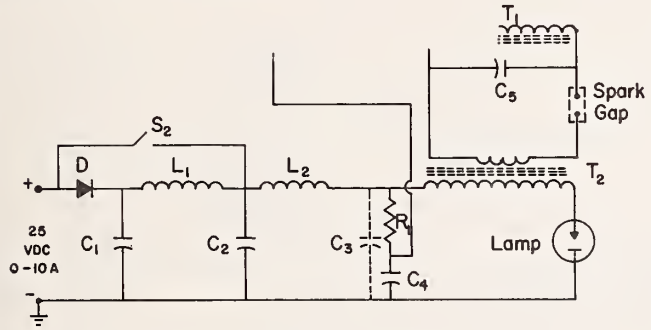

FIGURE 7. Starter circuit for xenon arc lamp (51).

C_1, C_2, C_3—0.5 μF (300 VDC)
C_4 —1300 μF (300 VDC)
C_5 —0.01 μF (30,000 VDC)
C_6 —100 μF (300 VDC)
R_1 —1 Ω
R_2 —1 k Ω
R_3 —1.8 k Ω
S_1 —Momentary contact switch
S_2 —15 Ampere switch—to be closed only after lamp ignites
L_1 —300 mH (10 A, hand wound on ferrite core)
L_2 —30 mH (15 A, hand wound on ferrite core)
D —Diode (15 A, 300 PIV)
T_1 —Autotransformer
T_2 —10 : 1 Ratio transformer

C. Decrease in Limits of Detection in Phosphorimetry

Limits of detection in phosphorimetry are reduced if either the signal level can be increased and/or the noise level can be reduced. By use of the more stable xenon lamp power supply, the elliptical source condensing system, the rotating sample cell assembly, and the improved cleanup procedure as well as the use of aqueous solutions for some molecules, the noise level is reduced and thus detection limits are also reduced. By use of more intense continuously operated or pulsed with gated detector, light sources phosphorescence signals can also be increased and detection limits are decreased even more.

TABLE 2. Comparision of signals and signal-to-noise ratios with rotating normal sample cell and with or without new cleanup procedure [55]

	Signal (nA)[a, b]	Signal-to-background fluctuation[b, c]	Signal-to-noise[b, d]
Conventional cleanup procedure	1.5(0.05)[e, f]	2.5	100[15][e]
New cleanup procedure	0.3[f]	25	45

[a] Signal is due to impurities in ethanol (solvent) background.
[b] All signals, signal-to-background fluctuations, and signal-to-noise ratios are approximate. Excitation is at 262 nm and emission is measured at 380 nm.
[c] Background fluctuation is percent standard deviation of five background readings.
[d] Time constant for all measurements was 0.3 s.
[e] Values in parentheses were obtained without the Aminco elliptical condensing system (American Instrument Co., Inc., Silver Spring, Maryland).
[f] Dark current is approximately 0.02 nA.

The improvement in detection limits, resulting primarily from noise reduction due to the processes described in the above paragraph, is given in table 3 for the measurement of several organic molecules using normal sample cells in the rotating sample cell assembly. Similarily, detection limits obtained for several organic molecules measured using the quartz capillary cells in the rotating sample cell assembly are given in table 4. The range of linearity and limits of detection reported in table 4 compare favorably with those previously obtained in clear, rigid glasses in the normal sample cell (see table 3), even though the sample volume is an order of magnitude smaller with the capillary cell. Because of the small volume of sample solution retained in the capillary tube, the total number of grams of analyte necessary for a determination is in the picogram region, and thus phosphorimetry can be considered both a trace and micro method of analysis. This should be of particular importance in biological and clinical applications where sample size is often limited. The average slopes of the analytical curves (logarithm of phosphorescence signal versus logarithm of analyte concentration) for the molecules in tables 3 and 4 are 0.94 which approaches the ideal slope of unity for phosphorescence signals in snowed matrices [51]. Both positive and negative deviations

TABLE 3. Phosphorescence characteristics of several organic molecules studied [51]

Compound	Solvent	Concentration range (M) of near linearity	Slope of linear portion	Relative percent standard deviation [a]	Linear correlation coefficient	Limit of detection (μg/ml [g])	Limit of detection (μg/ml [h])
Toluene	Ethanol [b]	10^3	0.94	1.5	0.9999	0.03	.....
Toluene	Propylene glycol: [c] water/ (9 : 1, *v/v*)	10^3	.76	[d] 2.5	.9999	.03	.....
Toluene	Isooctane [c]	10^3	.89	[e] 0.9 [f] (6.1)	.9998	.02	.....
Sulfanilamide	Isooctane: [c] Ethanol/ (4 : 1, *v/v*)	10^5	.96	[e] .8 [a] (1.1)	.9998	.0004	[i] .012
Oxythiamine HCl	Isooctane: [c] Ethanol/ (4 : 1, *v/v*)	10^2	1.01	1.9	1.0000	.34	.....
3-Acetylpyridine	Isooctane [c]	10^5	1.03	1.9	1.0000	.012	[i] 3.6

[a] For samples giving signals 5 times the limit of detection.
[b] Formed clear glasses.
[c] Formed snowed samples.
[d] Harrison power supply not used.
[e] Linear portion of the analytical curve.
[f] Nonlinear portion of the analytical curve.
[g] Limits of detection in this study [51].
[h] Best previous limits of detection using standard commercial phosphorimetric equipment.
[i] From Reference 57.

TABLE 4. Phosphorescence characteristics of molecules studied [54]

Compound	Slope of linear portion	Limit of detection (μg/ml)	Number of grams [b] at limit of detection	Concentration range of near linearity
p-Nitrophenol [c]	0.88	7×10^{-3}	1.24×10^{-10}	10^4
Sulfamethazine [a]	1.01	6×10^{-3}	1.07×10^{-10}	10^4
2-Thiouracil [a]	0.81	7×10^{-4}	1.24×10^{-11}	10^4

[a] Solvent 10 percent (*v/v*) methanol water, all solutions formed snowed samples.
[b] Volume of sample retained in capillary tube calculated as 17.8 μl.
[c] Solvent 10 percent (*v/v*) methanol water with 1 percent by volume saturated NaOH added.

from a slope of unity have been observed; however, much more data is necessary before a conclusion can be drawn as to whether an individual molecule perturbs the crystalline matrix and alters the slope or whether the deviations can be attributed to instrumental parameters influencing the precision and accuracy of signal measurements. Present theory assumes the scattering coefficient of the sample is not a function of solute molecule or concentration [51, 53].

D. Pulsed-Source Gated-Detector Phosphorimetric System

Fisher and Winefordner [58] have described a pulsed-source gated-detector system for phosphorimetry; such a system was shown to allow an increase in selectivity of analysis due to the use of time resolution [59], which will not be discussed here, and an increase in sensitivity of analysis due to the increased signal-to-noise ratio. The latter increase is a result of an increased signal and a decreased noise. The basis of pulsed-source systems and the system of Fisher and Winefordner [58] will be briefly described in the following paragraphs.

A pulsed-source gated-detector phosphorimetric system consists of much of the same equipment found in the commercial continuously operated source mechanically modulated phosphorimeters; the exception being that no mechanical phosphoroscope is required in the pulsed system. Also, the source of excitation energy is a short-arc high-pressure xenon flashtube rather than a continuously operated xenon arc lamp (usually 150 W); pulsed sources are operated from rather simple electronic circuits and power supplies and have operating characteristics suitable for the excitation of (fast) phosphors, e.g., a blackbody temperature of around 7000 K, a pulse rate as high as several thousand hertz, and most important, a pulse duration on the order of several microseconds (a duty cycle of about 10^{-3}). With too short a pulse, not enough molecules will be excited per excitation-emission cycle to permit the observation of analytically useful phosphorescence signals. With too long a pulse, the early portions of the emission decay curves of fast phosphors will be buried in source scatter noise. Also, with long pulses, the phosphorescence background signal, often a result of slow phosphor species in the sample mixture, may become increasingly significant.

Readout devices for pulsed-source systems are more complex than dc systems employed in commercial phosphorimeters; three principal readout methods have been used. The method proposed by O'Haver and Winefordner [60], involved phototube pulsing (gating) as well as source pulsing and is schematically illustrated in figure 8; it is seen that the first event in the excitation-observation-of-emission cycle for a pulsed-source system is the intense burst of energy from the source with a flash duration half-width, t_f. During this time, the phosphorescence intensity climbs to a value I_0 and begins to decay exponentially. At a delay time, t_d, preferably after the source flash has decayed significantly, the multiplier phototube is turned on (a high-voltage negative pulse is applied to the dynode chain), and the luminescence signal is monitored. The phototube is then turned off by termination of the negative "on" pulse: if an integrating dc measurement system is used to monitor its output, the integrated luminescence intensity I is measured during the on-time t_p of the phototube. If desired, t_d may be varied in such a manner that the gate t_p is scanned along the decay curve, providing the readout device with a display of the phosphorescence decay. This method was more difficult to achieve instrumentally than the other two methods discussed in the following paragraph.

Two other readout methods for observation of fast phosphor emissions were used by Fisher and Winefordner [58]. In the *first* method, the phototube was operated continuously in the conventional manner, but an electronic gate examined the integrated phosphorescence intensity after a time delay of t_d over the time period t_p; this gate may also be scanned to display the decay curve. This method is termed the *box-car integrator method.* In the *second* method, the phototube was also continuously operated, but the signal for the entire decay curve was presented to a fast multichannel readout device. This method is called the *signal averager method.* The latter method is the simplest one of the three to use for pulsed source studies although the problems of measurement of fast electronic signals accompanied by noise are more important with this method.

The integrated luminescence intensity I (cross-hatched area in fig. 8) achieved with a pulsed-source gated-detector system is given [6] by

$$I = \frac{I_0 f t_f [\exp(-t_d/\tau)]\,[1-\exp(t_p/\tau)]}{[1-\exp(-1/f\tau)]}$$

assuming a dc type readout is used to measure I within the phototube "on" time t_p (terms are defined in fig. 8). If an ac system is used, I will not be directly proportional to f, the source pulse repetition frequency. Figure 9 gives the variation of relative re-

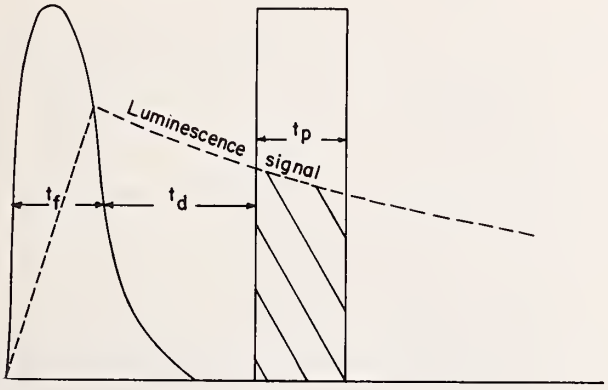

FIGURE 8. Schematic diagram of events occurring during one cycle of sample excitation and observation in a pulsed source phosphorimeter system [60].

Key to Symbols and Lines in Diagram

t_f = half-intensity width of the source flash

t_d = delay time after the end of the excitation pulse (assuming excitation pulse to be a rectangular) to the beginning of observation of the phosphorescence signal ("on" time of the detector or the readout system)

t_p = "on" time of detector or readout system

Dashed line represents buildup and decay of phosphorescence

Solid line tailing peak represents flash intensity temporal distribution

Solid line rectangular peak represents "on" time of detector or readout system

Cross-Hatched area represents measured integrated luminescence signal per source pulse

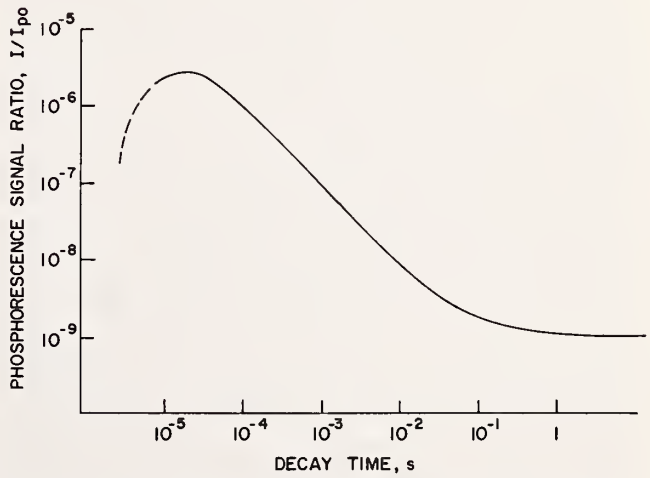

FIGURE 9. Plot of phosphorescence signal ratio (ratio of integrated intensity I to the steady state integrated intensity I_{po}) *versus* sample phosphorescence decay time τ[60] for case of pulsed source gated detector (see text for values of t_f, t_p, and t_d).

sponse (ratio of integrated luminescence intensity I to the steady state integrated intensity I_0) with phosphor decay time τ for parameters typical of an analytically useful pulsed-source gated-detector system ($t_f = 10^{-6}$ s, $t_p = 10^{-5}$ s, $t_d = 10^{-5}$ s). It is evident by the existence of the maxima in figure 9, that the pulsed-source system is capable of providing selective response to short-lived phosphors over long-lived phosphors. This is of considerable importance, because the background phosphorescence signal, which often defines the limits of detection and precision for fast phosphors in alcoholic/hydrocarbon/ether solutions, is usually due to a long-lifetime phosphor impurity. For example, the pulsed system (represented in fig. 9) for a typical fast ($\tau = 1$ ms) sample phosphor in the presence of a slow ($\tau = 1$ s) background phosphor interferent should have a 200-fold greater rejection of background than the commercial mechanical phosphoroscope phosphorimeter.

Therefore, the principle advantages of pulsed-source phosphorimetry over conventional continuous operating sources with mechanical modulation are: the possibility of achieving higher peak source intensities during the measurement period and thus lower detection limits and the possibility of achieving greater selectivity for a given short-τ phosphor over a long-lived interferent. Lesser advantages also exist. For example, since a flashtube pulse may terminate in several microseconds, whereas a typical phosphoroscopic mechanical disk chopper has a termination time (transit time) t_t of 3×10^{-5} and a typical phosphoroscopic mechanical can chopper has a t_t of 1×10^{-4} s, shorter-lived phosphors (τ's as short as 10 μs) can be measured. In addition, since the temporal parameters t_f, t_d, and t_p may be more readily varied with a pulsed-source gated-detector system, larger signals can be measured and greater selectivity achieved. Gating the detector so that it is on for only a predetermined time results in an improvement of the signal-to-noise ratio and a reduction in detection limits, an increase in precision, and an improvement in the accuracy of measurement. Finally, because it is easy to determine the linearity of a log I versus t_d plot, a rapid check on the purity of the phosphor under study can be obtained as well as an estimate of the phosphor decay time, which may be useful for structural (qualitative) studies.

A block diagram of the pulsed-source gated-detector phosphorimeter used by Fisher and Winefordner [58] is given in figure 10; a schematic diagram of the flashtube trigger circuit is shown in figure 11. To compare the standard commercial (AMINCO in our case) spectrophotofluorimeter with rotating can phosphoroscope with the pulsed-source gated-detector system, it was decided to measure the limit of detection of a fast phosphor (4-bromoacetophenone, $\tau = 6.8$ ms) in purified ethanol which was known to contain a phosphorescence background due to a slow phosphor (unknown material, $\tau = 0.8$ s) having phosphorescence excitation and emission spectra which overlapped considerably the corresponding spectra of the fast phosphor. The limit of detection of 4-bromoacetophenone was 10^{-6} M when measured using the standard commercial spectrophotofluorimeter with rotating can phosphoroscope. However, with the pulsed-source gated-detector system of Fisher and Winefordner [58], the detection limit was found to be 10^{-8} M, even though

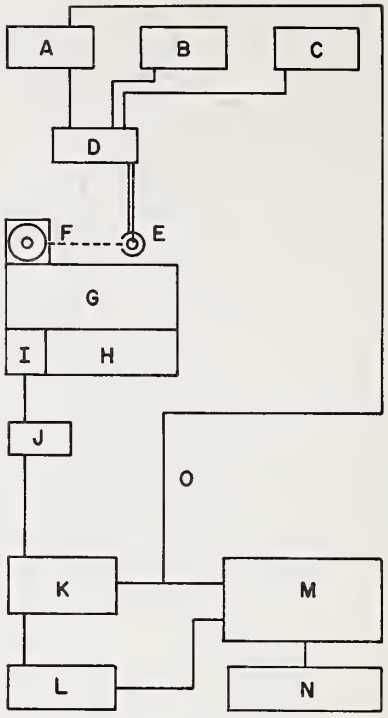

FIGURE 10. Block Diagram of Pulsed Source Phosphorimeter [58].

Key to Symbols

A. Pulse generator (Model 100, Datapulse Inc., Culver City, Calif.)
B. 300 V power supply (Model C–281, Lambda Electronics, Melville, N.Y.)
C. 1400 V power supply (Model 403 M, John Fluke Mfg., Co., Seattle, Washington)
D. Trigger circuit (see fig. 11)
E. Xenon flashtube compartment (Laboratory Constructed)
F. Sample cell compartment (identical to Aminco phosphoroscope accessory minus rotating phosphoroscope can)
G. Emission monochromator (Model EU–700, Heath Co., Benton Harbor, Michigan)
H. Phototube power supply (Model EU–701–30, Heath Co., Benton Harbor, Michigan)
I. RCA 1P28 photomultiplier tube
J. Load resistors (500 Ω to 3M Ω) and fast switching diodes
K. Oscilloscope (Model 545,Tektronix Inc., Orlando, Florida)
L. Preamplifier (Model 465A, Hewlett-Packard, Orlando, Florida)
M. Signal averager (Biomac Model 1000, Data Laboratories, Ltd., London, England), or Boxcar Integrator (Model 160, Princeton Applied Research, Princeton, New Jersey)
N. *x-y* Recorder

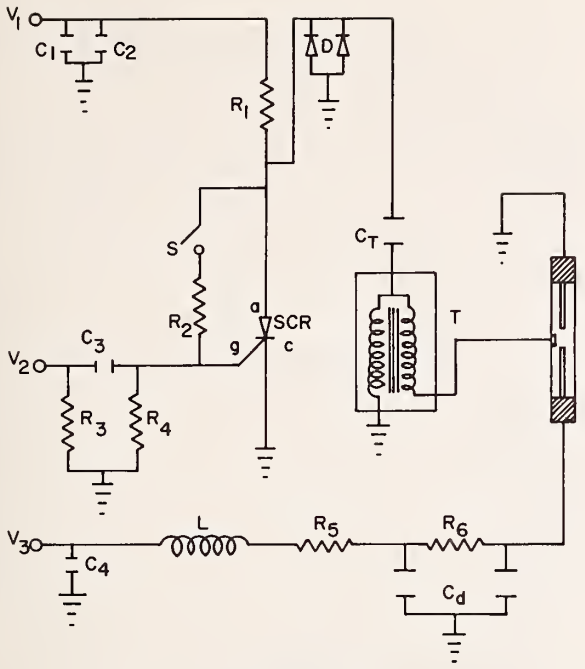

FIGURE 11. Schematic diagram of flashtube trigger circuit [58].

Value of Components

C_1 0.001 μF	R_1 100 kΩ	L ~100 μh
C_2 0.1 μF	R_2 33 kΩ	S SPST switch
C_3 0.022 μF	R_3 56 Ω	T EG & G TR 132 Trigger Transformer
C_4 0.002 μF	R_4 1.1 kΩ	V_1 300 V dc power supply
C_t 1.0 μF (600 V)	R_5 6.8 kΩ	V_2 15 V dc power supply
C_d 0.1 μF (5000 V)	R_6 190 kΩ	V_3 1400 V pulse power supply

the average power of the continuously operated xenon source in the commercial system (150 W) was 75 times as great as the average power of the pulsed xenon flashlamp (2 W). The main reason for the 100-fold reduction in the limit of detection with the pulsed system is the reduction in noise, i.e., essentially no phosphorescence signal due to the long-lived background component was observed with the pulsed system, and so the noise level was only about twice the dark current shot noise level.

One other factor which contributes to phosphorescence background should be mentioned. The diethyl ether used in the Fisher and Winefordner [58] studies was Baker and Adamson anhydrous reagent grade. Listed as impurities in this solvent are "0.001 percent carbonyl (as $>C=0$)." As expected, this also produced a fast decaying phosphorescence background to which the pulsed instrumentation was responsive. Fortunately, the ether background was *very* short-lived, and this interferent decayed before introducing error into the phosphorescence signal of the analyte with the pulsed-source system.

IV. Noninstrumental Improvements in Phosphorimetry

Lukasiewicz, Rozynes, Sanders, and Winefordner [52] showed that phosphorescence signals remain nearly constant for a variety of analytes in snowed matrices of mixtures of ethanol/water (methanol/water) at 77 K over the range of 10 to 50 percent *v/v*; as the volume percent of ethanol (or methanol) increased from 0 percent to about 10 percent, the phosphorescence signals of 2-thiouracil, *p*-nitrophenol, or sulfamethazine increased by about 3 orders of magnitude and simultaneously the physical appearance of the frozen matrix changed from a translucent severely cracked medium to an opaque completely snowed matrix. The phosphorescence signal levels were nearly the same in either methanol/water or ethanol/water (10–50) percent *v/v* of alcohol/water), but the phosphorescence background level was considerably lower in the former than the latter solvent mixture (spectrograde methanol versus 95 percent ethanol). The increased phosphorescence signals of analytes in 10 to 50 percent *v/v* of alcohol/water mixtures at 77 K as compared to those in pure aqueous solutions was correlated with the physical nature (snow versus cracked glass) rather than with chemical properties of the analyte and/or the solvent as has been further verified by Lukasiewicz, Mousa, and Winefordner [53] (see below).

Lukasiewicz, Mousa, and Winefordner [53], in a more recent study, have made careful phosphorescence measurements of the influence of solvent (methanol/water and alkali-halide salt solutions) composition upon the phosphorescence of 3-indole acetic acid, hippuric acid, and sulfacetamide at 77 K. Typical results for the methanol/water mixtures at 77 K are shown in figure 12. The three analytes all show the same solvent dependency, i.e., a region where there is an abrupt increase in phosphorescence signal between 0 and 3 percent *v/v* methanol/water, followed by a plateau region between about 5–30 percent *v/v*, and a region where the phosphorescence signal decreases slightly for solutions with more than 30 percent methanol. Little or no spectral shift was observed for the phosphorescence excitation and emission spectra as a function of solvent composition. Perhaps the most significant observation was that each region corresponded to a visible change in the nature of the matrix. Pure water solutions were severely cracked, but nearly transparent. Addition of small amounts of methanol to water produced an opaque matrix which corresponded to the region of greatest slope in the solvent dependency curves. Between approximately 5 and 30 percent *v/v* methanol/water, the frozen matrix became completely snowed, and the signal remained nearly constant. Increasing the percentage of methanol even more resulted in a signal decrease which corresponded to the reappearance of a cracked, translucent,

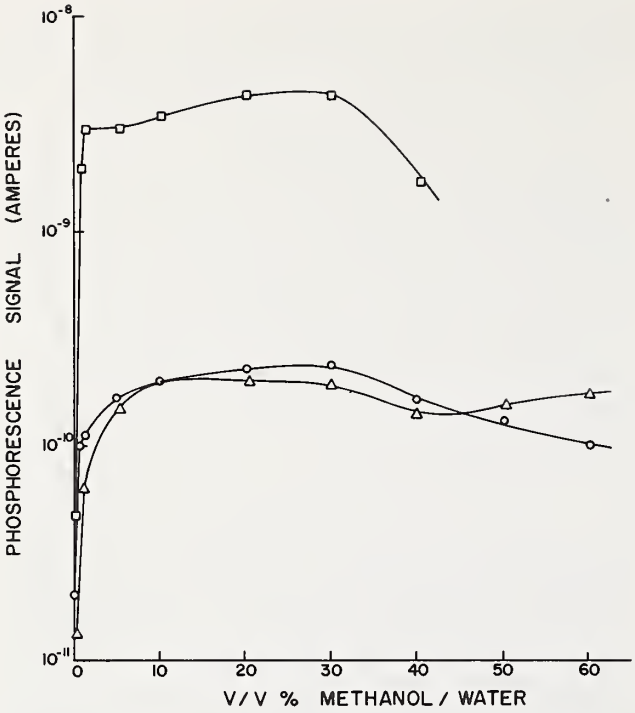

FIGURE 12. Phosphorescence Signal as Function of Solvent Composition (methanol-water) [53].

○ $2.0\times10^{-6}M$ 3-indole acetic acid
△ $4.7\times10^{-6}M$ hippuric acid
□ $1.7\times10^{-6}M$ sulfacetamide

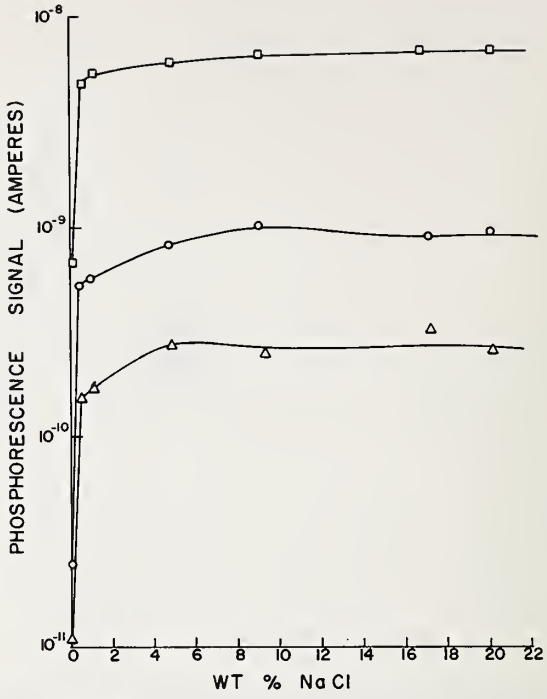

FIGURE 13. Phosphorescence Signal as Function of Solvent Composition (sodium chloride-water) [53].

○ $3.7\times10^{-6}M$ 3-indole acetic acid
△ $1.8\times10^{-6}M$ hippuric acid
□ $3.9\times10^{-6}M$ sulfacetamide

rigid matrix; the precision of measurement of phosphorescence signals for methanol/water solutions with 40 percent *v/v* or more methanol is poor because of the nonrandom cracking of the frozen solvent.

The shapes of the phosphorescence signal versus solvent composition curves when sodium chloride is added to water rather than methanol (or ethanol) are identical to those for the alcoholic solutions (fig. 13), and the previous conclusions regarding the physical nature of the matrix seem to be justified. It should be stressed, however, that the maximum phosphorescence signal for the NaCl solutions is about 3 times greater than the methanol/water solutions (the salt solutions at 77 K result in a rigid, snowed matrix with more finely divided particles than the snowed matrix for the methanolic solutions).

The use of the external heavy-atom effect to increase the transition probability from the first excited-singlet to the first excited-triplet state and therefore, to increase the sensitivity of phosphorescence, has also been reported [62, 63]. However, in the *past*, results obtained using the external heavy-atom effect have been of limited analytical value because of the following restrictions. First of all, the heavy-atom perturbant had to be appreciably soluble in the solvents used for phosphorimetry and also had to form clear, rigid glasses with the solvent. Second, the perturbant should not absorb in the same spectral regions as the compounds being studied. Third, the perturbant had to be available in extremely pure form, since impurities could cause a large background signal. Ethyl iodide has been most commonly used as an external perturbant; however, results obtained were limited because ethyl iodide did not fulfill all the requirements stated above, especially the last two. In aqueous solutions, however, the use of simple perturbants, such as alkali halide salts is possible. Solubility and purity of these salts make them desirable for phosphorimetric studies of aqueous solutions.

The effect of adding the alkali halide salts, NaI, NaBr, and NaCl to pure water solutions of 3-indole acetic acid, is shown in figure 14. The combined physical matrix and heavy-atom effect result in the greatest phosphorescence signals with added NaI. All three salts (see background spectra in fig. 14) result in significant phosphorescence background—NaBr giving the largest. Also, both NaBr and NaI solutions result in the same general shaped composition curve as for NaCl and alcohol with water, except that the NaI-water curve in figure 14 is somewhat sharper than the others. An increase in phosophorescence

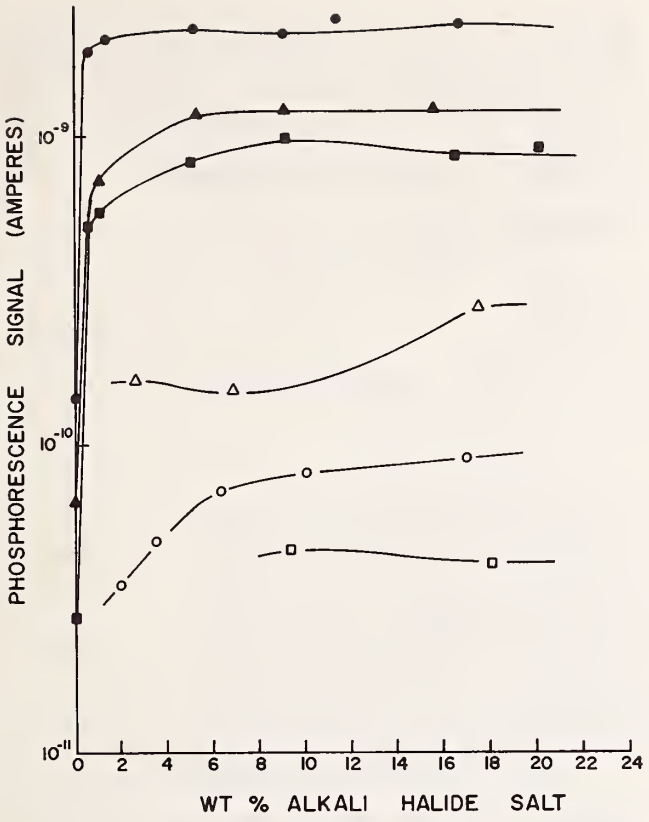

FIGURE 14. Phosphorescence Signal of $3.7 \times 10^{-6} M$, 3-indole Acetic Acid in Alkali Halide Salt Solution:

● aqueous NaI solution as solvent

▲ aqueous NaBr solution as solvent

■ aqueous NaCl solution as solvent

Phosphorescence background of alkali halide salt crystals:

○ NaI crystals

△ NaBr crystals

□ NaCl crystals

Excitation Wavelength 285 nm, emission wavelength 435 nm [53]. Reprinted from Anal. Chem. **44**, 965 (1972). Copyright (1972) by the American Chemical Society. Reprinted by permission of the copyright owner.

signal occurred for concentrations of NaI up to 1 *M*.

Therefore, the use of alkali-halide/water solutions as solvents for phosphorimetric analysis of polar organic molecules is advantageous for a number of reasons: alkali-halide salts may be obtained in ultrapure form, and thus phosphorescence background may be reduced to extremely low levels; salt solutions have the same matrix effect as alcohol/water solutions, while producing a much lower background signal; and, in the case of sodium iodide, an additional factor, namely the heavy-atom effect, enhances the phosphorescence signal. In some cases, however, use of aqueous sodium iodide solvents may be less desirable than other alkali halide salts. Phosphorescence decay time measurements for the compounds studied in this study by Lukasiewicz, Mousa, and Winefordner [53] indicated that decay times in aqueous sodium iodide solutions were considerably shorter than in methanol/water solutions. The changes in decay times for the compounds studied in aqueous sodium iodide and alcohol/water solutions are summarized in table 5. These observations are consistent with the heavy-atom perturbation theory [61]. Phosphorescence signals, however, did not increase for all three compounds listed in figure 13. A sixfold increase in phosphorescence signal was observed for 3-indole acetic acid, and a threefold increase for hippuric acid in 1 *M* sodium iodide. Sulfacetamide, on the other hand, showed a threefold decrease in signal even though the phosphorescence decay time was lower.

TABLE 5. Phosphorescence decay times in aqueous sodium iodide and aqueous alcohol solutions

Compound	Lifetime(s)	
	Solvent 10 percent *v/v* methanol-water	Solvent 1 *M* aqueous sodium iodide
3-Indole Acetic Acid	7.0	0.90
Sulfacetamide	1.7	0.83
Hippuric Acid	3.0	0.97

It is therefore quite evident that proper selection of the solvent for phosphorimetry can lead to an appreciable increase in phosphorescence signals of some species and in some cases an increase in selectivity of analysis. The advantages of using alkali-halide salt solutions over alcohol/water solutions as phosphorimetric solvents include: the availability and low cost of high purity salts; increased signal levels; and the high solubility of many biochemically related species.

V. References

[1] Hercules, D. M., Fluorescence and Phosphorescence Analysis, D. M. Hercules, Ed. (Wiley, Interscience, New York, 1966).

[2] Parker, C. A., Photoluminscence of Solutions (Elsevier, New York, 1968).

[3] Becker, R. S., Theory and Interpretation of Fluorescence and Phosphorescence (Wiley, Interscience, New York, 1969).

[4] Zander, M., The Application of Phosphorescence to the Analysis of Organic Compounds (Academic Press, New York, 1968).

[5] Winefordner, J. D., McCarthy, W. J., and St. John, P. A., Methods of Biochemical Analysis, D. Glick, Ed., Vol. **15** (Interscience, New York, 1967).

[6] Winefordner, J. D., St. John, P. A., and McCarthy, W. J., Chapter on Phosphorimetry, in Fluorescence Assay in Biology and Medicine, Vol. **II**, S. Udenfriend, Ed. (Academic Press, New York, 1969).

[7] McCarthy, W. J., Phosphorimetry, Chapter in Spectrochemical Methods of Analysis, J. D. Winefordner, Ed. (Wiley, New York, 1970).

[8] Winefordner, J. D., Schulman, S. G., and O'Haver, T. C., Luminescence Analysis in Analytical Chemistry (Wiley, New York, 1972).

[9] Zander, M., Angew. Chem. Intern. Ed. Engl. **4**, 930 (1965).

[10] Zander, M., Z. Anal. Chem. **226**, 251 (1967).

[11] Clar, E., and Zander, M., Chem. Ber. **89**, 749 (1956).

[12] Zander, M., Erdoel Kohle **19**, 279 (1966).

[13] Sawicki, E., Chemist-Analyst **53**, 88 (1964).

[14] Sawicki, E., and Johnson, H., Microchem. J. **8**, 85 (1964).

502-591 O - 73 - 13

[15] Sawicki, E., Stanley, T. W., Pfaff, J. D., and Elbert, W. C., Anal. Chim. Acta **31**, 359 (1964).
[16] Sidorov, N. K., and Rodomakina, G. M., Uch. Zap. Saratovsk Gos. Univ. **69**, 161, (1960).
[17] Drushel, H. V., and Sommers, A. L., Anal. Chem. **38**, 101 (1966).
[18] Drushel, H. V., and Sommers, A. L., Anal. Chem. **38**, 19 (1966).
[19] Drushel, H. V., and Sommers, A. L., Anal. Chem. **36**, 836 (1964).
[20] McCarthy, W. J., and Winefordner, J. D., J. Assoc. Offic. Agr. Chemists. **48**, 915 (1965).
[21] Winefordner, J. D., and Moye, H. A., Anal. Chim. Acta **32**, 278 (1965).
[22] Moye, H. A., and Winefordner, J. D., J. Agr. Food Chem. **13**, 516 (1965).
[23] Moye, H. A., Winefordner, J. D., J. Agr. Food Chem. **13**, 533 (1965).
[24] Moye, H. A., J. Assoc. Off. Anal. Chem. **51**, 1260 (1968).
[25] Latz, H. W., and Hurtabise, R. J., J. Agr. Food Chem. **17**, 352 (1969).
[26] Latz, H. W., Madsen, B. C., Anal. Chem. **41**, 1180 (1969).
[27] Freed, S., and Salmre, W., Science **128**, 1341 (1958).
[28] Freed, S., Turnbull, J. H., and Salmre, W., Nature. **181**, 1831 (1958).
[29] Freed, S., and Vise, M. H., Anal. Biochem. **5**, 338 (1963).
[30] Hollifield, H. C., and Winefordner, J. D., Anal. Chim. Acta **36**, 362 (1966).
[31] Hollifield, H. C., and Winefordner, J. D., Talanta **14**, 103 (1967).
[32] Winefordner, J. D., and Tin, M., Anal. Chim. Acta **32**, 64 (1964).
[33] Hollifield, H. C., and Winefordner, J. D., Talanta **12**, 860 (1965).
[34] Hood, L. V. S., and Winefordner, J. D., Anal. Biochem. **27**, 523 (1969).
[35] Hood, L. V. S., and Winefordner, J. D., Anal. Chim. Acta **42**, 199 (1968).
[36] McCarthy, W. J., Parsons, M. L., and Winefordner, J. D., J. Chem. Educ. **44**, 136 (1967).
[37] St. John, P. A., McCarthy, W. J., and Winefordner, J. D., Anal. Chem. **38**, 1828 (1966).
[38] Winefordner, J. D., and St. John, P. A., Anal. Chem. **35**, 2211 (1963).
[39] Scott, D. R., and Allison, J. B., J. Phys. Chem. **66**, 561 (1962).
[40] Smith, F. J., Smith, J. K., and McGlynn, S. P., Rev. Sci. Instr. **33**, 1367 (1962).
[41] Kanda, Y., and Shimada, R., Spectrochim. Acta. **17**, 279 (1961).
[42] Sponer, H., Kanda, Y., and Blackwell, L., ibid. **16**, 1135 (1960).
[43] Kanda, Y., Shimada, R., and Saka, Y., ibid. **17**, 1 (1961).
[44] Kanda, Y., Shimada, R., Honada, K., and Kajigaeshi, S., ibid. **17**, 1268 (1961).
[45] Von Foerster, G., Z. Naturforsch. **18a**, 6201 (1963).
[46] Kubelka, D., and Munk, F., Z. Techn. Physik **12**, 593 (1931).
[47] Parker, C. A., and Hatchard, G., Trans. Faraday Soc. **57**, 1894 (1961).
[48] Klasen, H. A., Philips Res. Rep. **2**, 68 (1947).
[49] Kortüm, G., Braun, W., and Herzog, G., Angew. Chem. Intern. Ed. **2**, 333 (1963).
[50] Hollifield, H. C., and Winefordner, J. D., Anal. Chem. **40**, 1759 (1968).
[51] Zweidinger, R. W., and Winefordner, J. D., Anal. Chem. **42**, 639 (1970).
[52] Lukasiewicz, R. J., Rozynes, P. A., Sanders, L. B., Winefordner, J. D., Anal. Chem. **44**, 237 (1972).
[53] Lukasiewicz, R. J., Mousa, J. J., and Winefordner, J. D., Anal. Chem. **44**, 963 (1972).
[54] Lukasiewicz, R. J., Mousa, J. J., and Winefordner, J. D., Anal. Chem. **44**, 1339 (1972).
[55] Zweidinger, R. W., Sanders, L. B., and Winefordner, J. D., Anal. Chim. Acta **47**, 558 (1969).
[56] Tin, M., and Winefordner, J. D., Anal. Chim. Acta **31**, 239 (1964).
[57] Sanders, L. B., Cetorelli, J. J., and Winefordner, J. D., Talanta **16**, 407 (1969).
[58] Fisher, R. P., and Winefordner, J. D. Anal. Chem. **44**, 948 (1972).
[59] Winefordner, J. D., Accnts, Chem. Res. **2**, 361 (1969).
[60] O'Haver, T. C., and Winefordner, J. D., Anal. Chem. **38**, 1258 (1966).
[61] McGlynn, S. P., Azumi, T., Kinoshita, M., Molecular Spectroscopy of the Triplet State (Prentice-Hall, Englewood Cliffs, New Jersey, 1969).
[62] Zander, M., Z. Anal. Chem. (Fresenius), **226**, 251 (1967).
[63] Hood, L. V. S., and Winefordner, J. D., Anal. Chem. **38**, 1922 (1966).

(Paper 76A6–743)

NATIONAL BUREAU OF STANDARDS SPECIAL PUBLICATION 378, Accurocy in Spectrophotometry ond Luminescence Meosurements, Proceedings of o Conference Held at NBS, Goithersburg, Md., Morch 22–24, 1972 (Issued Moy 1973).

Measurements of Absolute Values in Biochemical Fluorescence Spectroscopy

Raymond F. Chen

National Heart Institute, National Institutes of Health, Bethesda, Maryland 20014

(July 19, 1972)

Fluorescence spectroscopy is an important tool of the biochemist studying the structure and interactions of proteins and nucleic acids. The four basic quantities to measure accurately are: 1. spectra (corrected excitation and emission), 2. quantum yields (Q), 3. fluorescence decay characteristics, and 4. polarization. Commercially available instruments, with little modification, can be used to obtain these measurements, but the biochemist in this field is very dependent on the accuracy of measurements of substances he uses as standards. Confusion arises from disagreement between reported values for standards which may be used to calibrate a detector system to obtain quantum yields, or to set up lifetime and polarization photometers. For instance, the protein chemist is fond of using tryptophan and quinine as quantum yield standards, but Q for tryptophan has been variously reported as 0.13 and 0.20, and Q values for quinine bisulfate range from 0.4 to 0.7. The biochemist should also be aware of the problems inherent in the use of commerically available instruments in absolute measurements, as well as the special complications arising in complex biochemical systems where the fluorescence is heterogeneous.

Key words: Absolute fluorometry; absolute fluorometry in biochemistry; standard reference materials in fluorometry.

I. Introduction

A. Applications of Fluorescence Spectroscopy in Biochemistry

Within the last dozen years, biochemists have generally become aware of the value of fluorescence spectroscopy as a tool for the study of macromolecules such as proteins and nucleic acids. The marked increase in the use of fluorescence during recent years has also been due to improvements in instrumentation and techniques. Before discussing the types of measurements which are needed, let us consider some of the applications of fluorescence spectroscopy in physical biochemistry:

1. Obtaining Information on the Size and Shape of Macromolecules.

In 1952, Weber [1, 2][1] pointed out that the polarization of fluorescence of dyes attached to proteins could be used to give information on rotational relaxation times. These times were an estimate of the Brownian motion occurring during the lifetime of the excited state; hence, information was obtained concerning the size and shape of the proteins. The equation derived by Weber [1] to correlate the degree of polarization, P, with the fluorescence decay time τ, and the relaxation time ρ_h, was based on similar equations originally formulated by Perrin [3] and Levshin [4] for simple organic fluorophors:

$$\frac{1}{P}-\frac{1}{3}=\left(\frac{1}{P_0}-\frac{1}{3}\right)\left(1+\frac{3\tau}{\rho_h}\right) \tag{1}$$

where P_0 is the limiting polarization. Because the quantity τ/ρ_h is proportional to the ratio T/η (T, absolute temperature; η viscosity), a "Perrin plot" of $1/P-1/3$ versus T/η obtained from polarization data with protein-dye conjugates at different temperatures and/or viscosities, contains all the information needed to calculate the rotational relaxation time of the molecule, provided the lifetime can be measured. Polarization data are also useful for following conformational changes such as unfolding or dissociation of a protein. Such events can frequently be monitored by no other known techniques [5]. Note that utilization of eq (1) requires both polarization and lifetime determinations.

2. Study of Binding Equilibria

The interaction of proteins with small ligands is a key function of proteins comprising certain physiological systems. This is especially true in the case of

[1] Figures in brackets indicate the literature references at the end of this paper.

enzymes, proteins with catalytic properties. Some of these ligands, such as coenzymes like reduced nicotinamide adenine dinucleotide (NADH) are naturally fluorescent, and the binding of the ligands is accompanied by a large (typically, 2- to 5-fold) enhancement of the quantum yield, alteration of the emission spectrum, and an increase in the polarization of fluorescence. Other ligands such as flavin coenzymes are quenched on binding to proteins. Also, Velick [6] showed that the ultraviolet fluorescence of proteins is often quenched on binding of certain ligands. Any or all of these changes in fluorescence parameters are useful in obtaining the stoichiometry and association constants of the binding.

3. Elucidation of the Nature of Binding Sites

The dielectric properties of different areas on proteins differ markedly; such differences can be signalled by the fluorescence behavior of fluorescent ligands bound to these areas. Dyes which have been useful in this regard have been dubbed "fluorescent probes". The Stokes shift and quantum yield of bound fluorescent probes have been used to estimate the microscopic dielectric constant of binding sites in proteins. An example of how the nature of the binding site affects fluorescence is given in figure 1. The 1-dimethylaminonaphthalene-5-sulfonyl (DNS) group has emission properties which make it useful for a variety of fluorescence studies, including polarization. When DNS is used as a probe, a high quantum yield and a small Stokes shift is indicative of a nonpolar environment. Absorbed onto the active site of the enzyme, carbonic anhydrase, DNS in the form of the sulfonamide has a smaller Stokes shift than it does when adsorbed to BSA (bovine serum albumin) or attached covalently to the enzyme (fig. 1).

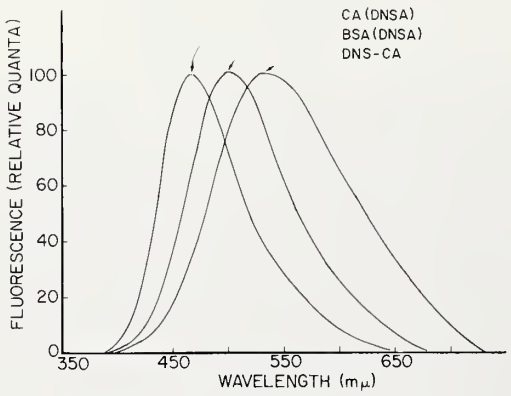

FIGURE 1. Corrected emission spectra of proteins containing the 1-dimethylamino-naphthalene-5-sulfonyl (DNS) group. CA(DNSA) and BSA(DNSA) are adsorbates of carbonic anhydrase and bovine serum albumin containing 1-dimethylamino-naphthalene-5-sulfonamide, and DNS–CA is a conjugate prepared by reacting carbonic anhydrase with DNS chloride. The curves are normalized to the same height. From Chen and Kernohan [7].

4. Study of the Environment Near Tryptophan and Tyrosine Residues in Proteins

Since it was discovered in the late 1950's that proteins have an ultraviolet fluorescence due to aromatic amino acids, much has been learned about the types of molecules or groups on a protein which can influence such fluorescence. The spectrum of tryptophanyl fluorescence is an indicator of the polarity of the environment near the emitting group. Changes in intrinsic fluorescence can be used to follow conformational changes or binding. Intrinsic fluorescence is a useful optical parameter for kinetic studies, including rapid reactions followed by stopped-flow or perturbation methods.

5. Determination of Intermolecular Distances by Energy Transfer

The radiationless transfer of energy from an excited chromophore to an acceptor molecule via a dipole-dipole resonance mechanism has been shown to occur in many intances. The theory of such energy transfer was studied by Förster [8] who developed a method for estimating the distance between donor and acceptor moieties based on their spectroscopic properties and the degree of energy transfer. Fluorometry is the best method for studying energy transfer, because this process is manifested by a quenching of the fluorescence of the donor and/or a sensitized fluorescence of the acceptor. A common example is that of a dye attached to a protein: the distance between the dye and the tryptophan residues may be estimated by the energy transfer from tryptophan to dye.

6. Study of the Orientation of Molecules Attached to Asymmetrical Macromolecules

By the use of polarized excitation, it is possible to obtain information on the orientation of ligands on a larger molecule. Using polarized photoselection, Lerman [9] determined that certain mutagenic dyes were attached with their planes perpendicular to the axis of deoxyribonucleic acid (DNA) molecules; this was the basis for his theory that mutagens intracalate between DNA base pairs. The orientation of dyes attached to proteins can similarly be studied by polarization measurements [10, 11]. The lack of a unique orientation of a dye fixed on a protein can also be detected. Such would be the case if dyes were attached in a random manner, or if a dye were attached to a flexible segment of the macromolecule.

7. Study of Changes in Conformation of Macromolecules

This is perhaps the most important use of fluorescence spectroscopy in biochemistry at present, and is accomplished by following changes in intrinsic fluorescence parameters as well as the fluorescence of attached groups. Such changes sometimes cannot be followed by other optical methods, and fluorescence

becomes the method of choice, especially for kinetic studies.

B. The Parallel Development of Fluorescence Spectroscopy and Instrumentation

From the preceding section, one can see that biochemical fluorescence spectroscopy requires the measurement of a variety of parameters: excitation and emission spectra, quantum yields, lifetimes, and polarization. The needs of biochemists often exceed those of individual physicists or physical chemists, although in biological fields investigators frequently are considerably less knowledgeable concerning instrumentation than physical scientists and are not qualified to construct their own instruments. However, commercially available instrumentation has improved and often has incorporated the best features of laboratory-built devices described in the literature. It is now possible to measure all of the above fluorescence parameters with available instrumentation. The development of such instrumentation has played an important role in the evolution of fluorescence techniques.

Following the description by Bowman et al. [12] in 1955 of the first spectrofluorometer, several instruments based on their design were produced commercially. Such instruments contain, basically, a xenon arc lamp, a sample compartment, two monochromators, and a photodetector system. The principal innovations by Bowman et al. were the introduction of the xenon arc as a source of energy continuum for fluorescence excitation, and the incorporation of two monochromators for excitation and emission. In this country, at least half a dozen spectrofluorometers of this type are marketed. There are probably thousands of these spectrofluorometers in use. They may serve as a basic tool for fluorescence spectroscopy and are of modest cost.

More sophisticated instruments are now available for determining spectra which have been designed to compensate for variations of exciting energy and photodetector response. These instruments generally cost 3 or 4 times as much as an uncompensated spectrofluorometer.

Polarization measurements have been made on light scattering photometers, filter fluorometers, and spectrofluorimeters [12]. Although specific instruments for fluorescence polarimetry do not seem to be generally used, the modification of other available instrumentation for such purposes poses no great problem. Even in the field of lifetime measurements there are commercial instruments available for the purpose. The TRW Instruments 75A (El Segundo, California)[2] fluorescence decay apparatus and the ORTEC Model 9200 fluorescence spectrometer are the first instruments for determining lifetimes, which were previously accessible only to those with considerable engineering skill.

II. Measurement of Fluorescence Parameters

A. Definition of the Term "Absolute"

The term "absolute" as used here refers to a property of a substance rather than its measurement. For example, the *absolute* quantum yield of a substance is the ratio of the photons emitted to the number of photons absorbed, in contrast to the *relative* quantum yield, the number of photons emitted by one substance as compared with another under specified conditions. Confusion may arise, because the phrase "absolute quantum yield" has been used by some workers to denote the quantum yield which has been measured by an "absolute" method; i.e., a method not requiring the use of a reference standard of known quantum yield. Absolute measurements are frequently required in certain biological fields like bioluminescence, but will not be treated here.

1. Excitation and Emission Spectra.

a. Definition.—The true, or absolute, fluorescence emission spectrum of a substance is a plot showing the relative number of photons emitted at different wavelengths; i.e., $dq/d\lambda$ versus λ, where q represents the total number of photons emitted and λ is the wavelength. Alternatively, the same information can be plotted on a frequency scale, $dq/d\nu$ versus ν in cm^{-1}. For simple organic compounds the emission spectrum is generally independent of the excitation wavelength, but for complex systems there is no single absolute emission spectrum since the emission may vary continuously with exciting light energy.

The excitation spectrum is a plot of the relative number of photons emitted at a given wavelength as a function of the exciting wavelength. The true, or corrected, excitation spectrum is compensated for any variations of excitation energy with wavelength. The corrected excitation spectrum is expected to coincide with the absorption spectrum in simple compounds, but this relationship may not hold in large biochemical systems.

b. Need for Corrected Spectra.—Absolute fluorescence spectra would be useful for comparing results from different laboratories and have long been advocated [14] as being the most suitable form of data presentation. Expensive spectrofluorometers are available for automatic recording of absolute fluorescence spectra. However, many uncorrected spectra are published even today, and some case can be made for continued use of uncorrected data. Thus, when the main point of a study is simply to show changes in fluorescence characteristics, there is little reason to take trouble to correct the spectra. The thousands of spectrofluorometers in use are equipped with similar

[2] In order to adequately describe materials and experimental procedures, it was occasionally necessary to identify commercial products by manufacturer's name or label. In no instances does such identification imply endorsement by the National Bureau of Standards, nor does it imply that the particular product or equipment is necessarily the best available for that purpose.

gratings and photomultiplier tubes, so that uncorrected spectra from one laboratory can, in fact, be used for comparison with results from another laboratory.

Absolute spectra are more informative, are required for quantum yield determinations, and are necessary for calculations of natural lifetimes or energy transfer distances. Nonetheless, one can confidently predict continued use of uncorrected spectra in the literature.

c. Calibration of Lamp Output and Detector Response.—Since most biochemists utilize uncompensated spectrofluorometers, it should be pointed out that procedures for calibrating these instruments have been published, e.g. [5, 15, 16]. The main steps involve (a) Calibration and alignment of the monochromators with a line source such as a mercury pen lamp, (b) Calibration of the exciting source with a fluorescent screen solution, such as Rhodamine B or some other dye, and (c) Calibration of the detector response by comparing the recorded signal from a standard lamp with its known output.

An example of a detector response calibration curve is given in figure 2. The response of an RCA 1P28

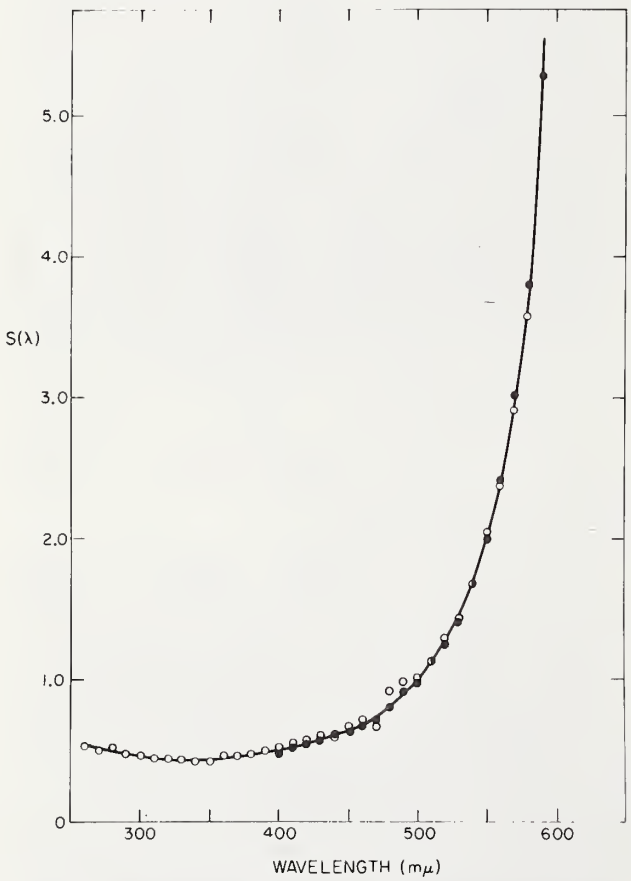

FIGURE 2. Detector calibration curve for Aminco-Bowman Spectrofluorometer fitted with 1P28 phototube and a grating blazed at 300 nm. Filled circles: data obtained with a National Bureau of Standards tungsten filament lamp. Open circles: data obtained with calibrated xenon arc lamp. $S(\lambda)$ is a function of the reciprocal of the sensitivity. From Chen [16]

Photomultiplier in an Aminco-Bowman spectrofluorometer fitted with a grating blazed for maximum response at 300 nm seems to be quite linear in the region from 290 nm to 400 nm. The detector system thus delivers "absolute" emission spectra for substances like proteins which emit in this range. By choosing suitable gratings and phototubes, it is sometimes possible to obtain linear response in regions of visible fluorescence as well, thus avoiding the need for point-by-point correction of spectra.

The accuracy of detector calibration depends on such factors as the photometric accuracy of the system and the accuracy of the standard lamp calibration. Lee and Seliger [17] have considered at length all the possible errors involved in *absolute* calibrations of detector systems. Their interest was principally the determination of chemiluminescent quantum yields, and it was necessary to know the relation between the number of photons and the detector response. In contrast, the determination of true emission spectra require that the relative detector response at different wavelengths be specified. Hence, the uncertainty in Lee and Seliger's absolute calibrations, ± 4.5 percent, is an upper limit in the more usual calibrations.

Calibration of spectrofluorometers by the use of "standard spectra" of well-known substances has been advocated [18]. In theory this would be a very convenient method. Comparison of the apparent excitation spectrum of a simple compound could be made with its absorption spectrum to yield the correction factors for lamp output. The method eliminates the need for a front-surface illumination attachment [15], which is needed for calibrations using the fluorescent screen method. Comparing absorption and emission spectra has the disadvantage that the same dispersion generally cannot be used in the absorption and fluorescence spectrometers. Other disadvantages make the comparison-of-spectra method less desirable than the fluorescent screen method. The latter results in a continuous plot of photon output versus wavelength compared with the discontinuous plot obtained by spectral comparison. Also, several absorption spectra are required to achieve a desired optical density at regions of maxima and minima, and several fluorescence excitation spectra at different gain settings will be needed as well.

The use of "standard spectra" to calibrate the detector response is becoming common practice as more corrected spectra are published. Unfortunately, the reliability of any given published spectrum is unknown, and it would perhaps be helpful if some spectra were certified by a committee of experts. In the past, there have been many discrepancies in published emission spectra of quinine [19], although more recent spectra seem to agree closely [20–23] and could be used for detector calibration. One complication which we pointed out several years ago is that the emission spectrum of quinine shows a red shift when excited in the long wavelength edge of the absorption band [21]. This effect is shown in figure 3. The emission shift has been postulated by Fletcher [22] to be related

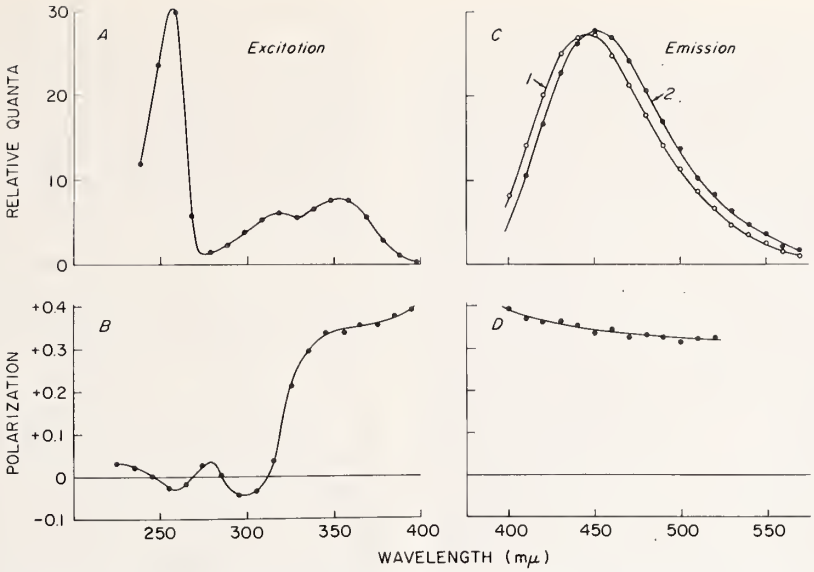

FIGURE 3. Fluorescence and polarization spectra of quinine in glycerol containing 0.1 N H_2SO_4 at 8 °C A. Excitation spectrum. B. Fluorescence polarization spectrum obtained with varied exciting wavelength and emission monochromator set at 450 nm. C. Corrected emission spectra obtained with excitation at 340 nm (curve 1) and 390 nm (curve 2). D. Variation of polarization in the emission band with constant excitation at 340 nm. From Chen [21].

to photoselection of quinine molecules with slightly different conformations. Other compounds also show this effect [21, 22, 24], which may involve what Fletcher calls rotatable auxochromes such as the methoxy group at the 6-position of the quinoline nucleus in quinine. At low temperatures, emission spectral shifts also occur due to the presence of different solvation states [25]. However, the spectrum of quinine under usual conditions of excitation should be suitable for a standard.

2. *Quantum Yield Measurements*

a. The Comparative Method of Determination.—In biochemistry, the quantum yield is most often obtained by comparison with a quantum yield standard. A spectrofluorometer is required, and the yield is calculated from the relation

$$\frac{Q_x}{Q_{st}}=\frac{F_x}{F_{st}}\times\frac{A_{st}}{A_x}\times\frac{\phi_{st}}{\phi_x}\times\frac{n_{st}^2}{n_x^2} \qquad (2)$$

where Q is the quantum yield, F is the area under the corrected emission spectrum, A is the optical absorbance at the exciting wavelength, ϕ is the relative photon output of the light source at that wavelength, and n is the refractive index. The subscripts x and st refer to the unknown and standard.

b. Factors Affecting the Accuracy.—

1. Accuracy of the emission detector response calibration. Any errors present may have little effect on the quantum yield calculations if the spectra of the standard and unknown are similar. One should not use fluorescein as a standard to determine quantum yields of ultraviolet fluorescence, for example.

2. "Bookkeeping" errors. Anyone who has attempted to perform quantum yield determinations must surely be impressed by the large number of factors which have to be inserted into the final calculations. Aside from the terms in eq (2), one must also remember that the photometer sensitivity may have been set at different values for standard and unknown, and the sensitivity scale may need recalibration. The absorbance, A, is usually read for concentrated solutions which then are diluted by some factor which renders self absorption unlikely in the fluorescence measurement; the dilution factor must be inserted. One can suspect that some of the large errors which have appeared in the literature are due to deficiencies in bookkeeping.

3. Determination of the absorbance. Although it would seem a simple matter to determine the absorbance of the test substances, errors arise because the wavelength calibrations of the spectrofluorometer and the spectrophotometer may be slightly incorrect. Excitation then may occur at a wavelength different from that at which the absorbance was measured. The bandwidth of the monochromators also are usually different, and the amount of error from this discrepancy depends on the spectral characteristics of the compounds. We have found that our average deviations for quantum yield determinations have been smaller when the unknown and standard are each excited at the peak of their long wavelength absorption bands. With

this method, one never need worry about slight monochromator alignment errors which would produce large errors in regions of sharply changing absorption.

4. Source output calibration. If sample and unknown are excited at the same wavelength, the term ϕ_{st}/ϕ_x of eq (2) reduces to one. However, since different wavelengths are usually used, some error may intrude. The lamp calibration curve for the xenon arc [16] is fairly smooth from 230–400 nm. In this region, if the exciting wavelengths for x and st are not too wide, one would not expect much error to be introduced if there is slight inaccuracy in the knowledge of the exciting wavelengths. Between 400 nm and 520 nm, however, there are some strong peaks in the xenon arc output. In this region, perhaps it would be best to use the same wavelength to excite both standard and unknown. The calibration curve itself might be erroneous due to factors such as impurities in the fluorescent screen substance. This may be checked by using several different screens, or by determining if the calibration curve allows for corrected excitation spectra which match the absorption spectra.

5. Polarization effects. In protein and nucleic acid fluorescence studies, the emission is frequently polarized due to the large size of the molecules. The resulting emission anisotropy can introduce an error into the quantum yield calculations even when unpolarized excitation is used, since even here, in instruments utilizing right-angle viewing geometry, the fluorescence is polarized. A number of papers have considered this problem [26–29]. Taking the worst possible case, Paoletti and Le Pecq [29] have estimated that a 15 percent error could occur in relative quantum yield measurements. However, an error this large could only occur with a sample showing maximum polarization in an instrument having large polarization artifacts, and where the fluorescence of standard and unknown were compared at individual emission wavelengths. Since the actual conditions for quantum yield assays are normally quite different, the errors are usually neglected, and indeed have never emerged as a great problem.

6. Accuracy of the value of the fluorescence standard.

a. Characteristics of quinine fluorescence. Recent reviews [30, 31] have pointed out the surprising discrepancies in reported quantum yields which exist in the literature and the controversy over the values of several well-known quantum yield standards. The most common standard is quinine in aqueous sulfuric acid solutions. An absolute yield of 0.55 for quinine in 1.0 N H_2SO_4 was reported by Melhuish [32, 33] as well as by Windsor and Dawson [30]. These workers employed absolute methods for the determination. A value of 0.58 for quinine in 0.1 N H_2SO_4 was reported by Eastman [34] using a technique which was probably less accurate. The report by Drobnik and Yeargers [35] that quinine probably had a yield of less than 0.4 must be dismissed, since Fletcher [36] was unable to duplicate their experiment and found a discrepancy of a factor of 6 in their reported Q for 2-aminopurine. Windsor and Dawson [30] pointed out that there were already literature reports that quinine yield was dependent on the concentration of sulfuric acid. Many investigators, including ourselves, were guilty of using 0.546 for the yield of quinine in 0.1 N H_2SO_4 rather than 1.0 N acid. We find that the quantum yield actually is 6 percent lower in the more dilute acid, so a yield of 0.51 should be used. The reason for the dependence of yield on acid concentration is not clear, but it must be an excited state phenomenon since we have been unable to demonstrate any significant change in absorption spectrum for quinine dissolved in 10 N H_2SO_4 compared with 0.1 N H_2SO_4.

Figure 4 shows the titration of quinine which has a midpoint at about pH 4.3 by absorption measurements. The optical density-pH titration curve shows the normal flattening at both ends, but the titration by fluorescence shows a slight continuing rise in the acid region, although the midpoint of the titration curve is the same. Figure 5 shows the variation of quinine fluorescence yield with sulfuric acid concentration. Several features may provide a clue as to the processes involved here. The fluorescence increases almost linearly from 0.1 N to 10 N H_2SO_4, although there is no change in absorption. However, we have also noted that $SO_4^=$ is a quencher of quinine fluorescence, although Stern-Volmer kinetics were not obtained. Thus the rise in quinine yield at high acid concentrations would be even larger except for the presence

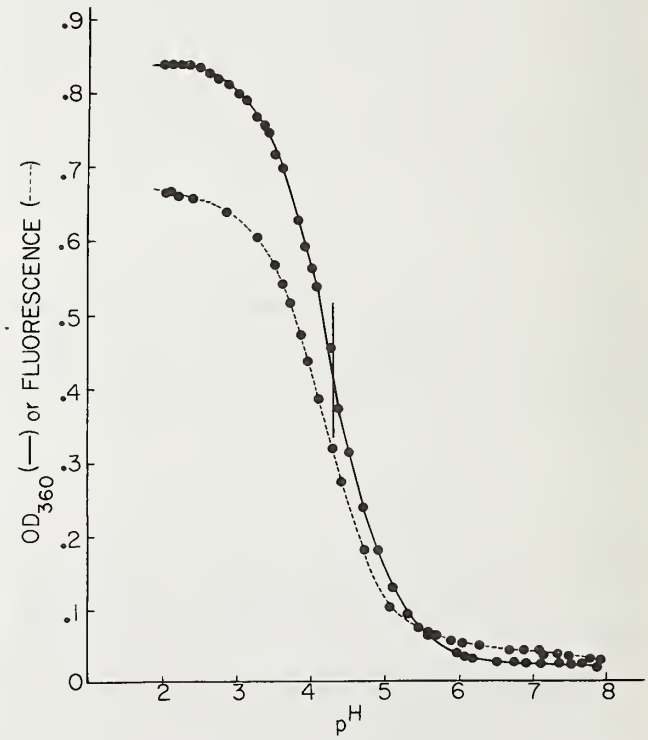

FIGURE 4. Titration of quinine monitored by fluorescence at 450 nm (---) or by optical density at 360 nm (—).

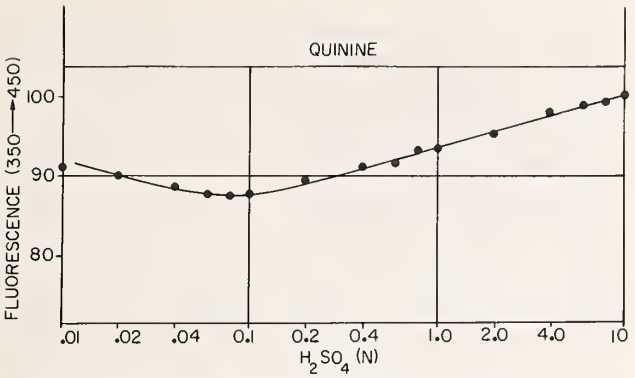

FIGURE 5. Effect of H_2SO_4 concentration on the fluorescence of quinine excited at 350 nm and monitored at 450 nm.

of sulfate ion. The slight increase in quinine yield at low acid concentration is reproducible and may be due to the lower concentration of sulfate ion.

Quinine is a good quantum yield standard for biochemical studies for several reasons. It is used in aqueous solutions. There is little overlap of absorption and emission spectra. The quantum yield is high. The material is obtained in pure form readily and is stable in acid solutions for months. There is little structure in the absorption spectrum and none in the emission spectrum, so high resolution equipment is not needed. The temperature dependence of the yield is relatively small. Figure 6 shows the temperature dependence of the yields of some compounds which might be useful as standards.

It is interesting that Rusakowicz and Testa [37] obtained a quantum yield of 0.46 for quinine in 0.1 N H_2SO_4 when comparing it with 9,10-diphenylanthracene, assumed to have a yield of 1.0 in cyclohexane. This value approaches Windsor and Dawson's value of 0.50 [30] and a value of 0.51 which we now favor. The value of 0.46 is fairly good since a very large refractive index correction (17%) was needed for comparing cyclohexane and water solutions. Nevertheless, there is no compelling reason to favor use of 0.46 rather than 0.51 as the yield for quinine in 0.1 N H_2SO_4.

The commonly accepted value for the quantum yield of quinine has also been challenged recently by Scott et al. [23], who claim that the yield in 0.1 N sulfuric acid is 0.70 ± 0.02. This value was determined from a comparison of measured lifetime with calculated natural lifetime, assuming the relation $Q = \tau/\tau_{nat.}$ This approach must be questioned, since the calculated natural lifetimes based on equations such as those of Förster [38] or Strickler and Berg [39] are quite approximate. Both Ware and Baldwin [40] and Birks and Dyson [41] noted the discrepancy between the measured and calculated lifetimes of quinine and have proposed explanations for this. The value of 0.70 must be too high, because many studies have used 0.55 as the value for quinine and have obtained values near unity for other compounds by comparison with quinine. Substitution of 0.70 for 0.55 would result in many quantum yields of greater than unity.

b. Controversy over the quantum yield of tryptophan. The most common quantum yield standard used in biochemistry for the ultraviolet region is tryptophan, because it has an emission which matches closely the tryptophanyl fluorescence of proteins. Here, too, there has been controversy over the quantum yield. Shore and Pardee [42] estimated Q to be 0.09, but used a rather crude method involving a spectrophotometer modified for fluorometry with filters. Teale and Weber [43] subsequently reported a value of 0.20, which has since been widely used. We reported that the value should be 0.13 [44] based on comparison with quinine in 0.1 N H_2SO_4 assumed (incorrectly) to have a yield of 0.55. Our value for tryptophan Q should be revised downward to 0.12 in view of the lower yield of quinine, 0.51. Also using quinine as a standard, Børresen [45] and Bridges and Williams [46] obtained tryptophan yields of 0.11 and 0.15. Eisinger [47] determined the tryptophan quantum yield to be 0.14 based on comparison with p-terphenyl, whose yield was 0.87. If Eisinger's data are correct, there can be no doubt that the value of 0.20 is much too high, for then the quantum yield of p-terphenyl would greatly exceed unity. We have convinced ourselves that 0.20 is, in fact, too high by similar comparisons with 9,10-diphenylanthracene and 2-aminopyridine (2AMP) which have very high quantum yields and have been recommended as standards [37, 48]. This simple experiment is recommended to anyone still in doubt concerning the quantum yield of tryptophan. While absolute measurements of quantum yield are difficult, relative quantum yields can easily be carried out with a precision of 5 percent. Therefore, if a standard with a supposed quantum yield of 1.0 is used, it is easy to determine an *upper limit* for the yield of any given unknown. Q determined in this way may be the real quantum yield, or, if the standard's Q turns out to be less than 1.0, some smaller value.

c. Other useful standards. Some quantum yields which have been measured in the author's laboratory are listed in table 1. Several values are at variance with those reported recently from Testa's laboratory [37, 48, 49]: 1. The yield of 2AMP is found to be 0.73 rather than 0.60. 2. The yield of 2AMP is found to be 6, rather than 13, times that of tryptophan. 3. A value of 0.55 for quinine in 1 N H_2SO_4 is consistent with our relative measurements, and is slightly higher than would be expected from the value of 0.46 reported for quinine in 0.1 N H_2SO_4.

Tryptophan with a quantum yield of 0.12 seems to be the best standard for protein quantum yields. The idea of using a protein as a quantum yield standard has occurred to us. However, when testing different commercial preparations of serum albumin, the most widely available protein in pure form, we have found wide variations in yield. Fresh tryptophan solutions are more suitable; solutions are not stable for more than one day.

There are, of course, many other compounds which might be suitable for standards, but the problem is to find compounds which have been examined in many

Table 1. Quantum yields of some possible standards

Compound	Q	Standard, Q_{st}
2-Aminopyridine, 0.1 N H_2SO_4	*0.74	9,10-diphenylanthracene, 1.0
Do.	.73	tryptophan, 0.12
Do.	.74	quinine, 1 N H_2SO_4, 0.55
Trytophan, water	*.12	9,10-diphenylanthracene, 1.0
Do.	.12	quinine, 1 N H_2SO_4, 0.55
1-dimethylaminonaphthalene-5-sulfonate, 0.1 M $NaHCO_3$	.34	Do.
4-Methylumbelliferone, 0.01 M NaOH	.64	Do.
4-Methylumbelliferone, 0.01 M HCl	.65	Do.
5-Hydroxyindole (serotonin), pH 7.4	.23	Do.
Tyrosine, water	.13	Do.
Phenylalanine, water	.022	Do.
Phenol, water	.13	Do.
1-dimethylaminonaphthalene-5-sulfonamide, pH 7.4	.051	Do.

All values were obtained by the author with the Aminco-Bowman spectrofluorometer and a Cary Model 11S spectrophotometer, except for those marked (*). The latter were determined with a Turner Model 210 spectrofluorometer. The author is indebted to Dr. H. Edelhoch for the use of this instrument.

different laboratories which agree on the quantum yield values. Fluorescein in aqueous base has frequently been used with a yield of 0.85 [cf. 50], and this is an excellent standard if the unknown has similar spectra. Biochemists will most often require aqueous standard solutions, since their samples are usually in water. The correction factor for refractive index differences between a given solvent and water may be quite large (+17% for cyclohexane solutions, for example). The correction factor is only approximate for the actual geometry existing in a given spectrofluorometer, and should be avoided wherever possible.

d. On the "certification" of quantum yield standards. In spite of our own confidence in the quantum yield data in table 1, we recognize that acceptance of compounds as standards comes only after agreement is reached between a number of reliable laboratories. Several studies have supported the values listed for tryptophan, 1-dimethylaminonaphthalene-5-sulfonate, quinine, 9,10-diphenylanthracene, and other compounds. Although a caveat has been issued [31] against the use of tryptophan as a standard, because of the controversy over its yield, a careful review of the data show that tryptophan Q is as well known as that of quinine. The use of quantum yield values for compounds over which controversy has not yet developed, because they have not been adequately investigated, seems irrational. The dearth of accepted quantum yield values is well brought out by the review of Demas and Crosby [31]. Perhaps one solution would be to carry out a cooperative study between several laboratories on a number of standards. This might speed the "certification" of standards.

3. Polarization Measurements

a. Definitions.—The degree of fluorescence polarization, P, is defined by

$$P=\frac{I_V-I_H}{I_V+I_H}.$$

If a fluorometer utilizes right-angle geometry, I_V and I_H refer to the intensities measured with the analyzer oriented normal and parallel to the direction of excitation. Fluorescence polarization is observed when the excitation is either polarized or unpolarized, provided that observation of the fluorescence is normal to the direction of excitation. If polarization observed with excitation polarized vertically (i.e., parallel to the orientation of the analyzer when measuring I_V) is p_p, the polarization observed with unpolarized, or natural, excitation, p_n, is given by

$$p_p=\frac{2p_n}{1+p_n}.$$

Most studies are carried out with polarized excitation because the absolute values of the polarization are higher ($-1/3 \leq p_p \leq +1/2$) than with natural light ($-1/7 \leq p_n \leq +1/3$). Perhaps the main reason for utilizing natural light is to obtain greater excitation intensities.

b. Measurement of polarization.—If a light-scattering photometer is adapted for polarization of fluorescence measurements, one is generally limited to excitation with certain mercury lines, and both excitation and emission are selected by filters. The use of a spectrofluorometer results in greater flexibility. There seem to be no commercially available instruments designed primarily for fluorescence polarimetry, but polarizing attachments are offered by makers of light-scattering photometers and spectrofluorometers.

c. Artifacts in polarization measurements.—

1. Defective collimation. The definition of P given above is based on the assumption that the exciting and emitted rays are perfectly collimated. In long path-length instruments, such a condition is nearly achieved. However, we have found that some simple filter fluorometers are quite unsuited for polarization measurements because the lamp is large and placed close to the sample, and the photodetector is also adjacent to the sample chamber. Large lenses which collect the fluorescence emitted at large angles to the axis connecting the sample and the photodetector may also invalidate the polarization data.

2. Polarizer defects. These can be several types. Azumi and McGlynn [51] found that improperly fabricated Glan prisms rotated the beam of light as the prisms were turned from one orientation to the other. Errors in mounting can cause the ordinary (unpolarized) ray to pass to the sample, or the polarizers may be set at some angle to the desired orientation. Some film polarizers may have incomplete polarization, especially at short wavelengths. Most polaroid film polarizers do not seem to be light-fast and will rapidly bleach when exposed to a high intensity source. However, some light-fast film polarizers of large aperture are available [13]. A convenient arrangement for spectrofluorometers is to use such filters in the exciting beam, and polaroid analyzers before the photodetector, as shown in figure 7. This arrangement has been used by many workers with good results.

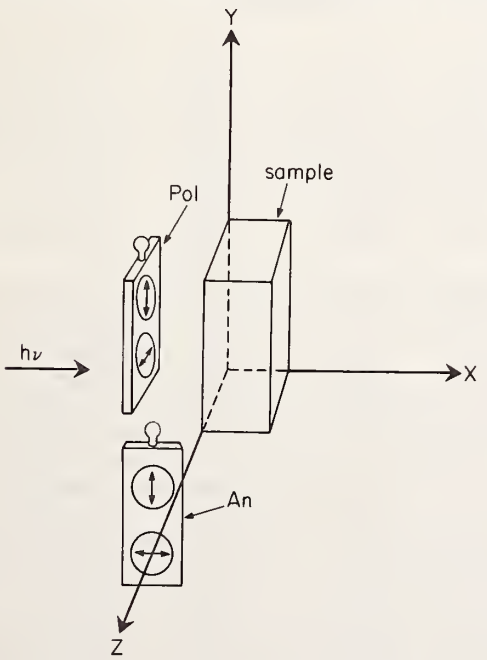

FIGURE 6. Recommended arrangement of polarizers in the Aminco-Bowman spectrofluorometer. The polarizers (Pol) and analyzers (An) are in sliding filter holders. From Chen and Bowman [13].

3. Spurious polarization introduced by the instrument. Light reflected from surfaces in a grating monochromator instrument becomes partly polarized, and such polarization must be corrected. In the exciting beam, this partial polarization is best rendered completely polarized; i.e., p_p rather than p_n is measured, especially in spectrofluorometers. The polarization introduced by the emission monochromator is wavelength dependent and related to variations in efficiency of the grating ("grating anomalies"). This artifact may be corrected by first determining the relative response of the detector system at any wavelength to horizontally and vertically polarized light. The grating correction factor, G, is obtained by observing a source of unpolarized light with the analyzer in the vertical and horizontal positions. A fluorescent sample can act as such a source if excited with horizontally polarized light. Polarization is then determined from

$$P=\frac{I_{VV}-GI_{VH}}{I_{VV}+GI_{VH}}$$

where $G=I_{HV}/I_{HH}$, and the subscripts refer to the orientations of the polarizer and analyzer.

G should depend only on the wavelength setting of the emission monochromator. For this reason, a calibration curve may be obtained with one or two highly fluorescent solutions and may be applied to measurements on other substances. The monochromator bandwidth should affect the G factor, but in our tests, the available bandwidths made very little difference in G [52]. Figure 8 shows the G factor

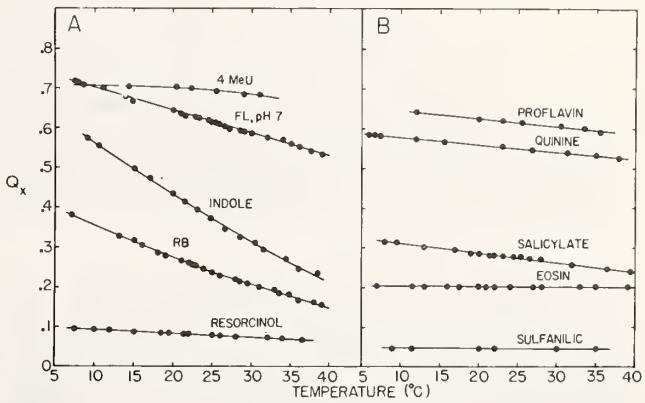

FIGURE 7. Variation of the quantum yield, Q_x, of some compounds with temperature. Abbreviations: 4 MeU, 4-methylumbelliferone; FL, fluorescein; RB, Rhodamine B.

calibration obtained with a spectrofluorometer. Although G could be measured for each sample, some solutions have very low fluorescence yield, and there may be large blank corrections required in determining I_{HV} and I_{HH}. A calibration curve obtained under better conditions is preferable. One of the interesting features of figure 8 is that G varies sharply with wavelength. Some authors [51] have suggested that G declines monotonically with wavelength, but this is clearly not the case.

4. Contributions from blanks. Like other measurements involving fluorescence intensity, polarization measurements should be rigorously corrected for blank contributions. If the G factor is known from prior calibration, polarization measurements still require four measured values: I_{VV} and I_{VH} for sample and blank. The magnitude of the blank relative to the sample signal can be large, as shown in figure 9 for the example involving bilirubin. Q for bilirubin bound to albumin is less than 0.01, and there is a background fluorescence due to impurities on albumin. There are relatively few instances where the blank can be neglected completely. Such might be the case of high quantum yield dyes dissolved in glycerol. A number of "automatic" fluorescence polarimeters have been described [53–55] in which I_{VH} and I_{VV} are measured simultaneously and ratioed electronically to give a function proportional to P. However, the common failing of these instruments is an inability to correct for the blank.

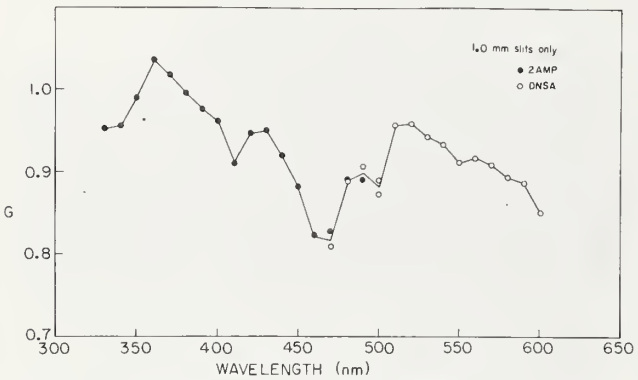

FIGURE 8. Dependence of the grating factor, G, with emission setting; i.e., calibration curve for G. The samples used were 10^{-4} M 2AMP in 0.1 N H_2SO_4 excited at 285 nm, and 10^{-3} M DNSA (1-dimethylaminonaphthalene-5-sulfonamide) in 50 percent ethanol, excited at 330 nm. G was calculated from I_{HV}/I_{HH}. From Chen [52].

5. Scattering. If scatter signal reaches the detector, the polarization will be anomalously high. Scatter can be corrected with a suitable blank, but such blanks may not be available. For example, in obtaining the polarization of the intrinsic emission from a protein, the blank should have the same light-scattering properties without being fluorescent. In turbid solutions, scatter may indirectly lower the observed fluorescence by causing the excitation to appear to reach the sample from many directions due to multiple reflections. For the most accurate measurements, the solutions should be clarified by centrifugation or filtration.

6. Depolarization by radiative energy transfer. In concentrated solutions of substances with considerable overlap of their absorption and emission spectra, depolarization can result from secondary fluorescence which has been excited by self-absorption of radiation. The effect can be detected by the increase in P upon dilution, and can be minimized by the use of small path length cells. Dyes with high absorption coefficients, like fluorescein and Rhodamine B, have been reported to exhibit concentration depolarization in solutions as dilute as 4×10^{-6} M [56].

d. Standards for Polarization.—Standards for fluorescence polarimetry would be helpful to evaluate the performance of a given instrument, but such well-defined standards do not appear to exist. There are considerable variations in reported polarization values for given solutions. The variations are as great as in the area of reported quantum yield values. In the absence of such standards, it is necessary to be certain that the apparatus registers zero polarization for nonviscous solutions of compounds with long lifetimes. Anthracene or other aromatic hydrocarbons in ethanol or cyclohexane may serve this purpose. At the other end of the scale, a sample having nearly the theoretical maximum polarization of 0.5 is desirable. An instrument could read zero for the polarization of a nonviscous solution, but might well give erroneously low polarizations for viscous solutions. Alkaline fluorescein, or Rhodamine B, in glycerol were reported to have polarizations between 0.4 and 0.5 and are therefore often used to test the performance of fluorescence polarimeters. The polarizations reported by various workers are given in table 2. Note

Table 2. Polarizations of dilute dye solutions in glycerol

Sample	Exciting wavelength (nm)	P	Reference
Fluorescein.....	366	0.28	Chen and Bowman [13]
Do.....	366	.424	Price at al. [57]
Do.....	430–520	.477±0.01	Chen and Bowman [13]
Do.....	436	.440	Weber [56]
Do.....	436	.446	Price et al. [57]
Do.....	436	.4922	Szalay et al. [58]
Rhodamine B.....	366	−0.17	Chen and Bowman [13]
Do.....	366	−.0655	Weber [56]
Do.....	366	−.091	Price et al. [57]
Do.....	366	−.17	Kaye[59]
Do.....	436	−.020	Chen and Bowman [13]
Do.....	436	−.0244	Weber [56]
Do.....	436	0.0	Price et al. [57]
Do.....	436	−0.03	Kaye [59]
Do.....	546	0.462	Chen and Bowman [13]
Do.....	546	.444	Weber [56]
Do.....	546	.441	Price et al. [57]
Do.....	546	.462	Singleterry and Weinberger [27]
Do.....	546	.44	Kaye [59]

that there is considerable variation in these values. The best agreement is for Rhodamine B excited at

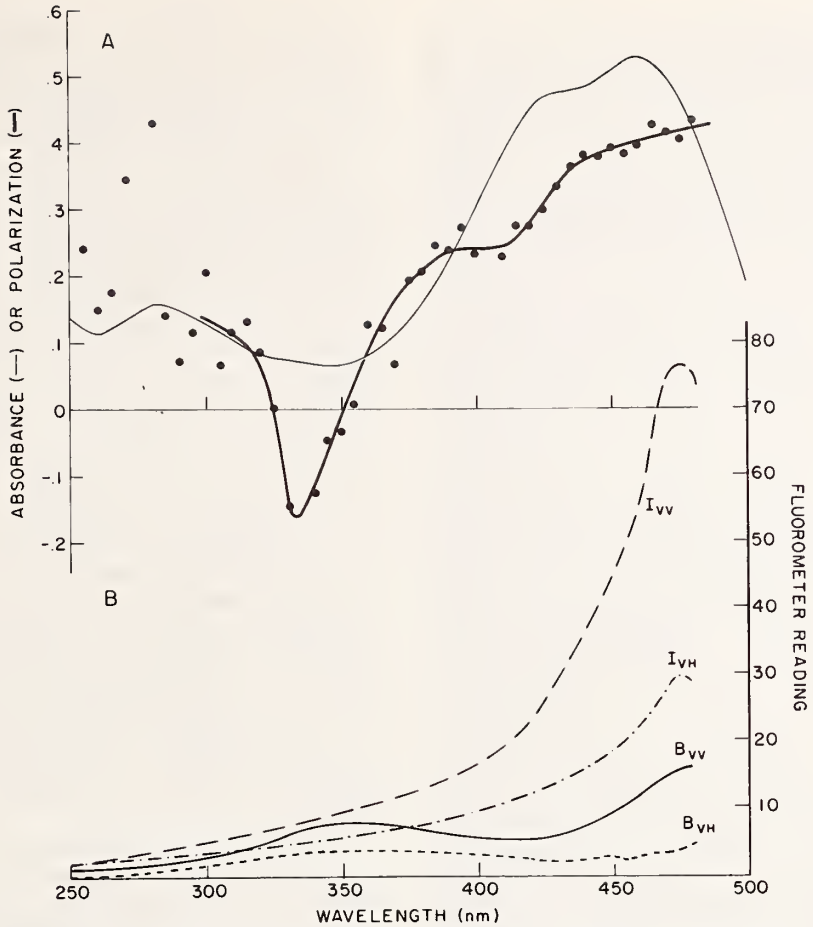

FIGURE 9. Example showing significance of blanks in polarization measurements. In A are shown the absorption (light line) and polarization spectrum (heavy line and points) of bilirubin bound to rabbit serum albumin. The polarization was calculated, using $G = 0.960$, from the data of Part B, which gives the apparent excitation spectra of the sample (I) and blank (B). Subscripts refer to orientation of the polarizer and analyzer. The emission was monitored at 520 nm. From Chen [52].

546 nm: the P values are 0.45 ± 0.01. Poor agreement is found for the values of polarization of Rhodamine B excited at 366 nm.

Useful polarization standards should have polarization which is independent of the emission wavelength. We have found this to be the case for Rhodamine B, fluorescein, and other compounds. However, we found [21] that quinine polarization decreases with wavelength in the emission band (fig. 3).

In many biochemical systems, the emission arises from several fluorophors such as dyes or tryptophans in different parts of a single protein. The polarization therefore depends on both the exciting and emission wavelengths. Much of the early work on the polarization of dye conjugates was obtained with fluorometers where the emission was isolated by a cut-off filter. Such data cannot be duplicated on a spectrofluorometer which detects only a segment of the emission band.

4. *Fluorescence Lifetimes.*

The fluorescence decay time, or lifetime, τ, is defined by $I = I_0 e^{-t/\tau}$ where I_0 is the fluorescence intensity at time $t = 0$ following a delta function exciting pulse, and I is the intensity at subsequent time t. The lifetime is thus the time required for decay of the fluorescence to a value of I_0/e.

The decay times of organic molecules in solution which are of interest to biochemists lie in the range of 0.1 to 100 ns. The accurate measurement of such short times requires complex electronic equipment, but there have been many recent advances in this field. There were no commercially produced instruments for the measurement of τ until 1966. However, numerous laboratory-built instruments had been designed and described. The features of such instruments have been reviewed by Birks and Munro [60].

Two basic types of instrument have been employed. (a) Phase and modulation fluorometers. Here the sample is excited by light which is sinusoidally modulated at megacycle frequencies. The fluorescence thus also fluctuates at these frequencies, but lags behind the excitation by a certain time which is detected electrically as a phase shift with reference to the exciting light. From the phase shift, one can calculate the lifetime value if fluorescence is assumed to decay as a single exponential. The fluorescence decay is also manifested as a decrease in the degree of modulation, and the lifetime can be obtained from this parameter quite apart from the electrical phase shift. Müller et al. [61] reported that a phase fluorometer could be constructed wholly from commercially available components. Spencer and Weber [62] have also constructed a modern phase and modulation fluorometer. Both of these instruments are said to have a very high time resolution, of the order of 0.02 ns. Therefore, the accuracy of lifetime measurements can be said to exceed the accuracy of absolute determinations of quantum yield. No phase fluorometers have ever been marketed. (b) Nanosecond pulse instruments. By repetitively exciting a sample with a short pulse of light, it is possible to obtain directly, with the aid of a fast oscilloscope, the curve of the fluorescence decay. Ideally, the light flash should be infinitely short; the observed fluorescence should then decay exponentially. Practically, lamp pulses have a finite duration with widths at half maximum intensity of 1 to 10 ns, and the pulse shape may be irregular. The fluorescence decay is also a complex function from which the lifetime must be extracted by any of several mathematical procedures. Advances in lamp design and the use of mode-locked lasers with picosecond pulses may in the future avoid the need for such manipulations, since the excitation will be much shorter than the fluorescence.

The two instruments which are currently available from commercial sources for lifetime determinations are both based on the nanosecond pulse method. In 1966, TRW Instruments introduced a decay time apparatus consisting of a nanosecond fluorometer with a "decay time computer" and requiring a dual-gun oscilloscope. One gun of the oscilloscope was used to display the signal from the sample chamber, while the other channel was connected to the computer, which in turn consisted of a variable waveform signal generator and an analog circuit. The computer was used to compare the shapes of the waveforms derived from the lamp pulse and from a fluorescent sample. The difference between the waveforms was analyzed by the computer to give the corresponding decay time directly. The instrument has been described in some detail [63, 64], is still available, and can be fitted with different kinds of lamps for excitation at different wavelengths. Although originally designed for long lifetimes such as those associated with solid laser materials, the instrument was shown to be capable of measuring lifetimes less than 2 ns [65].

Recently, ORTEC, Inc. (Oak Ridge, Tenn.) has produced a nanosecond pulse instrument based on the so-called single photon counting principle. The important feature of the system is the method used to detect and record the signal from the sample chamber. The low intensity, very fast, nanosecond flash lamp is made weaker still by attenuators so that for each repetitive pulse, no more than one photon which leaves the fluorescent sample causes a response in the photodetector. By timing the interval between the flash and the arrival of the photon at the detector, a histogram of counts versus time is built up and stored in a multichannel analyzer. After sufficient counts have been accumulated, the curve can be displayed on an oscilloscope or digitized for computer analysis. The advantage of the system is the extreme sensitivity, the good time resolution, the use of a lamp, which because of its low output can be made very fast, and then recording the actual undistorted decay. The system theoretically can be used to determine multiple lifetimes present in the fluorescence.

Lifetime measurements by any of the instruments mentioned require only a single standard, namely, a reflecting or scattering substance serving as a standard with $\tau=0$. No comparison with substances of known lifetimes is needed, so each lifetime measurement is, in fact, an absolute determination. There are now several compilations of lifetimes which can be used by investigators to test the accuracy of their instruments [60, 66].

Some lifetimes of fluorescence standards are listed in table 3. Many developers of lifetime instruments have examined fluorescein in aqueous base, and a lifetime of 4.5 ± 0.3 ns agrees with most of the values listed. Curiously, the value of 3.83 ns was obtained by Müller et al. [61] with an instrument estimated to be accurate to 0.02 ns. Several values for quinine lifetime have been reported and are listed in table 3. In 1.0 N H_2SO_4 the lifetime of quinine obtained by averaging the tabulated data is 19.9 ns with an average deviation of 0.5 ns or 2.5 percent. The agreement for this compound is as impressive as any listed by Birks and Munro [60], so quinine is probably the best lifetime standard now available.

However, some caution is required in the use of quinine, because we have now found that not only the quantum yield, but the lifetime too, is dependent on the concentration of sulfuric acid (table 3) present.

III. Summary and Conclusions

In biochemistry, many of the same principles for measuring absolute fluorescence parameters are used which are employed in any other area of physical chemistry. Perhaps the only differences are the general use of aqueous solutions, the greater need for commercially available instrumentation, and the diverse types of measurement needed. The range and quality of available instruments have improved. There are still many problems regarding standards to be used for quantum yields, polarization, and spectra. Quinine,

Table 3. Lifetimes of some fluorescence standards

Sample	Lifetime (ns)	Reference
Quinine, 0.1 *N* H_2SO_4	19.5	Weber [67]
Quinine, 1.0 *N* H_2SO_4	19.2	Berlman [66]
Do	19.4	Ware and Baldwin [40]
Do	20.1	Birks and Dyson [41]
Do	20.5	Metcalf, cited in [41]
Quinine, 10.0 *N* H_2SO_4	21.8	Present work
Quinine, 1.0 *N* H_2SO_4	20.4	Do.
Quinine, 0.1 *N* H_2SO_4	19.0	Present work, also [65]
Quinine, 0.2 *M Tris*-NO_3^-, pH 8	17.2	Do.
Fluorescein, dilute NaOH or KOH.	4.62	Ware and Baldwin [40]
Do	4.6	Szymanowski [68]
Do	4.6	Metcalf [69]
Do	4.8	Bennett [70]
Do	4.8	Brody [73]
Do	4.8	Kirchhoff [74]
Do	4.8	Maercks [75]
Do	4.5	Bailey and Rollefson [71]
Do	4.5	Chen et al. [65]
Do	4.2	Weber [67]
Do	4.0	Brewer et al. [72]
Do	4.0	Strickler and Berg [39]
Do	3.83	Müller et al. [1]
9,10-Diphenylanthracene, cyclohexane, not de-aerated.	6.7	Present work
9,10-Diphenylanthracene, cyclohexane, de-aerated.	9.35	Berlman [66]
Do	10.0	Amata et al. [76]
2-Aminopyridine, 0.1 *N* H_2SO_4	12.7	Present work
1-Dimethylaminonaphthalene-5-sulfonate, 0.1 *M* $NaHCO_3$.	13.8	Chen et al. [65]
Do	13.6	Förster and Rokos [77]

the universal standard, has been shown to undergo changes in emission spectrum, quantum yield, polarization, and lifetime depending on factors such as the wavelength of excitation and the sulfuric acid concentration. To determine what the "true" values are for a given compound, further reporting of such values is to be encouraged. It is suggested that collaborative efforts might speed up the "certification" of values for fluorescence standards.

IV. References

[1] Weber, G., Biochem. J. **51**, 145 (1952).
[2] Weber, G., Biochem. J. **51**, 155 (1952).
[3] Perrin, F., J. Phys. **7**, 390 (1926).
[4] Levshin, V. L., Z. Physik **26**, 274 (1924).
[5] Chen, R. F., Edelhoch, H., and Steiner, R. F., in Physical Principles and Techniques of Protein Chemistry, Part A, S. J. Leach, Ed., pp. 171–244 (Academic Press, N.Y., 1969).
[6] Velick, S. F., J. Biol. Chem. **233**, 1455 (1958).
[7] Chen, R. F., and Kernohan, J. C., J. Biol. Chem. **242**, 5813 (1967).
[8] Förster, T., Ann. Phys. (Leipzig) **2**, 55 (1948).
[9] Lerman, L. S., Proc. Nat. Acad. Sci. **49**, 94 (1963).
[10] Weber, G., and Anderson, S., Biochemistry **8**, 361 (1969).
[11] Witholdt, B, and Brand, L., Biochemistry **9**, 1948 (1970).
[12] Bowman, R. L., Caulfield, P. A., and Udenfriend, S., Science **122**, 32 (1955).
[13] Chen, R. F., and Bowman, R. L., Science **147**, 729 (1965).
[14] Chapman, J. H., Förster, T., Kortum, G., Parker, C. A., Lippert, E., Melhuish, W. H., and Nebbia, G., Appl. Spectroscopy **17**, 171 (1963).
[15] Melhuish, W. H., J. Opt. Soc. Am. **52**, 1256 (1962).
[16] Chen, R. F., Anal, Biochem. **20**, 339 (1967).
[17] Lee, J., and Seliger, H. H., Photochem. Photobiol. **4**, 1015 (1965).
[18] Argauer, R. F., and White, C. E., Anal. Chem. **36**, 368 (1964).
[19] Børresen, H. C., Acta Chem. Scand. **19**, 2089 (1965).
[20] Gill, J. E., Photochem. Photobiol. **9**, 313 (1969).
[21] Chen, R. F., Anal. Biochem. **19**, 374 (1967).
[22] Fletcher, A. N., J. Phys. Chem. **72**, 2742 (1968).
[23] Scott, T. G., Spencer, R. D., Leonard, N. J., and Weber, G., J. Am. Chem. Soc. **92**, 687 (1970).
[24] Hughes, E., Jr., Wharton, J. H., and Nauman, R. V., J. Phys. Chem. **75**, 3097 (1971).
[25] Galley, W. C., and Purkey, R. M., Proc. Nat. Acad. Sci. **67**, 1116 (1970).
[26] Weber, G., and Teale, F. W. J., Trans. Faraday Soc. **53**, 646 (1957).
[27] Singleterry, C. R., and Weinberger, L. A., J. Am. Chem. Soc. **73**, 4574 (1951).
[28] Almgren, M., Photochem. Photobiol. **8**, 231 (1968).
[29] Paoletti, J., and LePecq, J.-B., Anal. Biochem. **31**, 33 (1969).
[30] Windsor, W. R., and Dawson, M. W., J. Phys. Chem. **72**, 3251 (1968).
[31] Demas, J. N., and Crosby, G. A., J. Phys. Chem. **75**, 991 (1971).
[32] Melhuish, W. H., J. Phys. Chem. **65**, 229 (1961).
[33] Melhuish, W. H., N. Zeal. J. Sci. Technol. **37B**, 142 (1955).
[34] Eastman, J. W., Photochem. Photobiol. **6**, 55 (1967).
[35] Drobnik, J., and Yeargers, E., J. Mol. Spectr. **19**, 454 (1966).
[36] Fletcher, A. N., J. Mol. Spectr. **23**, 221 (1967).
[37] Rusakowicz, R., and Testa, A. C., J. Phys. Chem. **72**, 793 (1968).
[38] Förster, T., Fluoreszenz Organischer Verbindungen, p. 158 (Vandenhoeck u. Rupprecht, Göttingen, 1951).
[39] Strickler, S. J., and Berg. R. A., J. Chem. Phys. **37**, 814 (1962).
[40] Ware, W. R., and Baldwin, B. A., J. Chem. Phys. **40**, 1703 (1964).
[41] Birks, J. B., and Dyson, D. J., Proc. Roy. Soc. **A274**, 135 (1963).
[42] Shore, V. G., and Pardee, A. B., Arch. Biochem. Biophys. **62**, 355 (1956).
[43] Teale, F. W. J., and Weber, G., Biochem. J. **65**, 476 (1957).
[44] Chen, R. F., Anal. Lett. **1**, 35 (1967).
[45] Børresen, H. C., Acta Chem. Scand. **21**, 920 (1967).
[46] Bridges, J. W., and Williams, R. T., Biochem. J. **107**, 225 (1968).
[47] Eisinger, J., Photochem. Photobiol. **9**, 247 (1969).
[48] Rusakowicz, R., and Testa, A. C., J. Phys. Chem. **72**, 2680 (1968).
[49] Weisstuch, A., and Testa, A. C., J. Phys. Chem. **72**, 1982 (1968).
[50] Parker, C. A., and Rees, W. T., Analyst **85**, 587 (1960).
[51] Azumi, T., and McGlynn, S. P., J. Chem. Phys. **37**, 2413 (1962).
[52] Chen, R. F., Anal. Lett. **4**, 459 (1971).
[53] Weber, G., and Bablouzian, B., J. Biol. Chem. **241**, 2558 (1966).
[54] Deranleau, D. A., Anal. Biochem. **16**, 438 (1966).
[55] Rosén, C.-G., Acta Chem. Scand. **24**, 1849 (1970).
[56] Weber, G., J. Opt. Soc. Am. **46**, 962 (1956).
[57] Price, J. M., Kaihara, M., and Howerton, H. K., Appl. Opt. **1**, 521 (1962).

[58] Szalay, L., Gáti, L., and Sárkány, B., Acta Phys. Acad. Sci. (Hungary) **14,** 217 (1962).
[59] Kaye, W., Appl. Spectr. **18,** 9 (1964).
[60] Birks, J. B., and Munro, I. H. in G. Porter, ed., Progress in Reaction Kinetics **4,** 239 (1967).
[61] Müller, A., Lumry, R., and Kokubun, H., Rev. Sci. Instr. **36,** 1214 (1965).
[62] Spencer, R. D., and Weber, G., Ann. N.Y. Acad. Sci. **158,** 361 (1969).
[63] Chen, R. F., Arch. Biochem. Biophys. **133,** 263 (1969).
[64] Meserve, E., in R. F. Steiner and I. Weinryb, eds., Excited States of Proteins and Nucleic Acids, Plenum Press, N.Y., 1971, p. 57.
[65] Chen, R. F., Vurek, G. G., and Alexander, N., Science **156,** 949 (1967).
[66] Berlman, I. B., *Handbook of Fluorescence Spectra of Aromatic Molecules*, Academic Press, N.Y. 1965; 2d Ed., 1971.
[67] Weber, G., Methods in Enzymol. **16,** 393 (1969).
[68] Szymanowski, W., Z. Physik **95,** 450 (1935).
[69] Metcalf, W. S., J. Chem. Soc. 3726 (1960).
[70] Bennett, R. G., Rev. Sci. Instr. **31,** 1274 (1960).
[71] Bailey, E. A., and Rollefson, G. K., J. Chem. Phys. **21,** 1315 (1953).
[72] Brewer, L., James, C. G., Brewer, R. G., Stafford, F. E., Berg, R. A., and Rosenblatt, G. M., Rev. Sci. Instr. **33,** 1450 (1962).
[73] Brody, S. S., Rev. Sci. Instr. **28,** 1021 (1957).
[74] Kirchhoff, W., Z. Physik **116,** 115 (1940).
[75] Maercks, O., Z. Physik **109,** 685 (1938).
[76] Amata, C. D., Burton, M., Helman, W. P., Ludwig, P. K., and Rodemeyer, S. A., J. Chem. Phys. **48,** 2374 (1968).
[77] Förster, Th., and Rokos, K., Chem. Phys. Lett. **1,** 279 (1967).

(Paper 76A6–744)

NATIONAL BUREAU OF STANDARDS SPECIAL PUBLICATION 378, Accuracy in Spectrophotometry and Luminescence Measurements, Proceedings of a Conference Held at NBS, Gaithersburg, Md., March 22–24, 1972 (Issued May 1973).

Newer Fluorometric Methods for the Analysis of Biologically Important Compounds

G. G. Guilbault

Department of Chemistry, Louisiana State University, New Orleans, La. 70122

(June 15, 1972)

Newer fluorometric methods for the analysis of biologically important compounds will be discussed: enzymes such as LDH, alkaline phosphatase, lipase and cholinesterase, and substrates such as glucose, urea and uric acid. These methods are based on the production of fluorescence initiated by an enzymic reaction.

New reagentless fluorescence methods will be described for enzymes and substrates. These methods are highly precise (1%), fast (less than 1 minute) and involve no preparation of reagents. These methods, as adapted to clinical laboratory procedures, will be discussed.

Key words: Enzymes, fluorometric analysis; fluorometry of enzymes; fluorometry of substrates; silicone pad; solid surface fluorometry.

I. General

Enzymes are biological catalysts which enable the many complex chemical reactions, necessary to the existence of life, to take place at ordinary temperatures. Because enzymes work in complex living systems, one of their outstanding properties is specificity. Thus, an enzyme is capable of catalyzing a particular reaction of a particular "substrate" to produce a characteristic and measurable reaction end product. This specificity of enzymes and their ability to catalyze reactions of substrates at extremely low concentrations is of significant use in biochemical analyses.

Enzyme catalyzed reactions have long been used for such analytical purposes for determining the presence of specific substrates, enzyme activators, enzyme inhibitors, and enzymes themselves, and in determining the concentration of these substances. Numerous methods have been described for the determination of enzymic activity between an enzyme and a substrate. Until recently, however, the disadvantages associated with the use of enzymes in these analytical techniques have seriously limited their usefulness.

A detailed discussion of the use of enzymes for analysis can be found in review articles by Guilbault [1–3] and books by Guilbault [4] and Bergmeyer [5].

The concentration of substrate participating in an enzyme reaction can be calculated in one of two general ways. The first method measures, by chemical, physical, or enzymatic analysis, either the total change that occurs in the end product or the unreacted starting material. In this method, large amounts of enzyme and small amounts of substrate are used to insure a complete reaction. In the second method, which is a kinetic method, the initial rate of reaction is measured, in one of many conventional ways, by following the production of product or the disappearance of the substrate. In this method, the rate of reaction is a function of the concentration of substrate, enzyme, inhibitor and activator.

On the other hand, because enzymes are catalysts, and as such affect the rate and not the equilibrium of reactions, their concentration and activity must be measured by the rate or kinetic method. Similarly, activators and inhibitors that affect the enzyme's catalytic effect can be measured only by the rate method. While, as pointed out above, the substrate can be measured either by a total change or a rate method, the latter method is faster because the initial reaction can be measured without waiting for equilibrium to be established. The accuracy and precision of both methods are comparable.

In the past, manometric methods, pH procedures, and spectrophotometry have been used for determining enzyme activity. Spectrophotometry has been generally preferred because of its simplicity, its rapidity and the capability of measuring lower enzyme and substrate concentrations. Spectrophotometry embraces the use of colorimetric methods where colored products are produced as a result of enzyme activity, and fluorescent methods where fluorescent compounds are produced as a result of enzyme activity. Fluorescent procedures are several orders of magnitude more sensitive than colorimetric methods and thus have replaced the colorimetric methods in numerous instances.

Previous fluorometric methods, although they have

502-591 O - 73 - 14

been improvements over other prior art methods of determining enzyme activity have not eliminated all of the problems associated with enzymic analyses. Fluorometric analysis depends on the production of a fluorescent compound as a result of enzyme activity between a substrate and enzyme. The rate of production of the fluorescent compound is related to both the enzyme concentration and substrate concentration. This rate can be quantitatively measured by exciting the fluorescent compound as it is produced and by recording the quantity of fluorescence emitted per unit of time with a fluorometer.

The prior methods for fluorometrically measuring enzyme reaction rates, however, have been wet chemical methods and rely on reacting a substrate solution with an enzyme solution. Wet chemical methods involve time-consuming and wasteful preparation of costly substrate solutions and enzyme solutions. For example, when determining the presence and concentration of an enzyme, a substantial amount of substrate must be accurately weighed and dissolved in a large amount of buffer solution usually about 100 ml to prepare a stock solution. The enzyme reaction is then usually carried out by measuring, for example, 3 ml of stock substrate solution into an optical cuvet, adding a measured amount of the enzyme solution to the substrate solution, and recording the change in fluorescence eminating from the resultant solution per minute with a fluorometer. This standard wet chemical method is costly and wasteful because laboratory trained technicians' time and relatively large quantities of expensive substrate are required.

II. Solid Surface Fluorescence Monitoring System

Solid-surface fluorometric methods, using a reagentless system, have been developed for the assay of clinically important enzymes, substrates, activators and inhibitors. The method comprises forming a solid reactant film of one of the reactants on an inert silicone matrix pad, contacting the film of the first reactant with a solution of the second reactant (substance to the measured) to produce a fluorescent material, and monitoring the change of fluorescence with time to determine the concentration of the second reactant.

The reactant film may be formed by dissolving the reagents in a solvent, depositing the reactant solution on the silicone pad so that the solution spreads evenly over the pad, and evaporating the solvent from solution. The reagent may be applied to the pad either from an acetone solution if a substrate or in a polymeric film such as polyacrylamide if an enzyme. Either substrate or enzyme and/or coenzyme can be deposited on the pad in film form depending upon whether the substance to be assayed is an enzyme or a substrate.

After the pad is formed (fig. 1), it is attached to a slide made of a rigid material, such as a glass or metal slide, by applying an adhesive to the slide and overlying the pad on the adhesive. The pads are placed approximately 1 or 2 cm from the bottom of the slide (fig. 2).

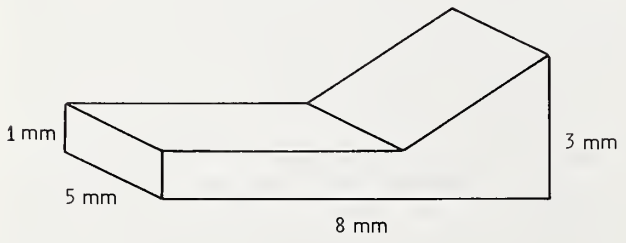

FIGURE 1. Pad support (all measurements are in mm).

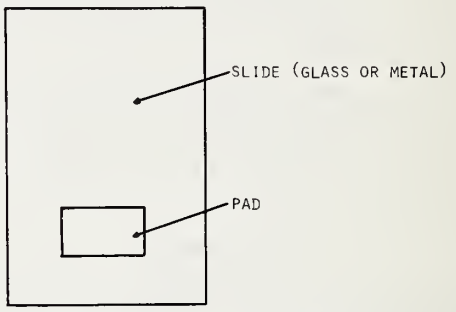

FIGURE 2. Slide support.

The fluorescent cell consists of a rectangular cell made of ordinary sheet metal, wood or plastic material (fig. 3), having portholes to allow radiation to enter and leave the cell cavity. The top of the cell is provided with guides at opposite sides so that the slide containing the reagents can be reproducibly placed within the cell. In order to obtain as low a background as possible, the cell is painted with a black optical paint having a dull finish.

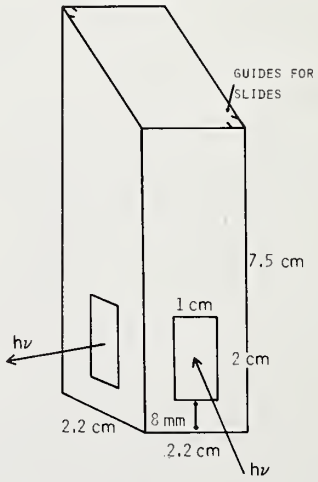

FIGURE 3. Fluorescence attachment used to hold pads.

Before the enzyme solution is added, the glass slide is put into the fluorometer and a background reading is taken. A blank rate is taken using all components of the system, except the unknown. The slide is then removed from the fluorometer and 20 μl of a solution of the substance to be assayed is applied to the slide. The recorder (100 mV input) is started immediately, the slide is placed back into the fluorometer, and the rate is recorded. A calibration plot of the change in fluorescence units per minute versus concentration is prepared and used for subsequent analyses of enzyme or substrate.

After a run is completed, the pad can be peeled from the slide, and the slide cleaned and stored for subsequent use.

The physical properties of the silicones and the stability of the reactant films of enzyme and substrate in the presence of silicones further make these materials ideally suited for use. The silicone materials can retain a reactant film on their surfaces for an indefinite time and permit the direct measurement of fluorescence from its surface when an appropriate second reagent solution is dropped onto the first reactant film. Background interference due to light scattering and nonspecific fluorescence are minimal compared to other materials.

The number of enzyme systems that could be monitored by this type of solid-surface device are as numerous as the number of enzyme systems known. Some of the more clinically important systems that will be studied and for which methods have been developed are as follows.

III. Assay of Clinically Important Enzymes

A. Cholinesterase

Low levels of cholinesterase (ChE) are found in individuals with anemia, malnutrition, and pesticide poisoning. High levels indicate a nephrotic syndrome.

Preliminary results have indicated that cholinesterase in solution can be monitored using a film of *N*-methyl indoxyl acetate on the surface of a silicone rubber pad:

$$N\text{-Methyl indoxyl acetate} \xrightarrow{\text{ChE}} N\text{-Methyl Indoxyl}$$

(Fluorescent—$\lambda_{ex}=495$ nm, $\lambda_{em}=525$ nm)

The rate of production of *N*-methyl indoxyl is followed and is proportional to the cholinesterase concentration. Attempts have been made to develop methods for the direct assay of ChE in blood and body tissue. The reproducibility and accuracy obtainable using several configurations of pad and various experimental conditions have been compared and the optimum system developed. A linear region of 10^{-4} to 1 unit has been obtained [6].

Preliminary studies have indicated that pads made from either method were stable for at least 60 days (table 1), if kept in a cold dark place.

TABLE 1. Pad stability data[a]

Day[b]	Rate, ΔF/min[c]
0	3.10
2	3.04
4	3.08
10	3.20
30	3.00
60	3.00

[a] A 500 μg/ml solution of cholinesterase was freshly prepared for each day. Twenty microliters of a 0.1 *M* substrate solution were applied to the pad and allowed to evaporate to dryness.

[b] Days after preparation of pad.

[c] Rates were an average of at least three runs.

B. Alkaline Phosphatase

High levels of alkaline phosphatase are observed in rickets, Paget's disease, obstructive pandicea, and metastatic carcinoma.

The fluorogenic substrate naphthol-AS-BI-phosphate was used for the assay of alkaline phosphatase in serum. Guilbault et al. [7, 8] found that this substrate is the best for the direct assay of alkaline phosphatase in serum. A solution method was used and an accuracy and precision of about 2 percent was obtained. The deep green fluorescent naphthol AS-BI formed is measured. Attempts have been made to monitor this reaction on a solid surface. A drop of serum to be assayed has been added directly to the naphthol AS-BI-phosphate on the surface and the rate monitored. No solutions are required. From 10^{-6} to 10 units are assayable [9].

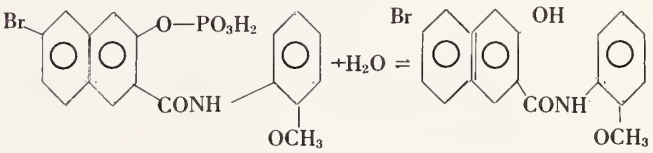

Naphthol AS-BI-Phosphate (Non-Fluorescent)

Naphthol AS-BI (Fluorescent)

Further attempts have been made to extend the usefulness of this method for a wide variety of biological samples.

The color of the silicone rubber however, affects both the background and reaction rates. With any of the filter systems, the background and reaction rates increase in the order black<grey<clear<white. Each possible combination of pad color and filter was examined and it was found that the most accurate results could be obtained if a combination of 7–54 filter and grey silicone rubber pads were used.

Table 2 shows the results obtained from a series of serum samples. Over 80 serum samples were analyzed with a relative error of ± 5 percent.

TABLE 2. Determination of serum alkaline phosphatase

Units alkaline phosphatase taken [a]	Units alkaline phosphatase found [a-c]
20	21.5
22	19
24	24.5
26	23
28	25
30	31
31	31
33	37
37	34
39	40
41	39
43	42
48	49
53	[d] 54
61	[d] 60
64	[d] 64

[a] Units expressed as μmol phenolphthalein liberated min^{-1} l^{-1} serum.

[b] Obtained by multiplying the rate by 31.5.

[c] Average from 3 or more different samples—each analysis in duplicate.

[d] One sample—average of 2 determinations.

Figure 4 shows the correlation between the serum alkaline phosphatase values obtained from the "solid surface" method and alkaline phosphatase values obtained from a solution method employing phenolphthalein phosphate. The graph shows good agreement between the two methods over a wide range of serum values. If the serum values are expressed as μmol phenolphthalein liberated min^{-1} l^{-1} serum, then normal serum has 27–105 units.

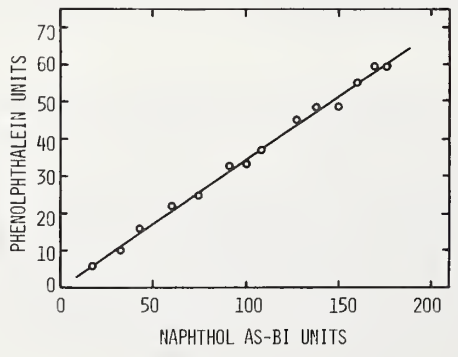

FIGURE 4. Correlation between results obtained with naphthol AS-BI method and phenolphthalein method.

Table 3 shows the alkaline phosphatase values obtained from highly jaundiced serum compared to the phenolphthalein phosphate method. All the results from these samples were low and implied a limitation on the method. It is, however, possible to predict which samples will give low results. Generally, it is those samples which are very dark yellow or orange-yellow in color. The light-yellow serum gave good results as did haemolyzed serum. The low values obtained from jaundiced serum is the main limitation of the method, but it is possible to recognize these solutions and carry out the analysis by an alternative method.

TABLE 3. Analytical results obtained from jaundiced serum samples

Units alkaline phosphatase taken [a]	Units alkaline phosphatase found [a, b]
27	18
34	21
59	30
86	21
135	44
185	115
200	138

[a] Units expressed as μmol phenolphthalein liberated min^{-1} l^{-1} serum.

[b] Average of 3 results.

C. Lipase

A low plasma lipase indicates vitamin A deficiency and some malignancies. Lipase assay is most important in diagnosis of pancreatitis.

Two fluorogenic substrates have been evaluated for the assay of lipase: *N*-methyl indoxyl myristate, a substrate developed by Guilbault and Hieserman [10], and 4-methyl umbelliferone myristate, a substrate recently prepared in our labs.

The production of the green fluorescent naphthol AS–BI or the blue 4-methyl umbelliferone myristate can be followed on the surface.

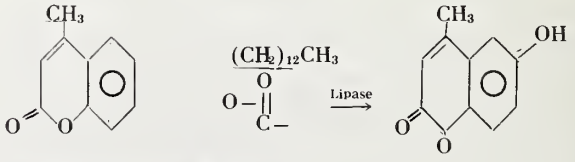

4-Methyl Umbelliferone Myristate ⟶

4-Methyl Umbelliferone $\lambda_{ex} = 340$ nm
$\lambda_{em} = 450$ nm

A direct assay of lipase (10^{-4} to 10 units) in serum and pancreas can be effected.

D. Lactate Dehydrogenase

Levels of this enzyme are elevated in individuals with acute and chronic leukemia in relapse, myocardial infarctions and carcinomatosis.

Fluorometric analysis of dehydrogenases in the past have been based on measurement of NADH fluorescence. Guilbault and Kramer [11] have described a fluorometric method of coupling reduced nicotinamide adenine dinucliotide (NADH) to an electron acceptor (resazurin) in the presence of the cofactor phenazine methosulfate (PMS).

$$\text{Lactate} + \text{NAD} \xrightarrow{\text{LDH}} \text{NADH} + \text{pyruvate}$$

$$\underset{\text{(Non-Fluorescent)}}{\text{NADH} + \text{Resazurin}} \xrightarrow{\text{PMS}} \underset{\text{(Fluorescent)}}{\text{Resorufin} + \text{NAD}}$$

A semisolid state fluorescence method for the analysis of lactic dehydrogenase (LDH) has been developed [12]. The commercially available enzyme in aqueous solution, and the enzyme in blood serum were studied. The serum analysis is compared to a method described by Bergmeyer, et al. [13]. As little as 160 units of LDH per milliliter of blood serum can be analyzed with an accuracy of better that 3 percent.

The reaction system used was:

$$\text{Li Lactate} + \text{NAD} \overset{\text{LDH}}{\rightleftarrows} \text{NADH} + \text{Pyruvic Acid.} \quad \text{(I)}$$

The rate of production of the fluorescent product NADH was monitored.

Some of the results obtained in the assay of LDH in serum using the solid surface method are shown in table 4. An average relative error of 2.3 percent was obtained.

IV. Assay of a Clinically Important Substrate

High levels of glucose may indicate diabetes.

Guilbault et al. [14] have described a fluorometric assay system for glucose using glucose oxidase, peroxidase, and *p*-hydroxyphenylacetic acid. The rate of production of fluorescence is proportional to the amount of glucose present.

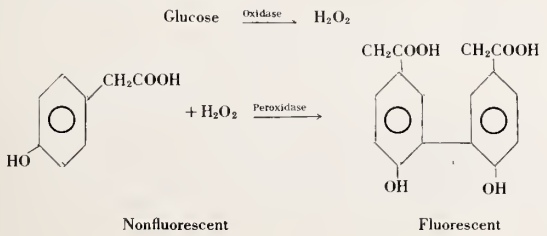

To develop a reagentless surface method for assay of glucose, the enzymes glucose oxidase and peroxidase, and the substrate *p*-hydroxyphenylacetic acid were placed on the surface. The addition of glucose initiates the reaction; fluorescence is produced and its rate of production will be proportional to the glucose present in blood [15]. A range of 10^{-5} to 10^{-1} M glucose can be assayed.

TABLE 4. Data and results of the assay of serum LDH using the proposed method

Rate, ΔF/min.	Concentration taken	u/ml found	Relative error (percent)
6.6	160	168	+4.9
7.3	190	189	−0.3
7.2	200	186	−6.5
10.1	280	276	−1.3
13.2	360	372	+3.3
13.9	380	394	+3.4
15.3	440	437	−0.6
16.0	460	459	− .2
17.2	500	496	− .8
18.8	560	546	−2.5
21.4	620	626	+1.0
		Average relative error	2.3

B. Advantages of Solid Surface Method

The advantages of this radically new system for the clinical laboratory are:

1. The time required for analysis by present methods is 30 to 60 min to prepare reagents plus 10 to 20 min per assay. If a sample is available at 1 a.m., the technician must proceed through the regular preparation and analysis routine. The solid surface method requires 10 bottles of pads, one for each of 10 common tests. The technician would open the bottle marked "LDH test," pick out a pad, put it in the instrument on the strip holder, add a 10 μl sample of blood or urine, and read out the results directly in mg percent urea. Total time is about 2 min.

2. The accuracy of current methods (mostly spectrophotometric) are limited to an error of about 2 to 3 percent over a narrow range (0.15 to 0.85 Abs units). Because fluorescence methods are based on the production of a signal over zero signal, the accuracy of these methods is independent of scale reading, and have an accuracy of 1 percent over a 3 to 4 fold linear range of concentrations.

3. Temperature must be controlled in all enzyme assays based on a kinetic approach. This is expensive and bothersome. The solid surface fluorescence method proposed is not temperature dependent, since the silicone rubber pad used to support the sample is nonheat conductive. Thus, provided the sample of blood is at the same temperature as used to prepare the calibration plot (generally room temperature, 25 °C) the temperature of the environment does not affect the results. For example, in the assay of alkaline phosphatase, we obtained the same rate at 10, 15, 20, 25, 30, 35, and 40 °C external temperature, provided

we added the blood from a sample kept at 25 °C. This represents a significant improvement.

4. The reagents used in present clinical procedures are unstable, and new solutions must be prepared daily. *o*-Toluidine and peroxidase in glucose assay, or NAD in LDH assay are examples of this. Yet when the reagents are placed in *solid form* on a surface, they can be kept for months with *no deterioration*. In our ChE, alkaline phosphatase and LDH assays, we found we could use our pads for 90 days, using the same calibration plot everyday.

5. Many clinical methods are subject to interferences because of (a) protein absorption in the near UV-visible or (b) absorbing impurities in the reagents. By using reagents that fluoresce in the visible, and reagents in a solid form, these two interferences are eliminated.

V. References

[1] Guilbault, G. G., Anal. Chem. **38**, 527R (1966).
[2] Guilbault, G. G., Anal. Chem. **40**, 459R (1968).
[3] Guilbault, G. G., Anal. Chem. **42**, 334R (1970).
[4] Guilbault, G. G., Enzymatic Methods of Analysis, (Pergamon Press, 1970).
[5] Bergmeyer, H., Methods of Enzymatic Analysis (Verlag Chemie, Germany, 1965).
[6] Guilbault, G. G., and Zimmerman, R., Anal. Letters **3**, 133 (1970).
[7] Guilbault, G. G., and Vaughn, A., Anal. Letters **3**, 1 (1970).
[8] Guilbault, G. G., and Vaughn, A., Anal. Chem. **43**, 721 (1971).
[9] Guilbault, G. G., and Vaughn, A., Anal. Chem. Acta **55**, 107 (1971).
[10] Guilbault, G. G., and Hieserman, J. Anal. Chem. **41**, 2006 (1969).
[11] Guilbault, G. G., and Kramer, D. N., Anal. Chem. **36**, 2497 (1964).
[12] Guilbault, G. G., and Zimmerman, R., Anal. Chim. Acta, **58**, 75 (1972).
[13] Bergmeyer, H., Bernt, E., and Hass, B., in Methods of Enzymatic Analysis, H. Bergmeyer, Ed, (Academic Press, New York, 1963), p. 736.
[14] Guilbault, G. G., Brignac, P., and Zimmer, M., Anal. Chem. **40**, 1256 (1968).
[15] Guilbault, G. G., and Tang, D., unpublished results.

(Paper 76A6–745)

NATIONAL BUREAU OF STANDARDS SPECIAL PUBLICATION 378, Accuracy in Spectrophotometry and Luminescence Measurements, Proceedings of a Conference Held at NBS, Gaithersburg, Md., March 22–24, 1972 (Issued May 1973).

Inorganic Ions in Glasses and Polycrystalline Pellets as Fluorescence Standard Reference Materials*

R. Reisfeld

Department of Inorganic and Analytic Chemistry, Hebrew University of Jerusalem, Jerusalem, Israel

(June 15, 1972)

The absorption and fluorescence of inorganic glasses and polycrystalline disks doped by heavy metal ions is discussed, and their use as fluorescence standards is evaluated. The advantages of the glass standards over other media is summarized.

The glass standards are divided into two groups (1) glasses doped by trivalent rare earths such as Gd^{3+}, Tb^{3+}, Eu^{3+}, Sm^{3+}, and Tm^{3+} which have narrow band optical spectra as a result of intraconfigurational transitions, and (2) glasses and polycrystalline disks doped by ions such as Tl^{+}, Pb^{2+}, Ce^{3+}, and Cu^{+} which have broad spectral bands since the optical spectra originate from interconfigurationally allowed transitions. Optical and physical parameters, including matrix effects, quantum efficiencies, decay characteristics, Stokes' shifts and spin-orbit versus orbit-lattice interactions due to the different transitions will be discussed.

Group (1) glasses are suitable for use as standards where a narrow well-defined fluorescence range is required, and group (2) glasses are suitable for use as standards whenever a substance with a wide range of fluorescence is measured. Special emphasis will be placed on energy transfer between donor and acceptor ions.

Key words: Fluorescence standards, inorganic ions; glass standards in fluorescence; rare-earth-doped glasses.

Introduction

The use of fluorescence and phosphorescence as experimental tools has increased immensely in the last decade. The fluorescence technique is used now as a common tool of research by physical chemists, physicists, analytical chemists, biochemists and biophysicists. The kinds of analyses which have been performed to date using fluorescence have varied, including such methods as trace metal determination, analysis for traces of organic materials and particularly for determination of trace constituents of biological systems. It provides some of the most sensitive and selective methods of qualitative and quantitative analysis. (Lower limits of detectability using fluorescence analysis lie often in subpart per million (ppm) and part per billion (ppb) range.) Fluoresence analysis especially, has many practical applications in the field of organic, inorganic, agricultural, biological and clinical chemistry.

The reader interested in the principles and applications of fluorescence in analysis is referred to two recently published books [1, 2][1] on this subject and to a very comprehensive review on measurements of photoluminescence quantum yield in solutions written by Demas and Crosby. [3]

The following are a few examples in which fluorescence is used in health and environmental problems.

Organic Compounds

Many organic compounds fluoresce and/or phosphoresce and these properties have been widely used for analysis. An understanding of the basic aspects of the luminescence of organic compounds can greatly enhance its efficiency as an analytical tool.

The ability of proteins to luminesce has now been fairly thoroughly investigated and is mostly due to the presence of the fluorescent aromatic amino acids tryptophan and tyrosine, [4, 5]. Any biological process can be inhibited, stimulated or altered through photochemical methods by inducing electronic excited states in proteins and nucleic acids. In the investigation of these excited states by photoabsorption and luminescence techniques, a great deal of information can be obtained, not only about the number of biopolymeric molecules in the system, but also about their environment.

Significant qualitative and quantitative information concerning molecular structure can be obtained through fluorescence. When one considers that information of this kind can be obtained rapidly from the interior of the undamaged, usually functioning cell, one realizes the special importance of spectral lumi-

* This work was performed under NBS contract C-103.

[1] Figures in brackets indicate the literature references at the end of this paper.

nescence research techniques in biology. An example of fluorimetric methods in this area is: the fluorescent tags for labeling proteins [6] and amino acids [7–10] which have proven useful in immunochemistry, virology, bacteriology, parasitology, and mycology.

Agriculture

Determining factors in the degree of pest control by chemicals are (1) efficiency of application, (2) the loss by spray particle drift to immediate areas not intended to be treated, and (3) the effective life of the chemical on plants, animals and in soils after application. In this respect, fluorescence has made an outstanding contribution in pesticide analysis. The excitation and emission spectra, decay times, analytical curves, and limits of detection, have been obtained for many pesticides in media such as milk, animal feeds, fruits and vegetables, tissues, etc. [11]. Fluorescent tracer studies of spray and dust deposits on plants and soils have been reported [12, 13].

Biomedical Research

In this area, fluorescence spectroscopy has been used largely as an analytical tool for the assay of many materials of biological origin, [14] such as the examination of carcinogenic materials in the environment, [15] in metabolic studies of aromatic hydrocarbon carcinogens [16] and the determination of drugs, enzymes and proteins.

Of great interest are the experimental observations of the luminescence of cells and tissues in such pathological states as carcinogenesis, inflammation, psychic diseases and muscle atrophy due to denervation. Investigators have sought a correlation between luminescence intensity and the pathological process. However, more information about the structural chemical organization of the protoplasm during the development of the pathological process will be obtained if the comparison involves, not merely the intensity of the fluorescence of various cells, but the magnitude of the changes in fluorescence intensity due to several factors. The use of luminescence to a successfully selected set of experimental treatments will prove to be a useful technique in the field of molecular and cell biology and primarily in the field of practical medicine [17].

The mechanism of cancer induction by aromatic hydrocarbons is of particular interest and it is possible that the initial interaction is a complex formation between the hydrocarbon and a vital cell constituent, such as the nucleic acids which may be determined by changes in fluorescence spectra and parameters [18–20]. Various aromatic hydrocarbons may fluoresce at widely differing frequencies, a fact which is of considerable analytical importance. A history of fluorescense work with carcinogenic hydrocarbons was included in a lecture by Cook in 1950 [21]. Presently, fluoroscence analysis is used in many studies to determine qualitatively and quantitatively the presence of polynuclear hydrocarbons in the environment, usually after separation by thin-layer chromatography [22].

A method for binding dyes to nucleic acids is widely used in staining biological tissues for fluorescence microscopic examination and is used as a screening procedure for cancerous tissue [23].

Fluorometric techniques have made great inroads in the clinical laboratory as the basis of sensitive analytical methods [24, 25].

A. General

In all research and measurements in which fluorescence is involved, it is of utmost importance to measure the true wavelength (energy) of excitation and emission, and the fluorescence efficiency. To determine fluorescence efficiency directly, it is necessary to measure the rate of emission at all wavelengths and in all directions. In practice, this is a difficult measurement to perform with accuracy. In view of the difficulties associated with absolute methods, and the ease with which the fluorescence efficiency may be determined by reference to a standard, a search for a suitable standard is of great importance in spectrofluorimetry. The requirements for a good reference compound to be used as a standard are stringent. It should have a well-defined fluorescence and excitation spectrum, a relatively high quantum efficiency, it should be of the same geometry as the samples to be measured and should be stable. There should be little or no overlap between the absorption and the emission spectrum. The reference compound used in any instance should have its absorption and fluorescence in the same general region as the compound being studied. This last restriction is needed because most spectrofluorimeters record spectra which are not corrected for instrumental parameters.

Fluorescence measurements are mainly made on liquids in aqueous or organic solvents, using glass or quartz cuvettes, and in the solid phase with single crystals, in pellets [26] and in solvent glasses [27]. It would therefore be desirable that the standard reference material also be made of the same or similar material having a similar refractive index, thus avoiding the refractive index correction (discussed later). It is also essential that the standard have a small absorption, since a higher absorption introduces an error in the efficiency determination. This arises from the following consideration: The optically dilute measurement rests on Beer's Law $I_0B = I_0(1-10^{-AL})$ where B is the fraction of light absorbed by the sample, I_0 (quanta/sec · cm^2) is the irradiance of incident light, A is the absorbance/cm, and L(cm) is the path length [3]. By expanding this expression in a power series we obtain $B = 1-[1-2.303\,AL]+[2.303\,AL]^2/2+ \ldots\ldots \simeq 2.303\,AL$. For solutions that are optically dilute, (absorbance less than 0.05) we can truncate the series and the following approximation is true: $B \simeq 2.303\,AL$. Thus at low solute concentrations, the fluorescence intensity is proportional to concentration.

With these criteria in mind we have attempted to prepare glass and pellet standards. The results of

our work are described in this paper. For the latest references to liquid standards the reader is referred to reference [3], for a sodium salicylate standard to reference [28], and for quantum yield determinations of powder phosphors to reference [29].

In this paper the physical parameters of doped glasses and alkali halides suggested as standards will be described. In order that such materials be used as standards, and the use be at optimal conditions for a fluorescence measurement, the following knowledge is needed:

1. Absorption and/or excitation spectrum.
2. Fluorescence spectrum.
3. Oscillator strength or molar absorptivity at the excitation wavelength.
4. Quantum efficiency for different excitation wavelengths.
5. Fluorescence output as a function of dopant concentration.
6. Lifetimes of fluorescence.
7. Quenching of fluorescence by additional processes such as energy transfer of radiation-induced color centers.
8. Stability.

The principles upon which the determination of quantum efficiencies is based will be discussed. Quantum yields of glasses and pellets prepared in this laboratory, for excitation to various electronic levels and the oscillator strengths of absorption to these levels will also be presented. The concentration dependence of quantum efficiency will be shown.

A short theory of the fluorescence of the material is also outlined for each group of proposed standards in order to simplify the choice of proper materials.

B. Determination of Quantum Yields

The luminescence quantum yield of a compound is defined as the fraction of excited molecules that luminesce after direct excitation by a light source.

The quantum yield, η, which is actually the ratio of probabilities of radiative transitions, ΣA_i^r to the sum of the probabilities of radiative and nonradiative transitions, A_i^{nr}, is defined as:

$$\eta = \frac{\text{number of photons emitted}}{\text{number of photons absorbed}} = \frac{\sum A_i^r}{\sum A_i^r + \sum A_i^{nr}} \qquad (1)$$

The quantum yield would equal unity if there were no nonradiative transitions.

The terms "quantum yield," "luminescence quantum efficiency," and "fluorescence yield" are used interchangeably.

Formula (1) serves as a basis of determination of quantum efficiency.

The determination of absolute quantum yields by this formula is difficult as mentioned in the introduction, hence a relative technique is often employed.

1. Comparative Method

Here, the fluorescence of an unknown is compared with the fluorescence of a compound whose fluorescence yield is well known. For dilute solutions, the following equation has been used [30]:

$$\eta_u = \eta_s \frac{n_u F_u A_s}{n_s F_s A_u} \qquad (2)$$

where η_u and η_s are quantum yields of unknown and standard respectively, n the index of refraction, A the absorbance at the wavelength of absorption and F the integrated fluorescence output in quanta/unit wavelength. This equation is valid for equal numbers of photons incident on u and s. More often the following equation is used:

$$\eta_u = \eta_s \frac{F_u A_s I(\lambda_s)}{F_s A_u I(\lambda_u)} \frac{n_u^2}{n_s^2} \qquad (3)$$

In this equation, F is the integrated area under the corrected emission spectrum, and $I(\lambda)$ is the relative irradiance of the exciting light at wavelength λ. A is the absorbance.

Equations (2) and (3) differ in the ratio $\frac{n_u}{n_s}$ and $\frac{n_u^2}{n_s^2}$. As we see by comparison of the two formulae, refraction corrections can be substantial, modifying quantum yield results by factors of 2 or more. Therefore, one should be especially careful when applying the refractive index correction. A comprehensive discussion on this correction can be found in reference [3, p. 1018]. As mentioned in the introduction, when the fluorescence of the unknown is compared with a standard of the same refractive index and geometry, the refractive index correction is avoided.

2. Determination of Quantum Yields from Lifetime Measurements

An alternative method is the determination of quantum yields by measurements of the lifetime of fluorescence and the natural lifetime of the state. Here we use the parameters appearing in eq (1)

$$\eta = \frac{\sum A_i^r}{\sum A_i^r + \sum A_i^{nr}} = \frac{\sum \frac{1}{\tau_{\text{nat}}}}{\frac{1}{\tau_{\text{exp}}}} = \sum \frac{\tau_{\text{exp}}}{\tau_{\text{nat}}} \qquad (4)$$

where τ_{exp} is the experimentally determined lifetime from the level in question and $\Sigma\tau_{\text{nat}}^{-1}$ is the sum of natural lifetimes, corresponding to the sum of the inverse of the radiative transition rates from this level. One term, A_i^r, appearing in the sum ΣA_i^r is equal to $\frac{1}{\tau_{i\text{nat}}}$ and is obtained directly from the absorbance spectra as shown below. The other terms in the sum are then obtained from the relative areas

in the corrected emission spectra. A detailed example of these calculations is presented below for Eu(III) doped glasses.

The natural radiative lifetime is related to the Einstein coefficient of spontaneous emission. Using this relation, several authors developed expressions relating the natural lifetime of fluorescence to the absorption spectrum of the compound [31].

Here, a distinction can be made between two cases: 1. When the absorption and emission of a compound occur at close wavelengths, that is, zero or very small Stokes shifts are observed, and the spectrum is narrow as in the cases of rare earths in various media, one can use an approximation developed for atomic spectra. Using this approximation [32], one obtains for the natural lifetime the following expression, which is valid for a transition between two levels:

$$\tau_{\text{nat}}^{-1} = 2.880 \times 10^{-9} n^2 (g_1/g_u) < \nu^2 > \int \epsilon(\nu)\, d\nu \qquad (5)$$

where n is the index of refraction, $< \nu^2 >$ the average squared wave number for the absorption maximum, g_u and g_1 the degeneracies in the upper and lower states, respectively, and $\epsilon(\nu)$ the molar absorptivity as a function of wave number.

In the case where there is a considerable Stokes shift between the absorption and emission as a result of strong vibronic coupling, for example in transition metal ions, mercury-like ions and organic compounds, a modified equation can be used for τ_{nat} [33], namely

$$\tau_{\text{nat}}^{-1} = 2.880 \times 10^{-9} n^2 < \nu_f^{-3} >_{\text{av}}^{-1} \frac{g_1}{g_u} \int \frac{\epsilon(\nu)\, d\nu}{\nu}. \qquad (6)$$

The quantity $< \nu_f^{-3} >_{\text{av}}^{-1}$ is given by

$$< \nu_f^{-3} >_{\text{av}}^{-1} = \frac{\int F(\nu)\ \alpha\nu}{\int F(\nu) \nu^{-3} d\nu} \qquad (7)$$

where $F(\nu)$ is the fluorescence output in photons as a function of wave number and ν is the wave number of $F(\nu)$.

3. Doped Glasses

The materials which we suggest as versatile standards for spectrofluorimetry and which were studied in this laboratory will be now described. They are divided in the text into four major groups: I. The rare-earth-doped glasses. II. Thallium-doped alkali halides. III. Glasses doped with thallium. IV. Glasses doped with Ce^{3+}, Pb^{2+}, and Cu^{+}.

I. The Rare-Earth-Doped Glasses

The characteristic spectra of the trivalent rare earths are attributable to the presence of deep lying $4f$ shells in the ions. The electrons of these shells are screened by the outer shell electrons, and as a result they give rise to a number of discrete energy levels. The presence of the surrounding lattice has little effect on the position of these levels; therefore, a close resemblance between the energy level diagram of the free ion and that of the incorporated ion exists (fig. 1).

Considerable attention has been paid in the past few years to the study of both the absorption and emission spectra of the rare earths [34, 35].

Trivalent rare-earth ions incorporated in inorganic solids exhibit luminescence owning to the intraconfigurational transitions of the $4f$ electron shell. The optical excitation of this luminescence can be governed by one of three possible mechanisms:

(a) excitation in the narrow $4f$ levels of the rare-earth ion;
(b) excitation in the broad levels due to $4f$-$5d^*$ transitions, or charge transfer processes;
(c) absorption of the host followed by energy transfer from the host to the rare earth activator.

While the first mechanism is operative in all the rare earths showing fluorescence, the second is well known mainly in europium and terbium. In the case of Eu^{3+}, this band is due to a charge transfer process between the Eu^{3+} ion and oxygen center. In the case of Tb^{3+}, however, the band is due to a $4f$-$5f$ transition in the Tb^{3+} ion. (Samarium also was found in some cases to exhibit a charge transfer type of excitation at wavelengths shorter than 220 nm.)

The narrow band emission of the trivalent rare earths in various media is always due to an inner f shell electronic transition. Intra-f-orbital transitions are parity forbidden in the free ion. In a solid, glass or liquid in the absence of a center of symmetry, the parity selection rule may be relaxed by the mixing of the $4f$ configuration with appropriate levels of configuration of opposite symmetry using odd terms in the static or dynamic crystal field expansion. There will also be an additional interaction owing to the influence of the crystal field of the host which produces broadening and splitting of the levels. As in the transition metal ions, which have been treated extensively by the ligand field theory, an increase in separation of a field-split degenerate level indicates an increase in the ligand field seen by the rare earth ion. The crystal field splittings in the rare earths are, however, much smaller than the transition ion splittings, and are not more than a few hundred wave numbers. For transitions between two nondegenerate levels, increasing the rare-earth-ligand interaction displaces both levels toward lower energies. The displacement of the upper, less shielded, level is usually greater, and thus the stronger perturbation causes shifts to longer wavelengths.

The electrostatic perturbation of a rare-earth ion should be directly related to its binding energy in the host medium. As a first approximation, this energy may be derived from a hard-sphere ionic model by the Born equation:

$$E = \sum \frac{Z_i Z_j}{r_{ij}} + \frac{b}{r^n} \qquad (8)$$

FIGURE 1. Energy level diagram of the rare-earth ions after G. H. Dieke, in Spectra and Energy Levels of Rare Earth Ions, H. M. Crosswhite and H. Crosswhite, Eds. (John Wiley & Sons, New York, N.Y., 1968), p. 142.

E = coulombic potential of the active ion; Z_i = charge on the active ion; Z_j = charge on the matrix ions: b = repulsion coefficient: r = distance between active ion and nearest anion; n = 4 to 10.

It was shown in a series of papers by Reisfeld et al. [36–40], that the behavior of rare earths in glasses is similar to that of rare earths in inorganic crystals of low symmetry except for inhomogeneous broadening of the spectra due to a multiplicity of rare-earth sites in glasses. According to our theory [39] a rare-earth ion occupies a center of a distorted cube comprised of four tetrahedra of borate, phosphate or silicate. Two oxygens belonging to such a tetrahedron produce an edge of the cube (fig. 2). The coordination

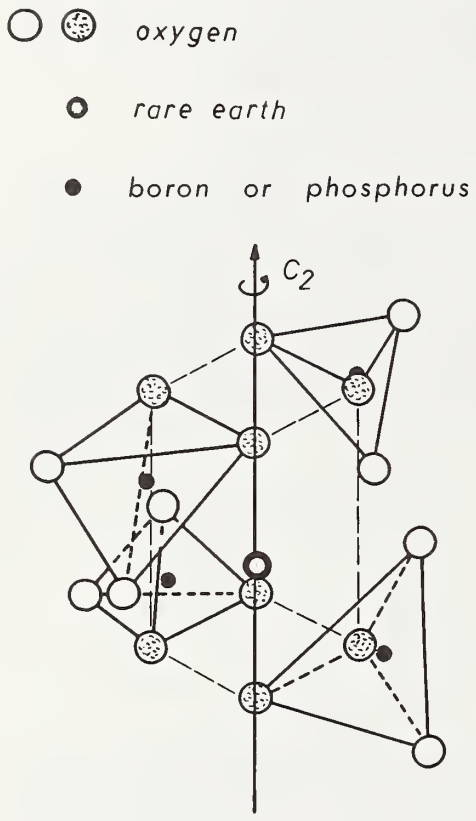

FIGURE 2. Proposed rare-earth site model.

of the rare earth in such an arrangement is with eight oxygens. The observed broadening in the spectrum can occur due to the existence of nonuniform, nonidentical ligand fields caused by slightly different values of rare-earth oxygen distances. An average rare-earth oxygen distance was calculated by assuming a rare-earth sits in a center of a regular cube. In a cube made of borate tetrahedra, in which the boron-oxygen distance is 1.48 Å and the oxygen-oxygen distance 2.4 Å, the rare-earth oxygen distance is 2.1 Å. In a cube made of phosphate tetrahedra in which the phosphorus-oxygen distance is 1.57 Å and the oxygen-oxygen distance is 2.56 Å, the rare-earth oxygen distance is 2.22 Å. It should be realized that in reality the symmetry is lower than cubic, and for the particular cases studied it was found to be of C_s symmetry Eu^{3+} in phosphate glass, [40] and C_2 for Tm^{3+} in phosphate and borate glasses [39]. As a result of this lower symmetry, forced electric dipole transitions become possible and absorption and fluorescence is observed.

The fluorescence can, in some cases, be quenched due to transfer of electronic excitation energy to the vibrations of the surrounding medium. Such interactions reduce the fluorescence quantum yield. In general the larger the energy difference between the two electronic states, the smaller the nonradiative transition probability between them [41]. For rare-earths, the energy difference between the electronic levels below which considerable quenching occurs is about four vibrational quanta (phonons). The nonradiative decay of the higher excited levels in the glasses is generally assisted by the phonons of the glass. The particular vibrational frequencies which are responsible for the quenching are the following:

bond	stretching frequency ν cm^{-1}	bond length Å
silicate, Si − 0	1010–1115	1.62
metaphosphate, P − 0	1140–1300	1.57
borate, B − 0	1310–1380	1.39 (trigonal) 1.48 (tetrahedral)

from which we conclude that in borate glasses, quenching will occur between levels that are separated by about 5000 cm^{-1}, while in silicate by about 4000 cm^{-1}.

We shall now show how this general theory works for specific cases.

A. Europium

The observed optical absorption and emission spectra of Eu^{3+} in glasses are characteristic of transitions between the lower energy levels of the $4f^6$ configuration of this ion. The oscillator strengths of the characteristic absorption bands in a phosphate glass together with the assignments of the transitions are given in table 1.

The oscillator strength was calculated from the well-known equation

$$f = 4.32 \times 10^{-9} \int \epsilon(\nu)\, d\nu \qquad (9)$$

where ϵ is the molar absorptivity at the energy ν (cm^{-1}). The values of f presented in table 1 were corrected for population distribution of total concentration in $^7F_0$, $^7F_1$, and $^7F_2$. Using a Boltzmann distribution correction, the relative concentration for the three levels at room temperature were $C_0 = 0.792$, $C_1 = 0.200$ and $C_2 = 0.008$, respectively.

TABLE 1. Oscillator strengths and quantum yields of fluorescence of Eu^{3+} in phosphate glass

Transition assignment	Wave number cm^{-1}	Wavelength nm	Oscillator strength $\times 10^7$	Percent quantum yield of D_0 fluorescence
$^7F_2 \rightarrow {}^5D_0$	16319	612.8	1.544	
$^7F_1 \rightarrow {}^5D_0$	16771	592.2	0.351	
$^7F_0 \rightarrow {}^5D_0$	17256	579.6	.006	0.95
$^7F_1 \rightarrow {}^5D_1$	18700	534.7	.505	
$^5F_0 \rightarrow {}^5D_1$	18993	526.4	.146	.91
$^7F_0 \rightarrow {}^5D_2$	21493	465.3	1.248	.88
$^7F_0 \rightarrow {}^5D_3$	24009	416.5	.547	.87
$^7F_0 \rightarrow {}^5L_6$	25380	394.0	8.981	.87
$^7F_1 \rightarrow {}^5G_5, {}^5G_6$	26041	384.0	6.019	
$^7F_0 \rightarrow {}^5G_3$	26507	377.2	2.726	
$^7F_1 \rightarrow {}^5L_8$	27285	366.5	.391	
$^7F_0 \rightarrow {}^5D_4$	27567	362.7	1.926	
$^7F_1 \rightarrow {}^5H_3$	30464	328.2	1.242	
$^7F_1 \rightarrow {}^5H_5$	31152	321.0	3.001	
$^7F_0 \rightarrow {}^5H_6$	31397	318.5	6.776	

Fluorescence was observed from the $^5D_0$ level and much weaker fluorescence (by a factor of three orders of magnitude) from the $^5D_1$ level. The corrected $^5D_0$ fluorescence to the ^7F ground state multiplet for Eu^{3+} in phosphate glass is given in figure 3. The corrected excitation spectrum of the fluorescence is also presented in this figure. The assignments, and relative intensities of the transitions are presented in table 2. (The transitions from the $^5D_0$ excited level to the $^7F_5$ and $^7F_6$ ground states are very weak, less than 1 percent of the total intensity, and are not included.) The $^5D_0 \rightarrow {}^7F_1$ emission band for Eu^{3+} are magnetic dipole-allowed transitions; the other fluorescence bands arise from forced electric-dipole transitions. The large ratio of the fluorescence intensities for the $^5D_0 \rightarrow {}^7F_2$ and $^5D_0 \rightarrow {}^7F_1$ transitions implies a low symmetry field at the europium sites.

Quantum efficiencies of fluorescence from the $^5D_0$ level of Eu^{3+} in phosphate [41] and silicate glasses [42] were obtained by two independent methods, (a) lifetime measurements, and (b) comparison with a liquid standard.

a. Lifetime measurements. The quantum yield determination based on lifetime measurements is calculated from eq (4). The measured lifetime of the $^5D_0$ excited state in silicate glass was 2.69 ± 0.03 ms

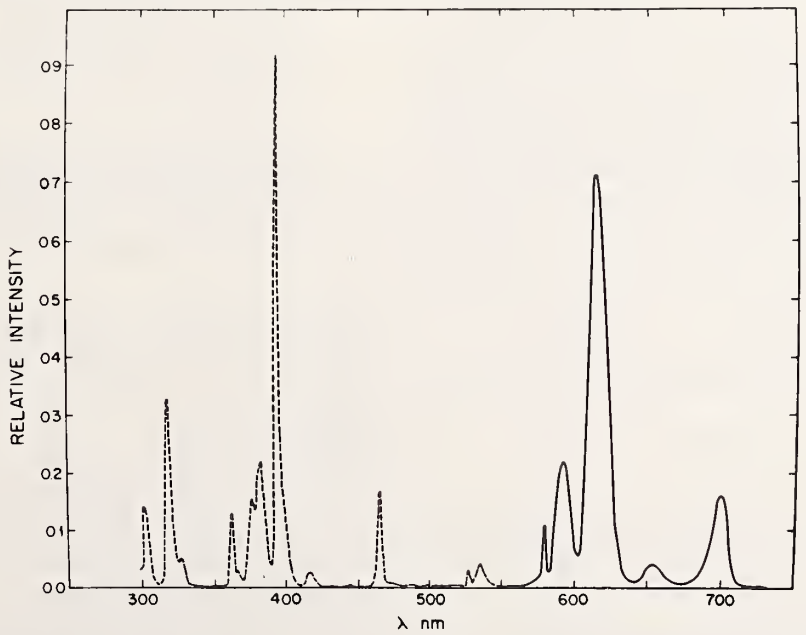

FIGURE 3. Corrected excitation (broken line) and emission (full line) spectrum of the $^5D_0$ fluorescence of Eu^{3+} in phosphate glass.

502-591 O - 73 - 15

and in phosphate glass was 2.83 ± 0.03 ms.

The natural radiative lifetime was calculated using eq (5). In this equation, ϵ was corrected for the relative population of the $^7F_0$ level, which was taken as 0.771 in silicate and 0.792 in phosphate. Using the calculated value for $A(^7F_0 \rightarrow {}^5D_0)$ the ratio of the intensities of fluorescence and the fact that $A(^7F_0 \rightarrow {}^5D_0) = A(^5D_0 \rightarrow {}^7F_0)$, the sum of radiative transition probabilities is expressed by:

$$\sum \frac{1}{\tau_{nat}} = \sum A_r = A(^5D_0 \rightarrow {}^7F_0) \left[1 + \frac{S(^5D_0 \rightarrow {}^7F_1)}{S(^5D_0 \rightarrow {}^7F_0)} + \frac{S(^5D_0 \rightarrow {}^7F_2)}{S(^5D_0 \rightarrow {}^7F_0)} + \frac{S(^5D_0 \rightarrow {}^7F_3)}{S(^5D_0 \rightarrow {}^7F_0)} + \frac{S(^5D_0 \rightarrow {}^7F_4)}{S(^5D_0 \rightarrow {}^7F_0)} \right] \quad (10)$$

where S is the area of the relevant emission bands obtained from the corrected emission spectrum.

TABLE 2. Emission wavelength and relative areas of the $^5D_0 \rightarrow {}^7F_i$ transitions for Eu^{3+} in phosphate glass

Transition assignments	Wavelength	Relative fluorescence (areas)
$^5D_0 \rightarrow {}^7F_0$	578.5	0.036
$^5D_0 \rightarrow {}^7F_1$	591.9	1.000
$^5D_0 \rightarrow {}^7F_2$	612.1	3.000
$^5D_0 \rightarrow {}^7F_3$	654.7	0.219
$^5D_0 \rightarrow {}^7F_4$	692.3	1.026

For Eu^{3+} in phosphate glass, the quantum yield obtained by this method was 0.95 [41] and for Eu^{3+} in silicate, 0.90 [42]. Europium-doped glasses do not show concentration quenching of the $^5D_0$ fluorescence [43].

b. Determination of Quantum Yield by Comparison Method. Here, the comparison was made with a solution of $Eu(NO_3)_3$ with a known quantum efficiency of 4 percent [41]. The fluorescence spectra were taken on a Turner Model 210 spectrofluorimeter[2] which gives corrected emission spectra in quanta/unit bandwidth, and excitation spectra corrected to constant energy [44]. The glasses were of the same geometry (standard cuvette form) as the cells in which the fluorescence of the solution of europium nitrate was measured.

Equation (11), which is a modification of eq (3) for use with a corrected spectrofluorimeter [45], was used:

$$\eta_u = \eta_s [(F_u A_s d_u \lambda_{ex.s} n_u^2)/(F_s A_u \lambda_{ex \cdot u} d_s \cdot n_s^2)] \quad (11)$$

where all the symbols have the same meaning as in eq (3); subscripts u and s refer to the unknown and standard, respectively; d is the dilution factor denoting the ratio of the fluorescence species concentration in the sample used for absorbance measurements to that used for fluorescence measurements: λ is the excitation wavelength.

The quantum efficiency determined by direct excitation to the $^5D_0$ level obtained by this method was 0.95 ± 0.03 for the phosphate glass, [41] and 0.93 ± 0.05 for the silicate glass [42].

The very similar values for the quantum yield obtained by the two independent methods suggests use of the phosphate glass as a reliable fluorescence standard at wavelengths similar to those for the fluorescence of europium, as summarized in table 2.

To obtain this quantum efficiency, it is necessary to excite the $^5D_0$ level of europium from the $^7F_0$ level at 580 nm, or from the $^7F_1$ level at 591 nm. Excitation to higher levels results in a decrease of fluorescence yield from the $^5D_0$ level, as additional paths for radia tive and nonradiative transitions become possible.

The quantum yields of fluorescence upon excitation to selected levels in phosphate glass are presented in table 1 [41]. The values of quantum efficiencies for fluorescence monitored by $^5D_0$ emissions when excited to higher levels, as listed in the table, were obtained from the ratio of the area under the excitation spectrum to the ratio of the area under the absorption band for a given level using eq (12). No corrections were made for the change of refractive index with wavelength.

$$\text{Q.Y.}^b = \frac{F_b/A_b}{F_a/A_a} \frac{\lambda_{ex\,a}}{\lambda_{ex\,b}} \text{Q.Y.}^a \quad (12)$$

Q.Y.^{b}	Quantum efficiency of $^5D_0$ fluorescence by excitation to a given level
Q.Y.^{a}	Quantum efficiency of $^5D_0$ fluorescence by excitation to the $^5D_0$ level
F_b	peak area of a given level in excitation spectrum
A_b	peak area of a given level in the absorption spectrum
F_a	peak area of $^5D_0$ in excitation spectrum
A_a	peak area of $^5D_0$ is absorption spectrum
$\lambda_{ex\,a}$	wavelength of $^5D_0$ absorption (581 nm)
$\lambda_{ex\,b}$	wavelength of absorption for given transition.

Therefore, europium glass is proposed as a standard where the emission of the unknown is close to the emission of Eu^{3+} (table 2) and the excitation wavelength is also near one of the excitation wavelengths of europium (table 1).

The fluorescence of europium shows a linear dependence on concentration up to 7 weight percent and no quenching is observed. Therefore, the concentration of the standard used will be governed by the desired wavelength of excitation because of different oscillator strengths. For excitation at 580 or 591 nm, 1–2 weight percent of Eu^{3+} in glass is suggested. The europium glass standard is suitable for compounds having narrow fluorescence in the wavelength range of 600–700 nm.

[2] In order to adequately describe materials and experimental procedures, it was occasionally necessary to identify commercial products by manufacturer's name or label. In no instances does such identification imply endorsement by the National Bureau of Standards, nor does it imply that the particular product or equipment is necessarily the best available for that purpose.

B. Gadolinium

Gadolinium has a comparatively simple optical absorption and emission spectrum because the trivalent gadolinium has a half-filled configuration corresponding to $7-4f$ electrons. The ground state is $^8S_{7/2}$, which is not split in a crystal field. Its first excited state lies around 3200 cm^{-1}, which corresponds to the 312 nm band. Gadolinium is the only rare-earth ion whose spectrum consists only of bands lying in the UV region. The emission spectrum of gadolinium in borate glass [46] has a major band with maximum at 312 nm due to the $^6P_{7/2}$–$^8S_{7/2}$ transition (fig 4), which is essentially unchanged in other matrices [47]. The oscillator strength of this transition and of transitions to higher levels from $^6P_{7/2}$ are tabulated in table 3. The quantum yield of the 312 nm fluorescence was computed by taking a ratio of the measured lifetime of $^6P_{7/2}$ fluorescence, which is 4.10 ± 0.01 ms, to the natural lifetime of this transition obtained by use of formula (5). The calculated lifetime was found to be 4.10 ms. The quantum yield thus obtained equals 1 with an estimated error of ± 1 percent. The quantum yield of $^6P_{7/2}$ fluorescence at excitation to higher levels was obtained relative to the quantum yield of excitation at $^6P_{7/2}$ using eq (12).

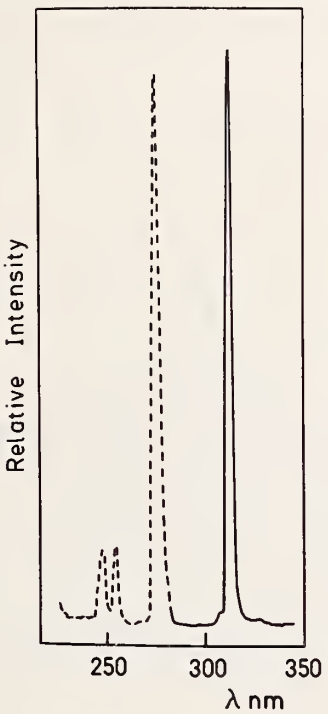

FIGURE 4. Corrected excitation (broken line) and emission (full line) spectrum of the $^6P_{7/2}$ fluorescence of Gd^{3+} in borate glass.

The quantum efficiencies of the 312 nm fluorescence of gadolinium in borate glass are tabulated in table 3.

Borate glass containing gadolinium can be used as a standard for fluorescent materials having emissions around 312 nm and excitation peaks around 250 and 273 nm. Because of the narrowness of the band, it is suitable for materials with narrow fluorescence. Gadolinium in borate glass shows a linear fluorescence output as a function of concentration from the ppm range [48] to 7 weight percent (the highest concentration introduced).

C. Terbium

The electronic configuration of Tb^{3+} is $4f^8$. The absorption spectrum of Tb^{3+} arises from the transitions from the ground $^7F_6$ state to higher levels of the f orbital giving rise to sharp bands of absorption due to f-f^* transitions. In glasses, an additional broad band occurs in the UV due to the $4f^8 \rightarrow 4f^75d$ transition. The oscillator strengths of Tb^{3+} together with the quantum efficiencies of the $^5D_4$ level are presented in table 4.

Terbium fluorescence is observed in the glass from the $^5D_4$ and $^5D_3$ excited states. The $^5D_3$ fluorescence, around 378–369 nm, is quenched at higher concentrations of Tb^{3+} due to $Tb^{3+} - Tb^{3+}$ interactions. The $^5D_4$ fluorescence consists of seven bands due to the transitions: $^5D_4 \rightarrow {}^7F_{6,5,4,3,2,1,0}$. The wavelengths for maxima of these bands together with their relative peak areas are presented in table 5. The corrected emission

TABLE 3. Oscillator strengths and quantum yields of fluorescence of Gd^{3+} in borate glass

Transition assignment	Wavelength nm	Wave number cm^{-1}	Oscillator strength $\times 10^6$	Quantum yield of $^6P_{7/2}$ fluorescence
$^8S_{7/2} \rightarrow {}^6P_{7/2}$	313.0	31949	0.176	1
$^6P_{5/2}$	307.0	32573	.074	
$^6I_{7/2}$	280.25	35682	.117	
$^6I_{9/2}$, $^6I_{17/2}$, $^6I_{11/2}$	277.0	36101	.781	
$^6I_{13/2}$	274.3	36456	1.679	0.870
$^6I_{15/2}$				
$^6D_{9/2}$	253.6	39432	0.406	.735
$^6D_{7/2}$	247.6	40388	.385	.735
$^6D_{3/2}$				
$^6D_{5/2}$	245.5	40733	.099	.590

TABLE 4. Oscillator strengths and quantum yields of $^5D_4$ fluorescence of Tb^{3+} in borate glass

Transition assignment	Wavelength nm	Wavenumber cm^{-1}	Oscillator strength $\times 10^7$	Quantum yield
$^7F_6 \rightarrow {}^5D_4$	485.5	20597	0.633	1
$^5D_3$, $^5G_6$	378.9	26392	3.812	0.60
$^5L_{10}$	368.7	26954	7.204	
$^5G_5$, $^5G_2$, $^5G_4$, $^5L_9$	352.5	28369	7.622	.62
$^5G_3$, $^5L_8$, $^5L_7$, $^5L_6$, $^5G_2$	340.6	29360	5.764	.256
$^5D_1$	325.7	30703	0.407	
$^5D_0$, $^5H_7$	318.5	31397	4.405	.197
$^5H_6$	303.4	32960	5.249	.06
$^5H_4$, $^5H_5$, $^5H_3$, $^5I_8$, $^5F_4$	283.6	35261	1.787	
$4f^8 \rightarrow 4f^7 5d$	220.5	45351	385×10^4	

TABLE 5. Emission wavelength and relative areas of the $^5D_4$ level of Tb^{3+} in borate glass

Transition assignments	Wavelength nm	Relative fluorescence (areas)
$^5D_4 \rightarrow {}^7F_6$	486	0.040
$^5D_4 \rightarrow {}^7F_5$	541	.150
$^5D_4 \rightarrow {}^7F_4$	585	.033
$^5D_4 \rightarrow {}^7F_3$	624	.019

spectrum from the $^5D_4$ level and the corrected excitation spectrum are presented in figure 5.

No quenching of the $^5D_4$ terbium fluorescence was observed in our work with borate glasses from the ppm range to 6 weight percent [49].

The lifetime of the $^5D_4$ fluorescence of terbium follows a simple exponential with an e^{-1} decay time of 2.80 ± 0.05 ms.

The quantum yields of $^5D_4$ fluorescence on excitation to this level were obtained using the measured

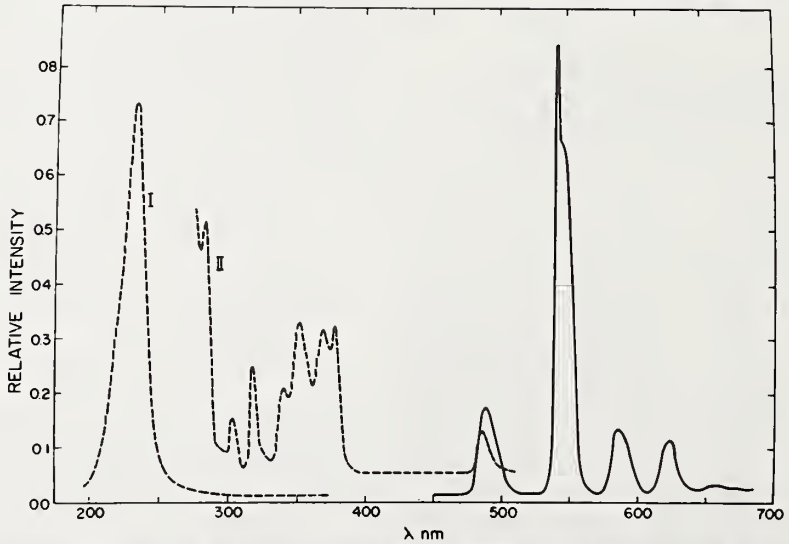

FIGURE 5. Corrected excitation (broken line) and emission (full line) spectrum of the $^5D_4$ fluorescence of Tb^{3+} in borate glass. I = the intensity decreased by a factor of 30.

lifetime and absorption and emission spectra in a similar way as the quantum yields for europium, using eqs (4), (5), and (10).

The radiative probability for the $^7F_6 \rightarrow {}^5D_4$ transition was calculated using eq (5) and equals 57.6 s^{-1}.

The total radiative transition probability, from the $^5D_4$ level, $\sum A_i' [^5D_4]$ is given by:

$$\sum A_i' [^5D_4] = \sum_{i=0}^{6} A [^5D_4 \rightarrow {}^7F_i].$$

From the emission spectrum we found that

$$\sum A_i' [^5D_4] = 6A [^5D_4 \rightarrow {}^7F_6];$$

thus, the total radiative transition rate from the $^5D_4$ level is 345 s^{-1}, which is equivalent to

$$\left[\sum \frac{1}{\tau_{nat}}\right]^{-1}$$

2.9 ms. Hence the quantum yield

$$\text{Q.Y.} = \frac{2.8}{2.9} = 0.97$$

with an estimated error of about 3 percent.

The quantum yields of the $^5D_4$ level on excitation to higher levels were obtained as they were for Eu^{3+} and Gd^{3+}; i.e., by taking ratios of the areas under the excitation spectrum to the areas in the absorption spectra, and multiplying by the ratio of excitation wavelength at 480 to the wavelength for the given excitation. Equation (12) was used for this calculation.

Terbium can be used as a standard for compounds which fluoresce at approximately 480, 543, 587, and 624 nm.

D. Samarium

The electronic configuration of Sm^{3+} is $4f^5$. Its absorption spectrum arises from transitions from the ground $^6H_{5/2}$ level to higher levels of the $4f^5$ configurations. The oscillator strengths of Sm^{3+} in phosphate glass are presented in table 6.

The excitation and emission spectra of Sm^{3+} in phosphate glass are presented in figure 6. The visible fluorescence of Sm^{3+} arises from the transitions from the $^4G_{5/2}$ level to the ground ^6H multiplet. The relative fluorescence intensities to each level in the multiplet are presented in table 7. The fluorescence arising from these transitions is linear with concentration up to about 0.6 weight percent. At higher concentrations an ion-ion energy transfer occurs. This multipolar interaction can be represented systematically (see ref. [35], p. 97):

$$[^4G_{5/2} \rightarrow {}^6F_{9/2}] \rightarrow [^6H_{5/2} \rightarrow {}^6F_{9/2}] \text{ or}$$

$$(Sm^{3+}\,{}^4G_{5/2})^* + (Sm^{3+}\,{}^6H_{5/2}) \rightarrow 2(Sm^{3+}\,{}^6F_{9/2})^*.$$

Therefore, if samarium glass is to be used as a fluorescence standard for the wavelength range presented in table 7, a glass containing less than 0.6 weight percent of this element should be used.

The quantum yield of the $^4G_{5/2}$ fluorescence of samarium in phosphate and borate glasses was calculated by use of eqs (4), (5), and (10). The radiative transition probability from $^6H_{5/2}$ to $^4G_{5/2}$ in phosphate glass as obtained from the absorption spectrum, using eq (5), is 41.3 s^{-1}. The total radiative transition probability from the $^4G_{5/2}$ level, $\Sigma A_i'[^4G_{5/2}]$, is given by

TABLE 6. Oscillator strengths and quantum yields of $^4G_{5/2}$ fluorescence of Sm^{3+} in phosphate glass

Energy level	Wave number cm^{-1}	Wavelength nm	Oscillator strength $\times 10^6$	Quantum yields
$^4G_{5/2}$	17467–18348	545.0–572.5	0.0476	0.950
$^6F_{3/2}$	18779–19047	525.0–532.5	.0115	
$^4G_{7/2}$	19800–20100	497.5–505.0	.0183	
$^4I_{9/2}$ $^4M_{15/2}$, $^4I_{11/2}$	20181–21621	462.5–496.0	1.5370	.653
$^4I_{13/2}$	21267–21978	455.0–470.0	0.1388	
$^4F_{5/2}$	21978–22346	447.5–455.0	.0273	.491
$^4M_{17/2}$, $^4G_{9/2}$, $^4I_{15/2}$	22321–23255	430.0–448.0	.2169	
$(^6P, {}^4P)_{5/2}$	23255–24630	406.0–430.0	1.0039	.213
$^4L_{17/2}$, $^6F_{7/2}$, $^6P_{3/2}$ $^4K_{11/2}$, $^4M_{21/2}$, $^4L_{15/2}$	24242–25316	395.0–412.5	4.0749	.264
$^4G_{11/2}$, $^4D_{1/2}$, $^6P_{7/2}$	25252–26109	383.0–396.0	0.2298	.249
$^4L_{17/2}$, $^4K_{13/2}$, $^6F_{9/2}$	26109–27173	368.0–383.0	1.2246	.224
$^4D_{3/2}$, $(^4D, {}^6P)_{5/2}$	27173–28089	356.0–368.0	1.2230	.226
$^4H_{7/2}$	27972–28368	352.5–357.0	0.0264	
$^4K_{15/2}$, $^4H_{9/2}$, $^4D_{7/2}$ $(^4K, {}^4L)_{17/2}$, $^4L_{19/2}$ $^4H_{11/2}$	28490–29450	340.0–351.0	.7457	.155

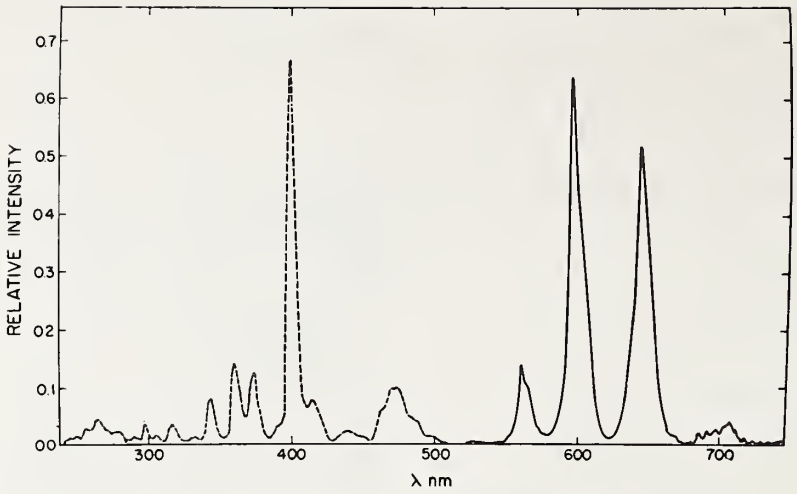

FIGURE 6. Corrected excitation (broken line) and emission (full line) of the $^4G_{5/2}$ fluorescence of Sm^{3+} in phosphate glass.

TABLE 7. Emission wavelength and relative areas of fluorescence from the $^4G_{5/2}$ level of Sm^{3+} in phosphate glass

Transition assignments	Wavelength nm	Relative areas
$^4G_{5/2} \rightarrow {}^6H_{5/2}$	562	1.000
$^4G_{5/2} \rightarrow {}^6H_{7/2}$	597	5.128
$^4G_{5/2} \rightarrow {}^6H_{9/2}$	645	4.856
$^4G_{5/2} \rightarrow {}^6H_{11/2}$	707	0.574
$^4G_{5/2} \rightarrow {}^6H_{13/2}$*	830	0.487
$^4G_{5/2} \rightarrow {}^6H_{15/2}$*	900	

* These two transitions were obtained by calculation assuming quantum yield of level $^4G_{5/2}$ to be 0.95.

$$\sum A_i^r[^4G_{5/2}^*] = \sum_{i=5/2}^{15/2} {}^4G_{5/2} \rightarrow \sum {}^6H_i.$$

The measured lifetime of the fluorescence from the $^4G_{5/2}$ level is 1.91 ms. By assuming the quantum efficiency of fluorescence from this level to be 0.95, we can calculate the transition rate $^4G_{5/2} \rightarrow {}^6H_{13}$, $^6H_{15}$, which is out of the range of measurements, by use of the formula[3]

$$\text{Q.Y.} = \tau_{\text{exp}}\left[A(^6H_{5/2} \rightarrow {}^4G_{5/2}) \times \left(1 + \frac{A(^4G_{5/2} \rightarrow {}^6H_{7/2})}{A(^6H_{5/2} \rightarrow {}^4G_{5/2})} + \frac{A(^4G_{5/2} \rightarrow {}^6H_{9/2})}{A(^6H_{5/2} \rightarrow {}^4G_{5/2})} + \frac{A(^4G_{5/2} \rightarrow {}^6H_{11/2})}{A(^6H_{5/2} \rightarrow {}^4G_{5/2})} + x\right)\right]$$

$$0.95 = 0.00191[41.3(1.000 + 5.128 + 4.856 + 0.5744 + x)].$$

$$x = \frac{A(^4G_{5/2} \rightarrow {}^6H_{13/2})}{A(^6H_{5/2} \rightarrow {}^4G_{5/2})} + \frac{A(^4G_{5/2} \rightarrow {}^6H_{15/2})}{A(^6H_{5/2} \rightarrow {}^4G_{5/2})}$$

The numbers in parenthesis are the relative fluorescence intensities of the transitions $^4G_{5/2} \rightarrow {}^6H_i$ as given in table 7. The relative areas of $^4G_{5/2} \rightarrow {}^6H_{13/2}$, $^6H_{15/2}$ thus calculated amount to about 4 percent of the total emission of the $^4G_{5/2}$, hence the assumption that the quantum yield equal 0.95 is justified. The estimated error in Q.Y. here is about 3 percent.

The quantum yields of the $^4G_{5/2}$ fluorescence on excitation to higher levels were calculated by eq (12) using as an internal standard the fluorescence yield on direct excitation to the $^4G_{5/2}$ level. They were independently calculated by use of Eu^{3+} glass as standard. The values of quantum yield are presented in table 6.

Glasses containing small concentrations of Sm^{3+} can be used as fluorescence standards for compounds which fluoresce at around 560, 602, and 640 nm.

By examining the quantum efficiencies of Eu^{3+}, Gd^{3+}, Tb^{3+}, and Sm^{+} in glasses, we see that the fluorescence quantum yields from the lowest excited fluorescing levels approach unity. This is because the differences between these levels and the ground levels (or multiplets) are more than five phonons. In such cases, the electronic transitions are almost totally radiative.

E. Thulium

The electronic configuration of trivalent thulium is $4f^{12}$. It possesses more than one strongly emitting level and selective excitation of the various fluorescent levels have been achieved in both phosphate and borate glasses [50]. Because part of the fluorescence occurs in the infrared, we were unable to obtain the relative quantum efficiency of fluorescence of thulium for various levels. It was found, however, that an estimation of an "apparent quantum efficiency" of these glasses could be of practical use if the materials are used as fluorescence standards. Therefore, these parameters will be presented here.

Oscillator strengths of Tm^{3+} in phosphate and borate glasses are presented in table 8. They were obtained by Gaussian analysis of the absorption spectrum.

TABLE 8. Oscillator strengths, f, of Tm^{+3} in borate and phosphate glasses

Transition assignments	Borate			Phosphate		
	Wave number cm^{-1}	Wavelength nm	$f \times 10^6$	Wave number cm^{-1}	Wavelength nm	$f \times 10^6$
$^3H_6 \rightarrow {}^3H_4$	5847 to 6134	1630.0 to 1710.0	3.94	5714	1750.0	.....
$^3H_6 \rightarrow {}^3H_5$	8257	1211.0	2.09	8250	1212.0	1.82
$^3H_6 \rightarrow {}^3F_4$	12626 to 12903	792.0 to 775.0	4.39	12626	792.0	3.00
$^3H_6 \rightarrow {}^3F_3$	14619	684.0	4.02	14550	687.2	2.53
$^3H_6 \rightarrow {}^3F_2$	15100	662.0	0.70	15060	664.0	0.22
$^3H_6 \rightarrow {}^1G_4$	21231 to 21505	471.0 to 465.0	2.19	21052	475.0	1.58
				21505	465.0	
$^3H_6 \rightarrow {}^1D_2$	27855 to 28050	356.5 to 355.0	3.75	27855	359.0	3.06
$^3H_6 \rightarrow {}^1I_6$	34246 to 34662	292.0 to 288.5		33057	302.5	
				34364	291.0	
			4.14			31.87
$^3H_6 \rightarrow {}^3P_0$	35082	285.0		35057	286.0	
$^3H_6 \rightarrow {}^3P_1$	36363	275.0		36166	276.5	
$^3H_6 \rightarrow {}^3P_2$	37950 to 38387	262.5 to 260.5	6.13	38095	262.5	14.46

The absorption occurs from the ground $^3H_6$ state. The emission spectra of Tm^{3+} at various excitation wavelengths are presented in table 9. The excitation spectrum of the 453 nm fluorescence

TABLE 9. Emission spectrum of Tm^{3+} at various excitation wavelengths

Excitation (nm)	Assigned transition	Emission			
		borate		phosphate	
		λ(nm)	R.A.*	λ(nm)	R.A.*
468.0($^1G_4$)	$^1G_4 \rightarrow {}^3H_4$			651.50	1.000
	$^1G_4 \rightarrow {}^3H_5$			752.75	0.114
	$^3F_2 \rightarrow {}^3H_6$			665.50	.083
	$^3F_3 \rightarrow {}^3H_6$			690.00	.708
358.0($^1D_2$)	$^1D_2 \rightarrow {}^3H_4$	456.00	1.000	453.00	1.000
	$^1D_2 \rightarrow {}^3H_5$	517.00	0.008	513.00	0.011
	$^1D_2 \rightarrow {}^3F_4$	665.00	.127	663.50	.034
	$^1G_4 \rightarrow {}^3H_6$	478.00	.118	478.00	.063
	$^1G_4 \rightarrow {}^3H_4$	652.50	.180	651.50	.074
	$^3F_2 \rightarrow {}^3H_6$	665.50	.014	665.50	.009
288.0($^3P_0$)	$^1I_6 \rightarrow {}^3H_4$	355.00	.446	350.00	1.000
	$^1I_6 \rightarrow {}^3H_5$	385.00	.125	383.00	0.094
	$^3P_0 \rightarrow {}^3F_4$, $^1I_6 \rightarrow {}^3F_4$	465.00	.155	463.00	.200
	$^1I_6 \rightarrow {}^3F_3$	500.00	.110	498.00	.060
	$^3P_0 \rightarrow {}^3F_3$, $^1I_6 \rightarrow {}^3F_2$	530.00	.061	521.50	.094
	$^3P_0 \rightarrow {}^1G_4$, $^1I_6 \rightarrow {}^1G_4$	705.00	.754	701.00	1.000
	$^1D_2 \rightarrow {}^3H_5$	367.50	.275	365.00	0.133
	$^1D_2 \rightarrow {}^3H_4$	456.00	1.000	453.00	.455
	$^1D_2 \rightarrow {}^3H_5$	517.00	0.067	513.00	.044
	$^1D_2 \rightarrow {}^3F_4$	.....			
	$^1G_4 \rightarrow {}^3H_6$	480.00	.190	478.00	.105
	$^1G_4 \rightarrow {}^3H_4$	.....			
	$^3F_2 \rightarrow {}^3H_6$	.....			
	$^3F_3 \rightarrow {}^3H_6$	.....			

*Relative areas; for each excitation the areas are given relatively to the strongest emission band which is taken as unity.

($^1D_2 \rightarrow {}^3H_4$) and the emission spectrum with excitation at 262 nm ($^3H_6 \rightarrow {}^3P_0$) are presented in figure 7.

The "apparent quantum yield," (A.Q.Y.), of 450–478 nm fluorescence of Tm^{3+} was calculated by the comparative method, using Tb^{3+} as a standard. The A.Q.Y. of Tm^{3+} is defined by eq [12a]:

$$\text{A.Q.Y. } Tm^{3+} = \left\{ \frac{F\left[(^1G_4 \rightarrow {}^3H_6) + (^1D_2 \rightarrow {}^3H_4)\right]\left[A(^7F_6 \rightarrow {}^5D_4)\right]}{\left[F\left(^5D_4 \rightarrow \sum_{i=6}^{i=0} {}^7F_i\right) A\,(^3H_6 \rightarrow {}^1D_2)\right]} (\text{Q.Y. } Tb^{3+}) \right\} \quad (12a)$$

in which $F[(^1G_4 \rightarrow {}^3H_6) + (^1D_2 \rightarrow {}^3H_4)]$ is the sum of the corresponding fluorescence intensities (expressed as areas under the emission spectrum) of Tm^{3+}: $A\,(^3H_6 \rightarrow {}^1D_2)$ is the absorbance for the 358 nm band of Tm^{3+}; $F(^5D_4 \rightarrow \Sigma\,{}^7F_i)$ is the sum of fluorescence intensities of the $^5D_4$ fluorescence of Tb; $A\,(^7F_6 \rightarrow {}^5D_4)$ is the absorbance for the Tb^{3+} band at 358 nm; and Q.Y. Tb^{3+} is the quantum efficiency of Tb^{3+} taken as 0.63. The apparent quantum efficiency for 10 weight percent of Tm^{3+}, calculated in this way, is 0.037 in borate and 0.043 in phosphate glasses.

Here, not all the transitions of Tm^{3+} were taken into account, but since the relative transitions to each level are constant for a given host, Tm^{3+} doped glasses can be used as standards for fluorescence around 450–480 nm and excitation around 358 nm. This small value of A.Q.Y. is not surprising since it is known [50] that at one weight percent of Tm^{3+} the concentration quenching of fluorescence is about 50 percent due to multipolar transitions between neighboring thulium ions. It should also be remembered that the fluorescence around 455–475 nm is one of seven transitions from $^1D_2$ and one of the six $^1G_4$ transitions.

Because of its low A.Q.Y. value, use of Tm^{3+} in the region of 450–480 nm fluorescence has no obvious advantage over Tb^{3+} as a standard. However, it can be used as an internal standard for Tm^{3+}. This fluorescence can be used to determine the apparent yield at 355 nm ($^1I_6 \rightarrow {}^3H_4$), 385 nm ($^1I_6 \rightarrow {}^3H_5$) and 367 nm ($^1D_2 \rightarrow {}^3H_6$), upon excitation to 288 nm ($^3P_0$) or 265 nm ($^3P_2$), which is of practical value as a standard in the UV region.

II. Thallium-Doped Alkali Halides and Glasses

While the rare-earth ions have characteristic sharp fluorescence bands largely independent of the host, due to f–f^* transitions, mercury-like ions in general and thallium in particular have much broader fluorescence, with the fluorescence maxima strongly dependent on the composition of the host matrix. The quantum efficiency also is dependent on the host as described below. Monovalent thallium is a well-known fluorescence emitter in the UV region and was used in our studies in various matrices as a possible standard for UV fluorescence.

The absorption spectrum of thallium consists of three main bands: A, B, and C. A review of the absorption and luminescence of this element can be found in references [51] and [52]. The absorption band A, which is discussed here, is assigned to the spin-forbidden transition $^1A_{1g} \rightarrow {}^3T_{1u}$ ($^1\Gamma_1 - {}^3\Gamma_4^\circ$), equivalent to $^1S_0 \rightarrow {}^3P_1$ in the free thallous ion (see fig. 8), which is triply degenerate. It can be split in a cubic field by a dynamic Jahn-Teller effect [54], or the degeneracy can be lifted when the symmetry is decreased in glasses [55] from cubic to tetragonal or lower. The oscillator strengths, f, for the maxima of the A bands are presented in table 10. It was shown by Scott and Hu [53] that when the chloride ligand is replaced by an oxygen ligand in aqueous solution, the maxima of the band is shifted towards a shorter wave-

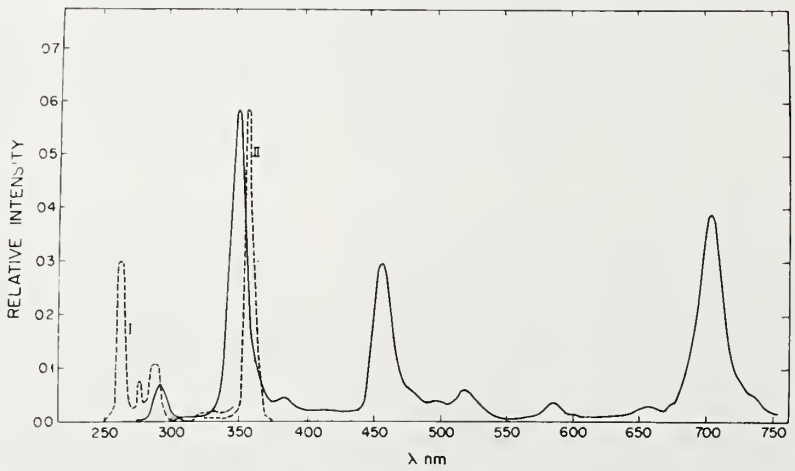

FIGURE 7. Corrected excitation spectrum of the $^1D_2$ fluorescence (broken line—II decreased by a factor of 2) and emission spectrum (full line) excited at $^3P_2$ band of thulium in phosphate glass.

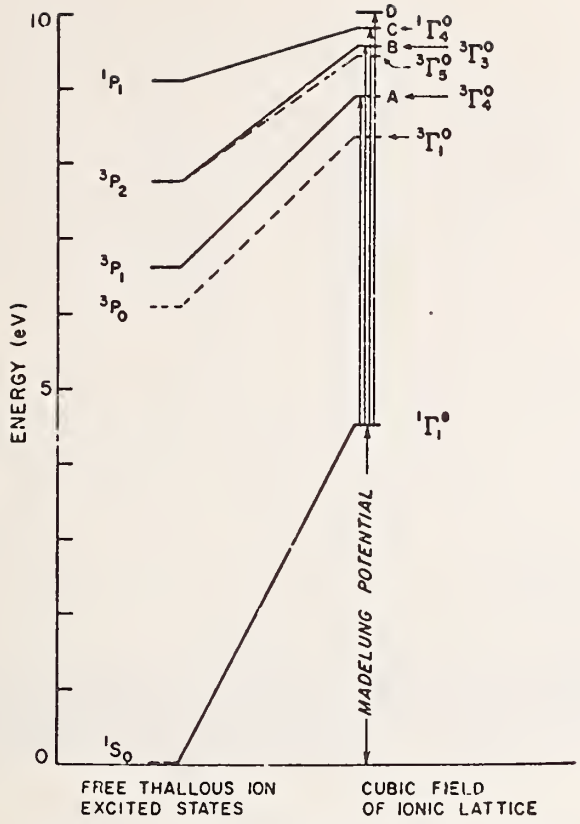

FIGURE 8. The energy of thallous ion in a cubic field.

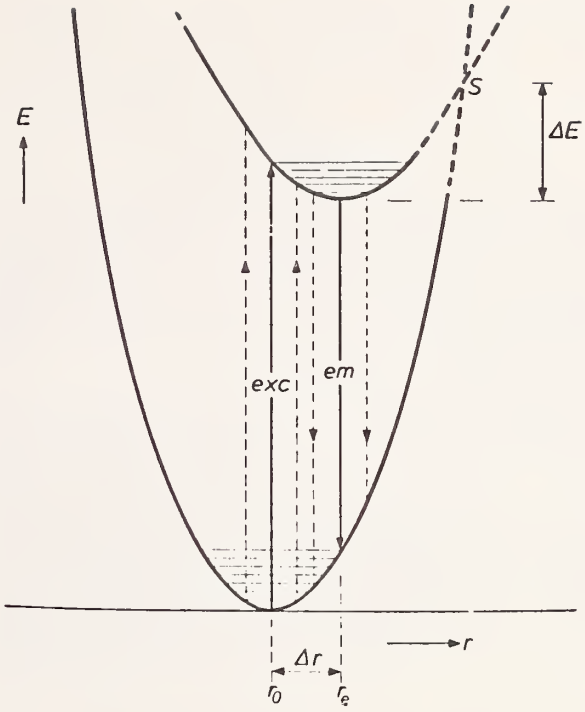

FIGURE 9. Configurational coordinate diagram of a luminescent center. The potential energy E of the center in the lattice is plotted as a function of the configurational coordinate r for the ground state and the first excited state. In practice, r is identified with the distance between the central cation and the surrounding anions. Vibrational states are represented schematically by horizontal lines in the parabolae. The excitation and emission transitions correspond to vertical transitions between the two curves. Since $\Delta r \neq 0$, the emission shows a Stokes' Shift (wavelength of the emission is longer than that of the excitation). Since the center can be in various vibrational states both at the ground level and at the excited level, and since $\Delta r \neq 0$, the transitions occur in a broad band of energies (schematically indicated by vertical dashed lines). Nonradiative return from the excited state to the ground state is possible via the point of intersection, S, of the two curves. This requires an activation energy ΔE, which can be supplied at higher temperatures (thermal quenching of the emission). In the region where the two parabolae intersect, the curve is marked by dashes since the situation is actually more complicated than is indicated here. This is due to interaction between the ground and the excited state at the situation of the intersection point. The present treatment is not invalidated by this.

length. The fluorescence occurs at a somewhat longer wavelength due to the Stokes' shift.

The relation between absorption and fluorescence can be most easily explained by the use of the configurational coordinate diagram, given in figure 9 [56]. The potential energy of the luminescent center in a crystal lattice is plotted here as a function of the configurational coordinate r. The quantity r represents a mean distance between the luminescence center and the surrounding ligands. The horizontal lines represent the vibrational states of the metal-oxygen bond vibrations.

At a temperature of absolute zero the luminescent center will occupy the lowest vibrational level of the ground state. The ions surrounding the central ion vibrate about their equilibrium positions situated at a distance r_0 from the central ion. At higher tempera-

TABLE 10. Quantum efficiencies (QE) of thallium in 4 matrices

Matrix	Max. absorption nm	Max. excitation nm	Max. emission nm	Oscillator strength, f [35]	QE	Stokes' shift (cm^{-1})
Borax	230	248	325	0.072	0.19	12709
Phosphate	212.5	230	300	.080	.23	13726
KCl	247	247	300	.074	.5	7153
KBr	261	261	320	.097	.44	7064

tures, higher vibrational levels may be occupied. In figure 9, the horizontal lines represent vibrational states. Due to the absorption of radiation of the appropriate wavelength (in this case UV radiation) the center is raised to an excited state. Since the equilibrium distance r_e of the excited state will not in general be equal to that of the ground state, and since the center may be at different vibrational levels, this transition will correspond to a fairly broad absorption band. The fact that the optical absorption corresponds to a vertical transition in figure 9 is attributable to the rapid nature of electronic transitions as compared to vibrational transitions which involve the heavier nuclei (Franck-Condon effect).

Once in an excited state, the system will relax towards the equilibrium state (of the excited level) by dissipation of heat. From this state or nearby levels the system returns to the ground state by emitting radiation. The emission, therefore, also consists of a broad band. Line emission is found only in the exceptional case where the configurational-coordinate curves are identical in shape and have the same equilibrium distance, as in the case of the rare-earth ions. Because of the heat dissipation, the emission always lies at a lower energy than the absorption. This displacement of emission with respect to absorption is known as the Stokes' shift.

With the aid of the simple model in figure 9 (the Mott-Seitz model) one can explain:

(a) the broad-band character of the emission and absorption of many centers;
(b) the shift of the emission to lower wavelengths; and,
(c) the temperature dependence of the emission.

If the equilibrium configuration of the excited state lies outside the curve of the ground state (fig. 10), then, after excitation, the intersection point of both curves is reached before the above-mentioned equilibrium configuration is reached, and the system relaxes nonradiatively to the ground state. No emission is then possible. The radiationless return to the ground state is temperature-independent. This is the model which Seitz proposed to explain the absence of luminescence in certain cases [57]. In other words, the condition for the absence of luminescence is a large difference between the equilibrium distance of the excited state and that of the ground state.

Dexter, Klick, and Russell later proposed a different model [58] which shows that even under less rigorous circumstances than in figure 10, nonradiative transitions to the ground state may occur (fig. 11). The characteristic feature of the situation in figure 11 is that the intersection point S of the two curves is lower than the level reached after excitation. When, after excitation, the system now relaxes while vibrating, to the equilibrium position of the excited state, the intersection point of the two curves is passed. Here too, a temperature-independent, radiationless return to the ground state can take place.

We learn from these models that the difference, Δr, between the equilibrium configuration of the excited

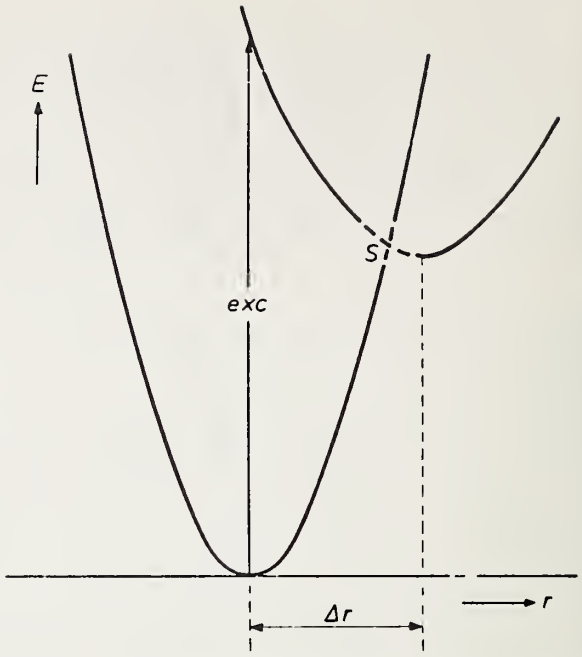

FIGURE 10. The Seitz model for explaining the absence of luminescence; see figure 9. The minimum of the curve for the excited state lies outside the curve for the ground state; luminescence is then not possible.

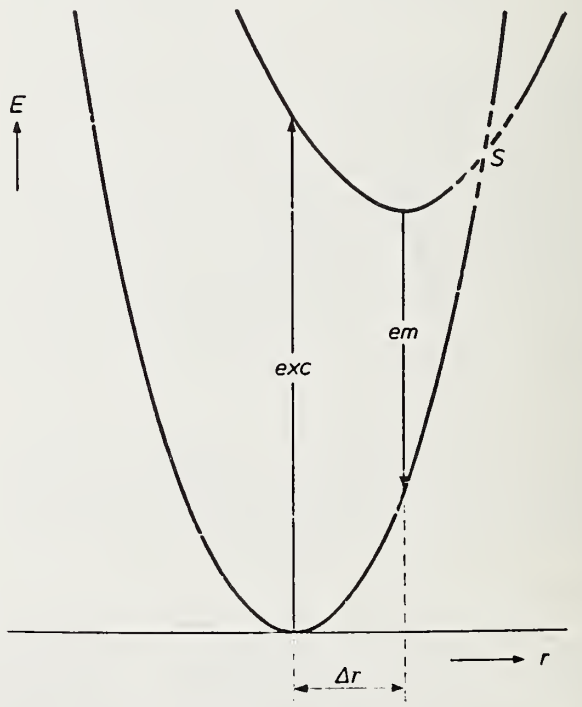

FIGURE 11. The Dexter-Klick-Russell model for explaining a low luminescence efficiency or the absence of luminescence. The intersection point S of the two curves lies below the vibrational level reached after excitation. The nonradiative return to the ground state requires no activation energy (as it did in fig. 9).

state and that of the ground state must be small if luminescence is to occur.

Because of the well-defined and broad fluorescence of thallium in the UV region, we have determined the optimum conditions for preparation of thallium doped alkali halide pellets in phosphate and borate glasses. Also, the dependence of fluorescence efficiency on concentration of Tl^+ was measured. It is shown that the thallium doped pellets and glasses can be used as fluorescence standards. The detailed results of the measurements are given.

A. Thallium Doped Potassium Chloride Disks

Polycrystalline pellets were used [52] as mentioned in the introduction. Such pellets are used in biomedical research for fluorescence measurements.

The optical absorption and fluorescence of alkali halides containing thallium has been widely studied; references can be found in a review paper by Teegarden [51].

The absorption band *A* with maximum around 247 nm in potassium chloride, arises from the spin-forbidden transition $^1A_g \rightarrow {}^3T_{1u}$ (corresponding to $^1S_0 \rightarrow {}^3P_1$ in a free thallous ion), and is accompanied by the fluorescence with band maximum at 300 nm. Because of large half-widths, the absorption and fluorescence are suitable for quantum-yield studies.

1. Preparation of Disks

Baker Analyzed KCl was ground for 1 h with an automatic mortar and pestle and dried for 48 h at 120 °C. TlCl (BDH Analytical Grade) was then added and the mixture was homogenized in an electric vibrator. In order to obtain low concentrations, the stock mixture was diluted twice with dry KCl powder. Prior to diffusion, the homogenized mixture was ground in an agate mortar with a small amount of triple-distilled water, and redried at 120 °C for 24 h.

As known from previous work [59, 60], only thallium that has undergone diffusion has an absorption band at 247 nm. The completeness of diffusion was checked by heating the mixtures at different temperatures for various periods and measuring the absorbance. The diffusion was then carried out by heating the mixtures at 400 °C for 4 h. Under these conditions, all of the thallium introduced diffuses into the KCl powder.

The absorption measurements were made on a Cary 14 spectrophotometer, with a KCl disk as blank. The effect of the emission on the absorbance readings was negligible, mainly because the solid angle subtended by the photomultiplier was small (0.005 rad), as compared to the full sphere (4π rad) over which emission occurs.

2. Preparation of Quinine Sulfate

Fisher Reagent Grade quinine sulfate was recrystallized from water five times and dried in a vacuum oven at 60 °C. Stock solutions were prepared by dissolving the purified quinine sulfate in 0.1 *N* H_2SO_4, analytical grade. The water used for the stock solutions was distilled, passed through an ion-exchange column, and then doubly distilled from a quartz still. Special low-fluorescence 1 mm quartz cells were used to hold the standard solutions.

3. Emission Measurements

The corrected emission was measured on a Turner 210 spectrofluorimeter in which the regular 1-cm cell was replaced by a special sample holder adapted to hold disks and cells of 1 mm thickness. The sample holder could be rotated to permit continuous variation of the angle of incidence of the exciting light. Because of the optical arrangement of the spectrofluorimeter, it was necessary to place a black-velvet screen between the sample and the collecting mirror to reduce reflections. All measurements were made at constant excitation energy and at room temperature.

Some representative A-band absorption curves are shown in figure 12. A plot of thallium concentration versus absorbance is linear, as can be seen in figure 13.

The oscillator strength, *f*, was calculated from the generalized formula of Smakula, (13), given by Patek (ref. [35, p. 72]).

$$f = 0.82 \times 10^{17} \frac{n}{(n^2+2)^2} \frac{V}{N} \alpha(E)\,dE \qquad (13)$$

where n is the refractive index, $\left(\frac{V}{N}\right)^{-1}$ the concentration of the ions per cm^3, α the absorbance in cm^{-1} and E the energy in electron volts. The refractive index of a KCl crystal was taken from Landodt-Bornstein [61] as 1.59. Multiplying 1.59 by the ratio of the pressed disk density (1.690 g/cm^3) to the crystal density (1.984 g/cm^3) yields an index of refraction value for the pressed disk of 1.57.

The oscillator strength was 0.074 ± 0.002. Figure 14 shows the corrected emission spectra. The linear concentration dependence of the emission-peak height is shown in figure 15.

The quantum yield was determined by use of eq (11) using quinine sulfate as a standard [52].

The quantum yield of 0.508 for quinine sulfate in 0.1 *N* H_2SO_4 used as a standard was taken from the data of Melhuish at $\lambda_{exc} = 366$ nm. Fletcher showed that the quantum yield was constant to within 5 percent over the wavelength range 240–290 nm, excluding a minimum at 270 nm. The refractive index n_s was taken as a weighted mean of the refractive indices of the standard solution and the quartz windows of the cell.

The excitation wavelength for the unknown and the standard was 247.5 nm. The emission-peak height was critically dependent on the angle of incidence of the exciting light, so that the small but inevitable difference of the angles of the sample and reference could cause a considerable error. On the other hand, the shape factor of the emission (ratio of emission-peak area to peak height) was independent of the angle. To eliminate the error, we found the maximum peak height by

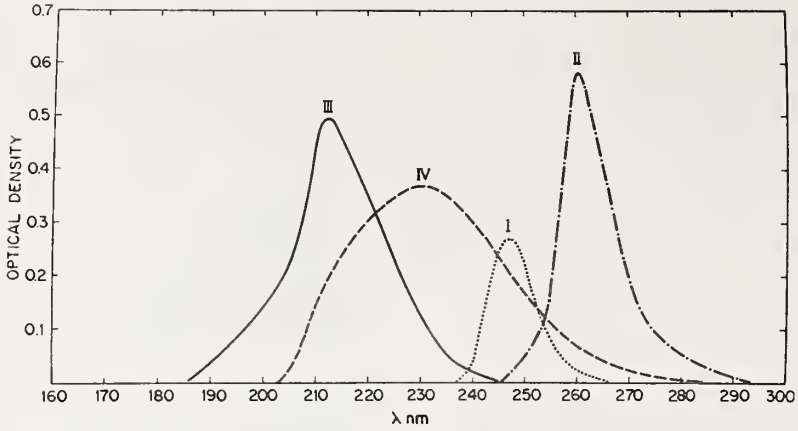

FIGURE 12. A band absorption spectra. I. KCl:Tl^+ 20 ppm; II. KBr:Tl^+, 20 ppm; III. Phosphate:Tl^+, 50 ppm; IV. Borax:Tl^+, 100 ppm.

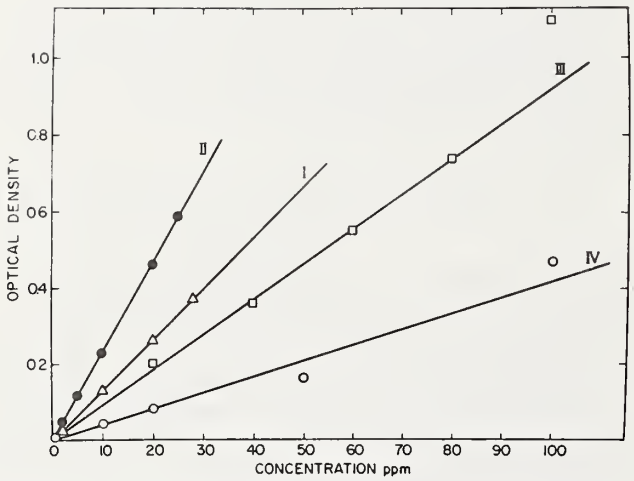

FIGURE 13. Absorbance versus concentration of Tl^+ in I. KCl; II. KBr; III. Phosphate; IV. Borax.

varying the angle of incidence and multiplied it by the shape factor to obtain the emission-peak area, A.

The quantum yield obtained in this way was 0.50 ± 0.03.

Pressed polycrystalline KCl:Tl disks differ only slightly in their density from KCl:Tl crystals, and they have the same optical characteristics. All of the thallium diffuses into the polycrystalline disks, and they can therefore be prepared to the predetermined uniform concentration. The linear concentration dependence of the absorbance (fig. 13) gives a check on the reproducibility of the samples, and the agreement of the oscillator strength of the disks with that of the crystals permits their use as a substitute for crystals. From the linear concentration dependence of the emission, it is concluded that the quantum yield is constant over the concentration range 2–30 ppm. Pressed polycrystalline KCl disks doped by diffusion with TlCl can therefore be used as UV luminescence standards at room temperature. The recommended

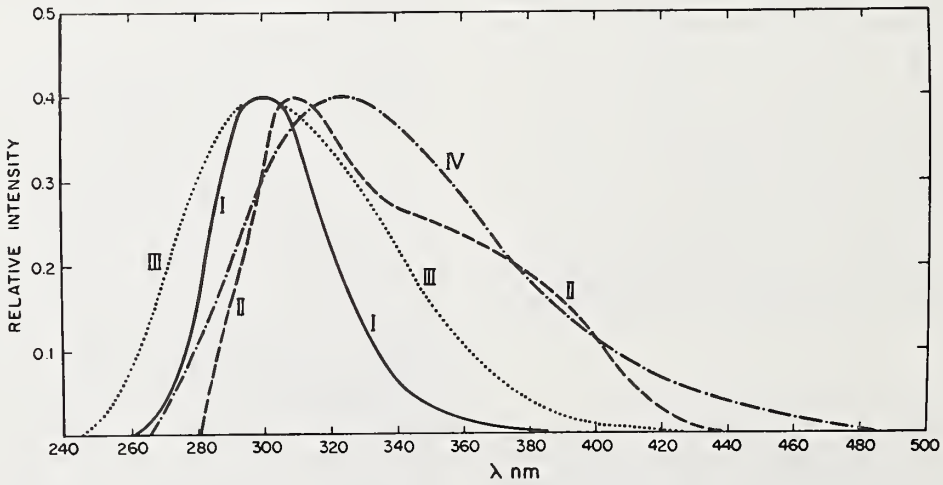

FIGURE 14. Corrected emission spectra I. KCl:Tl^+; II. KBr:Tl^+; III. Phosphate:Tl^+; IV. Borax:Tl^+.

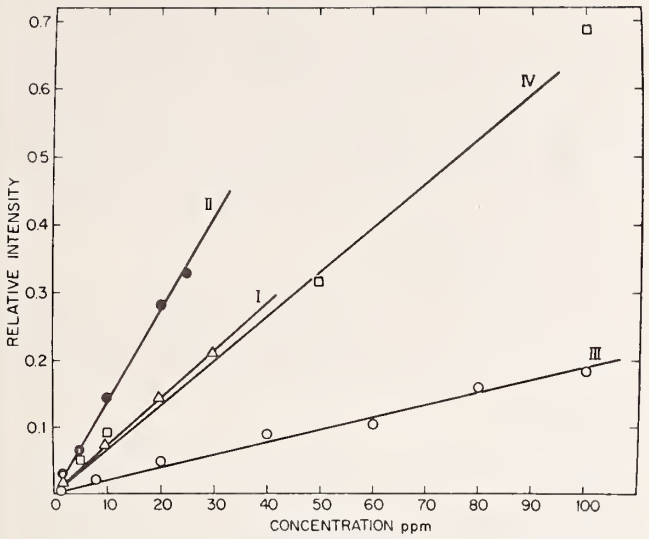

FIGURE 15. The dependence of fluorescence output on Tl^+ concentration: I. KCl; II. KBr; III. Phosphate; IV. Borax.

concentration is 2 ppm, corresponding to 0.624×10^{-6} mol/mol.

B. Thallium-Doped Potassium Bromide Disks

The absorption spectrum of KBr : Tl in polycrystalline disks and single crystals is well known [60, 62] and is presented in figure 12. The concentration dependence of the absorption maximum is presented in figure 13. The corrected emission spectrum of the A band is presented in figure 14. The dependence of fluorescence intensity on concentration is presented in figure 15.

The oscillator strength was calculated by use of Smakula's equation (13), and was found to be 0.097 ± 0.003. The quantum yield of the A band in KBr : Tl was calculated using KCl : Tl as a standard.

The emission and excitation spectra of the disks were measured on a spectrofluorimeter built in this laboratory, the description of which may be found in reference [36]. The emission spectra were corrected using standard compounds and their reported spectra. To correct for the difference of excitation energy in the standard and the unknown, a correction factor was introduced into eq (11).

The refined formula for the use with this spectrofluorimeter is of the form:

$$\eta_u = \eta_s \frac{F_u A_s d_s \lambda_s n_u^2}{F_s A_u d_u \lambda_u n_s^2} \times \frac{F_s^B F_u^T}{F_s^T F_u^B} \qquad (14)$$

in which the parameters have the same meaning as in (11). F_S^B is the relative fluorescence output at peak maximum in the excitation spectrum of the standard measured with our apparatus; F_S^T is the relative fluorescence output at peak maximum in the excitation spectrum of the standard measured on the Turner Model 210 spectrofluorimeter; F_u^B is the output at peak maximum of the unknown in the excitation spectrum of the standard measured in our apparatus; F_u^T is the output at peak maximum of the unknown measured in the excitation spectrum of the standard on the Turner Model 210 spectrofluorimeter. The density of the pressed KBr disk is 2.67 g/cm³.

We used as a standard a KCl:Tl disk with a quantum yield of 0.50. The quantum yield obtained for the KBr : Tl disk is 0.44 ± 0.03. All data concerning KBr : Tl disks are presented in table 10.

Because of the linear dependence of absorption and emission on the Tl^+ concentration, it is concluded that the quantum yield is independent of the concentration in the 0.5–25 ppm range. Pressed polycrystalline KBr:Tl and KCl:Tl disks can easily be prepared to predetermined concentrations for use as UV fluorescence standards at room temperature. The recommended Tl concentration is 2 ppm, corresponding to 0.837×10^{-6} mol/mol KBr:Tl and 0.624×10^{-6} mol/mol in KCl.

III. Thallium-Doped Glasses

To compare our results in glasses with the corresponding data of alkali halides, we have prepared and measured glasses doped with thallium.

Glasses were prepared from sodium phosphate monobasic and from borax. Glasses, 1 mm thick and 12 mm in diameter were obtained by molding the melt on a tile.

The absorption spectra were recorded on a Cary 14 spectrophotometer using undoped glasses or disks as blanks, and are presented in figure 12. The concentration dependence of the absorption is presented in figure 13.

1. Excitation and Emission Spectra

Excitation and emission spectra were taken on a spectrofluorimeter built in this laboratory [36]. The spectra were corrected with respect to light characteristics and spectral distribution of the photomultiplier by comparison with a similar spectrum taken on the Turner Model 210 spectrofluorimeter using standard compounds (quinine sulfate, fluorescein, etc.).

The corrected emission spectra are presented in figure 14. The concentration dependence of the emission is presented in figure 15. The quantum efficiencies were obtained by comparison of the glasses with alkali halide-thallium-doped disks using eq (14), the results of which are presented in table 10.

When a pellet or a glass containing thallium is excited through absorption into the A band at room temperature, the emission is composed of two time components, one with a short lifetime of about 25 ns and one with a long component of 400 ns. We have proposed an explanation for the two decay constants [55].

The proposed explanation is as follows: The absorption is from $^1S_0$ ground state to $^3P_1$ excited state. The emission occurs also between these two levels and is followed by a Stokes' shift (see table 10). It is an allowed emission with a short lifetime. However, part

of the population of the $^3P_1$ level is rapidly depleted by a radiationless process to the metastable $^3P_0$ state (see fig. 16). This assumption is proven by an experiment of Tomura [63], who had observed a decay of 2 − 1 ms at 20 K due to this transition. At an elevated temperature, the vibronic modes promote tunnelling from $^3P_0$ back to $^3P_1$. This process occurs with an activation energy of 0.06 eV in KCl. The next process is the delayed emission from $^3P_1$. The rate of this process is the rate of tunnelling which controls the population of $^3P_1$. Since both the instant and delayed emission occurs from the $^3P_1$ state, the wavelength of emission for both decays is the same. Also, the delayed fluorescence is not polarized [63] because the memory of polarization is lost during tunnelling. To determine the quantum yield from the lifetime measurement, additional calculations have to be made because of this delayed fluorescence.

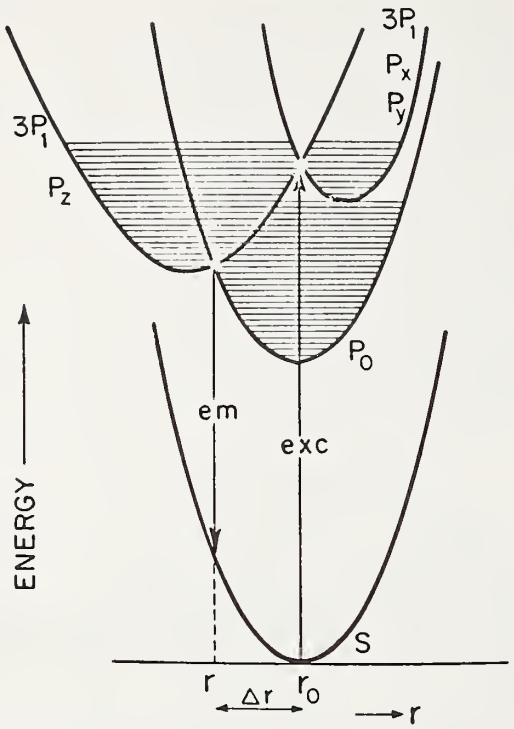

FIGURE 16. Configurational coordinate diagram of Tl^+ in a tetragonal symmetry.

In this mechanism, for all four cases described here, the broadening of the emission in KBr:Tl is due to emission from P_x, P_y and another emission from P_z, and not from P_0. Splitting of the various P orbitals by the Jahn-Teller effect is stronger the heavier the anion of the host lattice.

The shift of the absorption band to longer wavelength in the order Tl^+-phosphate, Tl^+-borax, Tl^+-KCl and Tl^+-KBr (also Tl^+-Kl) indicates that the ligand field acting on Tl^+ increases in the same order. The stronger the ligand field the smaller the difference between the excited and ground state and hence the absorption occurs at longer wavelengths. This also indicates that, in the case of borax, the electrons of the oxygen participating in the thallium-oxygen bond are shifted more to the Tl (stronger polarization of the bond), which is due to stronger electron affinity of phosphorus (0.78 eV) than of boron (0.33 eV).

IV. Glasses Doped by Pb^{2+}, Ce^{3+}, and Cu^+

In a search for standards to cover the fluorescence range from the UV region to the red region, it was found that in addition to thallium doped glasses [64], glasses containing Ce^{3+} [65], Pb^{2+} [66], and Cu^+ [67] are suitable for standards. considering the positions of their emission wavelengths and half bandwidths.

The corrected emission spectra of various glasses containing these ions are presented in figure 17. The

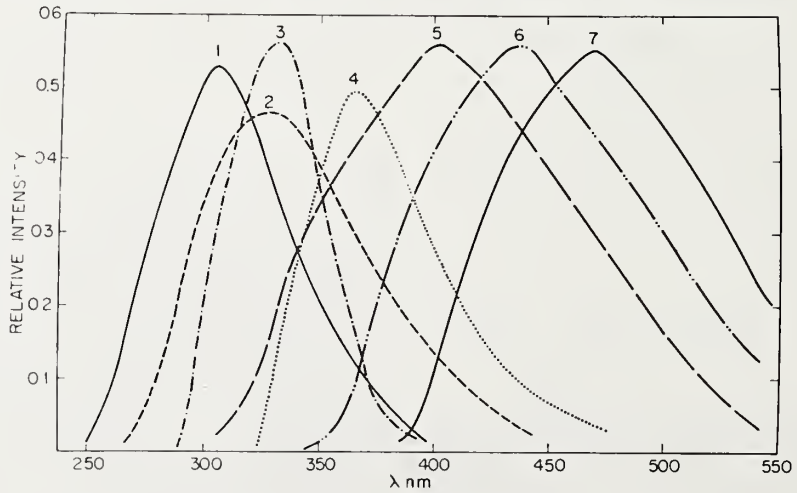

FIGURE 17. Matrix effects on position of emission band of Tl^+, Ce^{3+}, Pb^{2+}, and Cu^+. I. Phosphate:Tl^+; II. Borax:Tl^+; III. Phosphate:Ce^{3+}; IV. Borax:Ce^{3+}; V. Borax:Pb^{2+}; VI. Germanate: Pb^{2+}; VII Phosphate: Cu^+.

absorption spectra of Ce^{3+} and Cu^{+} in phosphate glass and Pb^{2+} in borax glass are presented in figure 18. The absorption is linear with concentration in the range measured (1–1000 ppm). The dependence of fluorescence on concentration is linear as shown in figure 19, and this range of concentration can be used for preparation of the standards. The maximum emission and excitation wave lengths of the glasses and the half bandwidths of the emission are presented in table 11.

The determinations of quantum yields of these glasses are now undergoing research. For these determinations, doped potassium chloride disks are used as standard references [64–67]. For the quantum yield determination of Tl in phosphate and borate glasses, and Ce^{3+} in phosphate glasses, quinine sulfate was used as a relative standard [68].

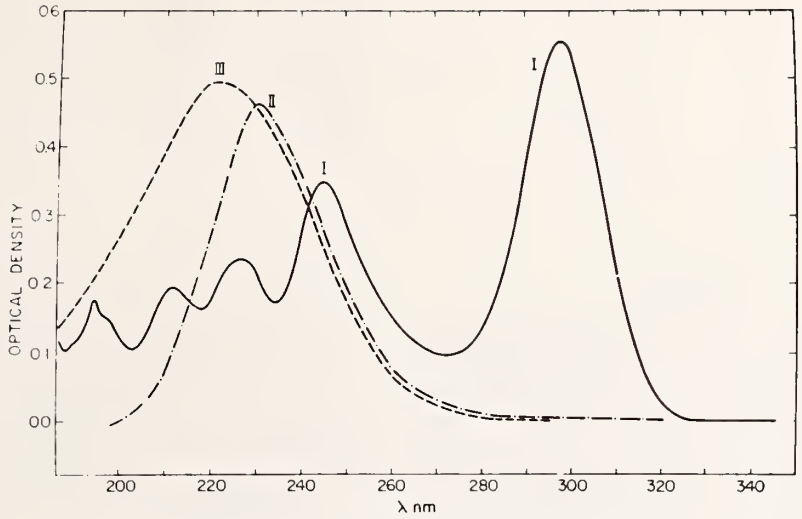

FIGURE 18. Absorption spectrum of I. Ce^{3+} in phosphate, 400 ppm; II. Pb^{2+} in borax, 100 ppm; III. Cu^{+} in phosphate, 50 ppm.

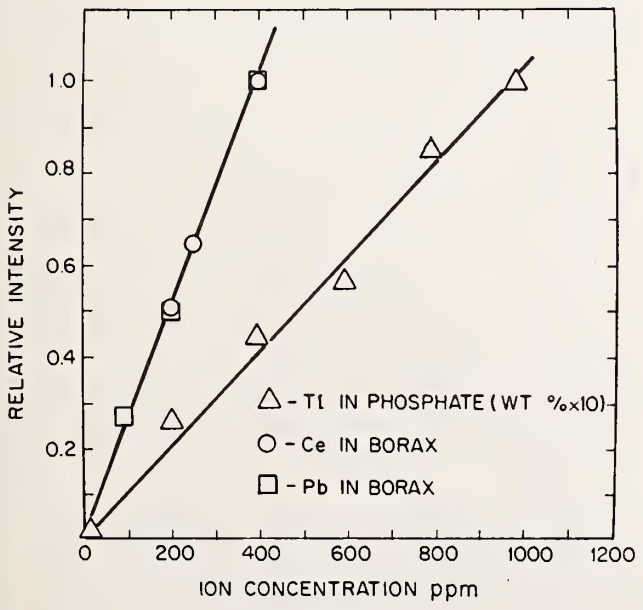

FIGURE 19. The dependence of fluorescence intensity on concentration I. Tl^{+} in phosphate; II. Ce^{3+} in borax; III. Pb^{2+} in borax.

Conclusions

Rare-earth-doped glasses are suggested as relative standards for use with compounds having narrow band excitation and emission of fluorescence. Thallium-doped alkali halides are standards suitable for determination of substances in alkali halide pellets, while thallium doped glasses can be used as standards for glassy substances or liquids in quartz cells. Other varieties of glass standards and pellets are now under investigation. Energy transfer studies which are of great importance in understanding quantum efficiencies will be summarized in a separate review.

The assistance of E. Greenberg in preparation of this paper is gratefully acknowledged. I wish also to express my thanks to Y. Eckstein and L. Boehm for fruitful discussions, and E. Hoffman for providing relevant literature on fluorescence in biomedical systems. I especially wish to express my gratitude to O. Menis who suggested the topic for this paper.

Table 11. Emission and excitation wavelength dependence on matrix for lead, cerium, thallium and copper

Ion	Matrix	Wavelength, nm		Emission half-bandwidths, nm
		Excitation	Emission	
Tl^{+}	KCl	247.5	300	40
Tl^{+}	Phosphate	219.0	302	70
Tl^{+}	Borate	233.0	325	90
Ce^{3+}	Phosphate	297.0	334	55
Ce^{3+}	Borate[a]	310.0	364	80
Ce^{3+}	Borax[b]	311.0	365	65
Ce^{3+}	Silicate	317.0	380	85
Pb^{2+}	Phosphate	241.5	309	70
Pb^{2+}	Borate[a]	261.0	424	140
Pb^{2+}	Borax[b]	241.0	425	165
Pb^{2+}	Germanate	295.0	440	125
Cu^{+}	Phosphate	270.0	445	120

[a] Mixture of boric acid and boric oxide. [b] Sodium borate only.

VI. References

[1] Parker, C. A., Photoluminescence of Solutions (Elsevier Publishing Co., New York, N.Y. 1968); Hercules, D. M. Ed., Fluorescence and Phosphorescence Analyses. (Interscience Publishing Co., New York, N.Y., 1966); B. Becker, R. S., Theory and Interpretation of Fluorescence and Phosphorescence (John Wiley & Sons, Inc., New York, N.Y., 1969).
[2] White, C. E., and Argaver, R. J., Fluorescence Analysis (M. Dekker, Inc., New York, N.Y. 1970); Berlman, I. B., Handbook of Fluorescence Spectra of Aromatic Molecules, (Academic Press, New York, N.Y., 2nd Edition 1971).
[3] Demas, J. N., and Crosby, G. A., J. Phys. Chem. **75**, 991 (1971).
[4] Edelman, G. M., and McClure, W. O., Accounts. Chem. Res. **1(3)**, 65 (1968).
[5] Strayer, L., Science **162**, 526 (1968).
[6] Rinder-Knecht, H., Nature **193**, 167 (1962).
[7] Hartley, B. S., and Massey, V., Biochim. Biophys. Acta **21**, 58 (1956).
[8] Deyl, Z., and Rosmus, J., J. Chromatogr. **20**, 514 (1965).
[9] Pataki, G., and Strasky, E., Chimia **20**, 361 (1966).
[10] Chen, R. F., Arch. Biochem. Biophys. **120**, 609 (1967).
[11] Moye, H. A., and Winefordner, J. D., J. Agr. Food Chem. **13**, 516 (1965).
[12] Staniland, L. N., J. Agr. Eng. Res. **4**, 110 (1959).
[13] Staniland, L. N., J. Agr. Eng. Res. **5**, 42 (1960).
[14] Udenfriend, S., Fluorescence Assay in Biology and Medicine (Academic Press, New York, N.Y., Vols. I and II, 1962, 1969).
[15] Van Duuren, B. L., J. Natl. Cancer Inst. Monograph No. 9, 135 (1962).
[16] Van Duuren, B. L., Acta Unio Intern. Contra Cancrum **19**, 524 (1963).
[17] Konev, S. V., Fluorescence and Phosphorescence of Proteins and Nucleic Acids, (Plenum Press, New York, 1967), p. 171.
[18] Booth, J., et al., J. Chem. Soc. 598 (1954).
[19] De Santis, F., et al., Nature **191**, 900 (1961).
[20] Liquori, A. M., et al., J. Mol. Biol. **5**, 521 (1962).
[21] Cook, J. M., J. Chem. Soc. London, 1210 (1950).
[22] Sawicki, E., et al., Talanta **14**, 431 (1967).
[23] Van Bertalanffy, L., et al., Cancer **11**, 873 (1958).
[24] Rubin, M., Fluorimetry in Clinical Chemistry, American Instrument Co., Silver Spring, Maryland.
[25] Phillips, R. E., Ed., Manual of Fluorimetric Clinical Procedures, G. K. Turner Assoc., Inc., Palo Alto, California.
[26] Van Duuren, B. L., and Bardi, C. E., Anal. Chem. **35**, 2198 (1963).
[27] Winefordner, J. D., and St. John, P. A., Anal. Chem. **35**, 2211 (1963).
[28] Samson, J. A. R., Techniques of Vacuum Ultraviolet Spectroscopy (John Wiley & Sons, Inc., New York, 1967), p. 212–216.
[29] Bril, A., Luminescence of Organic and Inorganic Materials (John Wiley & Sons, Inc., New York, N.Y. 1962), p. 477.
[30] Birks, J. B., and Dyson, D. J., Proc. Roy. Soc. **275A**, 135 (1963).
[31] Seybold, P. G., Gouterman, M., and Callis, J., Photochemistry and Photobiology **9**, 229 (1969).
[32] Lewis, G. N., and Kasha, M., J. Am. Chem. Soc. **67**, 994 (1945).
[33] Strickler, S. J., and Berg, R. A., J. Chem. Phys. **37**, 814 (1962).
[34] Wybourne, B. G., Ed., Spectroscopic Properties of the Rare Earths (Interscience Publ., New York, N.Y. 1965).
[35] Patek, K., Glass Lasers, Edwards, J. G., Ed., London (Butterworth & Co., 1970).
[36] Reisfeld, R., Honigbaum, A., Michaeli, G., Harel, L., and Ish-Shalom, M., Israel J. Chem. **7**, 613 (1970).
[37] Reisfeld, R., Greenberg, E., Kirshenbaum, L., and Michaeli, G., Proc. 8th Rare Earth Conference **2**, 743 (1970).
[38] Reisfeld, R., and Hormadaly, J., Proc. 9th Rare Earth Conference, **1**, 123 (1971).
[39] Reisfeld, R. and Eckstein, Y., Solid State Chem. **5**, 174 (1972).
[40] Reisfeld, R., Velapoldi, R. A., Boehm, L., and Ish-Shalom, M., J. Phys. Chem. **75**, 3981 (1971).
[41] Reisfeld, R., Velapoldi, R. A., and Boehm, L., J. Phys. Chem. **76**, 1293 (1972).
[42] Velapoldi, R. A., Reisfeld, R., and Boehm., L., Proc. 9th Rare Earth Res. Conf. **2**, 488 (1971).
[43] Reisfeld, R., and Greenberg, E., Anal. Chem. **47**, 155 (1969).
[44] Turner, G. K., Science **146**, 183 (1964).
[45] Fletcher, A. N., J. Mol. Spectry. **23**, 221 (1967).
[46] Reisfeld, R., Greenberg, E., Velapoldi, R. A., and Barnett, B., J. Chem. Phys. **56**, (4) 1698 (1972).
[47] Reisfeld, R., Glasner, A., and Mustaki, A., Proc. Int. Colloqu. Optic and Spectroscopic Phenomena in Ionic Crystals, Bucharest, 1968; Mustachi, A., Reisfeld, R., and Glasner, A., Israel J. Chem. **7**, 627 (1970).
[48] Reisfeld, R., and Biron, E., Talanta **17**, 105 (1970).
[49] Reisfeld, R., Arye, Z. Gur., and Greenberg, E., Anal. Chim. Acta **50**, 249 (1970).
[50] Reisfeld, R., and Eckstein, Y., Anal. Chim. Acta **56**, 461 (1971).
[51] Teegarden, T., in Luminescence of Inorganic Solids, Goldberg, P., Ed. (Academic Press, New York, N.Y., 1966), p. 83.
[52] Reisfeld, R., Honigbaum, A., and Velapoldi, R. A., J. Opt. Soc. Am. **61**, 1422 (1971).
[53] Scott, A. B., and Hu, K. H., J. Chem. Phys. **23**, 1830 (1955).
[54] Sturge, M. D., Solid State Physics **20**, 91 (1967).
[55] Reisfeld, R., Greenberg, E., Deinum, T., Werkhoven, C. J., and van Voorst, J. D. W., to be published.
[56] Blasse G., and Bril, A., Philips Technical Review **31**, 304 (1970).
[57] Seitz, F., Trans. Faraday Soc. **35**, 74 (1939).
[58] Dexter, D. L., Klick, C. C., and Russell, G. A., Phys. Rev. **100**, 603 (1955).

[59] Glasner A., and Reisfeld, R., J. Phys. Chem. Solids **18**, 345 (1961).
[60] Glasner, A., Rejoan, A., and Reisfeld, R., J. Phys. Chem. Solids **19**, 331 (1961).
[61] Landolt-Bornstein, Zahlenwerte und Funktionen, Bd. **2**, Teil 8, Optische Konstanten (Springer, Berlin, 1962).
[62] Reisfeld, R., and Honigbaum, A., 1972, unpublished results.
[63] Tomura, M., and Nishimura, H., J. Phys. Soc. Japan, **21**, 2081 (1966).
[64] Reisfeld, R., and Morag, S., J. Appl. Phys. Letters **21**, 57 (1972).
[65] Reisfeld, R., Hormodaly, J., and Barnett, B., Chem. Phys. Letters.
[66] Reisfeld, R., and Lieblich, N., unpublished results.
[67] Reisfeld, R., and Kosloff, R., unpublished results.
[68] Reisfeld, R., Velapoldi, R. A., and Greenberg, E., unpublished results.

(Paper 76A6–746)

502-591 O - 73 - 16

NATIONAL BUREAU OF STANDARDS SPECIAL PUBLICATION 378, Accuracy in Spectrophotometry and Luminescence Measurements, Proceedings of a Conference Held at NBS, Gaithersburg, Md., March 22–24, 1972 (Issued May 1973).

Development of a New Fluorescent Reagent and Its Application to the Automated Assay of Amino Acids and Peptides at the Picomole Level *

Sidney Udenfriend

Roche Institute of Molecular Biology, Nutley, New Jersey 07110

(June 15, 1972)

Methods for the assay of amino acids and peptides are most important in elucidating the structure of proteins and peptides. In many important areas of research such as in endocrinology, neurobiology, and genetics, methods are needed with sensitivity higher than is available with the widely used colorimetric ninhydrin procedure. A short while ago, we noted that all primary amines react with ninhydrin and phenylacetaldehyde to give a ternary product which is highly fluorescent. The chemistry of that reaction has now been elucidated and the conditions have been modified and improved so that essentially quantitative yields of fluorescent products are formed with all primary amines. The reaction has been automated and is being used as the detecting system for chromatography of amino acids, peptides and amines in the 10 to 100 picomole range. Problems concerning the fluorescence instrumentation and the isolation and chromatography of these compounds in the picomole range will be discussed.

Key words: Fluorometry, amino acids; fluorometry, peptides; picomole fluorometry.

Collaborative studies by biologists and chemists at Nutley have led to the development of a new fluorometric reagent for amino acids and peptides and its application to their automated assay at the picomole level. The origin of these studies, as well as the chemistry and the analytical applications, are presented in this report.

A number of years ago McCaman and Robins [1][1] reported a highly specific and sensitive fluorometric method for blood phenylalanine assay. The procedure is now generally used for the diagnosis of phenylketonuria. In this method, fluorescence develops when phenylalanine is treated with ninhydrin and a peptide. The other amino acids which are normally found in plasma and protein hydrolyzates give no fluorescence. On the other hand, almost any peptide can be used in the phenylalanine assay.

These very unusual requirements led us to investigate the reaction with the possibility of reversing the conditions to assay peptides fluorometrically by adding ninhydrin plus phenylalanine. When this was tried it worked. Other than phenylalanine, the only α-amino acid which yielded fluorescence (although of far less intensity) was α-aminobutyric acid. This amino acid is not normally present in tissues.

On further investigation, it was found that phenylalanine itself was not the active agent, but was first oxidized and decarboxylated by ninhydrin to phenylacetaldehyde. The latter, in the presence of additional ninhydrin, combined with primary aliphatic amines to yield highly fluorescent derivatives. It was found that several other aldehydes yielded fluorophors with ninhydrin and amines but that the most intense fluorescense by far was obtained with phenylacetaldehyde.

The products obtained on reacting amines, amino acids and peptides with ninhydrin and phenylacetaldehyde all exhibit the same excitation and emission spectra (fig. 1). Excitation maxima are at 275 nm and 390 nm with emission at 480 nm.

To investigate the mechanism of the reaction further, the fluorophor formed on reacting phenylacetaldehyde and ninhydrin with a simple amine, such as ethylamine, was prepared. The purified product could not be obtained in crystalline form, but was shown to be in equilibrium with a nonfluorescent congener which was apparently a lactone. The latter was crystallized and yielded a molecular ion with the highest mass at 305. This and other findings suggested that the product was the result of a ternary reaction involving one molecule each of amine, phenylacetaldehyde and ninhydrin.

The purified fluorophor obtained with ethylamine was used as a standard to show that under the conditions of the reaction the yield of fluorescent product was about 50 percent. There was considerable variation in the fluorescence obtained with various other amino acids. Much of this was due to differences in quantum yield as well as to completeness of reaction.

* This article is based on studies carried out in collaboration with Wallace Dairman, Keijiro Samejima, Manfred Weigele, Willy Leimgruber, Stanley Stein, and Peter Böhlen.

[1] Figures in brackets indicate the literature references at the end of this paper.

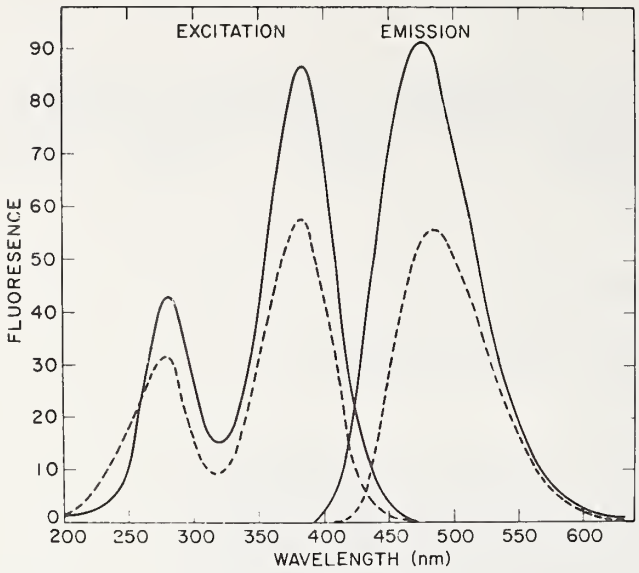

FIGURE 1. Spectral properties of fluorophor obtained on reacting an amino acid with ninhydrin and phenylacetaldehyde.

The procedure was automated with the use of appropriate pumps and a flow cell cuvette in an Aminco Microfluorometer.[2] Application of this automated procedure was made for amino acid analysis. The sensitivity at this stage with most amino acids was found to be below the nanomole level. This compares to a limit of 10 nanomoles for most commercial amino acid analyzers which utilize the colorimetric ninhydrin procedure.

Details of the procedure utilizing ninhydrin and phenylacetaldehyde have been published [2, 3]. It possesses the sensitivity and many other qualities which could have made it a useful analytical procedure. However, elucidation of the mechanism of the reaction [4] led to the development of a new reagent and made it obsolete.

Weigele and Leimgruber and their colleagues at Hoffmann-La Roche in Nutley had been collaborating with us in our studies. They concentrated on the mechanism of the ninhydrin phenylacetaldehyde reaction utilizing mass spectrometry, x-ray crystallography and other procedures on a number of crystalline derivatives. The structure of the fluorophor obtained with ethylamine was proven to be as shown in figure 2. The condensation with ninhydrin and phenylacetaldehyde also yielded two nonfluorescent products which could be converted to the fluorophor by treatment with base.

Brilliant deduction led Weigele and Leimgruber[3] to synthesize the compound, 4-phenylspiro[furan-2(3H), 1[1]-phthalan]-3,3[1]-dione, RO 20–7234. This compound was found to react with amines to form the identical

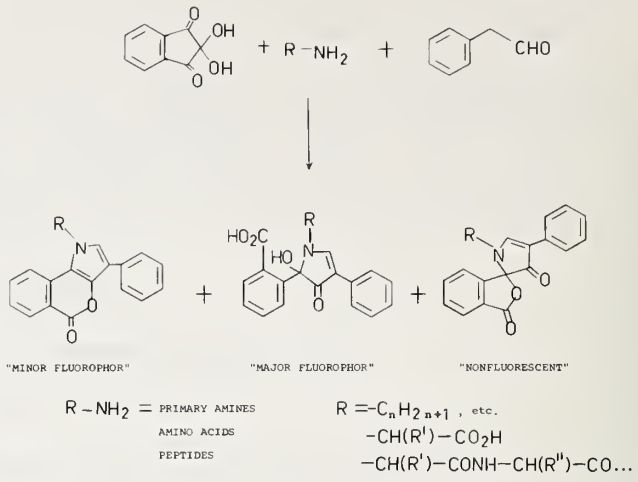

FIGURE 2. Formation of fluorophor from ninhydrin, phenylacetaldehyde and ethylamine.

fluorophor obtained with ninhydrin and phenylacetaldehyde (fig. 3). With this new reagent the reaction is a

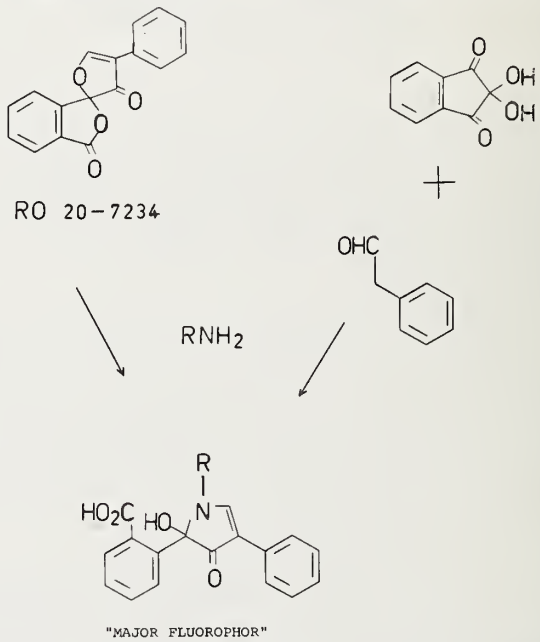

FIGURE 3. Comparison of reactions of amines with RO 20–7234 and with ninhydrin and phenylacetaldehyde.

binary one rather than a ternary one. The resulting advantages are many-fold. The ternary reaction with ninhydrin does not go to completion; about 45 percent with ethylamine and much less for aspartic acid. Yields with the new reagent are almost quantitative with all amines, amino acids and peptides. The ternary reaction is run at 65° for 25 min. The binary reaction is instantaneous at room temperature. In both cases the reagents are nonfluorescent. In the ternary reaction, ammonia does not react at all. With the new reagent, ammonia reacts to a slight extent (one thousandth as

[2] In order to adequately describe materials and experimental procedures, it was occasionally necessary to identify commercial products by manufacturer's name or label. In no instances does such identification imply endorsement by the National Bureau of Standards, nor does it imply that the particular product or equipment is necessarily the best available for that purpose.

[3] Weigle, M., and Leimgruber, W., to be published.

much as a typical amino acid). The conditions of the binary reaction lead to several times more intense fluorescence for the same amount of fluorophor.

The fluorophor obtained with peptides (fig. 4) are

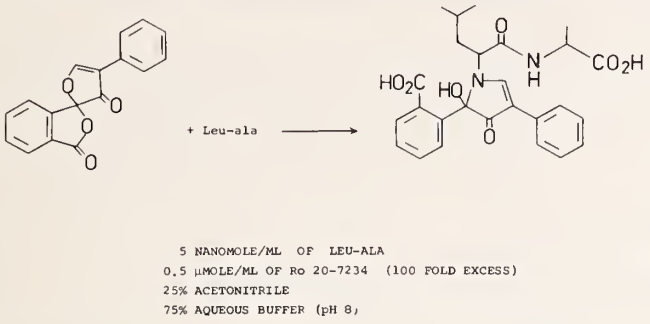

FIGURE 4. Formation of fluorophor with a peptide and the reagent RO 20–7234.

more intensely fluorescent than the fluorophors formed from the corresponding amino acids. This may be due to a greater quantum yield. The free carboxyl group close to the fluorophoric group may quench the fluorescence. Whatever the reason, this is a decided advantage for peptide assay.

The new reagent is ideally suited to detect amino acids and peptides in the automated assay of column effluents. Such assays have now been set up and even with relatively unsophisticated pumping systems and fluorescence instrumentation, it has been possible to carry out analyses in the picomole range. Figure 5 shows the chromatographic separation of an amino acid mixture (neutral and acidic), 250 picomoles of each. Figure 6 shows the chromatographic separation of 50 picomoles each of the basic amino acids.[4]

A number of applications have already been made which make use of this great sensitivity. It has been possible to measure the peptides oxytocin and vasopressin in an aliquot of an extract of a *single* rat pituitary (fig. 7). Thus, the method will be of great

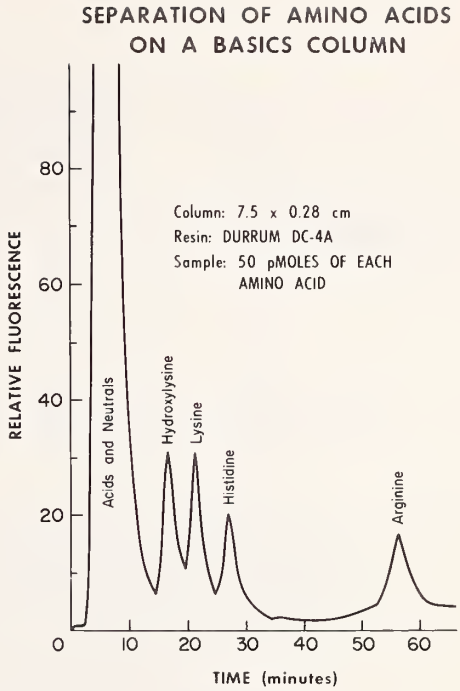

FIGURE 6. Chromatography of basic amino acids in the picomole range.

importance in the isolation and characterization of physiologically active peptides and their metabolites. Another important application has been to the assay of spermine and spermidine. The sensitivity in this case is so great and the tissue levels so high that microgram quantities of brain tissue are sufficient for assay. Most important, the simplicity of the apparatus required to operate in the picomole region using fluorescence should make it possible to devise relatively inexpensive commercial equipment. It is hoped that commercial instruments, which make use of this reagent, will soon be available.

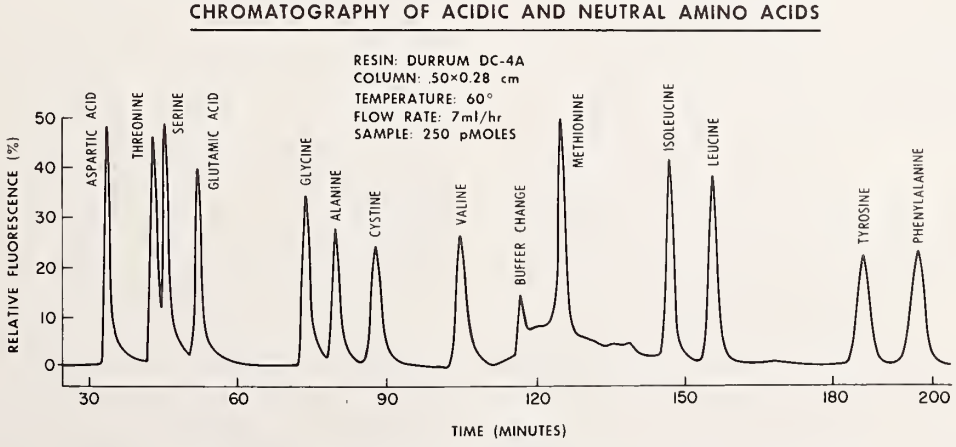

FIGURE 5. Chromatography of neutral and acidic amino acids in the picomole range.

[4] Details of these procedures will be published in a subsequent paper.

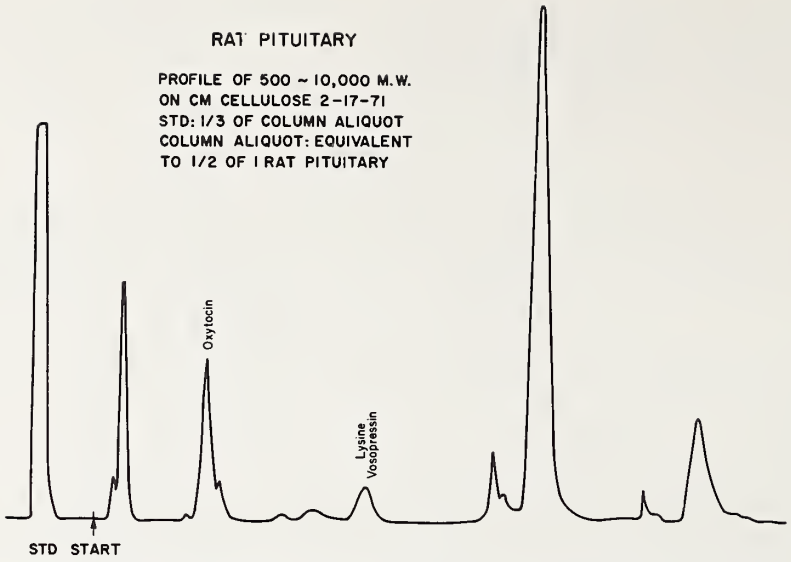

FIGURE 7. Chromatographic separation of the oxytocin and vasopressin in an extract of one rat pituitary.

References

[1] McCaman, M. W., and Robins, E., J. Lab. Clin. Med. **59,** 885 (1962).

[2] Samejima, K., Dairman, W., and Udenfriend, S., Anal. Biochem. **42,** 222 (1971).

[3] Samejima, K., Dairman, W., Stone, J., and Udenfriend, S., Anal. Biochem. **42,** 237 (1971).

[4] Weigele, M., Blount, J. F., Tengi, J. P. Czajkowski, R. C., and Leimgruber, W., J. Am. Chem. Soc. **94,** 4052 (1972).

(Paper 76A6–747)

NATIONAL BUREAU OF STANDARDS SPECIAL PUBLICATION 378, Accuracy in Spectrophotometry and Luminescence Measurements, Proceedings of a Conference Held at NBS, Gaithersburg, Md., March 22–24, 1972 (Issued May 1973).

Considerations on Organic Compounds in Solution and Inorganic Ions in Glasses as Fluorescent Standard Reference Materials

R. A. Velapoldi

Institute for Materials Research, National Bureau of Standards, Washington, D.C. 20234

(June 30, 1972)

The use of various organic compounds in solution and inorganic ions in glasses has been investigated as possible fluorescence Standard Reference Materials. Emphasis was placed on measuring physical and chemical parameters such as stability, reproducibilities of absorbance and fluorescence measurements, relative quantum efficiencies as a function of excitation wavelength, etc., for quinine derivatives and selected organic compounds. A brief discussion is included on the use of rare earth and non-rare earth inorganic ions in glasses as standards.

Key words: Emission spectra; excitation spectra; fluorescence; fluorescence standards; glass standards; quinine derivatives; rare earths; relative quantum efficiencies; solution standards.

I. Introduction

The rapid growth of publications in fluorimetric research and applications during the last two decades, and the variability of data and results in those publications, underline the need for standardization of fluorescence nomenclature and data presentation. These needs were discussed previously by investigators [1–3][1], who collectively presented a proposal for fluorescence standardization [4]. The main objective of this proposal was to supply a firm basis for reporting fluorimetric results so that comparisons of data among laboratories would be meaningful.

There are basically two methods which can be used for the presentation of data: (a) in absolute radiative or energy units, and (b) by comparing fluorescence data of the compound under study with data obtained for an accepted standard. Very few laboratories are equipped to make absolute radiant energy measurements; however, comparative spectra of standards run under the same experimental conditions on the same instrument can be easily done. This latter method, which effectively corrects for instrumentally dependent perturbations on the true fluorescence spectra is most widely used and applicable provided the users know the limitations, not only of their instrumentation, but also of the standard.

Not included here are fluorimetric measurements obtained on "uncorrected" instruments which are presented without units of intensity or benefit of comparative measurements. Many of these types of published results have led to confusion and are often of no quantitative value.

Fluorescence standards can be used to (a) correct spectra for instrumental parameters such as the wavelength dependence of exciting lamp intensity, monochromator transmission and detector response, (b) determine comparative quantum efficiencies, (c) compare data among laboratories, (d) determine periodically "in house" instrumental stabilities, (e) calibrate fluorescent lifetime determinations, and (f) calibrate polarization value measurements.

The requirements for a "general" fluorescence standard are quite specific. It should:

(a) have broad fluorescence spectra,
(b) be easily purifiable,
(c) be stable in solution or as the solid,
(d) have as little overlap as possible between the excitation (absorbance) and emission spectra,
(e) not be subject to oxygen quenching,
(f) have a constant quantum efficiency as a function of exciting wavelength,
(g) have isotropic emission,
(h) have the same emission spectrum shape independent of exciting wavelength,
(i) be soluble in aqueous and organic solvents, and
(j) absorb and emit in the same general regions as the compound under study.

No single compound exhibits all these desirable characteristics. In fact, the last requirement precludes the use of a single standard, for although absorbance may occur over a wide range (e.g. rhodamine B absorbs from 200 nm to about 560 nm), emission is usually limited to one small wavelength interval (for rhodamine B, 550 nm to 650 nm with maximum at 573 nm).

For this reason, in addition to the fact that fluores-

[1] Figures in brackets indicate the literature references at the end of this paper.

cence spectra are composites of true spectra and instrumental parameters dependent on wavelength, it is necessary to have available a series of fluorescence standards with emission maxima that covers the wavelength range of current interest. With the wide use of lasers and interest in radiative measurements in the near-infrared, this range now extends from 250 nm to 1100 nm.

One of the major objectives of the fluorescence program at the National Bureau of Standards is the selection, production, and certification of a series of fluorescence standards (Standard Reference Materials) which can be used for the standardization and comparison of data and methodologies among laboratories [5, 6]. It is essential that these Standard Reference Materials (SRM's) be certified with absolute values. Data reported here, however, are in relative units and not absolute since instrumentation for absolute measurements is not available at the present time. Absolute measurements will be made and values assigned to the SRM's as soon as instrumentation becomes available.

The work at NBS is following two parallel investigative paths: (a) the use of solutions of organic molecules and metal chelates in various solvents, and (b) in close collaboration with Reisfeld, The Hebrew University, Jerusalem, the use of inorganic ions in solid matrices. Group (b) may be further split into rare earth and nonrare earth inorganic ions. The investigative work on the inorganic ions has been covered extensively earlier in this series of papers by Reisfeld [7]. Discussion here, then, will be restricted primarily to the use of comparative standards in solution and some of the factors which affect quantum yields and spectra.

Since quinine and its derivatives are probably the most widely used comparative standards [13], and since a great deal of controversy exists as to their usefulness as standards, the emphasis of this paper is on the reproducibility, stability, and effects of wavelength excitation and acid concentration on the spectra and quantum efficiencies of the quinines.

I would like to digress briefly and discuss some of the equations and assumptions which have to be made in using comparative techniques and standards. Two types of solutions may be employed: optically dense and optically dilute. With optically dense solutions and front surface excitation and emission, Vavilov's experimental set up with some modifications is generally used [1, 8–12]. This method is not as widely utilized as the optically dilute method since stray light is high, compounds with large emission and excitation overlap give erroneous results, and only compounds with a high molar absorptivity can be used easily [13].

The optically dilute method is based on the Beer-Lambert Law and several assumptions. Combining the definition of quantum efficiency [14], eq (1),

$$Q=\frac{I_F}{I_A} \tag{1}$$

where Q = luminescence quantum efficiency
I_F = rate of fluorescence emission in quanta/s.
I_A = rate of light absorption in quanta/s.

with the Beer-Lambert Law, eq (2),

$$\frac{I_T}{I_0}=e^{-\epsilon cl} \tag{2}$$

where I_0 is the radiative flux of the exciting light in quanta/s,
I_T is the radiative flux of the transmitted light in quanta/s.
ϵ is the molar absorptivity in liter, mole^{-1}, cm^{-1},
c is the concentration in moles/liter,
l is the path length of the cell in cm,

and expanding the exponential term in a power series, the expression for the rate of light emission becomes [3, 13, 15]:

$$I_F=I_0(2.3\epsilon cl)\left[1-\frac{2.3\epsilon cl}{2}+\frac{(2.3\epsilon cl)^2}{6}-\cdots\right]Q. \tag{3}$$

For dilute solutions (i.e. absorbances less than 0.05), eq (3) may be approximated with only slight error by eq (4) [15],

$$I_F=I_0(2.3\epsilon cl)\,Q. \tag{4}$$

In determining comparative quantum efficiencies, a term for the index of refraction of the solvent is added [16–18], resulting in the final form of the applicable equation:

$$Q_u=Q_s\left(\frac{FA_u}{FA_s}\right)\left(\frac{A_s}{A_u}\right)\left(\frac{I_{0s}}{I_{0u}}\right)\left(\frac{\eta_u^2}{\eta_s^2}\right) \tag{5}$$

where Q is the quantum efficiency,
FA is the integrated fluorescence area (Σ quanta/unit bandwidth),
I_0 is the radiative flux of the exciting light in quanta/s,
η is the average refractive index of the solvent over the emission wavelength range, and
u and s refer to the unknown and standard, respectively.

In the studies reported here, comparative quantum efficiencies were calculated using eq (6) [20]:

$$Q_u=Q_s\left(\frac{FA_u}{FA_s}\right)\left(\frac{A_s}{A_u}\right)\left(\frac{\lambda_{ex_s}}{\lambda_{ex_u}}\right)\left(\frac{\eta_u^2}{\eta_s^2}\right) \tag{6}$$

where $\lambda_{ex_s}/\lambda_{ex_u}$ replaces I_0 and converts from an instrumentally produced constant energy to quanta/s.

The assumptions have been made, however, that (a) instrumental geometries are the same for the unknown and standard, (b) emission is isotropic, (c) the exciting light is monochromatic if excitation for both samples is

at different wavelengths, (d) no reabsorption and re-emission occur, and (e) the absorption is less than 0.04. (Recent work permits solutions with absorbances of 0.2 to 1.0 to be measured by the sideview technique [21, 22].) In addition, use of dilute solutions minimizes factors (d) and (e), and use of the same instrument and cuvette minimizes factor (a). Anisotropic emissions (polarization effects) may cause large measurement errors which may be corrected [13, 23]; but the easiest way to avoid polarization problems is to use a standard which emits isotropically.

Assuming then that corrected spectra may be obtained [11, 12, 15], the fundamental problem in spectrofluorimetry is the lack of well-characterized standards. Table 1 lists various organic compounds which have been suggested for possible inclusion in a series of

TABLE 1. Compounds proposed as fluorescence standards [1, 3, 8–10]

Compound	Emission maxima (nm)
β-Naphthol	354, 402
2-Aminopyridine	368
Anthracene	383, 404, 428, 454
Pyrene	390
Quinine sulfate	454
Quinidine sulfate	454
3-Aminophthalimide	510[a]
Fluorescein	518
N,N-Dimethylamino-*m*-nitrobenzene	542
Rhodamine 6G	557
Aluminum(III)-PBBR-chelate	635
4-Dimethylaminonitrostilbene	742

[a] Value is average.

fluorescence standards [1, 3, 10, 24, 25]. Some may not be suitable as general standards. Fluorescein undergoes degradation in sodium hydroxide, and solutions should be prepared and used within 12 hours. The purification of β-naphthol by recrystallization in air results in some discoloration due probably to oxidation. Aromatics such as anthracene and pyrene have narrow emission and/or excitation spectra (25 nm or less) and are not suitable as standards for fluorimeters which use wide slits since fluorescence spectra, as absorption spectra [26], are bandpass dependent [27, 28]. Other factors, such as acid concentration or excitation wavelength, are reported to affect the fluorescence of quinine and quinidine sulfates [21, 28–37] and 3-aminophthalimide [38]. The presentation and discussion of some of these factors and their effects, follow. The experimental section is presented as addendum A.

The following abbreviations are used in this paper: Q – quinine; QS – quinine sulfate; QDS – quinidine sulfate; 3-APT–3-aminophthalimide; N,N-DMAMNB–*N,N*-dimethylamino-*m*-nitrobenzene. Quinine samples are designated A, B, C, etc. and are listed in addendum A.

II. Results and Discussion

A. Quinine Sulfate and Related Compounds

1. Physical and Chemical State

It has been reported that the history of the quinine determines its optical characteristics [24, 35]. A report by Fletcher [28], however, suggests this is not the case, and that the observed differences were probably due to the presence of varying amounts of hydrated water. Although quinine sulfate is obtained as the dihydrate, varying amounts of water are definitely present. Table 2 summarizes the weight losses as determined by thermogravimetric (TGA) measurements for various quinine derivatives before and after vacuum drying. It can be seen that with no

TABLE 2. Water weight losses of various quinine derivatives as a function of pretreatment

Sample[a]		Percent weight loss	Calculated molecular formula
F	No drying	4.24	$QS^{b} \cdot 5.4H_2O$
C	No drying	4.96	$QS \cdot 5.7H_2O$
E	No drying	[c]4.37	$QS \cdot 5.0H_2O$
E	Vacuum dried, in desiccator for 6 months	0.18	$QS \cdot 2.1H_2O$
E	Vacuum dried within 24 hours	.03	$QS \cdot 2.0H_2O$
H	No drying	4.36	$QDS^{d} \cdot 5.4H_2O$
H	Vacuum dried within 24 hours	0.02	$QDS \cdot 2.0H_2O$
J	No drying	.00	$Q^{e} \cdot 2.0H_2O$

[a] See experimental section for designation.
[b] QS = quinine sulfate.
[c] Average of two determinations.
[d] QDS = quinidine sulfate.
[e] Q = quinine.

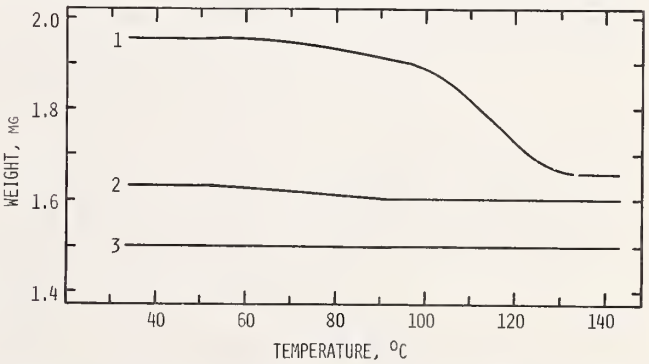

FIGURE 1. Thermogravimetric analyses of quinine sulfate (Sample E). 1. undried after recrystallization; 2. dried in vacuo at 55 °C for 18 hours, placed in desiccator, removed periodically to obtain sample; 3. freshly dried as 2. Heating rate was 5.0 °C/min in dry air. Weight scale offset 10 mg.

drying, approximately 5 to 6 waters of hydration per molecule rather than 2 are actually present. Figure 1 shows three TGA curves obtained for $QS \cdot 2H_2O$, sample E. There is a slight loss of water for the vacuum dried sample that had been kept in a desiccator for six months and removed periodically to obtain samples which shows the hygroscopic nature of $QS \cdot 2H_2O$. As pointed out by Fletcher [28], insufficient drying can cause variations in absorbance values, leading investigators to propose the inequivalence of quinine derivatives. For this reason, samples used for the following studies were predried as outlined in the experimental section.

2. *Absorbance Measurements*

Average weight absorptivities for various $QS \cdot 2H_2O$ samples from different suppliers with varying recrystallizations were calculated from eq (7), and the results are summarized in table 3.

$$WA = \frac{A}{cl} \tag{7}$$

where WA is the weight absorptivity.
A is the absorbance.
c is the sample concentration in grams solute/gram solvent.
l is the path length of the cell in cm.

Sample F gave consistently high weight absorptivities, but was included in the statistical analyses. The average weight absorptivities at 317.0, 347.5, and 365.0 nm for samples A to F differ from previous data [28] by −1.2 percent, +0.5 percent, and −2.3 percent in that order. Values for the average of all samples, including E, differ from previous data by −1.0 percent, −0.5 percent, and −1.0 percent in that order.

TABLE 3. Determination of weight absorptivities for quinine sulfate with varying recrystallizations in 0.1 N H_2SO_4 from different suppliers

Sample[a,b]	Rx[c]	Weight absorptivities × 10^4			
		365.0 nm	347.5 nm	317.0 nm	250.0 nm
A	0	0.922	1.430	1.148	7.720
B	0	.916	1.418	1.146	7.700
C	0	.918	1.428	1.145	7.710
D	3	.922	1.438	1.140	7.820
F	4	.941	1.454	1.162	7.920
E	6	.925	1.436	1.152	7.820
E'[d]	6	.947	1.445	1.146	7.717
Average[e]		0.924	1.434	1.149	7.782
σ		.009	0.012	0.008	0.086
Percent σ		.97	.84	.66	1.12

[a] All samples vacuum dried at 50–60 °C for 24 hours.
[b] See experimental section for sample designation.
[c] Times recrystallized.
[d] Absorbances measured on Cary 16, others on Cary 14, see addendum A.
[e] For samples A–F only (excluding E').

Determination of the weight absorptivities at 347.5 nm for three individual weighings of sample E yielded a value of 1.436 ± 0.005. Weight absorptivities and molar absorptivities are also given for $QDS \cdot 2H_2O$ in

TABLE 4. Molar and weight absorptivities (× 10^4) of quinine and quinidine sulfates in 0.1 N H_2SO_4

Compound	Concentration $M \times 10^{-5}$	Sample	Wavelength							
			365.0 nm		347.5 nm		317.0 nm		250.0 nm	
			ϵ[c]	WA[d]	ϵ[c]	WA[d]	ϵ[c]	WA[d]	ϵ[c]	WA[d]
Quinine sulfate[a]	2.554	E	0.7235	(0.924)	1.1228	(1.434)	0.8996	(1.149)	6.0930	(7.782)
Quinidine sulfate[b]	3.269	H	.7189	(0.918)	1.1257	(1.438)	.8902	(1.138)	6.0110	(7.676)

[a] Average for 6 determinations, samples A–F, table 2.
[b] Average for two determinations.
[c] l, mol^{-1}, $cm^{-1} \times 10^4$.
[d] $g_{solvents}, (g_{solute})^{-1}$, $cm^{-1} \times 10^4$.

table 4. As expected, the molar and weight absorptivities for QS·$2H_2O$ agree with those for QDS·$2H_2O$ since they are stereoisomers (structures for quinine and quinidine are I and II, respectively).

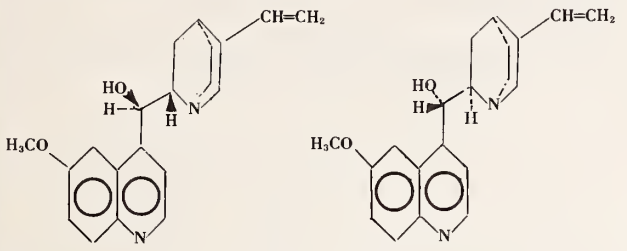

I. Quinine II. Quinidine

A single determination for the molar or weight absorptivities for quinine dihydrate gave results which, as a function of wavelength, were consistently 3 to 5 percent low as compared to the values for QS and QDS after correction for the difference in molecular weights. Plotting relative absorbances, i.e. A_λ/A_{250nm} versus wavelength, however, resulted in good agreement among the three spectra, figure 2, indicating the probable presence of a systematic error in the determination of the absorptivities for quinine dihydrate. These values are being redetermined.

Values of the ratios for several absorbance peaks of QS in 0.1 *N* sulfuric acid have been calculated from the literature [28–30, 33, 36, 46–48], and these values and those from the present work are reported in table 5. Although systematic errors exist since various spectrophotometers were used, comparison of the average of the literature values and the present work show differences to be +2.77, +0.25 and +0.62 percent. The first value is for the A_{250}/A_{347} ratio, and measurements in the ultraviolet are usually not as accurate or precise as those in the visible. Statistical evaluation (again

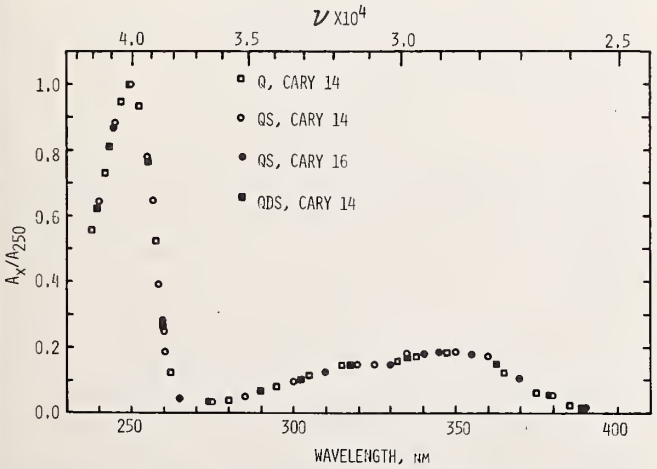

FIGURE 2. Normalized absorbance spectra of quinine (Q), quinine sulphate (QS), and quinidine sulfate (QDS) in 0.1 *N* H_2SO_4 using absorbance at 250.0 nm as 1.0. Temperature, 25.0 °C.

TABLE 5. Absorbance ratios for quinine sulfate dihydrate in 0.1 *N* sulfuric acid

Spectrophotometer	A_{250}/A_{346}	A_{317}/A_{346}	A_{365}/A_{346}	Ref.
Cary 16	5.340	0.793	0.655	this work
Cary 14	5.43	.80	.64	this work
Cary 14	5.38	.78	.65	[33]
Cary 14	5.36	.80	.62	[30]
Beckman D.U.		.82	.63	[47]
Beckman D.U.	5.43	.80	.59	[29]
Bausch and Lomb	5.23	.80	.63	[30]
Turner 210	5.4	.82	.66	[28]
	5.0	.75		[46]
	5.25	.80	.65	[48]
	5.10	.82	.69	[36]

including systematic errors) of all the ratios shows, however, that any individual ratio may be as much as 4 or 5 percent high or low at only the 68 percent confidence level. It is essential that accurate data be obtained for absorbance measurements, especially since the determinations of relative quantum efficiencies depend on these measurements, eqs (5) and (6).

The instruments used for the absorbance measurements in the present work were checked for accuracy by comparison against optically neutral filters supplied by Mavrodineanu [26]. Absorbance measurements were also made on solutions of QS and 3-APT in 0.1 *N* sulfuric acid at peak maxima using various instruments. The results are summarized in table 6. Good agreement was observed for these solutions. No

TABLE 6. The determination of absorbances of quinine sulfate and 3-aminophthalimide in 0.1 *N* H_2SO_4 using various spectrophotometers

QS A, 250.0 nm	3-APT A, 385.0 nm	Instrument
	0.9164	NBS [26]
0.7506	.9158	Cary 16
.751	.919	Cary 14
.749	.914	Turner 210

apparent fluorescence artifact was observed as shown by comparing absorbances from the first three instruments with those of the last instrument which has a monochromator between the sample and the detector [20, 23].

Differences as large as 8 percent, however, were observed when absorbances were measured on slopes in absorbance spectra. Care must therefore be used when absorbance measurements are made on slopes of peaks since small errors in wavelength (and also large bandwidths if the slope is steep) result in inaccurate absorbance values.

3. *Fluorescence Measurements*

Studies were made to determine fluorescence reproducibility of measurements on quinine sulfate dihydrate (sample E) in 0.1 *N* sulfuric acid. Table 7 summarizes results of repetitive measurements on five different quinine sulfate solutions.

Table 7. Reproducibility of repetitive fluorescence measurements on different solutions of quinine sulfate dihydrate

(Sample E) in 0.1 *N* sulfuric acid[d]

Concentration (ppm)	Average emission peak area	σ	Percent σ
0.5[a]	0.053	0.002	2.83
1.0[a]	.104	.002	1.92
1.0[b]	.104	.001	1.09
2.5[a]	.260	.002	0.85
5.0[a]	.706	.003	.42
5.0[b]	.518	.001	.22
10.0[a]	.915	.007	.78
10.0[b]	.911	.003	.32
5.0[c]	.517	.003	.59

[a] Dilution by volume, four sample weighings.
[b] Dilution by weight, three sample weighings.
[c] Quinidine sulfate dihydrate (Sample H) dilution by weight.
[d] λ_{ex}, 350 nm.

Fairly large standard deviations were obtained with the 0.5 and 1.0 ppm solutions, probably due to instrumental noise resulting from increased instrumental sensitivity. As can be seen, dilution by weight yields results for which standard deviations are approximately two times lower than those for dilution by volume. Similar results were obtained for solutions of quinidine sulfate [38]. All weighings of the vacuum-dried solid samples were made in air. Weighing in a dry nitrogen atmosphere should result in lower percent standard deviations since the dried material is somewhat hygroscopic.

Similar fluorescence measurements made on solutions of quinine sulfate samples from two different sources (samples A, B, D, and F), results summarized in table 8, show that the relative integrated area under the fluorescence peak may be considered to be the same if percent standard deviations of 1 to 3.0 percent are acceptable.

Table 8. Measurement of fluorescence peak areas using quinine sulfate dihydrate from two sources[a]

Sample	Emission peak areas: One day average	Emission peak areas: Three day average
A	0.555	0.554
B	.542	.544
D	.552	.556
F	.564	.558
Average	.553	.553
σ	.009	.006
Percent σ	1.64	1.12

[a] λ_{ex}, 350.0 nm; °C = 25.0.

Studies were also initiated to determine the stability of quinine sulfate (sample E) in 0.1 *N* sulfuric acid since little definitive data exist concerning the stability of QS in solution [43, 44, 49]. Table 9 summarizes results for "stabilities" during two "short time" (1 to 10 h) tests, while table 10 and figure 3 summarize results for longer periods of time (25 to 35 days). As might be expected, the results in table 9 show stabilities are better for the 1 hour determinations than for those stretching over a 10 hour period. From table 10, it is observed that glasses give more repeatable values and thus lower percent standard deviations. It is evident from the data in tables 9 and 10 and figure 3 that the results are actually composites of quinine sulfate solution stability and instrumental stability. The latter was maximized by using the overlapping solution method, and the results from this study are graphically illustrated in figure 4.

Table 9. Statistical analyses for fluorescence determinations[c] of quinine sulfate dihydrate (Sample E) in 0.1 *N* H_2SO_4 during two "short" time intervals

Concentration (ppm)	1.0[a]	5.0[a]	10.0[a]	1.0[b]	2.0[b]	2.0[b]
H_2SO_4, *N*	0.1	0.1	0.1	0.1	0.1	0.01
$\bar{A}$, peak area	.105	.557	1.116	.411	.816	.848
σ	.004	.003	.005	.001	.002	.001
Percent σ	4.34	.59	.49	.21	.24	.14

[a] Eleven determinations during a 10 hour span (same solution).
[b] Four determinations during a 1 hour span (same solution).
[c] λ_{ex} = 350.0 nm; °C = 25.0.

Table 10. Fluorescence peak areas of quinine sulfate and a uranium doped glass as a function of time on corrected and uncorrected instruments

	Instrument A, corrected [20] QS, Sample E[a,b]	Instrument B, uncorrected QS, Sample E[a,c]	Instrument B, uncorrected Uranium glass[c]
Average peak area	0.739	0.398	0.383
σ	.011	.027	.018
Percent σ	1.49	6.89	4.80

[a] 2.0 ppm in 0.1 *N* H_2SO_4.
[b] Fifteen measurements covering 26 days.
[c] Fourteen measurements covering 37 days. The uranium glass was too concentrated for use in the corrected instrument.

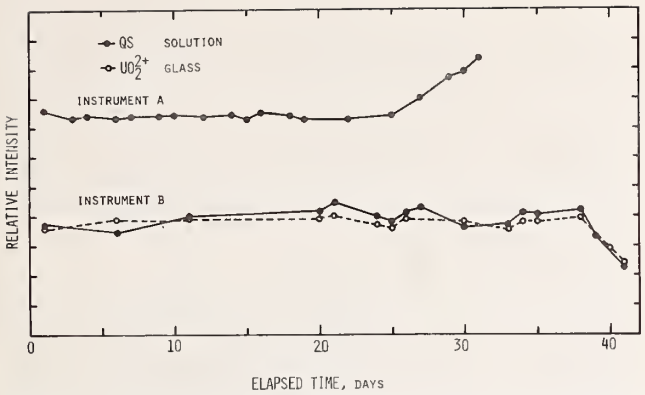

FIGURE 3. Instrumental and compound stability determinations using 2 ppm (μg solute/g solvent, 2.55×10^{-6} M) quinine sulfate in 0.1 N H_2SO_4 and a uranyl glass on corrected (instrument A) and uncorrected (instrument B) spectrofluorimeters.

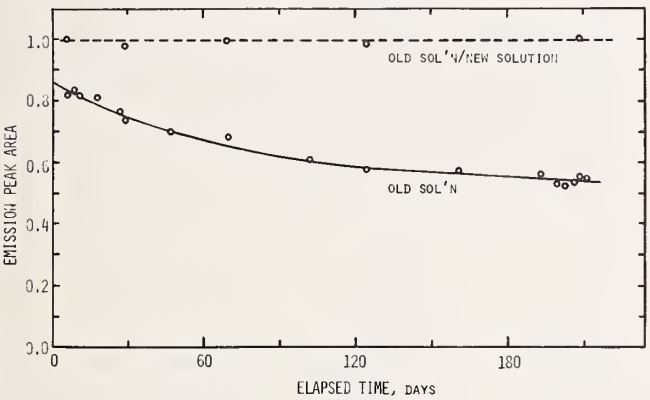

FIGURE 4. 2 ppm (2.55×10^{-6} M) quinine sulfate stability test in 0.1 N H_2SO_4 using relative emission peak areas as a function of time, designated by solid line and overlapping solution method (peak area original solution/peak area fresh solution), designated by broken line.

A 37 percent decrease in relative peak area as a function of time was observed (solid line) which, on face value, would indicate instability of the quinine sulfate in solution. Preparing new solutions, however, and comparing the peak areas to those of the "aged" solution gave ratios of one (designated by dashed line) proving quinine sulfate stability in solution over this period of time. The assumption was made that dried QS in a desiccator in the dark was stable over the 6-month period of time. Absorbance measurements for the freshly prepared QS solutions agreed within the standard deviations presented in table 3. The observed 37 percent decrease in peak area was due therefore to an instrumental factor and not QS instability.

No long term data as to the stability of quinine sulfate in a 0.1 N sulfuric acid solution in light have been established; however, preliminary results indicate that a 2 ppm solution is stable for 2 weeks if irradiated by typical laboratory fluorescent lighting [38]. Excitation in this study was done at 350 nm and emission peak areas were measured in the usual manner. However, Melhuish [50] reports a 25 percent decrease in fluorescence intensity upon irradiation of the QS solution with 313 nm light (and excitation at 313 nm). Excitation at this wavelength also resulted in a deviation of quantum efficiency as a function of excitation wavelength [13, 21]. The problems which arise when this wavelength is used should be investigated.

4. *Corrected Excitation and Emission Spectra*

To insure consistency in relative quantum efficiency measurements with instruments that give corrected spectra, the excitation spectrum should be compared with the absorbance spectrum and the emission spectrum compared with corrected spectra obtained by other investigators.

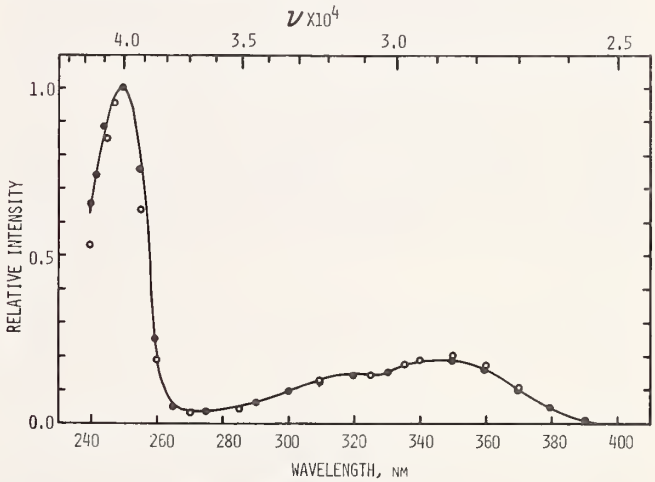

FIGURE 5. Normalized intensities which show equivalency of absorbance spectrum (solid line) and excitation spectrum (circles). Quinine sulfate solution 20 ppm (2.55×10^{-5} M) for absorbance spectrum and 2 ppm (2.55×10^{-6} M) for excitation spectrum, both in 0.1 N H_2SO_4; excitation bandwidth, 25 Å, emission bandwidth, 100 Å; temperature, 25.0 °C.

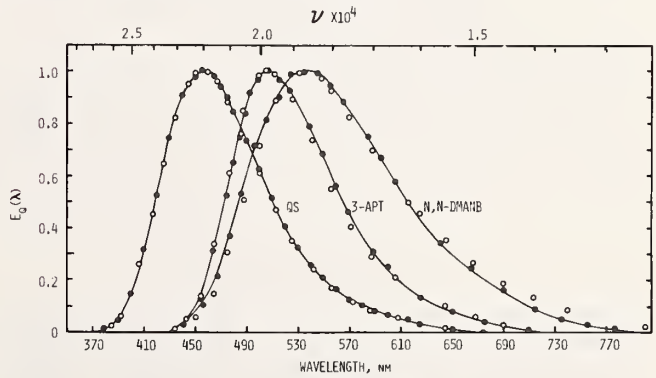

FIGURE 6. Relative $E_q(\lambda)$ versus wavelength for quinine sulfate [2 ppm (2.55×10^{-6} M) in 0.1 N H_2SO_4], 3-aminophthalimide [5.64 ppm (2.68×10^{-5} M) in 0.1 N H_2SO_4], and N,N-dimethylamino-m-nitrobenzene [2.76 ppm (9.34×10^{-6} M) in 70 percent n-hexane: 30 percent benzene, V/V] ●= this study, ○=Lippert, et al., [1] corrected from $E_q(\nu)$ to $E_q(\lambda)$ [50].

The equivalency of the excitation spectrum and absorbance spectrum is shown in figure 5, which has, as a direct consequence, the constancy of quantum efficiency as a function of excitation wavelength (discussed later). Some deviation is seen at wavelengths >350 nm as might be expected with the reported shift in emission maximum as a function of excitation wavelength [29, 31]. The emission spectra of QS and 3-APT in 0.1 *N* sulfuric acid and N,N-DMAMNB are given in figure 6 as $E_q(\lambda)$ versus λ in which $E_q(\lambda)_{max}=1$. Data show good agreement with those taken from Lippert, et al. [1] which were corrected to $E_q(\lambda)$ from $E_q(\nu)$ by multiplying $E_q(\nu)$ by λ^{-2} [50].

5. *Relative Quantum Efficiencies*

a. Intercomparative Study.—To verify the validity of the relative quantum efficiency (QE) measurements, an intercomparative study was undertaken using QS, fluorescein, pyrene, rhodamine B, and 3-APT in various solvents as comparison "standards." Table 11 summarizes the results of this study. The values of the quantum efficiencies for quinine or its derivatives in sulfuric acid have been reported to be in the range 0.40 to 0.70 [12, 21, 32, 34, 35, 37, 43–45]. Melhuish [43] and Dawson and Windsor [21] have measured the absolute quantum efficiency for QS in 1.0 *N* sulfuric acid and obtained excellent agreement (0.546 and 0.54 ± 0.02, respectively, $\lambda_{ex}=365$ nm). Measurements by Eastman [35] tend to support these findings. Systematic errors [13] have been suggested to explain low values of 0.46 or less by Rusakowicz and Testa [24] and Drobnik and Yeargers [34]. The quantum efficiencies chosen for this comparative study are the widely used and accepted values of 0.55 and 0.51 in 1.0 and 0.1 *N* sulfuric acid, respectively [43].

It is difficult to reconcile the results of this intercomparative study and many others with those of Scott, et al. [37], who recently reported the quantum efficiency of QS in 0.1 *N* sulfuric acid, based on lifetime measurements, as 0.70. It has been reported that QS has an anomalous lifetime [45, 51], and thus basing quantum efficiencies on this measurement alone is questionable. In addition, Scott, et al., suggest that the discrepancies in quantum efficiencies may be explained if previous investigators had ignored the red "tail" (>550 nm) of the corrected emission spectrum. An examination of the corrected emission spectra, however, figure 6 [1], shows that the spectra extend quite far into the red (>650 nm).

Quantum efficiencies for fluorescein in sodium

TABLE 11. Results of the intercomparative quantum efficiency (QE) study [e]

	Solvent	QE	QE (lit.)
QS[a]	0.1 *N* H_2SO_4	0.51 ± 0.01	0.508[43]
QDS[b]	.1 *N* H_2SO_4	$.52\pm0.01$	
Fluorescein[c]	.1 *N* NaOH	$.87\pm0.03$	[d].88
Pyrene[b]	Toluene	$.57\pm0.04$	.60[21], 0.32[51]
Rhodamine B [b]	Ethanol	$.72\pm0.02$	.69[3], 0.71[13]
3-Aminophthalimide[b]	0.1 *N* H_2SO_4	$.47\pm0.02$	

[a] Determined by intercomparison study with fluorescein, pyrene and rhodamine B.
[b] Duplicate determinations, duplicate measurements.
[c] Quadruplicate determinations, duplicate measurements.
[d] Average of 16 literature values, see text.
[e] Temperature, 25.0 ± 0.1 °C.

TABLE 12. Dependence of the relative quantum efficiencies of quinine and quinidine sulfates on sulfuric acid concentrations [a]

	Quantum efficiencies				
	$QS\cdot2H_2O$				$QDS\cdot2H_2O$
$[H^+]$, *N*	This work	[21]	Percent [c]	Percent [32]	This work
0.01	0.52 ± 0.01		+1.97		
.02	.52		+1.57		
.10	[b].51	0.50	—		0.52
.50	.54		+5.71		
1.02	$.55\pm0.01$	.54	+7.68	6	.55
2.00	.57		+9.84		
3.56	$.60\pm0.01$	.60	+17.72	13	.59

[a] Temperature, $25.0\pm.1$ °C, $\lambda_{ex}=350.0$ nm.
[b] Reference.
[c] Using 0.51 as 100 percent.

hydroxide have been reported to cover the range 0.76 to 0.96 [3, 9, 21, 23, 52–61]; however, the most widely accepted value is 0.90 plus or minus five percent [13]. The values quoted for pyrene and rhodamine B are less widely accepted: e.g. values of 0.97 and 0.92 have been reported for rhodamine B [23, 57], although it was reported the measurements in these cases were not made with a red-sensitive photomultiplier [13].

b. Acid Concentration.—The variability of quantum efficiency of quinine sulfate as a function of three sulfuric acid concentrations has been reported [21, 32]. These studies were extended to cover eight acid concentrations, as summarized in table 12. The results for the 0.1, 1.0, and 3.5 *N* sulfuric acid concentrations agree well with those reported by Dawson and Windsor [21] and Eisenbrand [32], although the latter reported a constant quantum efficiency for sulfuric acid concentrations from 0.01 to 0.2 *N*. The increases for acid concentrations less than 0.1 *N* are small, but apparently real, since Chen also observed this same phenomenon and suggested that this was due to less quenching by the sulfate ion at low acid concentrations [62]. Although the weight absorptivities of QS and QDS in three different acid concentrations agree within experimental error, table 13, a slight trend towards lower absorbances

TABLE 13. Weight absorptivities [a] of quinine and quinidine sulfates as a function of H_2SO_4 concentration [b]

	WA [a] × 10^4 at 347.5 nm	
$[H_2SO_4]$ *N*	QS	QDS
0.10	1.43	1.44
1.02	1.40	1.41
3.55	1.39	1.40

[a] See equation (7).
[b] Temperature 25.0 °C.

may be noted. Coupled with the increased fluorescence area as $[H^+]$ increases, the observed increase in quantum efficiency may be explained simply by ionization changes; however, discussions by Chen [29, 62] appear to negate this explanation. Further work is being done to resolve these discrepancies.

The increase in quantum yield of QS as a function of acid concentration is paralleled by QDS as might be expected due to their similarities in spectra, figure 2 [30, 47] and molar absorptivities, tables 4 and 13.

c. Excitation Wavelength.—The quantum efficiencies of quinine sulfate, figure 7, rhodamine B, and rhodamine 6G, figure 8 (others discussed later) were found to be independent of excitation wavelength (±5 percent). The largest deviations for QS were found from 260 to 280 nm where the absorbance is at a minimum and larger errors would be expected. Several investigators [21, 29, 36] reported a variation in quantum efficiency of fluorescence intensity as a

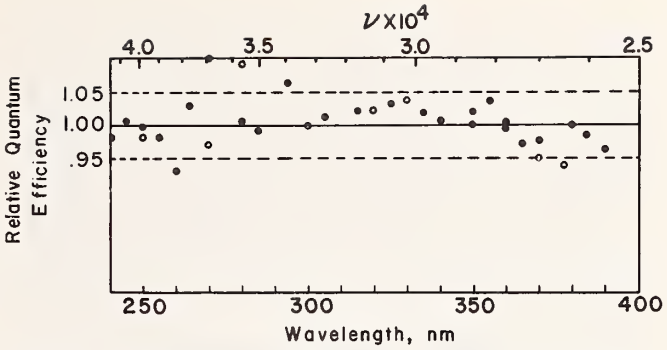

FIGURE 7. Relative quantum efficiencies of quinine sulfate as a function of excitation wavelength (● = this work), quinine sulfate concentrations: λ_{ex} = 240–290 nm, 0.1 ppm (1.28×10^{-7} *M*) and 0.5 ppm in 0.1 *N* H_2SO_4; λ_{ex} = 260–390 nm, 2.0 and 2.5 ppm (6.39×10^{-7} *M*) in 0.1 *N* H_2SO_4; excitation bandwidth, 25 Å; emission bandwidth, 100 Å; temperature, 25.0 °C; O=Fletcher [28].

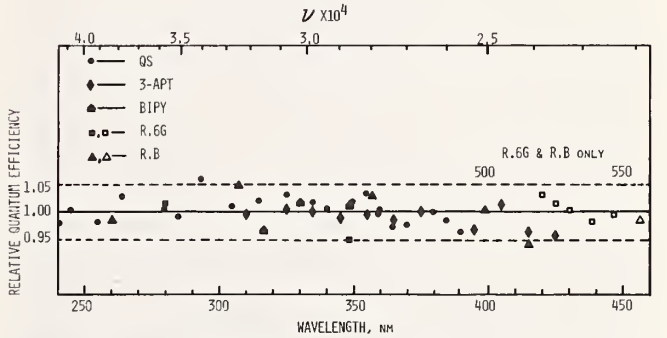

FIGURE 8. Relative quantum efficiencies as a function of excitation wavelength: quinine sulfate—same conditions as figure 7;3-aminophthalimide, 5.64 ppm (2.68×10^{-5} *M*) in 0.1 *N* H_2SO_4; bipyrenyl (BIPY), 0.14 ppm (2.98×10^{-7} *M*) in toluene; rhodamine 6G (R.6G), 0.12 ppm (2.08×10^{-7} *M*) and 0.025 ppm (4.43×10^{-8} *M*) in ethanol; rhodamine B (R.B.), 0.13 ppm (2.15×10^{-7} *M*) in ethanol. Emission bandwidth, 100 Å; excitation bandwidth, 25 Å; temperature, 25.0 °C.

function of excitation wavelength. Fletcher [28], however, found no more than ±5 percent quantum yield deviation for excitation wavelengths from 240 to 400 nm (except for 272 nm region, selected values in fig. 7), and other investigators also report essentially no variation in quantum yield at two excitation wavelengths [33–35].

B. Aromatic Hydrocarbons

Another large group of compounds with relatively high quantum yields are the aromatic hydrocarbons. Series of possible standards may be made by simply adding aromatic rings to the base compound, e.g. benzene and naphthalene fluoresce in the UV, anthracene exhibits blue fluorescence, naphthacene fluoresces in the green, and pentacene in the red. Anthracene has been studied quite extensively in ethanol and benzene, and the quantum efficiencies

reported from these studies vary from 0.25 to 0.33 [3, 18, 21, 23, 43, 57, 63–67].

We have studied pyrene derivatives [42] to determine if these compounds are suitable as fluorescence standards and to determine if substituents on more condensed systems exhibit the same trends in emission wavelengths, intensities and quantum efficiencies as the substituted naphthalenes. Corrected excitation and emission spectra for the pyrene derivatives are presented in figure 9. The 1-chloro-, 1-bromo-, and 1-nitropyrene compounds showed little, if any, fluorescence but would be expected to phosphoresce at low temperatures if the substituent "heavy atom" effect is followed for the substituted pyrenes as in the case of the naphthalenes [68]. The results for the quantum efficiency calculations and data taken from Berlman [51] for the naphthalenes and pyrenes are summarized in table 14. As can be seen, fairly good agreement was obtained with the quantum efficiency values from Berlman for the bipyrenyl. Better agreement for pyrene, however, was obtained with values from Förster and Seidel [69], probably due to the use of the same solvent, toluene, rather than benzene. The value for the quantum efficiency of pyrene by Dawson and Windsor [21] was obtained using ethanol as the solvent. The differences observed here may be due to some of the problems associated in the general use of aromatic hydrocarbons as standards since aromatics (a) usually show oxygen quenching, (b) have fairly large emission-excitation spectra overlap, (c) are very sensitive to extremely small amounts of impurities, (d) have narrow emission bandwidths, necessitating use of narrow slits, and (e) must have large index of refraction corrections made (as in this work) when quantum efficiencies are compared to compounds dissolved in aqueous media.

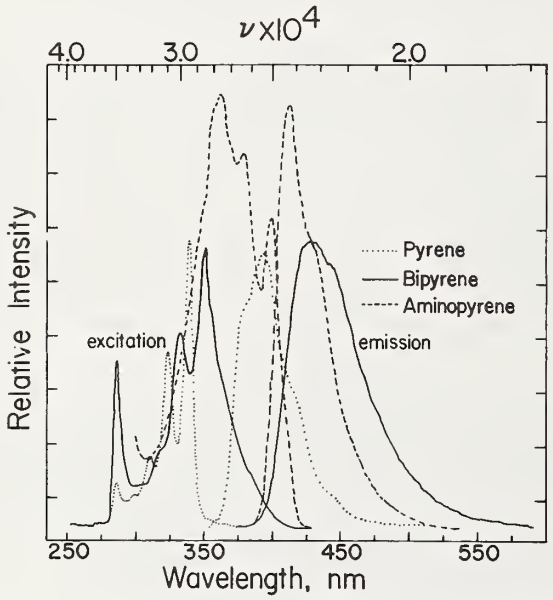

FIGURE 9. Relative intensities (emission spectra: quanta/unit bandwidth) versus wavelength for 0.13 ppm (5.69×10^{-7} *M*) pyrene, 0.47 ppm (1.84×10^{-6} *M*) 1-aminopyrene and 0.14 ppm (2.98×10^{-7} *M*) bipyrenyl in toluene. Excitation bandwidth, 25 Å, emission bandwidth, 100 Å; temperature, 25.0 °C.

Similar trends in quantum efficiencies are noted upon comparing pyrene and naphthalene to bipyrenyl and binaphthalenyl. The dimeric species have quantum efficiencies that are higher than the monomeric species which may be directly attributable to the lifetimes—i.e. 2 to 3 ns for the dimers and 100 to 600 ns for the monomers [51, 70]. The dimeric species have more asymmetry than the monomeric species and thus possess higher transition probabilities.

C. 3-Aminophthalimide

Although the compound 3-APT in 0.1 *N* sulfuric acid has been suggested as a fluorescence standard [1], care should be taken in its use. We have found that the absorption (excitation) spectrum, figure 10, and the quantum efficiency, table 15, are dependent on the acid concentration [38]. The decrease in the weight absorptivities at 385 nm with increasing acid concentration, coincides with the increased absorbance of a peak at 296 nm.

The quantum efficiency of 3-APT in ethanol reported by Alentsov [52] was 0.6. A quantum efficiency of 0.47 in 0.1 *N* sulfuric acid is not unreasonable in view of the difference in solvent. The observed decreases in the quantum efficiencies as a function of acid concentration are consistent with the presence of more than one species, allowing additional radiationless transitions such as energy transfer between the species to occur.

TABLE 14. Quantum efficiencies (QE) of some pyrene derivatives compared to similar naphthalene derivatives

Compound	Solvent	λ_{ex}	$\lambda_{em(max)}$	QE
Pyrene	Toluene	338.5	394	0.48, [a]0.52, [b]0.32, [c]0.53
1-Aminopyrene	Toluene	401	413	.43
1,1′-Bipyrenyl	Toluene	349	428	.78, [b]0.84
Naphthalene[a]	Cyclohexane	276	322	.23
1-Aminonaphthalene[a]	Cyclohexane	319	376	.46
1,1′-Binaphthyl[a]	Cyclohexane	284, 294	361	.77

[a] Ref. [70].
[b] Ref. [51].
[c] Ref. [21].

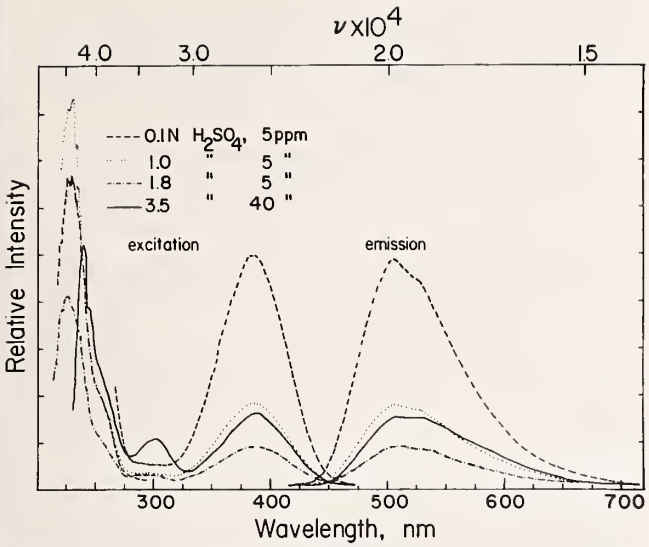

FIGURE 10. Relative intensities (emission spectra: quanta/unit bandwidth) versus wavelength for 5 ppm (2.38×10^{-5} *M*) and 40 ppm (1.90×10^{-4} *M*) 3-aminophthalimide in 0.1 *N*----, 1.0 *N*·····, 1.8 *N* -·-·- and 3.5 *N*—H_2SO_4. Excitation bandwidth. 25 Å; emission bandwidth, 100 Å; temperature, 25.0 °C.

TABLE 15. Dependence of absorbance at 385 nm and quantum efficiency for 3-aminophthalimide as a function of sulfuric acid concentration

	$WA^a \times 10^4$		
$[H_2SO_4]$, *N*	385 nm	296 nm	Quantum efficiencies[b]
0.10	2.36	0.39	0.45 ± 0.01
1.02	1.29	.78	$.31 \pm 0.02$
1.75	0.82	.94	$.23 \pm 0.02$
3.55	.32	1.02	$.15 \pm 0.01$

[a] See equation (7).
[b] λ_{ex}=385 nm; °C=25.0; reference=QS · $2H_2O$ in 0.1 *N* H_2SO_4.

This work is in progress and will be reported later in more detail. The quantum efficiency for 3-APT in 0.1 *N* sulfuric acid is constant witl in ±5 percent over the excitation wavelength range of 310 to 425 nm, figure 8.

D. Other Fluorescence Standards

N,*N*-dimethylamino-*m*-nitrobenzene has also been suggested as a standard [1] and, although the quantum efficiency appears to be relatively constant as a function of excitation wavelength [38], it is quite low and not very suitable as a standard. In addition, as mentioned before, a solvent system of 70:30, V:V of hexane:benzene is not desirable since fluorescence analyses in the biochemical areas [71] require use of compounds which are soluble in aqueous media.

Chen [62] has suggested standards which can be used in aqueous solutions and are suitable for biochemical applications. Other compounds which might be added to this list that cover the "red" region, include rhodamine B and rhodamine 6G, both used as quantum counters and both having relatively constant quantum efficiencies over a wide excitation wavelength range (250 to 600 nm), figure 8 [13, 72]. Studies should be made of these compounds in aqueous rather than alcoholic media, although aggregation in water has been reported [73].

E. Inorganic Ions in Glass or Polycrystalline Matrices

The use of inorganic ions in glass matrices as cuvette or disc shaped samples, figure 11, is attractive, especially when one considers ease of handling which may result in decreased methodological errors [74, 75]. The inorganic ions may be split into two classes determined by their absorption and emission spectra.

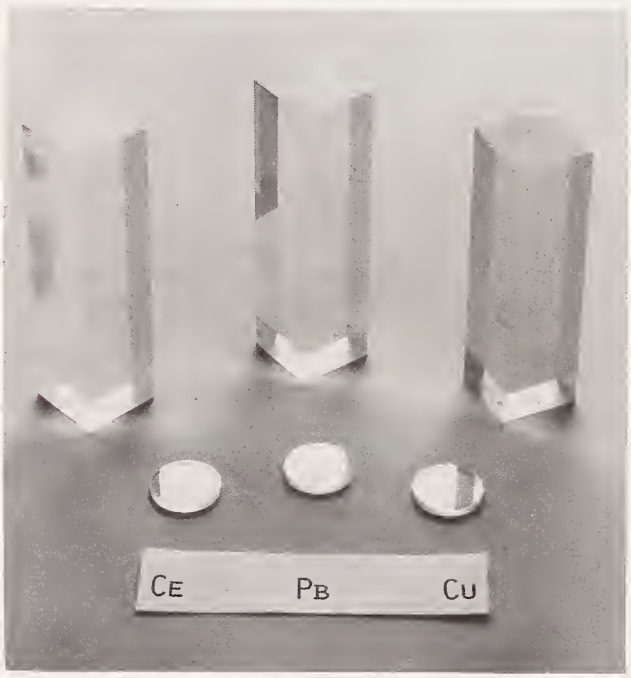

FIGURE 11. Cuvette and disc shaped cerium, lead, and copper doped silicate glasses.

The non-rare earths and cerium(III) have broad spectra with little structure due to interconfigurational electronic transitions, making them prime candidates for fluorescence standards. The rare earths in the +3 oxidation states, on the other hand, have sharp spectra due to intraconfigurational transitions (less than 25 nm bandwidths), and may be used for wavelength calibration, spectral resolution of instruments, and, in special cases, as quantum yield standards.

The non-rare earth inorganic ions interact to a greater extent with the matrix than the rare earth ions. Thus changing the glass matrix from borate to silicate results in fairly large shifts of emission maxima.

502-591 O - 73 - 17

Figure 12 shows these shifts for lead-doped phosphate, borate, and silicate glasses.

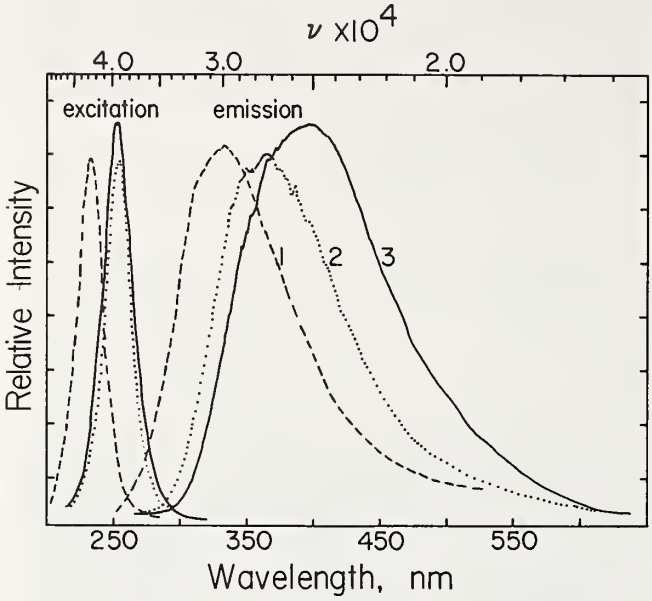

FIGURE 12. Relative intensity (emission spectra: quanta/unit bandwidth) versus wavelength for lead doped phosphate, 1; borate, 2; and silicate, 3; discs. Emission and excitation bandwidths, 100 Å; temperature, 25.0 °C; angle of disc with exciting beam, 15° [74, 75].

Table 16 summarizes ranges of emission maxima for the non-rare earth ions in glass or polycrystalline matrices. For an in-depth discussion of these effects and information concerning the rare earths, see reference [7] and the references listed therein.

TABLE 16. Ranges of emission maxima for cerium and non-rare earth inorganic ions in various solid matrices [a]

Inorganic Ion	Emission Range (nm)
Tl^{+}	290–325
Ce^{3+}	325–400
Pb^{2+}	350–450
UO_2^{2+}	475–550
Cu^{+}	475–550
Mn^{2+}	500–600

[a] For emission spectra, see reference [7].

F. Summary

In summary then, substantiative data are being accumulated as to the applicability of various compounds for use as fluorescence standards. The next major step would appear to be interlaboratory testing and comparison of data leading to the acceptance of either a single or a series of standards which are widely available for general use. Quinine sulfate, due to its desirable fluorescence characteristics, overall applicability, and widespread use and study, should probably be the first material selected for an interlaboratory comparison study.

III. Addendum A. Materials and Instrumentation

In order to adequately describe materials and experimental procedures, it was occasionally necessary to identify commercial products by manufacturer's name or label. In no instances does such identification imply endorsement by the National Bureau of Standards, nor does it imply that the particular product or equipment is necessarily the best available for that purpose.

A. Materials

The following reagents were used in this study:

Perchloric Acid: National Bureau of Standards, purified reagent, double distilled, lot 111103 [39].

Sulfuric Acid: Ultrex Grade, J. T. Baker Chemical Co., Phillipsburg, N.J. Used as obtained.

Sodium Hydroxide: Reagent Grade, J. T. Baker Chemical Co., address above. Used as obtained.

Distilled Water: Distilled water was passed through an ion exchange column (IWT Research Column, Rockford, Illinois), followed by double distillation from a quartz still.

Toluene: Certified, Fisher Chemical Co., Fairlawn, N.J., was shaken with cold concentrated sulfuric acid, water, aqueous 5 percent sodium hydroxide, water, and dried over calcium sulfate in that order. It was then distilled from sodium under nitrogen.

Benzene and *n*-Hexane: Spectrograde, Eastman Chemical Co., Rochester, N.Y. Used as obtained.

Ethanol, 95 and 100 percent: Pharmco Distributing Co., Publicker Industries, Philadelphia, Pa. Used as obtained.

Quinine Sulfate Dihydrate: Sample A—Aldrich Chemical Co., lot 032007; sample B—N. F. Grade, Fisher Chemical Co.; sample C—Pfalz and Bauer, 31–20 College Point Causeway, Flushing, N.Y.; sample D—sample A recrystallized three times from warm water; sample E—sample A recrystallized six times from warm water; sample F—sample B recrystallized four times from warm water.

Quinidine Sulfate Dihydrate: Sample G—Aldrich Chemical Co., lots 032781 and 062607; sample H—sample G recrystallized four times from warm water.

Quinine Dihydrate: Sample J—Aldrich Chemical Co., lot 071491 dissolved in dilute sulfuric acid, precipitated by neutralizing with dilute ammonium hydroxide. Washed with water twice.

All quinine derivatives were dried at 55–60 °C under vacuum for a minimum of 18 h before use [28].

Fluorescein: Aldrich Chemical Co., purified three times by the method of Koch [40].

Rhodamine B and Rhodamine 6G: Samples obtained from R. A. Keller [41]. Rhodamine 6G was purified by repeated recrystallizations, using ethyl acetate:

ethanol followed in one case by elution from a silica column (purification by R. A. Keller).

3-Aminophthalimide: Eastman Organic Chemicals. Recrystallized three times from ethanol, mp-260 °C [1].

N,N-Dimethylamino-*m*-nitrobenzene: Eastman Organic Chemicals. Recrystallized twice from chloroform and once from acetone-benzene [1].

Pyrene, bipyrenyl, 1-aminopyrene, 1-chloropyrene, and 1-nitropyrene prepared as designated [42].

B. Instrumentation

Absorbance spectra were obtained using Cary 14 and Cary 16 spectrophotometers, and a Turner Model 210 "Spectro" in the absorbance mode [20]. The spectrophotometers (except Model 210) were equipped with constant temperature cell blocks. Spectra were recorded or read at 25.0 ± 0.1 °C. Matched quartz cuvettes of 0.1, 1.0, and 5.0 cm were used.

Fluorescence spectra were obtained using a Turner Model 210 "Spectro" which gives corrected excitation and emission spectra [20], and a Farrand spectrofluorimeter which gives uncorrected spectra. Unblackened quartz spectrofluorimeter cells were used. Solvents were always run to determine baselines.

Before quantum efficiencies or band positions were measured, the accuracy of the wavelength scales for the emission and excitation monochromators were checked using a mercury lamp. A polished aluminum block cut at an angle of 45° was placed in the sample compartment. The monochromators were calibrated at 253.6, 435.8, and 546.1 nm. If necessary, the wavelength scales were adjusted so that accuracies of ±0.2 nm over the 253.6 to 546.1 nm range were obtained. A special Schlenk type [76] quartz cell was constructed, figure 13, by H. Deleonibus, Glassblowing Section, 129.06, National Bureau of Standards.

Stopcock and stopper were of polytetrafluoroethylene to avoid contamination. The solution was placed in the cylindrical sidearm and alternately frozen using liquid nitrogen and evacuated and thawed at room temperature at least five times to deoxygenate the solution. A test which repeated this cycle ten times resulted in a solution weight loss of less than 0.1 percent. Fluorescence studies, unless noted, were made on the corrected instrument. Quantum efficiencies were determined in duplicate, except where noted. All fluorescence measurements were made with 25 Å excitation bandwidth, 100 Å emission bandwidth, and at 25.0 ± 0.1 °C, except where noted.

Thermogravimetric measurements were run using dry nitrogen on a Model 950 TGA, E. I. DuPont de Nemours & Co., Wilmington, Delaware, by T. Sterling or S. Wicks, Section 310.04, Analytical Chemistry Division, National Bureau of Standards.

The glasses mentioned were prepared by the Inorganic Glass Section, 313.02, W. Haller, head, National Bureau of Standards. They were cut to size and polished by the Optical Shop, Section 129.05, S. Gerner, National Bureau of Standards.

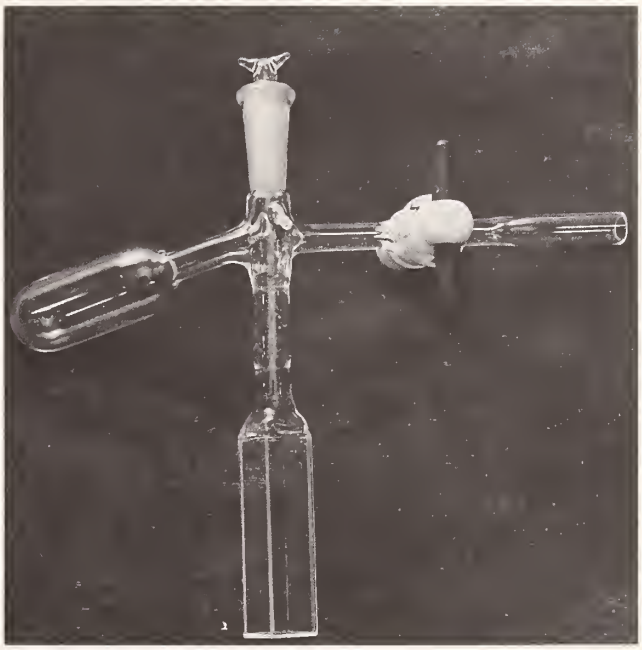

FIGURE 13. Schlenk type [76] spectrofluorimeter cell used with nitrogen manifold for degassing solutions.

The author would like to acknowledge the useful discussions in fluorescence with G. H. Atkinson, NBS, and the encouragement and support of O. Menis and J. I. Shultz, NBS.

IV. References

[1] Lippert, E., Nägele, W., Seibold-Blankenstein, I., Staiger, W., and Voss, W., Z. Anal. Chem. **170**, 1 (1959).
[2] Melhuish, W. H., J. Phys. Chem. **64**, 762 (1960).
[3] Parker, C. A., and Rees, W. T., Analyst **85**, 587 (1960).
[4] Chapman, J. H., Förster, Th., Kortüm, G., Lippert, E., Melhuish, W. H., Nebbia, G., and Parker, C. A., Z. Anal. Chem. **197**, 431 (1963).
[5] Velapoldi, R. A., Nat. Bur. Stand. (U.S.), Tech. Note 544 (O. Menis and J. I. Shultz, Eds.) 151 pages (Sept. 1970).
[6] Velapoldi, R. A., Nat. Bur. Stand. (U.S.), Tech. Note 584 (O. Menis and J. I. Shultz, Eds.) 175 pages (Dec. 1971).
[7] Reisfeld, R., "Inorganic Ions in Glasses and Polycrystalline Pellets as Fluorescence Standard Reference Materials, J. Res. Nat. Bur. Stand. (U.S.), **76A** (Phys. and Chem.), No. 6, (Nov.–Dec. 1972).
[8] Vavilov, S. I., Z. Phys. **22**, 266 (1924).
[9] Vavilov, S. I., Z. Phys. **42**, 311 (1927).
[10] Melhuish, W. H., J. Opt. Soc. Amer. **54**, 183 (1964).
[11] Melhuish, W. H., J. Opt. Soc. Amer. **52**, 1256 (1962).
[12] Melhuish, W. H., New Zealand J. Sci. Tech. **37**, 142 (1955).
[13] Demas, J. N. and Crosby, G. A., J. Phys. Chem. **75**, 991 (1971).
[14] No distinction is made here between luminescence quantum yield, quantum efficiency, or quantum yield.
[15] Parker, C. A., Photoluminescence of Solutions (Elsevier Publishing Co., New York, N.Y., 1968).
[16] Förster, Th., Fluoreszenz Organischer Verbindungen (Vandenhoeck-Ruprecht, Göttingen, Germany, 1951).
[17] Gilmore, E. H., Gibson, G. E., and McClure, D. S., J. Chem. Phys. **23**, 399 (1955).
[18] Fletcher, A. N., J. Mol. Spectry. **23**, 221 (1967).
[19] Hermans, J. J. and Levinson, S., J. Opt. Soc. Amer. **41**, 460 (1951).
[20] Turner, G. K., Science **146**, 183 (1964).

[21] Dawson, W. R. and Windsor, M. W., J. Phys. Chem. **72,** 3251 (1968).
[22] Gill, J. E., Appl. Spectry. **24,** 588 (1970).
[23] Weber, G. and Teale, F. W. J., Trans. Faraday Soc. **53,** 646 (1957).
[24] Rusakowicz, R. and Testa, A. C., J. Phys. Chem. **72,** 2680 (1968).
[25] Argauer, R. J. and White, C. E., Anal. Chem. **36,** 368 (1964).
[26] Mavrodineanu, R., Nat. Bur. Stand. (U.S.), Tech. Note 544, 151 pages, Sept. 1970 and 584, 175 pages, Dec. 1971 (O. Menis and J. I. Shultz, Eds.).
[27] Dawson, W. R. and Kropp, J. L., J. Opt. Soc. Amer. **55,** 822 (1965).
[28] Fletcher, A. N., Photochem. Photobiol. **9,** 439 (1969).
[29] Chen, R. F., Anal. Biochem. **19,** 374 (1967).
[30] Gill, J. E., Photochem. Photobiol. **9,** 313 (1969).
[31] Fletcher, A. N., J. Phys. Chem. **72,** 2742 (1968).
[32] Eisenbrand, J., Z. Anal. Chem. **179,** 170 (1961).
[33] Rosen, P., and Edelman, G. M., Rev. Sci. Instrum. **36,** 809 (1965).
[34] Drobnik, J., and Yeargers, E., J. Mol. Spectry. **19,** 454 (1966).
[35] Eastman, J. W., Photochem. Photobiol. **6,** 55 (1967).
[36] Börreson, H. C., Acta Chem. Scand. **19,** 2089 (1965).
[37] Scott, T. G., Spencer, R. D., Leonard, N. J., and Weber, G., J. Amer. Chem. Soc. **92,** 687 (1971).
[38] Velapoldi, R. A., and Kenigsberg, D. R., unpublished results.
[39] Murphy, T. J., Section 310.06, Analytical Chemistry Division, National Bureau of Standards, Washington, D.C. 20234.
[40] Koch, L., J. Assoc. Off. Agr. Chem. **42,** 149 (1959).
[41] Samples obtained from R. A. Keller, Section 316.03, Physical Chemistry Division, National Bureau of Standards, Washington, D.C. 20234.
[42] Fatiadi, A., and Velapoldi, R. A., unpublished data.
[43] Melhuish, W. H., J. Phys. Chem. **65,** 229 (1961).
[44] G. K. Turner Associates, Notes on the Determination of Quantum Efficiency with the Model 210 "Spectro", Feb. 1966.
[45] Birks, J. B., and Dyson, D. J., Roy. Soc. (London) Proc. **A275,** 135 (1963).
[46] Moss, D. W., Clin. Chim. Acta **5,** 283 (1960).
[47] Grant, H. S., and Jones, J. H., Anal. Chem. **22,** 679 (1950).
[48] Bartholomew, R. J., Rev. Pure Appl. Chem. Australia **8,** 265 (1958).
[49] Bowman, E. J., and Wokes, F., Fluorescence of Solutions (Longmans Green, London, p. 77, 1953).
[50] Ejder, E., J. Opt. Soc. Amer. **59,** 223 (1969). See also Discussion by W. H. Melhuish, Absolute Spectrofluorometry, J. Res. Nat. Bur. Stand. (U.S.), **76A** (Phys. and Chem.), No. 6, 547–560 (Nov.–Dec. 1972).
[51] Berlman, I. B., Handbook of Fluorescence Spectra of Aromatic Molecules, 2d ed., p. 383 (Academic Press, New York, N.Y., 1971).
[52] Alentsov, M. A., National Res. Council of Canada. Tech. Trans., TT–433 from Zhur. Eskp. i. Teoret. Fiz. **21,** 133 (1951).
[53] Forester, L. S., and Livingston, R., J. Chem. Phys. **20,** 1315 (1952).
[54] Hellstrom, H., Arkiv. Kemi. Mineral. Geol. **12A,** 17 (1937).
[55] Umberger, J., and LaMer, V., J. Amer. Chem. Soc. **67,** 1099 (1945).
[56] Bridges, J. W., and Williams, R. T., Nature **196,** 59 (1962).
[57] Roberts, B. G., and Hirt, R. C., Ann. ISA Conf. Proc. **19** (III), 2.2.2.64 (1964).
[58] Hercules, D. M., and Frankel, H., Science **131,** 1611 (1960).
[59] Latimer, P., Bannister, T. T., and Rabinowitch, E., Science **124,** 585 (1956).
[60] Forester, L. S., and Dudley, D., J. Phys. Chem. **66,** 838 (1962).
[61] Seybold, P. G., Gouterman, M., and Callis, J., Photochem. Photobiol. **9,** 229 (1969).
[62] Chen, R. F., Measurements of Absolute Values in Biochemical Fluorescence Spectroscopy, J. Res. Nat. Bur. Stand. (U.S.), **76A** (Phys. and Chem.), No. 6, 593–606 (Nov.–Dec. 1972).
[63] Parker, C. A., and Joyce, T., Trans. Faraday Soc. **62,** 2785 (1966).
[64] Medinger, T., and Wilkinson, F., Trans. Faraday Soc. **61,** 620 (1965).
[65] Drushel, H. V., Sommers, A. L., and Cox, R. C., Anal. Chem. **35,** 2167 (1963).
[66] Bridges, J. W., and Williams, R. T., Nature **196,** 59 (1962).
[67] Himel, C. M., and Mayer, R. T., Anal. Chem. **42,** 130 (1970).
[68] Wehry, E. L., and Rogers, L. B., in Fluorescence and Phosphorescence Analyses, D. M. Hercules, Ed., p. 81 (Interscience Publishers, New York, N.Y., 1966).
[69] Förster, Th., and Seidel, H. P., Z. Phys. Chem. (N.F.) **48,** 58 (1965).
[70] Birks, J. B., Photophysics of Aromatic Molecules, p. 128 (J. Wiley & Sons, Ltd., New York, N.Y., 1970).
[71] Udenfriend, S., Fluorescence Assay in Biology and Medicine (Academic Press, New York, N.Y., Vols. I and II, 1962, 1969).
[72] Yguerabide, J., Rev. Sci. Instrum. **39,** 1048 (1968).
[73] Selwyn, J. E., and Steinfeld, J. I., J. Phys. Chem. **76,** 762 (1972).
[74] Velapoldi, R. A., and Reisfeld, R., Nat. Bur. Stand. (U.S.), Tech. Note 584 (O. Menis and J. I. Shultz, Eds.) 175 pages (Dec. 1971).
[75] Reisfeld, R., Honigbaum, A., and Velapoldi, R. A., J. Opt. Soc. Amer. **61,** 1422 (1971).
[76] Schlenk, W., and Thal, A., Ber. Deut. Chem. Ges. **46,** 2840 (1913).

(Paper 76A6–748)

Author Index

C

D

E

F

M

N

O

P

Q

R

Subject Index

This brief Subject Index should be considered as a complement to the Table of Contents located at the beginning of this publication. The reader should use the Table and the Subject Index to find the information of interest.

FORM NBS-114A (1-71)

U.S. DEPT. OF COMM. BIBLIOGRAPHIC DATA SHEET	1. PUBLICATION OR REPORT NO. NBS SP-378	2. Gov't Accession No.	3. Recipient's Accession No.

4. TITLE AND SUBTITLE
Accuracy in Spectrophotometry and Luminescence Measurements, Proceedings of the Conference Held at NBS, Gaithersburg, Md., March 22-24, 1972.

5. Publication Date
May 1973

6. Performing Organization Code

7. AUTHOR(S)
R. Mavrodineanu, J. I. Shultz, and O. Menis, eds.

8. Performing Organization

9. PERFORMING ORGANIZATION NAME AND ADDRESS

NATIONAL BUREAU OF STANDARDS
DEPARTMENT OF COMMERCE
WASHINGTON, D.C. 20234

10. Project/Task/Work Unit No.

11. Contract/Grant No.

12. Sponsoring Organization Name and Address

Same as 9.

13. Type of Report & Period Covered
Final

14. Sponsoring Agency Code

15. SUPPLEMENTARY NOTES

16. ABSTRACT (A 200-word or less factual summary of most significant information. If document includes a significant bibliography or literature survey, mention it here.)

This volume contains the 18 papers presented at the Conference on Accuracy in Spectrophotometry and Luminescence Measurements organized by the Analytical Chemistry Division of the National Bureau of Standards and held from March 22 to 24, 1972.

These papers discuss the problems encountered in accurate spectrophotometry and luminescence measurements of materials. They also define the status of these competences from the standpoint of basic principles, critical factors involved in the measurements, and the instrumental conditions which must be fullfilled to assure accurate measurements. Particular attention is given to the selection, production and use of Standard Reference Materials in spectrophotometry and spectrofluorometry. Problems related to health are also covered in six of the papers, two of which include original contributions to the application of luminescence techniques to specific biochemical problems.

17. KEY WORDS (Alphabetical order, separated by semicolons)
Accuracy; critical parameters; instrumentation; linearity; quantum efficiency; spectrofluorometry; spectrophotometry; standards.

18. AVAILABILITY STATEMENT

[X] UNLIMITED.

[ ] FOR OFFICIAL DISTRIBUTION. DO NOT RELEASE TO NTIS.

19. SECURITY CLASS (THIS REPORT)
UNCLASSIFIED

21. NO. OF PAGES
268

20. SECURITY CLASS (THIS PAGE)
UNCLASSIFIED

22. Price
4.85, domestic postpaid
4.50, GPO Bookstore

☆U.S. GOVERNMENT PRINTING OFFICE : 1973 O—502-591

USCOMM-DC 66244-P71